Frank Wiese, Mike Reich and Gernot Arp (Eds.)

"Spongy, slimy, cosy & more"

Commemorative Volume in Celebration of the
60th Birthday of Joachim Reitner

Universitätsverlag Göttingen

Frank Wiese, Mike Reich and Gernot Arp (Eds.)
"Spongy, slimy, cosy & more"

Frank Wiese, Mike Reich and
Gernot Arp (Eds.)

"Spongy, slimy, cosy & more"

Commemorative Volume in Celebration
of the 60th Birthday of Joachim Reitner

Göttingen Contributions to Geosciences
Volume 77

Contents

Preface

Bent T. Hansen[1]

[1]Department of Isotope Geology, Geoscience Centre, Georg-August University Göttingen, Goldschmidtstr. 3, 37077 Göttingen, Germany; Email: bhansen@ gwdg.de

Göttingen Contributions to Geosciences (GCG), yet another new journal for earth science? The answer is no, the issue you are watching on your screen or holding in your hand is the new version of the well-known *Göttinger Arbeiten zur Geologie und Paläontologie (GAGP).* After 45-year-long presence as printed version, the *GAGP* goes online as an Open Access journal and from now on available as both printed and online. The journal intends to cover a wide range of different geo-scientific subjects and is dedicated to disseminate and share selected research achievements, offering a convenient access to interested researchers in geoscience and related communities.

The Geoscience Centre of the Georg-August University of Göttingen (GZG) acts as the publisher of the *GCG* represented by the present director. The first editors in chief will be J. Reitner and M. Reich both also responsible for the museum, exhibitions and the geopark of the GZG. The editorial board is primarily built by the professors from the eight divisions within the Geoscience Center, and therefore a very broad spectrum of geological themes like geology, sedimentology, structural geology, mineralogy, geochemistry, paleontology, environmental geology and geobiology are covered, but also guides to special exhibitions as well as contributions to the history of geolog-

ical sciences are welcome. Like in the *Göttinger Arbeiten zur Geologie und Paläontologie* the *Göttingen Contributions to Geosciences* will also be open for conference abstracts, contributions from workshops, PhD dissertations, excursion guides and further related monographs.

The cooperation with the *Göttingen University Press (Universitätsverlag Göttingen)* not only guaranties a professional handling of the new releasing issues, but also the Open Access to the 76 regular and 5 special issues of the *Göttinger Arbeiten zur Geologie und Paläontologie* already published. The publication of these former issues would not have been possible without the highly appreciated work of Helga Groos-Uffenorde, who was the responsible editor of the journal from 1969 to 2003.

The continuation of the *GAGP* as an Open Access journal has been the aim of Joachim Reitner for many years, so we are happy the realize his ambition on the occasion of his 60th birthday. I am well aware that the celebration took place two years ago, but as a geochronologist I am used to work with ages including a certain limit of error. Nevertheless, I am convinced that the *Göttingen Contributions to Geosciences* will have an excellent future as it is based on a long and successful tradition.

Professor Dr Bent T. Hansen

(Deputy Dean of the Faculty of Geoscience and Geography)

Introduction

Frank Wiese[1]; Mike Reich[1,2] & Gernot Arp[1]

[1]*Department of Geobiology, Geoscience Centre, Georg-August University Göttingen, Goldschmidtstr. 3, 37077 Göttingen, Germany; Emails: frank.wiese-1@geo.uni-goettingen.de & garp@gwdg.de*
[2]*Geoscience Museum, Georg-August University Göttingen, Goldschmidtstr. 1-5, 37077 Göttingen, Germany; Email: mreich@gwdg.de*

This issue of *"Göttingen Contributions to Geosciences"* is a continuation of the „*Göttinger Arbeiten zur Geologie und Paläontologie"*, founded in 1969. It contains 18 contributions of colleagues, companions and friends of Professor Dr. Joachim Reitner, and it is a convolute of subjects, most of which Joachim worked on during one of his numerous scientific phases of his career. We are glad having received so many scientific contributions, which are thematically very diverse and extremely interesting. Especially in times, where Hirsch and impact factors are the Golden Calf, it is not always easy to convince scientists to publish in a small journal. But those who contributed know that it is not the index what this issue is about. It is about and it is for Joachim Reitner in the occasion of his 60th birthday.

Joachim Reitner (JR), born 1952-05-06 in Garmisch-Partenkirchen, studied geology and palaeontology at the Eberhard Karls University in Tübingen, where he received his diploma and, later, his dissertation in 1984. He finished his postdoctoral qualification with the habilitation at the Freie Universität Berlin in 1991, and in 1994, Joachim followed the offer of a professorship in palaeontology from the Georg August University of Göttingen. For his seminal work on biomineralisation and evolution of coralline sponges, he was – as the first palaeontologist – rewarded the "Leibniz-Preis", the highest-ranked German sponsorship award for German scientists. Since 1998, Joachim is member of the Göttingen Academy of Sciences.

Fig. 1:   Joachim Reitner (Nanjing 2011).

When looking at the huge number of publications it becomes obvious that Joachim's scientific activities cover a broad field. Starting with coleoid palaeontology and tectono-sedimentary evolution of Cretaceous carbonate systems, he then focused on sponges and their biomineralisation. Proterozoic life, microbial early life, rock-forming microbial activities, biomineralisation, methane, deep biosphere, critical intervals or Fossil-Lagerstätten and astrobiology, are only some of the keywords that might sum up his research interest and publication topics. Field trips in the context of his study took him to any imaginable areas of the world (wherever rocks are accessible...), and his almost obsession-like sampling is legendary (we are not talking about kg or tens of kg per field trip....).

Apart from his professional career, Joachim also left a trace as an artist, as can be seen by his work in the Ars Natura and his participation in numerous exhibitions, and, of course, as a palaeontologist, he worked with sculpturing and natural stones.

Finally, we thought to add a complete list of Joachim's publications. This, however, turned out to be impossible because not even Joachim seems to have the entire overview over his numerous papers. But we know the problem now and start to collect the things together; maybe, we will be successful until his 70th birthday...

Fig. 2:   Selection of photographs of J. Reitner: **(A)** Berlin (1988); **(B)** Dolomites, Italy (1997); **(C)** Styria, Austria (2005); **(D)** Yichang, Hubei, P. R. of China (2011).

We wish JR all the best for his future research and life.

Frank Wiese

Mike Reich

Gernot Arp

Different regeneration mechanisms in the rostra of aulacocerids (Coleoidea) and their phylogenetic implications

Helmut Keupp[1] * & Dirk Fuchs[2]

[1]*Freie Universität Berlin, Institut für Geologische Wissenschaften (Fachrichtung Paläontologie), Malteser-Str. 74-100, Haus D, 12249 Berlin, Germany; Email: keupp@zedat.fu-berlin.de*
[2]*Freie Universität Berlin, Institut für Geologische Wissenschaften (Fachrichtung Paläontologie), Malteser-Str. 74-100, Haus D, 12249 Berlin, Germany; Email: drig@zedat.fu-berlin.de*

* corresponding author

Shells with growth anomalies are known to be important tools to reconstruct shell formation mechanisms. Regenerated rostra of aulacocerid coleoids from the Triassic of Timor (Indonesia) are used to highlight their formation and regeneration mechanisms. Within Aulacocerida, rostra with a strongly ribbed, a finely ribbed, and a smooth surface are distinguishable. In the ribbed rostrum type, former injuries are continuously discernible on the outer surface. This observation implicates that this type thickens rib-by-rib. In contrast, in the smooth rostrum type, injuries are rapidly covered by subsequent deposition of concentric rostrum layers.

This fundamentally different rostrum formation impacts the assumed monophyly of Aulacocerida. According to this phylogenetic scenario, either the ribbed rostrum type (and consequently also the strongly folded shell sac that secrets the rostrum) of Hematitida and Aulacocerida or the smooth rostrum type of xiphoteuthidid aulacocerids and belemnitids evolved twice. Assumption of a paraphyletic origin of aulacocerid coleoids might resolve this conflict since the ribbed rostrum could have been inherited from Hematitida and gradually smoothened within the lineage Aulacoceratidae—Dictyoconitidae—Xiphoteuthididae—Proostracophora.

Introduction

Palaeopathology usually involves individual growth irregularities of mainly mineralised hard parts. Causes for these anomalies can be endogene (genetical, pathological, parasitic) or exogene (abiotic or biotic interactions like injuries or epibionts) factors. Palaeopathological phenomena are therefore adequate sources for aut- and synecological interpretations. Essential aspects for autecology are formation mechanisms und functionality of characters, whose modification boundaries are often determinable only after comparisons with anomalies. Such information is furthermore very useful for an objective evaluation whether characters possess a taxonomic/systematic significance or not.

Table 1: Age, number of studied specimens, number of anomalies, family assignment, and rostrum morphology of examined aulacocerids.

Taxon	Stage	number of specimens	number of anomalies	family	rostrum surface
Aulacoceras sulcatum v. Hauer, 1860 var. *timorensis* Wanner, 1911	Carnian/Norian	236	3	Aulacoceratidae	ribbed
Aulacoceras sulcatum v. Hauer, 1860 var. *elliptica* v. Bülow, 1915		2	0	Aulacoceratidae	finely ribbed
Buelowiteuthis plana (v. Bülow) Jeletzky, 1966		7	0	Dictyoconitidae	finely ribbed
Dictyoconites multisulcatus v. Bülow, 1915		1	0	Dictyoconitidae	finely ribbed
Dictyoconites elegans v. Bülow, 1915		58	0	Xiphoteuthididae	smooth
Atractites gracilis v. Bülow, 1915			0		
Atractites parvus v. Bülow, 1915			0		
Atractites lanceolatus v. Bülow, 1915	Ladinian	53	1	Xiphoteuthididae	smooth
		357	4		

The variety of possible interpretations of palaeopathological phenomena in ectocochleate Cephalopoda have been recently summarised by Keupp (2012). As a result of their different bauplans, regeneration mechanisms of shells or shell parts considerably differ in ecto- and endocochleate cephalopods. In the former, the regenerative mantle epithelium is located inside the shell, whereas in the latter it is located both inside and outside. Within the endocochleate Coleoidea, whose shell is fully covered by regenerative epithelium (the so-called shell sac), different healing modifications can additionally indicate different soft part constructions, which itself might bear a systematic relevance. A good example for the systematic significance of shell anomalies is given for the case of aulacocerid rostra from the Middle and Upper Triassic of Timor (Indonesia).

Material

During a field campaign in summer 2007 to the river system of the Oë Bihati near Baun (SW Timor), the senior author, together with W. Weitschat (Hamburg) and R. Veit (Velden), collected numerous aulacocerid rostra from Middle and Upper Triassic (and Lower Jurassic) erratic boulders (see also Keupp 2009).

Three rostra (= 1.3 %) among in total 236 studied rostra of *Aulacoceras sulcatum* showed regenerated shell injuries (Table 1). Within the few records of dictyoconitid aulacocerids there was no evidence of anomalies. Similarly, 111 atractid rostra from the Ladinian and Carnian/Norian lack any evidence of shell repairs. However, a single specimen collected during an earlier field trip at Bekal–Nassi (Timor) was available for the present study. The rostrum of *Atractites lanceolatus* exhibits a knee-like fracture (Mietchen et al. 2005).

The present material is deposited in the collection H. Keupp (SHK) at the Freie Universität Berlin.

General morphology, stratigraphy and systematic position of Aulacocerida within Coleoidea

The order Aulacocerida Stolley, 1919 is typified by a longiconic phragmocone, which is covered from outside by a thin primordial rostrum and a solid rostrum proper (Jeletzky 1966; Bandel 1985). In contrast to Belemnitida, both rostral layers have been described as originally aragonitic (Cuif & Dauphin 1979; Bandel & Spaeth 1988). More aulacocerid key characters are a tubular body chamber (or final chamber) without evidence of a forward projecting proostracum typical of belemnitids and obviously widely spaced (i.e., remarkably long) chambers. The initial chamber (protoconch) is spherical and completely sealed by a closing membrane (Jeletzky 1966; Bandel 1985). The primary phragmocone wall (conotheca) is 4-layered (a thin inner prismatic layer, a thick middle layer of tabular nacre, a thin outer prismatic layer, an outermost organic layer). The marginal siphuncle is located ventrally. Aulacocerid soft parts are unknown.

Unambiguous aulacocerids shells are recorded from the Early Triassic to the Late Jurassic. Some shells tentatively interpreted as belonging to aulacocerids have been described also from Permian (e.g., Gordon 1966) and Carboniferous deposits (Flower & Gordon 1959; Jeletzky 1966; Doyle 1990; Doguzhaeva et al. 2010). Owing to slight differences in shell morphologies, some of these presumed Palaeozoic aulacocerids have been later removed from Aulacocerida and placed within Hematitida (Doguzhaeva et al. 2002). Despite of this systematic separation, Aulacocerida is very similar to Hematitida in having a longiconic phragmocone, a tubular body chamber, and an aragonitic rostrum proper, which is why a reliable distinction is very difficult and only possible in well preserved material.

In the past, aulacocerids have often been considered as hook-less (Engeser 1990). Indeed, hooks (micro-onychites) and aulacocerid shells have never been observed associated. However, if the abovementioned Palaeozoic coleoids indeed represent early aulacocerids, the abundant presence of hooks in Carboniferous, Permian and Triassic deposits would indicate that aulacocerid arms were likewise armed with hooks – as in belemnitids.

The aulacocerid/hematitid character combination "longiconic phragmocone with a tubular body chamber, a small spherical protoconch, a marginal siphuncle, and tabular nacre in the conotheca" suggest a primitive character state and therefore a close phylogenetic relationship with ectocochleate Bactritida (Kröger et al. 2011).

Traditionally, Aulacocerida (and Hematitida) has been grouped together with Phragmoteuthida (Middle Triassic–Lower Jurassic), Belemnitida (Upper Triassic–Upper Cretaceous), and Diplobelida (Upper Jurassic–Upper Cretaceous) as Belemnoidea. However, the latter taxon most probably represents a paraphylum (Fuchs 2006; Fuchs et al. 2010; Kröger et al. 2011).

Phragmoteuthida is characterised by a ventrally opened body chamber, which resulted in the development of a weakly mineralised proostracum (Donovan 2006; Doguzhaeva & Summesberger 2012). Apart from this, phragmoteuthids lack a solid rostrum. Belemnitida mainly differ from Aulacocerida/Hematitida by the possession of a proostracum and a predominantly calcitic rostrum proper. Diplobelida can be easily distinguished from Aulacocerida by the presence of a narrow proostracum and the absence of a rostrum proper (Fuchs 2012; Fuchs et al. 2012). Non-belemnoid coleoids such as Vampyropoda (absence of mineralised shell parts) and early spirulid/sepiids (absence of a solid rostrum proper) are usually not subject to misinterpretations.

General morphology of the aulacocerid/hematitid rostrum proper

The function of the aulacocerid/hematitid as well as the belemnitid rostrum is commonly regarded as a counterweight to bring the animal into a horizontal swimming position (Spaeth 1975; Bandel 1989; Monks et al. 1996; Hewitt et al. 1999; Fuchs et al. 2007; Keupp 2012). Moreover, rostra have also been interpreted to serve as fin attachment sites (Bandel 1989).

Basically, the aulacocerid/hematitid rostrum proper (= telum in other terminologies, e.g., Jeletzky 1966) appears in two different morphologies; one with a smooth and one with a longitudinally ribbed surface (Fig. 1).

Both types are of course formations of the shell sac and therefore homologous. However, they must have been formed in clearly differentiated shell sacs.

Ribbed rostra of *Hematites* and *Aulacoceras* consist of radially arranged longitudinal ribs or folds. Adjoining ribs are in contact (or with very narrow interspaces) and each rib shows a lamellar growth pattern (Figs. 1a, g, j). Accordingly, the ribbed rostrum must have been formed in a radially folded shell sac. Whereas the latter rostra can be described as strongly ribbed, some aulacocerid forms such as *Dictyoconites* exhibit very fine-ribbed rostra (Fig. 1b–d, h). On the other hand, smooth rostra – like in belemnitid rostra – consist of lamellar layers, which must have been successively formed in an unfolded shell sac (Fig. 1e–f, i, l). Hence, the ribbed rostrum type thickens rib-by-rib, whereas the smooth type concentrically grows around a nucleus. Smooth rostra characterises the aulacocerid family Xiphoteuthididae (e.g., *Atractites*).

Owing to this fundamentally different formation strategy, both rostrum types should have a very high systematic (and phylogenetic?; see discussion below) value. Both rostral growth modalities must have additionally a strong influence on shell regenerations so that their differences should especially become evident in repaired rostra.

Regeneration patterns after traumatic injuries

Similar to sepiids, whose cuttlebone is well known to show shell regenerations caused by unsuccessful predator attacks (Ruggiero 1980; Wiedmann & von Boletzky 1982; Battiato 1983; Bello & Paparella 2002), aulacocerid (and belemnitid) rostra yield traces of regenerations (Fig. 2a–d). Repaired fractures, which are often concentrated on the dorsal sides of the rostra, were most likely caused by large predators (vertebrates?).

In the smooth rostrum type, injuries regenerated during early ontogenetical stages are hardly visible in later stages as post-traumatic layers mask the former injury. An apically knee-like rostrum of *Atractites* sp. from the Sinemurian of Enzesfeld figured by Mojsisovics (1871) and later by Mariotti & Pignatti (1993: pl. 2, figs. 1–2) represents a good example for a regenerated smooth rostrum. The actual fracture is no more visible since subsequent layers cover and thereby bond the dislocated fragments of the injured juvenile rostrum. Similarly, the S-like bended rostrum of *Atractites lanceolatus* from the Ladinian of Timor indicates a repaired double-fracture (Fig. 2d). As demonstrated in Fig. 2f, analogous malformations in belemnite rostra can be visualised by the help of magnetic resonance techniques (Mietchen et al. 2005). This method is unfortunately not applicable in those strongly re-crystallised (originally aragonitic) rostra from Timor. Slight deformations on the outer surface of smooth rostra might therefore indicate former regenerations inside the rostrum.

Fig. 1: Regular rostra of Middle and Late Triassic Aulacocerida (a–k). **(a)** *Aulacoceras sulcatum*, dorsal view, SHK MB-644. **(b–d)** *Dictyoconites multisulcatus*, SHK MB-535; **(b)** ventral view; **(c)** lateral view; **(d)** close up of (b). **(e)** *Atractites gracilis*, SHK MB-517. **(f)** *Atractites lanceolatus*, lateral view, SHK MB-12. **(g)** same specimen as in (a), cross-fracture in alveolar view. **(h)** same specimen as in (b-d), cross-fracture in alveolar view. **(i)** same specimen as in (f), cross-fracture. **(j)** *Aulacoceras sulcatum*, SHK MB-738, cross-section to show the growth pattern of the ribbed rostrum type. **(k)** *Aulacoceras sulcatum*, longitudinal section through alveolar part of rostrum. **(l)** *Passaloteuthis* sp. (Belemnitida), SHK MB-739, cross-section to show concentric growth of the smooth rostrum type. Triassic; Oë Bihati near Baun, SW Timor, Indonesia (a–k). Early Jurassic: Toarcian; Bollernbank Buttenheim, Germany (l). All scale bars = 10 mm.

Fig. 2: Aulacocerid rostra (a, d–f) with regenerated injuries. **(a)** *Atractites lanceolatus*, with healed fracture of the juvenile rostrum, SHK PB-262. **(b–c)** *Gonioteuthis quadrata* (Belemnitida), SHK PB-246; **(b)** dislocated fractures are covered by post-traumatically deposited rostrum layers [see also Mietchen et al. 2005]; **(c)** same specimen with magnetoresonance signatures. **(d)** *Aulacoceras sulcatum*, the former cut remains discernible after regeneration, SHK PB-420. **(e)** close up of (a). **(f)** *Aulacoceras sulcatum*, SHK PB-445. Triassic; Oë Bihati near Baun, SW Timor, Indonesia (a, d–f). Late Cretaceous: Campanian; Alemania clay-pit, Höver, Germany (b–c). All scale bars = 10 mm.

In the ribbed rostrum type, in contrast to the smooth type, older injuries are at all times visible on the outer surface since each rib grows independently (Figs. 2d–f). As Fig. 3a demonstrates, growth of a fractured area is temporally interrupted, whereas adjoining uninjured areas proceed in growth. Growth of the concerned ribs initiates again as soon as the injured parts of the shell sac is healed. Hence, the growth of injured areas stays behind the growth of unfractured areas. The "scar" is therefore transferred in each rib from inside to outside (compare Figs. 3a–b).

Phylogenetic implications

Jeletzky (1966: fig. 2), Engeser & Bandel (1988: fig. 4), Engeser (1990: p. 137) and Fuchs (2006: fig. 4.1-1) considered Aulacocerida as a monophylum, however, without providing convincing autapomorphies for this assumption. Engeser (1990) found the presence of an aragonitic rostrum to be an autapomorphy, although aragonitic rostra are also known within Belemnitida (e.g., *Belemnoteuthis*, *Acanthoteuthis*).

Owing to the apparent lack of unequivocal autapomorphies, Haas (1989: fig. 8) and Doyle et al. (1994: fig. 1) doubted a monophyletic origin of Aulacocerida, and Pignatti & Mariotti (1995: p. 37) discussed at least a paraphyletic grouping ("…*we think that it should not be discarded a priori.*").

Assumption of a monophyletic origin of Aulacocerida produces a character conflict, which has been neglected in previous works. Apart from the systematic problem whether Hematitida represents an independent group or a subgroup within Aulacocerida, either the ribbed rostrum (Hematitida and Aulacoceratidae/Dictyoconitidae) or the smooth rostrum (Xiphoteuthididae and Belemnitidae) must have developed twice, independently from each other (Fig. 4a).

A paraphyletic origin of Aulacocerida resolves this conflict, as an originally ribbed rostrum of Hematitida might have become progressively smoothened in the lineage Aulacoceratidae—Dictyoconitidae—Xiphoteuthididae (Fig. 4b). Hence, the shift in rostrum mineralogy from aragonite to calcite occurred later in phylogeny, after the separation of Belemnitida.

Accordingly, Xiphoteuthididae represent the sister-taxon of all proostracum-bearing coleoids (= Proostracomorpha: Phragmoteuthida, Belemnitida, Diplobelida, Vampyropoda, Decabrachia?); Dictyoconitidae the sister-taxon of Xiphoteuthididae/Proostracomorpha; Aulacoceratidae the sister-taxon of Dictyoconitidae/Xiphoteuthididae/Proostracomorpha; and Hematitida the sister-taxon of Aulacoceratidae/Dictyoconitidae/Xiphoteuthididae/Proostracomorpha.

A smooth rostrum might therefore be considered a synapomorphy of Xiphoteuthididae and Proostracomorpha. In this case, the ribbed rostrum is a symplesiomorphy of Aulacoceratidae and Dictyoconitidae, since it derived from Carboniferous Hematitida.

Alternative phylogenies usually led to new character conflicts. However, the assumption of a paraphyletic origin has no impact on key characters and their polarisation (e.g., developments of a proostracum and a closing membrane remain single events).

Nevertheless, one enigmatic character conflict, which is evident also in previous phylogenetic scenarios, still exists: the orientation of the septal necks. According to the relationships outlined above, originally retrochoanitic septal necks (Hematitida) became prochoanitic ("Aulacocerida") and later again retrochoanitic (Proostracomorpha).
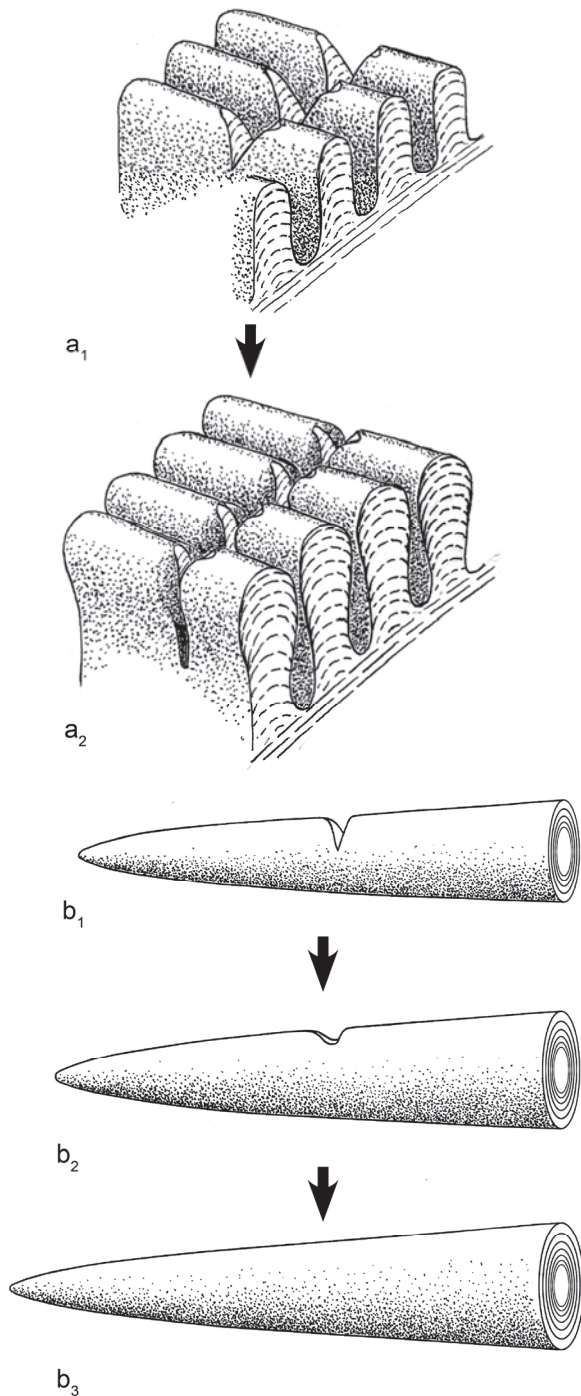
Fig. 3: Regeneration mechanisms in aulacocerid rostra. (a₁–a₂) ribbed type (in detailed aspect), (a₁) traumatic stage, (a₂) later regenerated stage. (b₁–b₃) smooth type (in general aspect); (b₁) traumatic stage; (b₂–b₃) later regenerated stages. Not to scale.
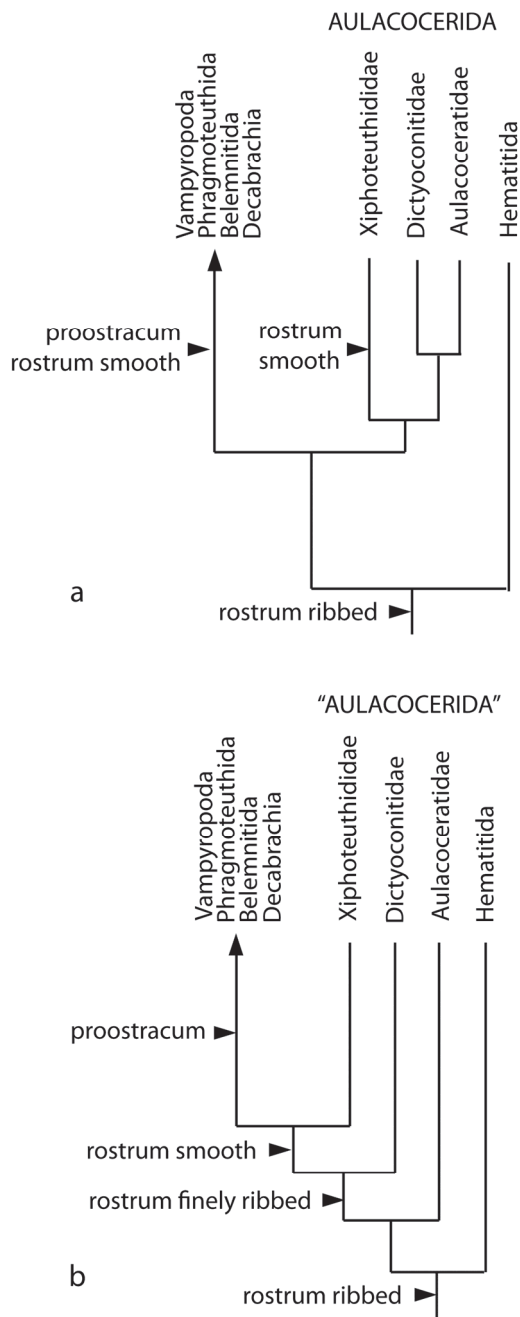
Fig. 4: Hypothetical higher level phylogenies of the Coleoidea. **(a)** phylogeny with Aulacocerida as a monophyletic group. **(b)** phylogeny with Aulacocerida as a paraphyletic group.

Conclusions

The present study on aulacocerid rostra from the Triassic of Timor provides striking evidence that both the smooth and ribbed rostrum types had different formation and regeneration mechanisms. The smooth rostrum-type grew by subsequent deposition of shell lamellae, whereas the ribbed type grew rib-by-rib. As a result, former fractures are obscured in the smooth rostrum-type, while in the ribbed one former fractures are transferred from inside to outside.

This difference is here considered to bear a phylogenetic impact on the previously presumed monophyly of Aulacocerida. Particularly, a convergent development of the ribbed rostrum-type in Aulacocerida and Hematitida, as a monophyletic origin of Aulacocerida would suggest, appears unlikely in the light of this study. The assumption of a paraphyletic origin resolves this problem. It is assumed that the originally ribbed rostrum of Hematitida has become progressively smoothened within the lineage Aulacoceratidae—Dictyoconitidae—Xiphoteuthididae—Proostracophora.

References

Bandel, K. (1985): Composition and ontogeny of *Dictyoconites* (Aulacocerida, Cephanlopoda). *Paläontologische Zeitschrift* **59**: 223-244.

Bandel, K. (1989): Cephalopod shell structure and general mechanisms of shell formation. In: Carter, J. G. (ed.): *Skeleton Biomineralization: Patterns, Processes and Evolutionary Trends*. New York (Van Nostrand Reinhold): 97-115.

Bandel, K. & Spaeth, C. (1988): Structural differences in the ontogeny of some belemnite rostra. In: Wiedmann, J. & Kullmann, J. (eds.): *Cephalopods – Present and Past*. Stuttgart (Schweizerbart'sche Verlagsbuchhandlung): 247-271.

Battiato, A. (1983): Su un sepiostario aberrante di *Sepia officinalis* L. (Cephalopoda, Sepiidae). *Thalassia Salentina* **12-13**: 152-153.

Bello, G. & Paparella, P. (2002): The "woundrous" cuttlebone of *Sepia orbignyana*. *Berliner Paläobiologische Abhandlungen* **1**: 10-11.

Bülow, E. U. von (1915). Orthoceren und Belemniten der Trias von Timor. *Paläontologie von Timor* **4**: 1-72.

Cuif, J.-P. & Dauphin, Y. (1979): Mineralogie et microstructures d'Aulacocerida (Mollusca - Coleoidea) du Trias de Turquie. *Biomineralisation* **10**: 70-79.

Donovan, D. T. (2006): Phragmoteuthida (Cephalopoda: Coleoidea) from the Lower Jurassic of Dorset, England. *Palaeontology* **49**: 673-684.   http://dx.doi.org/10.1111/j.1475-4983.2006.00552.x

Doguzhaeva, L. A.; Mapes, R. H. & Mutvei, H. (2002): Shell Morphology and Ultrastructure of the Early Carboniferous Coleoid *Hematites* Flower & Gordon 1959 (Hematitida ord. nov.) from the Midcontinent (USA). In: Summesberger, H.; Histon, K. & Daurer, A. (eds.): Cephalopods – Present & Past. *Abhandlungen der geologischen Bundesanstalt* **57**: 299-320.

Doguzhaeva, L. A.; Mapes, R. H. & Mutvei, H. (2010): Evolutionary patterns of Carboniferous coleoid cephalopods based on their diversity and morphological plasticity. In: Tanabe, K.; Shigeta, Y.; Sasaki, T. & Hirano, H. (eds.): *Cephalopods – Present & Past*. Tokyo (Tokai University Press): 171-180.

Doguzhaeva, L. A. & Summesberger, H. (2012): Pro-ostraca of Triassic belemnoids (Cephalopoda) from Northern Calcareous Alps, with observations on their mode of preservation in an environment of northern Tethys which allowed for carbonization of non-biomineralized structures. *Neues Jahrbuch für Geologie und Paläontologie, Abhandlungen* **266**: 31-38. http://dx.doi.org/10.1127/0077-7749/2012/0266

Doyle, P. (1990): The biogeography of the Aulacocerida (Coleoidea). In: Pallini, G. (ed.): *Fossili Evoluzione Ambiente. Atti II Convegno Piccinni*. Pergola: 263-271.

Doyle, P.; Donovan, D. T. & Nixon, M. (1994): Phylogeny and systematics of the Coleoida: *The University of Kansas Paleontological Contributions* **5**: 1-15.

Engeser, T. (1990): Phylogeny of the fossil coleoid Cephalopoda (Mollusca). *Berliner geowissenschaftliche Abhandlungen (A: Geologie und Paläontologie)* **124**: 123-191.

Engeser, T. & Bandel, K. (1988): Phylogenetic classification of cephalopods. In: Wiedmann, J. & Kullman, J. (eds.): *Cephalopods - Present and Past*. Stuttgart (Schweizerbart'sche Verlagsbuchhandlung): 105-115.

Flower, R. H. & Gordon, M. jr. (1959): More Mississipian Belemnites. *Journal of Paleontology* **33**: 809-842.

Fuchs, D. (2006): Fossil erhaltungsfähige Merkmalskomplexe der Coleoidea (Cephalopoda) und ihre phylogenetische Bedeutung. *Berliner Paläobiologische Abhandlungen* **8**: 1-115.

Fuchs, D. (2012): The "rostrum"-problem in coleoid terminology - an attempt to clarify inconsistences. *Geobios* **45**: 29-39. http://dx.doi.org/10.1016/j.geobios.2011.11.014

Fuchs, D.; Boletzky, S. von & Tischlinger, H. (2010): New evidence of functional suckers in belemnoid coleoids (Cephalopoda) weakens support for the „Neocoleoidea" concept. *Journal of Molluscan Studies* **76**: 404-406. http://dx.doi.org/10.1093/mollus/eyq032

Fuchs, D.; Keupp, H.; Mitta, V. & Engeser, T. (2007): Ultrastructural analyses on the conotheca of the genus *Belemnoteuthis* (Belemnitida: Coleoidea). In: Landman, N. H.; Davis, R. A. & Mapes, R. H. (eds.): *Cephalopods Present and Past: New Insights and Fresh Perspectives*. Dordrecht (Springer): 299-314.

Fuchs, D.; Keupp, H. & Wiese, F. (2012): Protoconch morphology of *Conoteuthis* (Diplobelida, Coleoidea) and its implications on the presumed origin of the Sepiida. *Cretaceous Research* **34**: 200-207. http://dx.doi.org/10.1016/j.cretres.2011.10.018

Gordon, M. J. (1966): Permian coleoid cephalopods from the Phosphoria Formation in Idaho and Montana. *Geological Survey Research* **28**: 28-35.

Haas, W. (1989): Suckers and arm hooks in Coleoidea (Cephalopoda, Mollusca) and their bearing for Phylogenetic Systematics. *Abhandlungen des naturwissenschaftlichen Vereins in Hamburg* **28**: 165-185.

Hauer, F. von (1860): Nachträge zur Kenntniss der Cephalopoden-Fauna der Hallstätter Schichten. *Sitzungsberichte der mathem.-naturw. Classe der kaiserlichen Akademie der Wissenschaften* **41**: 113-150.

Hewitt, R. A.; Westermann, G. E. G. & Judd, R. L. (1999): Buoyancy calculations and ecology of Callovian (Jurassic) cylindroteuthid belemnites. *Neues Jahrbuch für Geologie und Paläontologie, Abhandlungen* **211**: 89-112.

Jeletzky, J. A. (1966): Comperative Morphology, Phylogeny, and Classification of Fossil Coleoidea. *The University of Kansas Paleontological Contributions, Mollusca, Article* **7**: 1-162.

Keupp, H. (2009): Timor: Bonanza nicht nur für Triasfossilien. *Fossilien* **26** (4): 214-220.

Keupp, H. (2012): Atlas zur Paläopathologie der Cephalopoden. *Berliner Paläobiologische Abhandlungen* **12**: 1-390.

Kröger, B.; Vinther, J. & Fuchs, D. (2011): Cephalopod origin and evolution: A congruent picture emerging from fossils, development and molecules. *BioEssays* **33**: 602-613. http://dx.doi.org/10.1002/bies.201100001

Mariotti, N. & Pignatti, J. S. (1993): Remarks on the genus *Atractites* Gümbel, 1891 (Coleoidea: Aulacocerida). *Geologica Romana* **29**: 355-379.

Mietchen, D.; Keupp, H.; Manz, B. & Volke, F. (2005): Non-invasive diagnostics in fossils - magnetic resonance imaging of pathological belemnites. *Biogeosciences* **2**: 133-140.

Mojsisovics, E. von (1871): Über das Belemnitiden-Geschlecht *Aulacoceras* Fr. v. Hauer. *Jahrbücher der kaiserlich-königlichen Geologischen Reichsanstalt Wien* **21**: 41-66.

Monks, N.; Hardwick, J. D. & Gale, A. (1996): The function of the belemnite guard. *Paläontologische Zeitschrift* **70**: 425-431.

Pignatti, J. S. & Mariotti, N. (1995): Systematics and phylogeny of the Coleoidea (Cephalopoda): a comment upon recent works and their bearing on the classification of the Aulacoceratida. *Palaeopelagos* **5**: 33-44.

Ruggiero, L. (1980): Un esemplare aberrante di *Sepia officinalis* L. (Cephalopoda, Sepiidae). *Thalassia Salentina* **10**: 131-132.

Spaeth, C. (1975): Zur Frage der Schwimmverhältnisse bei Belemniten in Abhängigkeit vom Primärgefüge der Hartteile. *Paläontologische Zeitschrift* **49**: 321-331.

Stolley, E. (1919): Die Systematik der Belemniten. *Jahresberichte des Niedersächsischen Geologischen Vereins* **11**: 1-59.

Wanner, J. (1911): Triascephalopoden von Timor und Rotti. *Neues Jahrbuch für Mineralogie, Geologie und Paläontologie* **32**: 177-196.

Wiedman, J. & Boletzky, S. von (1982): Wachstum und Differenzierung des Schulps von *Sepia officinalis* unter künstlichen Aufzuchtbedingungen – Grenzen der Anwendung im palökologischen Modell. *Neues Jahrbuch für Geologie und Paläontologie, Abhandlungen* **164**: 118-133.

First evidence of *Mastigophora* (Cephalopoda: Coleoidea) from the early Callovian of La Voulte-sur-Rhône (France)

Dirk Fuchs[1]

[1]*Freie Universität Berlin, Institut für Geologische Wissenschaften (Fachrichtung Paläontologie), Malteser-Str. 74-100, Haus D, 12249 Berlin, Germany; Email: drig@zedat.fu-berlin.de*

A 3-dimensionally preserved coleoid cephalopod from the Lower Callovian La Voulte-sur-Rhône *lagerstätte* is described. The comparison with *Mastigophora brevipinnis* from the Upper Callovian Oxford Clay of Christian Malford (U.K.) revealed remarkable similarities in their soft part morphologies. The shared presence of conspicuously short arms, one pair of near-terminal and ear-shaped fins, and an unusual thickening of the anterior mantle margin led the author to determine the specimen under investigation as *Mastigophora* aff. *brevipinnis*. The presence of uniserial and ringless suckers in *Mastigophora* aff. *brevipinnis* support a phylogenetic relationship with the Vampyropoda rather than with the Decabrachia. The previously discussed presence or non-presence of tentacles in *Mastigophora* is re-evaluated.

Introduction

Besides the Nusplingen (Upper Kimmeridgian), Solnhofen (Lower Tithonian) and Hakel (Cenomanian) Plattenkalks, other *fossil lagerstätten* such as the Oxford Clay of Christian Malford (Upper Callovian) and the La Voulte-sur-Rhône *lagerstätte* (Lower Callovian) belong to the most important evolutionary windows through which observation of ancient life is possible. Such *lagerstätten* are outstanding not only due to their high diversity, but also due to their extraordinary preservation of fossilised soft tissues. Particularly, teuthologists benefit from these enormous information sources (e.g., Fischer & Riou 1982; Donovan 1983; Fischer & Riou 2002; Klug et al. 2005; Fuchs 2006a; Fuchs et al. 2009; Klug et al. 2010; Fuchs & Larson 2011a, 2011b). Remarkably, the Christian Malford *lagerstätte* even became famous through its excellent soft

part preservation of *Mastigophora*, a gladius-bearing coleoid previously known only from the Oxford Clay (Owen 1856; Donovan 1983; Wilby et al. 2008). Based on its unique gladius morphology, Engeser & Reitner (1985) established the family Mastigophoridae. The Mastigophoridae are today grouped together with the Loligosepiidae and Leptotheuthididae in the Loligosepiina. Owing to conspicuous gladius similarities, the Loligosepiina is often regarded as a stem-group of the Vampyromorpha with its only living representative *Vampyroteuthis infernalis*, the vampire squid (Engeser 1988; Page & Doyle 1994; Doyle et al. 1994; Fuchs 2006a, 2006b; Fuchs & Weis 2008).
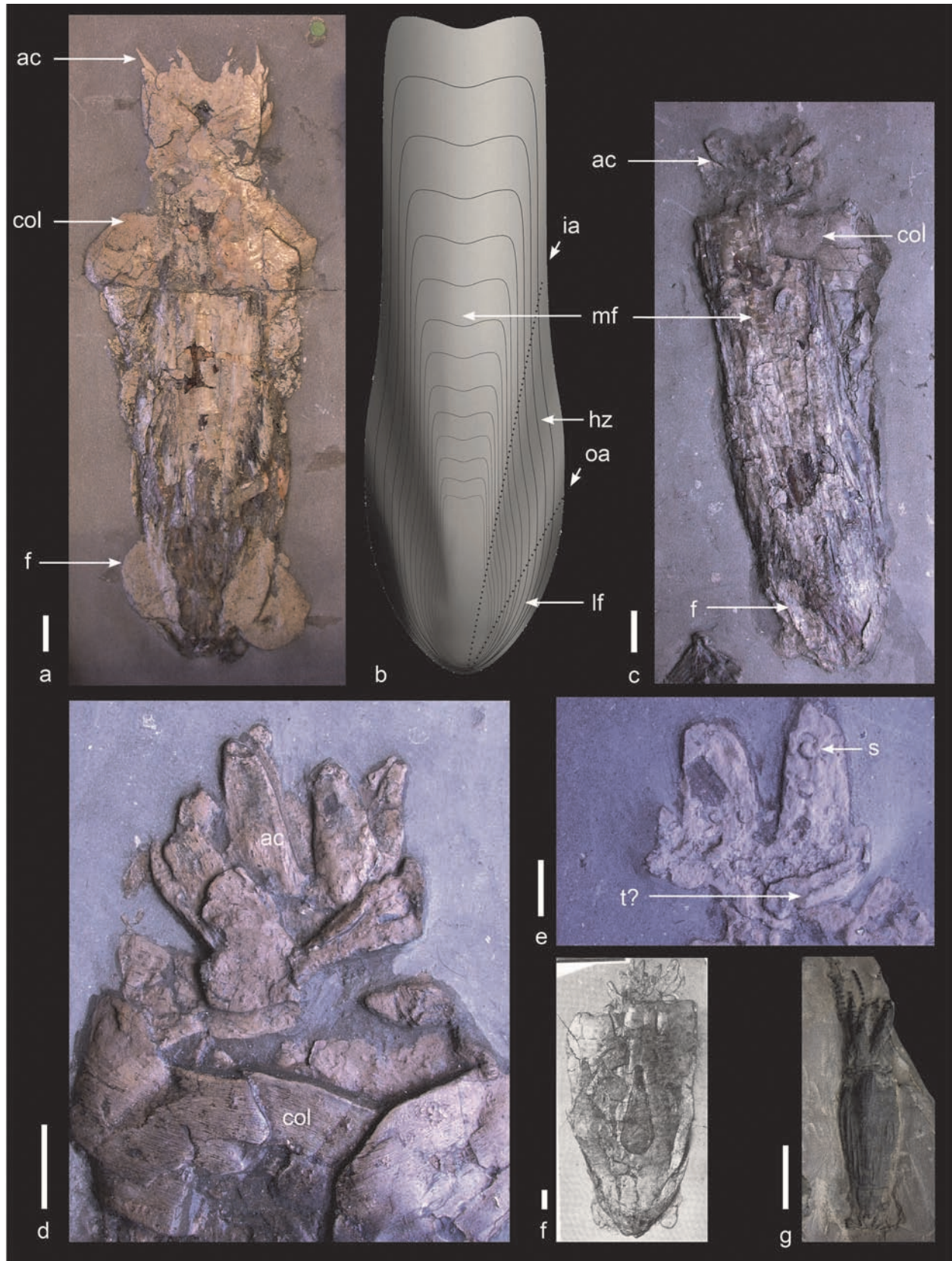
Fig. 1: **(a–f)** *Mastigophora brevipinnis* Owen, 1856, Christian Malford (U.K.), Upper Callovian, *athleta* Zone. **(a)** BMNH C.25288 [original of Donovan 1983: fig. 2], dorsal view; **(b)** gladius reconstruction, dorsal view; **(c)** BMNH C.88606, dorsal view; **(d)** BMNH C.25287 [original of Donovan 1983: fig. 7b], ventral view; **(e)** BMNH C.32352 [original of Vecchione et al. 1999: fig. 5]; **(f)** BMNH C.2695 [neotype, original of Donovan 1983: fig. 1], ventral view. **(g)** *Mastigophora* aff. *brevipinnis*, La Voulte-sur-Rhône (France), Lower Callovian, *koenigi* Zone, MNHN 74241 [original of Fuchs 2006a: pl. 21, fig. D], dorsal view. All scale bars: 10 mm. Abbreviations: ac = arm crown, col = collar, f = fins, hz = hyperbolar zone, ia = inner asymptote, lf = lateral field, mf = median field, oa = outer asymptote, s = sucker, t = tentacle.

This systematic assignment implicates that *Mastigophora* belongs to the "pseudo-eight-armed" (8 plus 2 rudimentary arms) lineage on the vampyropod branch. This attribution is challenged by findings made by Owen (1856) and more recently by Vecchione et al. (1999), who presumed that tentacles were present in *Mastigophora*. The presence of a strongly modified arm pair in ventrolateral position would strongly suggest decabrachian affinities rather than octobrachian. In the light of this controversy, *Mastigophora* is – similar to other taxa such as *Plesioteuthis* (see discussions in Fuchs et al. 2007b) and *Palaeololigo* (see Donovan & Strugnell 2010) – a key taxon in the principle discussion on whether Mesozoic gladius-bearing coleoids represent fossil vampyropods or teuthids.

In the paleontological collection of the Musée National d'Histoire Naturelle Paris (MNHN), an undetermined specimen from the La Voulte *lagerstätte* attracted my interests because it shows soft-tissue features typical for slightly younger *Mastigophora brevipinnis* from the Oxford Clay (Figs. 1a–f). It is hence the aim of the present article to describe and discuss this 3-dimensionally preserved specimen with a special focus on the arms and thus the systematic assignment of the genus.

Material

The specimen (MNHN 74241) comes from La Voulte-sur-Rhône (Ardèche, France), a locality of Early Callovian age (*koenigi* Zone; Fig. 2) and famous for its 3-dimensional soft part preservation. According to Wilby et al. (1996: 848), "*The soft tissues in the specimens are replaced mainly by apatite and pyrite, intervening areas are filled with calcite.*" The specimen co-occurred with other gladius-bearing coleoids such as *Romaniteuthis gevreyi*, *Rhomboteuthis lehmani*, *Vampyronassa rhodanica*, and *Teudopsis* sp. (Fischer & Riou 1982, 2002; Fischer 2003). These taxa were likewise studied during my stay at the MNHN.
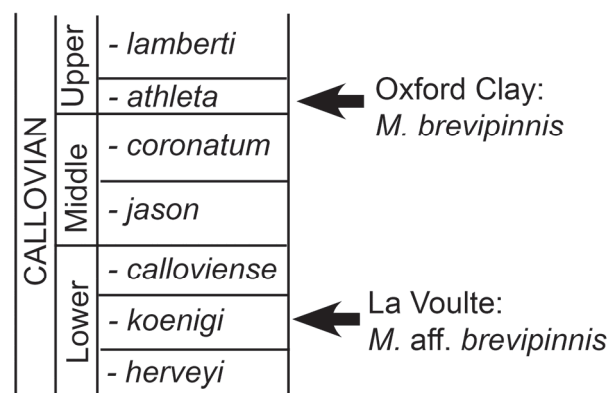
Fig. 2: Stratigraphic occurrences of *Mastigophora brevipinnis* and *Mastigophora* aff. *brevipinnis*.

Sixteen specimens of *Mastigophora brevipinnis* from the Upper Callovian Oxford Clay of Christian Malford (*athleta* Zone) were subject to morphological comparisons. The latter specimens are housed in the palaeontological collection of the British Museum of Natural History (BMNH).

Systematic palaeontology

Superorder **Vampyropoda** von Boletzky, 1992
Order **Vampyromorpha** Robson, 1929
Suborder **Loligosepiina** Jeletzky, 1965

Included families. – Loligosepiidae Van Regteren Altena, 1949; Leptotheuthididae Naef, 1921; Mastigophoridae Engeser & Reitner, 1985.

Family **Mastigophoridae** Engeser & Reitner, 1985

Diagnosis (after Fuchs 2006b). – Mastigophoridae includes forms with short lateral fields and particularly broad and elongated (outstretched) hyperbolar zones. "Hyperbolar" growth lines are almost straight, i.e. only weakly curved inwards. Hyperbolar zones are therefore not developed as furrows. As a result, transition from the short lateral fields into the longer hyperbolar zone is smooth. Inner and outer asymptotes are therefore indistinct.

Type genus. – *Mastigophora* Owen, 1856.

Included genera. – *Mastigophora* Owen, 1856; *Doryanthes* Münster, 1846; *Bavaripeltis* Engeser & Keupp, 1997.

Geographical and stratigraphical occurrence. – Middle Jurassic (Callovian) – Late Jurassic (Tithonian) of Europe.

Remarks. – Originally, the Mastigophoridae included only the genus *Mastigophora* (Engeser & Reitner 1985: 248; Engeser 1988: 25). Engeser & Keupp (1997) later added the genera *Bavaripeltis* Engeser & Keupp, 1997 and *Donovaniteuthis* Engeser & Keupp, 1997. Fuchs (2006b: 87), in his revision of the family, mentioned doubts about the classification of *Donovaniteuthis*. He removed *Donovaniteuthis* and instead included the genus *Doryanthes* Münster, 1846. Additionally, Fuchs (2006b: 82) preliminarily included the genus *Boreopeltis* Engeser & Reitner, 1985. Fuchs et al. (2007b) and Fuchs & Larson (2011a), however, followed Engeser (1988) and placed *Boreopeltis* in the prototeuthid Plesioteuthididae. Fuchs (2006b: 87) also mentioned the possibility of a mastigophorid record from the Aptian of Central Russia (see Hecker & Hecker 1955: fig. 1), but re-investigation of this specimen has shown more similarities with a plesioteuthid gladius (unpublished data).

Fig. 3: **(a–f)** *Mastigophora* aff. *brevipinnis*, La Voulte-sur- Rhône (France), Lower Callovian, *koenigi* Zone), MNHN 74241 [original of Fuchs 2006a: pl. 21, fig. D]. **(a)** specimen in dorsal view; **(b)** head and arm region in dorsal view; **(c)** dorso-lateral view of the funnel; **(d)** posterior mantle in dorsal view; **(e)** arm crown in anterior view; **(f)** arm crown in lateral view. Scale bars: (a) = 10 mm, (b–d) = 1 mm.

Genus *Mastigophora* Owen, 1856

Type species. – *Mastigophora brevipinnis* Owen, 1856.

Included species. – Only *Mastigophora brevipinnis* Owen, 1856.

Geographical and stratigraphical occurrence. – Oxford Clay of Christian Malford, Wiltshire, U.K. (Upper Callovian, *athleta* Zone) and La Voulte-sur-Rhône (Lower Callovian, *koenigi* Zone).

Mastigophora aff. *brevipinnis* Owen, 1856

Fig. 3

Material. – 1 specimen (MNHN 74241; original of Fuchs 2006a: pl. 21, fig. D).

Origin. – La Voulte-sur-Rhône (Lower Callovian, *koenigi* zone).

Description. – Specimen MNHN 74241 shows a 3-dimensionally preserved soft body including mantle, head and arm crown (Fig. 3a). The posteriorly rounded mantle has a maximum length of 29 mm and a maximum width of 7 mm. Vague imprints on both sides of the posterior mantle suggest a pair of near-terminal and ear-shaped fins (Fig. 3d). A gladius is not visible; it is most probably covered by mantle musculature. Close to the collar-like thickened anterior mantle margin, a median elevation withdrawn from the muscular mantle is interpreted as the funnel (Figs. 3b–c). The fossil is hence exposed in ventral view. This interpretation is supported by the position of the eyes, which are perceptible on both dorso-lateral sides of the head (Fig. 3f). The head is separated from the collar-like thickened anterior mantle margin by a distinct furrow (Fig. 3b). The arm crown preserves 5–6 short arms (length 8 mm; ratio arm length / mantle length = 0.26) with noticeably thick arm bases (Figs. 3b, e–f). Two further arms are distinctly longer (12 mm). According to the ventral view, this elongated arm pair is unambiguously in dorsal position. Oral surfaces of both dorsal arms indicate the presence of uniserial circular suckers (Figs. 3b, e–f). The latter arm pair clearly lacks tentacular clubs. There is no evidence of cirri or hooks (onychites).

Comparison with *Mastigophora brevipinnis* *from the Upper Callovian Oxford Clay of Christian Malford*

A mantle length of less than 30 mm is noticeably shorter than in *M. brevipinnis* from the Oxford Clay (compare mantle lengths in Figs. 1f, g). Mantle lengths in *M. brevipinnis* range from 120 to 300 mm. Hence, one might regard *Mastigophora* aff. *brevipinnis* as a juvenile (see discussion below). Admittedly, Recent squids are known to exhibit significant morphological differences during their ontogeny so that a meaningful comparison is certainly problematic. On the other side, a congeneric (if not con-

specific) affinity appears comprehensible since morphological similarities are striking.

Similar to *M.* aff. *brevipinnis*, the body of *M. brevipinnis* is mainly characterised by obviously short arms and a pair of near-terminal and ear-shaped fins. Moreover, both taxa under discussion share an unusual thickening of the anterior mantle margin. Although the gladius cannot be studied, it is obvious that the gladius shape of *M. brevipinnis* matches well within the tubular mantle outline of the La Voulte specimen (Fig. 1b).

A distinctly elongated arm pair has also been described in the British *M. brevipinnis* by Vecchione et al. (1999: 115). However, those arms appear considerably longer than in the French specimen. Besides, these strongly extended structures lack suckers, in contrast to the dorsal elongated arm pair of the La Voulte specimen.

Comparison with other loligosepiids

A comparison with closest relatives of *Mastigophora*, *Doryanthes* and *Bavaripeltis,* is unfortunately impossible as soft parts are still unknown in the latter genera.

Among other loligosepiids, comparatively short arms and a pair of near-terminal and ear-shaped fins are known in *Leptotheuthis gigas*, a gigantic loligosepiid from the Upper Jurassic of Solnhofen (South Germany). Lower Jurassic *Loligosepia aalensis*, on the other hand, has been recently described to have evidently longer arms (Fuchs et al. 2013). Although mantle musculature is commonly preserved in Lower Jurassic loligosepiids such as *Jeletzkyteuthis, Geopeltis* and *Parabelopeltis,* nothing is known about their arm- or fin- morphology (Fuchs & Weis 2008).

Discussion

The taxonomy of Mesozoic gladius-bearing coleoids is exclusively based on gladius morphologies. However, it is worthwhile to note that with increasing knowledge about soft part morphologies, we are more and more realising that soft parts are often highly congruent within subgroups. The possession of two pairs of fins, for instance, is unique for *Trachyteuthis* as well as for its closest relative *Glyphiteuthis* (Donovan 2002; Fuchs et al. 2007a; Fuchs & Larson 2011b). Both genera additionally exhibit a moderate arm length. On the other hand, closely related taxa with a similar gladius morphology and a strikingly dissimilar soft-part morphology are unknown. In the light of this, it is conceivable to consider the shared presence of very short arms, one pair of near-terminal and ear-shaped fins, and an unusual thickening of the anterior mantle margin at least as congeneric characters.

Accordingly, two alternative interpretations are possible: 1) early Callovian *Mastigophora* from La Voulte is either a juvenile very similar to its adult stage or 2) the latter is an adult (or subadult) significantly smaller than their late

Callovian descendants. Both ideas extend the stratigraphic and biogeographic distribution of the genus *Mastigophora*. What can Lower Callovian *Mastigophora* from La Voulte contribute to the principle discussion on the total number of arms in Mesozoic gladius-bearing coleoids? Fact is that despite the outstanding state of preservation there is no evidence of ventro-lateral tentacles, which typify decabrachian coleoids; and also in Upper Callovian *Mastigophora*, the presence of tentacles is questionable. Donovan (1983), who counted only eight arms in the neotype of *Mastigophora brevipinnis*, could not confirm true tentacles described by Owen (1856). Interestingly, Donovan (1983: 491) stated: *"One or two examples, such as 25288 (...) which appear to show the filaments, probably do so either, because the outline of the arms has been carved in order to produce a more acceptable fossil. This problem exists with a number of specimens in which it is not possible to be quite certain that the outline of the head and arms has not been affected by attempts to prepare the fossil when the shale was fresh and soft."*

Hence, coleoids from Christian Malford have unfortunately been "improved" through idealised carving, leaving slightly falsified soft tissue outlines (see also Wilby et al. 2008: 95). This becomes a particular problem in questions concerning the total number of arms.

Later, Vecchione et al. (1999) based on new material recognised structures that appear to represent the stalks of tentacles. However, similar to Haas (2002: 344), I have some doubts about their interpretation (see Fuchs 2006a: 74), because the presumed existence rests upon slightly thinner arm bases (see Fig. 1e). Indeed, these presumed tentacular stalks appear to lack suckers. On the other side, this is the case in most arms of *Mastigophora* from the Oxford Clay, where suckers are preserved only sporadically (compare Figs. 1d–e).

In the distal region of regular arms, Vecchione et al. (1999) additionally observed strongly wrapped filamentous structures. To me, these "filaments" seem to be much too long and too thin for true tentacles. Since their exact position within the arm crown is difficult to determine, the "filaments" might anyway represent the second dorsolateral arm pair of a vampyromorph stem-lineage representative.

Apart from these uncertainties, it is even unclear whether those filamentous structures belong to *Mastigophora*. Wilby et al. (2004) have impressively demonstrated the occurrence of very closely associated individuals at Christian Malford. At least two examples show *Mastigophora* and *Belemnotheutis* in a head to head position. It is therefore conceivable that the "filaments" described for *Mastigophora* represents the arm crown of a small *Belemnotheutis* specimen.

Finally, apart from the (non-)existence of true tentacles, the presence of uniserial suckers challenges a classification as Decabrachia, too, and instead clearly supports vampyropod affiliations. Decabrachians are well known to possess bi- or even multiserial longitudinal rows of suckers (Young and Vecchione 1996: 97). In the light of this, it

is worthwhile to note that La Voulte as well as Christian Malford fossils are known to preserve chitinous (or "horny") structures. Hence, if *Mastigophora* is a decabrachiate, teeth- or hook-bearing rings should have been preserved in close association with the suckers. However, there is no evidence of these structures neither in La Voulte nor in Christian Malford.

Conclusions

Based on the shared presence of very short arms, one pair of near-terminal and ear-shaped fins, and an unusual thickening of the anterior mantle margin, specimen MNHN 74241 from the Lower Callovian of La Voulte is determined as *Mastigophora* aff. *brevipinnis*. A more precise determination is currently hampered by the lack of gladius characteristics as well as significant size differences. *Mastigophora* aff. *brevipinnis* represents the first record of its genus outside the U.K. and therefore slightly extents the biogeographic as well as the stratigraphic distribution. *Mastigophora* aff. *brevipinnis* is classified as a vampyropod mainly due to the presence of uniserial suckers without horny rings and the absence of ventro-lateral tentacles; a phylogenetic relationship with decabrachian coleoids – as suggested by Vecchione et al. (1999) – is hence rejected. As a result, the existence of Mesozoic Teuthida is still unconfirmed.

Acknowledgements

References

Boletzky, S. von (1992): Evolutionary aspects of development, life style, and reproduction mode in incirrate octopods (Mollusca, Cephalopoda). *Revue de Suisse Zoologie* **4**: 755-770.

Donovan, D. T. (1983): *Mastigophora* Owen 1856: a little known genus of Jurassic coleoids. *Neues Jahrbuch für Geologie und Paläontologie, Abhandlungen* **165**: 484-495.

Donovan, D. T. (2002): *Trachyteuthis* (Upper Jurassic): two pairs of fins and their phylogenetic significance. *Berliner Paläobiologische Abhandlungen* **1**: 43-46.

Donovan, D. T. & Strugnell, J. (2010): A redescription of the fossil coleoid cephalopod genus *Palaeololigo* Naef, 1921 and its relationship to recent squids. *Journal of Natural History* **44**: 1475-1492. http://dx.doi.org/10.1080/00222931003624838

Doyle, P.; Donovan, D. T. & Nixon, M. (1994): Phylogeny and systematics of the Coleoidea. *The University of Kansas Paleontological Contributions (New Series)* **5**: 1-15.

Engeser, T. (1988): Vampyromorpha ("Fossile Teuthiden"). In: Westphal, F. (ed.): *Fossilium Catalogus (I: Animalia)* **130**: 1-167.

Engeser, T. & Keupp, H. (1997): Zwei neue Gattungen und eine neue Art von vampyromorphen Tintenfischen (Coleoida, Cephalopoda) aus dem Untertithonium von Eichstätt. *Archaeopteryx* **15**: 47-58.

Engeser, T. & Reitner, J. (1985): Teuthiden aus dem Unterapt ("Töck") von Helgoland (Schleswig-Holstein, Norddeutschland). *Paläontologische Zeitschrift* **59**: 245-260.

Fischer, J.-C. (2003): Invertébrés remarquables du Callovien inférieur de la Voulte-sur-Rhône (France). *Annales de Paléontologie* **89**: 223-252. http://dx.doi.org/10.1016/j.annpal.2003.09.001

Fischer, J.-C. & Riou, B. (1982): Les teuthoïdes (Cephalopoda, Dibranchiata) du Callovien inférieur de la Voulte-sur-Rhône (Ardèche, France). *Annales de Paléontologie* **68**: 295-325.

Fischer, J.-C. & Riou, B. (2002): *Vampyronassa rhodanica nov. gen. nov. sp.*, vampyromorphe (Cephalopoda, Coleoidea) du Callovien inférieur de la Voulte-sur-Rhône (Ardèche, France). *Annales de Paléontologie* **88**: 1-17. http://dx.doi.org/10.1016/S0753-3969(02)01037-6

Fuchs, D. (2006a): Fossil erhaltungsfähige Merkmalskomplexe der Coleoidea (Cephalopoda) und ihre phylogenetische Bedeutung. *Berliner Paläobiologische Abhandlungen* **8**: 1-115.

Fuchs, D. (2006b): Re-description of *Doryanthes munsterii* (d'Orbigny, 1845), a poorly known vampyropod coleoid (Cephalopoda) from the Late Jurassic Solnhofen Plattenkalks. *Archaeopteryx* **24**: 79-88.

Fuchs, D.; Bracchi, G. & Weis, R. (2009): New octopods (Cephalopoda: Coleoidea) from the Late Cretaceous (Upper Cenomanian) of Hâkel and Hâdjoula, Lebanon. *Palaeontology* **52**: 65-81. http://dx.doi.org/10.1111/j.1475-4983.2008.00828.x

Fuchs, D.; Engeser, T. & Keupp, H. (2007a): Gladius shape variation in coleoid cephalopod *Trachyteuthis* from the Upper Jurassic Nusplingen and Solnhofen Plattenkalks. *Acta Palaeontologica Polonica* **52**: 575-589.

Fuchs, D.; Keupp, H. & Schweigert, G. (2013): First record of a complete arm crown of the Early Jurassic coleoid *Loligosepia* (Cephalopoda). *Paläontologische Zeitschrift* **87** (3): 431-435. http://dx.doi.org/10.1007/s12542-013-0182-4

Fuchs, D.; Klinghammer, A. & Keupp, H. (2007b): Taxonomy, morphology and phylogeny of plesioteuthidid coleoids from the Upper Jurassic (Tithonian) Plattenkalks of Solnhofen. *Neues Jahrbuch für Geologie und Paläontologie, Abhandlungen* **245**: 239-252. http://dx.doi.org/10.1127/0077-7749/2007/0245-0239

Fuchs, D. & Larson, N. L. (2011a): Diversity, morphology, and phylogeny of coleoid cephalopods from the Upper Cretaceous Plattenkalks of Lebanon - Part I: Prototeuthidina. *Journal of Paleontology* **85**: 234-249. http://dx.doi.org/10.1666/10-089.1

Fuchs, D. & Larson, N. L. (2011b): Diversity, morphology and phylogeny of coleoid cephalopods from the Upper Cretaceous Plattenkalks of Lebanon - Part II: Teudopseina. *Journal of Paleontology* **85**: 815-834. http://dx.doi.org/10.1666/10-159.1

Fuchs, D. & Weis, R. (2008): Taxonomy, morphology and phylogeny of Lower Jurassic loligosepiid coleoids (Cephalopoda). *Neues Jahrbuch für Geologie und Paläontologie, Abhandlungen* **249**: 93-112. http://dx.doi.org/10.1127/0077-7749/2008/0249-0093

Haas, W. (2002): The evolutionary history of the eight-armed Coleoidea. In: Summesberger, H.; Histon, K. & Daurer, A. (eds.): Cephalopods - Present & Past. *Abhandlungen der Geologischen Bundesanstalt* **57**: 341-351.

[Hecker, E. L. & Hecker, R. F.] Геккер, Е. Л. & Геккер, Р. Ф. (1955): Остатки Teuthoidea из верхней юры и нижнего мела Поволжья. [Ostatki Teuthoidea iz verhnej ûry i nižnego mela Povolž'ã; Remains of Teuthoidea from the Upper Jurassic and Lower Cretaceous of the Volga region]. *Вопросы палеонтологии [Voprosy paleontologii]* **2**: 36-44.

Jeletzky, J. A. (1965). Taxonomy and Phylogeny of fossil Coleoidea (=Dibranchiata). *Geological Survey of Canada, Papers* **65** (2): 76-78.

Klug, C.; Schweigert, G.; Dietl, G. & Fuchs, D. (2005). Coleoid beaks from the Nusplingen Lithographic Limestone (Late Kimmeridgian, SW Germany). *Lethaia* **38**: 173-192. http://dx.doi.org/10.1080/00241160510013303

Klug, C.; Schweigert, G.; Fuchs, D. & Dietl, G. (2010): First record of a belemnite preserved with beaks, arms and ink sac from the Nusplingen Lithographic Limestone (Kimmeridgian, SW Germany). *Lethaia* **43**: 445-456. http://dx.doi.org/10.1111/j.1502-3931.2009.00203.x

Münster, G. G. zu (1846). Über die schalenlosen Cephalopoden des oberen Juragebirges, der lithographischen Kalkschiefern von Bayern. *Beiträge zur Petrefaktenkunde* **7**: 51-65.

Naef, A. (1921). Die Cephalopoden. *Fauna e Flora del Golfo di Napoli, Monografia* **35**: 917 pp.

Owen, R. (1856): *Descriptions of Cephalopoda, Descriptive catalogue of the fossil organic remains of Invertebrata contained in the Museum of the Royal College of Surgeons of England*. London (Taylor & Francis): 260 pp.

Page, K. & Doyle, P. (1994): Dibranchiate Cephalopoden und Nautiliden. In: Martill, D. M. & Hudson, J. D. (eds.). *Fossilien aus dem Ornatenton und Oxford Clay*. Korb (Goldschneck-Verlag): 150-160.

Regteren Altena, C. O. van (1949). Teyler's Museum systematic catalogue of the palaeontological collection – sixth supplement (Teuthoidea). *Archives du Musee Teyler* **3**: 53-62.

Robson, G. C. (1929). The rare Abyssal Octopod *Melanoteuthis beebei* (n. sp.): a Contribution to the Phylogeny of the Octopoda. *Proceedings of the Zoological Society of London* **99** (3): 469-486.

Vecchione, M.; Young, R.; Donovan, D. & Rodhouse, P. (1999): Reevaluation of coleoid cephalopod relationships based on modified arms in the Jurassic coleoid Mastigophora. *Lethaia* **32**: 113-118. http://dx.doi.org/10.1111/j.1502-3931.1999.tb00529.x

Wilby, P. R.; Briggs, D. E. G. & Riou, B. (1996): Mineralization of soft-bodied invertebrates in a Jurassic metaliferous deposit. *Geology* **24**: 847-850. http://dx.doi.org/10.1130/0091-7613(1996)024<0847:MOSBII>2.3.CO;2

Wilby, P. R.; Duff, K.; Page, K. & Martin, S. (2008): Preserving the unpreservable: a lost world rediscovered at Christian Malford, UK. *Geology Today* **24**: 95-98. http://dx.doi.org/10.1111/j.1365-2451.2008.00666.x

Wilby, P. R.; Hudson, J. D.; Clements, R. G. & Hollingworth, T. J. (2004): Taphonomy and origin of an acumulate of soft-bodied cephalopods in the Oxford Clay Formation (Jurassic, England). *Paleontology* **47**: 1159-1180. http://dx.doi.org/10.1111/j.0031-0239.2004.00405.x

Young, R. E. & Vecchione, M. (1996): Analysis of morphology to determine primary sister-taxon relationships within coleoid cephalopods. *American Malacological Bulletin* **12**: 91-112.

Preservation of organic matter in sponge fossils: a case study of 'round sponge fossils' from the Cambrian Chengjiang Biota with Raman spectroscopy

Luo Cui[1] *; Nadine Schäfer[1]; Jan-Peter Duda[1] & Li Li-xia[2]

[1]Department of Geobiology, Geoscience Centre, Georg-August University Göttingen, Goldschmidtstr. 3, 37077 Göttingen, Germany; Email: cluo@gwdg.de
[2]State Key Laboratory of Palaeobiology and Stratigraphy, Nanjing Institute of Geology and Palaeontology, Chinese Academy of Sciences, 39 East Beijing Road, Nanjing 210008, P. R. of China

* corresponding author

Understanding the taphonomy of organic matter of sponges will be helpful in reconstructing a more exhaustive picture of the evolutionary history of these organisms from fossil records. The so-called 'round sponge fossils' (RSF) from the Burgess Shale-type (BST) Chengjiang Lagerstätte predominantly yield explicit organic remains, which seem more durable than the carbonaceous components of other fossils in the same Lagerstätte. In order to characterize these carbonaceous remains with Raman spectroscopy, a quick and non-destructive technique with the ability of analyzing the molecular composition and crystal structure in high resolution, 5 RSF specimens were examined in this study. Another Cambrian sponge fossil from the Xiaoyanxi Formation and a few algal remains from the Ediacaran Wenghui Biota were also measured for comparison.

The resulting Raman spectra of the macroscopic fossils confirmed previous observations on microfossils by Bower et al. (2013) that carbonaceous material with compositionally complex precursor material and low diagenetic thermal affection will plot in a certain region in a Γ_D over R1 diagram. The results also successfully differentiated the sponge material from the algal material, as well as the fossil-derived signal from the background. However, it is still uncertain whether the different clustering of the RSF data and the algal data reflects the variance of precursor material or only the diagenetic and geological history. The variance within the RSF data appears to be larger than that within the algal data. Considering the similar diagenetic history of the RSF, this is possibly reflecting the difference in precursor material. Nonetheless, further measurements on other fossil algal and poriferan material must be involved in the future, in order to improve and testify the current interpretation.

Despite the properties revealed by Raman spectroscopy, the taphonomy of carbonaceous material in RSF has not been investigated. According to our observation, as well as the phenomenon described in previous studies, the preservation of the carbonaceous material in RSF does not show obvious taxonomical preferences. Because the RSF are polyphylogenetic and currently lack evidence to indicate that they represent any special development stage of sponges, we infer that this unusual carbonaceous preservation is due to diagenetic bias relating to their specific morphology, which in turn is possibly controlled by similar living environments. Again, to test these inferences, more detailed taxonomical and paleoecological studies are necessary.

Introduction

Porifera is the known most primitive lineage of Metazoa (e.g., Philippe et al. 2009; Sperling et al. 2009) and is now suspected having originated as early as Cryogenian (Peterson et al. 2008; Sperling et al. 2010). However, the commonly acknowledged fossil record of this lineage is not older than the Early Cambrian, although a group of unusual structures from Precambrian rocks have been proposed as candidates of early sponges (e.g., Maloof et al. 2010; Brain et al. 2012). This is partly because spicules, the traditionally adopted criteria for setting up a poriferan affinity, may have not been evolved in Precambrian, or the taphonomical windows at that time were not favorable for the spicular material (Sperling et al. 2010). Therefore, a revaluation of the taphonomical potential of sponges may lead to a new understanding on the early evolutionary history of Porifera.

One aspect of this question is the preservation of the sponge-derived organic matter. It was generally believed that the soft part is of low potential to be fossilized as macroscopic fossils, and the poriferan fossil record has therefore a strong bias toward mineral skeletons (Pisera 2006). However, at least the Burgess Shale-type (BST) Lagerstätten yield exceptions. From the Middle Cambrian Burgess Shale (Rigby & Collins 2004), *Vauxia* has been identified as the earliest fossil of ceractinomorph demosponge due to the preservation of carbon remains in the coring fibers of these fossils. Li et al. (1998) also mentioned an observation of a single specimen of keratose sponge in their collection from Chengjiang fauna.

The so-called 'round sponge fossils' (RSF) from the Chengjiang Biota are another example. They are always circular to sub-circular in shape, small in size (3–40 mm in diameter, mostly <10 mm) and exhibiting an intensive or even continuous carbonaceous cover on the surface. Because of these morphological similarities, they were loosely mentioned as a group under the name RSF by Wu (2004), although they seem polyphyletic and the affinity is still unresolved. Compared to most other fossils from the same locality, which are strongly weathered and exhibit very few organic remains (e.g., Zhu et al. 2005), the dense carbonaceous cover of RSF appears quite unique.

Raman spectroscopy is a valuable tool for almost non-destructive high resolution analysis of the molecular composition and crystal structure of samples. It does not need extensive sample preparation and can give comparatively quick information. However, when applying this method in fossil studies, the interpretation of the data is not always clear and often critically discussed (e.g in case of putative microfossils in Archaean rocks; Kudryavtsev et al. 2001; Brasier et al. 2002; Pasteris & Wopenka 2002; Schopf et al. 2002; Schopf et al. 2005). Already Marshall et al. (2012) made an approach for investigating BST type preservation on a fossil from the Cambrian Spence Shale with Raman spectroscopy. They focused on mineral replacement on different parts of the fossil and the associat-

ed thermal history. Only recently Bower et al. (2013) published comprehensive results concerning the interpretation of carbon signals from microfossils, in regard of tracing the differences in the putative precursor material. The most promising parameters turned out to be the full width at half height of the D-band (Γ_D) and the intensity ratio of the D- and the G-band (R1). As in our case the biogenicity of the sponge fossils is not questionable, the application of Raman spectroscopy serves the purpose of revealing the nature of the carbon cover of the RSF and at the same time extending the results to macroscopic fossils following the work of Bower et al. (2013).

In this study, a few specimens of RSF were examined with a short description and discussion on their taphonomy and taxonomical affinity. The Raman spectra of their carbonaceous cover were illustrated and analyzed. In order to identify the characters of these RSF-derived spectra, a sponge fossil from Cambrian Xiaoyanxi Formation and several algal remains from the Ediacaran Wenghui Biota were also examined for comparison.

Material and Methods

All the specimens studied in this paper are from the collection of Professor Zhu Mao-Yan's group in the Nanjing Institute of Geology and Palaeontology, Chinese Academy of Sciences, including five RSF from the Cambrian Chengjiang Biota (inventory numbers no. 41047, no. 42436, no. 42446, no. 42952 and no. 42982; Fig. 2), one sponge fossil from the Cambrian Xiaoyanxi Formation (inventory name XYX) and several algal fossils from the Wenghui Biota (inventory name WH). These fossils were observed with a ZEISS Stemi 2000-C microscope and photographed with a CANON EOS 500D. For Raman spectroscopic analysis a confocal Horiba Jobin-Yvon LabRam-HR 800 UV Raman spectrometer attached to an Olympus BX41 microscope was used. The excitation wavelength for the Raman spectra was the 488 nm line of an Argon Ion Laser (Melles Griot IMA 106020B0S) with a laser power of 20 mW. A detailed description of the spectrometer is given in Beimforde et al. (2011). All spectra were recorded and processed using LabSpec™ version 5.19.17 (Horiba Jobin-Yvon, Villeneuve d'Ascq, France). Mineral identification was performed on the basis of the Horiba Jobin-Yvon database for minerals.

The RSF were collected from fossil sites near Chengjiang County, mainly from Maotianshan and Xiaolantian (Wu 2004). They are preserved in the yellowish-green shale from the Maotianshan Shale Member of the Yu'anshan Formation (Fig. 1). The age of the fossiliferous layer has been estimated as ca. 520 Ma (Hu 2005). Previous research distinguished two types of sediments from the Maotianshan Shale: the slowly deposited background
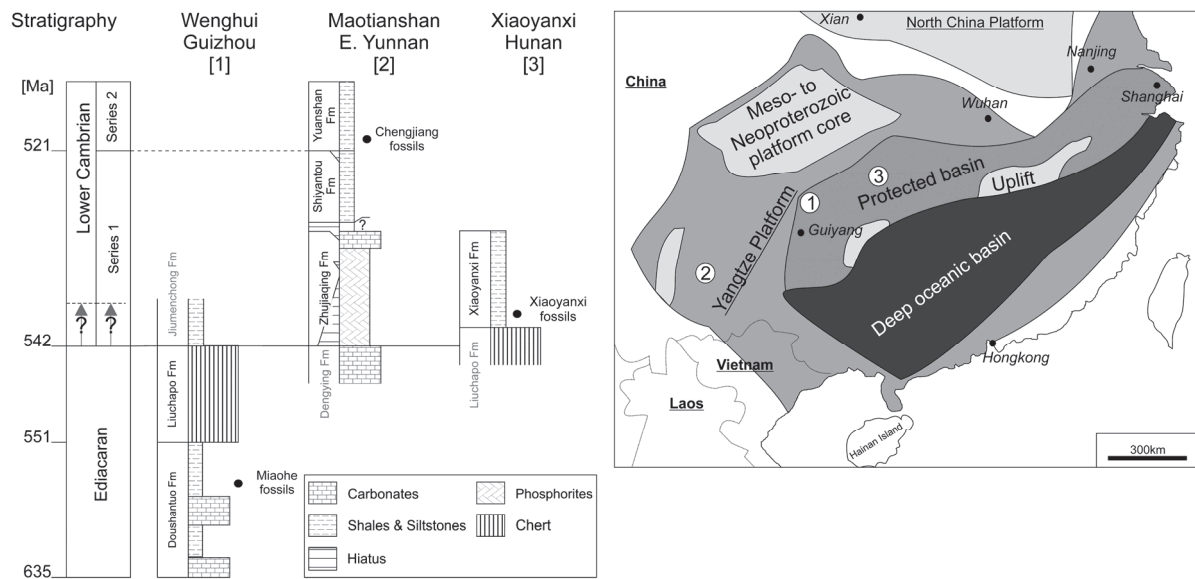
Fig. 1: Stratigraphy, locality and depositional environments of the sampled sections. Numbers of sections refer to the marked positions on the map [stratigraphy based on Steiner et al. 2001, 2005; Condon et al. 2005; Guo et al. 2007; Zhu et al. 2007; map based on Steiner et al. 2001].

beds and the rapidly deposited event beds which probably represent storm-induced distal tempestites (Hu 2005). Because the collection of these RSF is contributed by several workers over a long period, it is now impossible to know the exact type of sediments in which each RSF was collected. However, it has been confirmed by quantitative analysis that the fossils in the two taphonomical facies originated from a single local community, because the two types of beds exhibit similar recurrent and abundant species, as well as similar temporal trends in evenness and richness (Zhao et al. 2009).

The sponge fossil from the carbonaceous black shale of Xiaoyanxi Formation in Yuanling, Hunan Province has not yet been taxonomically described (Figs. 1, 3a). Similar to other Lower Cambrian sequences in South China, the fossiliferous black shale is successively underlain by a layer of Ni–Mo ore, a phosphorite layer and then Precambrian sedimentary rocks. The absolute age of the fossil horizon was evaluated as younger than 532 Ma (Jiang et al. 2012).

The algal remains are of Ediacaran age and were collected from the Wenghui Biota in Guizhou Province (Zhao et al. 2004; Wang et al. 2007). This fossil assemblage is composed of dominantly algal organisms preserved in the black shale of the upper Doushantuo Formation (Figs. 1, 3b–d). These algae appear to be benthic and buried *in situ*, therefore considering the paleogeography of the Doushantuo Formation, the sedimentary environment of these rocks was believed as on the slope, below the storm wave base but still within the photic zone (Jiang et al. 2011; Zhu et al. 2012).

Results

Preservation of carbonaceous remains in studied fossils

Except one incomplete specimen (no. 41047), the other four RSF studied in this paper have an elliptical outline and a diameter of 0.6–0.8 cm. No. 42952 maintains the thickest carbonaceous remains. Polygonal cracks are developed on the upper surface of the carbonaceous cover while traces of spicules are absent (Figs. 2a–c). However, the carbonaceous cover on this fossil can be removed quite easily, and where the cover is absent, impressions of a hexactinellid skeleton similar to that of *Triticispongia diagonata* turns out to be quite clear (Fig. 2b). By comparison, no. 42436 (Figs. 2d–f) and no. 42446 (Figs. 2g–i) show a thinner but also continuous carbonaceous cover, which is more tightly compacted to the siliciclastic matrix and not easy to remove. Some small and faint marks, resembling moulds of hexactinellid spicules, are distributed on parts of the fossil surface (Figs. 2e, 2h–i). The carbonaceous cover of no. 41047 (Fig. 2j) is not continuous as those of the aforementioned three specimens, although it looks also intensive. The siliceous skeleton of this specimen is distinctly preserved as mould and shows characters of a hexactinellid, whose skeleton seem denser and better interconnected than *T. diagonata*. No. 42982 exhibits a reddish surface with weakly preserved moulds of spicules and only scattered carbonaceous remains (Figs. 2k–l), generally resembling the surface of no. 42952 after removal of the carbonaceous cover. In the research of Wu (2004) on ca. 270 RSF specimens, it has been described that in these fossils the conspicuousness of the spicules decreases with increasing density of the carbonaceous cover.
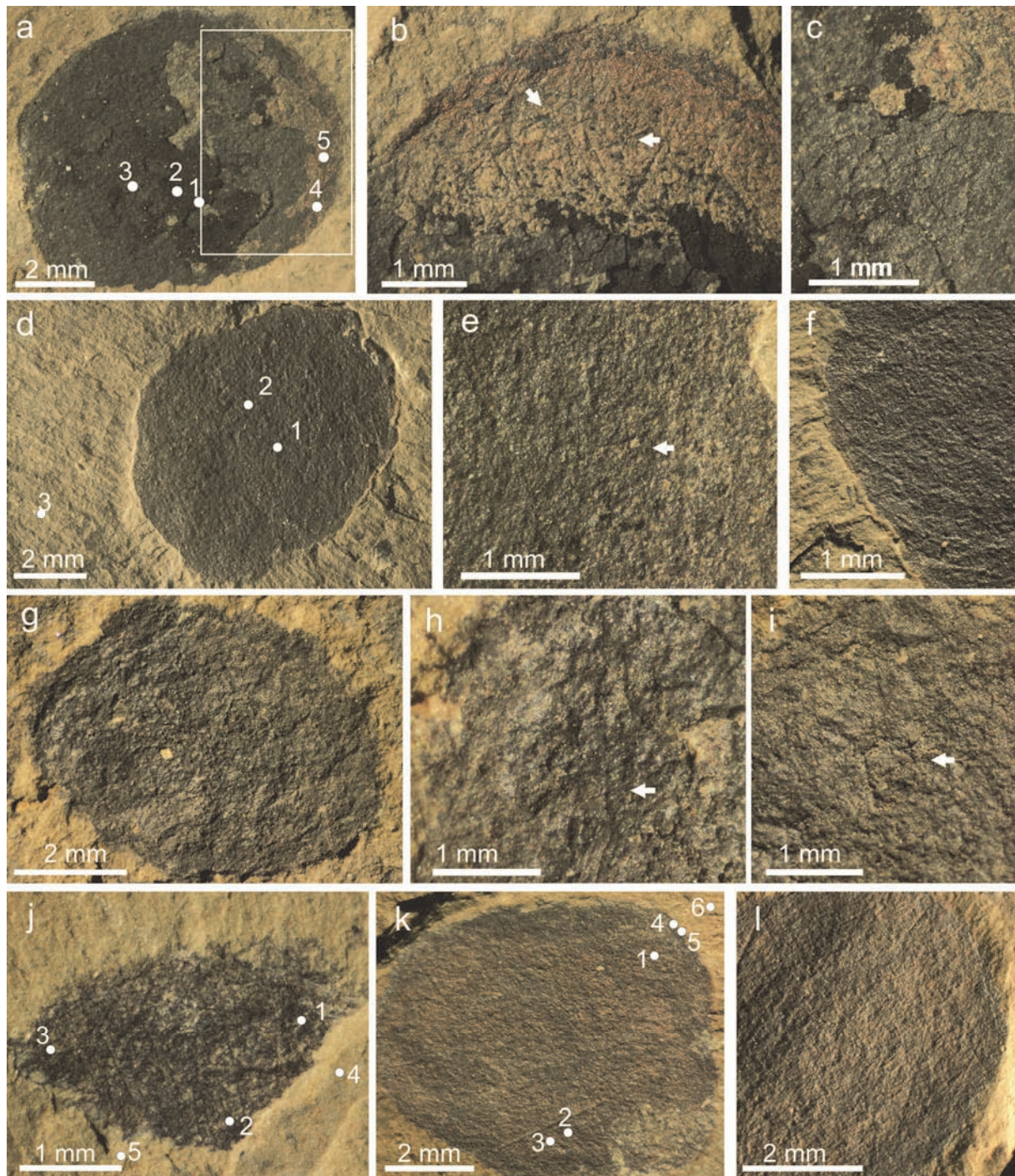
Fig. 2: 'Round sponge fossils' (RSF) from the Cambrian Chengjiang Biota. **(a–c)** Specimen no. 42952; **(b–c)** details of **(a)**, note cracks on the surface of the carbonaceous film. The white arrows in **(b)** point to marks of spicules. **(d–f)** Specimen no. 42436; **(e–f)** show details of **(d)**, the white arrow in **(e)** points to a possible mark of spicule. **(g–i)** Specimen no. 42446; **(h-i)** details of **(g)**, white arrows pointing to possible mineral skeleton marks. **(j)** Specimen no. 41047. **(k–l)** Specimen no. 42982; **(l)** detail of **(k)**, note apparent spicular structures. Number marks in **(a)**, **(d)**, **(j)** and **(k)** show the Raman spectra sample spots.

However, our observations indicate there may not be any definite relationship between the preservational qualities of the carbonaceous remains and the spicules.

In contrast to the RSF, the sponge specimen from Xiaoyanxi Formation does not have an obvious carbonaceous cover. Though, the fossil region appears generally darker than the background, the boundary between them can be quite obscure in many places (Fig. 3a).

The Ediacaran algal specimens show high morphological diversity within only square-decimeter scale. Although the thickness of carbonaceous remains of these fossils varies between different morphological taxa (Figs. 3b–d) and between different parts of a single individual (Fig. 3e), the boundary between fossil and background is mostly distinct.
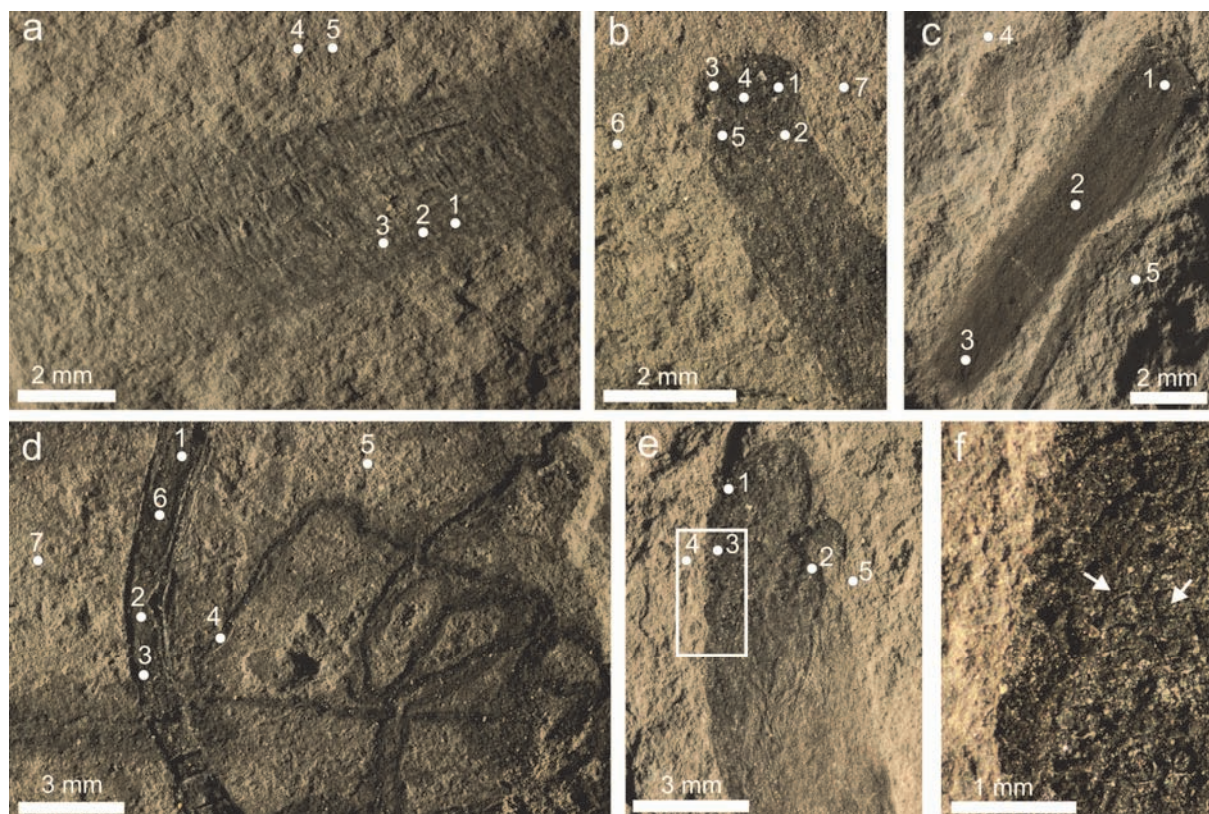
Fig. 3: **(a)** The sponge fossil from the Early Cambrian Xiaoyanxi Formation. **(b–e)** Algal fossils from the Ediacaran Wenghui Biota; **(b)** corresponds to algae 2; **(c)** corresponds to algae 4; **(d)** corresponds to algae 1 and **(e)** corresponds to algae 3 in Fig. 5; **(f)** Detail of **(e)**, white arrows pointing to polygonal cracks in the densely preserved carbon film. Number marks in **(a–e)** represent the location of Raman spectra sample spots.

In some individuals, the carbonaceous remains are extremely thick and form polygonal fractures on the surface like those in RSF no. 42952 (Figs. 3d, f).

Raman spectra

Totally 46 Raman spectra have been obtained from four of the Chengjiang fossils, the sponge fossil from the Xiaoyanxi Formation and a few algal remains from Wenghui Biota (Fig. 4). The most prominent signals from all the samples are typical for amorphous carbon, characterized by two prominent bands in the lower wavenumber region around 1600 cm^{-1}(G-band; graphite-band) and around 1350 cm^{-1} (D-band; disorder-band) (cf. Tuinstra & Koenig 1970; Wopenka & Pasteris 1993; Quirico et al. 2009). Sometimes additional bands for minerals also occur, which are a good sign for influence of the background material. Furthermore, especially the background shale material exhibits a high fluorescence, which can be caused by the extremely fine grained clay minerals, resulting in a reduction of the Raman signal (Wang & Valentine 2002). Since this study is focused on the analysis of the carbon signal, the mineral- and fluorescence-influenced spectra are not shown in this paper.

On first sight, the results for all samples look quite similar, with the exception of XYX (Fig. 4), in which the D-band is always higher than the G-band. The differences between the fossil and background material are also difficult to recognize. However, it is well known that peak intensities of the two bands can vary in a small range due to several independent factors, e.g., thermal alteration, the original carbonaceous material, and crystallinity of the carbon (Robertson 1986; Pasteris & Wopenka 2003; Busemann et al. 2007; Marshall et al. 2010). Therefore, geologically valuable information was extracted by calculating the relative intensity ratio between the D- and the G-band (R1) and the full width at half height of the D-band (Γ_D). Both parameters seem to be suitable to differentiate between different samples as well as between fossil and background material (Fig. 5; Table 1). The 'round sponge fossils' from the Chengjiang Biota show mean R1 values of 0.79 (no. 42952), 0.69 (no. 42436), 0.81 (no. 42981) and 0.74 (no. 41407). The sample XYX from the Xiaoyanxi Formation is characterized by signals with higher D- than G-band, with an average R1 value of 1.08. The different algal fossils from the Wenghui Biota have mean R1 values of 0.90 (algae 1), 0.88 (algae 2), 0.91 (algae 3) and 0.97 (algae 4). In all samples except XYX, there is a clear difference between the R1 values of the fossils and those of the background material. When plotting the average Γ_D values over the average R1 values becomes even clearer (Fig. 5a). The carbonaceous remains of XYX seem too thin and discontinuous, so that the carbon signals of the fossil do not differ from those of the background. Additionally, this sample is the only one with a mean R1

value greater than 1, suggesting intensive diagenesis and/or metamorphism (cf. Wopenka & Pasteris 1993; Rahl et al. 2005; Bower at al. 2013; Foucher & Westall 2013), which may have caused an equalization between the fossil-derived carbon and the carbon from the matrix. Because the signals from this sample cannot reflect the nature of sponge-derived carbon, it is not considered in the further discussion of the Raman signals.
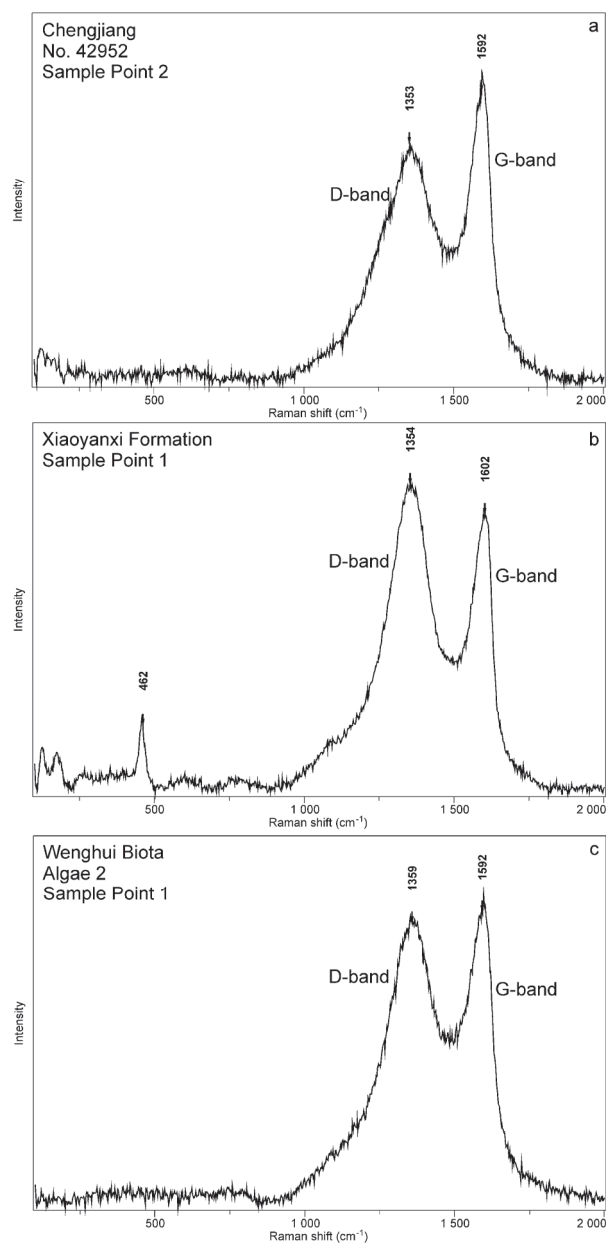
Fig. 4: Representative Raman spectra measured on sponge fossil from the Chengjiang Biota **(a)** and the Xiaoyanxi Formation **(b)** as well as algal fossils from the Wenghui Biota **(c)**; see Figs. 2–3 for position of sample spots. The small band centered at 462 cm^{-1} in **(b)** is attributed to the main SiO$_2$ vibration in quartz. Note the changing intensity relation of the D- and G-bands in each sample, resulting in different R1 values (cf. Table 1).

Discussion

BST preservation was firstly defined as '*exceptional organic preservation of non-mineralizing organisms in fully marine siliciclastic sediments*', with '*some degree of early diagenetic mineralization*' (Butterfield 1995). Following this definition, the algal fossils studied in this paper should also be regarded as a representative of BST preservation, as what has been figured out by Xiao et al. (2002) for the algal fossils from the equivalent Miaohe Biota. Although the mechanisms causing exceptional BST preservation are still under debate (e.g., Butterfield 1990; Petrovich 2001; Gaines et al. 2005), it is obvious that materials of different taphonomical resistance are preserved in different states in BST Lagerstätten. It has been summarized by Butterfield et al. (2007) that the two-dimensional carbonaceous compressions represent relatively recalcitrant extracellular components (e.g., cuticles and chaetae), while former labile soft-tissues may result in three-dimensional mineralization of either carbonates or phosphates, and the early diagenetic pyrite incidentally distributes in all Burgess Shale fossils.

In the Chengjiang Biota, most 2-D soft-bodied fossils are originally preserved in organic carbon, although due to intensive weathering the carbon material is largely diminished (Zhu et al. 2005). Compared with these fossils, the durability of carbonaceous material in the RSF appears unusual. As examples for diagenetically recalcitrant organic material, the taphonomy of collagenous periderm of *Rhabdopleura* (an extant close relative of graptolites) and the cuticle of arthropods composed of wax and chitin have been comprehensively studied (Gupta & Briggs 2011). Although received much less attention and having not been studied by taphonomical experiments, sponges possess diagenetic-recalcitrant organic material as well. Collagen distribute pervasively in sponges as either supplementary or main components in the skeletal frame (Bergquist 1978). Furthermore, chitin was recently detected in the skeleton of some hexactinellids (Ehrlich et al. 2007) and as a scaffold material tangling with collagen in the spongin skeleton of Verongida (Ehrlich et al. 2010).

In the case of algae, algaenan has been identified as a material with high fossilizing potential. However, the known occurrence of this material is restricted to Chlorophyta and some unicellular algae (Collinson 2011). Because the phylogeny of these Ediacaran macroscopic algae is uncertain (Xiao & Dong 2006), it is currently impossible to postulate the original material of the algal carbonaceous remains from Wenghui Biota.

The Raman signals from these recalcitrant carbonaceous materials are clearly distinguishable from those of their backgrounds in the Γ_D –R1 diagram (Fig. 5a), supporting the fossil-derived nature of these carbon remains. When the data points of the background material are removed, it is obvious that the signals from Chengjiang sponge fossils and those from Wenghui algal fossils do cluster separately (Fig. 5b).

Table 1: Average Γ_D and R1 values measured on the investigated fossils and the associated background materials.

	Sample Point	Description	average Γ_D	average R1
Chengjiang Biota				
No. 42952	1–3	fossil	157	0.79
	4–5	rim	212	0.90
No. 42436	1	fossil + background	257	0.82
	2	fossil	204	0.69
	3	background	195	0.71
No. 42982	1 + 3	fossil	239	0.81
	4–5	background	229	0.78
No. 41407	1–3	fossil	215	0.74
	4–5	background	121	0.56
Xiaoyanxi Fm	1–3	fossil	187	1.08
	4–5	background	187	1.07
Wenghui Biota				
algae 1	1–4 + 6	fossil	182	0.90
	5 + 7	background	147	0.76
algae 2	1–5	fossil	170	0.88
	6–7	background	171	0.82
algae 3	1–3	fossil	172	0.91
	4–5	background	141	0.71
algae 4	1–3	fossil	178	0.97
	4–5	background	148	0.80

Comparing with the data published by Bower et al. (2013), all our fossil signals fall into the region in which other samples containing compositionally complex precursor material plot (Γ_D between 100 and 250 cm⁻¹; R1 0.5 to 1.4). Bower et al. (2013) suggested that an extensive analysis of the carbon signature can reveal information on the precursor material, when other influences like a high thermal maturity can be ruled out. In our data, the Γ_D and R1 values of the algal fossils are very similar to each other, while the carbon of the sponge fossils shows a greater variability. Since the sponge fossils are from the same age and region, as well as preserved in similar yellowish-green shales, indicating a similar thermal diagenetic impact, it could be possible that a bigger variance of precursor material is responsible for the higher variance in the Raman signal of the carbonaceous remains. The values of the sponge sample no. 42952 show a higher similarity to those of the algae, with a slightly narrower D-band. The narrowing of the D-band could mean that this sample was either influenced by a thermal event (Wopenka & Pasteris 1993; Bower et al. 2013) or that the thick carbon cover has a different origin than the thinner covers of the other sponge fossils. Although these data show a clear differentiation between the carbon cover of the BST sponge fossils and the Ediacaran algal fossils, it is still hard to judge whether this phenomenon is caused by a divergent diagenetic history or the different source of organic carbon (sponge vs. algae).

Anyhow, the data presented here, support the observations of Bower et al. (2013) that the evaluation of the D- and G-band parameters of carbonaceous material can give a clue on different precursor materials. For a more detailed evaluation it would be necessary to apply Raman spectroscopy on a greater variety of sponge and algae fossils from different environments and, if possible, with known precursor materials.

Despite the information revealed by Raman spectroscopy, the unordinary occurrence of the diagenetically robust organic material in RSF raises questions. In sponges, the enrichment of diagenetic-durable organic material (collagen and chitin) varies between taxa and physiological structures. In keratose sponges, spongin composes the skeletal framework and collagen may be enriched as a complement in the mesohyl (Bergquist 1978). In demosponges, the fibrillar collagen is still pervasive and often forms dense binds between spicules, while in hexactinellids, collagen only forms a thin sheath wrapping the spicules but does not occur massively (Bergquist 1978). Additionally, the shell of sponge gemmules and the sponge base which attaches to the substratum can also be specially enhanced by spongin (Ehrlich 2010). However, the RSF studied here yield indisputable hexactinellid spicules (Fig. 2), although RSF possessing only diactines have also been mentioned by Wu (2004).

Therefore, the thick carbonaceous remains on the hexactinellid RSF may indicate that either these fossils represent a special part or developing stage of the sponges, or some hexactinellids once possessed enriched collagen/spongin in the evolutionary history, or there is a special taphonomical mechanism in Chengjiang Biota, which selectively benefit the preservation of organic matter in RSF.
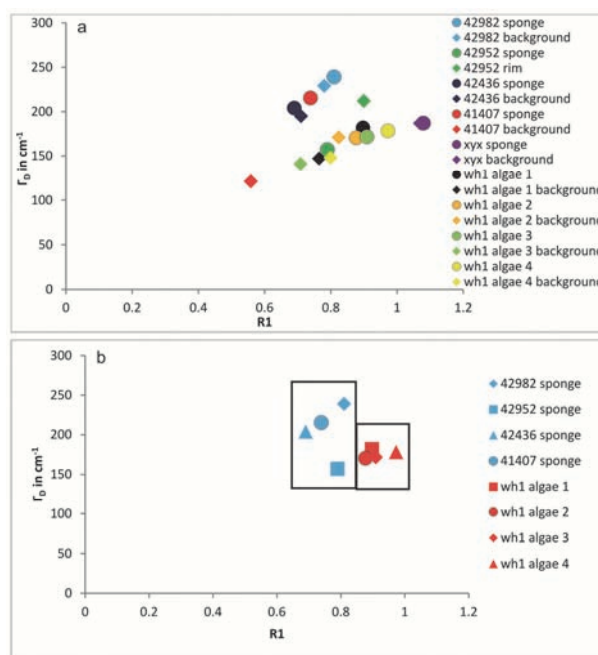
Fig. 5: Cross plots of the average values of the full width at half maximum of the D-band (Γ_D) over the intensity ratio of the D- and the G-band (R1) (cf. Table 1). **(a)** Values of the sponge fossils from Chengjiang and the Xiaoyanxi Formations (XYX), the algal fossils from the Wenghui Biota (WH), as well as the associated background materials. Fossil points are marked with circles and the associated background materials with diamonds. Except for samples from the Xiaoyanxi Formation, fossil values are clearly distinguishable from the respective background values. **(b)** Exclusively values of sponges from the Chengjiang Biota (blue symbols) and algae from the Wenghui Biota (red symbols); note the apparent clustering of the data (see squares).

Wu (2004) regarded the RSF as sponge gemmules because of the exceptionally recalcitrant organic matter and the round shape. But this interpretation is not in line with the character of modern and confirmed fossil sponge gemmules, which are at largest only about 1 mm in diameter (Fell 1993; Petit & Charbonnier 2012) and thus much smaller than the RSF. When erecting some RSF from Sancha as genera (*Triticispongia* and *Saetaspongia*), Steiner et al. (1993) interpreted *T. diagonata* as juveniles because their size hardly exceeds 10 mm, although adult forms have not been discovered then. But the juvenile theory cannot contribute directly to the interpretation of the thick carbon cover, because to our knowledge, the juvenile sponges do not necessarily have enriched spongin as in the case of gemmules.

On the other hand, based on the material from Chengjiang Biota, some other researchers tended to interpreted *T. diagonata* as adult precursor of reticulosid sponges, considering the missing adults and its well-organized skeletal structures (Rigby & Hou 1995). Larger specimens of *T. diagonata* (2.5–3 cm) were further discovered in the Niutitang Formation in Guizhou (Zhao et al. 2006). They are more probably giant individuals relating to certain environment or evolutionary stage than adult forms of the Hunan and Chengjiang analogues, because none of these three fossil communities contain big and small specimens at the same time. However, interpreting *T. diagonata* as a specific evolutionary stage of hexactinellids also could not help to explain the intensive carbon preservation of RSF, because RSF are polyphylogenetic. Wu (2004) has described sponges which possess only diactinal spicules in the RSF, indicating a demosponge population in them. And in this study, the observed specimens appear to belong to different hexactinellid morphotypes (Fig. 2).

For these reasons, we prefer to suggest that the unusual preservation of the organic carbon in RSF is probably due to some specific processes during early diagenesis, e.g., more effective adsorption of clays relating to the specific size and shape of these fossils. Furthermore, we attribute the exclusively small and round shape of these sponges to similar environmental controls. It has been observed in modern examples, that the exterior morphology of sponges can be strongly affected by environment, while the skeletal construction is still controlled by gene expression. The juvenile theory cannot be completely excluded as an interpretation of the specific morphology of RSF. However, the difficulty here is that the RSF are composed of various biological taxa, and it seems unlikely to expect that the juvenile of all the sponges possessed a similar morphology when the influence from the environment is absent. Furthermore, there has not been any reconstruction on the ontogenies of Chengjiang sponges, which could relate RSF to any potential adult forms. Nevertheless, to test proofing these postulations further investigations on the taxonomy of the RSF and precise observations in the outcrops are required.

Conclusions

Our observations show that the recalcitrant organic material from sponges, most probably being collagen and chitin according to current knowledge, can be preserved as dense carbonaceous remains in macroscopic fossils in BST Lagerstätten. The present application of Raman spectroscopy with the interpretation of the Γ_D and R1 values of the carbon signal still cannot directly reveal the nature of the precursor of the carbonaceous remains. However, our results confirmed suggestions by Bower et al. (2013) that carbonaceous material from complex precursor material with low thermal affection cluster in a certain area in the Γ_D-R1 plot (Γ_D between 100 and 250 cm^{-1}; R1 0.5 to 1.4). As the study of Bower et al. (2013) deals with microfossils, our findings represent first evidence that this approach could also be applied to macrofossils. This method also appears to be able to differentiate several sources of carbon in macroscopic fossil samples: between the fossil and the background, between the fossil material from Cambrian RSF and Ediacaran algal fossils, and between different specimens of RSF. It is still uncertain whether the separate clustering of the RSF data and the algal data reflects the variance of precursor material or only the diagenetic or geological history. However, the larger variance within the RSF data compared to the algal data probably is caused by different precursor material, because the RSF derive from the same setting and thus have a similar diagenetic and geological history. Nonetheless, further measurements on other fossil algal and poriferan material must be involved in the future, in order to improve and testify the current interpretations.

The taphonomical mechanism of the dense carbonaceous material in RSF is also interesting. Because the RSF are polyphylogenetic and there is currently no evidence to support their nature as any special development stage of sponges, we infer that this unusual carbonaceous preservation is due to a diagenetic bias relating to their specific morphology, which in turn is possibly controlled by similar living environments. Again, to test these inferences, more detailed taxonomical and paleoecological studies are necessary.

Acknowledgements

References

Beimforde, C.; Schäfer, N.; Dörfelt, H.; Nascimbene, P. C.; Singh, H.; Heinrichs, J.; Reitner, J.; Rana, R. S. & Schmidt, A. R. (2011): Ectomycorrhizas from a Lower Eocene angiosperm forest. *New Phytologist* **192** (4): 988-996. http://dx.doi.org/10.1111/j.1469-8137.2011.03868.x

Bergquist, P. R. (1978): *Sponges*. Berkeley & Los Angeles (University of California Press): 267 pp.

Bower, D. M.; Steele, A.; Fries, M. D. & Kater, L. (2013): Micro Raman spectroscopy of carbonaceous material in microfossils and meteorites: Improving a method for life detection. *Astrobiology* **13** (1): 103-113. http://dx.doi.org/10.1089/ast.2012.0865

Brain, C. K. B.; Prave, A. R.; Hoffmann, K.-H.; Fallick, A. E.; Botha, A.; Herd, D. A.; Sturrock, C.; Young, I.; Condon, D. J. & Allison, S. G. (2012): The first animals: Ca. 760-million-year-old sponge-like fossils from Namibia. *South Africa Journal of Sciences* **108** (1/2): 658-665.

Brasier, M. D.; Green, O. R.; Jephcoat, A. P.; Kleppe, A. K.; Van Kranendonk, M. J.; Lindsay, J. F.; Steele, A. & Grassineau, N. V. (2002): Questioning the evidence for Earth's oldest fossils. *Nature* **416** (6876): 76-81. http://dx.doi.org/10.1038/416076a

Busemann, H.; Alexander, C. M. O. D. & Nittler, L. R. (2007): Characterization of insoluble organic matter in primitive meteorites by microraman spectroscopy. *Meteoritics & Planetary Science* **42** (7/8): 1387-1416. http://dx.doi.org/10.1111/j.1945-5100.2007.tb00581.x

Butterfield, N. J. (1990): Organic preservation of non-mineralizing organisms and the taphonomy of the burgess shale. *Paleobiology* **16** (3): 272-286.

Butterfield, N. J. (1995): Secular distribution of Burgess-Shale-type preservation. *Lethaia* **28** (1): 1-13. http://dx.doi.org/10.1111/j.1502-3931.1995.tb01587.x

Butterfield, N. J.; Balthasar, U. W. E. & Wilson, L. A. (2007): Fossil diagenesis in the Burgess Shale. *Palaeontology* **50** (3): 537-543.

Collinson, M. (2011): Molecular taphonomy of plant organic skeletons. In: Allison, P. & Bottjer, D. (eds.): *Taphonomy: Process and Bias through time*. Dordrecht etc. (Springer): 223-247. [= *Topics in Geobiology* **32**]

Condon, D.; Zhu, M.; Bowring, S.; Wang, W.; Yang, A. & Jin, Y. (2005): U-Pb ages from the Neoproterozoic Doushantuo Formation, China. *Science* **308** (5718): 95-98. http://dx.doi.org/10.1126/science.1107765

Ehrlich, H. (2010): Spongin. In: Ehrlich, H.: *Biological Materials of Marine Origin*. Dordrecht etc. (Springer): 245-256. [= *Biologically-Inspired Systems* **1**]

Ehrlich, H.; Ilan, M.; Maldonado, M.; Muricy, G.; Bavestrello, G.; Kljajic, Z.; Carballo, J. L.; Schiaparelli, S.; Ereskovsky, A.; Schupp, P.; Born, R.; Worch, H.; Bazhenov, V. V.; Kurek, D.; Varlamov, V.; Vyalikh, D.; Kummer, K.; Sivkov, V. V.; Molodtsov, S. L.; Meissner, H.; Richter, G.; Steck, E.; Richter, W.; Hunoldt, S.; Kammer, M.; Paasch, S.; Krasokhin, V.; Patzke, G. & Brunner, E. (2010): Three-dimensional chitin-based scaffolds from Verongida sponges (Demospongiae: Porifera). Part I: Isolation and identification of chitin. *International Journal of Biological Macromolecules* **47** (2): 132-140.

Ehrlich, H.; Krautter, M.; Hanke, T.; Simon, P.; Knieb, C.; Heinemann, S. & Worch, H. (2007): First evidence of the presence of chitin in skeletons of marine sponges. Part II: Glass sponges (Hexactinellida: Porifera). *Journal of Experimental Zoology (B: Molecular and Developmental Evolution)* **308** (4): 473-483.

Fell, P. E. (1993): Porifera. In: Adiyodi, K. G. & Adiyodi, R. G. (eds.): *Reproductive Biology of Invertebrates VI (A: Asexual propagation and reproductive strategies)*. Chichester (Wiley): 1-44.

Foucher, F. & Westall, F. (2013): Raman imaging of metastable opal in carbonaceous microfossils of the 700-800 Ma old Draken Formation. *Astrobiology* **13** (1): 57-67. http://dx.doi.org/10.1089/ast.2012.0889

Gaines, R. R.; Kennedy, M. J. & Droser, M. L. (2005): A new hypothesis for organic preservation of Burgess Shale taxa in the Middle Cambrian Wheeler Formation, House Range, Utah. *Palaeogeography, Palaeoclimatology, Palaeoecology* **220** (1-2): 193-205. http://dx.doi.org/10.1016/j.palaeo.2004.07.034

Guo, Q.; Shields, G.; Liu, C.; Strauss, H.; Zhu, M.; Pi, D.; Goldberg, T. & Yang, X. (2007): Trace element chemostratigraphy of two Ediacaran–Cambrian successions in South China: Implications for organosedimentary metal enrichment and silicification in the Early Cambrian. *Palaeogeography, Palaeoclimatology, Palaeoecology* **254** (1-2): 194-216. http://dx.doi.org/10.1016/j.palaeo.2007.03.016

Gupta, N. & Briggs, D. E. G. (2011): Taphonomy of animal organic skeletons through time. In: Allison, P. & Bottjer, D. (eds.): *Taphonomy: Process and Bias through time*. Dordrecht etc. (Springer): 199-221. [= *Topics in Geobiology* **32**]

Hu, S. (2005): Taphonomy and palaeoecology of the Early Cambrian Chengjiang Biota from eastern Yunnan. *Berliner Paläobiologische Abhandlungen* **7**: 1-189.

Jiang, G.; Shi, X.; Zhang, S.; Wang, Y. & Xiao, S. (2011): Stratigraphy and paleogeography of the Ediacaran Doushantuo Formation (ca. 635-551 Ma) in South China. *Gondwana Research* **19** (4): 831-849. http://dx.doi.org/10.1016/j.gr.2011.01.006

Jiang, G.; Wang, X.; Shi, X.; Xiao, S.; Zhang, S. & Dong, J. (2012): The origin of decoupled carbonate and organic carbon isotope signatures in the Early Cambrian (ca. 542–520 Ma) Yangtze Platform. *Earth and Planetary Science Letters* **317-318** (0): 96-110. http://dx.doi.org/10.1016/j.epsl.2011.11.018

Kudryavtsev, A. B.; Schopf, J. W.; Agresti, D. G. & Wdowiak, T. J. (2001): In situ laser-Raman imagery of Precambrian microscopic fossils. *Proceedings of the National Academy of Sciences (PNAS)* **98** (3): 823-826.

Li, C. W.; Chen, J. Y. & Hua, T. E. (1998): Precambrian sponges with cellular structures. *Science* **279** (5352): 879-882. http://dx.doi.org/10.1126/science.279.5352.879

Maloof, A. C.; Rose, C. V.; Beach, R.; Samuels, B.; Calmet, C. C.; Erwin, D. H.; Poirier, G. R.; Yao, N. & Simons, F. J. (2010): Possible animal-body fossils in pre-Marinoan limestones from South Australia. *Nature Geoscience* **3** (9): 653-659. http://dx.doi.org/10.1038/ngeo934

Marshall, A. O.; Wehrbein, R. L.; Lieberman, B. S. & Marshall, C. P. (2012): Raman spectroscopic investigations of Burgess Shale-Type preservation: A new way forward. *Palaios* **27** (5): 288-292.

Marshall, C. P.; Edwards, H. G. M. & Jehlicka, J. (2010): Understanding the application of Raman spectroscopy to the detection of traces of life. *Astrobiology* **10** (2): 229-243. http://dx.doi.org/10.1089/ast.2009.0344

Pasteris, J. D. & Wopenka, B. (2002): Laser-Raman spectroscopy (Communication arising): Images of the Earth's earliest fossils? *Nature* **420** (6915): 476-477. http://dx.doi.org/10.1038/420476b

Pasteris, J. D. & Wopenka, B. (2003): Necessary, but not sufficient: Raman identification of disordered carbon as a signature of ancient life. *Astrobiology* **3** (4): 727-738.

Peterson, K. J.; Cotton, J. A.; Gehling, J. G. & Pisani, D. (2008): The Ediacaran emergence of bilaterians: Congruence between the genetic and the geological fossil records. *Philosophical Transactions of the Royal Society (B: Biological Sciences)* **363** (1496): 1435-1443. http://dx.doi.org/10.1098/rstb.2007.2233

Petit, G. & Charbonnier, S. (2012): Fossil sponge gemmules, epibionts of *Carpopenaeus garassinoi* n. sp. (Crustacea, Decapoda) from the Sahel Alma Lagerstätte (Late Cretaceous, Lebanon). *Geodiversitas* **34** (2): 359-372.

Petrovich, R. (2001): Mechanisms of fossilization of the soft-bodied and lightly armored faunas of the Burgess Shale and of some other classical localities. *American Journal of Science* **301** (8): 683-726.

Philippe, H.; Derelle, R.; Lopez, P.; Pick, K.; Borchiellini, C.; Boury-Esnault, N.; Vacelet, J.; Renard, E.; Houliston, E.; Quéinnec, E.; Da Silva, C.; Wincker, P.; Le Guyader, H.; Leys, S.; Jackson, D. J.; Schreiber, F.; Erpenbeck, D.; Morgenstern, B.; Wörheide, G. & Manuel, M. (2009): Phylogenomics revives traditional views on deep animal relationships. *Current Biology* **19** (8): 706-712. http://dx.doi.org/10.1016/j.cub.2009.02.052

Pisera, A. (2006): Palaeontology of sponges - a review. *Canadian Journal of Zoology* **84** (2): 242-261.

Quirico, E.; Montagnac, G.; Rouzaud, J. N.; Bonal, L.; Bourot-Denise, M.; Duber, S. & Reynard, B. (2009): Precursor and metamorphic condition effects on Raman spectra of poorly ordered carbonaceous matter in chondrites and coals. *Earth and Planetary Science Letters* **287** (1-2): 185-193. http://dx.doi.org/10.1016/j.epsl.2009.07.041

Rahl, J. M.; Anderson, K. M.; Brandon, M. T. & Fassoulas, C. (2005): Raman spectroscopic carbonaceous material thermometry of low-grade metamorphic rocks: Calibration and application to tectonic exhumation in Crete, Greece. *Earth and Planetary Science Letters* **240** (2): 339-354. http://dx.doi.org/10.1016/j.epsl.2005.09.055

Rigby, J. K. & Collins, D. (2004): Sponges of the Middle Cambrian Burgess Shale and Stephen Formations, British Columbia. *ROM Contributions in Science* **1**: 1-155.

Rigby, J. K. & Hou, X. (1995): Lower Cambrian demosponges and hexactinellid sponges from Yunnan, China. *Journal of Paleontology* **69** (6): 1009-1019.

Robertson, J. (1986): Amorphous carbon. *Advances in Physics* **35** (4): 317-374.

Schopf, J. W.; Kudryavtsev, A. B.; Agresti, D. G.; Wdowiak, T. J. & Czaja, A. D. (2002): Laser-Raman imagery of Earth's earliest fossils. *Nature* **416** (6876): 73-76. http://dx.doi.org/10.1038/416073a

Schopf, J. W.; Kudryavtsev, A. B.; Agresti, D. G.; Czaja, A. D. & Wdowiak, T. J. (2005): Raman imagery: A new approach to assess the geochemical maturity and biogenicity of permineralized Precambrian fossils. *Astrobiology* **5** (3): 333-371.

Sperling, E. A.; Peterson, K. J. & Pisani, D. (2009): Phylogenetic-signal dissection of nuclear housekeeping genes supports the paraphyly of sponges and the monophyly of Eumetazoa. *Molecular Biology and Evolution* **26** (10): 2261-2274. http://dx.doi.org/10.1093/molbev/msp148

Sperling, E. A.; Robinson, J. M.; Pisani, D. & Peterson, K. J. (2010): Where's the glass? Biomarkers, molecular clocks, and microRNAs suggest a 200-myr missing Precambrian fossil record of siliceous sponge spicules. *Geobiology* **8** (1): 24-36. http://dx.doi.org/10.1111/j.1472-4669.2009.00225.x

Steiner, M.; Mehl, D.; Reitner, J. & Erdtmann, B.-D. (1993): Oldest entirely preserved sponges and other fossils from the lowermost Cambrian and a new facies reconstruction of the Yangtze Platform (China). *Berliner Geowissenschaftliche Abhandlungen (E: Paläobiologie)* **9**: 293-329.

Steiner, M.; Wallis, E.; Erdtmann, B.-D.; Zhao, Y. & Yang, R. (2001): Submarine-hydrothermal exhalative ore layers in black shales from South China and associated fossils - insights into a Lower Cambrian facies and bio-evolution. *Palaeogeography, Palaeoclimatology, Palaeoecology* **169** (3-4): 165-191. http://dx.doi.org/10.1016/S0031-0182(01)00208-5

Steiner, M.; Zhu, M.; Zhao, Y. & Erdtmann, B.-D. (2005): Lower Cambrian Burgess shale-type fossil associations of South China. *Palaeogeography, Palaeoclimatology, Palaeoecology* **220** (1-2): 129-152. http://dx.doi.org/10.1016/j.palaeo.2003.06.001

Tuinstra, F. & Koenig, J. L. (1970): Raman spectrum of graphite. *The Journal of Chemical Physics* **53** (3): 1126-1130.

Wang, A. & Valentine, R. B. (2002): Seeking and identifying phyllosilicates on mars – a simulation study. In: *33rd annual lunar and planetary science conference. March 11-15, 2002, Houston, Texas*: [Abstract no 1370].

Wang, Y.; Wang, X. & Huang, Y. (2007): Macroscopic algae from the Ediacaran Doushantuo Formation in Northeast Guizhou, South China. *Earth Science (Journal of China University of Geosciences)* **32** (6): 828-844.

Wopenka, B. & Pasteris, J. D. (1993): Structural characterization of kerogens to granulite-facies graphite: applicability of Raman microprobe spectroscopy. *American Mineralogist* **78** (5-6): 533-557.

Wu, W. (2004): Fossil sponges from the Early Cambrian Chengjiang Fauna, Yunnan, China. *Unpublished PhD-thesis, Nanjing Institute of Geology and Palaeontology, Chinese Academy of Sciences*. Nanjing (NIGPAS): 179 pp.

Xiao, S. & Dong, L. (2006): On the Morphological and Ecological History of Proterozoic Macroalgae. In: Xiao, S. & Kaufman, A. (eds.): *Neoproterozoic Geobiology and Paleobiology*. Dordrecht etc. (Springer): 57-90. [= *Topics in Geobiology* **27**]

Xiao, S.; Yuan, X.; Steiner, M. & Knoll, A. H. (2002): Macroscopic carbonaceous compressions in a terminal Proterozoic shale: A systematic reassessment of the Miaohe Biota, South China. *Journal of Paleontology* **76** (2): 347-376.

Zhao, F.; Caron, J.-B.; Hu, S. & Zhu, M. (2009): Quantitative analysis of taphofacies and paleocommunities in the Early Cambrian Chengjiang Lagerstätte. *Palaios* **24** (12): 826-839.

Zhao, Y.; He, M.; Chen, M.; Peng, J.; Yu, M.; Wang, Y.; Yang, R.; Wang, P. & Zhang, Z. (2004): Discovery of a Miaohe-type biota from the Neoproterozoic Doushantuo Formation in Jiangou County, Guizhou Province, China. *Chinese Science Bulletin* **49** (18): 1916-1918.

Zhao, Y.; Yang, R.; Yang, X. & Mao, Y. (2006): Globular sponge fossils from the Lower Cambrian in Songlin, Guizhou Province, China. *Geological Journal of China Universities* **12** (1): 106-110.

Zhu, M.; Babcock, L. E. & Steiner, M. (2005): Fossilization modes in the Chengjiang Lagerstätte (Cambrian of China): Testing the roles of organic preservation and diagenetic alteration in exceptional preservation. *Palaeogeography, Palaeoclimatology, Palaeoecology* **220** (1-2): 31-46. http://dx.doi.org/10.1016/j.palaeo.2003.03.001

Zhu, M.; Yang, A.; Yang, X.; Peng, J.; Zhang, J. & Lu, M. (2012): Ediacaran succession and the Wenghui Biota in the deep-water facies of the Yangtze Platform at Wenghui, Jiangkou County, Guizhou. *Journal of Guizhou University (Natural Sciences)* **29** (1): 133-138.

Zhu, M.; Zhang, J. & Yang, A. (2007): Integrated Ediacaran (Sinian) chronostratigraphy of South China. *Palaeogeography, Palaeoclimatology, Palaeoecology* **254** (1-2): 7-61. http://dx.doi.org/10.1016/j.palaeo.2007.03.025

A brief synopsis on the history of sponge research in the Upper Triassic St. Cassian Formation (Dolomites, NE Italy)

Francisco Sánchez-Beristain[1] *; Jan-Peter Duda[2]; Laura López-Esquivel Kransksith[3] & Pedro García-Barrera[1]

[1]*Museo de Paleontología, Facultad de Ciencias, UNAM, Av. Universidad 3000, Circuito Exterior S/N, Coyoacán 04510 México, D.F., Mexico; Email: sanchez@ciencias.unam.mx*

[2]*Department of Geobiology, Geoscience Centre, Georg-August University Göttingen, Goldschmidtstr. 3, 37077 Göttingen, Germany*

[3]*Instituto de Ciencias Nucleares, UNAM, Av. Universidad 3000, Circuito Exterior S/N, Coyoacán 04510 México, D.F., Mexico*

* corresponding author

The St. Cassian Formation (Lower Carnian, Upper Triassic) of the Dolomites, northeastern Italy, has been the focus of wide scientific research since its discovery about 180 years ago. The main reason is the vast amount of well-preserved fossil invertebrates in the respective Fossil Lagerstätten. This is particularly important in case of Porifera since the fossil record of well-preserved specimens of this phylum is comparatively poor. Aim of this paper is therefore a brief outline of the history of research and a review of the current knowledge about fossil sponges in the St. Cassian Formation.

Introduction

The St. Cassian Formation is geographically part of the Dolomites (Fig. 1). It was firstly termed *'Cassianer Schichten'* (i.e., Cassian Beds) by zu Münster (1841), referring to the town of San Cassiano in the province of Bolzano, and cartographically recognized by von Hauer (1858). Subsequently extensive stratigraphic, sedimentological, and palaeontological studies were conducted by various scientists (e.g., von Richthofen 1860; Stur 1868; von Mojsisovics 1879; Ogilvie 1893; Pia 1937; Leonardi 1961; Fürsich & Wendt 1977; Wendt & Fürsich 1980; Russo et al. 1991, 1997; Stanley & Swart 1995; Nützel et al. 2010; Bernardi et al. 2011; Kroh 2011; Kroh et al. 2011; Tosti et al. 2011). Fossil groups such as cnidarians (e.g., Volz 1896); echinoderms (e.g., Hagdorn 2011; Kroh 2011); mollusks (e.g., Bandel 2007), plants (Kustatscher et al. 2011) and vertebrates (Bernardi et al. 2011) have been reviewed.

Aim of this paper is a brief review of respective findings with particular focus on exceptionally well-preserved remains of fossil sponges in this formation. In order to honour Professor Reitner's great contributions to the palaeontology of sponges in the St. Cassian Formation, findings of his respective studies are outlined separately.
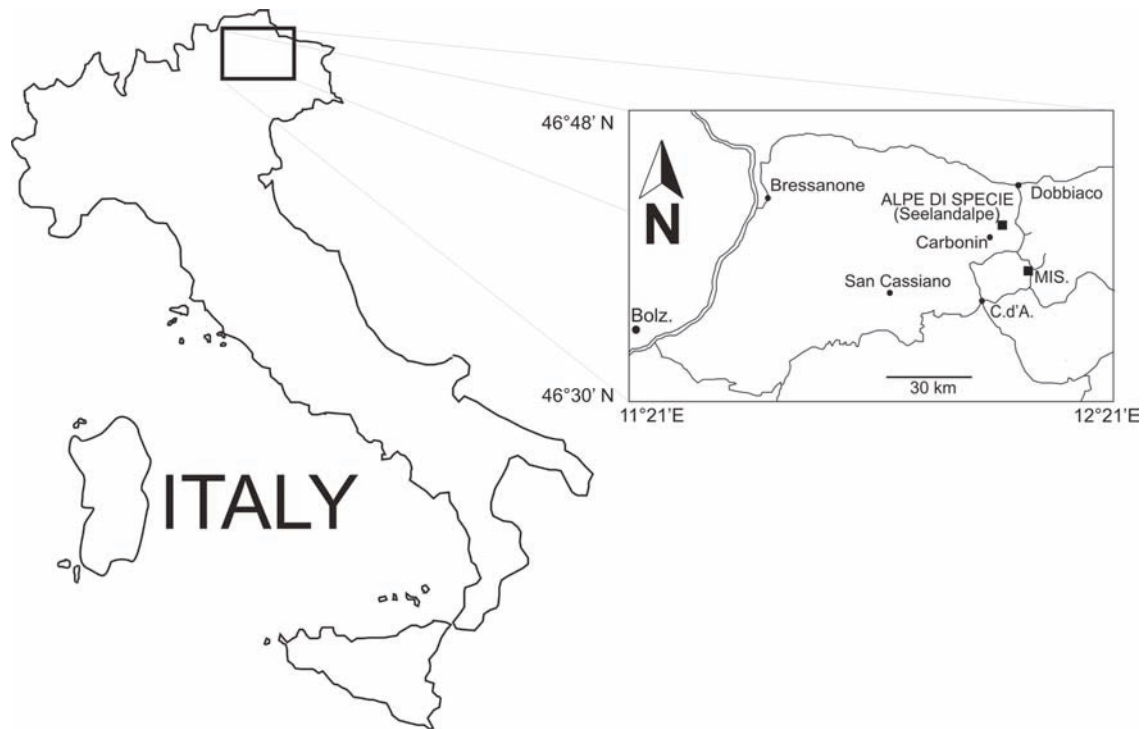
Fig. 1: Geographic positions of St. Cassian Formation outcrops. **Bolz.** = Bolzano; **C.d'A.** = Cortina d'Ampezzo; **Mis.** = Misurina [from Müller-Wille & Reitner 1993, modified].

Stratigraphy

The Carnian deposits of the Dolomites are represented by the huge carbonate platform sediments of the Cassian Dolomite and their contemporaneous basinal equivalents of the St. Cassian Formation (Russo et al. 1991). The St. Cassian Formation spans the time from the Middle to Upper Triassic (Ladinian–Carnian; Fig. 2) and comprises basin sediments (i.e., mostly marlstones and shales) deposited between carbonate buildups and locally back reef areas (Wendt & Fürsich 1980).

The first type section of the St. Cassian Formation was defined by Ogilvie (1893) by integration of several sections obtained between the regions of Stuores Wiesen and Pralongia. Ogilvie-Gordon (1929) later defined two sub-units in the St. Cassian Formation. This division was later confirmed by Mutschlechner (1933), Pia (1937), and Urlichs (1974) in several areas. However, Bizzarini & Braga (1978) performed a division into three levels: a lower level comprising a pseudo-flysch facies superposed on the Wengen Formation, a middle level with a sandy-tuffaceous lithology and rare fossils, and an upper level consisting of marls and gray-brown marly limestones with many fossiliferous beds ('*Seelandschichten*' *sensu* Pia 1937). It is also important to take into account that other authors (Stur 1868; von Mojsisovics 1874) had assigned the marly and tuffitic Wengen Strata to the St. Cassian Formation. However, Müller-Wille & Reitner (1993) compiled a stratigraphical section of the St. Cassian Formation where they accept the original model from Urlichs (1974), and place

the formation from the *aon* Zone in the Cordevolian to the *aonoides* and *austriacum* Zones in the Julian.

In the last two decades, some studies concerning the Carnian GSSP have been carried out (Gianolla et al. 1998; Broglio Loriga et al. 1999; Mietto et al. 2007, 2012). For the present work, the section of Müller-Wille & Reitner (1993) is taken as reference, considering that a deep stratigraphic review is not within the scope of this contribution.

Sedimentological considerations

A new stage of the research of the St. Cassian Formation started in the beginning of the 1960s. Leonardi (1961) recognized for the first time presence of lagoonal facies within an atoll/barrier. Baccelle (1965) described four Cassian lithofacies which she attributed to shallow water environments of narrow interreefal basins at the Sella Joch. Leonardi (1967) summarized the main outcrops where the authochthonous Cassian reef deposits can be found, which are mainly situated at Pralongia, Paso di Falzarego and Seiser Alm. However, based on investigations on some carbonate buildups, Bosellini & Rossi (1974) proposed that some of them may not have been ecological reefs in origin, but represent the indented edge of a broad shallow-water carbonate platform which had grown under

cyclically repeated subtidal, intertidal and supratidal conditions. This conclusion was shared by Leonardi (1979) concerning the Marmolada and Latemar buildups. His observations were corroborated by Russo et al. (1997), Keim & Schlager (2001) and Emmerich et al. (2005), who recognized the abundance of micrite produced in place (automicrite) for the Punta Grohmann, the Sella Massif, and the Latemar buildup. Regarding the variability of facies in the Dolomites, the most extensive analyses of the St. Cassian Formation was conducted by Fürsich & Wendt (1976, 1977) and Wendt & Fürsich (1980), who recognized four depositional environments, mainly based on their biofacies: deeper and shallow basinal, slope and shallow water facies. These papers underlined the diversity and complexity of facies, and among them 'Cipit boulders' have been given special attention (e.g., Russo et al. 1991; Russo et al. 1997; Rech 1998; Sánchez-Beristain & Reitner 2008; see below).

The Cipit boulders

Because of the abundance of publications dealing with calcareous blocks that originated from the Cassian carbonate platforms it is necessary to define and delineate the terms used in reference to these blocks. The term *'Kalkstein von Cipit'* (i.e., 'limestone from Cipit') was first used by von Richthofen (1860) to name calcareous blocks deposited within tuffitic marine beds in the Cassian Beds at the Seiser Alm. He described them as brown, partially crystallized bituminous limestones of an extraordinary tenaciousness, which he attributed to the abundant presence of celestine. The assignment of the name is toponymic and refers to the typical locality for such masses is in the vicinity of the Tschapit (*'Ciapit'*) Creek. He also pointed out that such blocks stratigraphically correspond to the base of the St. Cassian Formation. Later, von Mojsisovics (1875) applied von Richthofen's definition to a wider assortment of limestones, including regularly deposited limestone strata (*'Kalkbänke'*) in the Cassian Beds as well as isolated blocks. However, he assigned the term reefstone (*'Riffstein'*) to most of the isolated blocks.

Subsequent studies were increasingly focused on the genetic interpretation of the isolated blocks. Ogilvie (1893) and Salomon (1895) interpreted these blocks as autochthonous remains of small coral patch reefs from a shallow water zone, and the same idea was presented by Nöth (1929), van Houten (1930), and Valduga (1962). However, Cros (1967, 1974) and Cros & Lagny (1972) proposed an allochthonous origin of the blocks. This was subsequently confirmed by Fürsich & Wendt (1977). Because of distinct microfacial features observed in these blocks (e.g., Fe-hydroxide crusts and solution cavities cutting primary textures) these authors concluded that the blocks slid from shallow water carbonate platforms into the basin after subaerial erosion.

One important characteristic of most Cipit boulders is an early diagenetic cementation and an absence of dolomitization (Fürsich & Wendt 1977; Biddle 1981). This observation was explained by complete lithification of limestones before they slid into the basin during the emersion and karstification of the platforms (Cros 1974; Biddle 1981). Since dolomitization in the autochthonous shallow water facies was destructive, the exceptional preservation of the Cipit boulders provides rare insights into facies and biota of the shallow water environments (Russo et al. 1991) With regard to sedimentary facies, Cipit boulders are predominantly composed of algal biolithites and less commonly of coral limestones, which are associated with pelletal or micritic limestones, and these are attributed to reef- or reef-like environments of the platforms (Fürsich & Wendt 1977). Furthermore, there are also some blocks at the Seelandalpe and in Misurina, which may have originated from larger reef knolls (Fürsich & Wendt 1977). Finally, reef building/dwelling faunal associations known from Cassian patch reefs were also identified in blocks at the Seelandalpe/Alpe di Specie (Wendt 1982).
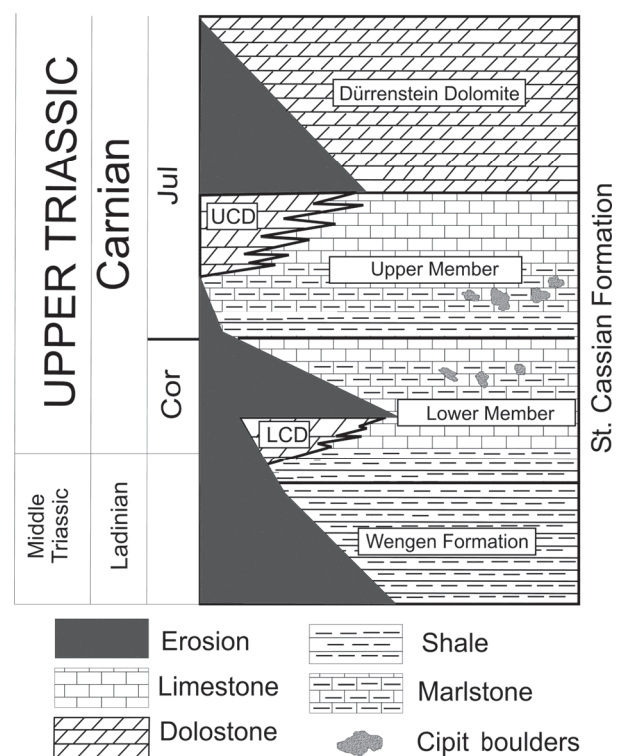
Fig. 2: Stratigraphic section of the St. Cassian Formation at Seelandalpe and Misurina. Abbreviations: **Cor** = Cordevolian; **Jul** = Julian; **LCD** = Lower Cassian Dolomite; **UCD** = Upper Cassian Dolomite [from Müller-Wille & Reitner 1993, modified].

Fossil Porifera

The St. Cassian Formation and its fauna has almost uninterruptedly been studied since the work of zu Münster (1834). Georg Graf zu Münster (1841) published the first encompassing monograph on the Cassian fauna and

reported a total of 79 genera and 422 species, mostly marine invertebrates. Von Klipstein (1843) and Laube (1864) provided encompassing revisions including several new taxa. Laube (1864) conducted the first study entirely focussed on the sponge fauna of the St. Cassian Formation. Many of the poriferan taxonomical classifications used by these authors are still valid. Loretz (1875) pinpointed the fossil richness of the Seelandalpe, highlighting the poriferan content, and Zittel (1879) took substantially into account sponge material from this locality for his work. Steinmann (1882) described also two new sponge species in the Cassian Beds (*Thaumastocoelia cassiana* and *Cryptocoelia zitteli*). Ogilvie-Gordon (1900) published an extensive list of fossils from various Cassian taxa from Falzarego Valley along with their stratigraphical distribution, though she did not include any poriferan.

An apparent gap in Cassian poriferan palaeontology exists from the beginning of the last century until the end of the 1960s, when Dieci et al. (1968) published a monograph on the sponges from the Cassian Formation. 23 species of "Inozoans" and "Sphinctozoans" are decribed here, including 10 new species. This publication represents a watershed for the investigation of Cassian poriferans. Following studies (e.g., Bizzarini & Braga 1978; Russo 1981) also account for some of the diversity of Cassian poriferans but they rather develop new trends in morphology and preservation of fossil sponges. Montanaro-Galitelli (1973) describes for the first time the microstructure of numerous Cassian corals. Dieci et al. (1974) perform studied the microstructure of selected poriferans from the Seelandalpe, distinguishing micritic, penicillate (clinogonal) and sphaerulitic types. Research on this issue continued to expand, and Cuif (1973, 1974) provided additional new descriptions and emphasized the role of the aragonitic sponges within the Triassic reefal fauna. However, some revolutionary issues emerged since Dieci et al. (1977) first reported the occurrence of spicules in Cassian chaetetids and ceratoporellids, thus assigning them to the "Sclerospongia". Parallel to these investigations, Wendt (1974) identified an orthogonal type (*sensu* Hudson 1959**)** as further microstructure for Cassian sponges. Moreover, he emphasized the extraordinary preservation of the aragonitic skeletons and included observations of spicules within their secondary skeletons, proposing for the first time the existence of such features within Cassian genera such as *Leiospongia*. Wendt (1975) determined the microstructural arrangement of Cassian stromatoporoids, which are, with exception of the sphaerulitic type, the same as in case of the poriferans. This topic was further discussed with regard to the stratigraphic distribution, associated diagenetic patterns, and comparability with recent forms (Wendt 1976, 1979, 1984; Veizer & Wendt 1976). Scherer (1976, 1977) achieved important breakthroughs in the geochemical analysis of Cassian samples and compared corals, sponges, and especially cements. In addition, he provided the first insights into the isotopic $\delta^{13}C$ and $\delta^{18}O$ records for Cassian sponges, by

assessing the first temperature data from these organisms, based on their excellent preservation state. They obtained temperatures ranging from 27 to 29°C, which are consistent with data obtained more recently from St. Cassian bivalves (Nützel et al. 2010) who reported a very high seasonal fluctuation of sea surface water temperatures based on high resolution sclerochronology of aragonitic bivalves.

Fürsich & Wendt (1977) performed the first encompassing quantitative palaeoecological analysis in the St. Cassian Formation. These authors described several associations and assemblages and characterized them with regard to palaeoecology. A particular feature of this study is the demonstration of specific and proportional abundances for each taxon, and that associations are referred to certain marine settings, ranging from shallow water to pelagic and basinal environments. Subsequently, Wendt & Fürsich (1980) carried out an exhaustive deep facies analysis, underlining the importance of poriferans in Cassian reefs. This was further pinpointed by Wendt (1982), who defined four community-types from the Cassian patch reefs from which one is dominated by poriferans, and by Russo (2005), who performed a study on the facies evolution within the Triassic platforms in the Dolomites. He also emphasized on the importance of sponges.

Engeser & Taylor (1989) reviewed the Klipstein collection at the British Museum of Natural History. They reassigned six poriferan type-specimens originally classified as bryozoans.

Finally, Belvedere & Bizzarini (2006) reported for the first time the occurrence of eleven sponge taxa from the St. Cassian outcrops of the Sappada area, in Veneto. Six of these taxa are included in the "Inozoa", whereas three are classified as "sphinctozoans" and two as "sclerosponges". Table 1 shows a list of type sponge species from the St. Cassian Formation.

J. Reitner's contributions to the palaeontology of Cassian sponges

Joachim Reitner has been working in the St. Cassian Formation since almost thirty years. He has described ten species of fossil poriferans mainly from Misurina (in the Rimbianco Valley) and the Seelandalpe (Alpe di Specie) near the town of Carbonin (Fig. 1). These species are: *Cassianothalamia zardinii* Reitner (Figs. 3–4), *Aka cassianensis* Reitner & Keupp (Fig. 5), *Murania kazmierczaki* Reitner (Fig. 6), *Hispidopetra triassica* Reitner (Fig. 7), *Ceratoporella breciacanthostyla* Reitner (Fig. 8), *Murania megaspiculata* Reitner (Fig. 9), *Hymedesmia mostleri* Reitner, *Chaetosclera klipsteini* Reitner & Engeser, *Petrosistroma stearni* Reitner and *Thalamnohaliclona amblysiphonelloides* Reitner. References to these species, as well as repository information can be found in Table 2.

Table 1: Overview of type-fossil Porifera from the St. Cassian Formation.

Species	Primary reference	Collection
Amblysiphonella loerentheyi	Dieci et al. 1968	Museo Paleontologico "Rinaldo Zardini", Cortina d'Ampezzo
Amblysiphonella strobiliformis	Dieci et al. 1968	Museo Paleontologico "Rinaldo Zardini", Cortina d'Ampezzo
Amblysiphonella timorica	Dieci et al. 1968	Museo Paleontologico "Rinaldo Zardini", Cortina d'Ampezzo
Atrochaetetes lagaaiji	Engeser & Taylor 1989	British Museum of Natural History
Atrochaetetes tamnifer	Engeser & Taylor 1989	British Museum of Natural History
Cassianochaetetes gnemidius	Engeser & Taylor 1989	British Museum of Natural History
Cassianochaetetes milleporatus	Engeser & Taylor 1989	British Museum of Natural History
Cassianochaetetes orbignyanus	Engeser & Taylor 1989	British Museum of Natural History
Celyphia submarginata	zu Münster 1841	Bayerische Staatssammlung für Paläontologie und Geologie
Colospongia dubia	zu Münster 1841	Bayerische Staatssammlung für Paläontologie und Geologie
Cryptocoelia zitteli	Steinmann 1882	Goldfuß-Museum, Bonn
Cystothalamia polysiphonata	Dieci et al. 1968	Museo Paleontologico "Rinaldo Zardini", Cortina d'Ampezzo
Enoplocoelia armata	von Klipstein 1843	British Museum of Natural History
Eudea polymorpha	von Klipstein 1843	British Museum of Natural History
Euepirrhysia montanaroae	Dieci et al. 1968	Museo Paleontologico "Rinaldo Zardini", Cortina d'Ampezzo
Euepirrhysia pusilla	Dieci et al. 1968	Museo Paleontologico "Rinaldo Zardini", Cortina d'Ampezzo
Leiospongia alpina	Laube 1865	British Museum of Natural History
Leiospongia polymorpha	Engeser & Taylor 1989	British Museum of Natural History
Leiospongia verrucosa	Laube 1865	British Museum of Natural History
Peronidella loretzi	Zittel 1879	Bayerische Staatssammlung für Paläontologie und Geologie
Peronidella rosetta	Dieci et al. 1968	Museo Paleontologico "Rinaldo Zardini", Cortina d'Ampezzo
Peronidella subcaespitosa	Dieci et al. 1968	Museo Paleontologico "Rinaldo Zardini", Cortina d'Ampezzo
Precorynella astroites	Dieci et al. 1968	Museo Paleontologico "Rinaldo Zardini", Cortina d'Ampezzo
Precorynella auriformes	Dieci et al. 1968	Museo Paleontologico "Rinaldo Zardini", Cortina d'Ampezzo
Precorynella capitata	Dieci et al. 1968	Museo Paleontologico "Rinaldo Zardini", Cortina d'Ampezzo
Precorynella pyriformis	von Klipstein 1843	British Museum of Natural History
Prosiphonella amplectens	Dieci et al. 1968	Museo Paleontologico "Rinaldo Zardini", Cortina d'Ampezzo
Sestrostomella aureolata	Dieci et al. 1968	Museo Paleontologico "Rinaldo Zardini", Cortina d'Ampezzo
Sestrostomella robusta	Zittel 1879	Bayerische Staatssammlung für Paläontologie und Geologie
Stellispongia manon	Dieci et al. 1968	Museo Paleontologico "Rinaldo Zardini", Cortina d'Ampezzo
Stellispongia subsphaerica	Dieci et al. 1968	Museo Paleontologico "Rinaldo Zardini", Cortina d'Ampezzo
Stellispongia variabilis	Dieci et al. 1968	Museo Paleontologico "Rinaldo Zardini", Cortina d'Ampezzo
Thaumastocoelia cassiana	Steinmann 1882	Goldfuß-Museum, Bonn
Zardinia perisulcata	Dieci et al. 1968	Museo Paleontologico "Rinaldo Zardini", Cortina d'Ampezzo
Zardinia platithalamica	Dieci et al. 1968	Museo Paleontologico "Rinaldo Zardini", Cortina d'Ampezzo

Table 2:   Overview of fossil Porifera from the St. Cassian Formation described by Joachim Reitner [GZG = depository Geoscience Museum Göttingen].

Species	Reference	Figure	Repository
Cassianothalamia zardinii	Reitner 1987	3-4	GZG
Aka cassianensis	Reitner & Keupp 1991	5	GZG
Murania kazmierczaki	Reitner 1992	6	GZG
Hispidopetra triassica	Reitner 1992	7	GZG
Ceratoporella breviacanthostyla	Reitner 1992	8	GZG
Murania megaspiculata	Reitner 1992	9	GZG
Hymedesmia mostleri	Reitner 1992		GZG
Chaetoslcera klipsteini	Reitner & Engeser 1989		GZG
Petrosiastroma stearni	Reitner 1992		GZG
Thalamnohaliclona amblysiphonelloides	Reitner 1992		GZG

Reitner (1987) noted for the first time the presence of spicules within sphinctozoans in the Cipit boulders from the St. Cassian Formation. The new 'sphinctozoan' species, *Cassianothalamia zardinii*, was thus assigned to the order Hadromerida due to the presence of aster microscleres and occasional monoaxonid megascleres. Keupp et al. (1989) firstly reported a Triassic hexactinellid in Cipit boulders.

Reitner & Engeser (1989) reported a chaetetid in the Cipit boulders. Because of its sphaerulitic microstructure and a primary skeleton with megascleres the authors assigned it to the *Halichondrida* Vosmaer *sensu* Levi. Later Reitner & Keupp (1991) described the new species *Aka cassianensis*. As later shown by Sánchez-Beristain (2010), this species is ecologically important with regard to the destruction and erosion of reef and reef-like communities from the St. Cassian Formation.

Summarizing, these findings contributed in a crucial way to the reassessment of organisms, formerly classified as 'sphinctozoans', 'chaetetids' and encrusting 'sclerosponges', to different families within the class Demospongiae. Since Reitner (1992) proposed his taxonomical-phylogenetical approach on coralline sponges, these terms are no longer valid. Based on cladistics (Hennig 1966) and several microscopical, histological and geochemical procedures, Reitner described seven new species of Cassian poriferans in this work (Table 2). Nevertheless, some St. Cassian taxa described by Reitner, such as *Cassianothalamia zardinii* are not considered as valid (Senowbari-Daryan 1990).

The work of Joachim Reitner on St. Cassian poriferans is not limited to taxonomy. Müller-Wille & Reitner (1993) described in detail the palaeobiology of four sponge taxa: *Cryptocoelia zitteli, Cassianothalamia zardini, Amblisyphonella strobiliformis* and *Thaumastocoelia cassiana*. This palaeobiological work is the first one dealing with the palaeobiology of St. Cassian sponges overall.

Reitner has furthermore been focused on the geobiology of Cassian sponges. He noted the presence of microbial crusts associated to some sclerosponges from the Cipit boulders. These microbial crusts/organomicrites (*sensu* Reitner 1993) are very important characteristics of many Cipit boulders (Brachert & Dullo 1994), and they are often closely associated with the sponge communities (Neuweiler & Reitner 1995). Due to the exceptional preservation of the material, it has even been possible to determine the presence of original organic matter in such organomicrites and even in sponges, such as *Cryptocoelia zitteli*, by means of epifluorescence microscopy at the surface of a *Cryptocoelia zitteli* specimen to detect organic matter.

Finally, Sánchez-Beristain & Reitner (2012) described the palaeoecological features of three sponge taxa: *Murania kazmierczaki, M. megaspiculata* and *Ceratoporella breviacanthostyla*. These encrusting 'coralline' sponges played an important role in the binding processes of the St. Cassian frameworks, along with microencrusters such as *Koskinobullina socialis, 'Tubiphytes'* cf. *T. obscurus* and *Ladinella porata*.

Conclusions

The history of research at the St. Cassian Formation spans a time period of ca. 180 years. In the beginning, research was focused on the general geology and the description of fossil taxa. In the first third of the 20th century, research focused more on geological and stratigraphical issues, though the study of fossil fauna was never abandoned. Regarding reef-building taxa, sponges constitute a considerable part. Joachim Reitner's contributions comprise the description of ten species of poriferans from the St. Cassian Formation as well as important findings about the taxonomy, palaeoecology palaeobiology, and even biogeochemistry of fossil sponges.
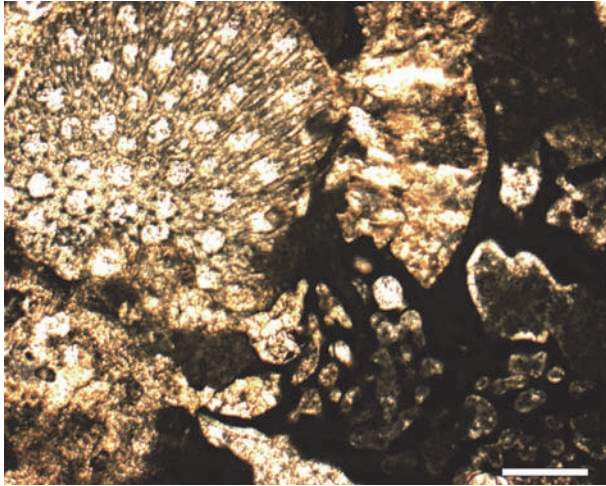
Fig. 3: The thalamid sponge *Cassianothalamia zardinii* Reitner (right), encrusting on top of a bryozoan. Cipit boulder from Seelandalpe. Thin section code: JRCas-22. Scale bar = 500 µm.
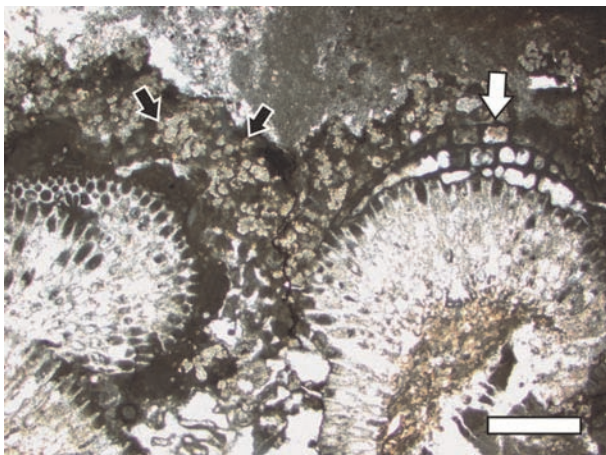
Fig. 4: *Cassianothalamia zardinii* Reitner (white arrow) on top of a ceratoporellid sponge. Black arrows point at the microencruster *Baccanella floriformis*, which are immerse in peloidal microbialite. Cipit boulder from Seelandalpe. Thin section code: CG-I-5. Scale bar = 5 mm.
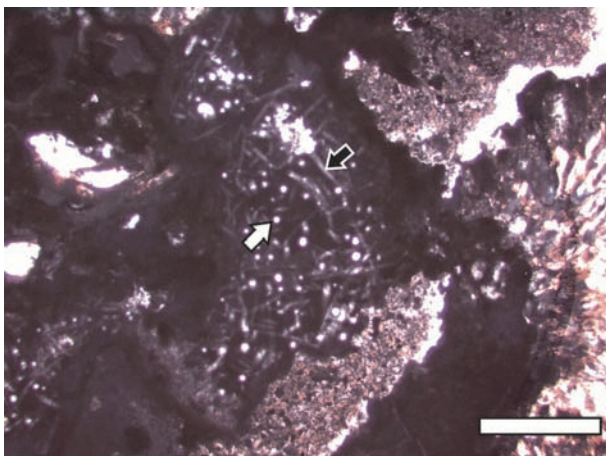
Fig. 5: The boring sponge *Aka cassianensis* Reitner & Keupp, revealed by the occurrence of monoaxonic spicules in longitudinal and transverse sections (black and white arrows, respectively), dwelling on peloidal microbialite. Cipit boulder from the Rimbianco Valley, Misurina. Thin section code: FSM-VI-11. Scale bar = 2 mm.
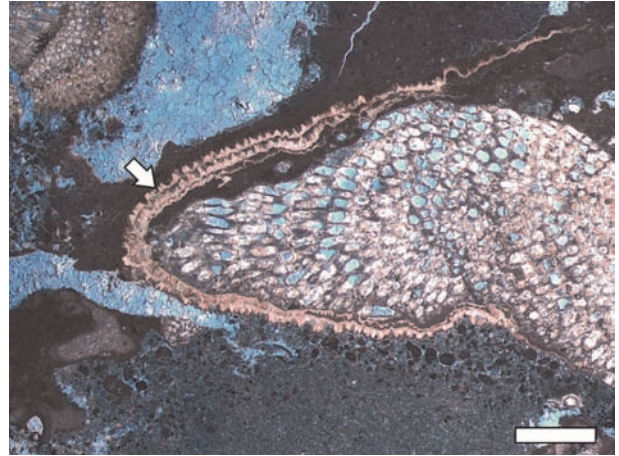
Fig. 6: The encrusting 'coralline' sponge *Murania kazmierczaki* Reitner (arrow), on top of an encrusting complex made of microbialite and foraminifers, all atop of a chaetetid sponge. Cipit boulder from the Rimbianco Valley, Misurina. Thin section code: FSM-IX-3. Scale bar = 2 mm. [from Sánchez-Beristain & Reitner 2012, modified]
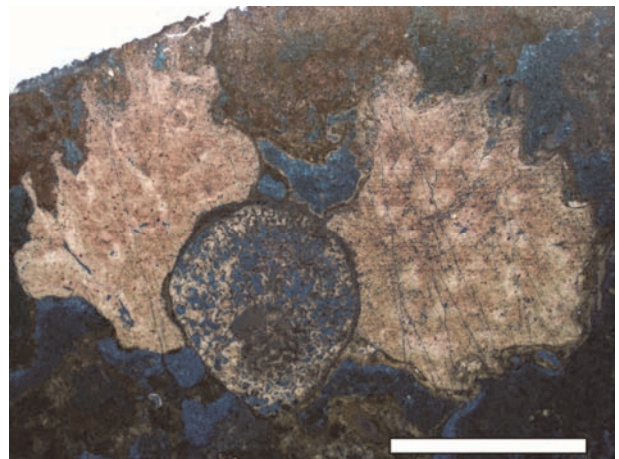
Fig. 7: The 'coralline' sponge *Hispidopetra triassica* Reitner, encrusting on a chaetetid? sponge. Cipit boulder from Seelandalpe. Thin section code: FSSA-V-4L. Scale bar = 5 mm.
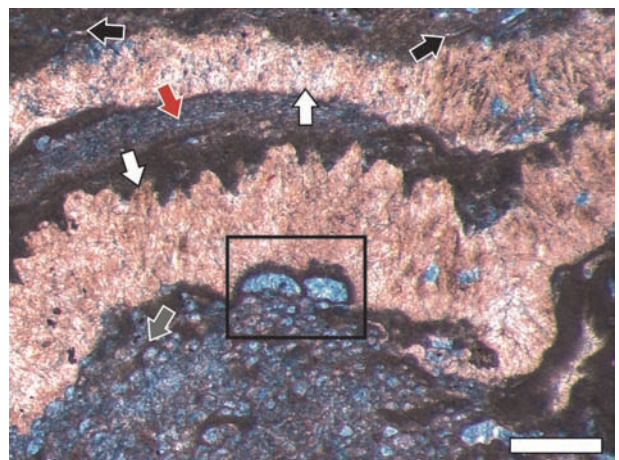
Fig. 8: The 'coralline' sponge *Ceratoporella breviacanthostyla* Reitner (white arrows), as a part of an encrusting complex consisting of colonies of *Koskinobullina socialis* (grey arrow), *Wetheredella*-like encrusters (red arrow), borings of *Microtubus communis* (black arrows) in peloidal microbialite, and thalamid sponges (black square). Cipit boulder from Seelandalpe. Thin section code: JRSA-19. Scale bar = 500 µm.
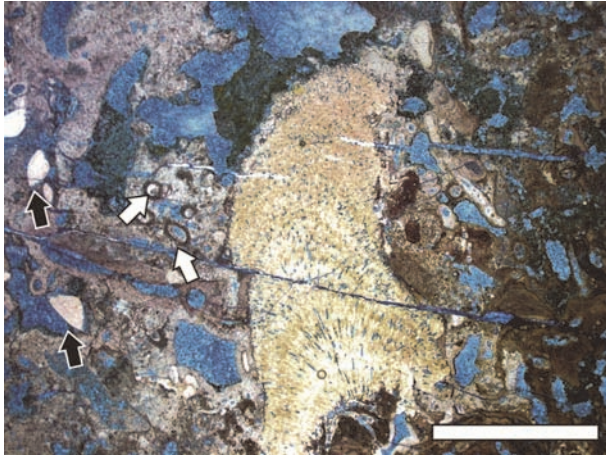
Fig. 9: The 'coralline' sponge *Murania megaspiculata* Reitner, as a part of a microbialitic boundstone where elements as *Terebella* cf. *lapilloides* (white arrows) and *Lamelliconus cordevolicus* (black arrows) can be seen. Cipit boulder from the Rimbianco Valley, Misurina. Thin section code: IP FUB J R/ 1992-PR-I-13. Scale bar = 1 mm.

Acknowledgements

References

Baccelle, L. (1965): Contributo alla conoscenza petrografica e Sedimentologica degli strati di S. Cassiano nelle Dolomiti. *Studi Trentini di Scienze Naturali Acta* **42** (2): 1-19.

Bandel, K. (2007): Description and classification of Late Triassic Neritimorpha (Gastropoda, Mollusca) from St. Cassian Formation, Italian Alps. *Bulletin of Geosciences* **82** (3): 215–274.

Belvedere, M. & Bizzarini, F. (2006): Prima segnalazione di Poriferi nel Carnico (Triassico Superiori) dei dintorni di Sappada. *Gortania. Atti del Museo Friuliano di Storia Naturale* **27**: 17-24.

Bernardi, M.; Avanzini, M. & Bizzarini, F. (2011): Vertebrate fauna from the San Cassiano Formation (early Carnian) of the Dolomites region. *Geo.Alp* **8**: 122-127.

Biddle, K. T. (1981): The basinal Cipit boulders: indicators of Middle to Upper Triassic buildup margins, Dolomite Alps, Italy. *Rivista Italiana di Paleontologia e Stratigrafia* **86**: 779-794.

Bizzarini, F. & Braga, G. (1978): Upper Triassic new genera and species of fair and questionable Bryozoa Chaetetida from the S. Cassiano Formation of the Dolomites (eastern Italy). *Bollettino della Società Paleontologica Italiana* **17** (1): 28-48.

Bosellini, A. & Rossi, D. (1974): Triassic Carbonate Buildups of the Dolomites, Northern Italy. In: Laporte, L. F. (ed.): Reefs in time and space: Selected examples from the recent and ancient. *Society of Economic Paleontologists and Mineralogists, Special Publication* **18**: 209-233.

Brachert, T. C. & Dullo, W. C. (1994): Micrite crusts on Ladinian foreslopes of the Dolomites seen in the light of a modern scenario from the Red Sea. *Abhandlungen der Geologischen Bundesanstalt* **50**: 57-68.

Broglio Loriga, C.; Cirilli, S.; De Zanche, V.; di Bari, D.; Gianolla, P.; Laghi, M. F.; Lowrie, W.; Manfrin, S.; Mastandrea, A.; Mietto, P.; Muttoni, C.; Neri, C.; Posenato, C.; Rechichi, M. C.; Rettori, R. & Roghi, G. (1999): The Prati di Stuores/Stuores Wiesen Section (Dolomites, Italy): a candidate Global Stratotype Section and Point for the base of the Carnian stage. *Rivista Italiana di Paleontologia e Stratigrafia* **105**: 37-78.

Cros, P. (1967): A propos de l'origine récifale de deux massifs ladino-carniens dans les Dolomites. *Compte rendu sommaire des séances de la Société géologique de France* **6**: 233.

Cros, P. (1974): Un modéle de sédimentation carbonatée marine: Les plateformes dites récifales du Trias des Dolomitees et leur environment. *Unpublished PhD thesis, Université de Paris*: 888 pp.

Cros, P. & Lagny, P. (1972): Die paleogeographische Bedeutung der pelagischen Ablagerungen im Anis und Ladin der Westlichen Karnischen Alpen und der Dolomiten (Norditalien). *Mitteilungen der Gesellschaft der Geologie- und Bergbaustudenten in Österreich* **21** (1): 169-192.

Cuif, J. P. (1973): Histologie de quelques sphinctozoaires (Poriferes) Triasiques. *Geobios* **6** (2): 115-125.

Cuif, J. P. (1974): Role des Sclérosponges dans la faune récifale du Trias des Dolomites (Italie du Nord). *Geobios* **7** (2): 139-153.

Dieci, G.; Antonacci, A. & Zardini, R. (1968): Le spugne cassiane (Trias medio-superiore) della regione dolomitica attorno a Cortina d´Ampezzo. *Bollettino della Società Paleontologica Italiana* **7** (2): 94-155.

Dieci, G.; Russo, A. & Russo, F. (1974): Nota preliminare sulla microstruttura di spugne aragonitiche del Trias medio-superiore. *Bollettino della Società Paleontologica Italiana* **13** (2): 99-107.

Dieci, G.; Russo, A.; Russo, F. & Marchi, M. S. (1977): Occurence of Spicules in Triassic Chaetetids and Ceratoporellids. *Bollettino della Società Paleontologica Italiana* **16** (2): 229-238.

Emmerich, A.; Zamparelli, V.; Bechstädt, T. & Zühlke, R. (2005): The reefal margin and slope of a Middle Triassic carbonate platform: the Latemar (Dolomites, Italy). *Facies* **50** (3-4): 573-614.

Engeser, T. S. & Taylor, P. D. (1989): Supposed Triassic bryozoans in the Klipstein collection from the Italian Dolomites redescribed as calcified demospongias: *Bulletin of the British Museum Natural History, Geology Series* **45**: 39-55.

Fürsich, F. T. & Wendt, J. (1976): Faziesanalyse und paläogeographische Rekonstruktion des Ablagerungsraumes der Cassianer Schichten (Mittel- bis Obertrias, Langobard-Cordevol, Jul? – Südalpen). In: Seilacher, A. (ed.): Palökologie. Konstruktionen, Sedimentologie, Diagenese und Vergesellschaftung von Fossilien. Bericht 1970-1975 des Sonderforschungsbereichs 53 Tübingen. *Zentralblatt für Geologie und Paläontologie (II: Paläontologie)* **[1976]** (5/6): 233-238.

Fürsich, F. T. & Wendt, J. (1977): Biostratinomy and Palaeoecology of the Cassian Formation (Triassic) of the Southern Alps. *Palaeogeography, Palaeoclimatology, Palaeoecology* **22** (4): 257-323. http://dx.doi.org/10.1016/0031-0182(77)90005-0

Gianolla, P.; De Zanche, V. & Mietto, P. (1998): Triassic sequence stratigraphy in the Southern Alps (northern Italy): definition of sequences and basin evolution. In: de Graciansky, P.-C.; Hardenbol, J.; Jacquin, T. & Vail, P. R. (eds.): Mesozoic and Cenozoic sequence stratigraphy of European basins. *Society of Economic Paleontologists and Mineralogists, Special Publication* **60**: 719-747.

Hagdorn, H. (2011): Benthic crinoids from the Triassic Cassian Formation of the Dolomites. *Geo.Alp* **8**: 128-135.

Hauer, F. von (1858): Erläuterungen zu einer geologischen Uebersichtskarte der Schichtgebirge der Lombardie. *Jahrbuch der Kaiserlich-königlichen geologischen Reichsanstalt* **9**: 445-496.

Hennig, W. (1966): Phylogenetic Systematics. Urbana, Ill. etc. (University of Illinois Press): 263 pp.

Hudson, R. G. S. (1959): A revision of Jurassic stromatoporoids *Actinostromina*, *Astrostylopsis*, and *Trupetostromaria*. *Palaeontology* **2** (1): 87-98.

Keim, L. & Schlager, W. (2001): Quantitative compositional analyses of a Triassic carbonate platform (Southern Alps, Italy). *Sedimentary Geology* **139** (3-4): 261-283.

Keupp, H.; Reitner, J. & Salomon, D. (1989): Kieselschwämme (Hexactinellida und "Lithistida") aus den Cipit-Kalken der Cassianer Schichten (Karn, Südtirol). *Berliner geowissenschaftliche Abhandlungen (A: Geologie und Paläontologie)* **106**: 221-241.

Klipstein, A. von (1843): Beiträge zur Geologischen Kenntnis der östlichen Alpen. Lieferung 1. Gießen (Heyen): 311 pp.

Kroh, A. (2011): Echinoids from the Triassic of St. Cassian − A review. *Geo.Alp* **8**: 136-140.

Kroh, A.; Nichterl, T. & Lukeneder, A. (2011): Type specimens from the Cassian Beds in the collection of the NHM Vienna. *Geo.Alp* **8**: 142-145.

Kustatscher, E.; Bizzarini, F. & Roghi, G. (2011): Plant fossils in the Cassian Beds and other Carnian formations of the Southern Alps (Italy). *Geo.Alp* **8**: 146-155.

Laube, G. (1864): Bemerkungen über die Münster'schen Arten von St. Cassian in der Münchener paläontologischen Sammlung. *Jahrbuch der Kaiserlich-königlichen geologischen Reichsanstalt* **14**: 402-412.

Leonardi, P. (1961): Triassic coralligenous reefs in the Dolomites. *Annali dell' Universitá di Ferrara* **8**: 127-157.

Leonardi, P. (1967): *Le Dolomiti: geologia dei monti tra Isarco e Piave; premio nazionale dei Lincei 1958 per la geologia e la paleontologia. Vol. 1 & 2*. Rovereto (R. Manfrini): 1-552 + 563-1019.

Leonardi, P. (1979): Sedimentological-stratigraphic considerations regarding the Triassic 'reefs' of the Dolomites (Italy). *Geologie en Mijnbouw* **58**: 139-144.

Loretz, H. (1875): Einige Petrefakten der alpinen Trias aus den Südalpen. *Zeitschrift der Deutschen Geologischen Gesellschaft* **27**: 784-842.

Montanaro Galitelli, E.; Morandi, N. & Pirani, R. (1973): Corallofauna triassica aragonitica ad alto contenuto in stronzio: studio analitico e considerazioni. *Bollettino della Società Paleontologica Italiana* **12**: 130-144.

Mietto, P.; Manfrin, S.; Preto, N. & Gianolla, P. (2007): Selected ammonoid fauna from Prati di Stuores/Stuores Wiesen and related sections across the Ladinian-Carnian boundary (Southern Alps, Italy). *Rivista Italiana di Paleontologia e Stratigrafia* **114** (3): 377-429.

Mietto, P.; Manfrin, S.; Preto, N.; Rigo, M.; Roghi, G.; Gianolla, P.; Posenato, R.; Muttoni, G.; Nicora, A.; Buratti, N.; Cirilli, S. & Spötl, C. (2012): The Global Boundary Stratotype Section and Point (GSSP) of the Carnian stage (Late Triassic) at Prati di Stuores/Stuores Wiesen section (Southern Alps, NE Italy). *Episodes* **35**: 414-430.

Mojsisovics, E. von (1874): Die Faunengebiete und Faciesgebiete der Triasperiode in den Ostalpen. *Jahrbuch der Kaiserlich-königlichen geologischen Reichsanstalt* **24**: 81-134.

Mojsisovics, E. von (1875): Über die Ausdehnung und die Structur der südtirolischer Dolomitstöcke. *Sitzungsberichte der Akademie der Wissenschaften in Wien, Mathematisch-Naturwissenschaftliche Klasse* **71**: 719-736.

Mojsisovics, E. von (1879): *Die Dolomit-Riffe von Südtirol und Venetien. Beiträge zur Bildungsgeschichte der Alpen*. Wien (A. Hölder): 552 pp.

Müller-Wille, S. & Reitner, J. (1993): Palaeobiological Reconructions of selected sphinctozoan sponges from the Cassian Beds (Lower Carnian) of the Dolomites (Northern Italy). *Berliner geowissenschaftliche Abhandlungen (E: Paläobiologie)* **9**: 253-281.

Münster, G. zu (1834): Über das Kalkmergel-Lager von St. Cassian in Tyrol und die darin vorkommenden Ceratiten. *Neues Jahrbuch für Mineralogie, Geognosie, Geologie und Petrefaktenkunde*, **[1834]**: 1-15.

Münster, G. zu (1841): Beschreibung und Abbildung der in den Kalkmergelschichten von St. Cassian gefundenen Versteinerungen. In: Wissmann, H. L., Münster, G. G (eds.): *Beiträge zur Geognosie und Petrefaktenkunde des Südöstlichen Tirols vorzüglich der Schichten von St. Cassian*. Bayreuth (Buchner): 25-152.

Mutschlechner, G. (1933): Geologie des Gebietes zwischen St. Cassian und Buchenstein (Südtiroler Dolomiten). *Jahrbuch der Geologischen Bundesanstalt* **83**: 199-232.

Neuweiler, F. & Reitner, J. (1995): Epifluorescence-microscopy of selected automicrites from lower Carnian Cipit-boulders of the Cassian Formation (Seeland Alpe, Dolomites). *Facies* **32**: 26-28.

Nöth, L. (1929): Geologie des mittleren Cordevolgebietes zwischen Vallazza und Cencenighe (Dolomiten). *Jahrbuch der Geologischen Bundesanstalt* **79**: 129- 202.

Nützel, A.; Joachimski, M. & López Correa, M. (2010): Seasonal climatic fluctuations in the Late Triassic tropics – High-resolution oxygen isotope records from aragonitic bivalve shells (Cassian Formation, Northern Italy). *Palaeogeography, Palaeoclimatology, Palaeoecology* **285** (3-4): 194-204. http://dx.doi.org/10.1016/j.palaeo.2009.11.011

Ogilvie, M. M. (1893): Contributions to the Geology of Wengen and St. Cassian Strata in Southern Tyrol. *Quarterly Journal of the Geological Society of London* **49**: 1-78.

Ogilvie-Gordon, M. M. (1900): On the fauna of the Upper Cassian Zone in Falzarego Valley, South Tyrol. *Geological Magazine* **4** (7): 337-348.

Ogilvie-Gordon, M. M. (1929): Geologie des Gebietes Von Piave (Buchenstein), St. Cassian und Cortina d´Ámpezzo. *Jahrbuch der Geologischen Bundesanstalt* **79**: 357-424.

Pia, J. (1937): *Stratigraphie und Tektonik der Pragser Dolomiten in Südtirol*. Wien (Selbstverlag): 248 pp.

Rech, H. (1998): Geobiologie der sogenannten „Cipit-Kalke" der Beckenfazies der Cassianer-Schichten, St. Kassian, Dolomiten. *Unpublished Diploma thesis, University of Göttingen*. Göttingen (IMGP): 136 pp.

Reitner, J. (1987): A new calcitic sphinctozoan sponge belonging to the Demospongiae from the Cassian Formation (Lower Carnian; Dolomites, Northern Italy) and its phylogenetic relationship. *Geobios* **20**: 571-589.

Reitner, J. (1992): "Coralline Spongien". Der Versuch einer phylogenetisch-taxonomischen Analyse. *Berliner geowissenschaftliche Abhandlungen (E: Paläobiologie)* **1**: 1-352.

Reitner, J. (1993): Modern Cryptic Microbialite/Metazoan Facies from Lizard Island (Great Barrier Reef, Australia): Formation and Concepts. *Facies* **29** (1): 3-40.

Reitner, J. & Engeser, T. (1989): *Chaetoclera klipsteini* n. gen. n. sp. (Halichondria, Demospongiae) aus dem Unterkarn der Cassianer-Schichten (Dolomiten, Italien). *Mitteilungen aus dem Geologisch-Paläontologischen Institut der Universität Hamburg* **68**: 159-165.

Reitner, J. & Keupp, H. (1991): The fossil record of the haplosclerid excavating sponge *Aka* de Laubenfels. In: Reitner, J. & Keupp, H. (eds.): *Fossil and Recent Sponges*. Berlin etc. (Springer): 102-120.

Richthofen, F. von (1860): *Geognostische Beschreibung der Umgegend von Predrazzo, Sanct Cassian und der Seiser Alpe in Süd-Tyrol*. Gotha (Perthes): xii + 327 pp.

Russo, F. (1981): Nuove spugne calcaree triassiche di Campo. (Cortina d'Ampezzo, Belluno). *Bollettino della Società Paleontologica Italiana* **20** (1/3): 3-17.

Russo, F. (2005): Biofacies evolution in the Triassic platforms of the Dolomites, Italy. *Annali dell' Università degli Studi di Ferrara, Volume Speciale:* 33-45.

Russo, F.; Neri, C.; Mastandrea, A. & Baracca, A. (1997): The Mud Mound Nature of the Cassian Platform Margins of the Dolomites. A Case History: the Cipit Boulders from Punta Grohmann (Sasso Piatto Massif, Northern Italy). *Facies* **36** (1): 25-36.

Russo, F.; Neri, C.; Mastandrea, A. & Laghi, G. (1991): Depositional and Diagenetic History of the Alpe di Specie (Seelandalpe) Fauna (Carnian, Northeastern Dolomites). *Facies* **25** (1): 187-210.

Salomon, W. (1895): Geologische und palaeontologische Studien über die Marmolata. *Palaeontographica* **42** (1-3): 1-210.

Sánchez-Beristain, J. F. (2010): Paleoecological and geochemical studies on sponge/microencruster -bearing communities contained in selected Cipit Boulders from the St. Cassian Formation (Lower Carnian, Upper Triassic) of the Dolomites, Northeastern Italy. *Unpublished PhD thesis*, University of Göttingen. Göttingen (GZG): 225 pp.

Sánchez-Beristain, J. F. & Reitner, J. (2008): Association diversity among sponge boundstones from the Lower Carnian Cassian Formation (Dolomites, Northern Italy). In: Löffler, S.-B. & Freiwald, A. (eds.): Jahrestagung der Paläontologischen Gesellschaft. 8.10. September 2008, Erlangen. *Erlanger Geologische Abhandlungen, Sonderband* **6**: 54.

Sánchez-Beristain, J. F. & Reitner, J.(2012): New occurrence of encrusting "coralline" sponges in selected erratic blocks from two localities at the Cassian Formation (Lower Carnian, Upper Triassic, Dolomites, Northern Italy) and their relation to associated microencrusters. *Paläontologische Zeitschrift* **86** (2): 113-133. http://dx.doi.org/10.1007/s12542-011-0124-y

Scherer, M. (1976): Diagenese aragonitischer Fossilien (Hexakorallen und Kalkschwämme) der Cassianer Schichten, Karn. In: Seilacher, A. (ed.): Palökologie. Konstruktionen, Sedimentologie, Diagenese und Vergesellschaftung von Fossilien. Bericht 1970-1975 des Sonderforschungsbereichs 53 Tübingen. *Zentralblatt für Geologie und Paläontologie (II: Paläontologie)* **[1976]** (5/6): 366-370.

Scherer, M. (1977): Preservation, alteration and multiple cementation of aragonitic skeletons from the Cassian Beds (U. Triassic, Southern Alps): Petrographic and geochemical evidence. *Neues Jahrbuch für Geologie und Paläontologie, Abhandlungen* **154** (2): 213-262.

Senowbari-Daryan, B. (1990): Die systematische Stellung der thalamiden Schwämme und ihre Bedeutung in der Erdgeschichte. *Münchner Geowissenschaftliche Abhandlungen (A: Geologie und Paläontologie)* **21**: 5-326.

Stanley, G. D. jr. & Swart, P. (1995): Evolution of the coralzooxanthellate symbiosis during the Triassic: A geochemical approach. *Paleobiology* **21** (2): 179-199.

Steinmann, G. (1882): Pharetronen-Studien. *Neues Jahrbuch für Geologie und Paläontologie, Abhandlungen* **[1882]** (2): 139-191.

Stur, D. (1868): Eine Exkursion in die Umgebung von St. Cassian. *Jahrbuch der Kaiserlich-königlichen geologischen Reichsanstalt* **18**: 529-568.

Tosti, F.; Guido, A.; Demasi, F.; Mastandrea, A.; Naccarato, A.; Tagarelli, A. & Russo, F. (2011): Microbialites as primary builders of the Ladinian-Carnian platforms in the Dolomites: Biogeochemical characterization. *Geo.Alp* **8**: 156-162.

Urlichs, M. (1974): Zur Stratigraphie und Ammonitenfauna der Cassianer Schichten von Cassian (Dolomiten/Italien). *Schriftenreihe der Erdwissenschaftlichen Kommissionen, Österreichische Akademie der Wissenschaften* **2**: 207-222.

Valduga, A. (1962): Osservazioni stratigrafico-paleontologiche sui rapporti fra la seria Raibliana dello Sciliar e i „Tufi a Pachicardie" dell'Alpe di Suisi. *Atti dell Istituto Veneto di scienze, lettere ed arti, Classe di Scienze Matematiche e Naturali* **120**: 165-189.

Van Houten, L. (1930): Geologie des Pelmo-Gebietes in den Dolomiten von Cadore. *Jahrbuch der Geologischen Bundesanstalt* **80**: 147-230.

Veizer, J. & Wendt, J. (1976): Mineralogy and chemical composition of Recent and fossil skeletons of calcareous sponges. *Neues Jahrbuch für Geologie und Paläontologie, Monatshefte* **[1976]** (9): 558-573.

Volz, W. (1896): Die Korallen der Schichten von St. Cassian in Süd-Tirol. *Palaeontographica* **43**: 1-124.

Wendt, J. (1974): Der Skelettbau aragonitischer Kalkschwämme aus der alpinen Obertrias. *Neues Jahrbuch für Geologie und Paläontologie, Monatshefte* **[1974]** (8): 498-511.

Wendt, J. (1975): Aragonitische Stromatoporen aus der alpinen Obertrias. *Neues Jahrbuch für Geologie und Paläontologie, Abhandlungen* **150** (1): 111-125.

Wendt, J. (1976): Der Skelettbau mesozoischer und rezenter Kalkschwämme. In: Seilacher, A. (ed.): Palökologie. Konstruktionen, Sedimentologie, Diagenese und Vergesellschaftung von Fossilien. Bericht 1970-1975 des Sonderforschungsbereichs 53 Tübingen. *Zentralblatt für Geologie und Paläontologie (II: Paläontologie)* **[1976]** (5/6): 321-325.

Wendt, J. (1979): Development of skeletal formation, microstructure, and mineralogy of rigid calcareous sponges from the Late Palaeozoic to Recent. *Colloques International du Centre National de la Recherche Scientifique Paris* **291**: 449-475.

Wendt, J. (1982): The Cassian Patch Reefs (Lower Carnian,. Southern Alps). *Facies* **6** (1): 185-202.

Wendt, J. (1984): Skeletal and spicular mineralogy, microstructure and diagenesis of coralline calcareous sponges. In: Oliver, W. A.; Sando, W. J.; Cairns, S. D.; Coates, A. G.; Macintyre, I. G.; Bayer, F. M. & Sorauf, J. E. (eds.): Fourth International Symposium on fossil Cnidaria (and Archaeocyathids and Stromatoporoids): *Palaeontographica Americana* **54**: 326-336.

Wendt, J. & Fürsich, F. T. (1980): Facies analysis and paleogeography of the Cassian Formation, Triassic, Southern Alps. *Rivista Italiana di Paleontologia e Stratigrafia* **85** (3/4): 1003-1028.

Zittel, K. A. (1879): Studien über fossile Spongien. Teil 3. *Abhandlungen der Bayerischen Akademie der Wissenschaften, Mathematisch-naturwissenschaftliche Classe* **13**: 91-138.

First report of sponge rhaxes in the Picún Leufú Formation (Tithonian–Berriasian), Neuquén Basin, Argentina

Filiz Afşar[1] *; Jan-Peter Duda[2]; Michael Zeller[3]; Klaas Verwer[4];
Hildegard Westphal[5] & Gregor P. Eberli[3]

[1]Department of Structural Geology and Geodynamics, Geoscience Centre, Georg-August University Göttingen,
Goldschmidtstr. 3, 37077 Göttingen, Germany; Email: filiz.afsar@geo.uni-goettingen.de
[2]Department of Geobiology, Geoscience Centre, Georg-August University Göttingen, Goldschmidtstr. 3, 37077 Göttingen,
Germany; Email: jan-peter.duda@geo.uni-goettingen.de
[3]Comparative Sedimentology Laboratory (CSL), Rosenstiel School of Marine and Atmospheric Science (RSMAS), University
of Miami, Miami, Florida, U.S.A.
[4]Statoil ASA, Bergen, Norway
[5]Leibniz Center for Tropical Marine Ecology (ZMT), Bremen, Germany

* corresponding author

The Picún Leufú Formation (Tithonian-Berriasian, Neuquén Basin, Argentina) comprises mixed carbonate-siliciclastic rocks. Here we report the occurrence of rhaxes (microscleres of the sponge genus *Rhaxella* Hinde, 1890) in the Picún Leufú Formation, which have formerly been misinterpreted as calcispheres. Furthermore, the meaning of the microscleres with respect to sedimentary environments and diagenesis in the Picún Leufú Formation is briefly evaluated. The rhaxes in the Picún Leufú Formation are highly abundant (up to 80–90 % of the components) and occur in various facies ranging from the proximal lagoon to the outer inner ramp, all representing shallow water environments. Diagenetic processes linked to the rhaxes probably have a significant impact on reservoir qualities in different parts of the Picún Leufú Formation.

Introduction

The Neuquén Basin is located on the eastern side of the Andes and is the most important hydrocarbon-producing province in southern South America (Howell et al. 2005) (Fig. 1). The Basin was characterised by a back-arc extension during the late Jurassic to early Cretaceous (e.g., Legarreta & Uliana 1991). Stratigraphical units in the southeastern margin of the basin were deposited on a ramp system (Legarreta & Uliana 1991; Schwarz & Buatois 2012) with a steeper depth gradient in the western part of the basin (Schwarz & Buatois 2012) and are characterised by multiple carbonate, clastic and evaporite intervals (e.g., Uliana & Legarreta 1993; Vergani et al. 1995; Howell et al. 2005).
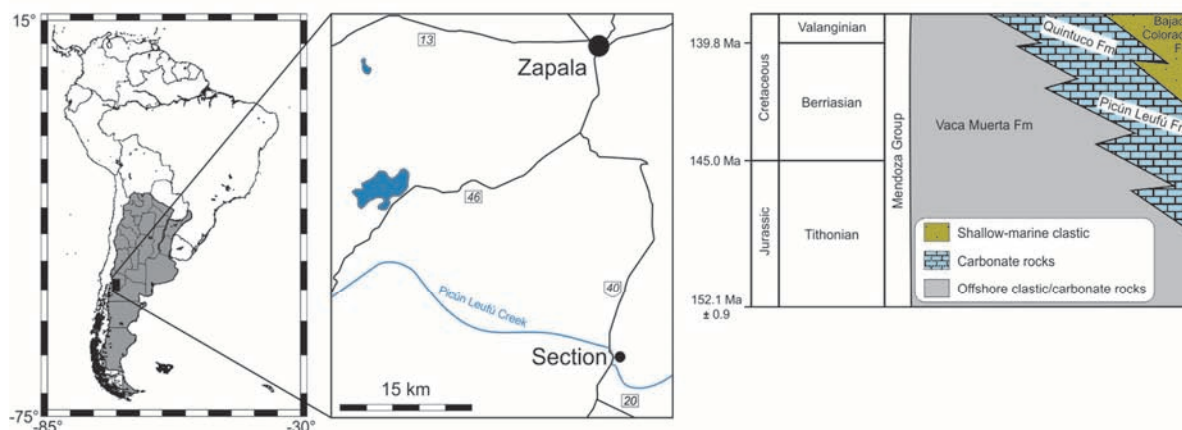
Fig. 1: Location of the study area and stratigraphy of the Tithonian–Valanginian strata in the Neuquén Basin (stratigraphy after Howell et al. 2005, modified).

In the study area the Tithonian to middle Valanginian interval is represented by the two marine lithostratigraphic Formations of the lower Mendoza Group, i.e. (from base to top) the Vaca Muerta Formation and the Picún Leufú Formation (Weaver 1931) (Fig. 1), with the Vaca Muerta Formation being the basinal equivalent to the shelf deposits of the Quintuco and Picún Leufú Formations.

Thin section analysis of mixed siliciclastic-carbonate rocks of the Picún Leufú Formation revealed highly abundant kidney-shaped microscleres ("*rhaxes*": Fig. 3.3., 3.4.), being characteristic for the genus *Rhaxella* Hinde, 1890. However, these components have been interpreted as calcispheres (Armella et al. 2007). Aim of this paper is the reinterpretation of these fossils in the Picún Leufú Formation. Furthermore, the meaning of the rhaxes with respect to sedimentary environments and diagenesis in the Picún Leufú Formation is briefly evaluated.

Methods

One section exposed along the Picún Leufú Creek in the southern part of the Neuquén Basin (Figs. 1–2) was documented and sampled. 75 thin sections were prepared for microfacies analyses. The microfacies was classified based on Dunham (1962). Field emission scanning electron microscopy (Fe-SEM) was conducted on selected samples, using a ZEISS Gemini Supra TM 40. For elemental analyses, an energy dispersive X-ray spectrometer (EDX) Oxford Inca 400 coupled to the SEM was used. The carbonate content was measured using the gas volumetric "Scheibler" method (cf. Kenter et al. 1997). For the identification of mineral phases a Philips PW1800 diffractometer (XRD) equipped with a Cu-tube (kα 1.541, 40 kV, 30 mA) was used. Based on these results, the weight-percent of stable carbonate minerals (dolomite and low-mg calcite) were calculated for each sample. The ratio between calcite and dolomite was calculated based on Royse et al. (1971).

Results and discussion

Rhaxes in the Picún Leufú Formation

Rhaxes observed in the Picún Leufú Formation have spherical and reniform shapes. The taxonomic interpretation of rhaxes is still controversially discussed since reniform shapes are characteristics of both selenaster- and sterraster-type microscleres (e.g., Reitner 1992; Wiedenmayer 1994; Pisera 1997; Rützler 2002; Reid 2004). But, selenasters are characteristic for the family Placospongiidae Gray, 1867 (Rützler 2002) while sterrasters are typical for the Geodiidae Gray, 1867 (Uriz 2002). However, the discussion of this taxonomic problem is not possible based on the investigated material and lies beyond the scope of this paper. For this reason, we will use the term "*rhaxes*" in the following.

The rhaxes observed in the Picún Leufú Formation occur abundantly in some samples (up to 80–90 % of the components: Fig. 3.1). Similar occurrences are e.g. known from the Portlandian of Dorset, were *Rhaxella* spicules make up to 70 % of the rocks (Townson 1975). The length of the spicules of the Picún Leufú Formation ranges between 103–127 µm, while the width ranges between 72–96 µm. This is comparable to the size range of *Rhaxella* spicules in the Portlandian of Dorset, which range between ~50–230 µm in length and ~50–170 µm in width (cf. Haslett 1992) (Fig. 4). The rhaxes in the Picún Leufú Formation are characterised by a clear rim which appears dark under transmitted light and spar cemented inner parts (Fig. 3.3.). EDX measurements show that the rim of the rhaxes is siliceous, while the core is made up of CaCO$_3$ (Fig. 5). In some samples, the rhaxes occur as nuclei of ooids (Fig. 3.4.).

Despite these characteristics, the rhaxes in the Picún Leufú Formation have been misinterpreted as calcispheres (Armella et al. 2007). Calcispheres are characterised by differentiated calcitic walls with or without openings and
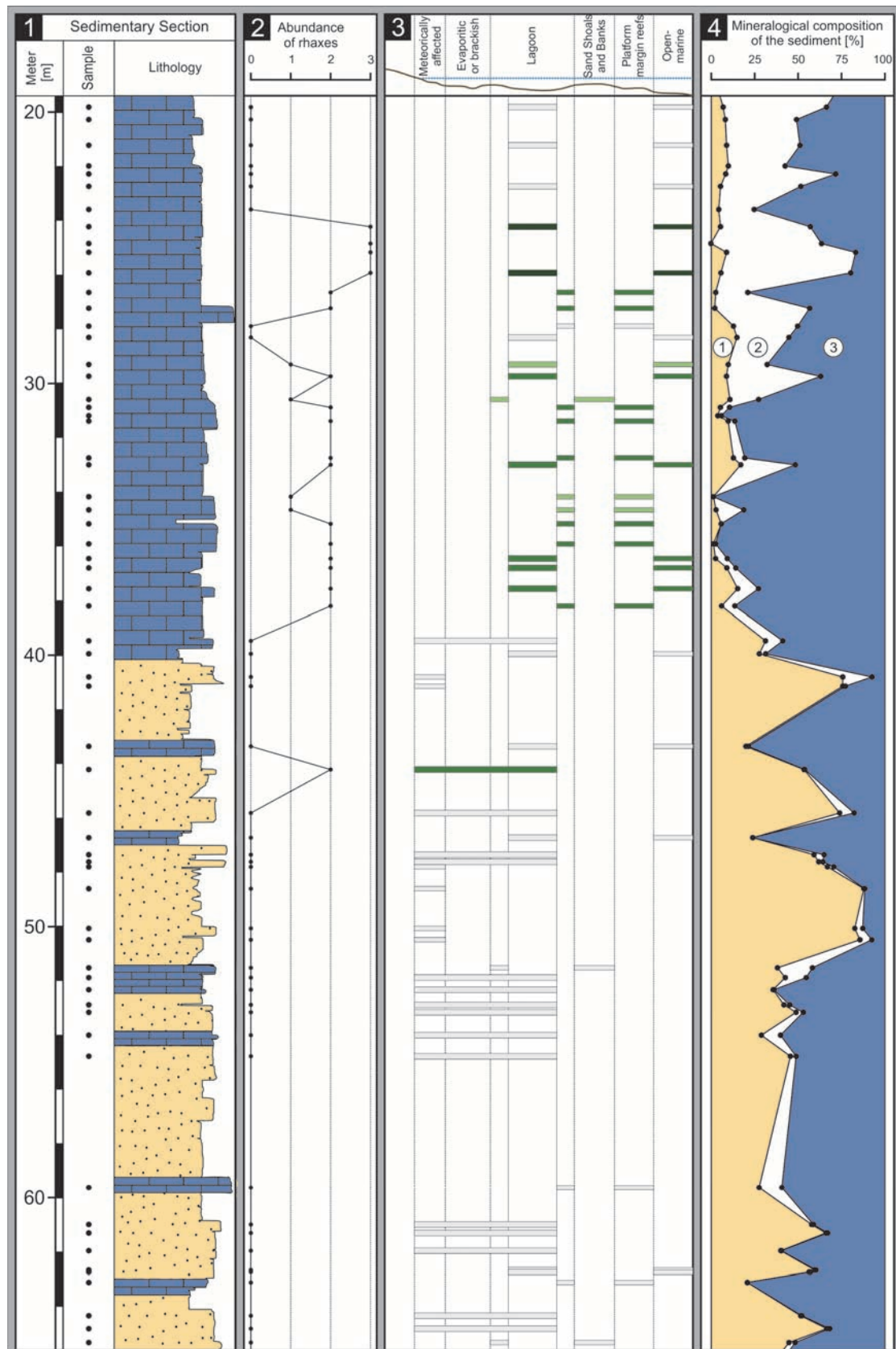
Fig. 2: Sedimentary section. **(A)** Lithology; **(B)** Estimated abundances of rhaxes in thin sections (0 = absent, 1 = rare, 2 = common, 3 = abundant); **(C)** Distribution of rhaxes in different palaeoenvironments of the Picún Leufú Formation, colours of bars indicate the petrographically estimated abundance of rhaxes in the respective facies (white bar = absent, light green bar = rare, middle green bar = common, dark green bar = abundant); **(D)** Mineralogical composition of the sediment (in %; 1 = silica, 2 = dolomite, 3 = low-magnesium calcite).
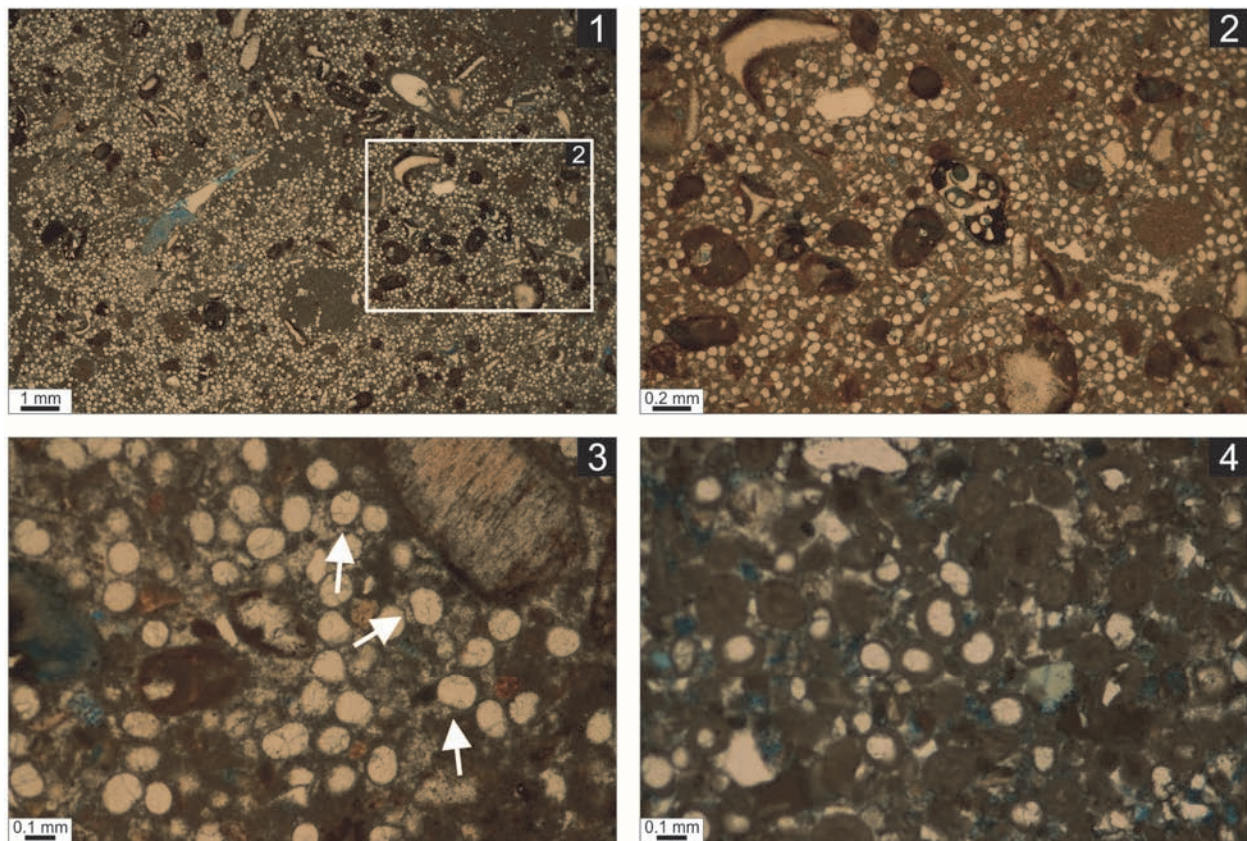
Fig. 3: **(1–4)** Thin sections photographs of sponge rhaxes – *Rhaxella* sp. **(1)** Example of sample with highly abundant rhaxes; **(2)** Detail of (1), note the spherical and reniform shapes of the rhaxes; **(3)** Rhaxes with a clear micritic rim (white arrows); **(4)** Rhaxes as nuclei of ooids. All from the Picún Leufú Fm. (Tithonian–Valanginian), south of Zapala, Neuquén Basin, Argentina.

pores (e.g., Keupp 1991; Flügel 2004; and references therein). But, transmitted light and scanning electron microscopy reveals that the objects do not exhibit typical wall structures of calcispheres (Figs. 3, 5) and, neither openings nor pores have been observed. These findings clearly support the interpretation as sponge rhaxes.

Palaeoenvironment and diagenesis

Sedimentary rocks of the Picún Leufú Formation were deposited on a tidally dominated, mixed carbonate-siliciclastic ramp (Spalletti et al. 2000). The studied interval of the Picún Leufú Formation, which is merely a small part of the whole Formation, can roughly be subdivided into two lithological intervals and range from siliciclastic rocks with intercalated carbonate beds to pure carbonates (Fig. 2). Six facies groups (FGs) have been distinguished (Fig. 2). The observed rhaxes occur in different facies ranging from the proximal lagoon to the outer inner ramp, with pure sandstones in the lower part of the section being the only exception (Fig. 2). And, the number of rhaxes increases with decreasing amounts of siliciclastic material (Fig. 2). This implies that the distribution of *Rhaxella* was strongly affected by impact of siliciclastic material.

In the Portlandian of Dorset, *Rhaxella* throve in low-to medium energy environments of the outer part of the carbonate shelf (i.e., seaward of the high energy ooid shoal), were facies transitionally changed downslope into open marine conditions (Townson 1975; Haslett 1992). This is in good accordance with the situation observed in the Picún Leufú Formation, since the rhaxes-bearing facies clearly represent shallow water environments. And, they are partly also abundant in relative deeper facies like lagoonal or marginal ramp facies (Fig. 2). Moreover, a close spatial association of environments with rhaxes and ooid shoals is evident in the Picún Leufú Formation as well, since rhaxes commonly occur as nuclei of ooids. Since rhaxes within ooids are commonly well-preserved (Fig. 3.4.), it appears that they have not been significantly transported or even reworked before ooid genesis. This observation further underlines the close spatial relationship between environments inhabited by *Rhaxella* and ooid shoals.

However, it appears that deep water depths were critical for *Rhaxella* as well. In the lower Oxfordian of north Yorkshire, the extensive development of *Rhaxella* generally went along with the establishment of shallow water marine conditions (i.e., the transition from Oxford Clay into

the Lower Calcareous Grit; Wright 1983). In case of the Neuquén Basin, the Los Catutos Member (middle Tithonian) of the Vaca Muerta Formation could help to evaluate this problem. In contrast to the Picún Leufú Formation, the Los Catutos Member was situated in the more distal part of the Neuquén Basin, representing deeper open marine parts of the ramp (e.g., Scasso et al. 2005). And, rhaxes also have been described in this Member though they are not abundant as in the Picún Leufú Formation (only 4–20 % rhaxes and radiolarians; Scasso et al. 2005). Furthermore, the preservation seems to be worse than in the Picún Leufú Formation, since the rhaxes are flattened or fragmented, only rarely preserved, and show other diagenetic features which could not be observed in the Picún Leufú Formation (e.g., syntaxial overgrowths; Scasso et al. 2005). And, they can easily be confused with spumellarian radiolarians (Scasso et al. 2005*)*, implying that the preservation of the rhaxes is not very good. For these reasons it appears much more probable that environments inhabited by *Rhaxella* were closer to the ones represented by the Picún Leufú Formation than to the environments represented by the Los Catutos Member.

This raises the question whether the shallow marine Picún Leufú Formation even directly represents the environment inhabited by *Rhaxella*. In some cases it is assumed that *Rhaxella* lived epifaunally attached to a fine sand substrate supported by a lime mud matrix (Townson 1975; Haslett 1992). Wholly preserved body fossils of *Rhaxella* have not been found in the Picún Leufú Formation so far. And, the rhaxes are not restricted to a muddy to fine sandy facies, but also occur within different types of coarser grained grainstones and packstones. Furthermore, the preservation of the rhaxes ranges from clearly recognisable (i.e., with well-defined silicified rims) to poorly recognisable shapes (i.e., with strongly altered rims). In sum this implies that the observed rhaxes are not entirely autochthonous, and that the environments inhabited by *Rhaxella* are not directly represented by the sedimentary facies of the Picún Leufú Formation. Thus, the respective environments have been very close to the ones represented by the Picún Leufú Formation or may just have been constantly reworked. However, both would imply that the environments inhabited by *Rhaxella* may have not been stable over a relative long time once they had been established, but rather changed dynamically on short term.

The preservation style of the investigated rhaxes has implications for diagenetic processes in the Picún Leufú Formation, particularly with regard to desilification- and silification-processes. In the Portlandian of Dorset (Portland Limestone Formation) e.g., spicules of *Rhaxella* are usually only preserved as casts and moulds, with the silica replaced by calcite (Townson 1975). The dissolution of the silica gives rise to thinly bedded chert horizons, which preserved these spicules in their original siliceous form (Wilson 1966). Similar processes are described for the Lower Calcareous Grit, were thin beds of cherts were sec-

ondarily formed because of *Rhaxella* (Powell 2010). This is in line with a proposed relation between presence of rhaxes and diagenetic quartz cementation during shallow burial, being important in hydrocarbon provinces with highly variable reservoir qualities such as e.g. the South Viking Graben (Williams et al. 1985; Hendry & Trewin 1995; Maast et al. 2011). Thus, the occurrence and distribution of rhaxes could have implications for reservoir qualities in different settings of the Picún Leufú Formation.
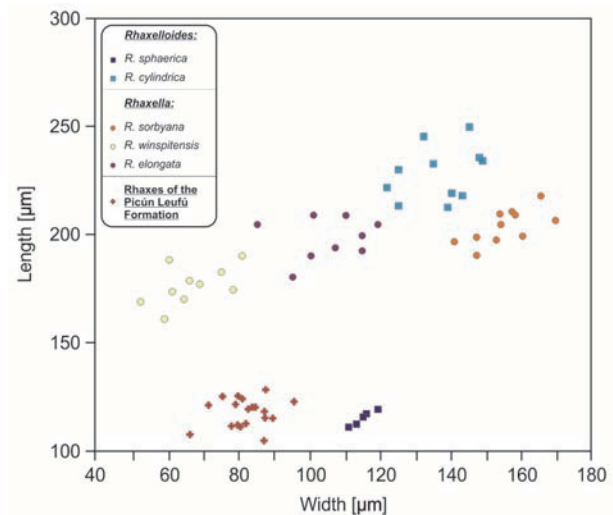
Fig. 4: Dimension of rhaxes in the Picún Leufú Formation compared to spicules of *Rhaxella sorbyana*, *R. winspitensis*, *R. elongata*, *Rhaxelloides sphaerica* and *R. cylindrica* (after Haslett 1992, modified). Note that the rhaxes in the Picún Leufú Formation are smaller than those of other species.

Conclusions

Rhaxes in the Picún Leufú Formation have formerly been misinterpreted as calcispheres (Armella et al. 2007). They are locally highly abundant in some samples (up to 80–90 % of the components). Dimensions of the rhaxes are comparable to the size range of *Rhaxella* spicules in the Portlandian of Dorset, while they are smaller than ones in the Ardassie limestone of Brora and in the Alness Spiculite of the Moray Firth (both Oxfordian Stage). Rhaxes in the Picún Leufú Formation occur in a wide range of facies ranging from the proximal lagoon to the outer inner ramp, all clearly representing shallow water environments. Although they are not originally preserved, they are commonly clearly recognisable due to the presence of a well-defined silicified rim. The rim could be explained by the depositional and diagenetic environments in which early diagenetic solution and re-precipitation of silica was temporarily favoured. This could be important with respect to reservoir qualities in different parts of the Picún Leufú Formation.
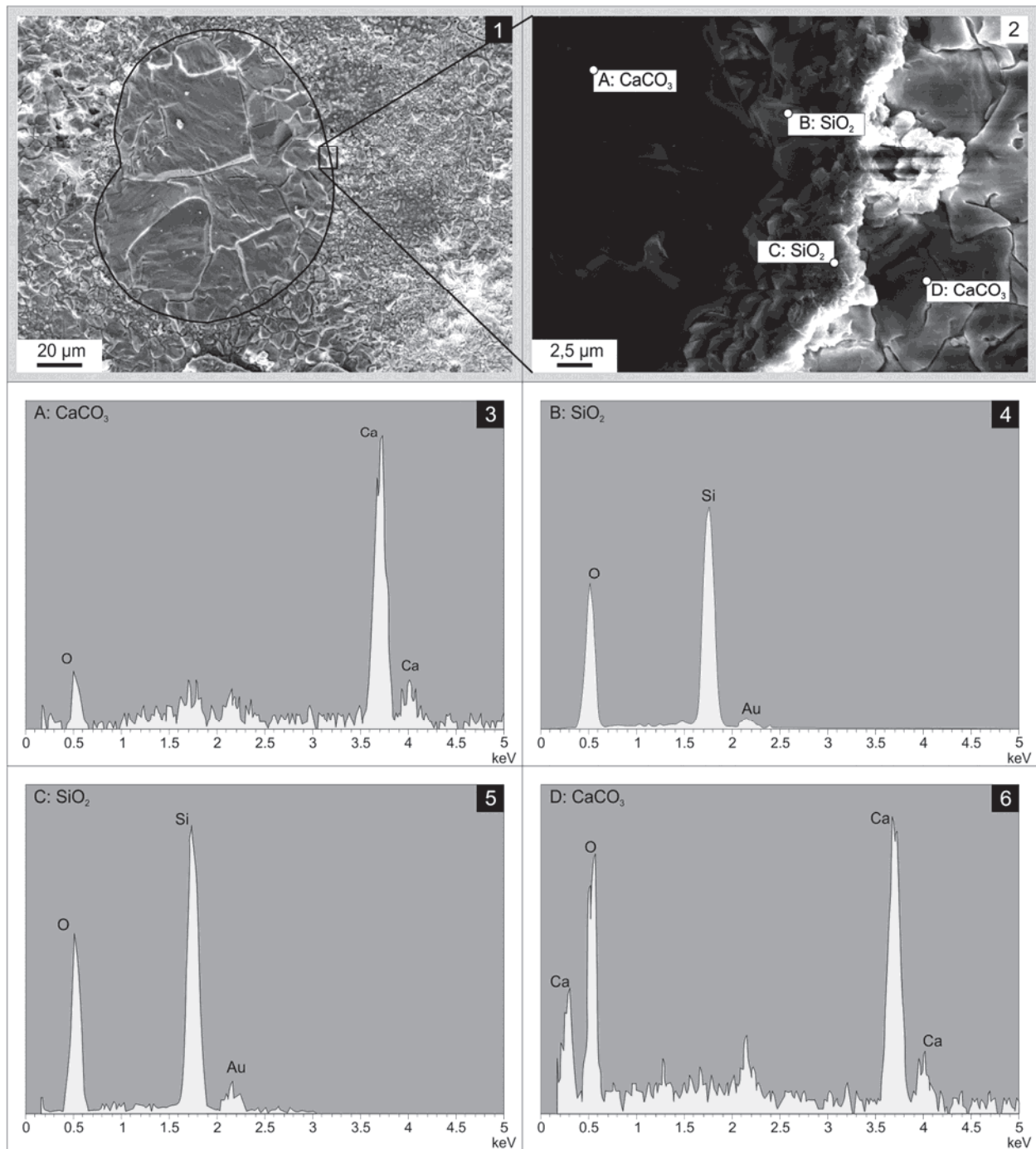
Fig. 5: **(1–6)** SEM pictures and respective EDX data of a *Rhaxella* rhax from the Picún Leufú Formation. **(1)** Rhax with clear reniform shape; **(2)** Detail of (1), the silicified rim is clearly distinguishable from the calcite because of etching; **(3–6)** EDX data [see (2) for positions]; CaCO₃ spar cemented inner part of the rhax]; **(4–5)** SiO₂ rim of the same rhax; **(6)** CaCO₃ matrix surrounding the rhax.

Acknowledgements

References

Armella, C.; Cabaleri, N. & Leanza, H. A. (2007): Tidally dominated, rimmed-shelf facies of the Picún Leufú Formation (Jurassic/Cretaceous boundary) in southwest Gondwana, Neuquén Basin, Argentina. *Cretaceous Research* **28** (6): 961-979. http://dx.doi.org/10.1016/j.cretres.2007.01.001

Dunham, R. J. (1962): Classification of carbonate rocks according to depositional texture. In: Ham, W. E. (ed.): Classification of carbonate rocks. *The American Association of Petroleum Geologists, Memoirs* **1**: 108-171.

Flügel, E. (2004): *Microfacies of Carbonate Rocks: Analysis, Interpretation and Application.* Berlin etc. (Springer): xix + 976 pp.

Gray, J. E. (1867): Notes on the Arrangement of Sponges, with the Descriptions of some New Genera. *Proceedings of the Zoological Society of London* **35** (2): 492-558.

Haslett, S. K. (1992): Rhaxellid sponge microscleres from the Portlandian of Dorset, UK. *Geological Journal* **27** (4): 339-347. http://dx.doi.org/10.1002/gj.3350270404

Hendry, J. P. & Trewin, N. H. (1995): Authigenic quartz microfabrics in Cretaceous turbidites: evidence for silica transformation processes in sandstones. *Journal of Sedimentary Research (A: Sedimentary Petrology and Processes)* **65** (2): 380-392. http://dx.doi.org/10.1306/D42680CC-2B26-11D7-8648000102C1865D

Hinde, G. J. (1890): On a new Genus of Siliceous Sponges from the Lower Calcareous Grit of Yorkshire. *Quarterly Journal of the Geological Society* **46** (1-4): 54-61. http://dx.doi.org/10.1144/GSL.JGS.1890.046.01-04.06

Howell, J. A.; Schwarz, E.; Spalletti, L. A. & Veiga, G. D. (2005): The Neuquén Basin: an overview. In: Veiga, G. D.; Spalletti, L. A.; Howell, J. A. & Schwarz, E. (eds.): The Neuquén Basin, Argentina: A Case Study in Sequence Stratigraphy and Basin Dynamics. *Geological Society London Special Publications* **252**: 1-14.

Kenter, J. A. M.; Podladchikov, F. F.; Reinders, M.; Van der Gaast, S. J.; Fouke, B. W. & Sonnenfeld, M. D. (1997): Parameters controlling sonic velocities in a mixed carbonate-siliciclastics Permian shelf-margin (upper San Andres formation, Last Chance Canyon, New Mexico). *Geophysics* **62** (2): 505-520. http://dx.doi.org/10.1190/1.1444161

Keupp, H. (1991): Fossil Calcareous Dinoflagellate Cysts. In: Riding, R. (ed.): *Calcareous Algae and Stromatolites.* Berlin & Heidelberg (Springer): 267-286.

Legarreta, L. & Uliana, M. A. (1991): Jurassic–Cretaceous marine oscillations and geometry of back-arc basin fill, central Argentine Andes. In: Macdonald, D. I. M. (ed.): Sedimentation, Tectonics, and Eustasy. Sea-level Changes at Active Margins. *Special Publication of the International Association of Sedimentologists* **12**: 429-450.

Maast, T. E.; Jahren, J. & Bjørlykke, K. (2011): Diagenetic controls on reservoir quality in Middle to Upper Jurassic sandstones in the South Viking Graben, North Sea. *AAPG Bulletin* **95** (11): 1937-1958. http://dx.doi.org/10.1306/03071110122

Pisera, A. (1997): Upper Jurassic Siliceous Sponges from the Swabian Alb: Taxonomy and Paleoecology. *Palaeontologia Polonica* **57**: 3-216.

Powell, J. H. (2010): Jurassic sedimentation in the Cleveland Basin: a review. *Proceedings of the Yorkshire Geological Society* **58** (1): 21-72. http://dx.doi.org/10.1144/pygs.58.1.278

Reid, R. E. H. (2004): Mesozoic and Cenozoic Choristid Demosponges. In: Finks, R.; Reid, R. E. H. & Rigby, J. K.: Porifera (Demospongea, Hexactinellida, Heteractinida, Calcarea). *Treatise on Invertebrate Paleontology, Part E: Porifera (Revised)* **3**. Boulder, Colo. (The Geological Society of America) & Lawrence, Kans. (The University of Kansas): 175-198.

Reitner, J. (1992): 'Coralline Spongien'. Der Versuch einer phylogenetisch-taxonomischen Analyse. *Berliner Geowissenschaftliche Abhandlungen (E: Paläobiologie)* **1**: 1-352.

Royse, C. F.; Wadell, J. S. & Petersen, L. E. (1971): X-ray Determination of Calcite-Dolomite: an Evaluation. *Journal of Sedimentary Petrology* **41** (2): 483-488. http://dx.doi.org/10.1306/74D722A7-2B21-11D7-8648000102C1865D

Rützler, K. (2002): Family Placospongiidae Gray, 1867. In: Hooper, J. N. A. & Soest, R. W. M. van (eds.): *Systema Porifera: A Guide to the Classification of Sponges.* New York, N.Y. (Kluwer Academic/Plenum Publishers): 196-200.

Scasso, R. A.; Alonso, M. S.; Lanés, S.; Villar, H. J. & Laffitte, G. (2005): Geochemistry and petrology of a Middle Tithonian limestone-marl rhythmite in the Neuquén Basin, Argentina: depositional and burial history. In: Veiga, G. D.; Spalletti, L. A.; Howell, J. A. & Schwarz, E. (eds.): The Neuquén Basin, Argentina: A Case Study in Sequence Stratigraphy and Basin Dynamics. *Geological Society London Special Publications* **252**: 207-229.

Schwarz, E. & Buatois, L. A. (2012): Substrate-controlled ichnofacies along a marine sequence boundary: The Intra-Valanginian Discontinuity in central Neuquén Basin (Argentina). *Sedimentary Geology* **277-278**: 72-87. http://dx.doi.org/10.1016/j.sedgeo.2012.07.014

Spalletti, L. A.; Franzese, J. R.; Matheos, S. D. & Schwarz E. (2000): Sequence stratigraphy of a tidally dominated carbonate–siliciclastic ramp; the Tithonian–Early Berriasian of the Southern Neuquén Basin, Argentina. *Journal of the Geological Society*, London **157** (2): 433-446. http://dx.doi.org/10.1144/jgs.157.2.433

Townson, W. G. (1975): Lithostratigraphy and deposition of the type Portlandian. *Journal of the Geological Society* **131** (6): 619-638. http://dx.doi.org/10.1144/gsjgs.131.6.0619

Uliana, M. A. & Legarreta, L. (1993): Hydrocarbons habitat in a Triassic-to-Cretaceous sub-Andean setting: Neuquén Basin, Argentina. *Journal of Petroleum Geology* **16** (4): 397-420. http://dx.doi.org/10.1111/j.1747-5457.1993.tb00350.x

Uriz, M. J. (2002): Family Geodiidae Gray, 1867. In: Hooper, J. N. A. & Soest, R. W. M. van (eds.): *Systema Porifera: A Guide to the Classification of Sponges.* New York, N.Y. (Kluwer Academic/Plenum Publishers): 134-140.

Vergani, G. D.; Tankard, A. J.; Belotti, H. J. & Welsink, H. J. (1995): Tectonic Evolution and Paleogeography of the Neuquén Basin, Argentina. In: Tankard, A. J.; Suárez S., R. & Welsink, H. J. (eds.): Petroleum Basins of South America. *American Association of Petroleum Geologists Memoir* **62**: 383-402.

Weaver, C. E. (1931): Paleontology of the Jurassic and Cretaceous of West Central Argentina. *Memoirs of the University of Washington* **1**: 1-469.

Wiedenmayer, F. (1994): Contributions to the knowledge of post-Palaeozoic neritic and archibenthal sponges (Porifera). The stratigraphic record, ecology and global distribution of intermediate and higher taxa. *Schweizerische Paläontologische Abhandlungen* **116**: 1-147.

Williams, L. A.; Parks, G. A. & Crerar, D. A. (1985): Silica diagenesis, I. Solubility controls. *Journal of Sedimentary Research* **55** (3): 301-311. http://dx.doi.org/10.1306/212F86AC-2B24-11D7-8648000102C1865D

Wilson, R. C. L. (1966): Silica diagenesis in Upper Jurassic Limestones of Southern England. *Journal of Sedimentary Petrology* **36** (4): 1036-1049. http://dx.doi.org/10.1306/74D715F0-2B21-11D7-8648000102C1865D

Wright, J. K. (1983): The Lower Oxfordian (Upper Jurassic) of North Yorkshire. *Proceedings of the Yorkshire Geological Society* **44** (3): 249-281. http://dx.doi.org/10.1144/pygs.44.3.249

The second fossil *Hyalonema* species (Porifera: Hexactinellida), from the Late Cretaceous Arnager limestone, Bornholm, Denmark

Dorte Janussen[1]

[1]*Forschungsinstitut und Naturmuseum Senckenberg, Senckenberganlage 25, 60325 Frankfurt am Main, Germany; Email: dorte.janussen@senckenberg.de*

The palaeontological history of the hexactinellid sub-class Amphidiscophora is little known and has been documented mainly by isolated spicules found in sediments. So far, only a few definite fossil records of rather complete body fossils of amphidiscophoran sponges, two from the Carboniferous and one from Late Cretaceous, have been published. A new finding of an entirely preserved fossil sponge described herein as *Hyalonema vetteri* sp. nov. in the Arnager Limestone on the isle Bornholm (Denmark) confirms the status of this lagerstätte as a unique window in the fossil record of the Porifera. The new species furthermore extend the record of the modern genus *Hyalonema* and family Hyalonematidae from Campanian back to the Coniacian.

Introduction

Hexactinellida (glass sponges) are Porifera with triaxial siliceous spicules, basically hexactins. Their fossil record goes back to the earliest Cambrian (Steiner et al. 1993; Reitner & Mehl 1995), or even late Proterozoic (Gehling & Rigby 1996), and their blossom time was in the late Mesozoic, especially Cretaceous, where the modern types of skeletal constructions radiated into the stem lineages of recent genera (Mehl 1992; Mehl-Janussen 1999; Dohrmann et al. 2013). Some hexactinellid taxa are characterised by rigid (dictyonal) skeletons of fused hexactins, or lychniscs (latern-like hexactine spicules), which are well represented in the fossil record. Together with "lithistid" demosponges they acted as important bioconstructors, e.g., in Late Jurassic siliceous sponge reefs (Krautter 2002). Non-rigid hexactinellida, today comprising the subclass Amphidiscophora and the order Lyssacinosida, are the oldest hexactinellids in the fossil record. Lyssacinosan sponges have been recorded with a worldwide distribution and in great numbers throughout the Paleozoic (e.g., Walcott 1920; Finks 1960; Rigby 1983, 1986; Rigby & Gosney, 1983). However, since the old sponge fossils with few exceptions are very different from recent sponges, furthermore they are normally found without any of the taxonomically important microscleres, the attribution of Pal-

aeozoic hexactinellids to recent taxa is normally not possible. In the Mesozoic record, we still have the problem of lacking microscleres in the fossil sponges, but since many of these body fossils are morphologically quite similar to recent representatives, a taxonomical attribution to recent sponge families, or even genera, is sometimes possible (e.g., Schrammen 1912; Salomon 1990; Mehl 1992).

The Mesozoic record of fossil nonrigid taxon Lyssacinosida is comparably poor. All together, about 28 more or less certain lyssacinosidan genera have been described mostly from the Late Cretaceous (e.g., Bowerbank 1869a, 1869b; Schrammen 1912; Rigby & Gosney 1983; Brückner 2006). The fact that the non-rigid hexactinellids are rarely found in Mesozoic strata is mainly due to their low preservation potiential. In most cases, after death of the sponge and decay of its soft body, the non-fused spicules of the skeleton will fall apart and be found only as isolated spicules. Complete sponge fossils of the sub-class Amphidiscophora are even more rare. Although isolated amphidiscs have been found in Silurian and younger sediments (Mostler 1986), reliable body fossils of Amphodiscophora are extremely rare and have been found only at a few localities. Completely preserved amphidiscophoran body fossils, with amphi- and hemidisc microscleres *in situ*, are known so far only from the Carboniferous of the Ural (Librovič 1929; Kling & Reif 1969). An almost complete sponge fossil from the Campanian of Münsterländer Basin (Germany) was described according to its outer morphology and megascleres as *Hyalonema cretacea* Mehl & Hauschke, 1995. Also from the Late Cretaceous some isolated root tufts have been recorded and attributed to *Hyalonema* sp. (Mehl 1992).

The Coniacian Arnager formation crops out as an about 150 m long and 4 m thick section at the southern coast of the Danish island of Bornholm, which is located SW of Sweden (for location map and further details, e.g., Brückner & Janussen 2005). The entire formation is between 12 and 20 m thick and belongs to a horst platform within the Fennoscandian Border Zone (Gravesen et al. 1982; Jørgart & Nielsen 1995). Several publications deal with the stratigraphy and facies of the Arnager Limestone Formation (Bromley 1979; Christensen 1984; Tröger & Christensen 1991), and the first palaeoecological interpretation of the sponge-rich limestone was given by Noe-Nygaard & Surlyk (1985), who considered it to be fossil sponge mounds. However, Mehl (1992) argued for a turbiditic origin of the Arnager limestone. The section at Arnager Pynt is known for its exceptionally preserved fossils, which were first described (Brongniart 1828) as plants and were later re-interpreted and described as hexactinellid lyssacinosidan sponges (Ravn 1918; Brückner & Janussen 2005; Brückner 2006), including three uncertain amphidiscophoran genera and species (Mehl 1992).

Material and Methods

The sponge fossil described in this paper was found on fallen down blocks from the Arnager limestone formation by Felix Vetter (Frankfurt a. M.) and given to the author for identification. It was studied and photo documented by light microscopy and compared with other described, complete *Hyalonema* species from Late Cretaceous (Mehl & Hauschke 1995). Spicule measurements, photographs and drawings were made using a Zeiss stereomicroscope with photo-equipment and ocular scale. The other specimen is deposited in Naturmuseum Senckenberg, Palaeobiology department (SMF), electronically catalogued (SESAM) and online available.

Systematic palaeontology

Class **Hexactinellida** Schmidt, 1870
Subclass **Amphidiscophora** Schulze, 1886
Order **Amphidiscosida** Schrammen, 1924

Family **Hyalonematidae** Gray, 1857

Genus ***Hyalonema*** Gray, 1832

Type species. – *Hyalonema sieboldi* Gray, 1832.

Diagnosis. – "Hyalonematidae with mainly bell-like or ovoid body; the everted (when known) atrialia do not form notable rise; basalia are gathered in a compact twisted (in grown specimens) tuft, being represented by toothed anchors" [from Tabachnick & Menshenina 2002].

Hyalonema vetteri sp. nov.
Figs. 1–2

Material. – One specimen, the holotype, SMF XXVI 528.

Type locality. – Near Arnager, Isle of Bornholm, Denmark.

Type horizon. – Arnager formation (Cretaceous: Coniacian).

Etymology. – This species is named in honour of Felix Vetter, finder of the holotype specimen.

Diagnosis. – *Hyalonema* with a cup- or calyx-formed body and unsegmented atrial cavity. Slender stalk of long thin root spicules twisted in clockwise direction. Body megascleres mainly diactins, also some hexactins/pentactins/stauractins and tauactins. Microscleres unknown.

Description. – The holotype is a small sponge, 58 mm in total length and 16 mm maximal width formed as a cup or calyx attached to a long stalk of basal spicules. Length of the stalk is 45 mm, but because it is somewhat curved, it may have been slightly longer in live position. The stalk proceeds 3–5 mm into basal part of the body. Its distal end-

ing is broken off and no basal anchors were observed. Its thickness is 5 mm at the top, narrowing to 4 mm in the middle, expanding to 6 mm towards the base. The calyx-shaped body is 15 mm high and 16 mm in width with a large shallow atrial cavity (osculum), 11 mm wide and about 8 mm deep.

Spicules: Only the long stalk spicules are well preserved, they measure about 50 µm in thickness. Because the distal ends are broken off, their length cannot be measured, but the spicules seem to continue along the entire length of the stalk (at least 45 mm), and they proceed ~3 mm into the basal part of the sponge body. Many diactins, mostly fragmental, are observed throughout the sponge body, especially near the base, and forming an indistinct marginal layer parallel to the surface. They are extremely variable, probably partly due to secondary diagenetic influence, and measure 0.5–2.0 mm in length and 50–100 µm in thickness. Near the osculum some larger diactins seem to protrude beyond the body wall by 0.5–1.0 mm. Further spicule types, recognisable only as indistinct imprints, are stauractins (or maybe obscure pentactins or hexactins) and few tauactins, ray lengths 150–250 µm, thickness ~30 µm. Because of the very incomplete fragmented condition of recognisable spicular structures, statistical spicule measurements were not possible.

Occurrence. – Hitherto known only from the type locality and type stratum.

Discussion and conclusions

This species is attributed to genus *Hyalonema*, in spite of the lack of preserved microscleres (as it is the normal case in fossil sponges), because of its very typical shape with a twisted stalk of long root spicules bearing a cup-formed body with a wide central atrial cavity (osculum). Its main skeleton of primarily diactine primary spicules corresponds to the definition of the recent genus *Hyalonema* Tabachnick & Menshenina 2002). Apart from the distance in geographical location and stratigraphical age, it differs from the only so far described fossil *Hyalonema* species, *H. cretacea* Mehl & Hauschke, 1995 from Campanian of Münsterland Basin (Germany), by its skeleton of the main body consisting of diactine primary spicules, whereas in *H. cretacea* stauractins and diactins were observed in equal proportions. *H. vetteri* smaller in size of both the body and spicules, the body form is roundish and possesses a thinner and more slender stalk of long root spicules, clearly clockwise twisted (not so in *H. cretacea*). Especially the root tuft spicules are much thinner, they measure only about 30 µm, whereas in *H. cretacea* they measure about 100 µm in diameter.

The recent genus *Hyalonema* is a deep-sea sponge taxon, as characteristic for the Hexactinellida in general, with worldwide distribution (Tabachnick & Menshenina 2002).

Fig. 1: *Hyalonema vetteri* sp. nov., holotype, SMF XXVI 528, from the Coniacian of Bornholm, Denmark. The stalk of long monaxone spicules proceeds well into the basal part of the clup-shaped body.

With its flexible long twisted and very resistant stalk of twisted anchoring root spicules, it is well adapted to life on soft bottoms in deep water, also in environments with strong current regimes and increased sedimentation rates. According to Noe-Nygaard & Surlyk (1985), the Arnager limestone is interpreted as fossil sponge mounds with the sponges preserved *in situ*. However, this interpretation is not consistent with the fast that mainly soft-bodied lyssacinosan and amphidiscophoran Hexactinellida are found in the Arnager chalk, because their fossil preservation requires a rapid embedding of the living sponges, e.g., by turbiditic sedimentation events (e.g., Mehl 1992; Mehl & Hauschke 1995), which rather corresponds to a lower slope than to a carbonate platform palaeoenvironment. Detailed sedimentological studies of the Arnager Pynt section later confirmed the interpretation of the Arnager Limestone as deposits of distal mud turbidites (Brückner 2006).
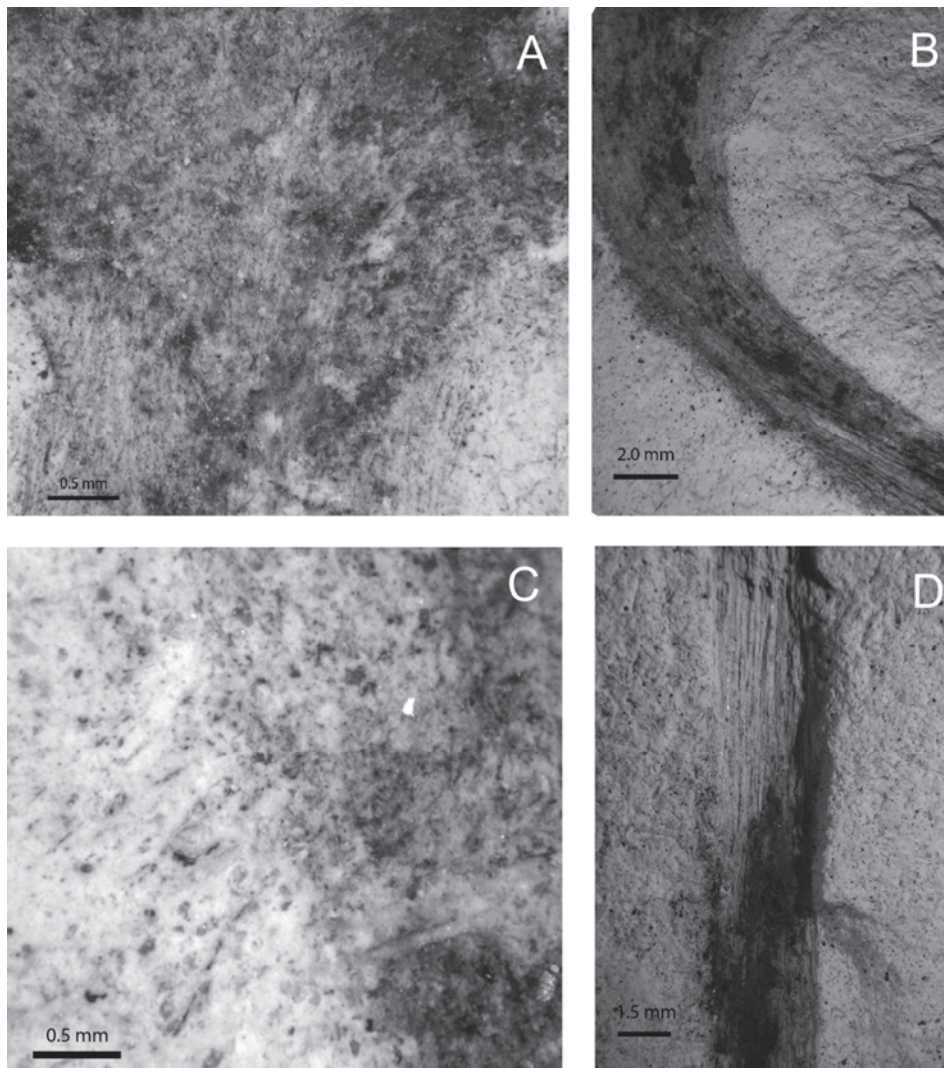
Fig. 2: **(A–D)** *Hyalonema vetteri* sp. nov., holotype, SMF XXVI 528 from the Coniacian of Bornholm, Denmark. **(A)** Detail of the basal part of the body; **(B)** Upper part of the stalk which is twisted in the clockwise direction; **(C)** Outer margin of the sponge body with remains of radially arranged diactins protruding beyond the dermal surface; **(D)** Lower part of the dense root tuft consisting of long, thin, monaxonal spicules.

The second finding in the fossil record of an almost complete *Hyalonema* specimen confirms this interpretation, as the body construction of the Hyalonematidae is extremely fragile and requires special conditions for preservation, including rapid embedding in live position. On the other hand, the rope-like stalks of long twisted monaxone spicules is fairly robust, and isolated root tufts are often caught in trawls, or by longline-fisheries, whereas complete *Hyalonama* specimens are rather rare, even in areas where the genus is common (such as the Japanese Sagami Bay, pers. obs.). Thus it is not unexpected that *Hyalonema* tufts have been reported from some sponge-rich localities, such as the Arnager Limestone (Mehl 1992), rather it is surprising that only few such occurrences are known from literature. However, it seems that such unspectacular fossils are not noticed or neglected by many collectors, misinterpreted as worthless plant-fossils fragments, and therefore not present in most of the Late Cretaceous sponge collections and also not mentioned in the corresponding literature (e.g., Schrammen 1912). The author of this article is aware of *Hyalonema* stalks, or stalk-fragments, from the Campanian of Höver, where they are probably even common (Janussen in prep.).

Thus, it can be expected that further fossil occurrences of *Hyalonema*, as well as other amphidiscophoran Hexactinellida will be discovered, to the degree that these become known and valued fossils both for science and for the amateur collectors.

Acknowledgements

References

Bowerbank, J. S. (1869a): A Monograph of the Siliceo-fibrous Sponges. *Proceedings of the Zoological Society of London* **37** (1): 66-100. http://dx.doi.org/10.1111/j.1469-7998.1869.tb07296.x

Bowerbank, J. S. (1869b): A Monograph of the Siliceo-fibrous Sponges. – Part II. *Proceedings of the Zoological Society of London* **37** (2): 323-351. http://dx.doi.org/10.1111/j.1469-7998.1869.tb07334.x

Bromley, R. (1979): Field meeting in southern Scandinavia, 18.-28. September 1975. *Proceedings of the Geologists' Association* **90** (4): 181-191. http://dx.doi.org/10.1016/S0016-7878(79)80004-8

Brongniart, A. (1828): *Histoire des Végétaux fossiles, ou recherches botaniques et géologiques sur les végétaux renfermés dans les diverses couches du globe.* Paris & Amsterdam (G. Dufour & d'Ocagne): 488 pp.

Brückner, A. (2006): Taxonomy and paleoecology of lyssacinosan Hexactinellida from the Upper Cretaceous (Coniacian) of Bornholm, Denmark, in comparison with other Postpaleozoic representatives. *Abhandlungen der Senckenbergischen Naturforschenden Gesellschaft* **564**: 1-103.

Brückner, A. & Janussen, D. (2005): The first entirely preserved fossil sponge species of the genus *Rossella* (Hexactinellida) from the Upper Cretaceous of Bornholm, Denmark. *Journal of Paleontology* **79** (1): 21-28. http://dx.doi.org/10.1666/0022-3360(2005)079<0021:RBNSTF>2.0.CO;2

Christensen, W. K. (1984): The Albian to Maastrichtian of Southern Sweden and Bornholm, Denmark: a review. *Cretaceous Research* **5** (4): 313-327. http://dx.doi.org/10.1016/S0195-6671(84)80027-0

Dohrmann, M.; Vargas, S.; Janussen, D.; Collins, A. G. & Wörheide, G. (2013): Molecular paleobiology of early-branching animals: integrating DNA and fossils elucidates the evolutionary history of hexactinellid sponges. *Paleobiology* **39** (1): 95-108. http://dx.doi.org/10.1666/0094-8373-39.1.95

Finks, R. M. (1960): Late Paleozoic sponge faunas of the Texas region. The siliceous sponges. *Bulletin of the American Museum of Natural History* **120** (1): 1-160.

Gehling, J. G. & Rigby, J. K. (1996): Long expected sponges from the Neoproterozoic Ediacara Fauna of South Australia. *Journal of Paleontology* **70** (2): 185-195.

Gravesen, P.; Rolle, F. & Surlyk, F. (1982): Lithostratigraphy and sedimentary evolution of the Triassic, Jurassic and Lower Cretaceous of Bornholm, Denmark. *Geological Survey of Denmark (Series B)* **7**: 1-51.

Gray, J. E. (1832): *Synopsis of the contents of the British Museum, 27th ed.* London (Woodfall): 212 pp.

Gray, J. E. (1857): Synopsis of the Families and Genera of Axiferous Zoophytes or Barked Corals. *Proceedings of the Zoological Society of London* **25**: 278-294. http://dx.doi.org/10.1111/j.1096-3642.1857.tb01242.x

Jørgart, T. & Nielsen, A. T. (1995): Geology of the island Bornholm (Denmark). In: Katzung, G.; Hüneke, H. & Obst, K. (eds.): Geologie des südlichen Ostseeraumes: Umwelt und Geologie. Exkursionsführer zur 147. Hauptversammlung der Geologischen Gesellschaft. *Terra Nostra* **95/6**: 115-135.

Kling, S. A. & Reif, W. E. (1969): The paleozoic history of amphidisc and hemidisc sponges: new evidence from the Carboniferous of Uruguay. *Journal of Paleontology* **43** (6): 1429-1434.

Krautter, M. (2002): Fossil Hexactinellida: an overview. In: Hooper, J. N. A. & Soest, R. W. M. van (eds.): *Systema Porifera. A Guide to the Classification of Sponges.* New York, N.Y. (Kluwer Academic/Plenum Publishers): 1211-1223.

[Либрович, Л. С.] Librovič, L. S. (1929): *Uralonema Karpinskii* nov. gen., nov. sp. и другие кремневые губки из каменноугольных отложений восточного склона Урала. [*Uralonema Karpinskii* nov. gen., nov. sp. i drugie kremnevye gubki iz kamennougol'nyh otloženij vostočnogo sklona Urala; *Uralonema Karpinskii* nov. gen., nov. sp. and other silicispongia from Car-

boniferous strata of the eastern slope of the Ural mountains]. *Труды Геологического комитета (новая серия) [Trudy Geologičeskogo komiteta (novaā seriā)]* **179**: 1-57.

Mehl, D. (1992): Die Entwicklung der Hexactinellida seit dem Mesozoikum. Paläobiologie, Phylogenie und Evolutionsökologie. *Berliner geowissenschaftliche Abhandlungen (E: Paläobiologie)* **2**: 1-164.

Mehl, D. & Hauschke, N. (1995): *Hyalonema cretacea* n. sp., first bodily preserved Amphidiscophora (Porifera, Hexactinellida) from the Mesozoic. *Geologie und Paläontologie in Westfalen* **38**: 89-97.

Mehl-Janussen, D. 1999: Die frühe Evolution der Porifera. *Münchner Geowissenschaftliche Abhandlungen (A: Geologie und Paläontologie)* **37**: 1-72.

Mostler, H. (1986): Beitrag zur stratigraphischen Verbreitung und phylogenetischen Stellung der Amphidiscophora und Hexasterophora (Hexactinellida, Porifera). *Mitteilungen der Österreichischen Geologischen Gesellschaft* **78**: 319-359.

Noe-Nygaard, N. & Surlyk, F. (1985): Mound bedding in a sponge-rich Coniacian chalk, Bornholm, Denmark. *Bulletin of the Geological Society of Denmark* **34**: 237-249.

Ravn, J. P. J. (1918): Kridtaflejringerne paa Bornholms sydvestkyst og deres fauna. II. Turonet. *Danmarks Geologiske Undersøgelse (II Række)* **31**: 7-37.

Reitner, J. & Mehl, D. (1995): Early Paleozoic diversification of sponges: New data and evidences. *Geologisch-Paläontologische Mitteilungen Innsbruck* **20**: 335-347.

Rigby, J. K. (1983): Sponges of the Middle Cambrian Marjum Limestone from the House Range and Drum Mountains of western Millard County, Utah. *Journal of Paleontology* **57** (2): 240-270.

Rigby, J. K. (1986): Sponges of the Burgess Shale (Middle Cambrian) British Columbia. *Palaeontographica Canadiana* **2**: 1-105.

Rigby, J. K. & Gosney, T. C. (1983): First reported Triassic lyssacid sponges from North America. *Journal of Paleontology* **57** (4):787-796.

Salomon, D. (1990): Ein neuer lyssakiner Kieselschwamm, *Regadrella leptotoichica* (Hexasterophora, Hexactinellida) aus dem Untercenoman von Baddeckenstedt (Nordwestdeutschland). *Neues Jahrbuch für Geologie und Paläontologie, Monatshefte* **[1990]** (6): 342-352.

Schmidt, O. (1870): *Grundzüge einer Spongien-Fauna des Atlantischen Gebietes.* Leipzig (W. Engelmann): iv + 88 pp.

Schrammen, A. (1912): Die Kieselspongien der oberen Kreide von Nordwestdeutschland. II. Triaxonia (Hexactinellida). *Palaeontographica, Supplements* **5**: 281-385.

Schrammen, A. (1924): Die Kieselspongien der oberen Kreide von Nordwestdeutschland. III. und letzter Teil. Mit Beiträgen zur Stammesgeschichte. *Monographien zur Geologie und Palaeontologie (Serie 1)* **2**: 159 pp.

Steiner, M.; Mehl, D.; Reitner, J. & Erdtmann, B.-E. (1993): Oldest entirely preserved sponges and other fossils from the Lowermost Cambrian and a new facies reconstruction of the Yangtze platform (China). *Berliner Geowissenschaftliche Abhandlungen (E: Paläobiologie)* **9**: 293-329.

Schulze, F. E. (1886): Über den Bau und das System der Hexactinelliden. *Abhandlungen der Königlichen Preußischen Akademie der Wissenschaften (Physikalisch-mathematische Classe)* **[1886]** (I): 1-97.

Tabachnick, K. R. & Menshenina, L. L. (2002): Family Hyalonematidae Gray, 1857. In: Hooper, J. N. A. & Soest, R. W. M. van (eds.): *Systema Porifera. A Guide to the Classification of Sponges. Vol. II.* New York, N.Y. (Kluwer Academic/Plenum Publishers): 1232-1263.

Tröger, K. A. & Christensen, W. K. (1991): Upper Cretaceous (Cenomanian-Santonian) inoceramid bivalve faunas from the island of Bornholm, Denmark. *Danmarks Geologiske Undersøgelse (A)* **28**: 7-45.

Walcott, C. D. (1920): Middle Cambrian Spongiae. *Smithsonian Miscellaneous Collection* **67**: 261-364.

Microphytoplankton from the Jena Formation (Lower Muschelkalk Subgroup, Anisian) in the forestry quarry at Herberhausen near Göttingen (Germany)

Walter Riegel[1,2] *; Frank Wiese[1]; Gernot Arp[1] & Volker Wilde[2]

[1]Abt. Geobiologie, Geowissenschaftliches Zentrum, Georg-August-Universität Göttingen, Goldschmidtstr. 3, 37077 Göttingen, Germany; Email: wriegel@gwdg.de
[2]Sektion Paläobotanik, Senckenberg Forschungsinstitut und Naturmuseum, Senckenberganlage 25, 60325 Frankfurt/M., Germany

* corresponding author

In a pilot project microphytoplankton has been studied from a 13 m thick section of carbonates from the upper part of the Anisian Jena Formation (Middle Triassic). The section is exposed in a small quarry near Göttingen, northern Germany, and located near the center of the Germanic Basin. The isolated phytoplankton assemblages consist exclusively of polygonomorph (*Veryhachium*) and acanthomorph (mainly *Micrhystridium*) acritarchs and prasinophytes, while dinoflagellates are still missing. The diversity of acritarchs and prasinophytes is high and particularly remarkable since the Anisian stage is just prior to the turnover from the "Phytoplankton Blackout" to the appearance of modern phytoplankton. New for the Middle Triassic is the diversity and abundance of very small acanthomorphs and prasinophytes (<15 μm) as revealed by SEM, which requires more detailed systematic study.

Considering acritarchs as the more stenohaline and the prasinophytes as a rather euryhaline segment of the phytoplankton their relative proportion can be interpreted as indicating changes in salinity. Thus, quantitative phytoplankton analysis of our section suggests alternations of normal marine conditions and conditions restricted by increased salinity, which can be related to changes in lithofacies. Problems of the biologic nature and mode of life of small acanthomorphs and prasinophytes are briefly discussed. The results of our study are promising to considerably refine environmental interpretations within the Muschelkalk Group of the Germanic Basin in general.

Introduction

The eukaryotic microphytoplankton is a crucial segment of aquatic primary production. It is not only an important basic driver of the marine food web, but, being dependent on dissolved nutrients, light and salinity, also provides deep insights into the physico-chemical environment of the marine realm and its variations in space and time. Indeed, the striking synchroneity of plate tectonic events, major faunal turnovers and changes in phytoplankton diversity is a clear signal of the pivotal role of microphytoplankton as a mediator between the biogeochemical cycle

and the development of marine biota in general as pointed out by a number of authors (e.g., Katz et al. 2004; Riegel 2008; Servais et al. 2008; van de Schootbrugge et al. 2005; Vecoli 2008). On a similar note, it has repeatedly been demonstrated that phytoplankton shows sensitive responses to changes in sedimentary environments and facies especially in coastal and shelf areas (e.g., Heunisch 1990; Loh et al. 1986; Prauss & Riegel 1989; Pross & Brinkhuis 2005).

Between the great end-Devonian demise of acritarchs and the mid-Mesozoic appearance of modern phytoplankton, primary productivity of late Palaeozoic and early Mesozoic seas appears to have been sustained on a relatively low level of diversity and abundance mainly by prasinophytes and a few survivors among the acritarchs. Therefore, the low microphytoplankton profile between the Devonian–Carboniferous boundary and the mid-Triassic has been somewhat provokingly termed the "Late Palaeozoic Phytoplankton Blackout" (Riegel 2008). Early Palaeozoic acritarchs and mid-Mesozoic to Cenozoic dinoflagellates and coccolithophorids proved to serve as excellent stratigraphic indices, while prasinophytes, main phytoplankton constituents during the gap in between, seemed to be rather long-ranging, less diversified morphologically, more facies dependent and highly vacillating in their occurrence. They seem to respond favourably to reduced salinity and temperature in surface waters and thrive particularly well under conditions of a stratified water column (Guy-Ohlson 1996; Prauss & Riegel 1989; Tappan 1980). Thus, the terms opportunistic or disaster species (Tappan 1980) have been commonly applied.

In this context, phytoplankton studies of the Germanic Muschelkalk Group (Anisian–Lower Ladinian, Triassic) are of particular interest since, for one, the Anisian is the last stage of the "Phytoplankton Blackout" immediately prior to the dawn of the modern phytoplankton (i.e., dinoflagellates, coccolithophorids and diatoms), and secondly, the Germanic Basin is an intracontinental, partially closed basin marginal to the Tethys Ocean, in which salinities, water column stability and benthic population density were highly variable.

The first unequivocal dinoflagellate cyst *Sahulodinium* appears in the Ladinian of Australia (Balme 1990; Stover & Helby 1987) and, little later, species of *Suessia, Rhaetogonyaulax* and other dinoflagellate genera invaded the Germanic Basin during marine ingressions of the Upper Triassic, reaching a notable diversity only by the middle Rhaetian (Heunisch 1996). The same factors which promoted the diversification of many fossil groups since the Middle Triassic and initiated the rise of dinoflagellates, may also have fueled the productivity and diversity of phytoplankton associations in the terminal stages of the "Phytoplankton Blackout" just prior to the dinoflagellate entry. Although related comparative studies are still lacking, it seems that acritarchs and prasinophytes have developed a remarkable increase in diversity during the middle Triassic.

A striking feature of Mesozoic phytoplankton assemblages appears to be the occurrence of what has previously been described as "small acritarchs" (Habib & Knapp 1982; Schrank 2003). Their occasional abundance in the Triassic of the Germanic Basin has been recorded before (Heunisch 1990; Reitz 1985), but their significance is largely neglected in routine studies, since their diagnostic morphology can only be resolved by scanning electron microscopy (SEM) and their stratigraphic utility has been considered rather limited.

Responses of phytoplankton assemblages to environmental changes have previously been observed in the Germanic Basin in particular at the boundary Muschelkalk to Keuper groups, where facies changes are most pronounced (Brocke & Riegel 1996; Duringer & Doubinger 1985; Heunisch 1986, 1990; Reitz 1985). For the Lower Muschelkalk, Götz (1996) and Götz & Feist-Burkhardt (1999) focused on the response of phytoplankton assemblages to sea level fluctuations and on palaeogeographic aspects (Götz & Feist-Burkhardt 2012).

Here, we present a cross section of the "old" phytoplankton just prior to the dawn of modern phytoplankton as a pilot study to trace phytoplankton responses to aquafacies changes as deduced from lithological and macrofaunal changes with a vertical lithologic column. We selected an interval within the Jena Formation (Anisian, Lower Muschelkalk Subgroup, Middle Triassic), which is favourably exposed at Joachim Reitner's backyard, the abandoned Herberhausen forestry quarry near Göttingen.

Geological framework

Generalities and lithostratigraphic context

The abandoned Herberhausen quarry is located about 1.3 km east of Göttingen and exposes parts of the Jena Formation (Anisian), which was deposited in an intracontinental sea marginal to the Tethys ("Germanic Basin", Fig. 1A). Traditionally, the Jena Formation is subdivided lithostratigraphically into a succession of platy, wavy and marly (often heavily bioturbated) limestones and marls ("Wellenkalk"), in which intervals of thick bioclastic/oolithic limestone beds are intercalated (Oolith Member, Terebratula Member, Schaumkalk Member; Fig. 1B). These serve basinwide as marker beds in lithostratigraphic correlation. Widespread yellow marls and limestones ("Gelbkalk": dedolomitised limestones and marls) are intercalated in some intervals, indicating short-term establishment of restricted hypersaline (lagoonal) environments in wide parts of the Germanic Basin.

A first description of the quarry with data on faunal assemblages was given by Hagdorn & Simon (1983), who figured a 15.5 m thick section from the middle of the Upper *Terebratula* Bed on (comp. Fig. 2). Together with the section given in Arp et al. (2004), a total thickness of ab-
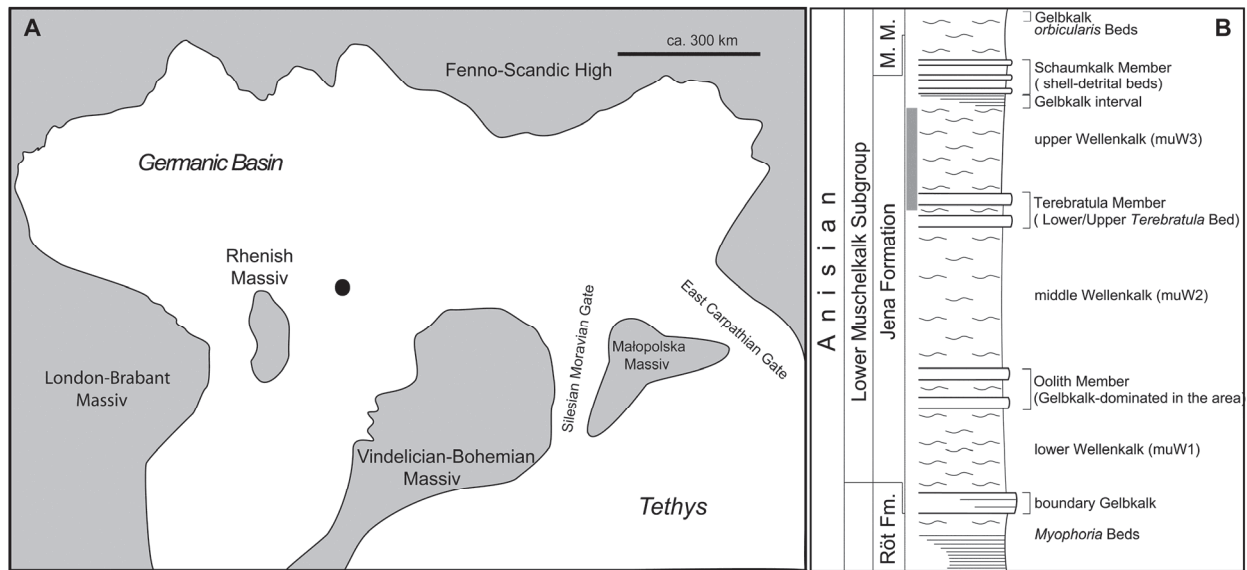
Fig. 1: **(A)** Anisian palaeogeography in Central Europe with location of studied section; **(B)** simplified lithostratigraphic subdivision of the Jena Formation (Lower Muschelkalk Subgroup, Anisian).

out 17 m (starting with wavy limestones separating the Lower and Upper *Terebratula* Beds: "Wellenkalkzwischenmittel") was exposed with time. Crucial for correlation with other sections and for fitting the Herberhausen section into the well-established regional lithostratigraphic frameworks of the Jena Formation (see Kramm 1997; Stein 1968; Schulz 1972) is the occurrence of a 1.5 m thick Gelbkalk at the top of the section (Hagdorn & Simon 1983), which is not exposed today. The succeeding massive Gelbkalk above the Upper *Terebratula* Bed occurs at the top of the Upper Wellenkalk muW3, below the base of the Schaumkalk Member in the wider area (Kramm 1997; Schulz 1972; comp. Fig. 1B). Thus, the Herberhausen section covered almost the entire muW3, but the base of the Schaumkalk Member was not reached. The thickness of muW3 at Herberhausen from the top of the Upper *Terebratula* Bed to the top of the previously exposed Gelbkalk is about 13 m, which equates circa with the thickness as described from other sections in southern Lower Saxony and Northern Hesse (Schulz 1972).

Sedimentary cycles

Numerous authors divide the Jena Formation into a number of sedimentary cycles (Fiege 1938; Götz 1994; Kedzierski 2002; Klotz 1990; Lippmann et al. 2005; Schulz 1972). Although sea level is believed to be the main trigger of this cyclicity, the interpretation of sediment geometries and geochemical trends remains ambiguous, and no generally valid triggering mechanism has been presented yet (see summary in Lippmann et al. 2005). For the Lower Muschelkalk, Kramm (1997) presented a synthesis of observed cycles.

For the muW3, three small-scale cycles are inferred (muW3 IIIb, IIIc, IIId; numbering after Schulz 1972), which should be also recognisable in the Herberhausen section (Hagdorn & Simon 1983). However, the application of the cyclic framework to the Herberhausen section is difficult exclusively based on schematic representation of Arp et al. (2004) (used here as a basis for Fig. 2) and the section of Hagdorn & Simon (2003). Unfortunately, the quarry walls are deteriorated today, why the cycle boundaries are not unequivocally detectable. Cycle IIIb starts at the base of the Upper *Terebratula* Bed and, after a short period of flooding at the top of the Upper *Terebratula* Bed (beds 12–17), an overall shallowing trend towards shell-detrital beds and the hardground in bed 39 occurs, which might be a candidate for the base of IIIc. The base of IIId cannot be recognised but might be located around bed 78. In the working area in southern Lower Saxony, cycles IIIc and IIId are developed as fining-upwards cycles, which likewise represent shallowing-upwards cycles, in some sections associated with Gelbkalk occurrences (see also Schulz 1972). In the case of the Hildesheim area (~80 km N of Göttingen), Gelbkalk development occurs at the contact between cycles IIIc and IIId. Between Hildesheim and northern Hesse, Gelbkalk terminates cycle IIId. The occurrence of Gelbkalk is not only an expression of shallowing, but sedimentary and biogenic structures (shrinkage cracks, microbial mat structures) witness increasing salinity in a progressively restricted depositional setting throughout wide parts of the Germanic Basin. The interpretation of the cyclicity to reflect salinity changes was, in agreement with Fiege (1938), Schüller (1967) and Schulz (1972) in the context of a discussion of the Gelbkalk as a deposit of hypersaline settings.
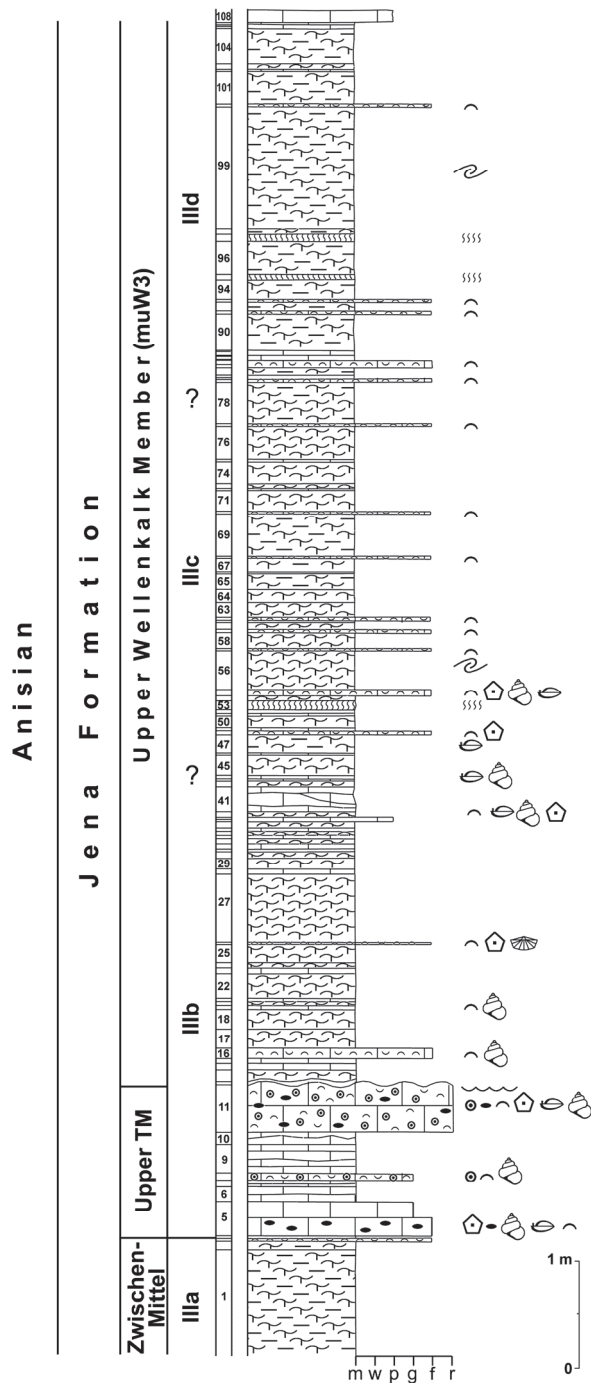
Fig. 2: Generalised overview of the lithology of the abandoned Herberhausen forestry quarry based on Arp et al. (2004). Numbering of cycles after Schulz (1972).

Lithology

Although monotonous at first sight, the Jena Formation represents a variable succession of lithoclastic, bioclastic and oolithic limestones, wavy limestones and marly limestones or marls with interbedded limestone layers. The base of the section (beds 5 to 10) consists of slightly bioturbated wavy mudstone and dense mudstones with some intercalated bioclastic event beds (mollusc floatstone,

cross-bedded oolithic mollusc-bearing grainstones). The top of the bioclastic Upper *Terebratula* Bed (bed 11) is characterised by a well-exposed bedding plane with large current ripples which are sealed by a micritic drape (bed 12). It likewise marks the base of the Upper Wellenkalk Member (muW3) which is characterised by an alternation of wavy, marly or platy limestones and dark grey marl intercalations. In distinct intervals shell-detrital beds occur (tempestites, lumachelles). Echinoderm macrofossils such as crinoids, echinoids, ophiuroids and asteroids are specifically concentrated in an obrution deposit (bed 38) above a hardground. Bivalves, favourably enriched in tempestites, occur scattered throughout the section (for further details on fauna see Hagdorn & Simon 1983 and Arp et al. 2004).

Materials and methods

For our pilot study, we concentrated on mapping palynofacies changes within cycle IIIb covered by 10 samples from beds 1 to 27, equivalent to the basal 5 m of the section and including the interval which has been proposed as maximum flooding surface in the sequence stratigraphic model of Götz (1994). Three additional approximately equidistant samples irrespective of possible cycle boundaries were processed to test whether any changes can be recognised approaching the Gelbkalk (lagoonal setting) at the top of cycle IIId.

50 to 100 g of solid pieces of carbonate rocks were cleaned from weathered clay and lichen growth on exposed surfaces by treating them with 15 % HCl for 5 to 10 minutes and carefully washing them. The cleaned pieces of rock were dissolved in 15 % HCl and concentrated HCl was added successively until all carbonate was dissolved. After removal of excessive HCl some HF was added to dissolve quartz and clay minerals and to separate organic particles from adhering minerals. The residue was finally sieved through a 10 μm mesh screen and the fraction >10 μm stored in glycerine. Mineral imprints on palynomorphs suggested that the original pyrite content (microcrystals and framboids) was already dissolved by surface weathering except for sample Her 18T, which contained abundant framboidal pyrite.

Preservation, assemblage composition and palynomorph diversity varies considerably within the section. Thus, pending further systematic scrutiny the observed palynomorph taxa have been grouped into broad systematic categories which were used as a basis for determining quantitative changes in assemblage composition throughout the section. 300 palynomorph specimens per sample have been counted for percentage calculations in the diagram (Fig. 3). Phytoclasts (black organic matter, e.g., charcoal particles) were also counted and calculated to 100 % of palynomorphs as additional percentages.
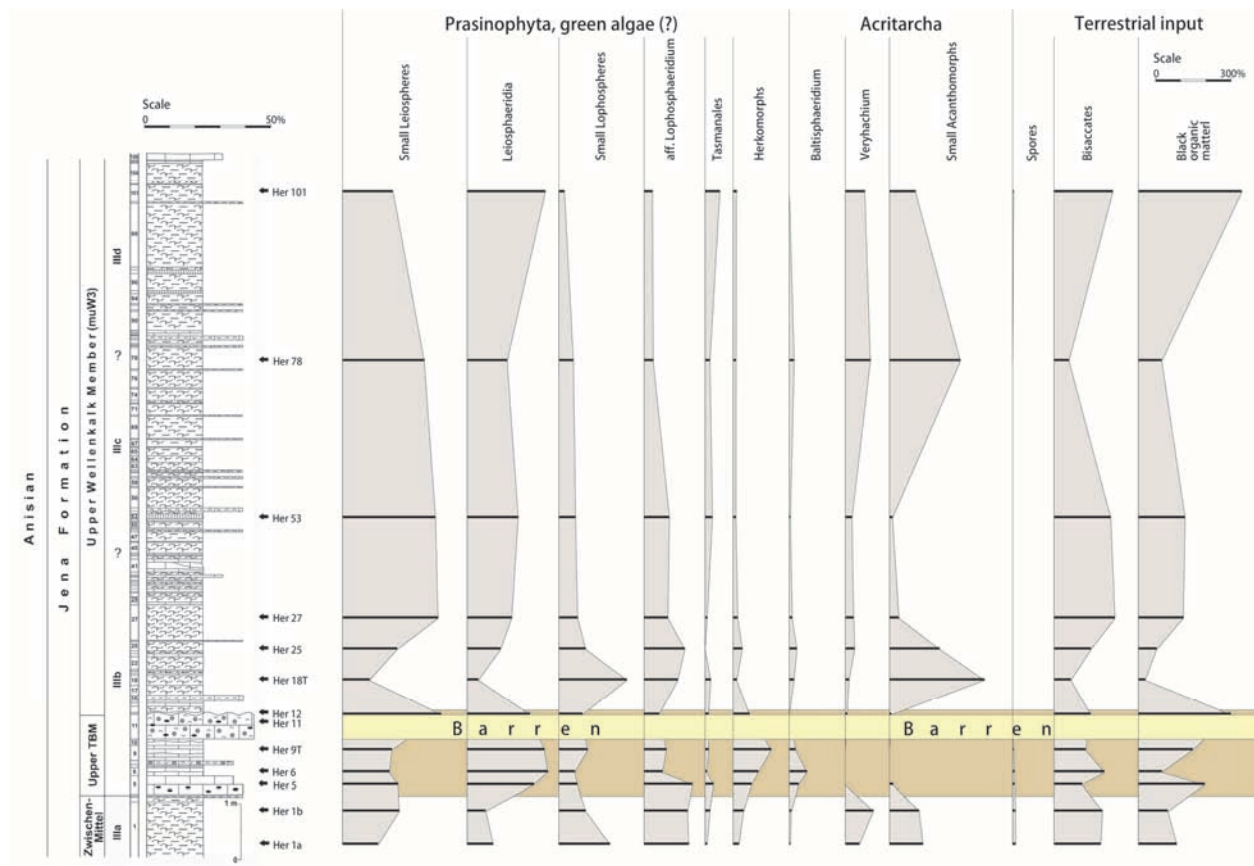
Fig. 3: Lithology, sample location and palynomorph spectrum of selected taxa or groups of taxa, respectively. Shaded area designates the Upper *Terebratula* Bed (TBM), the barren interval corresponds to the porous coquina at the top of the Upper *Terebratula* Bed. Sample Her 12 is from a thin, finely laminated micritic drape, which covers a ripple field, representing the top of the Upper *Terebratula* Bed. [Please note: 10 times reduced scale for black organic matter!]

Light microscope (LM) photographs of representative palynomorph taxa were taken in part from single grain mounts with a LEICA DFC 490 digital camera attached to a LEICA Metallux 3 microscope, SEM micrographs were made from strew mounts of samples Her 18T and Her 25 on a JEOL FM-6490LV, both at the Senckenberg Forschungsinstitut und Naturmuseum, Frankfurt.

The material described herein is deposited in the collections of the Geoscience Centre (GZG.PB), Georg-August University Göttingen (publication no. #1614).

Results

Twelve samples have yielded phytoplankton, pollen and spores in various degrees of abundance and preservation sufficient for quantitative analysis. A sample of bed 11, a highly porous coquina with iron oxide drapes, proved to be barren. Diversity and abundance is highest and preservation best in samples Her 18T and Her 25.

Since very few rigorous systematic studies of Triassic phytoplankton are available thus far, and preservation is rather variable, taxonomic assignment has been kept to a minimum at this stage. Thus, palynomorphs have been divided into broad morphologic groups as listed below.

Phytoplankton

Leiosphaeridia group: All spherical to lenticular laevigate forms regardless of size, wall thickness and preservation are included here. Small vesicles clearly less than 20 μm in diameter and often with a median split or lateral rupture are quite abundant in some samples and may be distinguished as a separate subgroup. Larger forms, with a diameter above 20 μm are also common and may actually be assigned to the genus *Leiosphaeridia* (e.g., Fig. 4.15). There is considerable variation in wall thickness. At this stage, however, it would be premature to distinguish different species on this basis. Some forms with a very irregular wall thickness are rather distinctive components in some samples. They may be considered as preservational variants of *Leiosphaeridia* and are included in this group with some reservation.

Lophosphaeridium group: Forms assigned to this group are mostly small, thin-walled and spherical and commonly show a median split or lateral rupture. They can be divided into two size classes above and below about 15 μm. The small forms generally appear ornamented with minute grains or very short spines under the light microscope and can not always be distinguished with certainty from small
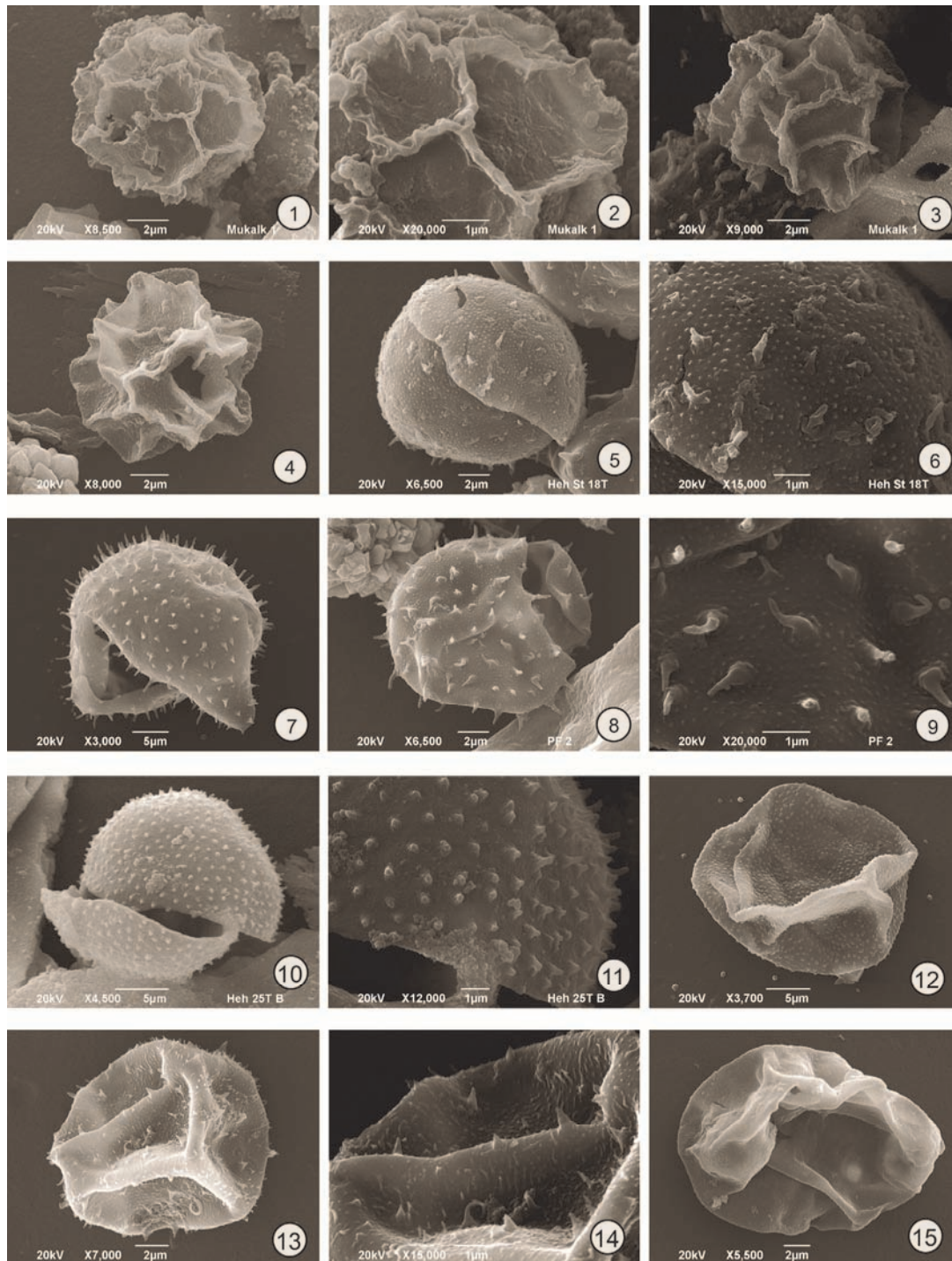
Fig. 4: SEM images of selected herkomorph and sphaeromorph acritarchs. **(1)** *Cymatiosphaera* sp. A, Her 18T, with crenulated crests of ridges, surrounding polygonal fields. ⌀ 9 μm, ridges about 1 μm high; **(2)** Detail of (1) showing fine perforation of fields and a central pore which is not elevated; therefore, the species is not assigned to Pterosphaeridia; **(3)** *Cymatiosphaera* sp. B, Her 18T, with more or less straight ridges surrounding non-perforated fields; Opening (pylome or "archeopyle"?) at top of specimen. ⌀ 10 μm, ridges low, <1 μm; **(4)** *Cymatiosphaera* sp. C, Her 18T, with opening in one field similar to C. sp. B but with higher ridges. ⌀ 10 μm including ridges; **(5)** *Lophosphaeridium* sp. A, Her 18T, with rigid vesicle wall and median split, surface ornamentation of very regular fine granulation and losely spaced coni with basal ringlike structure. ⌀ 14 μm, length of coni up to 1 μm; **(6)** Detail of (5) illustrating surface ornamentation; **(7)** *Lophosphaeridium* sp. B, relatively thick-walled vesicle with lateral rupture and dense surface ornamentation of thin short spines about 2 μm in length; **(8)** *Lophosphaeridium* sp. C, Her 18T, similar to *L.* sp. A, but with lateral rupture and flexible vesicle wall. ⌀ 15 μm; **(9)** Detail of (8) illustrating surface ornamentation consisting of very fine granulation and loosely spaced flexible spines 1 μm or slightly more in length; **(10)** *Lophosphaeridium* sp. D, Her 25, with relatively rigid vesicle wall and median split. ⌀ 20 μm; **(11)** Detail of (10) illustrating surface ornamentation of regularly spaced small coni (<1 μm) and very fine subordinate granulation; **(12)** *Lophosphaeridium* sp.?, Her 18T, strongly folded compressed specimen, originally nearly spherical, with thin wall and very finely granular surface ornamentation which would not be recognisable in transmitted light; the specimen would therefore be identified as *Leiosphaeridia*; **(13)** *Lophosphaeridium* sp. E, Her 18T, folded specimen with thin wall and complex surface ornamentation consisting of fine granulation and irregularly spaced, in part flexible spines of varying size up to 0.5 μm. ⌀ 14 μm; **(14)** Detail of (13) illustrating the type of surface ornamentation; **(15)** *Leiosphaeridia* sp., Her 18T, strongly folded compressed specimen, originally spherical, with thin nearly smooth wall. ⌀ 18 μm.
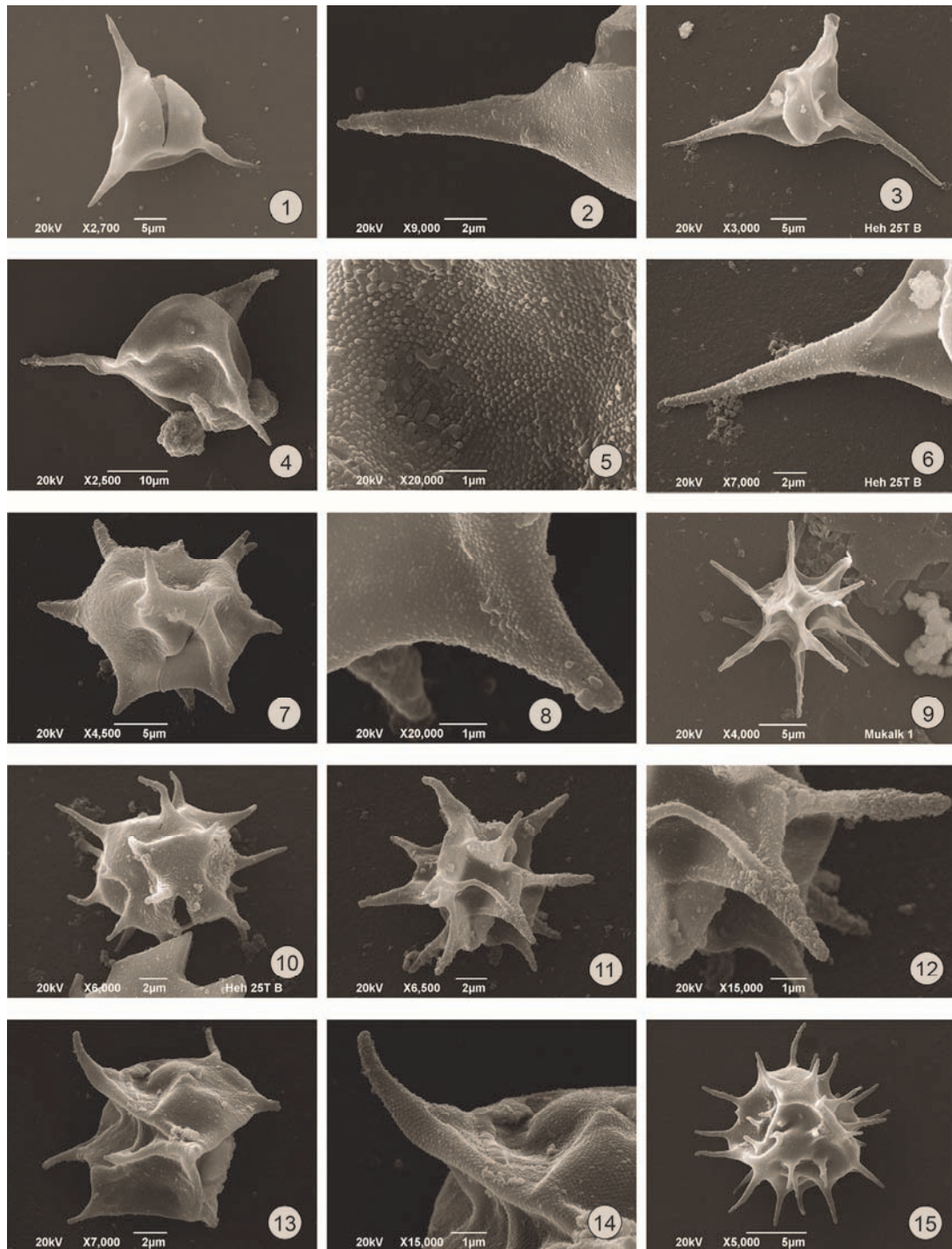
Fig. 5: SEM images of selected polygonomorph and acanthomorph acritarchs. **(1)** *Veryhachium reductum*, Her 18T, with short horns, triangular vesicle 15 µm in ∅ with accidental split; **(2)** Detail of (1) showing very fine granulation increasing in density on horn; **(3)** *Veryhachium trispinosum*, Her 25, with long horns, length of horns and vesicle ∅ equal (about 15 µm), horns hollow as shown by broken off tip of upper horn; **(4)** *Veryhachium* sp., Her 18T, large form, vesicle with strongly convex sides, ∅ ~25 µm; **(5)** Detail of (4) showing very regular dense and fine granulation on central body, granules <0.1 µm in ∅; **(6)** Detail of (3) showing increasing density of granulation on horn; **(7)** *Micrhystridium* sp. A, Her 18T, central body about 15 µm in ∅, with stout short horns about 3 to 4 µm long; **(8)** Detail of (7) showing very fine granulation on horn; **(9)** *Micrhystridium* sp. B, Her 18T, with very long horns, central body about 9 µm, horns 7 to 8 µm, surface of wall more or less smooth; **(10)** *Micrhystridium* sp. C, Her 25, subrounded central body about 12 µm in ∅, with relatively slender horns up to 5 µm long. Opening by damage, not preformed; **(11)** *Micrhystridium* sp. D, Her 18T, with collapsed polygonal central body and conical horns, central body 8 µm in ∅, horns about 5 µm long and up to 2 µm wide at base; **(12)** Detail of (11) showing fine irregular granulation on horns; **(13)** *Micrhystridium* sp. E, Her 18T, with polygonal central body and broad-based horns of variable size, central body about 11 µm in ∅; **(14)** Detail of (13) showing very regular fine granulation extending over both, central body and horns; (15) aff. *Baltisphaeridium* sp. with spherical central body and slender flexible spines, central body 10 µm in ∅, horns up to 4 µm long.

leiospheres at 400 times magnification in quantitative counts. In SEM (Figs. 4.5–9, 4.13) they clearly show a loosely spinose ornamentation superimposed on very fine granulation. Some of the larger forms (20–25 μm) are distinctive by their rigid wall facilitating three-dimensional preservation and a rather regular arrangement of grana (Figs. 4.10–11).

Tasmanites group: Relatively thick-walled tests often with recognisable pore canals can be assigned to the genus *Tasmanites*, however, pore canals may be obscured by poor preservation. Some forms assignable to *Pleurozonaria* may be preservational states of *Tasmanites* (Guy-Ohlson 1996) and are therefore included here. Also added to this group may be relatively large specimens with an irregularly thick wall vaguely suggesting a coarse rugulate sculpture thus far not assignable to any previously described taxon.

Herkomorph group: Most of the discoidal forms with a distinct reticulate ornamentation are assignable to the genus *Dictyotidium* which is represented in our section by several species differing in size and type of reticulation. The genus *Cymatiosphaera* is characterised by wider lumina separated by high walls and mainly represented by very small specimens of less than 20 μm in diameter. Two types can be distinguished: one with crenulated wall tops and perforated lumina with central pore (Figs. 4.1–2) and another with more or less straight walls and smooth lumina (Figs. 4.3–4). *Pterosphaeridia* is recorded in rare cases (Fig. 6.12) but often not distinguishable from *Cymatiosphaera* and *Dictyotidium* due to marginal preservation and limited optical resolution in routine studies. Further SEM studies have to confirm, whether taxa with perforated lumina and central pore (Figs. 4.1–2) should be assigned to *Pterosphaeridia*.

Polygonomorph acritarchs: *Veryhachium* is present to common in all samples above and below the Terebratula horizon but absent from within (samples Her 5, Her 6, Her 9T and Her 11). All specimens are triangular in outline with either short horns (Figs. 5.1–2; *V. reductum*) or long horns (Figs. 5.3, 5.6; *V. trispinosum*) at their corners. In either case, the vesicle surface is rather smooth and the horns are finely ornamented. A third somewhat larger type can be recognised on the basis of high resolution SEM images by the dense granulation which is evenly distributed over vesicle and horns (Figs. 5.4–5).

Acanthomorph acritarchs: Most of the acanthomorph acritarchs are represented by exceptionally small forms in considerable diversity. They are even abundant in samples Her 18T and Her 25 but, together with *Veryhachium*, they are absent from within the Upper *Terebratula* Bed.

The majority is broadly assignable to the genus *Micrhystridium* sensu Sarjeant (1967), but in contrast to other authors (e.g., Courtinat 1983), we excluded taxa with very small spines, coni or grana and included them with the lophospheres. At this stage, no attempt has been made to assign the observed taxa to established species. The selection shown in Figs. 5.7–14 illustrates the observed variation involving size, length, number and distribution of horns, ratio of vesicle size to length of horns and type and distribution of surface ornamentation. Detailed SEM studies are required for closer taxonomic resolution. By their small size the acanthomorph acritarchs in our section and of the Triassic in general represent a unique population differing from their generally larger Palaeozoic counterparts.

Baltisphaeridium group: Small thin-walled spherical vesicles in the order of 10 to 20 μm in diameter with slender flexible appendages exceeding 2 μm in length (Fig. 5.15) are common only within the Terebratula horizon and are tentatively classified with this group.

Pollen and spores

Trilete spores are exceptionally rare and generally without noteworthy diagnostic features, except for a few specimens of zonate forms resembling *Aequitriradites*. *Aratrisporites*, a monolete spore of lycopod affinity (Traverse 2007), has been occasionally recorded in samples Her 1b and Her 78. Very common are bisaccate pollen, the poor preservation of which, however, defies closer taxonomic assignment in most cases. The vast majority has sacci broadly attached to the central body similar to *Alisporites* (e.g., Fig. 6.10), ut in some relatively well-preserved specimens the genera *Vitreisporites, Protodiploxypinus* and *Platysaccus* have been identified.

► **Fig. 6:** LM images of selected acritarchs and prasinophytes. **(1, 3–4, 8)** Various types of *Lophosphaeridium*. (1, 4) corresponding to *Lophosphaeridium* sp. B in Fig. 4.7; (3) corresponds to *Lophosphaeridium* sp. A or sp. C in Figs. 4.5–6 and Figs. 4.8–9; (8) corresponds to *Lophosphaeridium* sp. D in Figs. 4.10–11; **(5)** *Cymatiosphaera* sp., corresponding to *Cymatiosphaera* sp. C in Fig. 4.4; **(2, 6, 9)** Various types of *Micrhystridium*. (2) corresponds to *Micrhystridium* sp. A in Fig. 5.7; (6) corresponds to *Micrhystridium* sp. C in Fig. 5.10; (9) not comparable to any figured specimens in Fig. 5; **(7)** *Cymatiosphaera* sp. with incomplete reticulum; **(10)** *Alisporites* sp.; **(11)** Bisaccate pollen indet.; **(12)** *Pterosphaeridia* sp.; **(13)** Tasmanalean prasinophyte with low rugulate surface ornamentation; **(14)** *Tasmanites* sp.

All correspondences between LM and SEM images are tentative. (7, 14) from Her 78, all others (1–6, 8–13) from Her 18T.
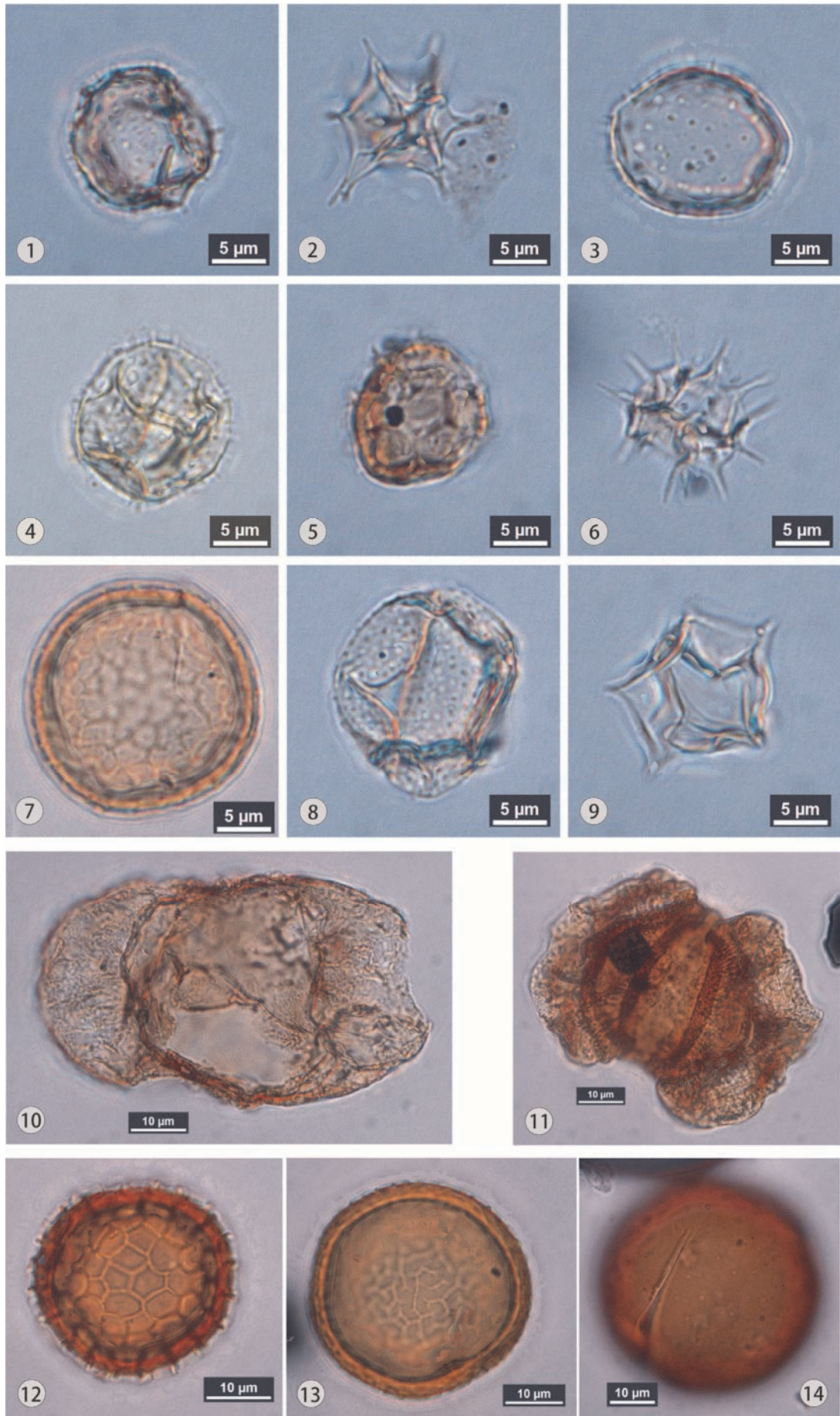
Black organic matter (BOM)

BOM occurs almost exclusively in small particles in the order of a few tens of microns as one of the major organic constituent in all samples except immediately above the Upper *Terebratula* Bed (sample Her 18T). More or less rectangular particles especially when showing traces of pitting are considered to be charcoal, irregularly shaped particles may be phytoclasts reworked from metamorphic rocks or aggregates of soot. In any case, they are terrestrially sourced and together with pollen and spores represent the terrestrial input.

Quantitative analysis

In order to detect any changes in assemblage composition in relation to lithofacies especially with respect to the Upper *Terebratula* Bed, a quantitative analysis based on a count of 300 specimens of total palynomorphs has been carried out on all productive samples. The dominant elements in most samples are very small spherical cysts most of them less than 15 μm in diameter. The majority of them appears entirely smooth and is listed in Fig. 3 as small leiospheres, but commonly a surface ornamentation by minute granules can be recognised in LM and demonstrated by SEM (Figs. 4.5–11, 4.13–14). The latter are then included within the *Lophosphaeridium* group as small lophospheres (Fig. 3). In routine quantitative analysis, however, the distinction between the smooth and granular forms remains rather arbitrary. At present, there seems to be an inverse relationship between the two groups, possibly an artefact due to differences in preservation and identification.

The most striking change in phytoplankton assemblages is shown by four samples from the Upper *Terebratula* Bed (Her 5, Her 6, Her 9T). *Veryhachium* is fairly abundant below the Upper *Terebratula* Bed ("Wellenkalk-Zwischenmittel", see Figs. 2–3), while *Veryhachium* and *Micrhystridium* – the most typically marine Triassic acritarch genera – are completely absent within the Upper *Terebratula* Bed (samples Her 5, Her 6, Her 9T, Her 12). The loss of *Veryhachium* and small acanthomorphs within the Upper *Terebratula* Bed is compensated by a marked increase in the abundance of larger leiospheres (*Leiophaeridia*), a moderate increase of the *Baltisphaeridium* group and a notable rise in diversity and abundance of herkomorphs, especially *Dictyotidium* and *Cymatiosphaera*.

Members of the *Tasmanites* group are conspicuous by their size and thick deep orange coloured wall, but appear quantitatively insignificant. They are somewhat more frequent in samples Her 5, Her 53 and Her 78 and quite common in sample Her 101, thus showing an increasing trend towards the top of the section.

Among terrestrial palynomorphs, bisaccate pollen are by far the most common element, but no clear vertical trend can be recognised in their distribution. BOM, i.e., charcoal and others, has been counted separately and calculated to 100 % of total palynomorphs. In Fig. 3 it is represented together with pollen and spores as terrestrial input but at a scale reduced by 10 times. As would be expected from terrestrially sourced components, bisaccate pollen and BOM show a remarkably parallel trend.

Discussion

Acritarchs and prasinophytes as indicators of salinity

Since the early Palaeozoic, the *Veryhachium-Micrhystridium* complex plays a unique role among acritarchs in its response to environmental changes such as bursting into abundance around the late Ordovician (Hirnantian) glaciation (Vecoli 2008) and at the base of the Carboniferous in widely spaced localities, e.g., Poland (Filipiak 2005) and Ohio, USA (Winslow 1962) subsequent to the extinction of most acritarch genera. The *Veryhachium–Micrhystridium* complex reaches up to 50 % of total palynomorph assemblages just above the Permian–Triassic boundary in several sections of Israel and is considered to signal the beginning recovery after the deep end-Permian ecological crisis (Eshet et al. 1995). Thus, *Veryhachium* and *Micrhystridium* display a similar opportunistic behaviour and broad ecologic tolerance as many of the prasinophytes. Nevertheless, for want of any more sensitive indices they are generally regarded and used here as the most typical marine phytoplankton in the Triassic (Visscher et al. 1993). Thus, their common presence respectively abundance below and especially above the Upper *Terebratula* Bed can be considered to indicate normal marine conditions, while their absence in an interval within the Upper *Terebratula* Bed suggests restricted conditions during this interval.

Among the acritarch taxa listed above, the genus *Baltisphaeridium* is considered as a fully marine acritarch on the basis of its Palaeozoic record, but assignments to this genus are still very tentative in our analysis and its ecologic signal remains rather doubtful. In fact, it shows a slight peak in abundance within the Upper *Terebratula* Bed and, thus, shows a reverse trend to *Veryhachium* and the small acanthomorphs.

Leiospheres are a broad, morphologically indistinct and therefore probably rather heterogeneous group which has been variously attributed to acritarchs or prasinophytes and may even include other unicellular organisms. A prasinophyte affinity is preferred here at least for the larger forms (clearly above 20 μm), which we assign to the genus *Leiosphaeridia*, but the biological source of the abundant small forms (mostly 15 μm or less) is rather doubtful. The same uncertainty exists for the abundant small granular forms included here in the *Lophosphaeridium* group. Since the emended diagnosis of *Lophosphaeridium* (Timofeyev) Lister 1970 is still rather broad and non-descript, we have loosely grouped all tuberculate spherical forms

and attributed them tentatively to the prasinophytes regardless of size. It is generally agreed that most of the larger sphaeromorphs such as *Tasmanites* and *Pleurozonaria* are fossilised phycomata of prasinophytes, originally containing numerous motile cells. Guy-Ohlson (1996), however, shows SEM images of small sphaeromorphs, leiospheres as well as lophospheres, and suggests that they may represent phycomata (respectively cysts?) of individual cells from an earlier still smaller stage in the life cycle of prasinophytes, an argument, which we accept here in view of the many open questions regarding the various stages in the life cycle of prasinophytes. Somewhat larger lophospheres have been previously recorded from the Jena Formation (Lower Muschelkalk) of northern Hesse (Reitz 1985), but erroneously assigned to the genus *Tytthodiscus,* which is considered to be a prasinophyte. Thus, in our study, we tentatively consider all sphaeromorph taxa as prasinophytes and, therefore, as potentially euryhaline.

Most members of the herkomorph group such as *Dictyotidium, Cymatiosphaera* and *Pterosphaeridia*, are generally considered to be prasinophyte phycomata. *Dictyotidium* and *Cymatiosphaera* are quite common throughout the section and even dominant within the Upper *Terebratula* Bed, in which *Veryhachium* and the small acanthomorphs are missing. Very small specimens of *Cymatiosphaera* (<15 μm) are infrequent but occur regularly throughout the section. They are listed as small acritarchs by Habib & Knapp (1982) and Schrank (2003), but from a morphological point of view it seems taxonomically and biologically inappropriate to separate them from the prasinophytes. They should, therefore, be also considered as part of the euryhaline phytoplankton.

Interpreting the proportion of the mainly prasinophycean euryhaline phytoplankton and the *Veryhachium–Micrhystridium* complex as essentially salinity controlled, the changes in salinity within the Herberhausen section can be summarised as follows: (1) Normal marine conditions existed at the base of the section ("Wellenkalk-Zwischenmittel", bed 1), where *Veryhachium* and small acanthomorphs are frequent and prasinophytes moderately present; (2) A marked change occurs in the slightly bioturbated calcareous mudstones above (Her 6, Her 5, Her 9), which are sandwiched between the two bioclastic limestone beds, bounding the Upper *Terebratula* Bed. Most striking there is the lack of both, *Veryhachium* and small acanthomorphs, which, together with a distinct increase of *Leiosphaeridia* and herkomorph prasinophytes (*Cymatiosphaera* and *Dictyotidium*), clearly indicates restricted conditions for this interval. A decrease of marine phytoplankton is also recorded by Rameil et al. (2000) from the base of the Upper *Terebratula* Bed of the Steudnitz quarry, Thuringia. These observation is in accordance with Lukas (1991, 1993), who demonstrated the strong lateral facies variability within the Terebratula Member, shifting between carbonate shoals and more lagoonal settings. Normal marine conditions were restored above the top of the Upper *Terebratula* Bed

as indicated by the peak abundance of small acanthomorphs in sample Her 18T. This interval corresponds to the position of a maximum flooding in the sense of the cycle model of Götz (1994), and corresponds to the data provided by Rameil et al. (2000). Our results, however, are in conflict with Götz & Feist-Burkhardt (2012), who show peak abundance of marine phytoplankton within the Terebratula Member and a decrease above.

Small acanthomorphs gradually decline as leiospheres become more abundant up to a point in the section, which may be identified as the top of cycle IIIb. The large sampling gaps in the upper part of the section limit identification of further trends, but the intermittent frequency of small acritarchs in sample Her 78 suggests that additional salinity fluctuations may eventually be revealed by higher resolution. Important to note is the numerically small but significant increase of *Tasmanites* and a distinct increase of *Leiosphaeridia* together with a concurrent decrease of small acanthomorphs in sample Her 101. This suggests a renewed trend towards restricted conditions as the previously exposed Gelbkalk is approached. Since Gelbkalk deposited under hypersaline conditions, it seems appropriate to generally interpret shifts towards euryhaline elements in phytoplankton assemblages of the Jena Formation as a response to increased salinities.

On a broader regional scale, Götz & Feist-Burkhardt (2012) suggest that marine phytoplankton selected for palaeogeographic realms during the Anisian. They show that acritarchs dominate over prasinophytes in the open Tethyan shelf and gateways to the Germanic Basin, while prasinophytes dominate in the Germanic Basin under conditions of varying salinity gradients including water column stratification and oxygen depleted bottom conditions. Furthermore, within the acritarch group *Micrhystridium* is characteristic of the shelf and gate areas, *Veryhachium* of the central basin. However, Götz & Feist-Burckhardt (2012) apparently did not take the abundance of small acanthomorph acritarchs into account, to which the micrhystridians in our section belong. Thus, the question of the preference of small acanthomorphs for more open marine environments requires additional comments.

Several authors interpreted palynological changes in the Muschelkalk Group in terms of sequence stratigraphy ("sequence palynology") at various levels of resolution (Götz 1996; Götz & Feist-Burkhardt 1999; Rameil et al. 2000; Visscher et al. 1993). Maximum abundance of acritarchs, mainly *Micrhystridium* with accessory *Veryhachium*, has previously been used to identify the maximum flooding surface of third order sequences of Aigner & Bachmann (1992) in the upper part of the Lower Muschelkalk Subgroup (Visscher et al. 1993), at a level presumably corresponding to the Terebratula Member, where Götz & Feist-Burkhardt (1999) placed their maximum flooding surface on the basis of peak abundance of marine phytoplankton, i.e., acritarchs plus prasinophytes. The succeed-

ing highstand systems tract within the muW3 is characterised by a general decrease of phytoplankton. Small cycles in the range of about 10 m are superimposed showing phytoplankton responses similar to those of the higher order systems tracts (Götz & Feist-Burkhardt 1999), however, this similarity appears rather vague.

Palynological results from the Herberhausen section (Fig. 3) rather suggest that changes in phytoplankton associations are primarily controlled by salinity changes, which in turn can be influenced by sea level fluctuations but other factors may be involved in salinity changes. An alternative view has, for instance, been presented by Brocke & Riegel (1996), interrelating repeated successions in the dominance of terrestrial input, prasinophytes and acritarchs as responses to pulses of delta advance at the top of the Muschelkalk Group.

Ecological role of "small acritarchs"

Small acritarchs form a unique segment of many microphytoplankton assemblages and appear to be abundant in special environments and at certain stratigraphic levels of the Mesozoic. Their ecological role and biological affinity, however, remain rather enigmatic. A possible biological link to prasinophytes has been discussed above. Taking up ideas expressed previously (Courtinat 1983; Dale 1977), Schrank (2003) argues in favour of a biologic affinity of small acritarchs to dinoflagellates for at least two of his genera (*Mecsekia* and *Recticystis*), which bear considerable similarity in size and morphology to the tiny lophospheres in our preparations. An affinity to dinoflagellates has even been suggested for some spiny acritarchs (Fensome et al. 1999). However, accepting that the adaptive radiation of dinoflagellates started in the Upper Triassic and Lower Jurassic (Fensome et al. 1996), a dinoflagellate affinity of the small lophospheres in our section seems highly unlikely and can be excluded for the spiny acritarchs on a morphological basis. Extending the idea of dinoflagellate affinity, Schrank (2003) points out that living dinoflagellates are concentrated in the upper centimetres of marine sands (Sarjeant & Taylor 1999), and he suggests an adaptation to a similar interstitial mode of life for the "small acritarchs" from the phosphoritic sands of the Upper Cretaceous of Egypt. This interpretation appears rather intriguing since a number of authors have observed that small acritarchs occur preferentially in relatively coarse-grained littoral sediments (Courtinat 2000; Fechner 1996; Sarjeant & Taylor 1999; Schrank 1984; Wall 1965). This can not, however, be applied to the small acritarchs of Habib & Knapp (1982) from the Lower Cretaceous oceanic clays and marls nor to the small acanthomorph acritarchs and small cymatiospheres in the mainly micritic limestones of the Jena Formation in our section, which might have been originally aragonite mud (Lippmann et al. 2005). Apparently, the phenomenon of "small acritarchs" can neither be explained by a single biological affinity or mode of life.

Habib & Knapp (1982) demonstrated that small acritarchs changed at relatively short intervals in Lower Creta-

ceous successions of the western North Atlantic (Continental slope, Bermuda Rise, Blake-Bahama Basin) and suggested that they provide a useful yet untapped biostratigraphic tool. But these changes may be facies controlled rather than the result of rapid evolutionary development, since at least some forms appear to be long-lived. For instance, forms shown in Figs. 5.7, 5.10 appear to be identical with *Micrhystridium karamurzae* from the late Permian of Australia (McMinn 1982), and others (e.g., Fig. 4.10) seems to correspond to cf. *Micrhystridium deflandrei* from the Upper Jurassic of France (Courtinat 1983). Very similar small acritarchs have also been reported from the Oxfordian (Upper Jurassic) of Lower Saxony, Germany (Kunz 1990).

Conclusions

In our pilot study on organic-walled microphytoplankton from a short section of the Jena Formation (Lower Muschelkalk Subgroup), we are able to show that changes in assemblage composition correspond well with changes in lithology and provide important additional evidence for environment interpretations. Assemblages are exclusively composed of prasinophytes and a relatively narrow segment of acritarchs, i.e., *Veryhachium* and small acanthomorphs. Despite limited quality of preservation and mostly low abundance, an unexpected high diversity has been observed, especially when SEM has been applied to the so-called small acritarchs, which demands further research.

Using the generally accepted euryhaline nature of prasinophytes and the stenohaline preference of *Veryhachium*, *Micrhystridium* and small acanthomorphs, respectively, we suggest that salinity changes were the main trigger for changes in phytoplankton assemblages. Increased salinities are indicated within the Upper *Terebratula* Bed and in the uppermost part of the succession (top of cycle IIId) below the Gelbkalk (comp. Figs. 1B, 2). Fully marine conditions may be interpreted for beds 1 and 18 to 27. The total lack of *Veryhachium* and small acanthomorphs within the Upper *Terebratula* Bed shows that these salinity trends are not necessarily straight forward, but may be interrupted by short-term events recognisable only at high resolution. Our results suggest that changes in composition of microphytoplankton assemblages are controlled directly by salinity and reflect evaporation cycles in the first place. However, sea level may be instrumental in as much as salinity is influenced by changes in sea level. Obviously, the sensitive response of microphytoplankton to facies changes observed at Herberhausen opens a promising new approach to the improvement of environment interpretations of the Muschelkalk Group in general.

Several problems surround the so-called small acritarchs, which are diverse and abundant in our section. Their taxonomy requires critical analysis by SEM, which has hitherto applied only to few occurrences in relatively

narrow stratigraphic intervals (Jurassic, France: Courtinat 1983; Lower Cretaceous, North Atlantic: Habib & Knapp 1982; Upper Cretaceous, Egypt: Schrank 2003) and never attempted for the Muschelkalk Group of the Germanic Basin. Much additional work is needed and intended to assess their stratigraphic ranges and possible evolutionary patterns. Various ideas have been proposed regarding their biological affinity and mode of life. But neither an affinity to dinoflagellates nor an interstitial mode of life can thus far be confirmed by our pilot study.

Acknowledgements

References

Aigner, T. & Bachmann, G. H. (1992): Sequence-stratigraphic framework of the Germanic Triassic. *Sedimentary Geology* **80** (1-2): 115-135. http://dx.doi.org/10.1016/0037-0738(92)90035-P

Arp, G.; Hoffmann, V.-E.; Seppelt, S. & Riegel, W. (2004): Exkursion 6: Trias und Jura von Göttingen und Umgebung. In: Reitner, J.; Reich, M. & Schmidt, G. (eds.): *Geobiology 2. 74. Jahrestagung der Paläontologischen Gesellschaft, Göttingen, 02. Bis 08. Oktober 2004. Exkursionen und Workshops. Universitätsdrucke Göttingen.* Göttingen (Universitäts-Verlag): 147-192.

Balme, B. E. (1990): Australian Phanerozoic Timescales: 9. Triassic Biostratigraphic Charts and Explanatory Notes. *Bureau of Mineral Resources, Australia, Record* **1989/37**: 1-28.

Brocke, R. & Riegel, W. (1996): Phytoplankton responses to shoreline fluctuations in the Upper Muschelkalk (Middle Triassic) of Lower Saxony (Germany). *Neues Jahrbuch für Geologie und Paläontologie, Abhandlungen* **200** (1/2): 53-73.

Courtinat, B. (1983): Évidence ou réalité chez le genre *Micrhystridium*. Un exemple par l'étude des quelques formes Jurassiques du Jura Francais. *Cahiers de Micropaléontologie* **1**: 1-32.

Courtinat, B. (2000): Review of the dinoflagellate cyst *Subtilisphaera inaffecta* (Grugg, 1978) Bujak and Davies, 1983 and *S.? paeminosa* (Drugg, 1978) Bujak and Davies, 1983. *Journal of Micropalaeontology* **19** (1): 165-175. http://dx.doi.org/10.1144/jm.19.2.165

Dale, B. (1977): New observations on *Peridinium faeroense* Paulsen (1905), and classification of small orthoperidinioid dinoflagellates. *British Phycological Journal* **12** (3): 241-253.

Duringer, P. & Doubinger, J. (1985): La palynologie: un outil de caractérisation des faciès marins et continentaux à la limite Muschelkalk supérieur – Lettenkohle. *Sciences Géologiques, Bulletin* **38** (1): 19-34.

Eshet, Y.; Rampino, M. R. & Visscher, H. (1995): Fungal event and palynological record of ecological crisis and recovery across the Permian-Triassic boundary. *Geology* **23** (11): 967-970. http://dx.doi.org/10.1130/0091-7613(1995)023<0967: FEAPRO>2.3.CO;2

Fechner, G. G. (1996): Septarienton und Stettiner Sand als Fazieseinheiten im Rupelium der östlichen Mark Brandenburg: Palynologisch-fazielle Untersuchungen bei Bad Freienwalde. *Berliner Geowissenschaftliche Abhandlungen (E: Paläobiologie)* **18**: 77-119.

Fensome, R. A.; Riding, J. B. & Taylor, F. J. R. (1996): Dinoflagellates. In: Jansonius, J. & McGregor, D. C. (eds.): Palynology: principles and applications. *American Association of Stratigraphic Palynologists Foundation* **1**: 107-169.

Fensome, R. A.; Saldarriaga, J. F. & Taylor, F. J. R. (1999): Dinoflagellate phylogeny revisited: reconciling morphological and molecular based phylogenies. *Grana* **38** (2-3): 66-80. http://dx.doi.org/10.1080/00173139908559216

Fiege, K. (1938): Die Epirogenese des Unteren Muschelkalkes in Nordwestdeutschland, I. Teil. *Zentralblatt für Mineralogie, Geologie und Paläontologie (B: Geologie und Paläontologie)* **[1938]**: 143-170.

Filipiak, P. (2005): Late Devonian and Early Carboniferous acritarchs and prasinophytes from the Holy Cross Mountains (central Poland). *Review of Palaeobotany and Palynology* **134** (1-2): 1-26. http://dx.doi.org/10.1016/j.revpalbo.2004.11.001

Götz, A. E. (1994): Feinstratigraphie und Zyklengliederung im Unteren Muschelkalk (Raum Creuzburg – Westthüringen). *Beiträge zur Geologie von Thüringen* **1**: 3-12.

Götz, A. E. (1996): Palynofazielle Untersuchungen zweier Geländeprofile im Unteren Muschelkalk Osthessens und Westthüringens. *Geologisches Jahrbuch Hessen* **124**: 87-96.

Götz, A. E. & Feist-Burkhardt, S. (1999): Sequenzstratigraphische Interpretation der Kleinzyklen im Unteren Muschelkalk (Mitteltrias, Germanisches Becken). In: Ricken, W. (ed.): Sediment '97. *Zentralblatt für Geologie und Paläontologie (Teil 1: Allgemeine, angewandte, regionale und historische Geologie)* **[1997]** (7/9): 1205-1219.

Götz, A. E. & Feist-Burkhardt, S. (2012): Phytoplankton associations of the Anisian Peri-Tethys Basin (Central Europe): Evidence of basin evolution and palaeoenvironmental change. *Palaeogeography Palaeoclimatology Palaeoecology* **337-338**: 151-158. http://dx.doi.org/10.1016/j.palaeo.2012.04.009

Guy-Ohlson, D. (1996): Prasinophycean algae. In: Jansonius, J. & McGregor, D. C. (eds.): Palynology: principles and applications. *American Association of Stratigraphic Palynologists Foundation* **1**: 181-189.

Habib, D. & Knapp, S. D. (1982): Stratigraphic utility of Cretaceous small acritarchs. *Micropaleontology* **28** (4): 335-371.

Hagdorn, H. & Simon, T. (1983): Ein Hartgrund im Unteren Muschelkalk von Göttingen. *Der Aufschluss* **34** (6): 255-263.

Heunisch, C. (1986): Palynologie des Unteren Keupers in Franken, Süddeutschland. *Palaeontographica (B: Paläophytologie)* **200**: 33-110.

Heunisch, C. (1990): Palynologie der Bohrung "Natzungen 1979" Blatt 4321 Borgholz (Trias; oberer Muschelkalk 2, 3, Unterer Keuper). *Neues Jahrbuch für Geologie und Paläontologie, Monatshefte* **[1990]** (1): 17-42.

Heunisch, C. (1996): Palynologische Untersuchungen im oberen Keuper Nordwestdeutschlands. *Neues Jahrbuch für Geologie und Paläontologie, Abhandlungen* **200** (1/2): 87-105.

Katz, M. E.; Finkel, Z. V.; Grzebyk, D.; Knoll, A. H. & Falkowski, P. G. (2004): Evolutionary Trajectories and Biogeochemical Impacts of Marine Eukaryotic Phytoplankton. *Annual Review of Ecology, Evolution and Systematics* **35**: 523-556.

Kedzierski, J. (2002): Sequenzstratigraphie des Unteren Muschelkalks im östlichen Teil des Germanischen Beckens (Deutschland, Polen). *Hallesches Jahrbuch für Geowissenschaften (B: Geologie, Paläontologie, Mineralogie), Beiheft* **16**: 1-52.

Klotz, W. (1990): Zyklische Gliederung des Unteren Muschelkalks ("Wellenkalk") auf der Basis von Sedimentations-Diskontinuitäten. *Zentralblatt für Geologie und Paläontologie (Teil 1: Allgemeine, angewandte, regionale und historische Geologie)* **[1989]** (9/10): 173-188.

Kramm, E. (1997): Stratigraphie des Unteren Muschelkalks im Germanischen Becken. *Geologica et Palaeontologica* **31**: 215-234.

Kunz, R. (1990): Phytoplankton und Palynofazies im Malm NW-Deutschlands (Hannoversches Bergland). *Palaeontographica (B: Paläophytologie)* **216**: 1-105.

Lippmann, R.; Voigt, T.; Lützner, H.; Baunack, C. & Föhlisch, K. (2005): Geochemische Zyklen im Unteren Muschelkalk (Typusprofil der Jena Formation, Steinbruch Steudnitz). *Zeitschrift für Geologische Wissenschaften* **33** (1): 27-50.

Loh, H.; Maul, B.; Prauss, M. & Riegel, W. (1986): Primary production, maceral formation and carbonate species in the Posidonia Shale of NW Germany. *Mitteilungen aus dem Geologisch-Paläontologischen Institut der Universität Hamburg* **60**: 397-421.

Lukas, V. (1991): Die Terebratel-Bänke (Unterer Muschelkalk, Trias) in Hessen – ein Abbild kurzzeitiger Faziesänderungen im westlichen Germanischen Becken. *Geologisches Jahrbuch Hessen* **119**: 119-175.

Lukas, V. (1993): Sedimentologie und Paläogeographie der Terebratelbänke (Unterer Muschelkalk, Trias) Hessens. In: Hagdorn, H. & Seilacher, A. (eds.): Muschelkalk. Schöntaler Symposium 1991. *Sonderbände der Gesellschaft für Naturkunde in Württemberg* **2**: 79-85.

McMinn, A. (1982): Late Permian acritarchs from the Northern Sydney Basin. *Journal and Proceedings of the Royal Society of New South Wales* **115**: 79-86.

Prauss, M. & Riegel, W. (1989): Evidence from phytoplankton associations for causes of black shale formation in epicontinental seas. *Neues Jahrbuch für Geologie und Paläontologie, Monatshefte* **[1989]** (11): 671-682.

Pross, J. & Brinkhuis, H. (2005): Organic-walled dinoflagellate cysts as paleoenvironmental indicators in the Paleogene; a synopsis of concepts. *Paläontologische Zeitschrift* **79** (1): 53-59. http://dx.doi.org/10.1007/BF03021753

Rameil, N.; Götz, A. E. & Feist-Burkhardt, S. (2000): High-resolution sequence interpretation of epeiric shelf carbonates by means of palynofacies analysis: an example from the Germanic Triassic (Lower Muschelkalk, Anisian) of East Thuringia, Germany. *Facies* **43**: 123-144. http://dx.doi.org/10.1007/BF02536987

Reitz, E. (1985): Palynologie der Trias in Nordhessen und Südniedersachsen. *Geologische Abhandlungen Hessen* **86**: 1-36.

Riegel, W. (2008): The Late Palaeozoic phytoplankton blackout – Artefact or evidence of global change? *Review of Palaeobotany and Palynology* **148** (2-4): 73-90. http://dx.doi.org/10.1016/j.revpalbo.2006.12.006

Sarjeant, W. A. S. (1967): Observations on the acritarch genus *Micrhystridium* (Deflandre). *Revue de Micropaléontologie* **9** (4): 201-208.

Sarjeant, W. A. S. (1973): Acritarchs and tasmanitids from the Mianwali and Tredian Formations (Triassic) of the Salt and Sugar Ranges, West Pakistan. In: Logan, A. & Hills, L. V. (eds.): Permian Triassic Systems and their mutual boundaries. *CSPG Special Publications, Memoir* **2**: 35-73.

Sarjeant, W. A. S. & Taylor, F. J. R. (1999): Dinoflagellates, fossil and modern: certain unresolved problems. *Grana* **38** (2-3): 186-192. http://dx.doi.org/10.1080/00173139908559227

Schrank, E. (1984): Organic-walled microfossils and sedimentary facies in the Abu-Tartur Phosphates (Late Cretaceous, Egypt). *Berliner geowissenschaftliche Abhandlungen (A: Geologie und Paläontologie)* **50**: 177-187.

Schrank, E. (2003): Small acritarchs from the Upper Cretaceous: taxonomy, biological affinities and palaeoecology. *Review of Palaeobotany and Palynology* **123** (3-4): 199-235. http://dx.doi.org/10.1016/S0034-6667(02)00228-2

Schüller, M. (1967): Petrographie und Feinstratigraphie des Unteren Muschelkalkes in Südniedersachsen und Nordhessen. *Sedimentary Geology* **1**: 353-401. http://dx.doi.org/10.1016/0037-0738(68)90022-5

Schulz, M.-G. (1972): Feinstratigraphie und Zyklengliederung des Unteren Muschelkalks in N-Hessen. *Mitteilungen aus dem Geologisch-Paläontologischen Institut der Universität Hamburg* **41**: 133-170.

Servais, T.; Lehnert, O.; Li Jun; Mullins, G. L.; Munnecke, A.; Nützel, A. & Vecoli, M. (2008): The Ordovician biodiversification: revolution in the oceanic trophic chain. *Lethaia* **41** (2): 99-109. http://dx.doi.org/10.1111/j.1502-3931.2008.00115.x

Stein, V. (1968): Stratigraphische Untersuchungen im Unteren Muschelkalk Südniedersachsens. *Zeitschrift der deutschen geologischen Gesellschaft* **117**: 819-828.

Stover, L. F. & Helby, R. (1987): Some Australian Mesozoic index species. In: Jell, P. A. (ed.): Studies in Australian Mesozoic palynology. *Memoir of the Association of Australasian Palaeontologists* **4**: 143-157.

Tappan, H. (1980): *The paleobiology of plant protists*. San Francisco (W. H. Freeman): xxi + 1028 pp.

Traverse, A. (2007): *Paleopalynology. 2nd edition*. Dordrecht (Springer): xviii + 813 pp.

Van de Schootbrugge, B.; Bailey, T. R.; Rosenthal, Y.; Katz, M. E.; Wright, J. D.; Miller, K. G.; Feist-Burkhardt, S. & Falkowski, P. G. (2005): Early Jurassic climate change and the radiation of organic-walled phytoplankton in the Tethys Ocean. *Paleobiology* **31** (1): 73-97.

Vecoli, M. (2008): Fossil microphytoplankton dynamics across the Ordovician-Silurian boundary. *Review of Palaeobotany and Palynology* **148** (2-4): 91-107. http://dx.doi.org/10.1016/j.revpalbo.2006.11.004

Visscher, H.; Brugman, W. A. & Houte, M. van (1993): Chronostratigraphical and sequence stratigraphical interpretation of the palynomorph record from the Muschelkalk of the Obernsees Well, South Germany. In: Hagdorn, H. & Seilacher, A. (eds.): Muschelkalk. Schöntaler Symposium 1991. *Sonderbände der Gesellschaft für Naturkunde in Württemberg* **2**: 145-152.

Wall, D. (1965): Microplankton, pollen and spores from the Lower Jurassic of Britain. *Micropaleontology* **11** (2): 151-190.

Winslow, M. (1962): Plant spores and other microfossils from the Upper Devonian and Lower Mississippian rocks of Ohio. *United States Geological Survey Professional Paper* **364**: 1-89.

Hydrochemistry, biofilms and tufa formation in the karstwater stream Lutter (Herberhausen near Göttingen)

Gernot Arp[1] * & Andreas Reimer[1] *

[1]Department of Geobiology, Geoscience Centre, Georg-August University Göttingen, Goldschmidtstr. 3, 37077 Göttingen, Germany; Email: garp@gwdg.de & areimer@gwdg.de

* corresponding authors

An actively forming tufa cascade at a tributary to the karstic stream Lutter in Herberhausen (backyard of Professor Reitner's stately home) was investigated with respect to hydrochemistry and biofilm calcification. The waters of the main stream Lutter are derived from the aquifer of the Lower Muschelkalk, whereas the tributary is characterised by an admixture of groundwaters from the Middle Muschelkalk Group. CO_2 degassing of the tributary results in a high supersaturation with respect to calcite, sustaining tufa formation at the cascade at the confluence with the stream Lutter. While top parts of the tufa cascade are currently dominated by poorly calcifying diatom-dominated and green algal biofilms, photosynthesis-induced formation of cyanobacterial tufa stromatolites was only observed at overhanging parts of the cascade. Despite the influx of the highly supersaturated tributary, the calcite supersaturation of the Lutter remains too low to sustain biofilm calcification in the main stream.

Introduction

Calcifying biofilms and associated tufa deposits are widespread in karstic springs and streams world-wide (for review see, e.g., Ford 1989; Ford & Pedley 1996; Pentecost 2005). In Germany, karstic springs and streams concentrate in areas where Devonian, Middle Triassic and Upper Jurassic carbonates crop out. This also applies to the area east of Göttingen, where limestones of the Middle Triassic Muschelkalk Group form the plateau of the eastern shoulder of the Leinetal Graben (von Koenen 1908; Stille 1932). Here, spring waters commonly discharge near main faults of the graben structure or at numerous smaller faults within the plateau, which is underlain by the impermeable claystones of the Lower Triassic Röt Formation.

Tufa formation is commonly considered to reflect inorganic CO_2 degassing of karstic waters and the concomitant rise in pH and calcite supersaturation (e.g., Jacobson & Usdowski 1975; Usdowski et al. 1979), although a number of earlier studies claimed a photosynthetic impact

by cyanobacteria, eukaryotic algae, or mosses (e.g., Wallner 1934; Golubić 1973).

Indeed, microsensor studies have shown that, wherever biofilms cover tufa surfaces and form laminated tufa stromatolites, calcification is controlled by the photosynthetic activity of the cyanobacterial biofilms (Bissett et al. 2008a, 2008b; Shiraishi et al. 2008a, 2008b). However, the relative importance of biofilm-controlled precipitation, abiotic calcite growth on moss of limestone surfaces, and precipitation within the water column probably varies with water chemistry and calcite supersaturation of the different springs and streams.

The aim of the study is to document a tufa stromatolite occurrence and its hydrochemical environment in the backyard of Professor Reitner's stately home in Herberhausen east of Göttingen, and to discuss factors of tufa stromatolite formation at this location.
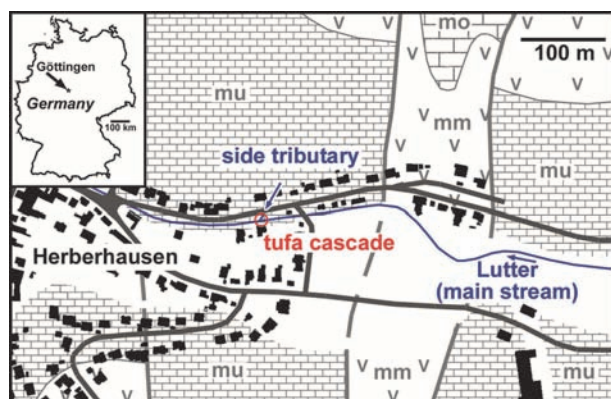

Fig. 1:   Geological map of Herberhausen with the location of the investigated tufa cascade site (arrow). **mu:** Lower Muschelkalk Group, **mm:** Middle Muschelkalk Group, **mo:** Upper Muschelkalk Group. **Black:** Buildings.

Location and geological overview

Herberhausen is a village located 2 km east of Göttingen on the eastern shoulder of the Leinetal Graben (Fig. 1). Here, flat lying to gently west dipping bedded carbonates of the Middle Triassic Muschelkalk Group form a karstic plateau, with the incised Lutter valley in its centre.

A number of minor faults in parallel to the SSW–NNE trending main graben faults transect the plateau. Major parts of the plateau are formed by limestones of the Lower Muschelkalk Group, overlain by dolomitic marlstones and evaporite residual sediments of the Middle Muschelkalk Group and patches of lime- and marlstones of the Upper Muschelkalk Group. Karstic springs are common near the basis of the Muschelkalk Group, where claystones of the Röt Formation form a water-impermeable horizon, at the margin of the Leinetal Graben, where equally impermeable strata of the Keuper and Lias

Groups force groundwaters to discharge near the main faults, and within the plateau, where minor faults cause deviations in groundwater pathways.

The stream Lutter originates about 1 km east of Herberhausen right within the Lower Muschelkalk Group. The spring discharges only seasonally when the water table is high, while a constant water flow is maintained by a number of fault-associated side tributaries. One of these tributaries flows into the Lutter right north of Professor Reitner's home. Here, tufa stromatolites form at a small waterfall into the Lutter, and these are the subject of this study (Fig. 2).

Material and methods

Water samples were either collected in pre-cleaned PE-bottles for the determination of cations, anions, and nutrients or in Schott glass bottles for titration of total alkalinity. Samples for cation analysis were filtered in the field through 0.8 μm membrane filters and fixed by acidification. Samples were stored cool and dark until laboratory measurements. Temperature, electrical conductivity, pH, redox potential, and oxygen were recorded in-situ using portable instruments (WTW GmbH). The pH-meter was equipped with a Schott pH-electrode calibrated against standard buffers pH 7.010 and pH 10.010 (HANNA Instruments). Total alkalinity was determined by acid-base titration immediately after sampling using a hand-held titrator and 1.6 N H_2SO_4 cartridges as titrant (Hach Corporation). Cations (Ca, Mg, Sr, Na, and K) were analysed by ion chromatography with conductivity detection (Metrohm) and anion concentrations (F, Br, Cl, SO_4, and NO_3) were measured by ion chromatography with suppressed conductivity detection (Metrohm). Dissolved phosphate and dissolved silica concentrations were measured by spectrophotometric methods (Unicam). Measured values were processed with the computer program PHREEQC (Parkhurst & Appelo 1999) in order to calculate ion activities, PCO_2 of the water samples, and saturation state with respect to calcite. Hydrochemical model calculations have been carried out using the same program.

Tufa biofilm samples were fixed with PBS (phosphate-buffered saline) buffered 3.7 % formaldehyde for 4–8 h, rinsed with filter-sterilised PBS-buffered sampling site water, and dehydrated in a graded ethanol series. The samples were finally embedded with LR White (LRWhite resin, medium grade; London Resin Company Ltd., Reading, UK) according to the manufacturer's instructions, cut with a saw microtome (Leica) to thickness of 70 μm, mounted on glass slides with Körapox (Kömmerling Chemische Fabrik GmbH, Pirmasens), and sealed by Biomount (ElectronMicroscopy Sciences, Hatfield, PA) and coverslips.
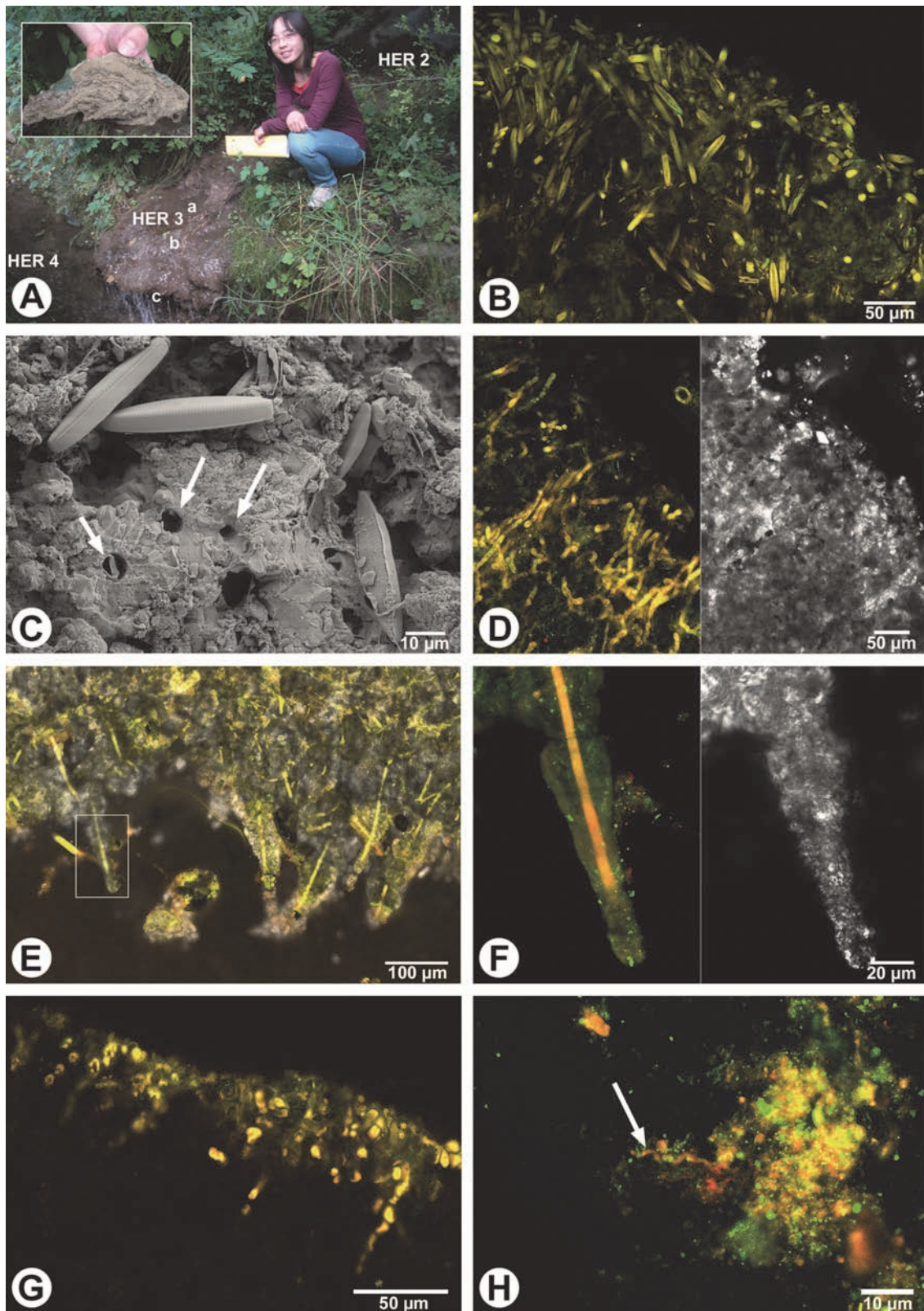
Fig. 2: **(A)** Field image of the Herberhausen tufa cascade with sampling sites HER 2, 3a–c, and 4. Luo Cui for scale. Insert shows tufa stromatolite sample from the overhanging part of the cascade; **(B)** LSM image (ex 488, 543, 633 / em 500–530, 565–615, 640–704) of the diatom biofilm at the top of the tufa cascade (sample HER 3a); **(C)** SEM image of the tufa surface at site HER 3a showing empty cyanobacterial calcite tubes (arrows) and diatoms; **(D)** LSM image (ex 488, 543, 633 nm / em 500–530, 565–615, 640–704 nm) and X Nicols view of a green algal biofilm with poorly calcified Ulvophyceae ("*Gongrosira*" morphotype) at site HER 3b; **(E)** Biofilm composed of calcified cyanobacteria at the overhanging part of the tufa cascade. Overlay of epifluorescence (ex 488, 543, 633 nm / em 500–530, 565–615, 640–704 nm) and X Nicols view. Sample HER 3c; **(F)** Detail of E showing calcite tube enclosing a filament of the *Phormidium incrustatum* morphotype. *Left:* LSM micrograph (ex 488, 543, 633 nm / em 500–530, 565–615, 640–704 nm), *Right:* X Nicols view. Sample HER 3c; **(G)** Endolithic biofilm on a limestone cobble of the stream bed with filaments of the cyanobacterium *Hyella*. LSM micrograph (ex 488, 543, 633 nm / em 500–530, 565–615, 640–704 nm). Sample HER 1; **(H)** Non-phototrophic spirillum-shaped bacterium (arrow) of soft stream bed sediments labelled by oligonucleotide probe EUB-Cy3. LSM micrograph (ex 488, 543 nm, em 500–530, 565–615, 640–700 nm).

Laser scanning microscopy (LSM) of hardpart biofilm sections was carried out using a Zeiss LSM 510 Meta NLO attached to a Zeiss Axiovert 200 M, equipped with an Ar-laser, two HeNe-lasers (Carl Zeiss MicroImaging, Jena). Scanning electron microscope (SEM) imaging was performed with a Zeiss LEO 1530 FE-SEM on platinum-coated samples.

Results and discussion

Hydrochemistry

Four water samples have been analysed: The main stream (HER 1), the side tributary (HER 2 and 3), and the main stream after the influx from side tributary (HER 4) (Table 1, Fig. 2A). All four waters analysed were cool (9.8–12.8°C), supersaturated with respect to calcite, highly oxygenated, and dominated by Ca^{2+} and HCO_3^-, i.e., typical karstic waters.

The stream and its side tributary, however, differed in a number of parameters: Main stream waters prior to mixing with the side tributary, had a lower pH (8.0) and lower concentrations of most cations and anions, except for Sr^{2+} and total alkalinity if compared to the side tributary. Strikingly, Mg^{2+}/Ca^{2+} and Cl^-/SO_4^{2-} ratios were higher in waters of the side tributary. Therefore, while the main stream represents water solely from the Lower Muschelkalk aquifer, the side tributary receives a significant influx of solutes from the dolomite- and gypsum-bearing Middle Muschelkalk Group. The composition of the main stream waters downstream from the side tributary finally reflects a mixing of 5 parts main stream waters with 1 part water from side tributary (Table 1).

Side tributary waters also exhibited a high supersaturation state with respect to calcite (SI_{Cc} = 1.14), higher than that of the main stream (SI_{Cc} = 0.86). Indeed, waters of the side tributary, within a distance of 2 m from site HER 2 to HER 3, exhibit a slight increase in pH and calcite supersaturation, due to CO_2 degassing and temperature increase. Simultaneously, a minor decrease in electrical conductivity EC reflecting a minor drop in Ca^{2+} and total alkalinity indicates an active precipitation of $CaCO_3$ at the tufa site between HER 2 and HER 3. In addition, a minor increase in O_2 was measured, substantiating a photosynthetic activity of the biofilms in the tributary.

Biofilms

Three types of biofilms could be distinguished at the tufa water fall (Fig. 2A): (1) Brownish biofilms dominated by pennate diatoms cover major parts of the top surfaces at the small tufa cascade (Figs. 2B–C). Most abundant are *Navicula veneta* and *Achnanthidium saprophilum*, while representatives of the genera *Nitzschia* and *Cocconeis* occur sporadically only. Calcification in the diatom biofilms is poor, although empty calcite tubes of cyanobacteria were locally observed in the calcite deposits.

(2) Green patches between that show biofilms with abundant, poorly calcified green algae of the Ulvophyceae ("*Gongrosira*" morphotype; see Hodac et al. subm.; Fig. 2D), also associated with diatoms, cyanobacteria and rod-shaped non-phototrophic bacteria.

(3) Overhanging parts of the cascade are characterised by conspicuous blue-green biofilms dominated by calcifying filamentous cyanobacteria of the *Phormidium incrustatum*-morphotype (see Arp et al. 2010) (Fig. 2E). Well developed calcite tubes enclosing the cyanobacterial filaments characterise the surface of this tufa stromatolite (Fig. 2F). In addition, *Pseudoanabaena* and few coccoid cyanobacteria occur.

The stream bed is covered by numerous limestone cobbles from the Muschelkalk Group and soft muddy sediment between them. Green, endolithic biofilms were observed on most surfaces of the limestone cobbles. Thin sections demonstrate that the main endolithic cyanobacterium is *Hyella fontana* (Fig. 2G). Calcite precipitates have not been observed at this site. Soft sediment shows various morphotypes of non-phototrophic bacteria, among them rods and spirillae (Fig. 2H).

Tufa formation

Active precipitation of $CaCO_3$ at the tufa cascade is indicated by the loss of Ca^{2+} and total alkalinity (TA) between the sites HER 2 and 3, associated with a drop in P_{CO_2} from 1549 to 1413 µatm over a distance of 2 m (Table 1). This is in accordance with the view that tufa formation is driven by physicochemical CO_2 degassing (Jacobson & Usdowski 1975; Chen et al. 2004) and externally forced calcite impregnation of the biofilms (e.g., Grüninger 1965; Riding 1991; Spiro & Pentecost 1991; Merz-Preiß & Riding 1999). However, microsensor studies have shown that biofilm photosynthesis controls the formation of laminated tufa deposits, i.e., tufa stromatolites (Bissett et al. 2008a, 2008b; Shiraishi et al. 2008a, 2008b, 2010; Arp et al. 2010), in parallel with calcite precipitation within the water column, driven by CO_2 degassing.

At Herberhausen, the three biofilm samples show different microbial communities and calcification pattern: Diatom dominated communities cover top parts of the tufa cascade and were poorly calcified at the time of sampling. Nonetheless, the tufa carbonate below shows abundant empty casts of former cyanobacterial filaments (Fig. 2C), suggesting a formerly more widespread cyanobacterial biofilm coverage. Green patches between the diatom-covered surfaces at the top side of the cascade also show only few cyanobacteria. Instead, green algae poorly encrusted by calcite dominate these places. The degree of biological control on calcite precipitation remains unclear for these biofilms. The only clear indication of photosynthesis-induced precipitation is provided by the tubular calcite encrustations of filamentous cyanobacteria in the intense blue-green biofilms at the overhanging part of the cascade, where currently major growth of tufa stromatolites occurs.

Table 1: Hydrochemical data of the karstic stream Lutter and its tributary at Herberhausen.

Date 2012/07/02	Sample Description	HER 01 main stream, before tributary	HER 02 tributary, end of tube	HER 03 tributary, tufa cascade	HER 04 main stream, after tributary	mixing 5 parts main stream plus 1 part tributary
$EC_{25°C}$	$\mu S\ cm^{-1}$	672	783	780	688	
pH		7.98	8.21	8.24	8.06	8.02
T	[°C]	9.8	12.6	12.8	10.2	10.3
$p\varepsilon$		8.05	7.45	6.99	5.98	
O_2	$mmol\ L^{-1}$	0.266	0.252	0.255	0.267	
O_2 Saturation	%	96.1	97.0	98.4	96.6	
Ca^{2+}	$mmol\ L^{-1}$	2.97	3.44	3.39	3.05	3.04
Mg^{2+}	$mmol\ L^{-1}$	0.63	0.89	0.89	0.68	0.67
Na^+	$mmol\ L^{-1}$	0.14	0.17	0.17	0.15	0.15
K^+	$\mu mol\ L^{-1}$	29.9	30.2	30.1	29.9	29.9
Li^+	$\mu mol\ L^{-1}$	0.7	1.4	1.3	0.9	0.8
Sr^{2+}	$\mu mol\ L^{-1}$	17.1	8.3	8.4	14.8	15.6
Si	$\mu mol\ L^{-1}$	47.1	70.4	68.8	49.9	50.7
TA	$meq\ L^{-1}$	5.82	5.40	5.28	5.76	5.73
Cl^-	$mmol\ L^{-1}$	0.14	0.26	0.26	0.16	0.16
SO_4^{2-}	$mmol\ L^{-1}$	0.62	1.49	1.49	0.75	0.76
NO_3^-	$mmol\ L^{-1}$	0.13	0.20	0.20	0.14	0.14
F^-	$\mu mol\ L^{-1}$	4.4	10.7	10.7	5.9	5.5
Br^-	$\mu mol\ L^{-1}$	0.2	0.2	0.2	0.2	0.2
PO_4^{3-}	$\mu mol\ L^{-1}$	0.4	0.2	0.2	0.3	0.4
PCO_2	μatm	2818	1549	1413	2344	2570
$SI_{Calcite}$	log IAP/KT	0.86	1.12	1.14	0.95	0.90

Conclusions

(1) Actively calcifying biofilms form tufa stromatolites in the backyard of Prof. Reitner's stately home.

(2) The karstic waters of the side tributary are derived from the Lower Muschelkalk aquifer, with an admixture of groundwater from the Middle Muschelkalk group. The mixing ratio of main stream waters and waters of the tributary at the confluence was 5:1 at the time of sampling.

(3) Similar to other tufa-forming karstic streams, physicochemical CO_2 degassing causes a rise in calcite supersaturation to high values permitting calcite precipitation in the water column and in biofilms of the side tributary. Calcite supersaturation of the main stream is less high, so that endolithic biofilms prevail.

(4) Currently, active photosynthesis-induced cyanobacterial calcification is restricted to the overhanging part of the tufa cascade, where blue-green biofilms cover the tufa stromatolite surfaces. Top parts of the cascade show only poorly calcifying diatom and green algal biofilms.

Acknowledgements

References

Arp, G.; Bissett, A.; Brinkmann, N.; Cousin, S.; Beer, D. de; Friedl, T.; Mohr, K. I.; Neu, T. R.; Reimer, A.; Shiraishi, F.; Stackebrandt, E. & Zippel, B. (2010): Tufa-forming biofilms of German karstwater streams: microorganisms, exopolymers, hydrochemistry and calcification. In: Pedley, H. M. & Rogerson, M. (eds.): Tufas and Speleothems: Unravelling the Microbial and Physical Controls. *Geological Society Special Publication* **336**: 83-118.

Bissett, A.; Beer, D. de; Schoon, R.; Shiraishi, F.; Reimer, A. & Arp, G. (2008a): Microbial mediation of stromatolite formation in karst-water creeks. *Limnology and Oceanography* **53** (3): 1159-1168. http://dx.doi.org/10.4319/lo.2008.53.3.1159

Bissett, A.; Reimer, A.; Beer, D. de; Shiraishi, F. & Arp, G. (2008b): Metabolic microenvironmental control by photosynthetic biofilms under changing macroenvironmental temperature and pH conditions. *Applied and Environmental Microbiology* **74** (20): 6306-6312. http://dx.doi.org/10.1128/AEM.00877-08

Chen, J.; Zhang, D. D.; Wang, S.; Xiao, T. & Huang, R. (2004): Factors controlling tufa deposition in natural waters at waterfall sites. *Sedimentary Geology* **166** (3-4): 353-366. http://dx.doi.org/10.1016/j.sedgeo.2004.02.003

Ford, T. D. & Pedley, H. M. (1996): A review of tufa and travertine deposits of the world. *Earth-Science Reviews* **41** (3-4): 117-175. http://dx.doi.org/10.1016/S0012-8252(96)00030-X

Ford, T. D. (1989): Tufa – the whole dam story. *Cave Science* **16**: 39-49.

Golubić, S. (1973): The relationship between blue-green algae and carbonate deposits. In: Carr, N. E. & Whitton, B. (eds.): *The Biology of Blue-Green Algae*. Oxford (Blackwell): 434-472.

Grüninger, W. (1965): Rezente Kalktuffbildung im Bereich der Uracher Wasserfälle. *Abhandlungen zur Karst- und Höhlenkunde (E: Botanik)* **2**: 1-113.

Hodač, L.; Brinkmann, N.; Mohr, K. I.; Arp, G.; Hallmann, C.; Ramm, J.; Spitzer, K. & Friedl, T. (subm.): Diversity of microscopic green algae (Chlorophyta) in calcifying biofilms of two karstic streams in Germany. *Geomicrobiology Journal.*

Jacobson, R. L. & Usdowski, E. (1975): Geochemical controls on a calcite precipitating spring. *Contributions to Mineralogy and Petrology* **51** (1): 65-74.

Koenen, A. von (1908): *Erläuterungen zur geologischen Specialkarte von Preussen und den Thüringischen Staaten. Blatt No. 28 Göttingen. [2nd ed.].* Berlin (Schropp): 58 pp.

Merz-Preiß, M. U. E. & Riding, R. (1999): Cyanobacterial tufa calcification in two freshwater streams: ambient environment, chemical thresholds and biological processes. *Sedimentary Geology* **126** (1-4): 103-124. http://dx.doi.org/10.1016/S0037-0738(99)00035-4

Parkhurst, D. L. & Appelo, C. A. J. (1999): User's guide to PHREEQC (version 2) – a computer program for speciation, batch-reaction, one-dimensional transport, and inverse geochemical calculations. *U.S. Geological Survey Water-Resources Investigations Report* **99–4259**: 312 pp.

Pentecost, A. (2005): *Travertine.* Berlin (Springer): 445 pp.

Riding, R. (1991): Classification of microbial carbonates. In: Riding, R. (ed.): *Calcareous algae and stromatolites.* Berlin (Springer): 21-51.

Shiraishi, F.; Bissett, A.; Beer, D. de; Reimer, A. & Arp, G. (2008a): Photosynthesis, respiration and exopolymer calcium-binding in biofilm calcification (Westerhöfer and Deinschwanger Creek, Germany). *Geomicrobiology Journal* **25** (2): 83-94. http://dx.doi.org/10.1080/01490450801934888

Shiraishi, F.; Reimer, A.; Bissett, A.; Beer, D. de & Arp, G. (2008b): Microbial effects on biofilm calcification, ambient water chemistry and stable isotope records (Westerhöfer Bach, Germany). *Palaeogeography, Palaeoclimatology, Palaeoecology* **262** (1-2): 91-106. http://dx.doi.org/10.1016/j.palaeo.2008.02.011

Shiraishi, F.; Okumura, T.; Takahashi, Y. & Kano, A. (2010): Influence of microbial photosynthesis on tufa stromatolite formation and ambient water chemistry, SW Japan. *Geochimica et Cosmochimica Acta* **74** (18): 5289-5304. http://dx.doi.org/10.1016/j.gca.2010.06.025

Spiro, B. & Pentecost, A. (1991): One day in the life of a stream – a diurnal inorganic carbon mass balance for a travertine-depositing stream (Waterfall Beck, Yorkshire). *Geomicrobiology Journal* **9** (1): 1-11. http://dx.doi.org/10.1080/01490459109385981

Stille, H. (1932): *Geologische Karte von Preußen und benachbarten deutschen Ländern. Erläuterungen zu Blatt Göttingen Nr. 2520. [3rd ed.].* Berlin (Preußische Geologische Landesanstalt): 40 pp.

Usdowski, E.; Hoefs, J. & Menschel, G. (1979): Relationship between ^{13}C and ^{18}O fractionation and changes in major element composition in a Recent calcite-depositing spring – A model of chemical variations with inorganic $CaCO_3$ precipitation. *Earth and Planetary Science Letters* **42** (2): 267-276. http://dx.doi.org/10.1016/0012-821X(79)90034-7

Wallner, J. (1934): Über die Beteiligung kalkablagernder Pflanzen bei der Bildung südbayrischer Tuffe. *Bibliotheca Botanica* **110**: 1-30.

Following the traces of symbiont bearing molluscs during earth history

Anne Dreier[1,2] * & Michael Hoppert[1,2]

[1]Institute of Microbiology and Genetics, Georg-August University Göttingen, Grisebachstr.8, 37077 Göttingen, Germany;
Email: anne.dreier@geo.uni-goettingen.de
[2]Courant Centre Geobiology, Geoscience Centre, Georg-August University Göttingen, Goldschmidtstr. 3,
37077 Göttingen, Germany

* corresponding author

Ivan E. Wallin (1883–1969) was among the first scientists who noticed the evolutionary impact of symbiotic events. He proposed that endosymbiosis was the principal source for speciation (Wallin 1927). Mitochondria and chloroplasts as symbiotic descendants of bacteria in a eukaryotic cell are the well-known and most important endosymbiotic key players, enabling and shaping the evolution of eukaryotes. In addition, a multitude of other symbioses between prokaryotes and Eukarya have been described so far. As an example, symbiosis between molluscs and sulphur- or methane-oxidising bacteria, is a widespread lifestyle in marine habitats (and perhaps yet undetected for other environments). These symbiotic associations occur worldwide at oxic–anoxic interfaces such as at the boundary layer of reducing sediments, in cold seeps, in hydrothermal vents or in mangrove peat. The symbiosis between marine molluscs and chemosynthetic bacteria increase the metabolic capabilities and therefore the possibilities to occupy ecological niches of both host and symbiotic prokaryote. Nowadays, due to molecular analyses and in situ hybridisation techniques, detection of symbioses in recent living organisms is not that difficult. But finding a path back to the point in Earth's history were symbiotic events took place is a tricky challenge. Not long ago only analyses of morphological features of shells and facies criteria were available for assessment of the lifestyle and the diet of extinct bivalves. Close phylogenetic relationships to recent symbiont bearing genera in a similar habitat make it likely that the extinct genera exhibited a similar lifestyle, but these indirect criteria are not sufficient to uncover ancient symbiosis in molluscs. In this review several approaches of "molecular palaeontology" are discussed, which allow for a direct determination of a symbiotic or non-symbiotic lifestyle in recent and fossil molluscs.

Introduction

"It is concluded that the evolutionary potential of symbiosis is great and that symbiosis serves as a supplementary speciation mechanism capable of producing directed evolutionary changes" (Taylor 1979). This conclusion may be particularly true for bivalves: bacteria and marine molluscs, often form mutualistic partnerships which markedly influence the physiology, ecology and evolution of both.

Autotrophic bacteria assimilate inorganic carbon as primary carbon source. The bacterium is chemoautotrophic when reducing power and energy needed for as-

similation of carbon dioxide derives from reduced inorganic compounds. The other important energy source is sunlight for photoautotrophic organisms. Chemoautotrophic or methanotrophic bacteria are found in a wide range of reducing habitats providing these coveted energy sources, in particular H_2, H_2S or CH_4. Most prominent sites are cold seeps and hydrothermal vents, but dysoxic conditions are frequent in marine environments, such as in seagrass beds, mangrove sediments or wood and whale falls. These habitats of free living autotrophic or methanotrophic bacteria are usually also inhabited by molluscs hosting symbiotic chemoautotrophs or methanotrophs (Lonsdale 1977; Corliss et al. 1979; Jannasch & Wirsen 1979; Van Dover 2000; Treude et al. 2009; Kiel & Tyler 2010). Though also bacteria of other metabolic types are symbionts of marine invertebrates, most of them are sulphur-oxidiser or methanotrophs belonging to the Gammaproteobacteria. According to phylogenetic analyses these symbioses have been established multiple times in earth history and evolved independently (Dubilier et al. 2008).

Several marine molluscs, especially some species of Cephalopoda, Gastropoda and Bivalvia, are known to cultivate symbiotic microbes. The basic feature of this relationship is that the symbionts need reduced substrates and electron acceptors for their metabolism, which do not occur in the same microenvironments (Zhang & Millero 1993). The molluscs are able to bridge the oxic–anoxic boundaries using behavioral, morphological or metabolic adaptations and supply substrates (e.g., reduced sulphur compounds) and electron acceptors (oxygen in most cases) to the microbes. In turn, most if not all organic carbon and also nitrogen compounds are provided by the symbiont (Cavanaugh et al. 2006; Dubilier et al. 2008).

Photosymbiosis is most successful in oligotrophic water under nutrient-limited conditions (Hallock & Schlager 1986; Hallock 1987; Schlager 2003). Eukaryotic algae of the genus *Symbiodinium* (zooxanthellae) are the most prevalent symbionts of molluscs. The zooxanthellae satisfy a major part of the host's energy demand (Trench et al. 1981; Klumpp et al. 1992; Hawkins & Klumpp 1995). In turn, zooxanthellae cover their nitrogen and phosphate demands mainly through their host's excretion products. Multiple studies provided insight into symbiont-host interaction, their metabolic features and how symbiotic partners are adapted to each other. Various approaches like 16S ribosomal DNA sequence analysis, fluorescence in situ hybridisation, transmission electron microscopy, stable isotope and fatty acid analysis were applied so far (Kharlamenko et al. 1995; McKenzie et al. 2000; Colaco et al. 2007). However, studies aiming at reconstruction of evolution of symbiotic molluscs were based on comparison of shell morphologies or were conducted in specific palaeoenvironments like vents and seeps (Fig. 1).

In order to get a better understanding of the evolutionary steps and to give an estimate for the time point when a representative of a mollusc taxon starts its cooperation with microbes and shifts its diet to chemo- or phototrophic we need to detect a direct symbiotic fingerprint of the investigated fossil. These fingerprints or biosignatures must be stable in geological timescales.
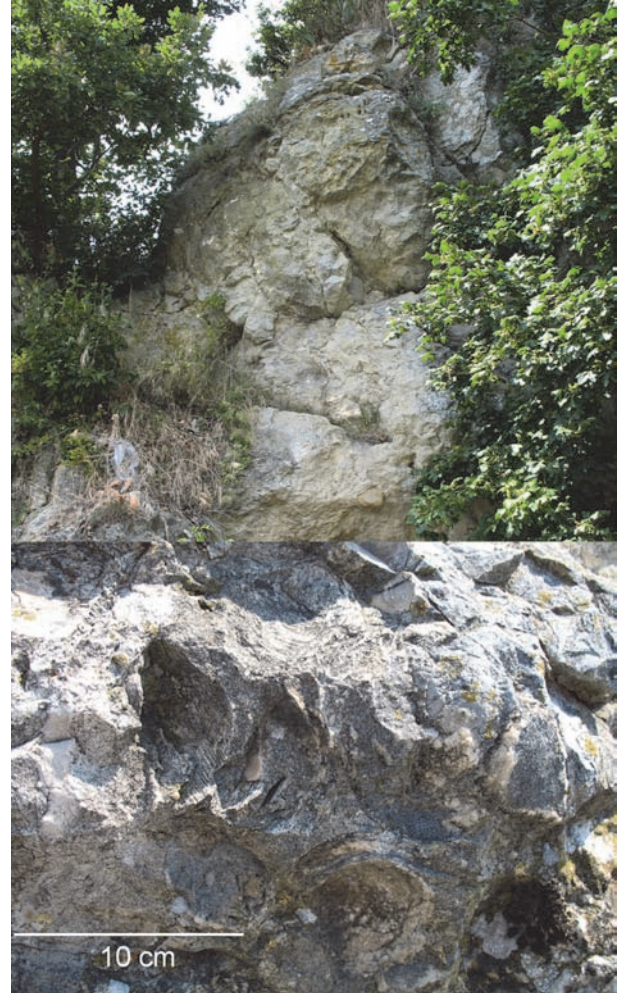
Fig. 1:   Late Miocene seep at Montepetra (Italy) with a mass occurrence of lucinid clams (Heterodonta: Lucinoida).

Endosymbiotic molluscs

Recent situation

Within the clades of recent molluscs, endosymbiosis with sulphur- or methane-oxidising (chemosynthetic) bacteria occur in seven bivalve families: Solemyidae, Nucinellidae, Montacutidae, Mytilidae, Thyasiridae, Lucinidae (being the most diverse familiy), Vesicomyidae (Taylor & Glover 2009, 2010; Taviani 2011, and references therein; Taylor et al. 2011; Oliver et al. 2013). In addition, the Teredinidae are known to harbour endosymbiotic cellulose-digesting symbionts (Distel et al. 2002).

The symbiosis seems to be obligate in all species of Lucinidae, Vesicomyidae and Solemyidae, while some species of Thyasiridae and Mytilidae are asymbiotic. Their life styles are highly diverse, ranging from epifaunal to deep infaunal (Taylor & Glover 2010). Lucinids occur also in the deep sea at cold seeps (Callender & Powell 1997), hydrothermal vents (Glover et al. 2004) and wood or whale falls (Dubilier et al. 2008). Though they appear to be rare on such sites, Kiel & Tyler (2010) stated that this might be a sampling artifact. Nevertheless, the more common molluscs of deep-sea habits are all three families of chemosynthetic gastropods, bathymodiolian mussels, vesicomyid clams and solemyids (Dubilier et al. 2008; Kiel & Tyler 2010).

A symbiotic relationship to chemosynthetic bacteria is also known from three gastropod families (Provannidae, Lepetodrilinae and Peltospiridae) and from one family of the Aplacophora (Simorthiellidae, Dubilier et al. 2008). These organisms are all inhabitants of deep sea seep and vent sites.

Deep sea hydrothermal vents with their rich and constant supply of reduced inorganic compounds are perfect niches for a chemosynthetic lifestyle, which leads to mass development of chemosymbiotic molluscs in such environments. They are less abundant in the photic zones. The primary production in shallow water is driven by phototrophy and is usually dominated by heterotrophic communities; however, in some cases chemosymbionts could also dominate in shallow water (Dando & Southward 1986; Little et al. 2002; Tarasov et al. 2005). Though, the role of chemosynthetic molluscs in shallow water systems like coral reef sediments, seagrass meadows or mangrove sediments is not that unimportant. The evolutionary radiation of Lucinidae, for example, seems to be linked to the emergence of seagrasses in the late Cretaceous (Heide et al. 2012; and references therein). Lucinids are very important for the stability of seagrass systems, because they detoxify the surrounding sediment from sulfide and lead to oxygenation, with a not negligible effect on seagrass (Heide et al. 2012). The highest diversity of recent Lucinidae was described for tropical reefal habitats (Glover & Taylor 2007); also some solemyids (Krueger et al. 1996) and thyasirids (Dubilier et al. 2008) occur in this environment as well as some photosynthetic Cardiidea and Tridacnidea.

Some bivalve species within the Trapeziidae and Cardiidea (Fig. 2) maintain symbiotic associations with *Symbiodinium* (Yonge 1936; Kawaguti 1950, 1968, 1983; Purchon 1955; Stasek 1961; Hartman & Pratt 1976; Jacobs & Jones 1989; Jones & Jacobs 1992; Ohno et al. 1995; Persselin 1998; Vermeij 2013). These bivalves exhibit specific characteristics of soft body but also microstructural and macroscopic adaptations in shell morphology. Tridacnidea have very large and thick shells, others exhibit semitransparent shells; all adaptations should improve the exposure of the mantle to sunlight (ref. above).
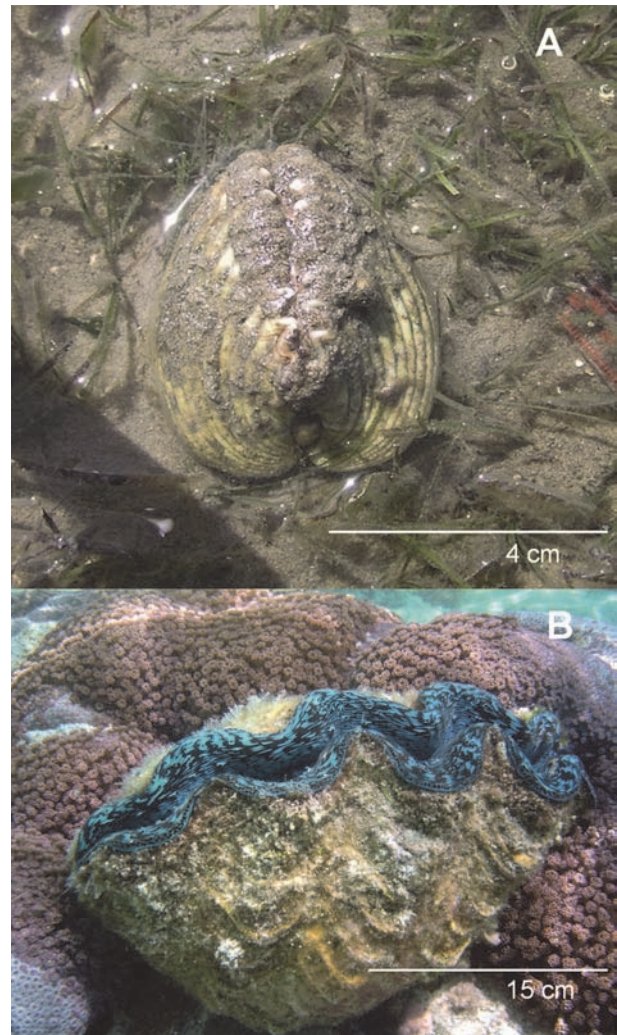
Fig. 2:   Two phototrophic bivalves in their natural habitats. **(A)** *Fragum unedo* (Heterodonta: Veneroida: Cardiidae) – mud flat of North Stradbroke Island, Queensland, Australia, and **(B)** *Tridacna maxima* (Heterodonta: Veneroida: Cardiidae) – coral reef of One Tree Island, Queensland, Australia.

Symbiont-bearing invertebrates in earth's history

Ancient shelled molluscs have a rich and well-documented fossil record; they are confirmed since the early Cambrian (Goedert & Squires 1990; Peel 1991; Gubanov et al. 2004; Vinther & Nielsen 2005; Skovsted et al. 2007; Kiel & Tyler 2010). The common method to detect ancient symbioses in some fossil bivalves/molluscs is based on structural features of their shells, e.g., the imprints of the elongated anterior adductor muscle and pallial blood vessels in the shells. In addition, palaeohabitat occupation patterns give important hints for symbiotic life styles (Taylor & Glover 2000; Amano et al. 2007). Indirect tools to date back symbiotic molluscs evolution (estimated molecular age) are molecular clocks (Baco et al. 1999; Shank et al. 1999; Distel et al. 2000; Kano et al. 2002). Upcoming direct molecular tools are biogeochemical analyses of biosignatures which are described in detail below.

The longest fossil record and hence the oldest supposed symbiotic bivalves are the Lucinidae and Solemyidae. The existence of fossil Solemyidae dates back to the Ordovician (Kiel & Tyler 2010), Lucinidae first appear during the Silurian (Taylor & Glover 2006). It was suggested that symbiotic relationship of both groups are ancient (Taylor & Glover 2000, 2006; Taylor et al. 2008). Thyasirids are possibly much younger; they were first described from the Early Cretaceous and were found at seeps and wood falls, which indicates possible symbiotic lifestyle (Kiel et al. 2008a, Kiel & Dando 2009). Vesicomyids are also associated with seep deposits from the beginning of their appearance in the Middle Eocene; from the Late Eocene onwards they could be found in large numbers at vents and seeps (Kiel & Tyler 2010 and references therein). Bathymodiolins also appear in the Middle to Late Eocene (Goedert & Squires 1990; Squires & Goedert 1991; Taviani 1994; Kiel & Goedert 2006a; Kiel & Little 2006). All of these fossil molluscs had recent relatives, thus an ancient symbiotic lifestyle of their ancestors living in similar environments was deduced (e.g., Goedert & Squires 1990; Taviani 1994; Goedert & Campbell 1995; Peckmann et al. 1999, 2002, 2004; Goedert et al. 2003; Gill et al. 2005; Majima et al. 2005; Campbell 2006; Kiel & Little 2006; Kiel & Peckmann 2007).

Inoceramidae disappeared at the end of Cretaceous (Dhondt 1983) and were first known from the Permian (Cramton 1988). Some authors also speculated about chemosynthetic or even photosynthetic lifestyles of some inoceramid species (MacLeod & Hoppe 1992).

The Cardiidea have a fossil record dating back to the Late Triassic (Keen 1980; Morton 2000; Coan et al. 2000; Schneider & Carter 2001). Recent members of Cardiidea with photosynthetic lifstyle like *Fragum* have a fossil record that dates back to Miocene/Holocene (Keen 1980), Tridacnids proliferate since the Eocene (Romanek et al. 1987). Futhermore, for the Neogen bivalve *Mercenaria "tridacnoides"* (Jones et al. 1988) for rudists and some other fossil bivalves a photosymbiotic lifestyle was postulated (Kauffman 1969; Philip 1972; Vermeij 2013).

It was speculated about symbiotic relationships in some extinct non-bivalve species like brachiopods which were associated with chemosynthesis-dominated environments in their fossil record (Sandy 2010) and even photosymbiosis was postulated for some fossil rostroconchia and brachiopods (Cowen 1970, 1982; Vermeij 2013). Fortey (2000) reported that olenid trilobites (Late Cambrian/Ordovician) lived under oxygen-poor and sulphur-rich conditions at the sea floor. Reduced oral structures and extended pleural areas were interpreted as an indication for a symbiotic relationship with sulphur bacteria.

Also fossil members of gastropods inhabiting chemosynthetic ecosystems, e.g., Provannids date back to the Late Cretaceous (Kiel & Tyler 2010).

Though fossil deep-sea chemotrophic molluscs are relatively well-documented, not much attention is given to the non-seep related shallow water chemo- or phototrophic molluscs. At seep and vent sites the epifaunal molluscs densely colonise the habitat. Detecting fossil endosymbiosis in shallow water molluscs by using biogeochemical techniques has an advantage that possibly different heterotrophic molluscs co-occur in the same substrate. Comparing different species in the same habitat gives a better indication of which might have had symbiotic associations with chemosynthetic bacteria or maybe phototrophic dinoflagellates. In the evolution of bathymodiolid bivalves, it was expected that the ancestors of this modern deep-sea mussels live in shallow water reducing sediments. Thus it is possible that "the first contact" between free-living chemosynthetic bacteria and heterotrophic bathymodiolids did not start in the deep-sea but in shallower marine environments (Duperron 2010). It will be really interesting to support these hypotheses by analysis of biosignatures. In shallower water habitats the probability to find fossils of definitive non-symbiotic molluscs among the putative symbiotic ancestor of bathymodiolids is much greater than at fossil seep and vent deposits. Here, it is possible to compare biosignatures of shell-fossils from different species of the same location, to evaluate their lifestyles (see below).

Molecular markers in tissue of chemo-symbiotic *vs.* heterotrophic bivalves

Prokaryotes are inhabitants of this planet long before the raise of eukaryotes and metazoans and consequently "invented" most of the biochemical key processes. They are the only organisms capable of primary energy production like chemosynthesis and photosynthesis; fixation of molecular nitrogen is unique to prokaryotes. Thus, all other living organisms are able to perform primary production only with support of their ancient or current endosymbiotic associations with prokaryotes. In any case, metazoans whose major diet is based on their autotrophic symbionts are closer to the bottom of the food chain than metazoans without relationship to such microbes. Some of the symbiotic bacteria in molluscs are located within specialised gill cells, so-called bacteriocytes. In other cases the bacteria are attached extracellularly at the gill tissue (Dubilier et al. 2008; Duperron 2008; Southward 2008).

Fluids, rich in oxygen and sulfide or methane, are drawn into the gill and are absorbed by the bacteriocytes. Furthermore, it was reported that *Calyptogena* use their foot to dig for sulfide in the sediment and then use specific transport proteins which transfer sulfide to symbionts in the gill tissue (Zal et al. 2000).

The majority of phototrophic symbionts, the zooxanthellae, are located within mantle tissue, sometimes within the gill filaments of the host bivalve (Yonge 1981), so that the symbionts are exposed to sunlight.

How may the lifestyle of symbiont bearing molluscs lead to identifiable features or even "patterns", identifiable in the fossil record?

In case that the major nutrients (carbon, nitrogen and sulphur) of molluscs derive from their prokaryotic symbionts, the host biomass is based on molecules built by the prokaryotic metabolism. In contrast, heterotrophic molluscs filter out or graze off particulate organic matter from their surrounding environment. Thus, search for fingerprints specific for either heterotrophic or chemo- and phototrophic molluscs must consider autotrophic and/or nitrogen metabolism of the symbionts.

Carbon fixation

Apart from the cellulose-degraders in Teredinidae and methanotrophs, all prokaryotic symbionts fix inorganic carbon autotrophically. The common pathway for CO_2 fixation in chemo- as well as in phototrophic symbionts is the Calvin-Benson cycle (Herry & Le Pennec 1989; Duperron & Fiala-Médioni 2007; Dreier et al. 2012). The key enzyme of this pathway is ribulose 1,5-bisphosphate carboxylase/oxygenase (RubisCO). RubisCO catalyses the fixation of $^{12}CO_2$ slightly faster than fixation of $^{13}CO_2$ (Purich & Allison 2000). This selection leads to an enrichment of ^{12}C in the biomass relative to ^{13}C (negative $\delta^{13}C$ value). The host obtains the organic carbon from its symbionts (Fiala-Médioni & Felbeck 1990; Childress & Fisher 1992), hence $\delta^{13}C$ ratios of host tissue reflect the carbon source. Mentionable is the fact that ^{13}C depletion by chemoautotrophic bacteria using the Calvin-Benson cycle for CO_2 fixation is higher than in photosynthetic algal organisms, because of different specificities of RubisCO form I and II enzymes (Ruby et al. 1987; Blumenberg 2010; see Table 1). Moreover, these distinct forms of RubisCO have been also described for chemoautotrophs (Robinson & Cavanaugh 1995). They show that form I RubisCO is expressed by the symbionts of *Solemya velum* and *Bathymodiolus thermophilus,* exhibiting relatively low $\delta^{13}C$ ratios, whereas form II RubisCO is expressed in the tubeworms *Riftia pachyptila* and *Tevnia jerichonana* with higher $\delta^{13}C$ ratios (Childress & Fisher 1992). However, the $\delta^{13}C$ ratios are also influenced by the ratios of source carbon (CO_2) and by translocation of carbon during uptake and transport from symbiont to host (Scott et al. 2004).

Symbionts that oxidise methane are related to type I methanotrophs within the Gammaproteobacteria (Petersen & Dubilier 2009). Methane serves as electron donor as well as carbon source. Biogenic methane exhibits highly $\delta^{13}C$ depleted signatures (Sugimoto & Wada 1995; Zyakun 1996). Type I methanotrophs use the ribulose monophosphate pathway for carbon fixation (Leak et al. 1985) and preferentially consume $^{12}CH_4$ which leads to a further depletion in $\delta^{13}C$ values (Coleman et al. 1981; Grossman et al. 2002).

In summary, $\delta^{13}C$ values of tissue from molluscs which harbor, chemoautotrophs and/or methanotrophs ("primary producers") are all significantly depleted relative to molluscs at higher trophic levels. This depletion pattern should also be expected for tissue of phototrophic molluscs

Nitrogen assimilation

The main nitrogen sources of bacterial biomass and hence host tissue in chemoautotrophic symbioses are ammonia (NH_4^+) and nitrate (Johnson et al. 1988; Conway et al. 1992; Lilley et al. 1993; Lee & Childress 1994; Lee et al. 1999). Ammonia and nitrate are used by bacteria for biosynthesis of amino acids and other nitrogen compounds (Payne 1973; Reitzer & Magasanik 1987). Molluscs receive their amino acids from their diet (e.g., Neff 1972), which is in case of chemosymbiosis mainly based on biomolecules from the symbionts.

Isotopic fractionation of nitrogen may occur during uptake and incorporation of nitrogen by bacterial symbionts (Hoch et al. 1992; Yoneyama et al. 1993; Dreier et al. 2012). Methane-oxidising bacteria, for instance, prefer assimilation of $^{14}NH_3$ (Lee & Childress 1994). Independent of the pathway of nitrogen assimilation, it is known that $\delta^{15}N$ ratio increases by about 3.4 ‰ per trophic level (Minagawa & Wada 1984; Peterson & Fry 1987). Accordingly, primary producers must show lower $\delta^{15}N$ in tissue than their consumers (Conway et al. 1989; Conway et al. 1992; Lee & Childress 1994; Colaco et al. 2002; Dreier et al. 2012).

Sulphur oxidation

Thiotrophic endosymbiosis is most common among molluscs (see above). Their energy source is sulfide, which originates from abiogenic reduction of sulfate or from microbial sulfate reduction (Kaplan et al. 1963; Aharon & Fu 2000; Joye et al. 2004). Sulfide in sediments mostly derives from microbial sulfate reduction; both biogenically and abiogenically generated sulfide is depleted in $\delta^{34}S$ (Kaplan et al. 1963; Kiyosu & Krouse 1993; Aharon & Fu 2000; Joye et al. 2004). The pathway of sulphur oxidation does not lead to a significant fractionation of sulphur isotopes. The depleted sulfide from sediment is possibly not just used as an energy source but is also assimilated by sulfide-oxidising symbionts and incorporated in their biomass (Dreier et al. 2012). In contrast, the sulphur compounds of non-thiotrophic molluscs derive from sea-water sulfates with $\delta^{34}S$ ratios being markedly different from that of sulfides in sediments (Kaplan et al. 1963; Trust & Fry 1992; Michener & Schell 1994).

Table 1: Some δ¹³C values of different chemoautotrophic symbioses and corresponding isotopic discrimination of different carbon fixing pathways (compiled after Roeske & O'Leary 1984; Brooks et al. 1987; Conway et al. 1989; Fisher 1990; Kennicutt et al. 1992; Guy et al. 1993; Goericke et al. 1994; Robinson & Cavanaugh 1995; Cavanaugh & Robinson 1996; Van Dover et al. 2003; Scott et al. 2004; Van Dover 2007).

δ¹³C	Organisms	Carbon assimilation	¹²C enrichment
-30 ‰ to -34 ‰	Bivalves with chemoautotrophic symbionts	CO_2 to organic C (RubisCO form I)	22–30 ‰, (24.4 ‰, form IA)
-8.8 ‰ to -16 ‰	Hydrothermal vent vestimentiferan tubeworms with chemoautotrophic symbionts	CO_2 to organic C (RubisCO form II)	18–23 ‰
-18 ‰ to -28 ‰	Phytoplankton	CO_2 to organic C (supposed RubisCO form IB)	22–30.3 ‰
-39.3 ‰ (thermogenic CH_4) to -76.0 ‰ (biogenic CH_4)	Bivalves with methanotrophic symbionts (in some cases additional chemoautotrophic symbionts)	CH_4 to organic C	5–30 ‰

Thus δ³⁴S ratios of biomass from thiotrophic molluscs are higher depleted than ³⁴S ratios of non-thiotrophic molluscs (Mizota & Yamanaka 2003; O'Donnell et al. 2003; Mae et al. 2007; Dreier et al. 2012).
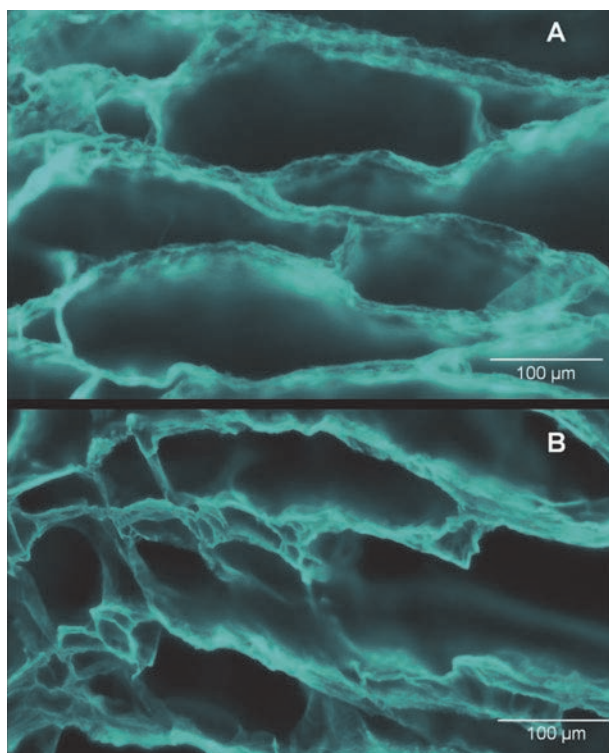

Fig. 3: Chitin staining of a cross section of *Tridacna maxima* decalcified shell. **(A)** Recent, One Tree Island, Queensland, Australia; **(B)** Pleistocene, north of Dahab, Sinai, Egypt. Cross sections were stained with Calcofluor White.

In summary, the isotopic compositions of the biological elements carbon, sulphur and nitrogen in biomolecules from host tissue are excellent biosignatures, providing information about an animal's diet and trophic level (Michener & Schell 1994; Casey & Post 2011). However, in order to determine diet of fossil molluscs, preserved biomolecules are needed. Here one may take benefit from the mineralised mollusc shells, which are perfect long term conservation wrappings for organic matter.

Different biosignatures and stability over geological timescales

Various techniques are used to detect symbiotic prokaryotes in mollusc tissue, such as 16S ribosomal DNA sequence analysis, fluorescent *in situ* hybridisation and transmission electron microscopy.

After death, soft tissue is degraded and only shells are left for incorporation into the fossil record. Mollusc shells are mainly composed of calcium carbonate in aragonite and calcite conformation; these crystals are formed between organic matrix layers. Frémy (1855) was the first who described conchiolin, the acid insoluble organic matrix in shells. Later, high proportions of acidic amino acids Asx (Asp+Asn) were found in soluble shell organics. X-ray/electron diffraction revealed matrix-crystal spatial relations protein structure (β-sheet), and the presence of chitin (Weiner & Traub 1980; Weiner et al. 1983).

Recent studies about shell proteins imply that the organic shell matrix is composed of a macromolecular framework consisting of a chitin-silk fibronin gel with acidic proteins (e.g., Marin & Luquet 2007; Evens 2008; Marin et al. 2008). To demonstrate the presence of chitin in shells, staining with the fluorescence dye Calcofluor White may be performed, which binds to cellulose and chitin. Obviously, also the remaining organic shell matrix of fossil shells could be stained. This could be a hint for the persistence of these biomolecules in the shell matrix. Fig. 3 shows a stained cross section of *Tridacna maxima* shells (recent and fossil) embedded in LR white resin. The cross section was decalcified with 0.5 M EDTA over night and then stained with Calcofluor White. To exclude unspecific binding to embedding resin, an untreated (unfixed, not embedded) piece of *Tridacna maxima* shell was decalcified and stained with Calcofluor White (Fig. 4). It is obvious that the Calcoflour-stained material in the fossil shell of *Tridacna maxima* (Fig. 4C) is different from the filamentous structure in the modern shell (Figs. 4A, 4C).

In addition, a cross section of a fossil (Upper Cretaceous) *Inoceramus* sp. shell was stained with Calcofluor White. Treatment of cross section was identical to that of *Tridacna* but without decalcification. Fig. 5 shows that maybe fossil chitin was stained between the calcium carbonate crystals of the *Inoceramus* sp. shell.

The preserved biomolecules of the shell will provide information about the mollusc's diet. In endosymbiont-bearing molluscs, carbon, nitrogen and sulphur are taken up by the symbionts, get an isotopic fingerprint and are then incorporated in mollusc biopolymers (see above). Since the remains of the organic shell matrix are preserved after death, stable isotope analysis of the matrix serves as valuable screening tool for detecting symbiotic association in living as well as in fossil molluscs. In many studies $\delta^{13}C$, $\delta^{15}N$ and sometimes $\delta^{34}S$ in soft tissue were determined in order to analyze dietary intake (Kennicutt et al. 1992; Dando & Spiro 1993; Conway et al. 1994; Dando et al. 1994; Fischer 1995; Colaco et al. 2002; Lorrain et al. 2002; Dattagupta et al. 2004; Carlier et al. 2007, 2009). However, only few studies describe these isotopic fingerprints with respect to the organic matrix of recent and fossil shells (O'Donnell et al. 2003; Mae et al. 2007; Dreier et al. 2012). Only the study by Dreier et al. provides $\delta^{34}S$ values of the organic matrix of empty shells from recent bivalves and subfossil (Late Pleistocene) shells.

It was shown that sulphur isotopes are not useful markers to detect ancient the thiotrophic lifestyle, because after death of the molluscs $\delta^{34}S$ values in the organic matrix will decrease. It was assumed that the reason could be the instability of sulphur-containing amino acids (Jones & Vallentyne 1960) or sulfides derived from proteolysis and from bacterial sulfate reduction during soft tissue degradation. New results confirm the latter hypothesis: the non-symbiotic bivalve *Venerupis aurea,* which was used in the study of Dreier et al. (2012), was degraded in original sediments under laboratory conditions in an aquarium. After

half a year the shells were analyzed and $\delta^{34}S$ as well as C/N ratios were measured. The C/N ratio is an expression for the grade of alteration and decay of the organic shell matrix (Ambrose 1994). The C/N ratio of the artificial degraded shells of *Venerupis* slightly increased from 3.15 (fresh shell) to 3.27 (degraded half a year), the $\delta^{34}S$ ratio dropped slightly from 7.8 ‰ to 7.5 ‰. Longer resting time in the sediment is needed to futher decrease the $\delta^{34}S$ ratio further (Dreier et al. 2012).
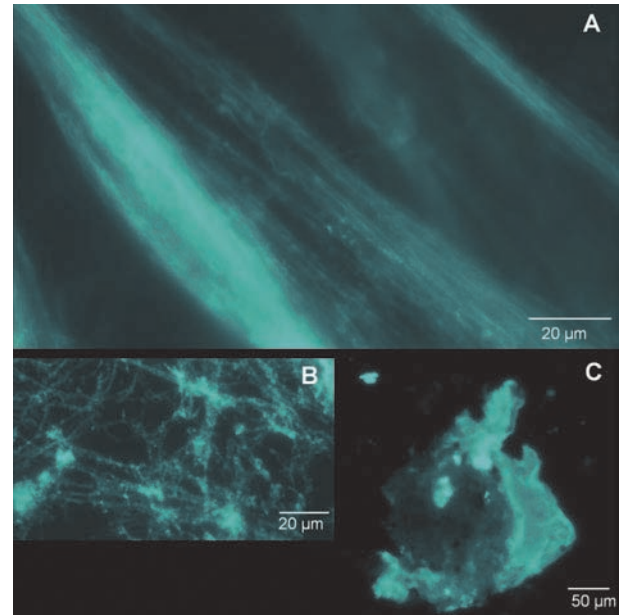
Fig. 4: Chitin staining of decalcified piece of *Tridacna maxima* shell. **(A–B)** Recent, One Tree Island, Queensland, Australia, filament like structures are visible; **(C)** Pleistocene, north of Dahab, Sinai, Egypt, no filaments could be detected. Cross sections were stained with Calcofluor White.
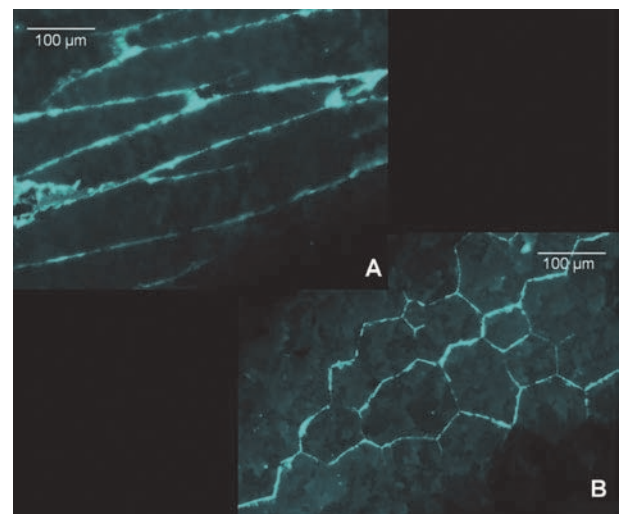
Fig. 5: Chitin staining of a section of fossil (Upper Cretaceous of the quarry Dammann South, Söhlde, Germany) *Inoceramus* sp. (Heterodonta: Veneroida: Cardiidae) shells. **(A)** Longitudinal section of shell stained with Calcofluor White. **(B)** Cross section of the same shell.

The enrichment of sulfides during degradation of soft tissue may be the cause of the framboidal pyrite formation (Fig. 5; Berner 1984; Wilkin 1995) and for the decreasing $\delta^{34}S$ ratio of shells after death.

Lipids are another prominent group of biochemical markers, which are analyzed to identify symbiosis in molluscs. Fatty acids as main building blocks of lipids have a characteristic distribution pattern. Short-chained monounsaturated fatty acids (MUFA) are of mainly prokaryotic origin (Bishop 1976) whereas the major component of eukaryotic lipids consist of long-chained polyunsaturated fatty acids (PUFA; Shaw 1974). Their specificity and structural diversity make them to important trophic biomarkers in marine ecology (Gehron & White 1982; Parkes & Taylor 1983; Guckert et al. 1985; Sargent et al. 1987; Wakeham & Canuel 1988; Findlay et al. 1990; Sargent et al. 1990; Bradshaw et al. 1991; Hopkins et al. 1993; Rajendran et al. 1993).

Lipids were also used to characterise symbiotic associations between prokaryotes and marine invertebrates (Berg et al. 1985; Conway & Capuzzo 1990, 1991; Ben-Mlih et al. 1992; Zhukova et al. 1992; Cobabe & Pratt 1995; Fullarton et al. 1995). In molluscs the lipid content depends on dietary lipid intake (Moreno et al. 1980; Piretti et al. 1987), thus lipid content of molluscs with autotrophic symbionts will reflect a diet based on the symbionts. It is known from bivalve shells that they contain lipids like fatty acids, cholesterol, phytandienes, ketones and sometimes *n*-alkanes. Lipids are geologically stable which make them well-suited for paleontological approaches. In addition, lipids have low solubility in water at low temperatures; hence in early diagenesis the level of contamination from surrounding pore fluids and the migration of lipids out of the shell is low. As mentioned above, the carbon of symbiont-derived compounds is depleted in $\delta^{13}C$, furthermore it is known that lipid carbon was found to be depleted by 3 ‰ relative to their dietary carbon (DeNiro & Epstein 1977; Crenshaw 1980). Consequently, $\delta^{13}C$ ratios of most molluscs shell-lipids may reflect if they are symbiont-bearing or not. Cobabe & Pratt (1995), Conway & Capuzzo (1991) and Dreier et al. (2012) found some fatty acids of chemotropic bivalves to be more depleted in $\delta^{13}C$ relative to heterotrophic bivalve. Lipids from fossil shells of two bivalve species about 1.4 million years old show a fatty acid distribution very similar to modern shells (with differences in their relative abundance; Cobabe & Pratt 1995). However, $\delta^{13}C$ values of fossil shell lipids have been not reported so far.

Future perspectives

In the light of recent climatic and global changes it will be more and more important to reconstruct environmental conditions of the past. Especially the marine environment represents an important climatic driving force and changing conditions could be recognised by a change in the benthic ecosystem. Today the stability of many ecosystems is in danger, also because of the breakdown of symbiotic interactions, just considering e.g. bleaching events in coral reefs (Carpenter et al. 2008).

Chemosymbiotic species are major players at oxic-anoxic interfaces of the sediment or at seep and vent sites, for example at sites of methane-hydrate breakdown. The influence and importance of chemosymbiotic species at places with high eutrophication, leading to anoxic events, is not well-understood, though one may expect that eutrophication also leads to mass development of chemosymbionts (Hesselbo et al. 2000).

If we even could identify the point where the lifestyle of a species switches from heterotrophic to symbiotic, we will be also able to find factors driving emergence of cooperative microbial-host associations, which will foster our understanding of this evolutionary driving force. Molluscs are very suitable model organisms, because they have a well-documented fossil history and provided mineralised tissue.

In some cases original organic matrix is preserved in fossil shells. By analyzing the isotopic composition of the remaining original organic matrix and of separately extracted lipids of fossil molluscs shells, it is possible to distinguish between "primary consumers" (chemo- and phototrophic) and molluscs from higher trophic levels.

In order to get trustworthy data it is recommendable to analyze at least two species with different diets from the same habitat or location, otherwise the reliability of isotopic dates are questionable (Dreier et al. 2012). For instance, Dreier et al. (2012) found $\delta^{13}C$ and $\delta^{15}N$ values for the heterotrophic bivalve *Venerupis (*$\delta^{13}C$ of -24.1 ‰ and $\delta^{15}N$ of +4.2 ‰) in the same range as for chemotrophic bivalves from other sites. But in contrast, compared to the values of the chemotrophic bivalves from the same site, the large differences between the isotopic signatures allowed to distinguish between the two lifestyles. With this respect it is also important to keep in mind that some diets of endosymbiotic molluscs are not completely based on their symbionts. Some of the molluscs still use filter-feeding as an additional option (Duplessis et al. 2004). To date no isotopic data are available for chemo-compared with phototrophic molluscs inhabiting the same site, so is not known if there is a resolution limit between the two different primary producer's lifestyles.

Generally it should be possible to confirm either autotrophy or heterotrophy by comparing carbon and nitrogen isotopies of the organic matrices from different candidate shell specimens from the same location. This method is not limited to molluscs – all invertebrates with mineralised tissue and embedded organic matrix could be analyzed, for example also shells of brachiopods and perhaps even organic matrices of tubeworm tubes.
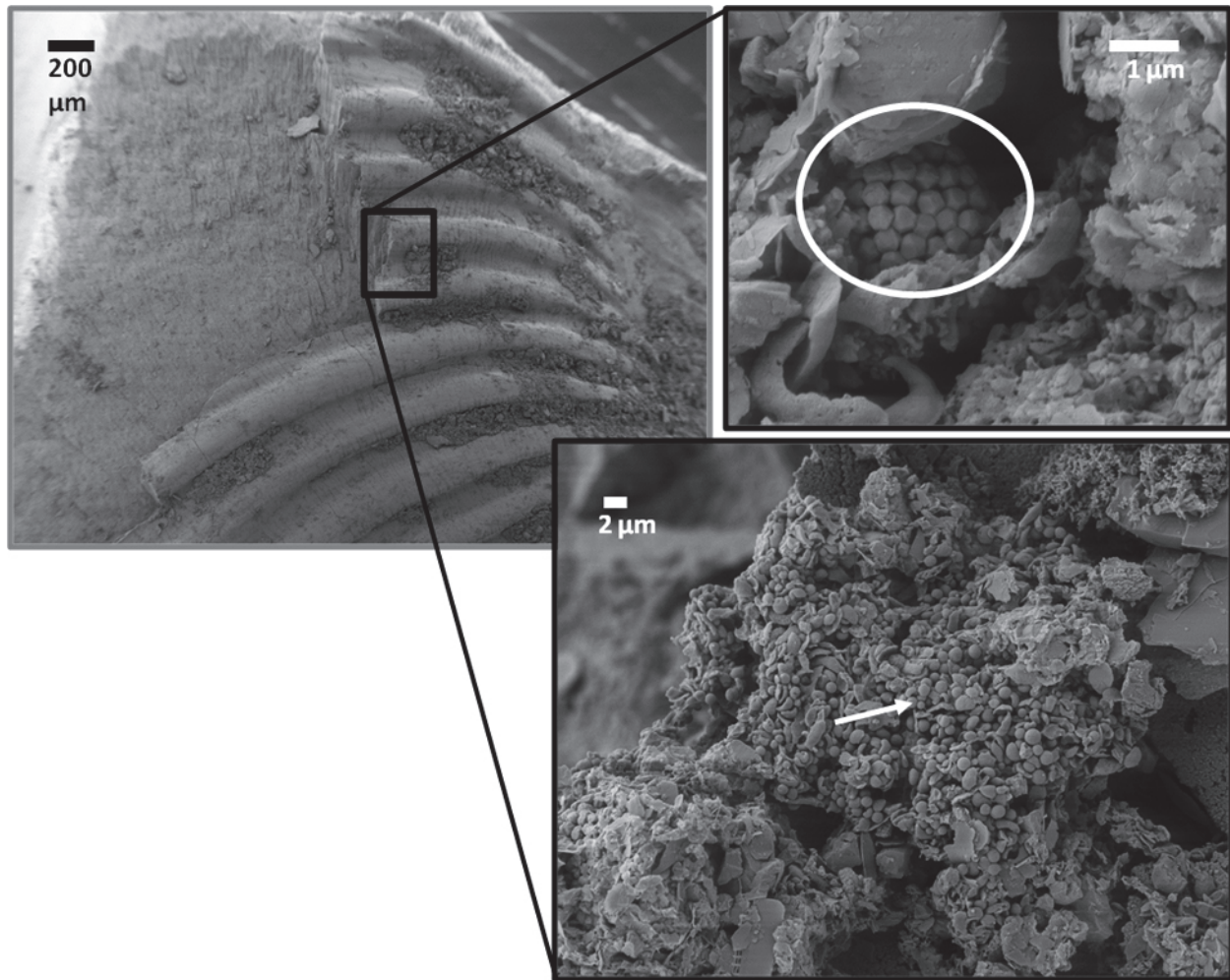
Fig. 6: Scanning electron micrographs of a *Venerupis* shell (Heterodonta: Veneroida: Veneridae) after 6 months incubation in sediment. **(A)** general view of the shell; **(B)** higher magnification, with framboidal pyrite [circle]; **(C)** higher magnification of left picture, with bacteria attached to the shell surface [arrow].

Acknowledgements

References

Aharon, P. & Fu, B. S. (2000): Microbial sulfate reduction rates and sulfur and oxygen isotope fractionations at oil and gas seeps in deepwater Gulf of Mexico. *Geochimica et Cosmochimica Acta* **64**: 233-246. http://dx.doi.org/10.1016/S0016-7037(99)00292-6

Amano, K.; Jenkins, R. G.; Kurihara, Y. & Kiel, S. (2007) A new genus for *Vesicomya inflate* Kanie & Nishida, a lucinid shell convergent with that of vesicomyids, from Cretaceous strata of Hokkaido, Japan. *The Veliger* **50**: 255-262.

Ambrose, S. H. (1994): Preparation and characterization of bone and tooth collagen for isotopic analysis. *Journal of Archaeological Science* **17**: 431-451.

Baco, A. R.; Smith, C. R.; Peek, A. S.; Roderick, G. K. & Vrijenhoek, R. C. (1999): The phylogenetic relationships of whale-fall vesicomyid clams based on mitochondrial COI DNA sequences. *Marine Ecology Progress Series* **182**: 137-147.

Ben-Mlih, F.; Marty, J. C. & Fiala-Médioni, A. (1992): Fatty acid composition in deep hydrothermal vent symbiotic bivalves. *Journal of Lipid Research* **33**: 1797-1806.

Berg, C. J. jr.; Krzynowek, J.; Alatalo, P. & Wiggin, K. (1985): Sterol and fatty acid composition of the clam, Codakia orbicularis, with chemoautotrophic symbionts. *Lipids* **20**: 116-120.

Berner, R. A. (1984): Sedimentary pyrite formation: An update. *Geochimica et Cosmochimica Acta* **48**: 605-615. http://dx.doi.org/10.1016/0016-7037(84)90089-9

Bishop, D. G. (1976): Lipids and lipid metabolism. *Comparative animal nutrition* **1**: 74-98.

Blank, R. J. (1986): Unusual chloroplast structures in endosymbiotic dinoflagellates: a clue to evolutionary differentiation within the genus *Symbiodinium* (Dinophyceae). *Plant Systematics and Evolution* **151**: 271-280. http://dx.doi.org/10.1007/BF02430280

Blumenberg, M. (2010): Microbial chemofossils in specific marine hydrothermal and cold methane cold seep settings. In: Kiel, S. (ed.): The Vent and Seep Biota: Aspects from Microbes to Ecosystems. Dordrecht etc. (Springer): 73-106. [= *Topics in Geobiology* 33]

Bradshaw, S. A.; O'Hara, S. C. M.; Corner, E. D. S. & Eglinton, G. (1991): Effects on dietary lipids of marine bivalve Scrobicularia plana feeding in different modes. *Journal of the Marine Biological Association of the United Kingdom* 71: 635-653. http://dx.doi.org/10.1017/S0025315400053200

Brooks, J. M.; Kennicutt, M. C.; Fisher, C. R.; Macko, S. A.; Cole, K.; Childress, J. J.; Bidigare, R. R. & Vetter, R. D. (1987): Deep-sea hydrocarbon seep communities: Evidence for energy and nutritional carbon sources. *Science* 238:1138-1142. http://dx.doi.org/10.1126/science.238.4830.1138

Callender, W. R. & Powell, E. N. (1997): Autochthonous death assemblages from chemautotrophic communities at petroleum seeps: palaeoproduction, energy flow and implications from the fossil record. *Historical Biology* 12: 165-198. http://dx.doi.org/10.1080/08912969709386562

Campbell, K. A. (2006): Hydrocarbon seep and hydrothermal vent paleoenvironments and paleontology: Past developments and future research directions. *Palaeogeography, Palaeoclimatology, Palaeoecology* 232: 362-407. http://dx.doi.org/10.1016/j.palaeo.2005.06.018

Carlier, A.; Riera, P.; Amouroux, J-M.; Bodiou, J-Y.; Escoubey-rou, K.; Desmalades, M.; Caparros, J. & Grémare, A. (2007): A seasonal survey of the food web in the Lapalme Lagoon (northwestern Mediterranean) assessed by carbon and nitrogen stable isotope analysis. *Estuarine, Coastal and Shelf Science* 73: 299-315.

Carlier, A.; Riera, P.; Amouroux, J. M.; Bodiou, J. Y.; Desmalades, M. & Gremare, A. (2009): Spatial heterogeneity in the food web of a heavily modified Mediterranean coastal lagoon: stable isotope evidence. *Aquatic Biology* 5: 167-179.

Carpenter, K.; Abrar, M.; Aeby, G.; Aronson, R. B.; Banks, S.; Bruckner, A.; Chiriboga, A.; Cortés, J.; Delbeek, J. C.; De-Vantier, L.; Edgar, G. J.; Edwards, A. J.; Fenner, D.; Guzmán, H. M.; Hoeksma, B. W.; Hodgson, G.; Johan, O.; Licuanan, W. Y.; Livingstone, S. R.; Lovell, E. R.; Moore, J. A.; Obura, D. O.; Ochavillo, D.; Polidoro, B. A.; Precht, W. F.; Quibilan, M. C.; Reboton, C.; Richards, Z. T.; Rogers, A. D.; Sanciangco, J.; Sheppard, A.; Sheppard, C.; Smith, J.; Stuart, S.; Turak, E.; Veron, J. E. N.; Wallace, C.; Weil, E. & Wood, E. (2008): One-third of reef-building corals face elevated extinction risk from climate change and local impacts. *Science* 321: 560-563. http://dx.doi.org/10.1126/science.1159196

Casey, M. M. & Post, D. M. (2011): The problem of isotopic baseline: reconstructing the diet and trophic position of fossil animals. *Earth-Science Reviews* 106: 131-148. http://dx.doi.org/10.1016/j.earscirev.2011.02.001

Cavanaugh, C. M.; McKiness, Z. P.; Newton, I. L. G. & Stewart, F. J. (2006): Marine chemosynthetic symbioses. In: Dworkin, M.; Falkow, S.; Rosenberg, E. & Stackebrandt, E. (eds.): *Prokaryotes. Volume 1: Symbiotic associations, Biotechnology, Applied Microbiology*. New York, N.Y. (Springer): 475-507.

Childress, J. J. & Fisher, C. R. (1992): The biology of hydrothermal vent animals: physiology, biochemistry, and autotrophic symbioses. *Oceanography and Marine Biology – An Annual Review* 30: 337-441.

Cobabe, E. A. & Pratt, L. M. (1995): Molecular and isotopic compositions of lipids in bivalve shells: a new prospect for molecular paleontology. *Geochimica et Cosmochimica Acta* 59: 87-95. http://dx.doi.org/10.1016/0016-7037(94)00374-U

Colaco, A.; Dehairs, F. & Desbruyéres, D. (2002): Nutritional relations of deep-sea hydrothermal fields at the Mid-Atlantic Ridge: a stable isotope approach. *Deep-Sea Research (I: Oceanographic Research Papers)* 49: 395-412. http://dx.doi.org/10.1016/S0967-0637(01)00060-7

Colaço, A.; Desbruyéres, D. & Guezennec, J. (2007): Polar lipid fatty acids as indicators of trophic associations in a deep-sea vent system community. *Marine Ecology* 28: 15-24. http://dx.doi.org/10.111/j.1439-0485.2006.00123.x

Coleman, D. D.; Risatti, J. B. & Schoell, M. (1981): Fractionation of carbon and hydrogen isotopes by methane-oxidizing bacteria. *Geochimica et Cosmochimica Acta* 45:1033-1037. http://dx.doi.org/10.1016/0016-7037(81)90129-0

Conway, N.; McDowe, J.; Capuzzo, J.; Fry, B. (1989): The role of endosymbiotic bacteria in the nutrition of *Solemya velum*: Evidence from a stable isotope analysis of endosymbionts and host. *Limnology and Oceanography* 34:149-155.

Conway, N. & Capuzzo, J. McD. (1990): The use of biochemical indicators in the study of trophic interactions in animal-bacteria symbiosis: Solemya velum, a case study. In: Barnes, M. & Gibson, R. N. (eds.): *Trophic relationships in the marine environment. Proceedings of the 24th European Marine Biology Symposium*. Aberdeen (University Press): 553-564.

Conway, N. & Capuzzo, J. McD. (1991): Incorporation and utilization of bacterial lipids in the *Solemya velum* symbiosis. *Marine Biology* 108: 277-291. http://dx.doi.org/10.1007/BF01344343

Conway, N. M.; Howes, B. L.; Capuzzo, J.; McDowell J. E.; Turner, R. D. & Cavanaugh, C. M. (1992): Characterization and site description of Solemya borealis (Bivalvia; Solemyidae), another bivalve–bacteria symbiosis. *Marine Biology* 112: 601-613. http://dx.doi.org/10.1007/BF00346178

Conway, N. M.; Kennicutt; M. C. & Van Dover, C. L. (1994): Stable isotopes in the study of marine chemosynthetic based ecosystems. In: Lajtha, K. & Michener, R. H. (eds.): *Stable Isotopes in Ecology and Environmental Science*. Oxford (Blackwell): 158-186.

Corliss, J. B.; Dymond, J.; Gordon, L. I.; Edmond, J. M.; Herzen, R. P. von; Ballard, R. D.; Green, K.; Williams, D.; Bainbridge, A.; Crane, K. & Andel, T. H. van (1979): Submarine thermal springs on the Galápagos rift. *Science* 203: 1073-1083. http://dx.doi.org/10.1126/science.203.4385.1073

Cowen, R. (1970): Analogies between the Recent bivalve *Tridacna* and the fossil brachiopods Lyttoniacea and Richthofeniacea. *Palaeogeography Palaeoclimatology Palaeooecology* 8: 329-344. http://dx.doi.org/10.1016/0031-0182(70)90105-7

Cowen, R. (1982): Algal symbiosis and its recognition in the fossil record. In: Tevesz, M. J. S. & McCall, P. L. (eds.): Biotic interactions in Recent and fossil benthic communities. New York, N.Y. (Plenum): 431-478. [= *Topics in Geobiology* 3]

Cramton, J. S. (1988): Comperative taxonomy of the bivalve families Isognomidae, Inoceramidae, and Retroceramidae. *Palaeontology* 31: 956-996.

Crenshaw, M. (1980): Mechanisms of shell formation and dissolution. In: Rhoads, D. & Lutz, R. (eds.): Skeletal Growth of Aquatic Organisms. New York, N.Y. (Plenum): 115-128.

Dando, P. R. & Southward A. J. (1986): Chemoautotrophy in bivalve molluscs of the genus *Thyasira. Journal of the Marine Biological Association of the United Kingdom* 66: 915-929. http://dx.doi.org/10.1017/S0025315400048529

Dando, P. R. & Spiro, B. (1993): Varying nutritional dependence of the thyasirid bivalves *Thyasira sarsi* and *T. equalis* on chemoautotrophic symbiotic bacteria, demonstrated by isotope ratios of tissue carbon and shell carbonate. *Marine Ecology Progress Series* 92: 151-158.

Dando, P. R.; Ridgway, S. A. & Spiro, B. (1994): Sulphide 'mining' by lucinid bivalve molluscs: demonstrated by stable sulphur isotope measurements and experimental models. *Marine Ecology Progress Series* 107: 169-175.

Dattagupta, S.; Bergquist, D. C.; Szalai, E. B.; Macko, S. A. & Fisher; C. R. (2004): Tissue carbon, nitrogen, and sulfur stable isotope turnover in transplanted *Bathymodiolus childressi* mussels: relation to growth and physiological condition. *Limnology and Oceanography* 49: 1144-1151.

DeNiro, M. J. & Epstein, S. (1977): Mechanism of carbon isotope fractionation associated with lipid synthesis. *Science* **197**: 261-263. http://dx.doi.org/10.1126/science.327543

Distel, D.; Baco, A.; Chuang, E.; Morrill, W.; Cavanaugh, C. & Smith, C. (2000): Do mussels take wooden steps to deep-sea vents? *Nature* **403**: 725-726. http://dx.doi.org/10.1038/35001667

Distel, D. L.; Morrill, W.; MacLaren-Toussaint, N.; Franks, D. & Waterbury, J. (2002): *Teredinibacter turnerae* gen. nov., sp. nov., a dinitrogen-fixing, cellulolytic, endosymbiotic γ-proteobacterium isolated from the gills of wood-boring molluscs (Bivalvia: Teredinidae). *International Journal of Systematic and Evolutionary Microbiology* **52**: 2261-2269.

Dhont, A. V. (1983): Campanian and Maastrichtian inoceramids: A review. *Zitteliana* **10**: 689-701.

Dreier, A.; Stannek, L.; Blumenberg, M.; Taviani, M.; Sigovini, M.; Wrede, C.; Thiel, V. & Hoppert, M. (2012): The fingerprint of chemosymbiosis: origin and preservation of isotopic biosignatures in the nonseep bivalve *Loripes lacteus* compared with *Venerupis aurea*. *FEMS Microbiology Ecology* **81**: 480-493. http://dx.doi.org/10.1111/j.1574-6941.2012.01374.x

Dubilier, N.; Bergin, C. & Lott, C. (2008): Symbiotic diversity in marine animals: the art of harnessing chemosynthesis. *Nature Reviews Microbiology* **6**: 725-740. http://dx.doi.org/10.1038/nrmicro1992

Duperron, S. & Fiala-Médioni, A. (2007): Evidence for chemoautotrophic symbiosis in a Mediterranean cold seep clam (Bivalvia: Lucinidae): comparative sequence analysis of bacterial 16S rRNA, APS reductase and RubisCO genes. *FEMS Microbiology Ecology* **59**: 1-11.

Duperron, S.; Halary, S.; Lorion, J.; Sibuet, M. & Gaill, F. (2008): Unexpected co-occurrence of six bacterial symbionts in the gills of the cold seep mussel *Idas* sp. (Bivalvia: Mytilidae). *Environmental Microbiology* **10**: 433-445. http://dx.doi.org/10.1111/j.1462-2920.2007.01465.x

Duperron, S. (2010): The diversity of deep-sea mussels and their bacterial symbioses. In: Kiel, S. (ed.): The Vent and Seep Biota: Aspects from Microbes to Ecosystems. Dordrecht etc. (Springer): 137-167. [= *Topics in Geobiology* **33**]

Duplessis, M. R.; Dufour, S. C.; Blankenship, L. E.; Feldbeck, H. & Yayanos, A. A. (2004): Anatomical and experimental evidence for particulate feeding in *Lucinoma aequizonata* and *Parvilucina tenuisculpta* (Bivalvia: Lucinidae) from the Santa Barbara Basin. *Marine Biology* **145**: 551-561. http://dx.doi.org/10.1007/s00227-004-1350-6

Evens, J. S. (2008): "Tuning in" to mollusc shell nacre- and prismatic-associated protein terminal sequences. Implications for biomineralization and the construction of high performance inorganic organic composites. *Chemical Reviews* **108**: 4455-4462. http://dx.doi.org/10.1021/cr078251e

Fiala-Médioni, A. & Felbeck, H. (1990): Autotrophic process in invertebrate nutrition: bacterial symbiosis in bivalve molluscs. In: Mellinger, J. (ed.): *Animal nutrition and transport processes. Volume 1: Nutrition in wild and domestic animals*. Basel etc. (Karger): 49-69.

Findlay, R. H.; Trexler, M. B.; Guckert, J. B. & White, D. C. (1990): Laboratory study of disturbance in marine sediments: response of a microbial community. *Marine Ecology Progress Series* **62**: 121-133.

Fisher, C. R. (1990): Chemoautotrophic and methanotrophic symbioses in marine invertebrates. *Reviews in Aquatic Sciences* **2**: 399-436.

Fischer, C. R. (1995): Toward an appreciation of hydrothermal-vent animals: their environment, physiological ecology, and tissue stable isotope values. *Geophysical Monograph Series* **91**: 297-316. http://dx.doi.org/10.1029/GM091p0297

Fortey, R. (2000): Olenid trilobites: The oldest known chemoautotrophic symbionts? *Proceedings of the National Academy of Sciences of the United States of America* **97**: 6574-6578. http://dx.doi.org/10.1073/pnas.97.12.6574

Frémy, M. E. (1855): Recherches chimiques sur les os. *Annales de Chimie et de Physique* **43**: 45-107.

Fullarton, J. G.; Dando, P. R.; Sargent, J. R.; Southward, A. J. & Southward, E. C. (1995): Fatty acids of hydrothermal vent *Ridgeia piscesae* and inshore bivalves containing symbiotic bacteria. *Journal of the Marine Biological Association of the United Kingdom* **75**: 455-468. http://dx.doi.org/10.1017/S0025315400018300

Gehron, M. J. & White, D. C. (1982): Quantitative determination of the nutritional status of detrital microbiota and the grazing fauna by triglycerides and glycerol analysis. *Journal of Experimental Marine Biology and Ecology* **64**: 145-158. http://dx.doi.org/10.1016/0022-0981(82)90150-2

Gill, F. L.; Harding, I. C.; Little, C. T. S. & Jonathan, A. T. (2005): Palaeogene and Neogene cold seep communities in Barbados, Trinidad and Venezuela: An overview. *Palaeogeography, Palaeoclimatology, Palaeoecology* **227**: 191-209. http://dx.doi.org/10.1016/j.palaeo.2005.04.024

Glover, E. A.; Taylor, J. D. & Rowden, A. A. (2004): *Bathyaustriella thionipta*, a new lucinid bivalve from a hydrothermal vent on the Kermadec Ridge, New Zealand and its relationship to shallow-water taxa (Bivalvia: Lucinidae). *Journal of Molluscan Studies* **70**: 283-295.

Glover, E. A. & Taylor, J. D. (2007): Diversity of chemosymbiotic bivalves on coral reefs: Lucinidae (Mollusca, Bivalvia) of New Caledonia and Lifou. *Zoosystema* **29**: 109-181.

Goedert, J. L. & Squires, R. L. (1990): Eocene deep-sea communities in localized limestones formed by subduction-related methane seeps, southwestern Washington. *Geology* **18**: 1182-1185. http://dx.doi.org/10.1130/0091-7631(1990)18<1182:EDSCIL>2.3.CO;2

Goedert, J. L. & Campbell, K. A. (1995): An Early Oligocene chemosynthetic community from the Makah Formation, Northwestern Olympic Peninsula, Washington. *The Veliger* **38**: 22-29.

Goedert, J. L.; Thiel, V.; Schmale, O.; Rau, W. W.; Michaelis, W. & Peckmann, J.; (2003): The Late Eocene 'Wiskey Creek' methane-seep deposit (Western Washington State). Part I: Geology, palaeontology and molecular geobiology. *Facies* **48**: 223-240.

Goericke, R.; Montoya, J. P.; & Fry, B. (1994): Physiology of isotopic fractionation in algae and cyanobacteria. In: Lajtha, K. & Michener, R. H. (eds.): *Stable Isotopes in Ecology and Environmental Science*. Oxford (Blackwell): 189-221.

Grossman, E. L.; Cifuentes, L. A. & Cozzarelli, I. M. (2002): Anaerobic methane oxidation in a landfill-leachate plume. *Environmental Science & Technology* **36**: 2436-2442.

Gubanov, A. P.; Skovsted, C. B. & Peel, J. S. (2004): Early Cambrian molluscs from Sierra de Cordoba (Spain). *Geobios* **37**: 199-215. http://dx.doi.org/10.1016/j.geobios.2003.04.003

Guckert, J. B.; Antworth, C. P.; Nichols, P. D. & White, D. C. (1985): Phospholipid, ester-linked fatty acid profiles as reproducible assays for changes in prokaryotic community structure of estuarine sediments. *FEMS Microbiology Letters* **31**: 147-158. http://dx.doi.org/10.1111/j.1574-6968.1985.tb01143.x

Guy, R. D.; Fogel, M. L. & Berry, J. A. (1993) Photosynthetic fractionation of stable isotopes of oxygen and carbon. *Plant Physiology* **101**: 37-47. http://dx.doi.org/10.1104/pp.101.1.37

Hallock, P. & Schlager, W. (1986): Nutrient excess and the demise of coral reefs and carbonate platforms. *Palaios* **1**: 389-398. http://dx.doi.org/10.2307/3514476

Hallock, P. (1987): Fluctuations in the trophic resource continuum: a factor in global diversity cycles? *Paleoceanography* **2**: 457-471. http://dx.doi.org/10.1029/PA002i005p00457

Hartman, M. C. & Pratt, I. (1976): Infection of the heart cockle, *Clinocardium nuttalli,* from Yaquina Bay, Oregon, with an endosymbiotic alga. *Journal of Invertebrate Pathology* **28**: 291-299. http://dx.doi.org/10.1016/0022-2011(76)90002-1

Hawkins, A. J. S.; & Klumpp, D. W. (1995): Nutrition of the giant clam *Tridacna gigas* (L.) II. Relative contribution of filter feeding and the ammonium acquired and recycled by symbi-

otic algae towards total nitrogen requirements for tissue growth and metabolism. *Journal of Experimental Marine Biology and Ecology* **190**: 263-290. http://dx.doi.org/10.1016/0022-0981(95)00044-R

Heide, T. van der; Govers, L. L.; de Fouw, J.; Olff, H.; Geest, M. van der; Katwijk, M. M. van; Piersma, T.; Koppel, J. van de; Silliman, B. R.; Smolders, A. J. P. & Gils, J. van (2012): A Three-Stage Symbiosis Forms the Foundation of Seagrass Ecosystems. *Science* **336**: 1432-1434. http://dx.doi.org/10.1126/science.1219973

Herry, M. D. & Le Pennec, M. (1989): Chemoautotrophic symbionts and translocation of fixed carbon from bacteria to host tissues in the littoral bivalve *Loripes lucinalis* (Lucinidae). *Marine Biology* **101**: 305-312. http://dx.doi.org/10.1007/BF00428126

Hesselbo, S. P.; Gröcke, D. R.; Jenkyns, H. C.; Bjerrum, C. J.; Farrimond, P.; Morgans Bell, H. S. & Green, O. R. (2000): Massive dissociation of gas hydrate during a Jurassic oceanic anoxic event. *Nature* **406**: 392-395. http://dx.doi.org/10.1038/35019044

Hoch, M. P.; Fogel, M. L. & Kirchman, D. L. (1992): Isotope fractionation associated with ammonium uptake by a marine bacterium. *Limnology and Oceanography* **37**: 1447-1459.

Hopkins, C. C. E.; Sargent, J. R. & Nilssen, E. M. (1993): Total lipid content, and lipid and fatty acid composition of the deep-water prawn *Pandalus borealis* from Balsfjord, northern Norway: growth and feeding relationships. *Marine Ecology Progress Series* **96**: 217-228.

Jacobs, D. K. & Jones, D. S. (1989): Photosymbiosis in *Clinocardium nuttalli*: a model for isotopic "vital effecs" with implications for the fossil record of photosymbiosis. *Geological Society of America, Abstracts with Program* **21**: A77.

Jannasch, H. W. & Wirsen, C. O. (1979): Chemosynthetic primary production at West Pacific sea floor spreading centers. *Bioscience* **29**: 592-598.

Johnson, K. S.; Childress, J. J.; Hessler, R. R.; Sakamoto-Arnold, C. M. & Beehler, C. L. (1988): Chemical and biological interactions in the Rose Garden hydrothermal vent field. *Deep-Sea Research (A: Oceanographic Research Papers)* **35**: 1723-1744. http://dx.doi.org/10.1016/0198-0149(88)90046-5

Jones, D. S.; Williams, D. F. & Spero, H. J. (1988): More Light on Photosymbiosis in fossil molluscs: The case of *Mercenaria "tridacnoides"*. *Palaeogeography, Palaeoclimatology, Palaeoecology* **64**: 141-152. http://dx.doi.org/10.1016/0031-0182(88)90003-X

Jones, D. S. & Jacobs, D. K. (1992): Photosymbiosis in *Clinocardium nuttalli*: implications for test of photosymbiosis in fossil molluscs. *Palaios* **7**: 86-95. http://dx.doi.org/10.2307/3514798

Jones, J. D. & Vallentyne, J. R. (1960): Biogeochemistry of organic matter. I. Polypeptides and amino acids in fossil and sediments in relation to geothermometry. *Geochimica et Cosmochimica Acta* **21**: 1-34. http://dx.doi.org/10.1016/S0016-7037(60)80002-6

Joye, S. B.; Boetius, A.; Orcutt; B. N.; Montoya, J. P.; Schulz, H. N.; Erickson, M. J. & Lugo, S. K. (2004): The anaerobic oxidation of methane and sulfate reduction in sediments from Gulf of Mexico cold seeps. *Chemical Geology* **205**: 219-238. http://dx.doi.org/10.1016/j.chemgeo.2003.12.019

Kano, Y.; Chiba, S. & Kase, T. (2002): Major adaptive radiation in neritopsine gastropods estimated from 28S rRNA sequences and fossil records. *Proceedings of the Royal Society (B: Biological Sciences)* **269**: 2457-2465. http://dx.doi.org/10.1098/rspb.2002.2178

Kauffman, E. G., (1969): Form, function and evolution. In: Moore, R. C. (ed.): *Treatise on Invertebrate Paleontology, Part N, Mollusca 6(1), Bivalvia*. Boulder, Colo. (Geological Society of America) & Lawrence, Kans. (University of Kansas): N129-N205.

Kaplan, I. R.; Emery, K. O. & Rittenberg, S. C. (1963): The distribution and isotopic abundance of sulphur in recent marine sediments off southern California. *Geochimica et Cosmochimica Acta* **27**: 297-331. http://dx.doi.org/10.1016/0016-7037(63)90074-7

Kawaguti, S. (1950): Observations on the heart shell, *Corculum cardissa* (L.), and its associated zooxanthellae. *Pacific Science* **4**: 43-49.

Kawaguti, S. (1968): Electron microscopy on zooxanthellae in the mantle and gill of the heart shell. *Biological Journal of Okayama University* **14**: 1-11.

Kawaguti, S. (1983): The third record of association between bivalve molluscs and zooxanthellae. *Proceedings of Japan Academic (B: Physical and Biological Sciences)* **59**: 17-20.

Keen, A. M. (1980): The pelecypod family Cardiidae: a taxonomic summary. *Tulane Studies in Geology and Paleontology* **16**: 1-40.

Kennicutt, M. C.; Burke, R. A. Jr.; MacDonald, I. R.; Brooks, J. M.; Denoux, G. J. & Macko, S. A. (1992): Stable isotope partitioning in seep and vent organisms: chemical and ecological significance. *Chemical Geology (including Isotope geoscience)* **101**: 293-310. http://dx.doi.org/10.1016/0009-2541(92)90009-T

Kharlamenko, V. I.; Zhukova, N. V.; Khotimchenko, S. V.; Svetashev, V. I. & Kamenev, G. M. (1995): Fatty acids as markers of food sources in a shallow water hydrothermal ecosystem (Kraternaya Bight, Yankich Island, Kurile Islands). *Marine Ecology Progress Series* **120**: 231-241.

Kiel, S. & Goedert, J. L. (2006a): Deep-sea food bonanzas: early Cenozoic whale-fall communities resemble wood-fall rather than seep communities. *Proceedings of the Royal Society of London (B: Biological Sciences)* **273**: 2625-2631. http://dx.doi.org/10.1098/rspb.2006.3620

Kiel, S. & Little, C. S. T. (2006): Cold-Seep molluscs are older than the general marine mollusc fauna. *Science* **313**: 1429-1431. http://dx.doi.org/10.1126/science.1126286

Kiel, S. & Peckmann, J. (2007): Chemosymbiotic bivalves and stable carbon isotopes indicate hydrocarbon seepage at four unusual Cenozoic fossil localities. *Lethaia* **40**: 345-357. http://dx.doi.org/10.1111/j.1502-3931.2007.00033.x

Kiel, S.; Amano, K. & Jenkins, R. G. (2008a): Bivalves from Cretaceous cold-seep deposits on Hokkaido, Japan. *Acta Palaeontologica Polonica* **53**: 525-537.

Kiel, S. & Dando, P. R. (2009): Chaetopterid tubes from vent and seep sites: Implications for fossil record and evolutionary history of vent seep annelids. *Acta Palaeontologica Polonica* **54**: 443-448.

Kiel, S. & Tyler, P. A. (2010): Chemosynthetically-driven ecosystems in the Deep Sea. In: Kiel, S. (ed.): The Vent and Seep Biota: Aspects from Microbes to Ecosystems. Dordrecht etc. (Springer): 1-14. [= *Topics in Geobiology* **33**]

Kiyosu, Y. & Krouse H. R. (1993): Thermochemical reduction and sulfur isotopic behavior of sulfat by acetic acid in the presence of native sulfur. *Geochemical Journal* **27**: 49-57.

Klumpp, D. W.; Bayne, B. L.; Hawkins, A. J. S. (1992): Nutrition of the giant clam *Tridacna gigas* (L.). I Contribution of filter feeding and photosynthates to respiration and growth. *Journal of Experimental Marine Biology and Ecology* **155**: 105-122. http://dx.doi.org/10.1016/0022-0981(92)90030-E

Krueger, D. M.; Dubilier, N. & Cavanaugh, C. M. (1996): Chemoautotrophic symbiosis in the tropical clam *Solemya occidentalis* (Bivalvia: Protobranchia): ultrastructural and phylogenetic analysis. *Marine Biology* **126**: 55-64. http://dx.doi.org/10.1007/BF00571377

Leak, D. J.; Stanley, S. H.; & Dalton, H. (1985): Implication of the nature of methane monooxygenase on carbon assimilation in methanotrophs. In: Poole, R. K. & Dow, C. S. (eds.): *Microbial Gas Metabolism, Mechanistic, Metabolic and Biotechnological Aspects*. London (Academic Press): 201-208.

Lee, R. W. & Childress, J. J. (1994): Assimilation of inorganic nitrogen by chemoautotrophic and methanotrophic symbioses. *Applied and Environmental Microbiology* **60**: 1852-1858.

Lee, R. W.; Robinson, J. J. & Cavanaugh, C. M. (1999): Pathways of inorganic nitrogen assimilation in chemoautotrophic bacteria-marine invertebrate symbioses: expression of host and symbiont glutamine synthetase. *Journal of Experimental Biology* **202**: 289-300.

Lilley, M. D.; Butterfield, D. A.; Olson, E. J.; Lupton, J. E.; Macko, S. A. & McDuff, R. E. (1993): Anomalous CH_4 and NH_4^+ concentrations at an unsedimented mid-ocean-ridge hydrothermal system. *Nature* **364**: 45-47. http://dx.doi.org/10.1038/364045a0

Little, C. T. S.; Campbell, K. A. & Herrington, R. J. (2002): Why did ancient chemosynthetic seep and vent assemblages occur in shallower water than they do today? *International Journal of Earth Sciences* **91**: 149-153. http://dx.doi.org/10.1007/s005310050273

Lonsdale, P. (1977): Clustering of suspension-feeding macrobenthos near abyssal hydrothermal vents at oceanic spreading centers. *Deep Sea Research* **24**: 857-863. http://dx.doi.org/10.1016/0146-6291(77)90478-7

Lorrain, A.; Paulet, Y-M.; Chauvaud, L.; Savoye, N.; Donval, A. & Saout, C. (2002): Differential d13C and d15N signatures among scallop tissues: implications for ecology and physiology. *Journal of Experimental Marine Biology and Ecology* **275**: 47-61.

MacLeod, K. G. & Hoppe, K. A. (1992): Evidence that Inoceramid bivalves were benthic and harbored chemosynthetic symbionts. *Geology* **20**: 117-120. http://dx.doi.org/10.1130/0091-7613(1992)020<0117:ETIBWB>2.3.CO;2

Mae, A.; Yamanak, T. & Shimoyama, S. (2007): Stable isotope evidence for identification of chemosynthesis-based fossil bivalves associated with cold seepages. *Palaeogeography, Palaeoclimatology and Palaeoecology* **245**: 411-420. http://dx.doi.org/10.1016/j.palaeo.2006.09.003

Majima, R.; Nobuhara, T. & Kitazaki, T. (2005): Review of fossil chemosynthetic assemblages in Japan. *Palaeogeography, Palaeoclimatology and Palaeoecology* **227**: 86-123. http://dx.doi.org/10.1016/j.palaeo.2005.04.028

Marin, F. & Luquet, G. (2007): Unusually acidic shell proteins in biomineralization. In: Bäuerlein, E. (ed.): *Handbook of Biomineralization* **1**: 273-290.

Marin, F.; Luquet, G.; Marie, B.; Medakovic, D. (2008): Molluscan shell proteins: primary structure, origin and evolution. *Current Topics in Developmental Biology* **80**: 209-276.

McKenzie, J. D.; Black, K. D.; Kelly, M. S.; Newton, L. C.; Handley, L. L.; Scrimgeour, C. M.; Raven, J. A. & Henderson, R. J. (2000): Comparisons of fatty acid and stable isotope ratios in symbiotic and nonsymbiotic brittlestars from Oban Bay, Scotland. *Journal of the Marine Biological Association of the United Kingdom* **80**: 311-320.

Michener, R. & Schell, D. (1994): Stable isotope ratios as tracers in marine aquatic food webs. In: Lajtha, K. & Michener, R. H. (eds.): *Stable Isotopes in Ecology and Environmental Science.* Oxford (Blackwell): 138-157.

Minagawa, M. & Wada, E. (1984): Stepwise enrichment of 15N along food chains: further evidence and the relation between d15N and animal age. *Geochimica et Cosmochimica Acta* **48**: 1135-1140. http://dx.doi.org/10.1016/0016-7037(84)90204-7

Mizota, C. & Yamanaka, T. (2003): Strategic adaptation of a deep-sea, chemosynthesis-based animal community: An evaluation based on soft body part carbon, nitrogen, and sulfur isotopic signatures. *Japanese Journal of Benthology* **58**: 56-69. [in Japanese with English summary]

Moreno, J.; Pollero, A. E.; Moreno, V. J.; Brenner, R. R. (1980): Lipids and fatty acids of the mussel (*Mytilus platensis* d'Orbigny) from South Atlantic Waters. *Journal of Experimental Marine Biology and Ecology* **48**: 263-276. http://dx.doi.org/10.1016/0022-0981(80)90081-7

Morton, B. (2000): The biology and functional morphology of *Fragum erugatum* (Bivalvia: Cardiidae) from Shark Bay, Western Australia: the significance of its relationship with entrained zooxanthelllae. *Journal of Zoology* **251**: 39-52.

Neff, J. (1972): Ultrastructure of the outer epithelium of the mantle in the clam *Mercenaria mercenaria* in relation to calcification of the shell. *Tissue Cell* **4**: 591-600. http://dx.doi.org/10.1016/S0040-8166(72)80032-6

O'Donnell, T. H.; Mackob, S. A.; Choub, J.; Davis-Harttenc, K. L. & Wehmillerc, J. F. (2003): Analysis of δ 13C, δ15N, and δ34S in organic matter from the biominerals of modern and fossil *Mercenaria* spp. *Organic Geochemistry* **34**: 165-183. http://dx.doi.org/10.1016/S0146-6380(02)00160-2

Ohno, T.; Katoh, T.; Yamasu, T. (1995): The origin of algal-bivalve photosymbiosis. *Palaeontology* **38**: 1-21.

Oliver, P. G.; Southward, E. C. & Dando P. R. (2013) Bacterial symbiosis in *Syssitomya pourtalesiana* Oliver, 2012 (Galeommatoidea: Montacutidae), a bivalve commensal with the deep-sea echinoid *Pourtalesia. Journal of Molluscan Studies* **79**: 30-41.

Parkes, R. J. & Taylor, J. (1983): The relationship between fatty acid distributions and bacterial respiratory types in contemporary marine sediments. *Estuarine, Coastal and Shelf Science* **16**: 173-189.

Payne, W. J. (1973): Reduction of nitrogen oxides by microorganisms. *Bacteriological Reviews* **37**: 409-452.

Peckmann, J.; Thiel, V.; Michaelis, W.; Clari, P.; Gaillard, C.; Martire, L.; Reitner, J. (1999): Cold seep deposits of Beauvoisin (Oxfordian; southeastern France) and Marmorito (Miocene; northern Italy): microbially induced authigenic carbonates. *International Journal of Earth Sciences* **88**: 60-75. http://dx.doi.org/10.1007/s005310050246

Peckmann, J.; Goedert, J. L.; Thiel, V.; Michaelis, W. & Reitner, J. (2002): A comprehensive approach to the study of methane-seep deposits from the Lincoln Creek Formation, western Washington State, USA. *Sedimentology* **49**: 855-873. http://dx.doi.org/10.1046/j.1365-3091.2002.00474.x

Peckmann, J.; Thiel, V.; Reitner, J.; Taviani, M.; Aharon, P. & Michaelis, W. (2004): A microbial mat of a large sulphur bacterium preserved in a Miocene methane-seep. *Geomicrobiology Journal* **21**: 247-255. http://dx.doi.org/10.1080/01490450490438757

Persselin, S. (1998): The Evolution of Shell Windows within the Fraginae (Bivalvia: Cardiidae) and the Origin of Algal Symbiosis in Cardiids. *MSc Thesis Publication. Mangilao, Guam: University of Guam Marine Laboratory*: 49 pp.

Peterson, B. J. & Fry, B. (1987): Stable isotopes in ecosystem studies. *Annual Review of Ecology and Systematics* **18**: 293-320.

Petersen, J. M. & Dubilier, N. (2009): Methanotrophic symbioses in marine invertebrates. *Environmental Microbiology Reports* **1**: 319-335. http://dx.doi.org/10.1111/j.1758-2229.2009.00081.x

Peel, J. S. (1991): Functional morphology of the Class Helcionelloida nov, and the early evolution of Mollusca. In: Simonetta, A. M. & Conway, S. (eds): *The early evolution of Metazoa and the significance of problematic taxa.* Cambridge (Cambridge University Press): 157-177.

Philip, J. (1972): Paléoécologie des formations á rudistes du Crétacé supérieur - l'example du sud-est de la France. *Palaeogeography, Palaeoclimatology, Palaeoecology* **12**: 205-222. http://dx.doi.org/10.1016/0031-0182(72)90060-0

Piretti, M. V.; Tioli, F. & Pagliuca, G. (1987): Investigation of the seasonal variations of sterol and fatty acid constituents in the bivalve molluscs *Venus gallina* and *Seapharca inaequivalsis* (Bruguiére). *Comparative Biochemistry and Physiology (B: Comparative Biochemistry)* **88**: 1201-1208. http://dx.doi.org/10.1016/0305-0491(87)90024-1

Purchon, R. D. (1955): A note on the biology of *Tridacna crocea* Lam. *Proceedings of the Malacological Society of London* **31**: 95-110.

Purich, D. L. & Allison, R. D. (2000): *Handbook of Biochemical Kinetics.* New York, N.Y. (Academic Press): xxii + 788 pp.

Rajendran, N.; Suwa, Y. & Urushigawa, Y. (1993): Distribution of phospholipid ester-linked fatty acid biomarkers for bacteria in the sediment of Ise Bay, Japan. *Marine Chemistry* **42**: 39-56. http://dx.doi.org/10.1016/0304-4203(93)90248-M

Reitzer, L. J. & Magasanik, B. (1987): Ammonia assimilation and the biosynthesis of glutamine, glutamate, aspartate, asparagine, L-alanine and D-alanine. In: Neidhardt, F. C.; Ingraham, J. L.; Low, K. B.; Magasanik, B.; Schaechter, M. & Umbarger, H. E. (eds.): Escherichia coli *and* Salmonella typhimurium*, Cellular and Molecular Biology.* Washington, D.C. (American Society for Microbiology): 302-320.

Robinson, J. J. & Cavanaugh, C. M. (1995) Expression of form I and form II Rubisco in chemoautotrophic symbioses: Implications for the interpretation of stable carbon isotope values. *Limnology and Oceanography* **40**: 1496-1502.

Roeske, C. A. & O'Leary, M. H. (1984) Carbon isotope effects on the enzyme-catalyzed carboxylation of ribulose bisphosphate. *Biochemistry* **23**: 6275-6284. http://dx.doi.org/10.1021/bi00320a058

Romanek, C. S.; Jones, D. S.; Williams, D. F.; Krantz, D. E. & Radtke, R. (1987): Stable isotopic investigation of physiological and environmental changes recorded in shell carbonate from the giant clam *Tridacna maxima*. *Marine Biology* **94**: 385-393. http://dx.doi.org/10.1007/BF00428244

Ruby, E. G.; Jannasch, H. W. & Deuser, W. G. (1987): Fractionation of stable carbon isotopes during chemoautotrophie growth of sulfur-oxidizing bacteria. *Applied and Environmental Microbiology* **53**: 1940-1943.

Sandy, M. R. (2010): Brachiopods from ancient hydrocarbon seeps and hydrothermal vents. In: Kiel, S. (ed.): The Vent and Seep Biota: Aspects from Microbes to Ecosystems. Dordrecht etc. (Springer): 279-314. [= *Topics in Geobiology* **33**]

Sargent, J. R.; Parkes R. J.; Mueller-Harviy, I. & Henderson, R. J. (1987): Lipid biomarkers in marine ecology. In: Sleigh, M. A. (ed.): *Microbes and the Sea.* Chichester (Ellis Horwood Ltd.): 119-138.

Sargent, J. R.; Bell, M. V.; Henderson, R. J. & Tocher, D. R. (1990): Polyunsaturated fatty acids in the marine and terrestrial food webs. In: Mellinger, J. (ed.): *Animal nutrition and transport processes. Volume 1: Nutrition in wild and domestic animals.* Basel etc. (Karger): 11-23.

Schlager, W. (2003): Benthic carbonate factories of the Phanerozoic. *International Journal of Earth Sciences* **92**: 445-464. http://dx.doi.org/10.1007/s00531-003-0327-x

Schneider, J. A. & Carter, J. G. (2001): Evolution and phylogenetic significance of Cardioidean shell microstructure (Mollusca: Bivalvia). *Journal of Paleontology* **75**: 607-643. http://dx.doi.org/10.1666/0022-3360(2001)075<0607:EAPSOC>2.0.CO;2

Scott, C. L.; Kwasniewski, S.; Falk-Petersen, S. & Sargent, J. R. (2000): Lipids and life strategies of *Calanus finmarchicus, Calanus glacialis* and *Calanus hyperboreus* in late autumn, Kongsfjorden, Svalbard. *Polar Biology* **23**: 510-516. http://dx.doi.org/10.1007/s003000000114

Scott, K. M.; Schwedock, J.; Schrag, D. P. & Cavanaugh, C. M. (2004) Influence of form IA RubisCO and environmental dissolved inorganic carbon on the $\delta^{13}C$ of the clam-chemoautotroph symbiosis *Solemya velum*. *Environmental Microbiology* **12**: 1210-1219.

Shank, T. M.; Black, M. B.; Halanych, K. M.; Lutz, R. A. & Vrijenhoek, R. C. (1999): Miocene radiation of deep-sae hydrothermal vent shrimp (Caridea: Bresiliidae): evidence from mitochondrial cytochrome oxidase subunit I. *Molecular Phylogenetics and Evolution* **13**: 244-254. http://dx.doi.org/10.1006/mpev.1999.0642

Shaw, N. (1974): Lipid composition as a guide to the classification of bacteria. *Advances in Applied Microbiology* **17**: 63-108.

Skovsted, C. B.; Brock, G. A.; Lindstroem, A.; Peel, J. S.; Paterson, J. R. & Fuller, M. K. (2007): Early Cambrian record of failed durophagy and shell repair in an epibenthic mollusc. *Biology Letters* **3**: 314-317. http://dx.doi.org/10.1098/rsbl.2007.0006

Southward, E. C. (2008): The morphology of bacterial symbioses in the gills of mussels of the genera *Adipicola* and *Idas* (Bivalvia: Mytilidae). *Journal of Shellfish Research* **27**: 139-146.

Squires, R. L. & Goedert, J. L. (1991): New Late Eocene Molluscs from localized limestone deposits formed by subduction-related methane seeps, southwestern Washington. *Journal of Paleontology* **65**: 412-416.

Stasek, C. R. (1961): The form, growth and evolution of the Tridacnidae (giant clams). *Archives de Zoologie expérimentale et générale* **101**: 1-40.

Sugimoto, A. & Wada, E. (1995): Hydrogen isotopic composition of bacterial methane: CO_2/H_2 reduction and acetate fermentation. *Geochimica et Cosmochimica Acta* **59**:1329-1337. http://dx.doi.org/10.1016/0016-7037(95)00047-4

Tarasov, V. G., Gebruk, A. V., Mironov, A. N. & Moskalev, L. I. (2005): Deep-sea and shallow-water hydrothermal vent communities: two different phenomena? *Chemical Geology* **224**: 5-39. http://dx.doi.org/10.1016/j.chemgeo.2005.07.021

Taviani, M. (1994): The "calcari a Lucina" macrofauna reconsidered: deep-sea faunal oases from Miocene-age cold vents in the Romagna Apennine, Italy. *Geo-Marine Letters* **14**:185-191. http://dx.doi.org/10.1007/BF01203730

Taviani, M. (2011): The deep-sea chemoautotroph microbial world as experienced by the Mediterranean metazoans through time. In: Reitner, J.; Queric, N-V. & Arp, G. (eds.): Advances in Stromatolite Geobiology. Berlin etc. (Springer): 277-295. [= *Lecture Notes in Earth Sciences* **131**] http://dx.doi.org/10.1007/978-3-642-10415-2_18

Taylor, F. J. R. (1979): Symbionticism Revisited: A Discussion of the Evolutionary Impact of Intracellular Symbioses. *Proceedings of the Royal Society of London (B: Biological Sciences)* **204**: 267-286. http://dx.doi.org/10.1098/rspb.1979.0027

Taylor, J. D. & Glover, E. A. (2000): Functional anatomy, chemosymbiosis and evolution of the Lucinidae. In: Harper, E. M.; Taylor, J. D. & Crame, J. A. (eds.): The Evolutionary Biology of the Bivalvia. *Geological Society of London, Special Publication* **177**: 207-225.

Taylor, J. D. & Glover, E. A. (2006): Lucinidae (Bivalvia) – the most diverse group of chemosymbiotic molluscs. *Zoological Journal of the Linnean Society* **148**: 421-438. http://dx.doi.org/10.1111/j.1096-3642.2006.00261.x

Taylor, J. D.; Glover, E. A. & Williams, S. T. (2008): Ancient chemosynthetic bivalves: systematics of Solemyidae from eastern and southern Australia (Mollusca: Bivalvia). *Memoirs of the Queensland Museum (Nature)* **51**: 75-104

Taylor, J. D. & Glover, E. A. (2009): A giant lucinid bivalve from the Eocene of Jamaica – systematic, life habitats and chemosymbiosis (Mollusca: Bivalvia: Lucinidae). *Palaeontology* **52**: 95 - 109.

Taylor, J. D. & Glover, E. A. (2010): Chemosymbiotic bivalves. In: Kiel, S. (ed.): The Vent and Seep Biota: Aspects from Microbes to Ecosystems. Dordrecht etc. (Springer): 107-135. [= *Topics in Geobiology* **33**]

Taylor, J. D.; Glover, E. A.; Smith, L.; Dyal, P. & Williams, S. T. (2011): Molecular phylogeny and classification of the chemosymbiotic bivalve family Lucinidae (Mollusca: Bivalvia). *Zoological Journal of the Linnean Society* **163**: 15-49. http://dx.doi.org/10.1111/j.1096-3642.2011.00700.x

Trench, R. K.; Wethey, D. S. & Porter, J. W. (1981): Observations on the symbiosis with zooxanthellae among the Tridacnidae (Mollusca: Bivalvia). *Biological Bulletin* **161**: 180-198.

Treude, T.; Smith, C. R.; Wenzhöfer, F.; Carney, E.; Bernardino, A. F.; Hannides, A. K.; Krüger, M. & Boetius, A. (2009): Biogeochemistry of a deep-sea whale fall: sulfate reduction, sulfide efflux and methanogenesis. *Marine Ecology Progress Series* **382**: 1-21.

Trust, B. A. & Fry, B. (1992): Stable sulphur isotopes in plants: review. *Plant, Cell & Environment* **15**: 1105-1110. http://dx.doi.org/10.1111/j.1365-3040.1992.tb01661.x

Van Dover, C. L. (2000): *The Ecology of Deep-Sea Hydrothermal Vents.* Princeton, N.J. (Princeton University Press): xx + 424 pp.

Van Dover, C. L.; Aharon, P.; Bernhard, J. M.; Caylor, E.; Doerries, M.; Flickinger, W.; Gilhooly, W.; Goffredi, S. K.; Knick, K. E.; Macko, S. A.; Rapoport, S.; Raulfs, E. C.; Ruppel, C.; Salerno, J. L.; Seitz, Sen Gupta B. K.; Shank, T.; Turnipseed, M. & Vrijenhoek, R. (2003): Blake Ridge methane seeps: characterization of a soft-sediment, chemosynthetically based ecosystem. *Deep-Sea Research (I: Oceanographic Research Papers)* **50**: 281-300. http://dx.doi.org/10.1016/S0967-0637(02)00162-0

Van Dover, C. L. (2007): Stable isotope studies in marine chemoautotrophically based ecosystems: an update. In: Michener, R. & Lajtha, K. (eds.): *Stable isotopes in ecology and environmental science. [2nd ed.].* Boston, Mass. (Blackwell Publishing): 202-237.

Vinther, J. & Nielsen, C. (2005): The Early Cambrian *Halkeria* is a mollusc. *Zoologica Scripta* **34**: 81-89. http://dx.doi.org/10.1111/j.1463-6409.2005.00177.x

Wallin, I. E. (1927): *Symbionticism and the Origin of Species.* London (Baillière, Tindall & Cox): x + 171 pp.

Wakeham, S. G. & Canuel, E. A. (1988): Organic geochemistry of particulate matter in the eastern tropical North Pacific Ocean: implications for particle dynamics. *Journal of Marine Research* **46**: 183-213. http://dx.doi.org/10.1357/002224088785113748

Weiner, S. & Traub, W. (1980): X-ray diffraction study of the insoluble organic matrix of mollusc shell. *FEBS Letters* **111**: 311-316. http://dx.doi.org/10.1016/0014-5793(80)80817-9

Weiner, S., Talmon, Y. & Traub, W. (1983): Electron diffraction of mollusc shell organic matrices and their relationship to the mineral phase. *International Journal of Biological Macromolecules* **5**: 325-328. http://dx.doi.org/10.1016/0141-8130(83)90055-7

Wilkin, R. T. (1995): Size distribution in sediments, synthesis, and formation mechanism of framboidal pyrite. *PhD. dissertation, The Pennsylvania State University*: 454 pp.

Yoneyama, T.; Kamachi, K.; Yamaya, T. & Mae, T. (1993): Fractionation of nitrogen isotopes by glutamine synthetase solated from spinach leaves. *Plant & Cell Physiology* **34**: 489-491.

Yonge, C. M. (1936): Mode of life, feeding, digestion and symbiosis with zooxanthellae in the Tridacnidae. *Great Barrier Reef Expedition, 1928–29, British Museum (Natural History), Scientific Report* **1**: 283-321.

Yonge, C. M. (1981): Functional morphology and evolution in the Tridacnidae (Mollusca: Bivalvia: Cardiaceae). *Records of the Australian Museum* **33**: 735-777.

Zhang, J. Z. & Millero, F. J. (1993): The products from the oxidation of H_2S in seawater. *Geochimica et Cosmochimica Acta* **57**: 1705-1718. http://dx.doi.org/10.1016/0016-7037(93)90108-9

Zhukova, N. V.; Kharlamenko, V. I.; Svetashev, V. I. & Rodionov, I. A. (1992): Fatty acids as markers of bacterial symbionts of marine bivalve molluscs. *Journal of Experimental Marine Biology and Ecology* **162**: 253-263. http://dx.doi.org/10.1016/0022-0981(92)90205-O

Zal, F. et al. (2000): Haemoglobin structure and biochemical characteristics of the sulphide-binding component from the deep-sea clam *Calyptogena magnifica. Cahiers de biologie marine* **41**: 413-423.

Zyakun, A. M. (1996): Potential of $^{13}C/^{12}C$ variations in bacterial methane in assessing origin of environmental methane. In: Schumacher, D. & Abrams, M. A. (eds.): Hydrocarbon migration and its near-surface expression. *AAPG Memoir* **66**: 341-352.

Chemolithotrophic microbial mats in an open pond in the continental subsurface – implications for microbial biosignatures

Christine Heim[1] *; Nadia-Valérie Quéric[1]; Danny Ionescu[2]; Klaus Simon[3] & Volker Thiel[1]

[1]Department of Geobiology, Geoscience Centre, Georg-August University Göttingen, Goldschmidtstr. 3, 37077 Göttingen, Germany; Email: cheim@gwdg.de

[2]Max-Planck Institute for Marine Microbiology, Celsiusstr. 1, 28359 Bremen, Germany

[3]Department of Geochemistry, Geoscience Centre, Georg-August University Göttingen, Goldschmidtstr. 1, 37077 Göttingen, Germany

* corresponding author

The 450 m deep Äspö Hard Rock Laboratory (Äspö HRL), run by the Swedish Nuclear Fuel and Waste Management Co. (SKB) offers a unique opportunity to access microbial systems within Precambrian, mostly granodioritic rocks of the Baltic Shield. Biofilms and microbial mats at a deep groundwater seepage site and an associated pond exhibit a large diversity of aerobic and anaerobic, often chemolithotrophic microorganisms. An open pond system consisting of several different subsystems was studied to explore the diversity and spatial distribution of microbial communities and associated mineral precipitates. A further focus was placed on the establishment of inorganic biosignatures (especially trace and rare earth element (TREE) fractionation patterns) for biogeochemical processes involving subsurface microorganisms.

Introduction

Biofilms cover almost every rock-water interface on Earth. Within biofilms and microbial mats, microorganisms often mediate (bio-)mineral formation due to their presence and metabolism that cause changes in the chemical equilibrium of the surrounding environment. While biologically induced mineralization pathways can be well specified in theory, they are often difficult to recognize and distinguish in natural samples. Nevertheless, such biogenic processes may produce minerals different from their inorganically formed varieties in shape, size, crystallinity, isotopic and trace element composition (Konhauser 1997; Ferris et al. 1999, 2000; Weiner & Dove 2003, Bazylinski et al. 2007; Haferburg & Kothe 2007; Takahashi et al. 2007; Templeton & Knowles 2009; Chan et al. 2011). Such inorganic 'biosignatures' may be specified and utilized for the identification of related biological processes in geological samples, even when organic biosignatures, namely lipid biomarkers, have not survived over geological time.
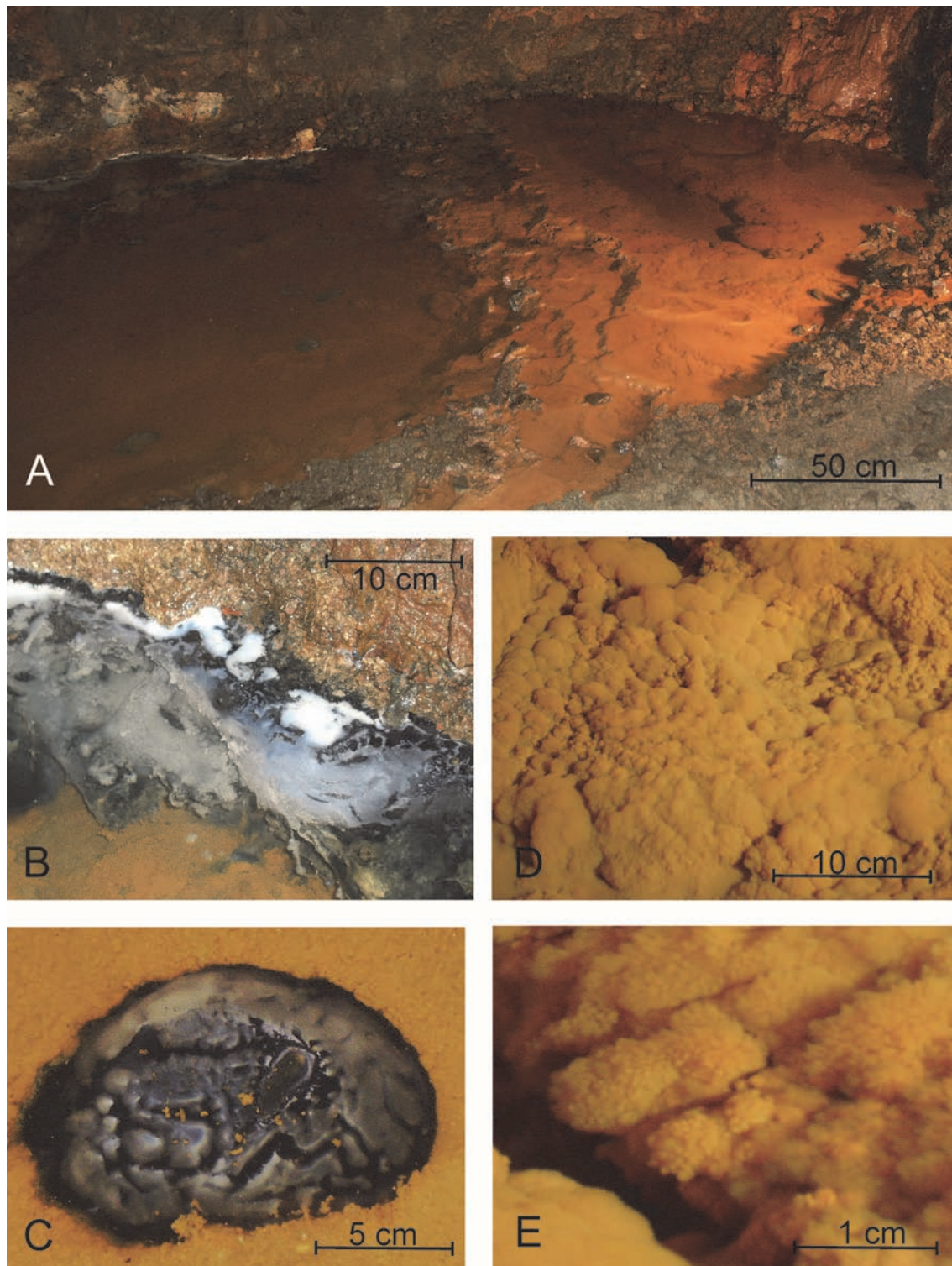
Fig. 1: The studied open pond at NASA 1127B in the Äspö HRL (**A**). The fluid inflow is located in the upper right corner and the outflow on the bottom left side (not visible). The ochre coloured, iron oxidizing microbial mats cover most of the pond area, whereas localized occurrences of white and black mats (**B, C**) are seen in the upper left corner. Details of ochre mat showing the internal cauliflower (**D**) and dendritic structures (**E**).

A better understanding of mineralizing microbial communities in the subsurface may furthermore provide insights and analogies to early Earth ecosystems. Early life on Earth probably developed in the subsurface, where it was protected from meteorite impacts and radiation penetrating the newly forming atmosphere (Trevors 2002; Russel 2003; Bailey et al. 2009).

In this study, mineralizing microbial mats were investigated from an open pond located at ca. 160 m depth in the Äspö Hard Rock Laboratory (HRL; north of Os-

karshamn, Sweden). The Äspö HRL was built as a testing environment for the disposal of nuclear waste and is operated by the Swedish Nuclear Fuel and Waste Management Co (SKB). In the Äspö HRL a wide spectrum of chiefly chemolithotrophically driven subsurface ecosystems is accessible (Pedersen 1997) that may offer a window into the microbial biosphere existing in continental vein systems. The study pond at the Äspö HRL site NASA 1127B (Fig. 1) exhibits a broad diversity of aerobic and anaerobic microorganisms, with iron/manganese oxidizing consortia forming a several cm thick microbial mat (Fig. 2). In our study, we paid particular attention to ion species involved in microbial mineralisation processes. To distinguish selective cation incorporation, three distinct types of microbial mats and the overlying water body were systematically analysed, and the in- and out-flows of the pond were compared. Especially trace and rare earth element (TREE) fractionation patterns were investigated to assess their potential utility as inorganic biosignatures for individual groups of microorganisms

Methods

Microbial mats

Microbial mats from the pond (Fig. 1A) were separated in three visually different mat types, (ochre, white and black). Whereas the ochre mat was mainly distributed over the whole pond, exhibiting a cauliflower structure (Figs. 1D, E), the black and the overlying white mat were contiguously distributed along the rim and at some localised spots in the pond (Figs. 1B, C). The mats were sampled with different devices, depending on the mat consistency, using spatulas, petri dishes and syringe cores. Additionally, an ochre mat core was taken with a plexiglas tube of 15 cm Ø and 25 cm length (Fig. 2). After sampling, the microbial mats were frozen, transported with dry ice, and stored at -20°C and -80°C (samples for DNA analysis) until further processing

Chemical analysis of the pond water and the microbial mats

Oxygen in the feeder fluids was measured using the Winkler method (Hansen 1999). Anion concentrations, measured by titration and ion chromatography, conductivity, pH and spectrophotometrical Fe_{total}/Fe(II) data were analysed immediately after sampling by the certified SKB chemistry lab.

For sample conservation and TREE measurements, concentrated, distilled HNO_3 was added to 50 ml water samples (final concentration 2 % HNO_3). In order to quantify the amounts of REE in the microbial mats, 4 ml of H_2O_2 and 2 ml of concentrated, distilled HNO_3[***] were added to 500 mg of lyophilised sample. The resulting solutions containing the dissolved mineral precipitates were diluted in 50 ml of deionised water (final concentration

4 % HNO_3). These solutions, a reference sample (blank) containing all chemicals used, and the water samples were spiked with internal Ge, Rh, In and Re standards and analysed by ICP-MS and ICP-OES. As a reference, Fe_{total} was also measured by ICP-OES and was in good agreement with the spectrophotometrical data (1 % deviation). TREE were analysed using Inductive Coupled Plasma Mass Spectrometry (ICP-MS; Perkin Elmer SCIEX Elan DRCII) and Optical Emission Spectroscopy (ICP-OES; PerkinElmer Optima 3300 DV).

Carbon (C_{tot}), total nitrogen (N_{tot}) and sulphur (S_{tot}) were analysed using a CNS Elemental Analyser (HEKAtech Euro EA). C_{inorg} and organic carbon (C_{org}) were analysed with a Leco RC 412 multiphase carbon analyzer. Double measurements were performed routinely, and appropriate internal standards were used for the C_{inorg} (Leco 502-030), C_{org} (Leco 501-034), and CNS (BBot and atropine sulphate, IVA Analysentechnik SA990752 and SA990753) analyses.

Microsensor measurements

The microenvironment was probed using glass microsensors for O_2, pH and H_2S as previously described in (Santegoeds et al. 1998; Wieland et al. 2005). Four different environments were chosen for analysis: (1) Fresh looking ochre coloured mats in the upper part of the pond; (2) Aged mats of darker colour in the lower part of the pond; (3) Small black mat spots in the lower part of the pond; (4) Large black mat zone containing a white microbial mat in the corner of the lower part of the pond.
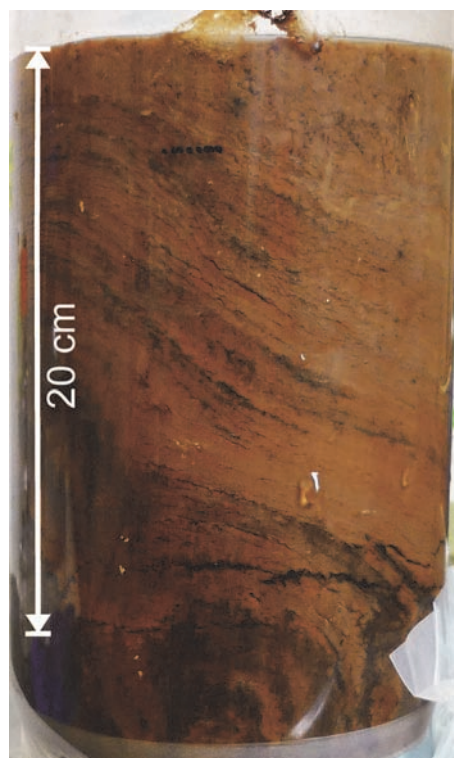

Fig. 2:   Push core of an iron oxidizing microbial mat taken from the central part of the pond. The colour zoning and the different layers within the profile are attributed to different mat generations.
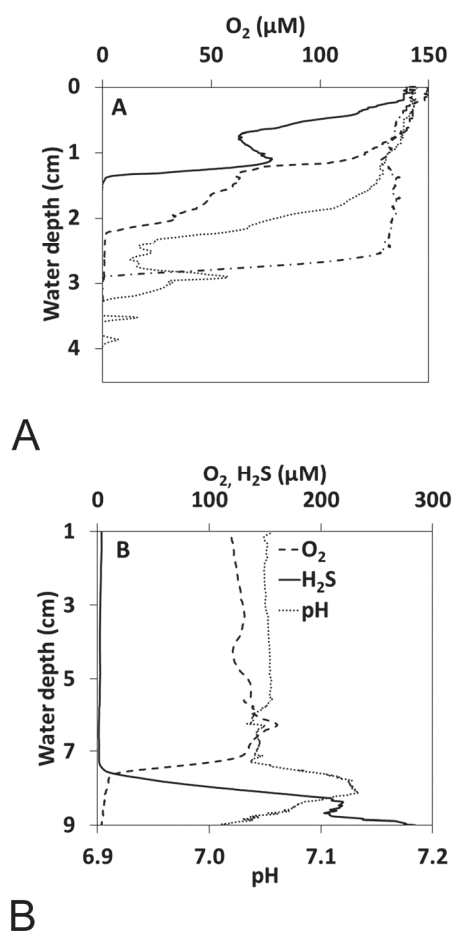
Fig. 3: Microsensor profiles into the ochre mat (**A**) and the black and white mat (**B**). The oxygen (O_2) concentration at different measurement points in the ochre mat decreases much faster in dense mat parts (continuous line) than in more fluffy mat parts (dashed lines, **A**). The O_2 and pH profiles penetrating the black and white mats show at first a roughly stable profile in the water column. At the mat surface (7 cm water depth) a sharp drop in O_2 concentration is visible, with a concurrent rise of the H_2S concentration and a pH shift by 0.1 (**B**).

Scanning Electron Microscopy and Energy Dispersive X-ray analysis (SEM-EDX)

For SEM-EDX analysis, the fresh samples were immediately fixed in 2 % glutardialdehyde and stored at 4°C until analysis. Prior to measurement, the samples were dehydrated in rising ethanol concentrations in 15 %, 30 %, 50 %, 70 % ethanol (30 min each), followed by 90 % and 99 % (60 min each), and 99 % ethanol (12 hrs). After the dehydration series, the samples were mounted on SEM sample holders and sputtered with Au-Pd (7.3 nm for 120 sec). Samples were analysed using a field emission SEM (LEO 1530 Gemini) combined with an INCA X-act EDX (Oxford Instruments).

Confocal Laser Scanning Microscopy (CLSM)

Structural characterization and localization of microbial cells and associated EPS structures within the mineralized ochre mats were examined by Laser Scanning Microscopy using a TCS SP1 confocal laser scanning microscope (Leica, Heidelberg, Germany).

Biofilm organisms were stained using nucleic acid-specific (Syto 9; Sybr Green) and protein-specific fluorochromes (Sypro Red). In addition, lectin-binding analysis was employed for the characterization of EPS glycoconjugates (PSA_Alexa568).

Fluorescence in situ hybridization (FISH)

Loosely attached microbial biofilms were carefully sampled by means of petridiscs with the aim to minimize biofilm destruction. Samples were fixed with 4 % paraformaldehyde (final concentration) for 4 hrs and carefully transferred to 1x PBS (10 mM sodium phosphate; 130 mM NaCl) three times before a final storage in 50 % ethanol/1x PBS at -20°C until further processing. Hybridization and microscopy visualisation of hybridized and 4-,6-diamidino-2-phenylindole (DAPI)-counterstained cells were performed as described previously (Snaidr et al. 1997). Cy3- and Oregon green monolabeled oligonucleotides were purchased from Metabion (Martinsried, Germany). Probes and formamide (FA) concentrations used in this study were as follows: EUB338 I-III targeting bacteria (Daims et al. 1999; 35 % FA), Non338 (negative control; Wallner et al. 1993; 10 % FA), Beta42 targeting Beta-Proteobacteria (Manz et al. 1992; 35 % FA), SRB385 targeting sulfate reducing bacteria (SRB) inclusive most species of the δ-group of purple bacteria (Amann et al., 1990; 35 % FA) and DSS658 targeting *Desulfosarcina* spp./*Desulfococcus* spp./*Desulfofrigus* spp. and *Desulfofaba* spp. (Manz et al. 1998; 35 % FA). Background signal of samples, observed with the nonsense probe NON338, was negligible (<0.1 %).

454 analysis

A DNA sample of the fresh looking ochre mat was sent for Roche 454 pyrosequencing at the MrDNA lab (Shallowater, TX, USA). Sequencing of the 16S rRNA gene was done using the 28F and 519R general primers (Lane 1991). 6500 sequences were obtained and were processed as described in Ionescu et al. (2012). Shortly, the sequences were checked for quality (length, homopolymers and ambiguous bases) and aligned against the SILVA ref database Sequences with poor alignment score were removed while the rest were dereplicated and clustered (per sample) into operational taxonomic units (OTUs) at a similarity value of 98 %. Reference sequences of each OTU were assigned to a taxonomy using BLAST against the SILVA ref database (Version 111; Quast et al. 2013). Full OTU mapping of the sample was done by clustering the reference sequences of each OTU at 99 % similarity.
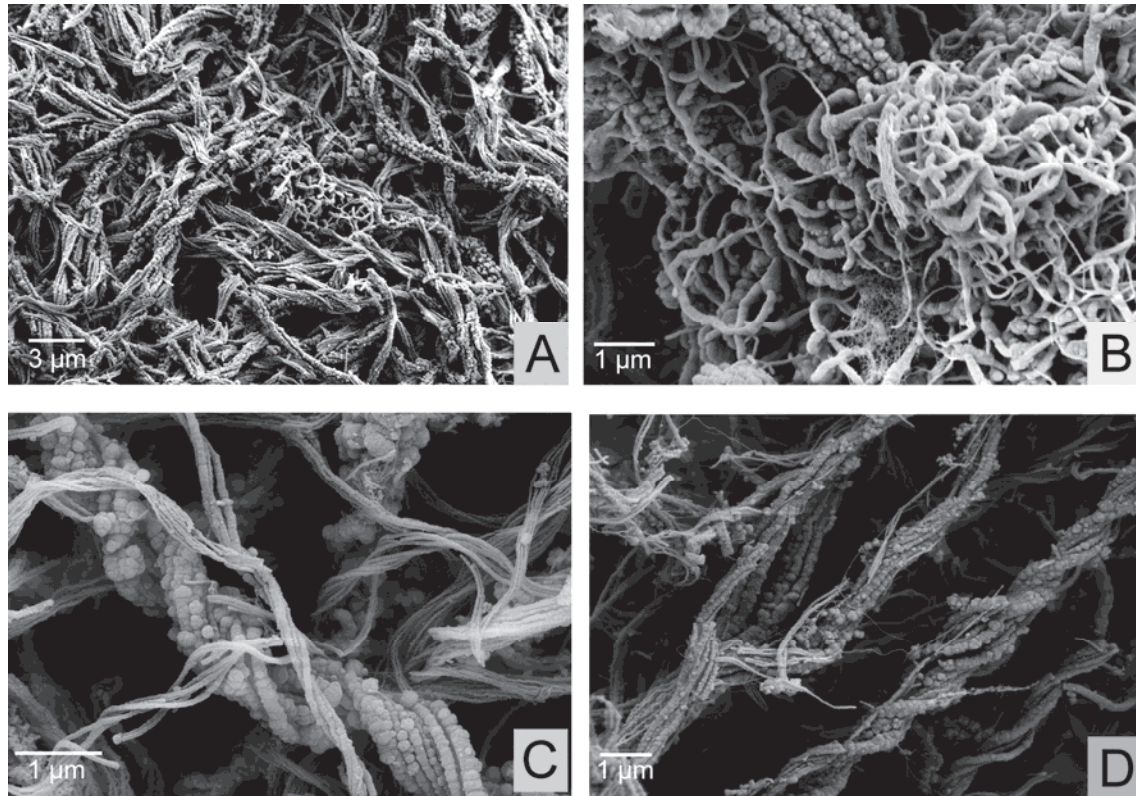
Fig. 4: SEM micrographs of the orange microbial mat, dominated by iron oxidizing bacteria (IOB). The microbial mat is visibly dominated by stalks produced by *Gallionella ferruginea* and *Mariprofundus* sp. (**A**). Iron oxyhydroxide precipitates resembling *Metallogenium*-like structures were occasionally observed (**B**). *Mariprofundus/Gallionella* EPS stalks show different stages of iron oxyhydroxide impregnation, most likely as a function of cell activity and age (**C**). The iron oxyhydroxide structures are connected via filigree structures similar to nanowires (**D**; Reguera et al. 2005).
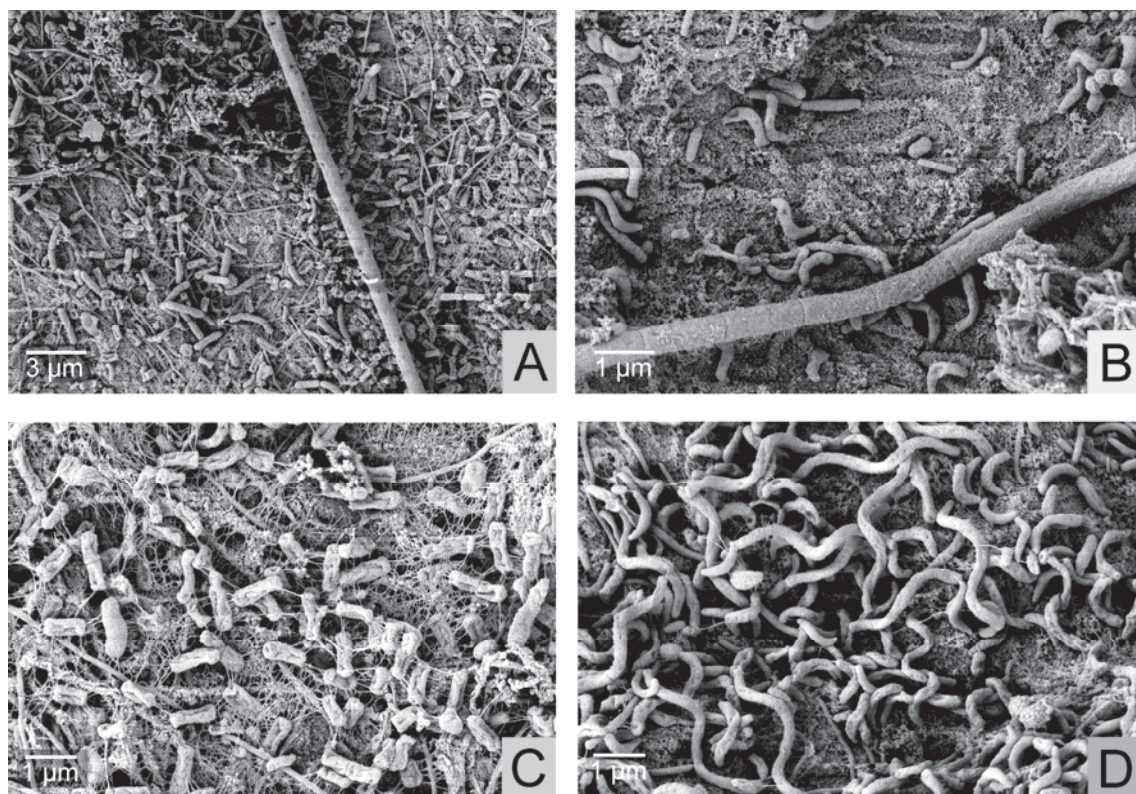
Fig. 5: SEM micrographs exhibiting different kinds of microbial cells and EPS structures of the white (**A**, **B**) and the black (**C**, **D**) microbial mats, mainly composed of rod shaped and spirally coiled cells; (**A**) rods, filaments, (**B**) rods, spirillum, (**C**) rods, (**D**) spirochaetes.

Table 1: Major physicochemical parameters of the pond water (NASA 1127B).

|	1127B inlet	1127B main	1127B outlet
PO$_4$ µg/l	44.8	54.8	50.4
NO$_3^-$	1.9	2.7	11.0
pH	7.2	7.3	7.2
kond, mS/m	1090	1074	1075
Alkalinity, mg/l	184.8	173.9	168.6
Uranine, %	0.2	0.2	0.2
Cl, mg/l	3461	3405	3409
Br mg/l	15.8	15.2	14.5
SO$_4$ mg/l	333.6	346.3	346.5
F mg/l	1.8	1.8	1.8
Ca mg/l	374.0	346.7	347.9
Na mg/l	1521	1511	1537
Mg mg/l	141.4	143.4	145.1
K mg/l	38.0	40.3	40.5
Fe tot mg/l	1.59	0.3	0.3
Fe(II) mg/l	1.51	0.3	0.1
Mn mg/l	0.8	0.8	0.8
Al mg/l	0.1	0.3	0.1
Sr mg/l	6.7	6.2	6.2
Ba mg/l	0.1	0.1	0.1
Si mg/l	4.5	4.3	4.3
O$_2$ mg/l	0.7	1.6	1.9
H$_2$S mg/l	0.04	0.08	0.02

DNA extraction, PCR amplification and Denaturing Gradient Gel Electrophoresis (DGGE)

Genomic DNA was extracted directly from environmental subsamples by using the Ultra Clean Soil DNA extraction kit (MOBIO Laboratories, Inc., CA) according to the manufacturer's protocol.

Partial 16S rRNA gene amplification from environmental DNAs for subsequent DGGE-analysis was performed using the primer sets GM5F (341F) with a GC clamp and 907R for bacteria (Muyzer et al. 1995), ARC344F-GC and 915R for archaea (Casamayor et al. 2000) as well as DSRp2060F-GC (Geets et al. 2006) and DSR4R (Wagner et al. 1998) targeting sulphate reducing bacteria, following the respective PCR protocols of the former authors. PCR products in an amount ranging from 300 to 500 ng was applied to DGGE as described by Schäfer & Muyzer (2001), using the D-Code system (Bio-Rad Laboratories, CA). Electrophoresis was performed with 6 % polyacryl-amide gels (ratio of acrylamide to bisacrylamide, 40:1) submerged in 0.75 x TAE buffer (40 mM Tris, 40 mM acetic acid, 1 mM EDTA, pH 7.5) at 60°C and run for 16 hrs at 100 V in a linear 20 to 70 % denaturant gradient. Stained with ethidium bromide (0.5 g/ml), individual bands were excised and re-suspended overnight at 4°C in 50 µl of Milli-Q water. After re-amplification with the original primer sets, PCR products were purified via the Qiaquick PCR purification kit (QIAGEN GmbH, Hilden, Germany) prior to direct sequencing by using an ABI Prism 3100 genetic analyser (PE Applied Biosystems).

The partial 16S rRNA sequences were assembled and manually corrected using the BioEdit sequence alignment editor (Hall 1999), and further compared to the Gen-Bank database by the BLAST analysis tools of the National Centre for Biotechnology Information (Altschul et al. 1990) in order to determine their phylogenetic affiliation and to identify their closest phylogenetic relatives.

The deduced, partial dsrB sequences of the environmental samples were implemented into the persisting dsrAB alignment of SRP references strains, including all full-length Dsr sequences available from the public databases. The data sets were phylogenetically analysed with the tree inference methods included in the ARB software package (Ludwig et al. 2004) and the Phylogeny Inference Package Version (PHYLIP) 3.5c (Felsenstein 1993).

Results

Water chemistry

Water chemistry data are given in Tables 1 and 2B. Our three-years-monitoring of the pond water chemistry did not reveal any extensive seasonal variation or other fluctuation. Therefore, data given in Table 1 and 2B are mean values of five sampling time points. Chemical variations observed between the inlet, main pond and outlet are rather small (Table 1). The concentration of dissolved iron (FeII) at the inlet (1.6 mg/l) is almost completely consumed in the pond (outlet: 0.1 mg/l). Alkalinity drops from 184.8 mg/l to 168.6 mg/l as does Ca^{2+} from 374 mg/l to 348 mg/l. On the other hand, the concentrations of PO_4^{3-} (44.8 mg/l), NO_3^- (1.9 mg/l), and SO_4^{2-} (333.6 mg/l) increase to 50.4 mg/l, 11.0 mg/l, and 346.5 mg/l, respectively. The oxygen (O_2) concentration in the water column varies between 1.2–4.8 mg/l (37–150 µmol/l), but closer to the mat surfaces the O_2 concentration rises from the 0.7 mg (21.1 mmol/l) at the inlet to 1.9 mg (58.0 mmol/l) at the outlet. Oxygen profiles starting at the water surface into the ochre mats (at 1 cm water depth) show a clear decrease in oxygen concentration (Fig. 3A). The decline depends on the density of the ochre mat. The fluffy nature of the mats is clear from the intrusion of water with a higher O_2 content to deeper parts in the mats. The oxygen consumption alters between the different layer of the mat and is much slower in the upper fluffy part than in the denser deeper parts. O_2 and pH profiles down into the white and black mat show a roughly stable water column above these mats, and a sharp drop in O_2 concentration at the mat surface (7 cm water depth). Concurrently the H_2S concentration rises significantly and the pH is shifted by 0.1 (Fig. 3B).
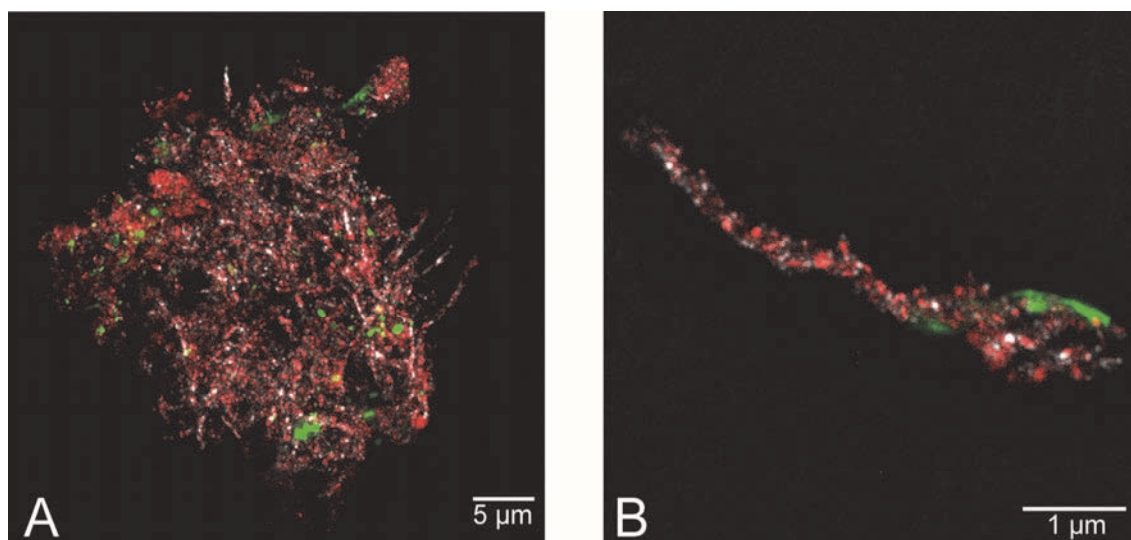
Fig. 6: Laser scanning microscopy (CLSM) of an ochre microbial mat. Fluorescence lectin-binding analysis was performed using nucleic acid and protein-specific fluorochromes (green) as well as the D-glucose and D-mannose staining lectin (red). Mineral precipitates are visible as white reflections. In the mat aggregate, a clear recognition of cells and their relation to appending stalks was impossible (**A**). In a partly mineral impregnated stalk fragment a smooth protein end was detected (**B**).

Table 2A: Major cation concentrations in the microbial mats. The thick ochre mats were analysed in three different sections (each 7cm), in order to check for potential stratifications.

g/kg	White mat	Black mat	Ochre core top	Ochre core middle	Ochre core bottom
Al	2.469	6.200	0.025	0.027	0.063
Ca	29.5	56.3	13.9	16.1	13.4
Cr	0.024	0.016	0.002	0.003	0.003
Fe	60.3	76.7	150.3	154.0	143.4
K	1.66	2.35	0.137	0.204	0.155
Mg	7.85	10.30	1.19	1.42	1.11
Mn	0.295	0.469	4.17	6.25	5.60
Na	53.6	30.8	5.49	7.97	4.46
Sr	0.326	0.368	0.473	0.567	0.489
Ti	0.678	1.629	0.003	0.004	0.010
Si	7.05	13.71	16.10	18.42	17.77

Microbial mat structure and community

The different mat types differ significantly in their content of organic matter. The ochre mat contains 5.1 to 5.8 % C_{org} (organic carbon), the black mat 15.4 % C_{org} and the white mat 17.6 % C_{org}.

Whereas the ochre mat consists mainly of iron oxyhydroxide impregnated stalks produced by iron oxidizing bacteria (IOB), numerous bacterial cells and EPS structures are visible in the black and white mat (SEM images, Figs. 4, 5). CLSM images from the lectine-stained ochre mat show a diffuse network of mineralized stalks without a clear relation to the stalk-producing cells (Fig. 6A). Some stalk fragments contained a non-encrusted protein band of unclear function (Fig. 6B).

The community compositions of the microbial mat at the inlet, outlet and in the main pond, respectively, were analysed by FISH, 16S rRNA gene analyses, and by 454 pyrosequencing. 454 pyrosequencing of the ochre mat resulted in 6500 sequences per sample, allowing a good overview of the large diversity of iron-oxidizing (deposit-ing) bacteria. Among the identified genera were *Gallionella, Sideroxydans, Crenothrix, Marinobacter, Acidithiobacillus, Thiobacillus, Acidovorax*, a large diversity of Hyphomicrobiaceae including *Pedomicrobium, Filomicrobium*, and the recently isolated marine iron oxidizing bacterium *Mariprofundus* (Emerson et al. 2007) that dominated this environment. Although an initial clone library (data not shown) several sequences were related to known *Leptothrix* sequences none could be detected in the 454 sequences.

In comparision to sequences published in the International Nucleotide Sequence Database GenBank (in the following, accession codes are put in parentheses), sequences obtained by DGGE band excision and reamplification inter alia showed high similarities to two alpha-proteobacteria: a mucus bacterium (AY654810.2) and *Citreicella thiooxidans* (AY639887.1), a lithoheterotrophic sulphur-oxidizing bacterium, which had been detected at first in the Black Sea (Sorokin et al. 2005). The ochre microbial mats also harboured the beta-proteobacterium *Nitrosomonas sp.* (AB113603.2, AJ275891.2) and *Thiocapsa sp.*

(AJ632077.2), a sulphur-oxidizing delta-proteobacterium. The sulphate-reducing bacteria, *Desulfolobus propionicus* (AY953411.1, AY354098.1, AY354099.1, AY953400.1, DQ250787.1, AY953399.1), *Desulfolobus rhabdoformis* (AB263181.1, DQ250778.1), *Desulfobacterium autotrophicum* (AB263151.1) and *Desulfotalea psychrophila* (AY354094.1) were found in all mat types (white, black and ochre). DGGE-derived sequences with high similarity to *Methylomonas sp* (EF212354.1, AY424847.1, AY550695.1) were found in both ochre mat consortia connected to in- and outlet, as well as in white and black mats. Only two out of six archaeal species present in the ochre mat types could be blasted (NCBI, Blastx) yet, one with an uncultured Crenarchaeote (AF201358.1) and one with a ferromanganous micronodule archeon (AF293019).

FISH was used to illustrate the relation between the autotrophic denitrifying *Thiobacillus denitrificans* and sulphate reducing bacteria by comparing the white and black mats, applying according probe combinations (Fig. 7). Both community compounds were densely packed, dominating within the white mat, while the underlying black mat aggregation was dominated by SRB, but also interspersed with minerals and bacteria other than beta-proteobacteria, as shown by pure DAPI signals (Figs. 7B-C)

Microbial mat chemistry

Microscopy and LA-ICP-MS were used to investigate TREE fractionations and accumulations within the different microbial mats. A distinctive TREE pattern of each mat type, if existing, can potentially serve as an inorganic biosignature for iron oxidizing, sulphate reducing bacteria and sulphur oxidizing bacteria (IOB, SRB, SOX) respectively. Major and trace element contents of the microbial mats are given in Tables 2A and 2B. In the ochre mat, Fe, Mn, and Si are considerably more abundant than in the white and black mats. These elements seem to be distributed evenly within the ochre mat as our analyses did not reveal any element accumulation in a particular zone of the mat profile (Table 2A; see also Fig. 2).

On the other hand, in the white and black mats, alkaline and alkaline earth metals (Ca, K, Mg, Na) and the elements Al, Cr and Ti are significantly enriched as compared to the ochre mat (Table 2A). In all microbial mat types, REE were enriched up to 10^4-fold compared to the pond water (Table 2B). Whereas some transition metals (Sc, V, Cr, Co) do not show significant accumulation in any of the microbial mats, other transition metals (Cu, Zn), as well as the elements Se, As, Rb, Cs, Cd, Mo, Bi are highly enriched in the black and white mat (Tables 2A-B).

When normalising the observed element accumulation patterns on the pond water, it is possible to distinguish individual fractionation behaviours of the different mat types. Fig. 9 shows the accumulation of individual elements in order of increasing enrichment.
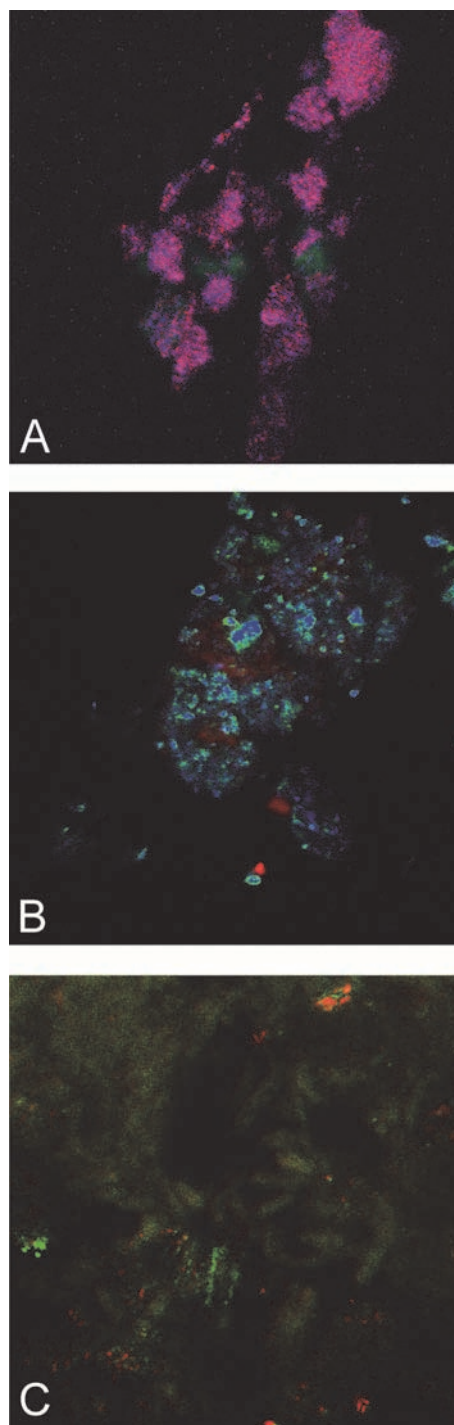
Fig. 7: Laser scanning microscopy coupled with fluorescent *in situ* hybridization (FISH) applying probes Beta42_og (Beta-proteobacteria, labeled with oregon green) and DSS658(cy3) (*Desulfosarcina/Desulfococcus*) on white consortia (**A**); Beta42(cy3) and SRB385(og) (sulfate reducing bacteria) applied to the black mat (**B, C**) from the main pond (abbreviations for fluorochromes cyanine 3 and oregon green in parentheses).
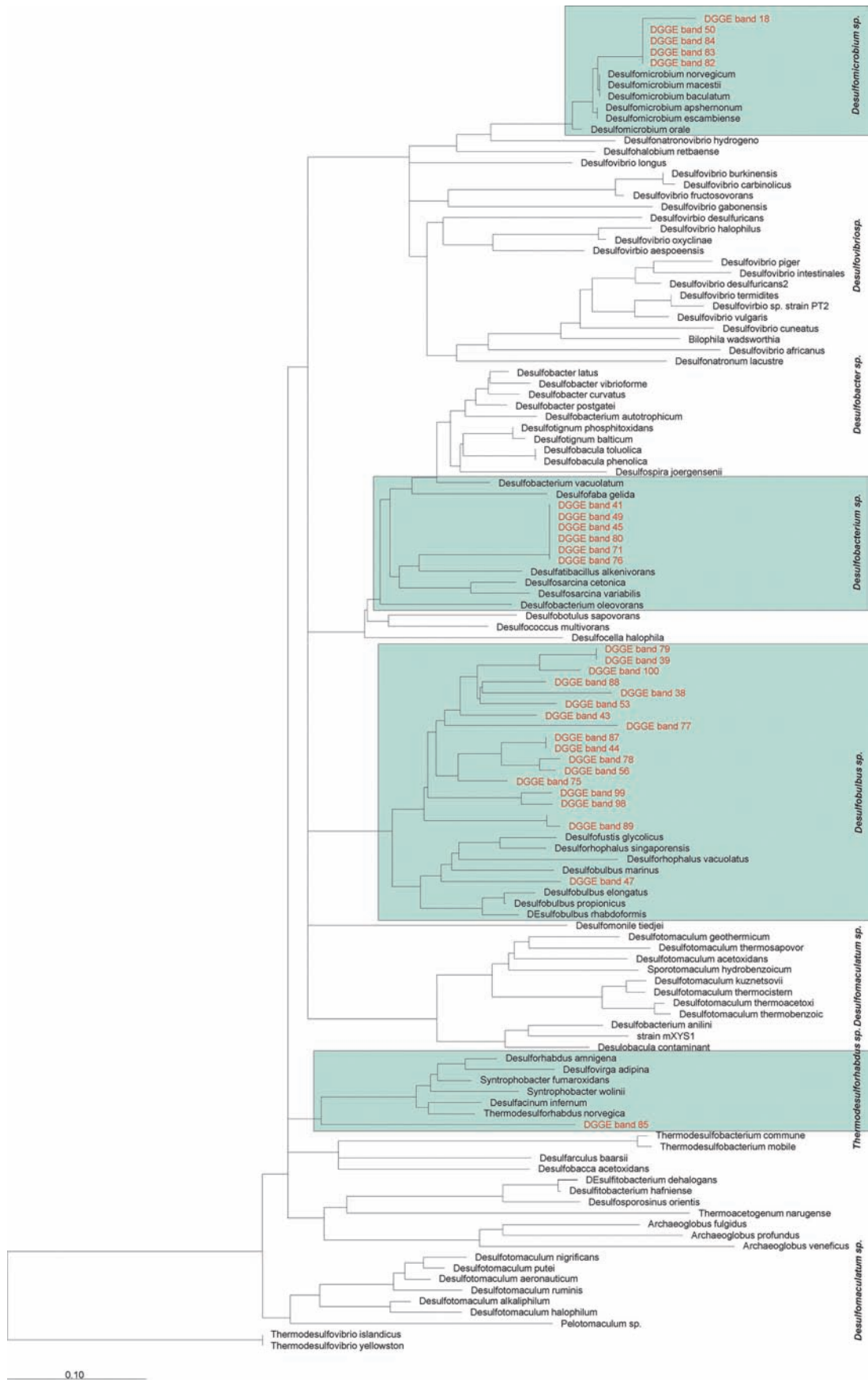
Fig. 8: Fitch-Margoliash tree (Consensus) of re-amplified DGGE-bands based on dsrB-derived PCR-products, indicating the encoding gene for the dissimilatory sulfate reductase. Areas indicate similarities to species matched by BLASTx (NCBI).

Table 2B: Trace element concentrations from the main pond water and from the black, white and ochre mats, respectively. TREE showed an even distribution along the ochre-mat profile, therefore, the data from this profile were merged (Table 2B) [b.d. = below detection limit].

|	Pond water mean mg/l	Ochre mat mg/kg	White Mat mg/kg	Black mat mg/kg
Li	155.7	35.43	342	193.4
Be	0.04	134.66	5.3	7.7
Sc	14.66	1283	b.d.	b.d.
V	78.7	272.35	246.8	224.3
Co	3.95	14.60	24.5	52.2
Ni	55.25	43.06	85.2	202.2
Cu	4.32	39.47	141	354
Zn	6.99	76.04	363	543
As	33.0	16.35	85.1	36.2
Se	13.1	4.69	51.3	17.3
Y	0.31	891	116	155
Zr	0.17	381	60.3	90.3
Nb	0.04	10.56	8.3	24.6
Mo	2.45	75.6	387	735
Cd	0.01	0.18	1.4	1.8
Sn	b.d.	2.49	12.9	27.0
Sb	0.16	0.77	1.8	2.0
Rb	48.1	25.8	75.9	166
Cs	5.43	3.26	101.2	91.8
Ba	1331	61457	977	1974
La	0.06	257.0	102.2	231.6
Ce	0.06	357	174.8	420
Pr	0.01	44.9	20.8	46.8
Nd	0.11	209.3	83.3	176.0
Sm	0.01	40.4	bd	4.32
Eu	b.d.	6.96	2.15	4.89
Gd	0.02	74.50	15.0	26.3
Tb	0.002	9.48	1.68	3.03
Dy	0.02	75.3	12.7	18.8
Ho	0.005	22.3	3.35	4.41
Er	0.02	80.6	9.86	12.7
Tm	0.003	11.5	1.43	1.97
Yb	0.03	84.4	9.64	13.5
Lu	0.01	16.7	1.95	2.45
Hf	0.001	1.33	1.01	1.74
Ta	b.d.	0.02	0.63	1.31
W	0.39	302	47.3	63.1
Tl	b.d.	0.11	0.33	0.85
Pb	b.d.	59.30	79.2	158.7
Bi	b.d.	0.24	1.01	2.81
Th	b.d.	2.56	18.4	26.3
U	1.28	21.82	21.1	39.3

Comparing the black and white mat, they show a similar fractionation pattern, but rather contrasting to the ochre mat. The white and black mats show a generally higher enrichment of most of the trace elements except for the REE. The highest REE accumulation rates were observed in the ochre mat. Furthermore, the even fractionation pattern shows that the REE distribution of the ochre mat mirrors quite exactly the major water chemistry, but with an enrichment factor of about 10^4. The white and black mats show a preferential enrichment of the light REE (La-Sm) over the heavy REE (Gd-Lu).

Discussion

The water chemistry of the pond remained quite stable over the three years, and no seasonal variations were detected. The interaction between the microbial mats and the pond water seem to be rather stable. A remarkable impact of the microbial mat activity on the pond fluid is the maintenance of hypoxic conditions close to the mats (Table 1), even though the large pond surface is exposed to a "normal" atmosphere. Although the oxygen concentration of the pond water is significantly higher close to the pond surface, the microbial community of the ochre mat seems to be able to maintain favouring conditions to oxidize Fe(II). Keeping the O_2 concentration below 5 mg/l (ca. 150 μmol/l) in the main pond water enables a half life time of Fe(II) of several minutes (Emerson et al. 2010 and references therein). These conditions still allow iron oxidizing microbial communities to thrive and form thick microbial mats all over the pond.

The pyrosequencing results indicate that *Gallionella* sp. is not as abundant in the ochre mat as it was anticipated from previous reports (Pedersen & Hallbeck 1985; Hallbeck et al. 1993; Pedersen et al. 1996; Anderson & Pederson 2003). Rather, *Mariprofundus ferrooxidans* was found to be the dominating stalk-producing IOB in the studied pond. Although a visual differentiation through comparison of the order and structures of the stalks between certain *Gallionella* and *Mariprofundus* species is possible (Comolli et al. 2011), such differences where not observed in our samples. Both *G. ferruginea* and *M. ferrooxidans* are able to cast off their old, mineral-covered stalks and replace them by fresh ones (Cholodny 1926; Emerson et al. 2007). Due to the effective production of iron oxyhydroxides and the permanent replacement of heavily encrusted stalks, the ratio of mineral precipitates to organic matter is extremely high in these IOB-dominated mats.

The TREE accumulation in the ochre mat shows a signature, conserving mostly the TREE pattern of the feeder fluid, especially the REE (Fig. 9) with a constant 10^4 enrichment. The iron oxidizing bacteria *Mariprofundus* sp. and *G. ferruginea* are able to control the iron mineralization process to some degree (Saini & Chan 2012). This would allow a localized distribution of the biotic and abiotic minerals formed. Although the stalk surface is smooth and pristine during the initial stage of formation, with increasing distance and age, the stalk becomes more and more coated with lepidocrocite (FeOOH) and two-line ferrihydrite (Chan et al. 2011).

The accumulation rates of REE, Be, Y, Zr, Nb, Hf and W in the ochre mat were as high as those of Fe (Tables 2A-B) indicating a co-precipitation with the iron oxyhydroxides. This strong metal sorption capacity of iron oxyhydroxides is also widely used in technical applications and remediation activities (de Carlo et al. 1998; Bau 1999; Cornell & Schwertmann 2004; Michel et al. 2007).
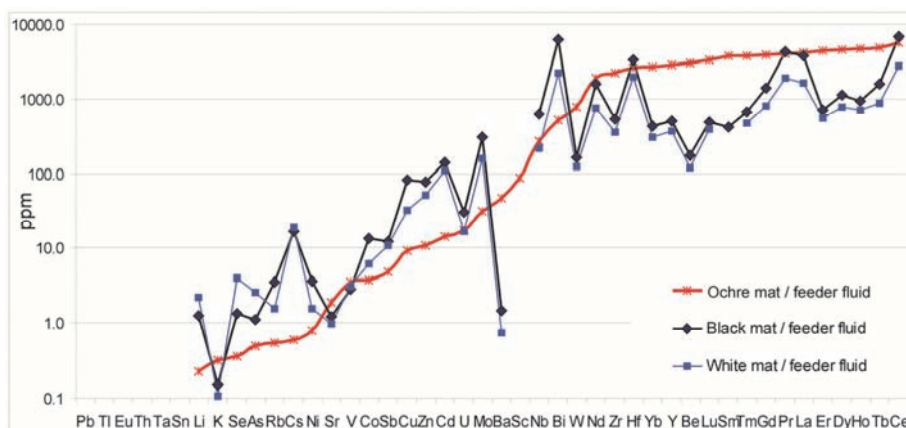
Fig. 9: Element fractionation in mineralized microbial mats normalised on the inflowing water. All data are mean values of five single samples from the same mat type. The elements are ordered according to the highest accumulation in the ochre mat. All microbial mat types (ochre, black and white) show an up to 10^6 fold accumulation of TREE compared to the TREE content in the aquifer. In addition, the TREE pattern ochre mat resembles quite exactly the pattern of the feeder fluid, whereas the black and white mats show more distinctive fractionations.

However, not only the microbial iron oxyhydroxides, but also the EPS-composed stalks play an important role in TREE precipitation as they offer large reactive surfaces for the biosorption of metals. Metals with a higher positive charge tend to show enhanced biosorption (Haferburg et al. 2007). This may also explain the higher enrichments observed for the 3- and 4-valent elements Si, Mn, REE, Y, Zr, Hf, U, and W compared to lower valent elements like Ca, K, Mg, Na, Cs, Rb and Li. However, although a preferential uptake of specific elements was not observed in the IOB dominated ochre mat, the general enrichment pattern seems to reflect the environmental conditions throughout the activity of the microbial mat.

According to DGGE as well as FISH results, the black and white mats seem to harbour similar community members mainly involved in sulphur oxidation, autotrophic denitrification, aerobic methylotrophy and sulphate reduction, which have been shown to build layers of dense aggregates (Fig. 6). Sulphur compounds are both used by SRB and autotrophic denitrifiers such as *Thiobacillus denitrificans* as electron donor, coupling the oxidation of inorganic sulphur compounds (such as hydrogen sulphide and thiosulphate) to the reduction of oxidized nitrogen compounds (such as nitrate, nitrite) to dinitrogen. This facultative anaerobic beta-proteobacterium was found also to couple the anaerobic oxidation of Fe(II) to denitrification, utilizing poorly-soluble minerals containing reduced iron and/or sulphur, such as pyrite (FeS_2) and FeS (Straub et al. 1996).

Overall, sulphate reducers are found in all type of mats presented here, while not all of them exhibited an active dissimilatory sulphate reduction; such, most sequences obtained by DGGE on the base of functional genes such as dsrB (Fig. 8) fall within the *Desulfobacterium* sp., *Desulfobulbus* sp. and *Desulfomicrobium* sp. clusters. However, any similarity to *Desulfobulbus* sp. might overlap with *Desulfocapsa* sp., which was not included in this analysis. Despite

their visual appearance, the microbial communities of the black and the white mat were rather similar, harbouring a significant amount of SRB, closely aggregated with beta-proteobacteria such as *Thiobacillus denitrificans* (Fig. 7). This is in good agreement with H_2S profiles (Fig. 3), in the white and black mat, showing a high concentration above the black mat and decreasing in the white mat. Although SEM analyses indicate the presence of filamentous, sulphur-oxidizing bacteria (Fig. 5), no respective sequences could be retrieved from DGGE band sequencing. In general, fingerprinting analyses need always careful interpretation, including the evaluation of bias of PCR primer-based strategies (Mahmood et al. 2006) and the fact of potentially poor amplicon separation by DGGE and re-amplification (Nikolausz et al. 2005). Consequently, the total of sequences obtained by DGGE band excision may not represent all members of the complete microbial community in the pond

Although a great similarity between the microbial communities at the in- and outflow were detected the localized occurrence of specialized mat types in the pond argues for different controlling factors for the microbial mat formation. The substrate could be such a controlling factor. Indeed, the analysis of rock samples showed that at the growth location of the black and white mats, the surrounding grano-dioritic host rock was covered with concrete. Apparently, the presence of concrete created a micro-environment within the pond that favoured the presence of SRB and SOX communities. Concretes and cements commonly contain considerable amounts of either gypsum or sulphate rich fly ash (e.g., Iglesias et al. 1999; Guo & Shi 2008; Camarini & De Milito 2011). Thus, the concrete may serve as a likely sulphate source for the microbial communities.

The high accumulation of Cu, Zn, Se, As, Rb, Cs, Cd, Mo, Bi in the black mat can be mainly attributed to the activity of SRB resulting in the production and precipita-

tion of iron sulphide minerals (Huerta-Diaz & Morse 1992; Watson et al. 1995; Beech & Cheung, 1995; Neumann et al. 2006). Studies showed that accumulations of TREE like Co, Cu, Mn and Ni with pyrite (FeS_2) are linear to the amount of pyrite produced, due to co-precipitation of these trace elements with biogenic pyrite (Huerta-Diaz & Morse 1992). Therefore, the TREE fractionation pattern observed in the black was related to the dominating SRB in this mat. Further comparison to TREE fractionation in SRB-derived iron sulphides is difficult due to sparse reference literature. In most contemporary palaeontological studies, the morphological occurrence (e.g., pyrite framboids) and or the fractionation of iron and sulphur isotopes is attributed to the activity of sulphate reducing prokaryotes (a.o., Beard et al. 1999; Icopini et al. 2004; Shen & Buik 2004; Fortin & Langley 2005; Watson et al. 2009; Canfield et al. 2010; Cavalazzi et al. 2012). However, a systematic evaluation of TREE fractionation in biogenic pyrite is necessary to allow a further differentiation from hydrothermal pyrite and its validation as a biosignature. As the white mat seem to consist of several dominating communities (sulphate reducing, sulphur oxidizing and methanotrophic bacteria) the TREE pattern of this mat will not be discussed further as clear attribution to a certain community is not possible.

Conclusions

Mineralizing microbial mats from an open pond in the subsurface were investigated. Although a visual differentiation of three different mat types (ochre, black and white) was possible, the microbial communities involved were much more complex and heterogeneous. However, a clear relation of a dominating microbial consortium to a respective mat type was partly possible, like the attribution of iron oxidizing bacteria to the ochre and sulphate reducing bacteria to the black mat. The microbial community of the white mat was rather complex and, unlike the other microbial mats, showed no indication for a clearly dominating metabolic group of microorganisms.

A clear relationship of between microbial key players and specific biogeochemical processes is necessary to evaluate microbially induced trace and rare earth element (TREE) accumulation and fractionation. These accumulation or fractionation patterns could therefore serve as potential biosignatures for the respective mat metabolism. The ochre mat dominated by iron oxidizing bacteria, showed an even 1000 fold accumulation of rare earth elements (REE), but still reflected the pattern of the feeder fluid. A similar behaviour is observed for the most higher valent trace metals that co-precipitated with the microbial iron oxyhydroxides. Therefore, the TREE enrichment pattern of the iron oxidizing microbial mat largely reflects the environmental conditions prevailing throughout the activity of the microbial mat. In contrast, the black mat,

dominated by sulphate reducing bacteria, showed a TREE fractionation that significantly differs from both, the iron oxidizing microbial mat and the pond water. The accumulated TREE can mainly be attributed to the microbially formed pyrite within this mat. These observations point at a potential utility of this fraction pattern as a distinctive biosignature, but a further validation and comparison with other microbial mats and biotically and abiotically formed pyrites is necessary.

Acknowledgements

References

Altschul, S. F.; Gish, W.; Miller, W.; Myers, E. W. & Lipman, D. J. (1990): Basic local alignment search tool. *Journal of Molecular Biology* **215**: 403-410. http://dx.doi.org/10.1016/S0022-2836(05)80360-2

Amann, R. I.; Krumholz, L. & Stahl, D. A. (1990): Fluorescent-oligonucleotide probing of whole cells for determinative, phylogenetic, and environmental studies in microbiology. *Journal of Bacteriology* **172**(2): 762-770.

Anderson, C. R. & Pedersen, K. (2003): *In situ* growth of *Gallionella* biofilms and partitioning of lanthanides and actinides between biological material and ferric oxyhydroxides. *Gebiology* **1**: 169-178. http://dx.doi.org/10.1046/j.1472-4669.2003.00013.x

Bailey, J. V.; Orphan, V. J.; Joye, S. B. & Corsetti, F. A. (2009): Chemotrophic Microbial Mats and Their Potential for preservation in the Rock Record. *Astrobiology* **9** (9): 843-859. http://dx.doi.org/10.1089/ast.2008.0314

Bau, M. (1999) Scavenging of dissolved yttrium and rare earths by precipitating iron oxyhydroxide: Experimental evidence for Ce oxidation, Y-Ho fractionation, and lanthanide tetrade effect. *Geochimica et Cosmochimica Acta* **63** (1): 67-77. http://dx.doi.org/10.1016/S0016-7037(99)00014-9

Bazylinski, D. A.; Frankel, R. B. & Konhauser, K. O. (2007): Modes of Biomineralization of Magnetite by Microbes. *Geomicrobiology Journal* **24** (6): 465-475. http://dx.doi.org/10.1080/01490450701572259

Beard, B. L.; Johnson, C. M.; Cox, L.; Sun, H.; Nealson, K. H. & Aguilar, C. (1999): Iron isotope biosignatures. *Science* **285** (5435): 1889-1892. http://dx.doi.org/10.1126/science.285.5435.1889

Camarini, G. & De Milito, J. A. (2011): Gypsum hemihydrate–cement blends to improve rendering durability. *Construction and Building Material* **25** (11): 4121-4125. http://dx.doi.org/10.1016/j.conbuildmat.2011.04.048

Canfield, D.; Farquhar, J. & Zerkle, A. L. (2010) High isotope fractionations during sulfate reduction in a low-sulfate euxinic

ocean analog. *Geology* **38** (5): 415-418. http://dx.doi.org/10.1130/G30723.1

Casamayor, E. O.; Schäfer, H.; Bañeras, L.; Pedrós-Alió, C. & Muyzer, G. (2000): Identification of and Spatio-Temporal Differences between Microbial Assemblages from Two Neighboring Sulfurous Lakes: Comparison by Microscopy and Denaturing Gradient Gel Electrophoresis. *Applied Environmental Microbiology* **66** (2): 499-508.

Cavalazzi, B.; Barbieri, R.; Cady, S. L.; George, A. D.; Gennaro, S.; Westall, F.; Luif, A.; Canteri, R.; Rossi, A. P.; Ori, G. G. & Taj-Eddie, K. (2012): Iron-framboids in the hydrocarbon-related Middle Devonian Hollard Mound of the Anti-Atlas mountain range in Morocco: Evidence of potential microbial biosignatures. *Sedimentary Geology* **263-264**:183-193. http://dx.doi.org/10.1016/j.sedgeo.2011.09.007

Chan, C. S.; Fakra, S. C.; Emerson, D.; Fleming, E. J. & Edwards K. J. (2011): Lithotrophic iron-oxidizing bacteria produce organic stalks to control mineral growth: implications for biosignature formation. *The ISME Journal* **5** (4): 717-727. http://dx.doi.org/10.1038/ismej.2010.173

Cholodny, N. G. (1926): Die Eisenbakterien - Beiträge zu einer Monographie. In: Kolkwitz, R. (ed.): *Pflanzenforschung* **4**. Jena (G. Fischer): vi + 162 pp.

Comolli, L. R.; Luef, B. & Chan, C. S. (2011): High-resolution 2D and 3D cryo-TEM reveals structural adaptations of two stalk-forming bacteria to an Fe-oxidizing lifestyle. *Environmental Microbiology* **13** (11): 2915-2929. http://dx.doi.org/10.1111/j.1462-2920.2011.02567.x

Cornell, M. & Schwertmann, U. (2004): *The Iron Oxides*. Weinheim (Wiley-VCH): 664 pp.

Daims, H.; Bruhl, A.; Amann, R.; Schleifer, K. H.; & Wagner, M. (1999): The domain-specific probe EUB338 is insufficient for the detection of all Bacteria: development and evaluation of a more comprehensive probe set. *Systematic and Applied Microbiology* **22**: 434-444. http://dx.doi.org/10.1016/S073-2020(99)80053-8

De Carlo, E. H.; Wen Xi-yuan & Irving, M. (1998): The Influence of Redox Reactions on the Uptake of Dissolved Ce by Suspended Fe and Mn Oxide Particles. *Aquatic Geochemistry* **3** (4): 357-389. http://dx.doi.org/10.1023/A:1009664626181

Emerson, D.; Flemming, E. J. & McBeth, J. M. (2010): Iron-Oxidizing Bacteria: An Environmental and Genomic Perspective. *Annual Reviews in Microbiology* **64**: 561-583. http://dx.doi.org/10.1146/annurev.micro.112408.134208

Emerson, D.; Rentz, J. A.; Lilburn, T. G.; Davis, R. E.; Aldrich, H.; Chan, C. & Moyer, C. L. (2007): A Novel Lineage of Proteobacteria Involved in Formation of Marine Fe-Oxidizing Microbial Mat Communities. *PLoS ONE* **2** (8): 1-9 [e667]. http://dx.doi.org/10.1371/journal.pone.0000667

Felsenstein, J. (1993): PHYLIP (Phylogeny Inference Package) version 3.5c. Distributed by the author. Department of Genetics, University of Washington, Seattle. (based on Felsenstein, J. 1989. PHYLIP -- Phylogeny Inference Package (Version 3.2). *Cladistics* **5**: 164-166. http://dx.doi.org/10.1111/j.1096-0031.1989.tb00562.x

Ferris, F. G.; Hallberg, R. O.; Lyvén, B. & Pedersen, K. (2000): Retention of strontium, cesium, lead and uranium by bacterial iron oxides from subterranean environment. *Applied Geochemistry* **15** (7): 1035-1042. http://dx.doi.org/10.1016/S0883-2927(99)00093-1

Ferris, F. G.; Kohnhauser, K. O.; Lyvén, B. & Pedersen, K. (1999): Accumulation of metals by bacteriogenic iron oxides in a subterranean environment. *Geomicrobiology Journal* **16** (2): 181-192. http://dx.doi.org/10.1080/014904599270677

Fortin, D.; Langley, S. (2005): Formation and occurrence of biogenic iron-rich minerals. *Earth-Science Reviews* **72**: 1-19. http://dx.doi.org/10.1016/j.earscirev.2005.03.002

Geets, J. B.; Borremans, L.; Diels, D.; Springael, J.; Vangronsveld, D.; Lelie, D. van der & Vanbroekhoven, K. (2006): DsrBgene-based DGGE for community and diversity surveys of sulfate-reducing bacteria. *Journal of Microbiology Methods* **66** (2):194-205. http://dx.doi.org/10.1016/j.mimet.2005.11.002

Guo, Xiao-lu & Shi, Hui-sheng (2008): Thermal treatment and utilization of flue gas desulphurization gypsum as an admixture in cement and concrete. *Construction and Building Materials* **22**: 1471-1476. http://dx.doi.org/10.1016/j.conbuildmat.2007.04.001

Haferburg, G. & Kothe, E. (2007): Microbes and metals: interactions in the environment. *Journal of Basic Microbiology* **47** (6): 453-467. http://dx.doi.org/10.1002/jobm.200700275

Haferburg, G.; Merten, D.; Büchel, G. & Kothe, E. (2007): Biosorption of metal and salt tolerant microbial isolates from a former uranium mining aerea. Their impact on changes in rare earth element patterns in acid mine drainage. *Journal of Basic Microbiology* **47** (6): 474-484.

Hall, T. A. (1999): BioEdit: a user-friendly biological sequence alignment editor and analysis program for Windows 95/98/NT. *Nucleic Acids Symposium Series* **41**: 95-98.

Hallbeck, L.; Ståhl, F. & Pedersen, K. (1993): Phylogeny and phenotypic characterization of the stalk-forming and iron-oxidizing bacterium *Gallionella ferruginea*. *Journal of General Microbiology* **139**:1531-1535. http://dx.doi.org/10.1099/00221287-139-7-1531

Hansen, H. P. (1999): Determination of oxygen. In: Grasshoff, K.; Kremling, K. & Ehrhardt, M. (eds.): *Methods of seawater analysis*. Hoboken (Wiley-VCH): 75-89.

Huerta-Diaz, M. A. & Morse J. W. (1992): Pyritization of trace metals in anoxic marine sediments. *Geochimica et Cosmochimica Acta* **56**: 2681-2702. http://dx.doi.org/10.1016/0016-7037(92)90353-K

Icopini, G. A.; Anbar, A. D.; Ruebush, S. S.; Tien, M. & Brantley, S. K. (2004): Iron isotope fractionation during microbial reduction of iron: The importance of adsorption. *Geology* **32** (3): 205-208. http://dx.doi.org/10.1130/G20184.1

Iglesias, J. G.; Álvarez, M. M. & Rodríguez, J. E. (1999): Influence of gypsum's mineralogical characteristics on its grinding behaviour applied to cement fabrication. *Cement and Concrete Research* **29** (5): 727-730. http://dx.doi.org/10.1016/S0008-8846(99)00038-1

Ionescu, D.; Siebert, C.; Munwes, Y. Y.; Lott, C.; Häusler, S.; Bizic-Ionescu, M.; Quast, C.; Peplies, J.; Glöckner, F. O.; Ramette, A.; Rödinger, T.; Dittmar, T.; Oren, A.; Geyer, S.; Stärk, H. J.; Sauter, M.; Licha, T.; Laronne, J. B. & De Beer, D. (2012): Microbial and Chemical Characterization of Underwater Fresh Water Springs in the Dead Sea. *PLoS ONE* **7** (6): 1-21 [e38319]. http://dx.doi.org/10.1371/journal.pone.0038319

Konhauser, K. O. (1997): Bacterial iron biomineralisation in nature. *FEMS Microbiology Reviews* **20** (3-4): 315-326. http://dx.doi.org/10.1016/S0168-6445(97)00014-4

Ludwig, W.; Strunk, O.; Westram, R.; Richter, L.; Meier, H.; Yadhukumar; Buchner, A.; Lai, T.; Steppi, S.; Jobb, G.; Förster, W.; Brettske, I.; Gerber, S.; Ginhart, A. W.; Gross, O.; Grumann, S.; Hermann, S.; Jost, R.; König, A.; Liss, T.; Lüßmann, R.; May, M.; Nonhoff, B.; Reichel, B.; Strehlow, R.; Stamatakis, A.; Stuckmann, N.; Vilbig, A.; Lenke, M.; Ludwig, T.; Bode, A. & Schleifer, K.-H. (2004): ARB: a software environment for sequence data. *Nucleic Acids Research* **32** (4): 1363-1371. http://dx.doi.org/10.1093/nar/gkh293

Mahmood, S.; Freitag, T. E. & Prosser, J. I. (2006): Comparison of PCR primer-based strategies for characterization of ammonia oxidizer communities in environmental samples. *FEMS Microbiology Ecology* **56** (3): 482-493. http://dx.doi.org/10.1111/j.1574-6941.2006.00080.x

Manz, W.; Amann, R.; Ludwig, W.; Wagner, M. & Schleifer, K. H. (1992): Phylogenetic Oligodeoxynucleotide Probes for the Major Subclasses of Proteobacteria: Problems and Solutions. *Systematic and Applied Microbiology* **15** (4): 593-600.

Manz, W.; Eisenbrecher, M.; Neu, T. R. & Szewzyk, U. (1998): Abundance and spatial organization of Gram-negative sulfate-reducing bacteria in activated sludge investigated by in situ probing with specific 16S rRNA targeted oligonucleotides. *FEMS Microbiology Ecology* **25** (1): 43-61. http://dx.doi.org/10.1111/j.1574-6941.1998.tb00459.x

Michel, M. F.; Ehm, L.; Antao, S. M.; Lee, P. L.; Chupas, P. J.; Liu, G.; Strongin, D. R.; Schoonen, M. A. A.; Phillips, B. L. & Parise, J. B. (2007): The structure of ferrihydrite, a nanocycrstalline material. *Science* **316** (5832): 1726-1729. http://dx.doi.org/10.1126/science.1142525

Muyzer, G.; Teske, A.; Wirsen, C. O. & Jannasch, H. W. (1995): Phylogenetic relationships of *Thiomicrospira* species and their identification in deep-sea hydrothermal vent samples by denaturing gradient gel electrophoresis of 16S rDNA fragments. *Archives of Microbiology* **164** (3):165-172. http://dx.doi.org/10.1007/BF02529967

Nikolausz, M.; Sipos, R.; Révész, S.; Székely, A. & Márialigeti, K. (2005): Observation of bias associated with re-amplification of DNA isolated from denaturing gradient gels. *FEMS Microbiology Letters* **244** (2): 385-390. http://dx.doi.org/10.1016/j.femsle.2005.02.013

Pedersen, K. (1997): Microbial life in deep granitic rock. *FEMS Microbiology Reviews* **20** (3-4): 399-414. http://dx.doi.org/10.1111/j.1574-6976.1997.tb00325.x

Pedersen K.; Arlinger, J.; Ekendahl, S. & Hallbeck, L. (1996): 16s rRNA gene diversity of attached and unattached bacteria in boreholes along the access tunnel to the Äspö Hard Rock Laboratory, Sweden. *FEMS Microbiology Ecology* **19**: 249-262. http://dx.doi.org/10.1111/j.1574-6941.1996.tb00217.x

Quast, C.; Pruesse, E.; Yilmaz, P.; Gerken, J.; Schweer, T.; Yarza, P.; Peplies, J. & Glöckner, F. O. (2013): The SILVA ribosomal RNA gene database project: improved data processing and web-based tools. *Nucleic acids research* **41** (Database issue): D590–6. http://dx.doi.org/10.1093/nar.gks1219

Reguera, G.; McCarthy, K. D.; Mehta, T.; Nicoll, J. S.; Tuominen, M. T. & Lovely, D. R. (2005): Extracellular electron transfer via microbial nanowires. *Nature* **435** (7045): 1098-1101. http://dx.doi.org/10.1038/nature03661

Russel, M. J. (2003): The importance of being alkaline. *Science* **302** (5645): 580-581. http://dx.doi.org/10.1126/science.1091765

Santegoeds, C. M.; Schramm, A. & de Beer, D. (1998): Microsensors as a tool to determine chemical microgradients and bacterial activity in wastewater biofilms and flocs. *Biodegradation* **9** (3-4): 159-167. http://dx.doi.org/10.1023/A:1008302622946

Schäfer, H. & Muyzer, G. (2001): Denaturing gradient gel electrophoresis in marine microbial ecology. *Methods in Microbiology* **30**: 425-468. http://dx.doi.org/10.1128/AEM.67.7.2942-2951.2001

Shen Yanan & Buick, R. (2004): The antiquity of microbial sulfate reduction. *Earth Science Reviews* **64** (3-4): 243-272. http://dx.doi.org/10.1016/S0012-8252(03)00054-0

Snaidr, J.; Amann, R.; Huber, I.; Ludwig, W. & Schleifer, K. H. (1997): Phylogenetic analysis and in situ identification of bacteria in activated sludge. *Applied Environmental Microbiology* **63** (7): 2884-2896.

Sorokin, D. Y.; Tourova, T. P. & Muyzer, G. (2005): *Citreicella thiooxidans* gen. nov., sp. nov., a novel lithoheterotrophic sulfur-oxidizing bacterium from the Black Sea. *Systematic and Applied Microbiology* **28** (8): 679-687. http://dx.doi.org/10.1016/j.syapm.2005.05.006

Straub, K. L.; Benz, M.; Schink, B. & Widdel, F. (1996): Anaerobic, nitrate-dependent microbial oxidation of ferrous iron. *Applied Environmental Microbiology* **62** (4): 1458-1460.

Takahashi, Y.; Hirata, T.; Shimizu, H.; Ozaki, T. & Fortin, D. (2007): A rare earth element signature of bacteria in natural waters? *Chemical Geology* **244** (3-4): 569-583. http://dx.doi.org/10.1016/j.chemgeo.2007.07.005

Templeton, A. & Knowles, E. (2009): Microbial Transformations of Minerals and Metals: Recent Advances in Geomicrobiology Derived from Synchrotron-Based X-Ray Spectroscopy and X-Ray Microscopy. *Annual Reviews in Earth and Planetary Sciences* **37**: 367-391. http://dx.doi.org/10.1146/annurev.earth.36.031207.124346

Trevors, J. T. (2002): The subsurface origin of microbial life on the Earth. *Research in Microbiology* **153** (8): 487-491. http://dx.doi.org/10.1016/S0923-2508(02)01360-8

Wagner, M. A.; Roger, J.; Flax, J. L.; Brusseau, G. A. & Stahl, D. A. (1998): Phylogeny of Dissimilatory Sulfite Reductases Supports an Early Origin of Sulfate Respiration. *Journal of Bacteriology* **180** (11): 2975-2982.

Wallner, G.; Amann, R.; Beisker, W. (1993): Optimizing fluorescent in situ hybridization with rRNA-targeted oligonucleotide probes for flow cytometric identification of microorganisms. *Cytometry* **14** (2): 136-143. http://dx.doi.org/10.1002/cyto.990140205

Watson, E. B.; Cherniak, D. J. & Frank, E. A. (2009): Retention of biosignatures and mass-independent fractionations in pyrite: Self-diffusion of sulfur. *Geochimica et Cosmochimica Acta* **73**: 4792-4802. http://dx.doi.org/10.1016/j.gca.2009.05.060

Weiner, S. & Dove, P. M. (2003): An Overview of Biomineralization Processes and the Problem of the Vital Effect. In: Dove, P. M.; De Yoreo, J. J. & Weiner, S. (eds.): Biomineralization. *Reviews in Mineralogy & Geochemistry* **54** (1): 1-29. http://dx.doi.org/10.2113/0540001

Wieland, A.; Zopfi, J.; Benthien, M. & Kühl, M. (2005) Biogeochemistry of an Iron-Rich Hypersaline Microbial Mat (Camargue, France). *Microbial Ecology* **49** (1): 34-49. http://dx.doi.org/10.1007/s00248-003-2033-4

Raman spectroscopy of biosignatures in methane-related microbialites

Tim Leefmann[1,2] *; Martin Blumenberg[3]; Burkhard C. Schmidt[4] & Volker Thiel[2] *

[1]Department of Earth and Planetary Sciences, Macquarie University, Sydney, NSW 2109, Australia;
Email: tim.leefmann@mq.edu.au

[2]Department of Geobiology, Geoscience Centre, Georg-August University Göttingen, Goldschmidtstr. 3,
37077 Göttingen, Germany; Email: Volker.Thiel@geo.uni-goettingen.de

[3]Federal Institute for Geosciences and Natural Resources (BGR), Stilleweg 2, 30655 Hannover, Germany;
Email: Martin.Blumenberg@bgr.de

[4]Department of Experimental and Applied Mineralogy, Geoscience Centre, Georg-August University Göttingen, Gold-
schmidtstr. 1, 37077 Göttingen, Germany

* corresponding authors

A major challenge in geobiological studies is the localization of organic compounds in a mineral matrix. Raman spectroscopy is here potentially powerful as it can be employed directly on rock surfaces and is capable of the characterization of organic and inorganic compounds in one analyzing step. In this study we tested Raman spectroscopy to approach the organic matter information locked in the complex mineral phase association of methane-related carbonate chemoherms of different age (Hydrate Ridge, Lincoln Creek, Münder Formation, Black Sea). Our data show that Raman spectroscopy allows detecting differences in the amount of organic material in geobiological samples on a micrometer scale. Particularly for the microbialites from Hydrate Ridge and the Lincoln Creek Formation, these studies were able to distinguish on a mm-scale fossilized biofilms of methanotrophic consortia from precipitates that were not directly mediated by microorganisms. However, Raman spectroscopy did not allow for a compound-class specific characterization of the organic material within the microbialite samples. A laser excitation wavelength of 244 nm was determined as most promising for the analysis of organic matter contents of carbonates, as it largely avoids autofluorescence. Comparisons with published extract-based studies (GC-MS) of the same samples demonstrate that the different techniques cannot replace each other, but should rather be used in conjunction in geobiological studies.

Introduction

In studies of microbially controlled systems such as biofilms, stromatolites and other microbialites on small scales, the exact localization of organic compounds represents a major analytical challenge. Because of the consumption of relatively high sample amounts (typically >1000 mg), extraction-based biomarker techniques provide bulk information, and their spatial resolution usually stands isolated from the microscopic and inorganic techniques that operate at the microscopic level (e.g., SEM/EDX, EMS, LA-ICP-MS). In geobiological studies this problem makes it difficult to associate distinctive mineral precipitates with the former presence of particular microbes and by implication, biogeochemical pathways. Likewise it is difficult to estimate as to what extent organic substances retain their once existing spatial association with an inorganic mineral phase during diagenesis. Ap-

proaching higher spatial resolution in the analysis of organic biomarkers in inhomogeneous samples is therefore a highly desirable goal and several recent biomarker studies aimed in that direction. These studies encompassed, for instance, the phase specific fatty acid analysis of fossil carbonate concretions using conventional gas chromatography-mass spectrometry (Pearson et al. 2005; Leefmann et al. 2008; Hagemann et al. 2013), microanalysis of organic fossils using laser pyrolysis-GC-MS (La-Py-GC-MS; Greenwood et al. 1998), and mapping of organic compounds using Time-of-Flight Secondary Ion Mass Spectrometry (ToF-SIMS, Toporski et al. 2002; Thiel et al. 2007).

Here we employed Raman spectroscopy to approach the organic matter information locked in complex mineral phase association of methane-related carbonate chemoherms. Methane–derived carbonate formation is particularly pronounced at cold seeps, areas on the ocean floor where methane-rich fluids or gas escapes from the sediment into the water column. It is commonly accepted that carbonate precipitation is due to the microbial anaerobic oxidation of upward migrating methane by downward migrating sulfate coming from the sea water (AOM; Iversen & Jörgensen 1985; Reeburgh 1976; Barnes & Goldberg 1976). The exact mechanisms of AOM have not been finally clarified, but probably involve the oxidation of methane (CH_4) to carbon dioxide (CO_2) by methanotrophic archaea via reverse methanogenesis (Gal'chenko 2004) and sulfate-reduction to hydrogen sulphide (HS^-) by sulfate reducing bacteria (SRB) according to the sum reaction

$$CH_4 + SO_4^{2-} \rightarrow HCO_3^- + HS^- + H_2O$$

(Valentine & Reeburgh 2000)
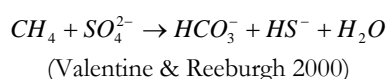
Since the mid 1980s active cold seeps have been discovered at various ocean margin settings (Suess et al. 1985; Polikarpov et al. 1992; Greinert et al. 2002; Werne et al. 2004). Beside the recent cold seeps, fossil counterparts of Cenozoic, Mesozoic and even Palaeozoic age have been found (Campbell et al. 2002; Peckmann & Thiel 2004; Birgel et al. 2008). At recent cold seep sites diverse types of carbonates occur (Greinert et al. 2001), but the most common chemoherm carbonates are aragonites and low Mg-calcites (Peckmann et al. 2001; Reitner et al. 2005; Teichert et al. 2005). Whether aragonite or low Mg-calcite is precipitated, is not yet understood but assumed to depend on sulfate and phosphate concentrations, carbonate supersaturation and the viscosity of the growth medium (Peckmann et al. 2001).

Our study aimed to test the utility of Raman spectroscopy for directly probing the distribution of organic matter in a number of methane-related carbonates, and to establish a linkage between the past activity of microorganisms and the precipitation of distinctive mineral phases at cold seeps. Modern micro-Raman systems comprise one or more lasers which are focused through a microscope on the sample. Such micro-Raman systems are capable of analyzing the organic and inorganic features of samples

with lateral resolutions at the micrometer scale. Moreover, by the introduction of confocal microscopy the spatial resolution along the optical axis has been additionally improved. However, the occurrence of high intensity fluorescence is the major problem in Raman spectroscopy, especially when applying this technique to biological samples containing fluorophores. As the Raman signal is usually comparatively low in intensity, the occurrence of fluorescence complicates the identification of individual Raman-active vibrational modes by masking the corresponding Raman bands. However, recent advances in technology have addressed this problem. Fluorescence effects may be decreased or avoided by using the Resonance Raman Effect (RRE; e.g., Kiefer 1995), Surface-Enhanced Raman Scattering (SERS; e.g., Kneipp et al. 1999), or deep ultra violet (UV) Raman spectroscopy (e.g., Frosch et al. 2007; Tarcea et al. 2007).

In this study we used deep UV-Raman spectroscopy, which allows to completely avoid interference of Raman and fluorescence signals, because the latter do not occur at excitation wavelengths below 250 nm. Furthermore, as many inorganic and organic materials have absorption bands in the deep UV-region, a laser excitation wavelength <250 nm will likely result in the resonance enhancement of certain Raman bands (e.g., Tarcea et al. 2007).

Using the deep UV-laser the small-scale distribution of organic matter within different mineral phases of methane-derived microbialites was analyzed for (1) Hydrate Ridge (Pleistocene, off Oregon, USA), (2) Lincoln Creek Formation (Oligocene, Washington State, USA), (3) Münder Formation (Late Jurassic, NW-Germany), and (4) modern methane seep associated microbial mats from the Black Sea. Published data obtained by our group from similar samples using coupled gas chromatography-mass spectrometry (GC-MS), were used as a reference and for comparing the analytical capabilities of both techniques (Leefmann et al. 2008; Hagemann et al. 2013).

Material and methods

Samples

– Hydrate Ridge, SE-Knoll chemoherm, NW-Pacific Ocean –

Hydrate Ridge is located 90 km offshore central Oregon, USA. The ridge, extending 25 km in N–S and 15 km in E–W direction, is morphologically divided into a northern and a southern summit. The up to 90 m high SE-Knoll chemoherm is located about 15 km SE from the southern summit of Hydrate Ridge. The samples were taken from a carbonate block collected during cruise SO165/2 of research vessel 'Sonne' in August 2002. The block was gathered directly from the top of the SE-Knoll chemoherm using a television grab (TVG; Station 230-1, TVG-13, 44:27.0440°N, 125:01.8000°W, 615 m water depth).
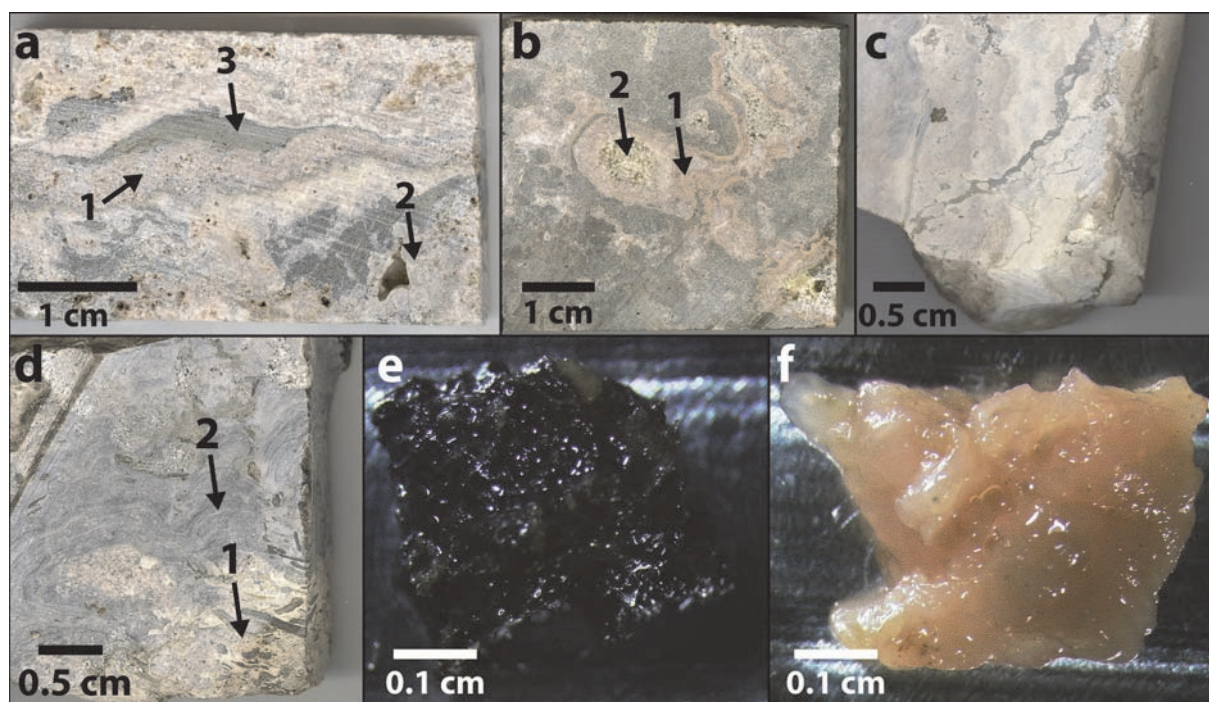
Fig. 1: Mineral phases and microbial mat types analyzed by Raman spectroscopy. (**a**) Hydrate Ridge sample with arrows marking (1) whitish aragonite, (2) lucent aragonite, and (3) gray micrite; (**b**) Lincoln Creek Formation sample with arrows marking (1) yellow aragonite, and (2) equant calcite spar; (**c**) initial clast of Münder Formation sample; (**d**) Münder Formation sample with arrows marking (1) growth phase 1, and (2) growth phase 2; (**e**) black microbial mat type of Black Sea samples; (**f**) pink microbial mat type of Black Sea samples.

From this block a core of 50 mm in diameter was drilled, which was later cut lengthwise resulting in two transverse sections. From one of these sections, the analyzed samples were taken.

The drill core section contains three closely interfingered, major carbonate types. These carbonate types (first described by Teichert et al. 2005) consist of a macroscopically opaque, cryptocrystalline variety of aragonite ranging in color from white to pinkish and brownish (*whitish aragonite*), a translucent, botryoidal aragonite consisting of fibrous, acicular crystals (*lucent aragonite*), and a gray, microcrystalline carbonate with varying content of Mg-calcite and various components, namely shell fragments, pellets containing pyrite, peloids and detrital quartz, and feldspar grains (*gray micrite*; Fig. 1a)

– Lincoln Creek Formation, USA –

Within the Oligocene Lincoln Creek Formation, which is exposed within river valleys of the south-eastern Olympic Peninsula, Washington, USA, several cold seep carbonate deposits have been observed (Peckmann et al. 2002). Samples of these cold seep carbonates were retrieved through an expedition to the Olympic Peninsula in September 2004. Within the cold seep carbonates several different phases, namely *gray micrite, yellow aragonite, clear aragonite*, and *equant calcite spar* were distinguished and analyzed for their biomarker content by GC-MS (Fig. 1b; Hagemann et al. 2013).

– Münder Formation, Germany –

A stromatolite sample was retrieved from a limestone quarry near the village of Thüste, located 30 to 50 km southeast of Hannover, Germany. The sample site is located in the centre of the Hils Syncline, a halotectonic depression that formed during the late Late Jurassic (Thitonian) to the lowermost Cretaceous (Berriasian). Within the quarries, oolithic limestones are overlain by a dark, well-stratified to laminated marlstone bed with prominent occurrences of stromatolites. The analyzed stromatolite sample was comprised of three distinct phases, namely the *initial clast*, and the *growth phases 1* and *2* (Figs. 1c, d; for a detailed description, see Arp et al. 2008). *Growth phase 1* shows irregular dendroid stromatolite columns and is composed of hemispheres with a vesicular, spar-cemented core veneered by brownish to dark gray microcrystalline laminae. In contrast *growth phase 2* is characterized by regular columns. This dark gray to gray phase includes stromatolithic lamination as a result of alternation of porous, clotted laminae with elongated, angular crystal traces. The microfabric of the *initial clast* is identical to the fabric of the *growth phases 1* and *2*, but discontinuities of growth are more abundant (for a detailed petrographic description see Arp et al. 2008).
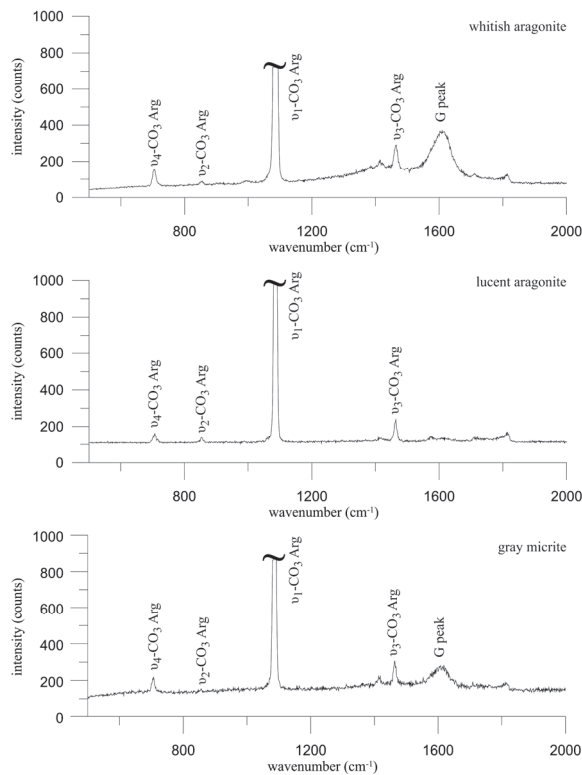
Fig. 2: UV-Raman spectra of distinct phases of samples from Hydrate Ridge, SE-Knoll chemoherm. (Arg = aragonite; peak assignments are discussed in text).
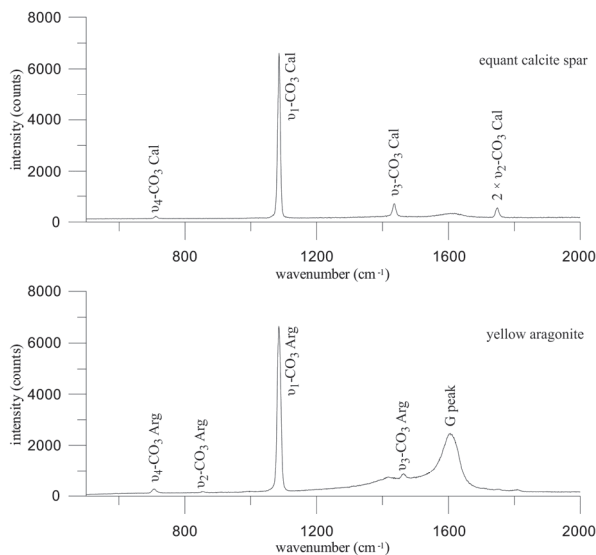

Fig. 3: UV-Raman spectra of distinct phases of samples from the Lincoln Creek Formation. (Cal = calcite; Arg = aragonite; peak assignments are discussed in text).

– Black Sea –

Several studies have reported the occurrence of methane seepage in the NW' Black Sea (e.g., Egorov et al. 1998). The combination of methane seepage and anoxic bottom water conditions results in the shifting of the AOM-activity from the sediments into the water column. As a consequence carbonate towers up to 4 m in height grow

into the anoxic water column (Pimenov et al. 1997; Michaelis et al. 2002; Reitner et al. 2005). Microbial mats mediating AOM were found to be associated with these carbonate build-ups. Samples were obtained from cruise 317-2 of research vessel 'Poseidon' to the lower Crimean shelf of the NW' Black Sea in September 2004. By using the manned submersible 'Jago', samples of microbial mats associated with carbonate towers were taken at water depths of 203 m (Station No.752; 44°46.41' N, 31°58.84' E), 235 m (Station No.744; 44°46.47' N, 31°59.52' E), 229 m (Station No.716; 44°46.49'N, 31°59.55'E), and 221 m (Station No.744; 44°46.48'N, 31°59.49'E), respectively. The samples were immediately frozen on board of RV Poseidon and stored at -20°C. Two different mat types were macroscopically distinguished, namely a *black* and a *pink mat* type (Figs. 1e, f). From each mat type, one sample was analyzed by means of Raman spectroscopy

Sample preparation

To avoid contamination of the sample surface by organic compounds, all preparation tools with direct sample contact (blade saw, spatula, pipettes, and object slides) were carefully pre-cleaned using acetone.

Using a rock saw 3 x 5 cm sized slabs were cut out of the original samples from Hydrate Ridge, Lincoln Creek, and Münder Formation. After preparation, the rock samples were stored enveloped in aluminium foil until measurement. Small pieces of the mat samples from the Black Sea were transferred on an object slide using a spatula, and immediately measured with the Raman spectrometer.

Raman spectroscopy

The micro-Raman system (Horiba Jobin Yvon LabRAM 800 UV; Table 1) used is equipped with a 244 nm UV-laser, which was operated at 25 mW at the laser exit. Depending on the sample the initial laser power was reduced to 1 %, 10 %, 25 %, or 50 % by using different filters. The laser beam was focused on the samples by an OFR LMV-40x-UVB objective with a numerical aperture of 0.5. The confocal hole diameter was set to 200 μm. The Raman scattered light was dispersed by a 2400 l/mm grating on a liquid nitrogen cooled CCD detector with 2048 x 512 pixels, yielding a spectral dispersion of better than 1.05 cm^{-1} per pixel. Raman spectra in the range from 300–4000 cm^{-1} were obtained in 2 spectral windows. Acquisition times were 2 times 5–300 s per window. A diamond standard with a major peak at 1332.0 cm^{-1} was used for calibration of the spectrometer.

Line profile measurements on Hydrate Ridge and Lincoln Creek Formation samples were carried out using a motorized xy-stage, controlled by the HORIBA Jobin Yvon LabSpec software version 5.19.17. Peak integrals of line profile measurements were calculated from the background corrected spectra.

Table 1: Hardware specifications of the used micro-Raman system (NA = numerical aperture).

	manufacturer	model / specifications
laser	COHERENT	Innova 90C FreD Ion Laser / λ=244 nm / output power up to 100 mW
microscope	Olympus	BX41
objectives	Optics For Research	LMV-10x-UVB, NA 0.25
	Optics For Research	LMV-40x-UVB, NA 0.50
x-y-stage	Märzhauser	EK32 75x50
spectrometer	HORIBA Jobin Yvon	LabRAM HR 800 UV / focal lenght: 800 mm /gratings: 600, 1200, 2400 / filter: D03=50 %, D06=25 %, D1=10 %, D2=1 %, D3=0.1 %, D4=0.01 % of laser output power
detector	HORIBA Jobin Yvon	CCD Symphony LN2-Series / 2048 × 512 Pixel / image area: 26.6 mm × 6.9 mm

Results

The peaks detected in the cold seep samples are exclusively located in the range between 700 cm⁻¹ and 1900 cm⁻¹. Peaks below 500 cm⁻¹ could not be detected by UV-Raman spectroscopy due to technical limitations of the UV-notch filter systems.

– Hydrate Ridge, SE-Knoll chemoherm, NW-Pacific Ocean –

All spectra obtained from the distinct phases of the Hydrate Ridge samples showed a similar peak pattern (Fig. 2).

In the UV-Raman spectra, strong peaks occurred around 1086 cm⁻¹ and 1609 cm⁻¹ and medium intensity peaks around 706 cm⁻¹ and 1464 cm⁻¹. Peaks of weak intensity were found around 854 cm⁻¹, 1415 cm⁻¹, 1710 cm⁻¹, and 1814 cm⁻¹. No fluorescence effects were observed when using 244 nm as excitation wavelength.

– Lincoln Creek Formation, USA –

The spectra from the *yellow aragonite* and the *equant calcite spar* were similar in peak distribution (Fig. 3). The UV-Raman spectra of both phases showed a strong band around 1083 cm⁻¹. Moreover, a band at 1606 cm⁻¹ was detected, which was strongly variable in intensity. Medium intensity bands at 1435 cm⁻¹ (*equant calcite spar*), 1463 cm⁻¹ (*yellow aragonite*) and 708 cm⁻¹, and weak peaks around 1749 cm⁻¹ complete the spectra.

– Münder Formation, Germany –

The UV-Raman spectra obtained from the Münder formation samples showed five distinct peaks (Fig. 4). Strong peaks were detected around 1085 cm⁻¹ and 1600 cm⁻¹. The latter peak is enclosed by two medium intensity peaks at 1434 cm⁻¹ and 1749 cm⁻¹, respectively. A weak peak was detected at 711 cm⁻¹. Notably, in spectra from the *growth phase 1* the peak at 1600 cm⁻¹ showed a higher intensity signal as the peak at 1085 cm⁻¹ (Fig. 4).

– Black Sea –

The UV-Raman spectra of the microbial mat samples from the Black Sea showed a high intensity peak with a maximum around 1605 cm⁻¹ and a broad shoulder towards lower Raman shifts (Fig. 5). In the pink mat type further medium intensity peaks were observed at 918 cm⁻¹ and 998 cm⁻¹ and 1090 cm⁻¹.
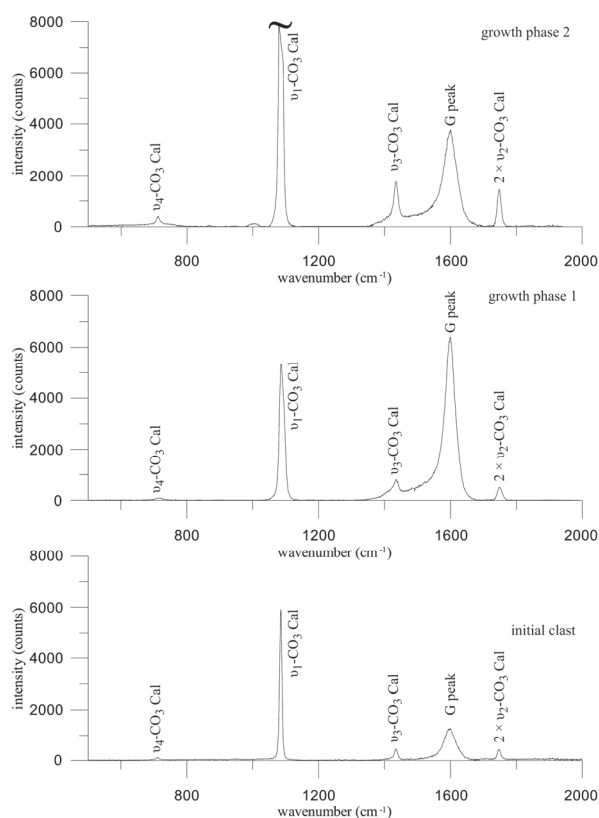

Fig. 4: UV-Raman spectra of distinct phases of samples from the Münder Formation. (Cal = calcite; peak assignments are discussed in text).
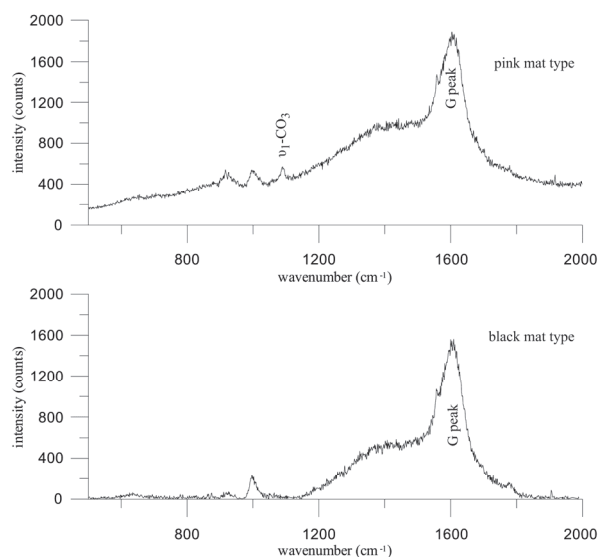

Fig. 5: UV-Raman spectra of distinct phases of microbial mat samples from the Black Sea. (peak assignments are discussed in text).
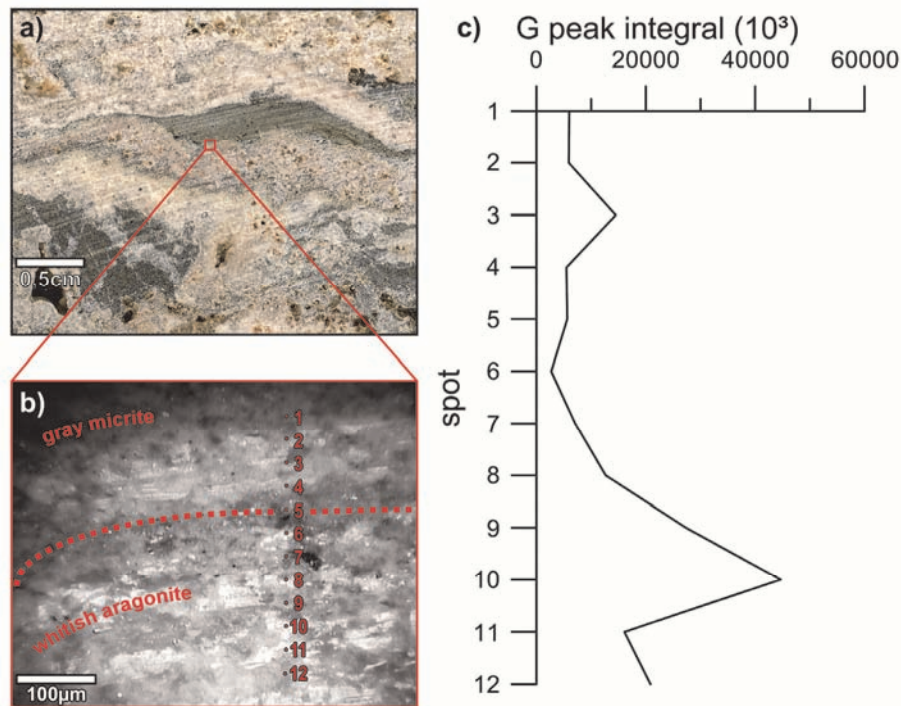
Fig. 6: Raman line profile of Hydrate Ridge microbialite using UV-laser (**a**) reflected light image of analyzed sample surface, (**b**) UV-camera image of gray micrite and whitish aragonite with marked line profile spots, (**c**) diagram of G peak integral *vs.* spot number, (G peak integral = 1548–1640 cm^{-1}).

Discussion

– Hydrate Ridge, SE-Knoll chemoherm, NW-Pacific Ocean –

Previous GC-MS studies of the analyzed Hydrate Ridge samples revealed strongly differing biomarker patterns in the three carbonate phases. This was interpreted to reflect different modes of formation (for a detailed discussion see Leefmann et al. 2008). Briefly, high amounts of AOM-specific lipid biomarkers observed in the *whitish aragonite*, such as archaeol, *sn*-2-hydroxyarchaeol, and non-isoprenoidal dialkyl glycerol diethers (DAGEs), indicate that microorganism mediating AOM were involved in the formation of this specific phase. Moreover, the abundance of *sn*-2-hydroxyarchaeol suggested that anaerobic methanotrophic archaea of the phylogenetic 'ANME-2' group played an important role among the ancient methane-consuming community (Blumenberg et al. 2004). The high amounts of DAGEs probably originated from the syntrophic SRBs of the AOM-consortia. By contrast, the *lucent aragonite* was found to be extremely lean in organic compounds, and even the lipid traces observed were probably due to contamination from other phases during sample preparation (Leefmann et al. 2008). The low biomarker concentrations reveal that this carbonate phase did not include fossilized microorganisms and suggests a mode of formation that was not directly mediated by microorganisms. The occurrence of both, AOM-specific (e.g., archaeol) and allochthonous (e.g., sterols, perylene) biomarkers in the *gray micrite* indicated, that this phase largely consists of allochthonous, i.e., sedimentary material

cemented by authigenic AOM-derived carbonates (Leefmann et al. 2008).

Most Raman signals observed in the analysis of three carbonate phases can be attributed to the carbonate mineralogy (Fig. 2). The peak at 706 cm^{-1} represents the υ_4 in-plane bending mode of the carbonate-ion. The weak peak at 854 cm^{-1} can be attributed to the υ_2 mode of the carbonate ion (Frech et al. 1980). The υ_1 mode of the carbonate ion is represented by the peak at 1086 cm^{-1}. According to Frech et al. (1980), the peak at 1464 cm^{-1} arises from the υ_3 mode of the carbonate ion. Frech et al. (1980) also mention a broad feature around 1420 cm^{-1}, which may correspond to the peak at 1415 cm^{-1} observed in the UV-Raman spectra. However, the band observed in the Raman spectra at 1415 cm^{-1} is rather sharp and might thus arise from a different source. The weak peaks around 1710 cm^{-1} and 1814 cm^{-1} could not be assigned to certain vibrational modes, but they were also observed within spectra of pure aragonite (not shown). The peak observed around 1609 cm^{-1} is attributed to C-C bonds, and most likely arises from carbonaceous matter bound in the samples. For ordered, graphite-like structures this peak (referred to as G peak in the following) occurs as a sharp peak at 1575 cm^{-1}, depending on the used laser excitation wave length. Broader G peaks around 1600 cm^{-1} are common features of disordered carbonaceous materials such as kerogens. In the spectra recorded in our study, the occurrence of such broad G peaks may indicate potential alteration of the organic matter from high laser power. In spectra of disordered carbonaceous materials, the G peak is accompanied by D peaks (Pasteris & Wopenka 2003).

When using UV-excitation wavelengths, however, the D peaks greatly decrease in intensity, and were below detection limit in the spectra recorded here.

Except for the G peak no peaks specific for individual functional groups of organic compounds were observed in the spectra of the Hydrate Ridge samples. The intensity of the G peak may thus be plausibly used as a measure of organic carbon content in the mineral phases. By the line profiles, the coupling of intensity of the G peak to the individual carbonate phases should be revealed. Fig. 6 shows the integral of the broad G peak as a function of the measurement spot. The figure clearly shows that the intensity of the broad G peak decreases towards the *gray micrite*. This may be due to higher organic carbon contents in the whitish aragonite than in the *gray micrite*.

In the second profile carried out at the interfaces of *whitish* and *lucent aragonite*, the G peak integral graph shows a decrease from the *whitish* towards the *lucent aragonite* phase (Fig. 7).
Both profiles (Figs. 6, 7) clearly support the GC-MS results with respect to the biomarker content reported in Leefmann et al. (2008). Based on this experiment, it is evident that Raman spectroscopy can reveal differences in the organic carbon content of the individual mineral phases at a microscopic scale.

Summarizing, the Raman analyses of the Hydrate Ridge samples clearly indicate preferred aragonite mineralogy of all phases studied, and considerable differences in the amounts of (disordered) organic material.

– Lincoln Creek Formation, USA –

Like for the Hydrate Ridge materials, GC-MS analysis conducted on the Lincoln Creek carbonates by Hagemann et al. (2013) revealed strong differences in the distribution of lipid biomarkers between the distinct phases. The high abundance of AOM-specific biomarkers in the *yellow aragonite* was interpreted as to reflect an AOM-derived precipitate, i.e., a fossilized AOM-biofilm. Accordingly, a low abundance of lipid biomarkers in the *equant calcite spar* was assumed to represent a late diagenetic origin.

In the Raman spectra of the *yellow aragonite* and the *equant calcite spar*, most peaks represent the aragonite or calcite mineralogy, respectively (Fig. 3). The peak at 1463 cm⁻¹ can be attributed to υ_3 mode of the carbonate ion in aragonite, whereas the peak at 1435 cm⁻¹ is consistent with the υ_3 mode of the carbonate ion in calcite. Likewise, the peaks at 708 cm⁻¹, and 1085 cm⁻¹ can be assigned to the carbonate ion. The peak at 1749 cm⁻¹ can be assigned to the $2x\upsilon_2$ mode of the carbonate ion (Urmos et al. 1991). The differences in lipid biomarker content between the phases revealed by GC-MS analysis were reflected in the Raman spectra by the strong differences in the abundance of the G peak at 1606 cm⁻¹. However, no further peaks representing organic compounds were observed.

– Münder Formation, Germany –

Previous GC-MS-analyses on the same Thüste stromatolites as analyzed in this study revealed strongly ¹³C-depleted sulfurized hydrocarbon biomarkers (Arp et al. 2008). In conjunction with other indications this was interpreted as to reflect stromatolithic carbonate $CaCO_3$ precipitation near the oxic–anoxic interface, as a result of intensive bacterial sulfur cycling and AOM, rather than of photosynthetic activity. Further GC-MS studies revealed a variety of biomarkers, but no systematic differences in the biomarker patterns between the individual growth phases were observed. However, the total amount of lipid biomarkers showed slight variations between the phases. In the Raman spectra, most peaks (711 cm⁻¹, 1085 cm⁻¹, 1434 cm⁻¹ and 1749 cm⁻¹) observed in the spectra of the samples from Thüste can be assigned to calcite (Fig. 4). The only signal interpreted to originate from organic compounds is the G peak around 1600 cm⁻¹, which is markedly strong in the spectra of *growth phase 1* and thus suggests a higher organic content of this phase compared to the initial clast and *growth phase 2*. However, in the absence of Raman line profile measurements crosscutting the three phases, this interpretation must remain speculative.

– Black Sea –

Previous GC-MS analyses and compound specific isotope analyses of biomarkers from similar Black Sea mats indicated that lipids in both black and the pink variety were sourced by Archaea and SRB involved in AOM (Blumenberg et al. 2004). Furthermore, the typical compounds observed were similar to those reported from Hydrate Ridge (see above), with somewhat different distributions of phylogenetic groups in the different mat types, respectively.

In the Raman spectra of the pink mat type, the peak observed around 1090 cm⁻¹ probably arises from carbonate particles within the mat (Fig. 5). The major peak at ~1605 cm⁻¹ found within the UV-Raman spectra corresponds to the peak of disordered carbonaceous material found in the microbialites. However, it should be noted that the peak shape is more asymmetric than the G peaks in the spectra from the microbialite samples from the Hydrate Ridge, Lincoln Creek and the Münder Formation (Figs. 2–4). Further peaks at 918 cm⁻¹ and 998 cm⁻¹ might reflect vibrational modes of organic molecules, as they were not observed within the UV-Raman spectra of the carbonate samples. The spectrum of the black microbial mat showed a slightly lower signal intensity of the G peak than the pink microbial mat. In contrast to biomarker differences as been obvious from GC-MS analyses, however, no major differences were found between both mat types by Raman spectroscopy.
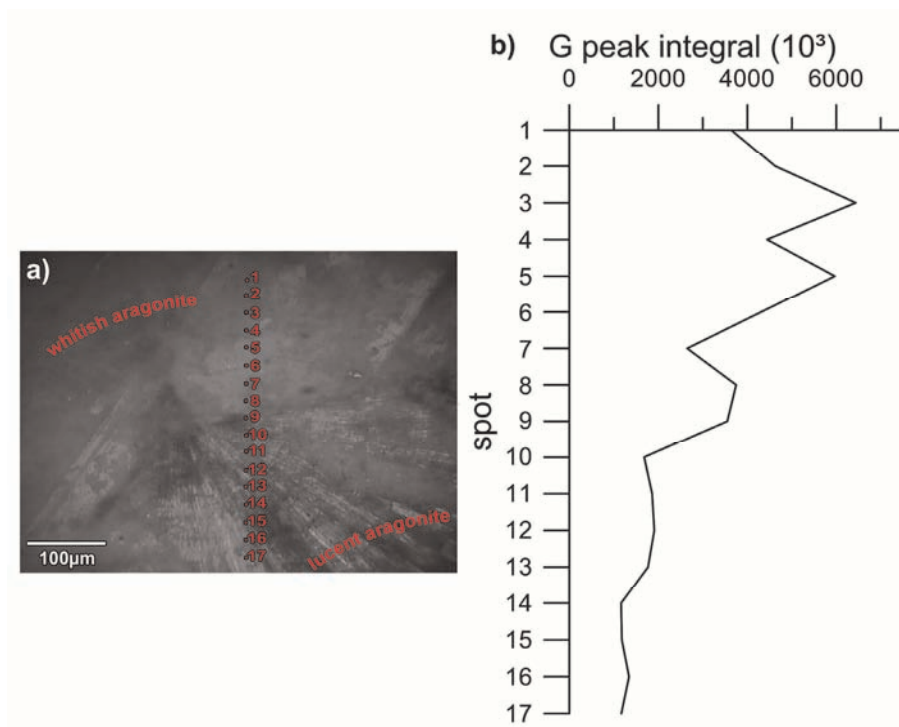
Fig. 7: Raman line profile of Hydrate Ridge microbialite using UV-laser: (**a**) UV-camera image of whitish aragonite and lucent aragonite with marked line profile spots, (**b**) diagram of G peak integral *vs.* spot number (G peak integral = 1548–1640 cm⁻¹).

Conclusions

Under the given analytical conditions UV-Raman spectroscopy does not allow for a detailed characterization of the biomarker content of carbonate microbialites. Except for the broad G peak representing disordered carbonaceous material, no peaks specific for individual functional groups or organic compound classes were detected within the carbonate microbialites studied. The difficulty to further characterize organic matter bound in sedimentary rocks might be regarded as a general drawback of current Raman spectroscopy. Similar problems were reported from the analysis of kerogens (Pasteris & Wopenka 2003). Comparison with published biomarker studies shows a much greater capability of GC-MS to identify distinctive biosignatures of methanotrophic consortia in the microbialite phases. On the other hand, Raman spectroscopy clearly resolved the differences in organic matter content of distinct microbialite phases. Raman spectroscopy can therefore be regarded useful to distinguish fossilized biofilms from precipitates that were not directly mediated by microorganisms. Another advantageous feature of Raman spectroscopy is its capability to simultaneously analyze the mineralogy and organic matter content of the microbialite phases at the microscopic level, and without the need of elaborate sample preparation. The results of this study thus demonstrate that the different techniques cannot replace each other, but should rather be used in conjunction in geobiological studies.

Acknowledgements

References

Arp, G.; Ostertag-Henning, C.; Yücekent, S.; Reitner, J. & Thiel, V. (2008): Methane-related microbial gypsum calcitization in stromatolites of a marine evaporative setting (Münder Formation, Upper Jurassic, Hils Syncline, north Germany). *Sedimentology* **55** (5): 1227-1251. http://dx.doi.org/10.1111/j.1365-3091.2007.00944.x

Barnes, R. O. & Goldberg, E. D. (1976): Methane production and consumption in anoxic marine sediments. *Geology* **4** (5): 297-300. http://dx.doi.org/10.1130/0091-7613(1976)4<297:MPACIA>2.0.CO;2

Birgel, D.; Himmler, T.; Freiwald, A. & Peckmann, J. (2008): A new constraint on the antiquity of anaerobic oxidation of methane: Late Pennsylvanian seep limestones from southern Namibia. *Geology* **36** (7): 543-546. http://dx.doi.org/10.1130/G24690A.1

Blumenberg, M.; Seifert, R.; Reitner, J.; Pape, T. & Michaelis, W. (2004): Membrane lipid patterns typify distinct anaerobic methanotrophic consortia. *Proceedings of the National Academy of Sciences* **101** (30): 11111-11116. http://dx.doi.org/10.1073/pnas.0401188101

Campbell, K. A.; Farmer, J. D. & Des Marais, D. (2002): Ancient hydrocarbon seeps from the Mesozoic convergent margin of California: carbonate geochemistry, fluids and palaeoenvironments. *Geofluids* **2** (2): 63-94. http://dx.doi.org/10.1046/j.1468-8123.2002.00022.x

Egorov, V. N.; Luth, U.; Luth, C. & Gulin, M. B. (1998): Gas seeps in the submarine Dnieper Canyon, Black Sea: acoustic, video and trawl data. In: Luth, U.; Luth, C.; & Thiel, H. (eds.): *Methane Gas Seep Explorations in the Black Sea (MEGASEEBS), Project Report. Berichte aus dem Zentrum für Meeres- und Klimaforschung* **14**: 11-21.

Frech, R.; Wang, E. C. & Bates, J. B. (1980): The i.r. and Raman spectra of $CaCO_3$ (aragonite). *Spectrochimica Acta Part A: Molecular Spectroscopy* **36** (10): 915-919. http://dx.doi.org/10.1016/0584-8539(80)80044-4

Frosch, T.; Tarcea, N.; Schmitt, M.; Thiele, H.; Langenhorst, F. & Popp, J. (2007): UV Raman Imaging - A Promising Tool for Astrobiology: Comparative Raman Studies with Different Excitation Wavelengths on SNC Martian Meteorites. *Analytical Chemistry* **79** (3): 1101-1108. http://dx.doi.org/10.1021/ac0618977

Gal'chenko, V. F. (2004): On the Problem of Anaerobic Methane Oxidation. *Microbiology* **73** (5): 698-707. [translation of *Microbiologyia*]

Greinert, J.; Bohrmann, G. & Elvert, M. (2002): Stromatolitic fabric of authigenic carbonate crusts: result of anaerobic methane oxidation at cold seeps in 4,850 m water depth. *International Journal of Earth Sciences* **91** (4): 698-711. http://dx.doi.org/10.1007/s00531-001-0244-9

Greenwood, P. F.; George, S. C. & Hall, K. (1998): Applications of laser micropyrolysis-gas chromatography-mass-spectrometry. *Organic Geochemistry* **29** (5-7): 1075-1089. http://dx.doi.org/10.1016/S0146-6380(98)0010-6

Greinert, J.; Bohrmann J. G. & Suess, E. (2001): Gas Hydrate-Associated Carbonates and Methane-Venting at Hydrate Ridge: Classification, Distribution, and Origin of Authigenic Lithologies. In: Natural Gas Hydrates: Occurrence, Distribution, and Detection. *Geophysical Monograph Series* **124**: 99-113. http://dx.doi.org/10.1029/GM124p0099

Hagemann, A.; Leefmann, T.; Peckmann, J.; Hoffmann, V.-E. & Thiel, V. (2013): Biomarkers from individual carbonate phases of an Oligocene cold-seep deposit, Washington State, USA. *Lethaia* **46** (1): 7-18. http://dx.doi.org/10.1111/j.1502-3931.2012.00316.x

Iversen, N. & Jörgensen, B. B. (1985): Anaerobic methane oxidation rates at the sulfate-methane transition in marine sediments from Kattegat and Skagerrak (Denmark). *Limnology and Oceanography* **30** (5): 944-955.

Kiefer, W. (1995): Special techniques and applications. In: Schrader, B. (ed.): *Infrared and Raman Spectroscopy - Methods and Applications*. Weinheim (VCH): 465-517.

Kneipp, K.; Kneipp, H.; Itzkan, I.; Dasari, R. R. & Feld, M. S. (1999): Surface-enhanced non-linear Raman scattering at the single-molecule level. *Chemical Physics* **247** (1): 155-162. http://dx.doi.org/10.1016/S0301-0104(99)00165-2

Leefmann, T.; Bauermeister, J.; Kronz, A.; Liebetrau, V.; Reitner, J. & Thiel, V. (2008): Miniaturized biosignature analysis reveals implications for the formation of cold seep carbonates at Hydrate Ridge (off Oregon, USA). *Biogeosciences* **5** (3): 731-738. http://dx.doi.org/10.5149/bg-5-731-2008

Michaelis, W.; Seifert, R.; Nauhaus, K.; Treude, T.; Thiel, V.; Blumenberg, M.; Knittel, K.; Gieseke, A.; Peterknecht, K.; Pape, T.; Boetius, A.; Amann, R.; Jørgensen, B. B.; Widdel, F.; Peckmann, J.; Pimenov, N. V. & Gulin, M. B. (2002): Microbial Reefs in the Black Sea Fueled by Anaerobic Oxidation of Methane. *Science* **297** (5583): 1013-1015. http://dx.doi.org/10.1126/science.1072502

Pasteris, J. D. & Wopenka, B. (2003): Necessary, but Not Sufficient: Raman Identification of Disordered Carbon as a Signature of Ancient Life. *Astrobiology* **3** (4): 727-738. http://dx.doi.org/10.1089/153110703322736051

Pearson, M. J.; Hendry, J. P.; Taylor, C. W. & Russell, M. A. (2005): Fatty acids in sparry calcite fracture fills and microsparite cement of septarian diagenetic concretions. *Geochimica et Cosmochimica Acta* **69** (7): 1773-1786. http://dx.doi.org/10.1016/j.gca.2004.09.024

Peckmann J.; Goedert, J. L.; Thiel, V.; Michaelis, W. & Reitner, J. (2002): A comprehensive approach to the study of methane-seep deposits from the Lincoln Creek Formation, western Washington State, USA. *Sedimentology* **49** (4): 855-873. http://dx.doi.org/10.1046/j.1365-3091.2002.00474.x

Peckmann, J.; Reimer, A.; Luth, U.; Luth, C.; Hansen, B. T.; Heinicke, C.; Hoefs, J. & Reitner, J. (2001): Methane-derived carbonates and authigenic pyrite from the northwestern Black Sea. *Marine Geology* **177** (1-2): 129-150. http://dx.doi.org/10.1016/S0025-3227(91)00128-1

Peckmann, J. & Thiel, V. (2004): Carbon cycling at ancient methane–seeps. *Chemical Geology* **205** (3-4): 443-467. http://dx.doi.org/10.1016/j.chemgeo.2003.12.025

Pimenov, N. V.; Rusanov, I. I.; Poglazova, M. N.; Mityushina, L. L.; Sorokin, D. Y.; Khmelenina, V. N. & Trotsenko, Y. A. (1997): Bacterial mats on coral-like structures at methane seeps in the Black Sea. *Microbiology* **66** (3): 354-360. [translation of *Mikrobiologiya*]

Polikarpov, G. G.; Egorov, V. N.; Gulin, S. B.; Gulin M. B.; Stokozov N. A. (1992): Gas seeps from the bottom of the Black Sea - A new object of molismology. In: Polikarpov, G. G. (ed.): *Molismology of the Black Sea*. Kiev (Nauka): 10-28.

Reeburgh, W. S. (1976): Methane consumption in Cariaco Trench waters and sediments. *Earth and Planetary Science Letters* **28** (3): 337-344. http://dx.doi.org/10.1016/0012-821X(76)90195-3

Reitner, J.; Peckmann, J.; Reimer, A.; Schumann, G. & Thiel, V. (2005): Methane-derived carbonate build-ups and associated microbial communities at cold seeps on the lower Crimean shelf (Black Sea). *Facies* **51**: 66-79. http://dx.doi.org/10.1007/s10347-005-0059-4

Suess, E.; Carson, B.; Ritger, S. D.; Moore, J. C.; Jones, M. L. & Kulm, L. D. (1985): Biological communities at vent sites along the subduction zone off Oregon. *Biological Society of the Washington Bulletin* **6**: 475-484.

Tarcea, N.; Harz, M.; Rosch, P.; Frosch, T.; Schmitt, M.; Thiele, H.; Hochleitner, R. & Popp, J. (2007): UV Raman spectroscopy – A technique for biological and mineralogical *in situ* planetary studies. *Spectrochimica Acta (A: Molecular and Biomolecular Spectroscopy)* **68** (4): 1029-1035. http://dx.doi.org/10.1016/j.saa.2007.06.051

Teichert, B. M. A.; Bohrmann, G. & Suess, E. (2005): Chemoherms on Hydrate Ridge – Unique microbially-mediated carbonate build-ups growing into the water column. *Palaeogeography, Palaeoclimatology, Palaeoecology* **227** (1-3): 67-85. http://dx.doi.org/10.1016/j.palaeo.2005.04.029

Thiel, V.; Heim, C.; Arp, G.; Hahmann, U.; Sjövall, P. & Lausmaa, J. (2007): Biomarkers at the microscopic range: ToF-SIMS molecular imaging of Archaea-derived lipids in a microbial mat. *Geobiology* **5** (4): 413-421. http://dx.doi.org/10.1111/j.1472-4669.2007.00119.x

Toporski, J. K. W.; Steele, A.; Westall, F.; Avci, R.; Martill, D. M. & McKay, D. S. (2002): Morphologic and spectral investigation of exceptionally well-preserved bacterial biofilms from the Oligocene Enspel formation, Germany. *Geochimica et Cosmochimica Acta* **66** (10): 1773-1791. http://dx.doi.org/10.1016/S0016-7037(01)00870-5

Urmos, J.; Sharma, S. K. & Mackenzie F. T. (1991): Characterization of some biogenic carbonates with Raman spectroscopy. *American Mineralogist* **76** (3-4): 641-646.

Valentine, D. L. & Reeburgh, W. S. (2000): New perspectives on anaerobic methane oxidation. *Environmental Microbiology* **2** (5): 477-484. http://dx.doi.org/10.1046/j.1462-2920.2000.00135.x

Werne, J. P.; Haese, R. R.; Zitter, T.; Aloisi, G.; Bouloubassi, I.; Heijs, S.; Fiala-Médioni, A.; Pancost, R. D.; Sinninghe Damsté, J. S.; De Lange, G.; Forney, L. J; Gottschal, J. C.; Foucher, J.-P.; Mascle, J. & Woodside, J. (2004): Life at cold seeps: a synthesis of biogeochemical and ecological data from Kazan mud volcano, eastern Mediterranean Sea. *Chemical Geology* **205** (3-4): 367-390. http://dx.doi.org/10.1016/j.chemgeo.2003.12.031

Mud volcanoes in onshore Sicily:
a short overview

Marianna Cangemi[1] * & Paolo Madonia[2]

[1]*Dipartimento DiSTeM, Università di Palermo, via Archirafi 36, 90123 Palermo (I), Italy; Email: marianna-cangemi@gmail.com*
[2]*INGV, Sez. di Palermo, via Ugo La Malfa 153, 90146 Palermo (I), Italy; Email: p.madonia@pa.ingv.it*

* corresponding author

A short overview on Sicilian mud volcanoes is given. A total of 8 sites are presently known and studied in Sicily, mainly located in central–southern Sicily (Caltanissetta basin). All of these are of small dimension and sometimes associated to water pools. Methane is the main emitted gaseous phase, with the exception of the Paternò site, dominated by CO_2 due to its proximity to Mt. Etna.

Emitted waters are of the chloride–sulphate–alkaline type, due to the dominance of NaCl as the main dissolved salt. Sicilian mud volcanoes represent a potential threat for humans but, at the same time, they are threatened by anthropic activities. The main risks are related to the damages produced by paroxysmal events, while their survival is threatened by illegal discharge of wastes, consumption of rural land and agricultural activities.

Introduction

Mud volcanoes are geological structures formed as a result of the emission of argillaceous material on the Earth's surface, which are commonly associated with compressive tectonics and sediment accretion at convergent margins (for a review, see Kopf 2002). Overpressured multiphase pore fluids incorporated in this material, mainly water and methane, make it semi-liquid and force it up through fissures in the crust, producing an outflowing mass of mud on the surface.

Mud volcanoes present characteristic isometric to elongated morphological structures, varying both in shape (from plano-conical shapes rising some hundred meters above the adjacent landscape to irregular shapes) and size (from tens of square meters to very large structures up to 100 km²), composed by "mud breccia" sharply contrasting to the surrounding host sediments (Dimitrov 2002).

Presently more than 1800 mud volcanoes are known from modern accretionary complex areas, with high sedimentation rates originating as a result of rapid overloading caused by structural or tectonic thickening (Dimitrov 2002). Mud volcanoes are normally in a quiescent stage because of the short duration of eruptions, often characterized by vigorous seepage of water, gas, and petroleum. Mud volcanoes in Sicily occur both onshore (Etiope et al. 2002) and offshore (Holland et al. 2003; Savini et al. 2009; Cangemi et al. 2010) in geological settings characterized
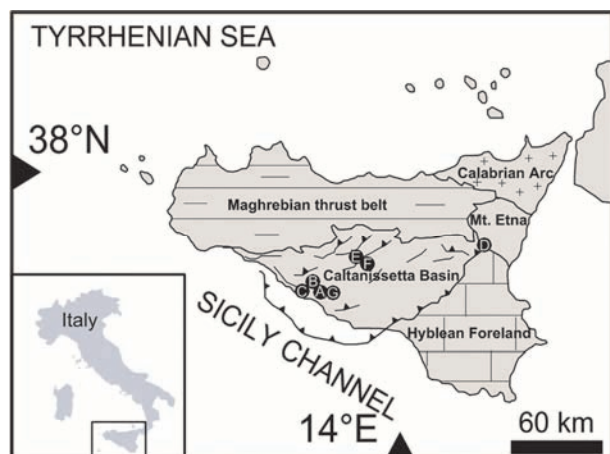
Fig. 1: Geological map of Sicily with locations of mud volcanoes: Bissana (**C**), Comitini (**G**), Fuoco di Censo (**B**), Maccalube (**A**), Marianopoli (**E**), Santa Barbara (**F**), Salinelle San Biagio and Salinelle Stadio at Paternò (**D**).

by a rapid sedimentation since the Late Cenozoic and intense neotectonics. These phenomena have been studied since the second half of the XIX century (Silvestri 1866). Comprehensive lists of Sicilian Mud volcanoes were reported by Etiope et al. (2002; 5 sites) and Martinelli & Judd (2004; 13 sites).

The present paper is aimed to give a short overview on Sicilian mud volcanoes. After the description of the general geological setting of Sicily, we will present the list of the known mud volcanoes together with a short description, and chemical and isotopic data of the emitted fluids, if available. We will complete our overview with the geochemical characterization of the emitted fluids and some considerations about environmental threats originating from or affecting Sicilian mud volcanoes.

Geological setting of Sicily

Sicily is a segment of the Alpine collisional belt along the Africa-Europe plate boundary that links the African Maghrebides to the west and southwest with the Calabria and the Appennines to the East and Northeast (Catalano et al. 1996, 2000; Avellone et al. 2010). The geological setting of Sicily (Fig. 1) is characterized by three main structural elements: (i) the Hyblean Plateau foreland in southeastern Sicily, constituted by Triassic–Liassic platform and scarp-basin carbonates overlain by Jurassic–Eocene pelagic carbonates and Tertiary open-shelf clastic deposits; (ii) the northwest-dipping foredeep north of the foreland, consisting of Plio–Pleistocene pelagic marly limestones, silty mudstones, and sandy clays overlying Messinian evaporites; and (iii) the complex chain composed of several imbricate units geometrically arranged in a thrust pile verging toward the east and the southeast, including the Calabro-Peloritani Units, located in northeastern Sicily, formed of

Hercynian crystalline units with a Mesozoic terrigenous cover and Plio–Pleistocene clastic and pelagic sediments and the Sicilian Maghrebian Units consisting of Meso–Cenozoic siliceous rocks, basin pelagic turbiditic carbonates, and platform and pelagic carbonates.

These units are tectonically overlain by a roof thrust formed of Oligo–Miocene turbiditic successions, or Lower–Middle Miocene glauconitic calcarenites and pelagic mudstones, or Lower Pleistocene foreland or satellite basin deposits, deformed and detached from the substratum (Catalano et al. 1996, 2000). The Maghrebian Units crop out along the northern Sicily belt in the Madonie, Palermo, and Trapani Mountains and in the western and southwestern sectors of the island. Southern and central Sicily are characterized by the presence of Cretaceous–Lower Pleistocene clastic-terrigenous deposits and Messinian evaporites.

Distribution and description of mud volcanoes in Sicily

Mud volcanoes are located in central-southern Sicily (Caltanissetta basin), with the only exception of the Paternò site, that lies at the contact between the eastern margin of the Sicilian foredeep and the volcanic edifice of Mt. Etna (Fig. 1). A total of 8 sites showing volcano-sedimentary activity are presently known and studied from the geochemical viewpoint (Table 1; with indication of the bibliographic sources used in the following descriptions).

All of these mud volcanoes are typically smaller than those generally occurring in other hydrocarbon-prone areas; some are characterized by water pools of several meters in diameter, where gases bubble vigorously (Etiope et al. 2002).

The **Bissana site** rises at the top of a hill and shows intermittent degassing activity, characterized by long periods of quiescence interrupted by violent emissions of mud and associated fluids (hereafter referred as "paroxysmal events"), that caused damages to local roads. A big pool (10 m of diameter and 20 m of depth) with gurgling gases and vents discharging mud and salty water is also present.

The **Comitini site** is located at the end of a hill and characterized by the presence of several active vents.

The **Fuoco di Censo** at Bivona is characterized by gas vents producing charming everlasting fires that occasionally burn with metre-high flames. No mud is emitted, causing the absence of cone-shaped structures.

Maccalube at Aragona is the biggest mud volcanism site in Sicily. It covers an area of about 1.4 km², where mud volcanoes are characterized by heights ranging from few centimeters to half a meter. Their eruptive style alternates during non-periodical paroxysmal episodes, not related to seismic activity, with expulsion of blast and burning of gases.

Table 1: Name, location (city and province), latitude and longitude (degrees and decimals, WGS84), elevation (m a.s.l.) of the presently known mud volcano sites in Sicily. Source of data are indicated in the last column. The Ids between brackets in the Name column refer to the locations reported in Fig. 1.

Name (Id)	Location	Latitude	Longitude	Elevation [m]	Reference
Bissana (C)	Cianciana (AG)	37.4833	13.3881	172	Etiope et al. (2002)
Comitini (G)	Comitini (AG)	37.4429	13.6519	210	Martinelli and Judd (2004), Heller (2011)
Fuoco di Censo (B)	Bivona (AG)	37.6250	13.3878	737	Etiope et al. (2002)
Maccalube (A)	Aragona (AG)	37.3757	13.5999	282	Etiope et al. (2002), Heller (2011)
Marianopoli (E)	Caltanissetta (CL)	37.6264	13.8936	374	Graziano (2009)
Santa Barbara (F)	Caltanissetta (CL)	37.4966	14.0907	528	INGV (2008), Madonia et al. (2011)
Salinelle S. Biagio (D)	Paternò (CT)	37.5449	14.9195	217	Etiope et al. (2002)
Salinelle Stadio (D)	Paternò (CT)	37.5726	14.8902	210	Etiope et al. (2002) Heller (2011)

In the Maccalube area there are also two main pools (about 3 m in diameter) with water and gurgling gases.

The Marianopoli site is presently characterized by a very residual activity, with few little mud pools (some square centimeters) and gas vents.

The Santa Barbara site at Caltanissetta occupies an area of about 12 km^2 and is characterized by cone-shaped structures tens of centimeters high, emitting mud and gases. Paroxysmal eruptions are not uncommon. The most recent one, preceded by a strong gas blast, occurred in August 2008 and caused severe damages to the surrounding roads and buildings.

The Salinelle S. Biagio and the Salinelle Stadio at Paternò strongly interact with anthropogenic activities that perturb their morphology and fluid emissions. Their activity is strongly influenced by seismic events and changes of volcanic degassing from Mt. Etna.

et al. 1997; Giammanco et al. 1998) the main emitted gas at Paternò is CO_2, along with a significant amount of H_2 and a mantle-derived helium signature that suggests a possible seismogenetic control on mud volcanoes (Etiope et al. 2002, Guliyev & Feizullayev 1995). The chemical compositions of venting gases from the different Sicilian mud volcanoes sites are summarized in Table 2 and in the ternary diagram CO_2–CH_4–N_2 illustrated in Fig. 2.

Chemical data of water emitted by Sicilian mud volcanoes are summarized in the Langelier–Ludwig diagram reported in Fig. 3. All the points decline in the chloride–sulphate–alkaline quadrant, due to the dominance of NaCl as the main dissolved salt. In particular for Santa Barbara (Madonia et al. 2011), the water has a salinity around 28 g l^{-1} and shows circumneutral pH values. Its chemical composition resembles that of seawater, with some modifications induced by both mixing with a low-Cl component (meteoric water) and water-clay interaction processes.

Geochemistry of fluid emissions from Sicilian mud volcanoes

In the following discussion we will give a summary of the geochemical data available for fluids emitted from Sicilian mud volcanoes from different bibliographic sources (Etiope et al. 2002 (sites A, B, C, D - gas), Graziano (2009; previously unpublished, site E - gas), Heller (2011; sites A, D, G - water and G - gas), INGV (2008; site F, gas), Madonia et al. 2011 (site F, water).

Sicilian mud volcanoes are characterized by a highly diffuse soil degassing. The emitted gaseous phase is normally dominated by CH_4. Carbon dioxide is subjected to dissolution in the underground aquifers underlying the emitting vents. However, due to the proximity of the Mt. Etna volcanic system (Chiodini et al. 1996; D'Alessandro


Fig. 2: Ternary diagram CO_2–CH_4–N_2 showing the chemical classification of gases emitted from Sicilian mud volcanoes.

Table 2: Chemical data of venting gases from mud volcanoes and ponds (b.d.l. = below detection limit). Data sources are listed in Table 1.

Site	He [ppm$_v$]	H$_2$ [ppm$_v$]	O$_2$ [%]	N$_2$ [%]	CH$_4$ [%]	CO$_2$ [%]	References
Bissana	501	15	b.d.l.	0.83	96.2	2.9	Etiope et al. (2002)
Comitini			2.12	5.47	91.62	0.68	Heller (2011)
Fuoco di Censo	367	59	2.03	9.66	86	2.2	Etiope et al. (2002)
Maccalube ponds	147	10	0.34	0.78	98.9	1.7	Etiope et al. (2002)
Maccalube MVs	71	10	0.29	1.15	98.8	0.9	Etiope et al. (2002)
Marianopoli	300	b.d.l.	0.48	2.12	93.39	2.93	Graziano (2009)
Santa Barbara					>95	<2	INGV (2008)
Salinelle S. Biagio	151	b.d.l.	b.d.l.	0.78	35.1	64.6	Etiope et al. (2002)
Salinelle Stadio	42	3	0.35	b.d.l.	4.2	95.5	Etiope et al. (2002)

Environmental threats affecting and/or originating from mud volcanoes

Mud volcanoes are a source of risks for anthropogenic activities but, at the same time, can be seriously threatened by these. The necessary condition for triggering this "two-ways" environmental treat, e.g., the close proximity between mud volcanoes and anthropized areas, is often found in Sicily.

The main risks for the population living close to mud volcanoes concern their paroxysmal events, during which strong gas blasts can produce seismic shocks able to damage buildings, roads and other facilities. Secondarily, the sudden expulsion and fallout of huge amounts of mud, mixed with soil and clay clots, can seriously injure persons present in their vicinity.

Fig. 3: Langelier–Ludwig diagram reporting the chemical data of waters emitted by Sicilian mud volcanoes. Composition of Mediterranean Sea Water is also given for comparison.

During the last paroxysm from Santa Barbara mud volcanoes, dated August 2008 and described by Madonia et al. (2011), damages of millions of Euros were caused by a near-surface seismic shock induced by the strong gas blast that shortly preceded the eruption. Within a radius of several hundreds of meters around the mud volcanoes, the walls of several buildings were damaged by the opening of wide cracks and many roads were interrupted by deep fractures. Similar problems were reported in 1999 at Bissana, where a paroxysm caused the damage of the local roads (Etiope et al. 2002).

Fortunately, no victims or injured people were reported during mud volcanoes paroxysms in Sicily, even if this potential risk is very high in some sites. Santa Barbara and Salinelle Stadio are located within heavily urbanized areas, and the immediate surroundings of these mud volcanoes are used as occasional playgrounds by children. Moreover, the Aragona site is the core of a natural reserve frequented by ecological tourism, especially during the warm season. On the opposite, the proximity to inhabited areas represents a serious problem for the survival of these geosites, threatened by the illegal discharge of wastes (Santa Barbara, Salinelle Stadio), the concreting of rural land due to the expansion of the city suburbs (Salinelle Stadio) and, when mud volcanoes are located in cultivated fields (Marianopoli), by the periodic plowing of the soil.

Acknowledgements

References

Avellone, G.; Barchi, M. R.; Catalano, R.; Gasparo Morticelli, M. & Sulli, A. (2010): Interference between shallow and deep-seated structures in the Sicilian fold and thrust belt, Italy. *Journal of the Geological Society* **167**: 109-126. http://dx.doi.org/10.1144/0016-76492008-163

Cangemi, M.; Di Leonardo, R.; Bellanca, A.; Cundy, A.; Neri, R. & Angelone, M. (2010): Geochemistry and mineralogy of sediments and authigenic carbonates from the Malta Plateau, Strait of Sicily (Central Mediterranean): Relationships with mud/fluid release from a mud volcano system. *Chemical Geology* **276**: 294-308. http://dx.doi.org/10.1016/j.chemgeo.2010.06.014

Catalano, R.; Di Stefano, P.; Sulli, A. & Vitale, F. P. (1996): Paleogeography and structure of the central Mediterranean: Sicily and its offshore area. *Tectonophysics* **260**: 291-323. http://dx.doi.org/10.1016/0040-1951(95)00196-4

Catalano, R.; Franchino, A.; Merlini, S. & Sulli, A. (2000): Central western Sicily structural setting interpreted from seismic reflection profiles. *Memorie della Società Geologica Italiana* **55**: 5-16.

Chiodini, G.; D'Alessandro, W. & Parello, F. (1996): Geochemistry of the gases and waters discharged by the mud volcanoes of Paternò, Mt. Etna (Italy). *Bulletin of Volcanology* **58**: 51-58. http://dx.doi.org/10.1007/s004450050125

D'Alessandro, W.; Giammanco, S.; Parello, F. & Valenza, M. (1997): CO_2 output and $\delta^{13}C$ (CO_2) from Mount Etna as indicators of degassing of shallow asthenosphere. *Bulletin of Volcanology* **58**: 455-458. http://dx.doi.org/10.1007/s004450050154

Dimitrov, L. I. (2002): Mud volcanoes – the most important pathway for degassing deeply buried sediments. *Earth-Science Reviews* **59**: 49-76. http://dx.doi.org/10.1016/S0012-8252(02)00069-7

Etiope, G.; Caracausi, A.; Favara, R.; Italiano, F. & Baciu, C. (2002): Methane emission from the mud volcanoes of Sicily (Italy). *Geophysical Research Letters* **29**: 56-1–56-4. http://dx.doi.org/10.1007/1-4020-3204-8_12

Giammanco, S.; Gurrieri, S. & Valenza, M. (1998): Anomalous soil CO_2 degassing in relation to faults and eruptive fissures on Mount Etna (Sicily, Italy). *Bulletin of Volcanology* **60**: 252-259. http://dx.doi.org/10.1007/s004450050231

Graziano, L. (2009): Manifestazioni di vulcanesimo sedimentario nel territorio di Marianopoli (CL). *Unpublished Thesis, Università di Palermo*: 48 pp.

Guliyev, I. S. & Feizullayev, A. A. (1995): *All about mud volcanoes.* Baku (Institute of Geology of the Azerbaijan Academy of Sciences): 52 pp.

Heller, C. (2011): Fluid venting structures of terrestrial mud volcanoes (Italy) and marine cold seeps (Black Sea) – Organogeochemical and biological approaches. *Doctoral Thesis, Georg-August University Göttingen:* 138 pp.

Holland, C. W.; Etiope, G.; Milkov, A. V.; Michelozzi, E.; Favali, P. (2003): Mud volcanoes discovered offshore Sicily. *Marine Geology* **199**: 1-6. http://dx.doi.org/10.1016/S0025-3227(03)00125-7

INGV [Istituto Nazionale di Geofisica e Vulcanologia, Sezione di Palermo] (2008): *Comunicato sull'eruzione di fango in C.da Terrapelata-Santa Barbara (Cl) 11 Agosto 2008.* http://193.206.213.9/intranet/gest_news/uploads/3929Comunicato_14_Agosto.pdf

Kopf, A. J. (2002): Significance of mud volcanism. *Reviews of Geophysics* **40**: 2-1–2-52. http://dx.doi.org/10.1029/2000RG000093

Madonia, P.; Grassa, F.; Cangemi, M. & Musumeci, C. (2011): Geomorphological and geochemical characterization of the 11 August 2008 mud volcano eruption at S. Barbara village (Sicily, Italy) and its possible relationship with seismic activity. *Natural Hazards and Earth System Sciences* **11**: 1545-1557. http://dx.doi.org/10.5194/nhess-11-1545-2011

Martinelli, G. & Judd, A. (2004): Mud volcanoes of Italy. *Geological Journal* **39**: 49-61. http://dx.doi.org/10.1002/gj.943

Savini, A.; Malinverno, E.; Etiope, G.; Tessarolo, C. & Corselli, C. (2009): Shallow seep-related seafloor features along the Malta plateau (Sicily channel – Mediterranean Sea): Morphologies and geo-environmental control of their distribution. *Marine and Petroleum Geology* **26**: 1831-1848. http://dx.doi.org/10.1016/j.marpetgeo.2009.04.003

Silvestri, O. (1866): *Le salse e la eruzione fangosa di Paternò (Sicilia); Osservazioni e ricerche, Stabilimento tipografico C Galatola, Catania*, p. 30.

Bojen-Seelilien (Scyphocrinitidae, Echinodermata) in neu-datierten Schichten vom oberen Silur bis untersten Devon Südost-Marokkos

Buoy crinoids (Scyphocrinitidae, Echinodermata) in newly dated Upper Silurian to lowermost Devonian strata of SE Morocco

Reimund Haude[1,3] *; Maria G. Corriga[2]; Carlo Corradini[2] & Otto H. Walliser†[1]

[1]Abt. Geobiologie, Geowissenschaftliches Zentrum, Georg-August-Universität Göttingen, Goldschmidtstr. 3, 37077 Göttingen; Email: rhaude@gwdg.de

[2]Dipartimento di Scienze Chimiche e Geologiche, Università di Cagliari, via Trentino 51, 09129 Cagliari, Italien; Emails: maria.corriga@unica.it & corradin@unica.it

[3]Geowissenschaftliches Museum, Georg-August-Universität Göttingen, Goldschmidtstr. 1-5, 37077 Göttingen

* corresponding author

In den Alaunschiefern des hohen Silurs – untersten Devons im Tafilalet-Gebiet von SE-Marokko sind mehrere Bänke und linsenförmige Lagen aus Massen von oft sehr gut erhaltenen Scyphocrinoiden eingeschaltet. Diese zu der Zeit weltweit verbreiteten großen Crinoiden hatten durch Umwandlung ihrer normalerweise als Verankerungsorgan dienenden Wurzel in eine gekammerte Schwimmboje („Lobolith") das Plankton-reiche Oberflächenwasser als neuen Lebensraum gewonnen. Die lagigen Massenvorkommen entstanden wahrscheinlich durch gelegentliche Sturmwetter-Ereignisse, bei denen viele Bojenwurzeln abgerissen wurden, so dass Kolonie-artige, wohl durch lange Algen miteinander verbundene Ansammlungen dieser Tiere ihren Gesamt-Auftrieb verloren und in ein eutrophiertes H$_2$S-reiches Milieu am Meeresboden absanken, wo sie oft in sehr guter Erhaltung fossilisierten. Obwohl sich im oberen Silur mehrere Scyphocrinoiden-Arten entwickelt hatten, bestehen die „Kolonien" jeweils nur aus einer Art. Die Conodonten-stratigraphische Untersuchung von drei Profilen in SE-Marokko zeigt, dass im oberen Silur zunächst nur Formen mit einem bautechnisch ursprünglicheren Cirren-Lobolithen vorkommen (*Scyphocrinites* und *Carolicrinus*); im höheren Bereich der Unteren *detortus*- und v. a. in der Oberen *detortus*-Conodonten-Zone kommen Lagen mit Scyphocrinoiden hinzu, die einen deutlich verbesserten Platten-Lobolithen entwickelt hatten: Arten von *Marhoumacrinus* und/oder *Camarocrinus*, die dann im untersten Devon (*hesperius*-Zone) als alleinige und letzte Vertreter dieser Crinoidengruppe nachzuweisen sind.

Stratigraphical occurrence and biology of the large pelagic scyphocrinoids (with their biostratinomically always separated buoy-like bulbous root, the lobolith) are investigated in three sections of the S–D boundary layers in the Tafilalet region. These successions of Přídolí–lower Lochkovian alum shales with several scyphocrinoid beds with crowns, stems and loboliths can be divided into four conodont zones. First scyphocrinoids appear in the *eosteinhornensis* s. l. Zone: species of *Scyphocrinites* and *Carolicrinus* in separate beds, both exclusively being associated (and, hence, to be anatomically combined) with the biotechnically relatively primitive type of buoy, the "cirrus lobolith".

In the Lower and Upper *detortus* Zones, such beds alternate with layers of species of either *Marhoumacrinus,* or *Camarocrinus*, both exclusively being associated (and thus, anatomically to be combined) with the biotechnically improved buoy, the "plate lobolith". Only a species of one of the latter passed into the *hesperius* Zone of the lowermost Lochkovian. The floating large crinoids profited as filter feeders from a highly increased contemporary microplankton productivity in the surface waters, thus, attaining considerable size, high reproductivity and wide distribution in the palaeoceans, forming colony-like aggregations, which enlarged by closely settling and developing juveniles. By occasional heavy weather events many loboliths in possibly with large algae entangled monospecific scyphocrinoid "colonies" were broken off, which thus lost their joint buoyancy and submerged into a eutrophic bottom facies.

Einleitung

Bei den in obersilurischen bis tief-unterdevonischen, fast weltweit nachgewiesenen, großen Scyphocrinoiden (Crinoidea, Echinodermata) ist die ursprüngliche Verankerungsstruktur (Wurzel) am Stielende in eine gekammerte gashaltige Schwimmboje umgewandelt. An diesem sog. Lobolith hängend lebten sie an der Wasseroberfläche – also in inverser Stellung – und erreichten so, ohne einschränkende Faziesgrenzen, in den Paläo-Ozeanen jener Zeit ihre weite Verbreitung. Nach dem fast weltweiten Vorkommen der Scyphocrinoiden (siehe z. B. Waagen & Jahn 1899; Schuchert 1904; Reed 1906, 1917; Springer 1917; Yakovlev 1953; Alleman 1958; Hollard 1962; Jaeger 1962; Legrand 1962; Prokop & Petr 1987; Chen & Yao 1990; Hess 1999) müssen in dem betreffenden Zeitraum im Oberflächenwasser für dort filtrierend lebende Tiere optimale Bedingungen geherrscht haben. Die Scyphocrinoiden erreichten so eine beträchtliche Größe mit Stielen von mehreren Metern Länge und Lobolithen von bis zu 30 cm Durchmesser (Hess 2010). Außerdem dürfte die Reproduktionsrate hoch gewesen sein (Haude 1972, 1992; Prokop & Petr 2001). Auch bei bester Erhaltung von Kronen, Stielen und Lobolithen wurden nie komplette Fossilien gefunden. Vielfach kommen exzellent erhaltene Kronen mit Stielteilen lagenweise, die Lobolithen oft bankbildend vor. Offenbar sind große Kolonie-artige Ansammlungen von Scyphocrinoiden nach Verlust ihrer Lobolithen-Bojen abgesunken, während die Lobolithen nekroplanktonisch weiterdrifteten und schließlich an anderer Stelle sedimentierten bzw. biostratinomisch angereichert wurden (Haude et al. 1994).

Andererseits zeigen die Vorkommen von Scyphocrinoiden-Lagen in z. T. bituminösen Alaun-/Graptolithenschiefern, dass durch den Planktonreichtum mit einem hohen Maß an absinkender organischer Substanz tiefere Wasserbereiche eutrophierten, so dass Bodenleben sehr eingeschränkt war oder unmöglich wurde. Dieses konservierende Bodenmilieu verhinderte auch weitgehend den gewöhnlich schnellen Zerfall der hochgegliederten Crinoidenskelette. So waren die Scyphocrinoiden einerseits durch Evolution der Bojenwurzel dem Bodenleben entzogen, täuschten andererseits als gut erhaltene Fossilien und besondere biostratinomische Befunde der Lobolithen ein solches aber vor (s. Springer 1917, der Lobolithen als Anpassung der Wurzel an weiches Sediment begründete).

Wegen der weiten Verbreitung der Scyphocrinoiden waren Funde der meist gut identifizierbaren Skelettteile – und damit der Nachweis eines „*Scyphocrinites*-Horizonts" – ein wichtiges stratigraphisches Kriterium für den Grenzbereich Silur–Devon (z. B. Beyer 1952; Jaeger 1962; Hollard 1977). Mit dem Nachweis von zwei deutlich verschiedenen Bautypen von Lobolithen, die in Spanien, Deutschland und China stets in verschiedenen Schichten und dort in charakteristischen Assoziationen mit jeweils nur einem Kronen-Taxon gefunden worden waren, schienen Formen mit dem bautechnisch „primitiveren" Cirren-Lobolith auf das Silur, solche mit optimiertem Platten-Lobolith auf das Devon beschränkt zu sein (Haude 1972, 1989, 1992; Jahnke & Shi 1989). Inzwischen hatten aber Prokop & Petr (1986, 1987) nachgewiesen, dass auch der Platten-Lobolith bereits im Silur entwickelt war. Außerdem sollten nach Beobachtungen dieser Autoren in Tschechien beide Lobolithen-Typen auch zusammen, in der gleichen Schicht, vorkommen (Prokop & Petr 1986: 207, 1994: 31: "presence of both lobolith types in all stratigraphical levels in the Silurian-Devonian boundary beds" ... "also in the lowermost levels"), so dass eine systematische Zuordnung dieser Skelettteile grundsätzlich nicht möglich wäre.

Zu einer Prüfung der widersprüchlichen Befunde boten sich die Scyphocrinoiden-Vorkommen in Nord-Afrika an, wo seit langem mehrere weit im Gelände zu verfolgende Lagen dieser Crinoiden bekannt waren (in Abfolgen, die z. B. Hollard 1977 als "scyphocrinitid layer" bzw. „*Scyphocrinites*-Schicht" bezeichnete), von denen nur einzelne lokale Vorkommen systematisch bearbeitet worden sind (Alleman 1958; Prokop & Petr 1987).

Im Tafilalet-Gebiet (SE-Marokko) wurden deshalb drei Profile mit jeweils mehreren Scyphocrinoiden-Lagen bearbeitet und zunächst nur teilweise und vorläufig biostratigraphisch interpretiert (Haude & Walliser 1998); eine vollständigere Untersuchung war erst in jüngster Zeit möglich (Corriga et al. 2014) und wird hier fortgesetzt.

[Gegen Ende der Profilaufnahmen durch O. H. W. und R. H. kam − programmgemäß − auch Joachim Reitner mit weiteren Forschungszielen in das Tafilalet. Für das Scyphocrinoiden-Projekt hatte die Aussicht auf diesen Besuch schon während eines Kurzaufenthalts in Sevilla fast existentielle Bedeutung gewonnen: Der für die Geländearbeiten ausgerüstete VW-Kombi, der scheinbar auch transzendental gut gesichert in der Straße Santo Paolo bei der Kirche Santa Maria Magdalena geparkt war, hatte das Interesse von Räubern geweckt, die ihn dann technisch perfekt öffneten und u. a. die Reisekasse stahlen. Praktisch ohne Geld, aber mit der hoffnungsvollen Gewissheit substantieller Unterstützung durch J. R., konnte die Fahrt fortgesetzt werden.]

Material

Nach früheren Profilaufnahmen (O. H. W.) wurden drei Profile in der Tafilalet-Region südöstlich von Erfoud für die Behandlung der latenten Fragen als besonders gut geeignet ausgewählt (Abb. 1): „Bou Tchrafine Nord 2" (474), „Atrous 3" (477) und „Atrous 7" (540). Kürzere Abschnitte mit mehreren Scyphocrinoiden-Lagen wurden per Metermaß, längere Strecken per Schrittmaß dokumentiert. Da das Einfallen in den jeweiligen Profilen weitgehend konstant war, wurde zur Umrechnung auf die Mächtigkeiten der einzelnen Profilabschnitte jeweils ein einheitlicher Winkel eingesetzt.

Alle kalzitischen Lagen, die meist als Rippen aus den weitgehend eingeebneten und selten freiliegenden, ungestörten Tonschichten heraustreten, wurden für Conodonten-Analysen beprobt. In den frühen 1970er Jahren waren auch die im Wesentlichen aus Scyphocrinoiden bestehenden Lagen noch gut sichtbar. Inzwischen verlaufen an ihrer Stelle oft Gräben oder Reihen von Gruben, die lokal mehrere Meter tief oder auch schon verschüttet sind. Wegen der vollständigen Blumen-artigen Erhaltung der Kronen auf den Bank-Unterseiten werden diese Lagen seit etwa Ende der 1970er Jahre ausgegraben oder bergmännisch abgebaut und dann stückweise oder als großflächige „Kolonien" in den Handel gebracht. Nur Lagen mit weitgehend zerfallenen Scyphocrinoiden und die Bänke aus Platten-Lobolithen haben (noch) keinen Handelswert und sind daher sichtbar. Von solchen Grabungen stammen die inzwischen in Museen oder privaten Sammlungen für Untersuchungen zur Verfügung stehenden großen Platten (siehe z. B. Haude et al. 1994; Plodowski 1996; Haude 1998; Hess 1999), so auch die Scyphocrinoiden-Kolonie (Abb. 2) im Museum des Göttinger Zentrums für Geowissenschaften. In dem Aushub der Gräben und Grubenreihen wurden Reste von Scyphocrinoiden in der Erwartung gesammelt, dass sie auch zu der jeweiligen Lage gehörten. Immerhin zeigte sich bereits dort, anhand der gewöhnlich gut erkennbaren Reste der beiden Lobolithen-Typen, dass bei den Grabungsarbeiten in der Regel keine Mischung von Aushub aus verschiedenen Lagen stattgefunden hatte.

Einige Grubenreihen scheinen anzuzeigen, dass dort nicht nur kleinere linsenförmige „Kolonien", sondern wohl auch in Suchgrabungen Detritus-Lagen abgebaut wurden, die wohl aus dem Randbereich von „Kolonien" stammen. Nur an einer Stelle in Profil Atrous 7 war noch eine dickere Bank mit Kronenteilen sichtbar („Hauptschurf", Profil-Bezeichnung nach O. H. W.), einer darunter mit radial ausgebreiteten Armen und danach einem Durchmesser der Krone von ca. 70 cm (Abb. 3).

Das untersuchte Material befindet sich unter den angegebenen Nummern mit dem Präfix GZG #1612 in der Originale-Sammlung des Zentrums für Geowissenschaften der Universität Göttingen, die Conodonten-Proben im dortigen Teilbereich Mikropaläontologie („Conodonten-Sammlung O.H. Walliser"; GZG.MP).
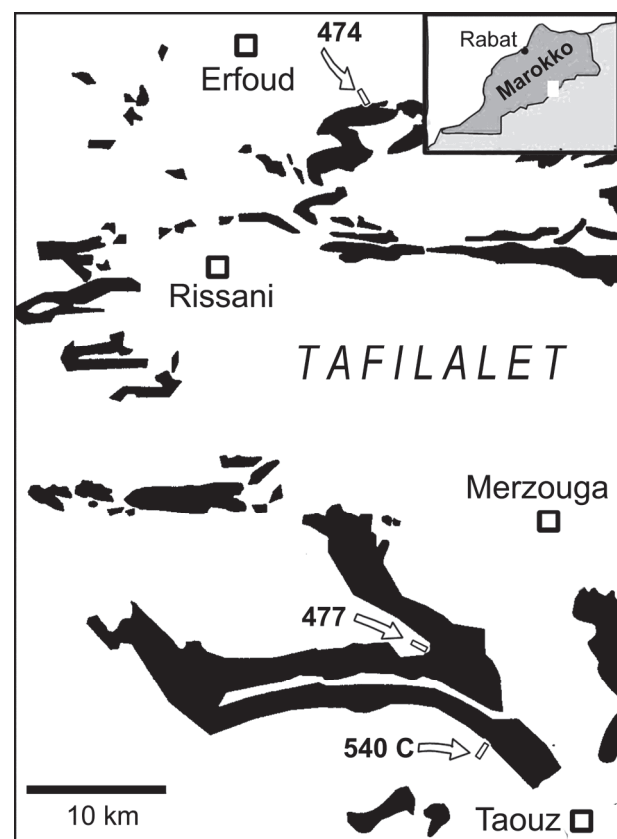
**Abb. 1:** Tafilalet-Region in Südost-Marokko mit der Lage der untersuchten Profile (Pfeile) im Grenzbereich Silur−Devon [474 = Bou Tchrafine N2, 477 = Atrous 3, 540 C = Atrous 7; schwarz = Devon].

Fig. 1: The Tafilalt region in SE Morocco with location of the investigated sections (arrows) in the Silurian−Devonian boundary beds [474 = Bou Tchrafine N2, 477 = Atrous 3, 540 C = Atrous 7; black = Devonian].
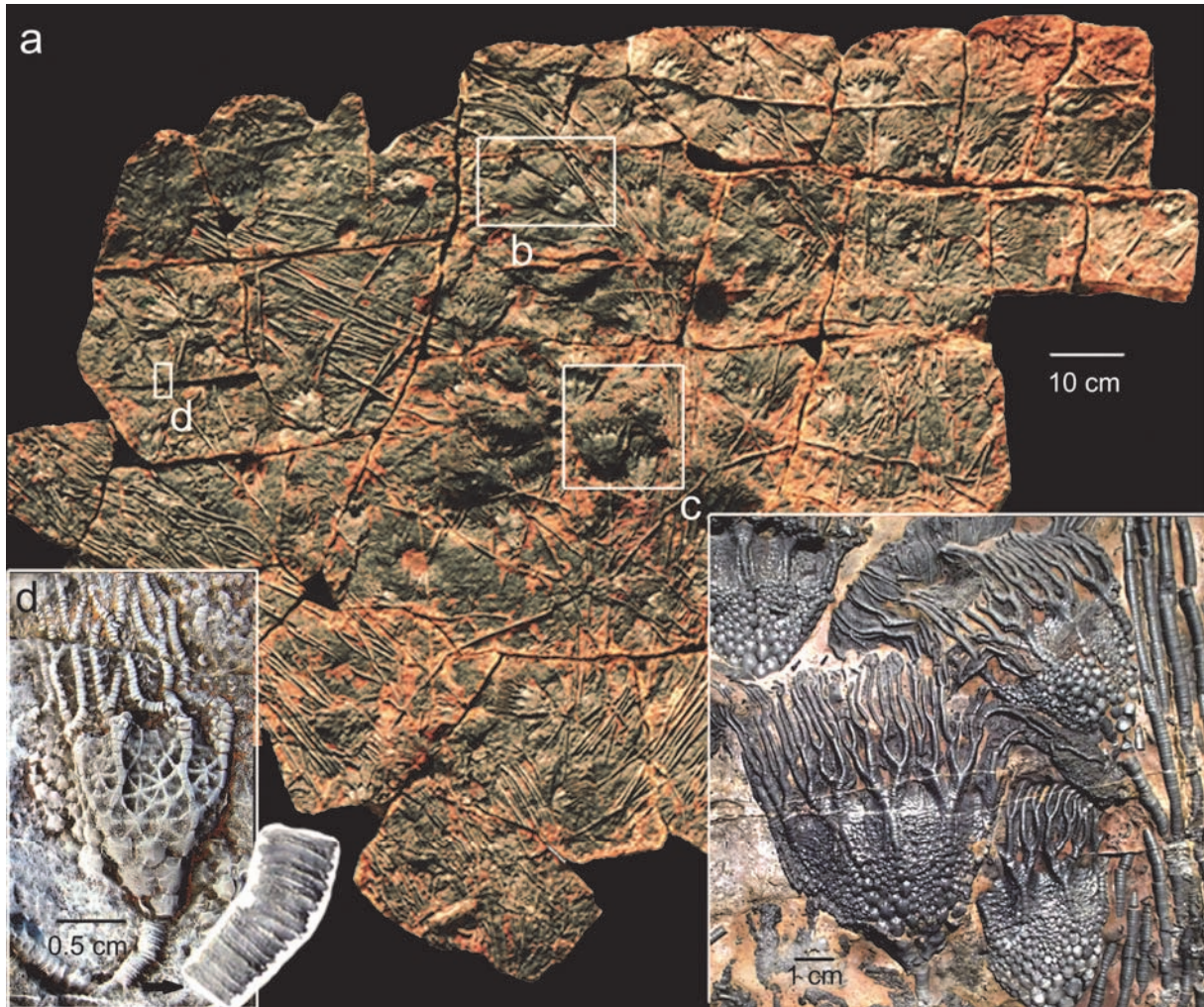
Abb. 2: (**a**) Göttinger Scyphocrinoiden-„Kolonie" mit zahlreichen Kronen unterschiedlicher Größe von *Camarocrinus*? n. sp.? aus der Unteren *detortus*-Zone (Unterseite; **GZG 103-1**; Ausgrabungsort wahrscheinlich ca. 7 km südöstlich von Erfoud im „Hauptschurf" [Lage 10] von Profil Bou Tchrafine N2); (**b**) Ausschnitt der Krone "Gö-3" in Abb. 9d; (**c**) Kronen "Gö-8, -12, -13" (**Ausschnitt c; GZG 103-1-8, -12, -13**); (**d**) juvenile Krone "Gö-15" (**Ausschnitt d; GZG 103-1-15),** daneben ihr vergrößerter Stielteil mit heteromorpher Struktur.

Fig. 2: (**a**) Large Göttingen scyphocrinoid "colony" with many crowns of different size of *Camarocrinus*? n. sp.? from the Lower *detortus* Zone (lower side; **GZG 103-1**; probably mined at about 7 km south-east of Erfoud in the "main trench" [bed 10] of section Bou Tchrafine N2); (**b**) crown "Gö-3" (see Fig. 9d); (**c**) crowns "Gö-8, -12, -13" (**detail c; GZG 103-1-8, -12, -13**); (**d**) juvenile crown "Gö-15" (**detail d; GZG 103-1-15)** and enlarged part of its stem with heteromorphic structure.

Die „*Scyphocrinites*-Schichten"

Die dunklen Schiefer („Alaun-/Graptolithenschiefer") mit eingeschalteten bituminösen Kalken und konkretionären Lagen des höheren Silurs im Tafilalet (SE-Marokko) erreichen Mächtigkeiten von mehreren 100 m (Hollard 1962; Legrand 1962). Durch die Erosion der weichen Schiefer bildeten sich weite Ebenen, in denen kalkige Lagen normalerweise als weit zu verfolgende Rippen hervortreten. Diese enthalten in der Regel orthocone Nautiliden („Orthocerenkalke"), Bivalven, vereinzelt kleine Brachiopoden; vor allem aber sind in der Přídolí-Stufe bis in das tiefe Devon weit verbreitet auch mehrere linsenförmige Lagen und dünne Bänke aus Skelettteilen von Scyphocrinoiden

eingeschaltet, die aber durch den fortgesetzten Abbau meist nur noch in Resten zu finden sind.

In den drei aufgenommenen Profilen hat die eigentliche „*Scyphocrinites*-Schicht" (Hollard 1977), also die Schichtfolge vom Přídolí bis ins unterste Lochkovium mit mehreren Scyphocrinoiden-Lagen, sehr verschiedene Mächtigkeiten (Abb. 4). In der kürzesten Abfolge, Atrous 7 (540), wurden sechs Lagen innerhalb von nur 3,50 m registriert; hier beträgt der Abstand der einzelnen Lagen 0,25–1,00 m. In der Abfolge Atrous 3 (477) hat sie eine Mächtigkeit von ca. 70 m und enthält sieben Scyphocrinoiden-Lagen, deren Abstände besonders im unteren Bereich viele Meter betragen.

Abb. 3: Teil einer großen Krone von *Marhoumacrinus* cf. *legrandi* mit radial ausgebreiteten Armen, ventrale Seite auf der Liegendfläche exponiert, d. h. nach unten gerichtet (Profil Atrous 7, Lage 21; GZG 1612-540-21-113).

Fig. 3: Part of large crown of *Marhoumacrinus* cf. *legrandi* with radially spreaded arms, ventral sinde, exposed on lower side oft he layer, i.e. directed downwards (section Atrous 7, bed 21; GZG 1612-540-21-113).

In der ca. 21 m mächtigen Abfolge von Profil Bou Tchra-fine Nord 2 (474) befinden sich neun Scyphocrinoiden-Lagen mit Abständen von meist 1–5 m.

Die abgebauten bzw. mehrere Meter tief ausgegrabenen Scyphocrinoiden-Lagen sind meist Linsen-artige, 2–20 cm dicke Kalke aus einem dichten Gemenge von Skelettteilen. Auf ihrer Unterseite sind oft vollständige Kronen mit langen Stielteilen exponiert, nach oben hin sind die Skelettteile weitgehend zerfallen. Nach den aufgelesenen Resten bestehen manche dünne Lagen aus Scyphocrinoiden-Detritus mit einigen stabileren größeren Skelettresten. Im obersten Bereich der Profile kann eine dicke Bank erhalten sein, deren Makrofossilinhalt gänzlich von Lobolithen geprägt wird.

Biostratinomische Beziehungen

Selbst bei bester Erhaltung der Kronen mit z. T. noch langem ansitzendem Stielteil ist noch nie ein (post-juveniler) vollständiger Scyphocrinoide − mit Lobolith am Stielende − gefunden worden. Das wäre wegen seiner Lebensweise im Oberflächenbereich des Wassers nach dem Absterben auch nicht zu erwarten; denn nach dem bald darauf erfolgenden Bruch des verwesenden Stiels in seinem dünnsten Bereich (nahe dem Lobolithen) sanken Krone und der lange Stielteil ab, während die Boje, vor allem jene mit dem sehr stabilen Platten-Bau, noch recht lange nekroplanktonisch weiterdriften konnte (s. u.). Immerhin ist inzwischen der Fund einer Scyphocrinoiden-Ansammlung mit einzelnen, fast vollständigen – allerdings juvenilen Exemplaren − mit noch relativ langem Stiel,

samt Lobolith bekannt geworden (Hess 1999); dessen Wand war so dünn, dass sie beim Ablagerungsprozess sofort kollabierte. Unter den jeweiligen regionalen biostratinomischen Bedingungen wurden die stabilen adulten (Platten-)Lobolithen zu dickeren Bänken konzentriert (z. B. in den USA, Schuchert 1904, Ray 1980; in Nord-Afrika, Poueyto 1952, Hollard 1977; in China, Chen & Yao 1990; in Tschechien, Prokop & Petr 1986).

Die ausgedehnten Lagen aus dort oft linsenförmig aneinander gereihten Massenvorkommen von Scyphocrinoiden lassen sich gut mit Sturm-Ereignissen und schwerem Seegang erklären, die zahlreiche benachbart treibende Individuen zum Absinken brachten. Die angenäherte Linsenform der fossilen Massen-Vorkommen und vor allem die Analyse der Lagerungsverhältnisse der Skelette auf der Göttinger Platte zeigen, dass hier die Crinoiden nicht einzeln, sondern als untereinander verbundene, Kolonie-artige Ansammlungen abgelagert wurden (Haude et al. 1994): Beim Bruch vieler Stiele und damit Verlust von Lobolithen als gemeinsame Schwimmbojen, wurde der Gesamt-Auftrieb unterschritten, so dass eine solche „Kolonie" absinken musste. Zweifellos hatten aber nicht alle der von einem solchen Event betroffenen Individuen in den absinkenden „Kolonien" ihren Lobolithen verloren, bzw. es waren nicht alle Kammern leck geschlagen. Bei beginnendem Zerfall der Skelette am Meeresboden lösten sich die Lobolithen dank des noch vorhandenen Auftriebs schon früh von dem dort relativ dünnen Stielbereich, stiegen auf und drifteten fort.
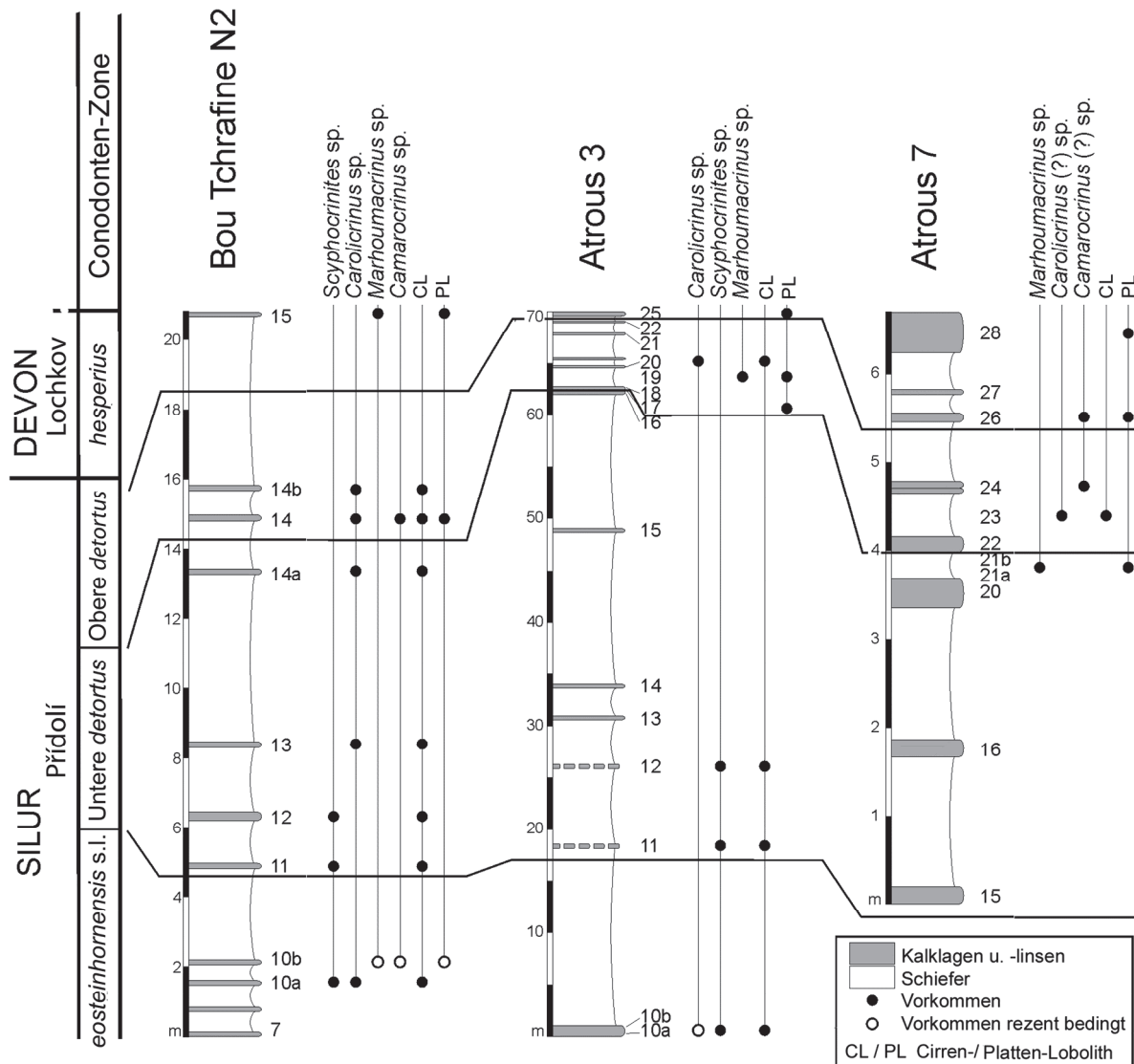
Abb. 4: Stratigraphie der Scyphocrinoiden-Lagen in den Profilen Bou Tchrafine N2, Atrous 3 und Atrous 7 [nach Corradini et al. 2013, verändert; verschiedene Maßstäbe].

Fig. 4: Stratigraphy of the scyphocrinoid beds in the sections Bou Tchrafine N2, Atrous 3, and Atrous 7 [from Corradini et al. 2013, modified; different scales].

Aber auch die nur undicht gewordenen Lobolithen einer nun am Meeresboden liegenden Menge dieser Crinoiden dürften aufgrund ihrer voluminösen Form, der bei Platten-Lobolithen besonders stabilen Wand und des insgesamt geringen spezifischen Gewichts (mikroporöser Stereom-Kalzit) nach einiger Zeit zwischen den zerfallenden anderen Skelettteilen herausgeragt haben. Derartig exponiert konnten sie bereits durch leichte Strömungen verlagert werden. Dennoch zeigen die Befunde an den großen Fossilplatten und auch an Bruchstücken aus dem Grabungsschutt, dass in der Regel defekte Lobolithen oder deren Wandteile in der Skelettmasse einer solchen Event-Lage zurückgeblieben sind.

Die Scyphocrinoiden sind aber kaum erst durch Sturmereignisse oder lokale Turbulenzen zu größeren lokalen Ansammlungen konzentriert worden; dazu wäre es wohl an Untiefen gekommen, was dann aber zu dicken Lagen Scyphocrinoiden-Detritus geführt hätte. An den marok-kanischen Scyphocrinoiden-Platten, z. B. der „Göttinger Kolonie", sind nur leichte Strömungseinwirkungen während des Ablagerungsvorgangs festzustellen; aber auch die hätten kaum zu so enormen Konzentrationen der Tiere geführt. Plausibler ist, dass die Scyphocrinoiden bereits zu „Normalzeiten" eng benachbart drifteten, wobei ihre Anzahl durch eine hohe Reproduktionsrate schnell gewachsen sein dürfte. Die Individuen in den Kolonie-artigen Ansammlungen wurden wahrscheinlich durch ein Netz langteiliger driftender Algen zusammen gehalten, wie sie in der heutigen Sargassosee bekannt sind (Haude et al. 1994). Das spricht für eher langdauernde Ursachen, etwa überregionale große Strömungswirbel („Gyren"), die zur Erklärung getrennter Vorkommen in den obersilurischen Alaunschiefern herangezogen werden können (Prokop & Petr (2001).

Stratigraphie der Scyphocrinoiden-Schichten

Nach den Conodonten-Daten kann im Tafilalet der Schichtbereich mit den Scyphocrinoiden-Lagen vom oberen Silur mit drei Zonen (Přídolí-Stufe) bis in das unterste Devon mit einer Zone (untere Lochkov-Stufe) gegliedert werden (Abb. 4) (Corradini et al. 2013; Corradini & Corriga 2012; Corriga et al. 2014): Die *eosteinhornensis* s. l. (Intervall-)Zone beginnt mit *Ozarkodina eosteinhornensis* s. l. (nicht aufgeschlossen in Profil Atrous 7). Darüber folgt mit dem Einsetzen von *Oulodus elegans detortus* die Untere *detortus*-Zone; diese enthält den *Ozarkodina eosteinhornensis* s. s.-Horizont, der im Bereich von Nord-Gondwana für Korrelationen wichtig ist und jetzt auch in Marokko nachgewiesen werden konnte. Der Beginn der Oberen *detortus*-Zone wird mit dem Erscheinen von *Zieglerodina remscheidensis* definiert; in ihr treten *Oul. el. detortus* und *Oul. el. elegans* letztmalig auf. Das Einsetzen des Index-Taxons *Icriodus hesperius* markiert den Beginn des Devons mit der *hesperius*-Zone (Corradini et al. 2013).

Im Tafilalet wurden die ersten Scyphocrinoiden-Lagen in der *eosteinhornensis* s. l.-Zone nachgewiesen (Abb. 5). Die nächsten Lagen folgen in der Unteren *detortus*-Zone, in Atrous 3 erst nach ca. 15 m Tonschiefern, in Bou Tchrafine N2 bereits nach ca. 2 m; die zwei bis drei Lagen dieser Zone sind jeweils durch zwei bis fünf Meter Tonschiefer getrennt. In der Oberen *detortus*-Zone wurden in allen drei Profilen jeweils zwei bis drei durch geringer mächtige Schiefer getrennte Lagen registriert. Erst in ziemlich großem Abstand von ca. 5 m folgen in der *hesperius*-Zone der unteren Lochkov-Stufe die letzten Scyphocrinoiden-Lagen, in Bou Tchrafine und Atrous 3 je eine in verschiedenen Abständen von der Grenze. In Atrous 7 sind es zwei Lagen, eine direkt über der Grenze, die zweite und letzte nach ca. 1 m.

Die beträchtlichen, durch die stratigraphische Vergleichsmöglichkeit noch auffälligeren Mächtigkeits-Unterschiede in den drei Profilen erscheinen zunächst als unrealistisch, so als ob sie durch Wechsel der als einheitlich eingesetzten Einfallswinkel bedingt wären. Die bei Legrand (1962) und Hollard (1962, 1977) angegebenen Mächtigkeiten des oberen Silurs in Nord-Afrika zeigen aber ebenfalls erhebliche Unterschiede an.

Assoziationen monospezifischer Scyphocrinoiden-Kronen mit typischen Skelettteilen – taxonomische Konsequenzen

Da die beiden Lobolithen-Bautypen (Abb. 6, 7) bzw. deren Reste meist leicht zu unterscheiden sind, zeigte es sich bereits im Gelände (bzw. im dortigen Grabungs-Aushub), dass sie oder ihre Teile in der Regel nicht in der gleichen Lage miteinander assoziiert sind – mit zwei deutlichen Ausnahmen: In dem (etwas kürzeren) Profil Bou Tchrafine N2 fanden sich im Aushub an einer Stelle der dort tiefsten (ältesten) Lage 10 [oder zwei Lagen, 10a (+b?) = „Hauptschurf" nach W.'s Geländeprofil] und in der höheren Lage 14a, b jeweils beide Lobolithen-Typen (zusammen mit verschiedenen Kronen-Taxa).
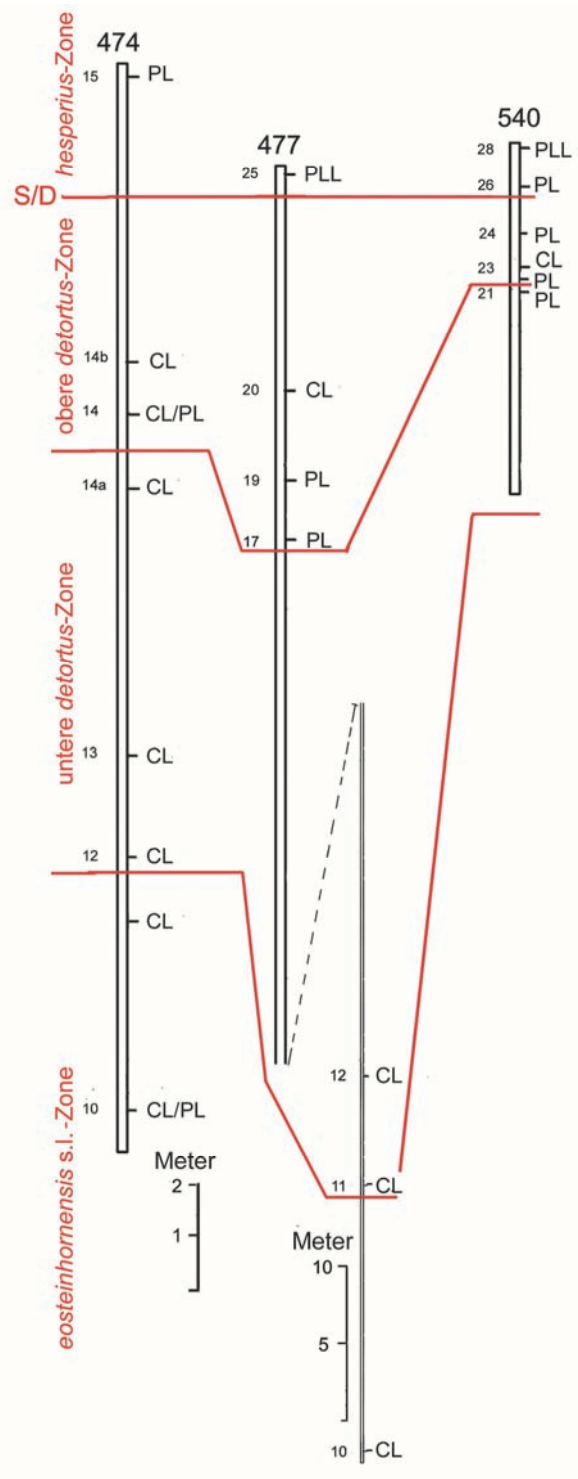
Abb. 5: Lagen mit Cirren- und Platten-Lobolithen (CL, PL) in den drei Profilen [gleiche Maßstäbe, außer im unteren Teil von Profil 477, zum Vergleich der sehr verschiedenen Mächtigkeiten; S/D = Silur–Devon-Grenze, PLL = dicke Bank aus Platten-Lobolithen].

Fig. 5: Layers with cirrus and plate loboliths (CL, PL) in the three sections [same scales, except in the lower part of section 477, for comparison of the great differences in thickness; S/D = Silurian–Devonian boundary, PLL = thick layer consisting of plate loboliths].
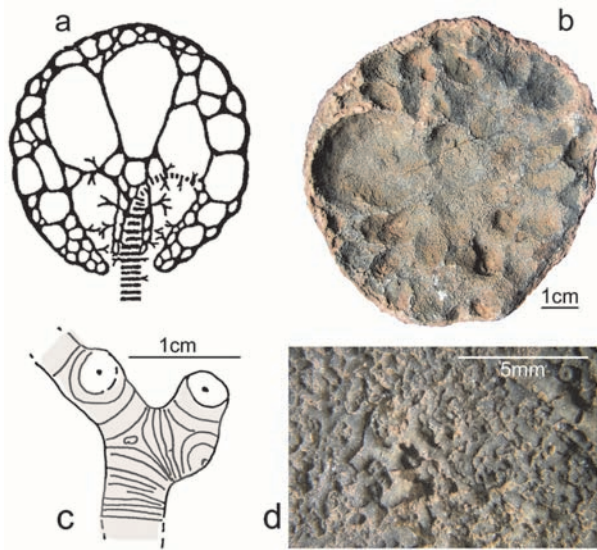
Abb. 6: Cirren-Lobolith. (**a**) Schematischer Vertikalschnitt, in der oberen, dem Stielansatz gegenüber liegenden Kugel-Kalotte und im Bereich der Wand ausschließlich geschlossene, Blasen-artige Kammern, in der unteren Kalotte mit dem Stielansatz auch einige nach unten offene Kammern; (**b**) Ansicht biostratinomisch freigelegter, Blasen-artiger Kammern der oberen Kalotte (untere Kalotte mit Stielansatz disartikuliert), in Lage 20 ausschließlich mit Kelch-/Kronen-Resten von *Carolicrinus* assoziiert (GZG 1216-477-20-107); (**c**) Stiel-Ansatz mit irregulär gesprossten Primär-Cirren einer disartikulierten Lobolithen-Kalotte, Pfeil: „Narbe" des Stielendes (GZG 1612-474-12-111); (**d**) Detail einer Cirrenwand, in Lage 10 ausschließlich mit Kelch-/Kronen-Resten von *Scyphocrinites* assoziiert (GZG 1612-474-10-131).

Fig. 6: Cirrus lobolith. (**a**) vertical cut (diagrammatic), with bubble-like closed chambers in the upper part (i.e. opposite to the stem trunk) and within the thick wall; several larger open chambers in the lower part (i.e. that with the trunk); (**b**) biostratinomically opened aspect of closed chambers of the upper hemisphere (lower hemisphere with stem trunk disarticulated); all cirrus loboliths from this layer associated with parts of crowns / calyces of *Carolicrinus* (GZG 1216-477-20-107); (**c**) stem trunk of disarticulated lower hemisphere with irregularly arranged primary cirri, arrow: cicatrix of distal end of stem (GZG 1612-474-12-111); (**d**) detail of wall of a lobolith, in this layer exclusively associated with parts of crowns / calyces of *Scyphocrinites* (GZG 1612-474-10-131).

Allerdings schienen die Mischfunde der Lage 10 hier auf die eine Stelle beschränkt zu sein, während im weiteren Verlauf des Aushubs nur zahlreiche Reste von Cirren-Lobolithen zusammen mit Kronenteilen von *Scyphocrinites* (und fraglichen *Carolicrinus*), aber keine weiteren Reste von Platten-Lobolithen gefunden wurden. Da die besagte Stelle nicht weit von Erfoud entfernt ist, könnte Grabungsmaterial von anderer Stelle hierher geraten sein (Corriga et al. 2014). Dennoch ist die Existenz einer dicht oberhalb einer Bank im „Hauptschurf" (aus dem viele große Scyphocrinoiden-Platten stammen, möglicherweise auch die in Göttingen befindliche) verlaufenden, stratigraphisch frühen Lage mit Platten-Lobolithen und zugehörigen Kronen-Taxa nicht auszuschließen. Die Mischfunde im Aushub bei „Lage 14" stammen sicher von den dicht darüber und darunter gelegenen Scyphocrinoiden-Lagen 14a/b.

Die zahlreichen, vollständig erhaltenen Kronen auf großen, in Museen und anderswo ausgestellten Platten [z. B. in Göttingen (Abb. 2); in Frankfurt/M.: Senckenberg-Museum (Plodowski 1996: Abb. 1); Basel: Naturhistorisches Museum (Hess 1999: Abb. 110); Tokyo: Planey Co. Ltd. (Haude 1998: Abb. 2)] gehören jeweils zu nur einer Gattung bzw. Art. Das zeigen auch die Kelch- bzw. Kronenreste, die im weiteren Verlauf von Scyphocrinoiden-Lagen, bzw. in deren Grabungs-Aushub aufgesammelt werden konnten. Eine sichere Bestimmung ist auch bei relativ gut erhaltenen Kelchresten z. T. problematisch. Denn einerseits zeigt sich an optimal erhaltenen Kelchen/Kronen großer „Kolonien" von Museums-Exponaten, dass systematisch wichtige Strukturen beträchtlich variieren. Andererseits handelt es sich bei den im Gelände bzw. Grabungs-Aushub aufgesammelten Proben meist um Fragmente, bzw. für kommerzielle Zwecke ungeeignete Stücke. Deshalb ist die Feststellung signifikanter Skelett-Assoziationen in Lagen monospezifischer Scyphocrinoiden von entscheidender Bedeutung: Ein in der betreffenden Lage assoziierter einziger Lobolithen-Typ kann somit den dortigen Kronen zugeordnet werden. Diese skelettale Beziehung wird noch durch bestimmte begleitende Stielreste gestützt: In den Lagen mit Platten-Lobolithen kommen außer Stielteilen mit rundem Querschnitt regelmäßig auch solche mit (primär) ovalem Querschnitt vor; sie wurden als Reste des Mittelstiels mancher Scyphocrinoiden erkannt Haude (1981), dann speziell bei *Marhoumacrinus* (Prokop & Petr 1987) und bei *Camarocrinus* (Haude 1992) beschrieben.

Ein weiterer Hinweis auf die taxonomische Zusammengehörigkeit von Scyphocrinoiden-Teilen in den einzelnen Lagen der Profile im Tafilalet − wie auch in anderen Regionen (Haude 1992) − sind häufige Funde von zwei permanent und selektiv auf verschiedenen Scyphocrinoiden parasitierenden platyceraten Schnecken: in Lagen mit Cirren-Lobolithen die hohe Zipfelmützen-förmige *Orthonychia*, in solchen mit Platten-Lobolithen der eingerollte *Platyceras* (vgl. auch Hess 1999, Abb. 110; zur Lebensweise dieser Platyceratidae s. Horný 2000 und Baumiller 2002). Danach gehören die hier − wie auch an anderen Vorkommen − mit diesen Schnecken assoziierten Lobolithen-Typen jeweils der betreffenden Scyphocrinoiden-Gattung bzw. -Art an [vgl. die Beobachtungen in anderen Vorkommen, etwa in Spanien, Deutschland, China, USA (Haude 1989, 1992)].

Anders verhält es sich mit der Möglichkeit solcher Zuordnungen im Barrandium: Die Silur–Devon-Übergangsschichten sind deutlich kondensiert (mdl. Mitteilung 2013 von Rainer Brocke, Frankfurt/M.). Die Scyphocrinoiden-Lagen folgen lokal − z. B. in dem Standard-Profil der Silur/Devon-Grenzschichten bei Karlstejn − sehr dicht aufeinander, und an der Fundstelle „Lobolith hillside" bei Prag scheint überhaupt keine Trennung möglich zu sein. Außerdem könnte es sich bei den Kalkbänken der Typlokalität der Silur/Devon-Grenze (bei Klonk) um distale Turbidite handeln (Chlupáč & Vacek 2003).
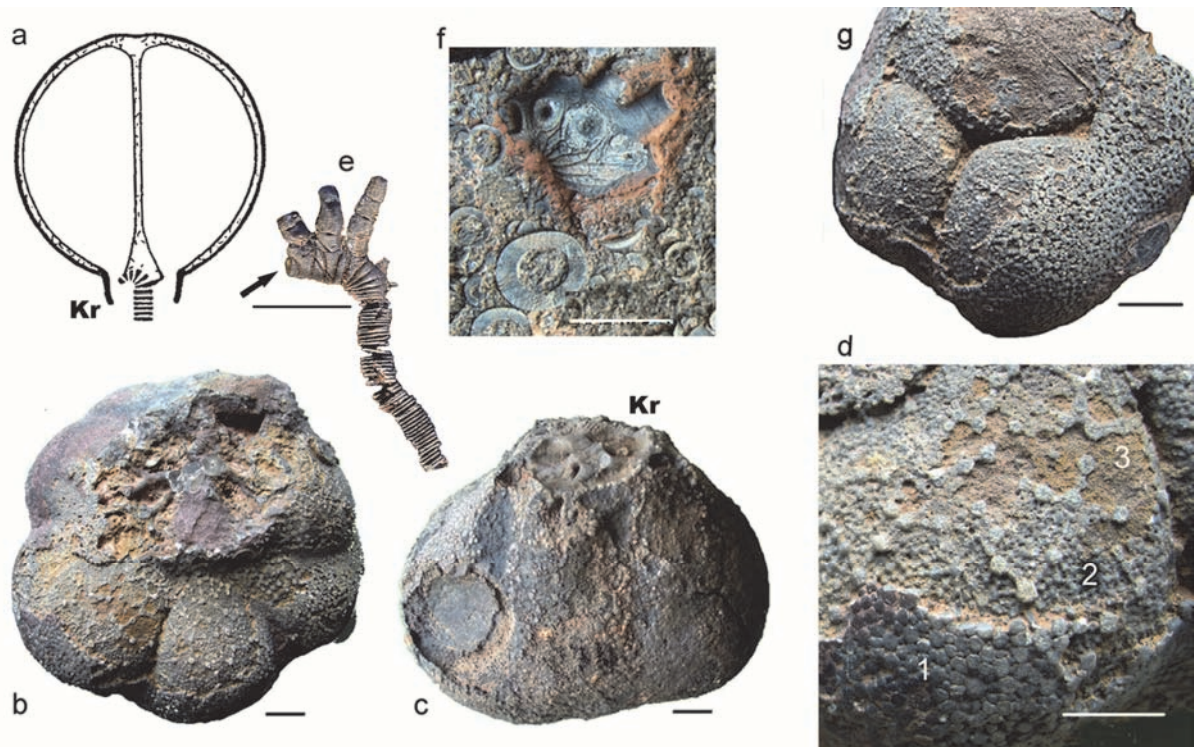
Abb. 7: Platten-Lobolith. (**a**) Schematischer Vertikalschnitt mit nach unten offenen Kammern, Stielansatz mit den Kammer-Öffnungen von einer Kragen-artigen Wand umgeben; (**b**) Lobolith mit dem (bilateral-symmetrischen) Stielansatz, die diesen Bereich umgebende Kragenwand ist nur in Resten erhalten (GZG-1612-474-x); (**c**) stark nach außen vorgewölbte Kammern, Kammer-Öffnungen in Gabelungen der Primär-Cirren nahe dem basalen Rest des Kragens, z. T. sichtbar (GZG 1612-474-10-124); (**d**) (Detail aus der nach oben orientierten Wand des Lobolithen in "c") Bereich der nach oben exponierten, partiell erodierten Plattenwand: (1) Platten der Außenfläche, (2) darunter freiliegende Internfläche der kammerseitigen Doppelwand, (3) Sedimentfüllung der betreffenden Kammer; (**e**) längerer distaler Stielteil mit Primär-Cirren eines disartikulierten juvenilen Lobolithen, Pfeil: Abbruchstelle des Stielendes (GZG-1612-540-21-105); (**f**) Skelettreste von *Camarocrinus* oder *Marhoumacrinus*: Stielansatz eines disartikulierten Lobolithen mit basal erhaltenen, regelhaft bilateral-symmetrisch angeordneten Primär-Cirren, einzelne ovale Stielglieder eines Mittelstiels (GZG 1612-477-19-106); (**g**) oberer Teil eines Lobolithen, Außenwand dort nicht erhalten, dadurch drei aneinander grenzende, nach oben gewölbte Kammern sichtbar (GZG 1612-474-10-127) [Kr = Kragenwand; Maßstäbe = 1 cm].

Fig. 7: Plate lobolith. (**a**) vertical cut (diagrammatic), distal stem trunk and openings of chambers surrounded by relicts of the collar-like wall; (**b**) lobolith with (bilaterally symmetrical) distal stem trunk, only fragments of the collar wall preserved (GZG-1612-474-x); (**c**) strongly bulging chamber walls, some chamber openings visible in bifurcations of primary cirri near only basally preserved collar wall (GZG 1612-474-10-124); (**d**) (detail from upper side of lobolith in "c") area of upwardly exposed, partly eroded tessellate layers of double wall: (1) plates of exterior wall, (2) below this an exposed part of the internal wall, (3) sedimentary contents of a chamber; (**e**) part of distally bent stem with primary cirri of a (disarticulated) juvenile lobolith, arrow: scar of broken-off distal part of stem (GZG-1612-540-21-105); (**f**) skeletal residues of *Camarocrinus* or *Marhoumacrinus*: distal part of stem with partly preserved typical, bilateral-symmetrically arranged primary cirri of disarticulated lobolith, some elliptical columnals of the middle part of a stem (GZG 1612-477-19-106); (**g**) upper part of a lobolith, external wall not preserved, thus the tessellate walls of three contiguous chambers visible (GZG 1612-474-10-127) [Kr = collar wall; scale bars = 1 cm].

So wären gleichzeitig lebende Scyphocrinoiden-„Kolonien" verschiedener taxonomischer Zugehörigkeit, die in anderen Regionen weit voneinander entfernt drifteten, im paläogeographischen Raum Böhmen in engere Nachbarschaft und − vor allem die beiden Lobolithen-Typen − biostratinomisch in die gleiche Lage geraten. Deshalb ist Prokop & Petr (1994, 2001) zuzustimmen, dass es − in Böhmen − nicht möglich sei, assoziierte verschiedene Skelettbereiche von Scyphocrinoiden einander sicher zuzuordnen.

Die Befunde in den marokkanischen Profilen bestätigen nun frühere Beobachtungen (Haude 1992), dass vier Scyphocrinoiden-Gattungen − in jeweils verschiedenen Lagen − mit ihren zugehörigen Skelettteilen hinreichend sicher belegt werden können (Abb. 8): *Scyphocrinites* Zenker, 1833 und *Carolicrinus* Waagen & Jahn, 1899, beide mit Cirren-Lobolith und einem im Querschnitt runden Stiel; *Marhoumacrinus* Prokop & Petr, 1987 und *Camarocrinus* Hall, 1879, beide mit Platten-Lobolith und einem im Mittelstiel-Bereich ovalen Querschnitt. Die Bestimmung der Arten ist einer Revision vorbehalten (Abb. 9).

Die früheste (älteste) Form in den marokkanischen Profilen ist *Scyphocrinites* sp. (in der tieferen *eosteinhornensis* s. l.-Zone, Profil Atrous 3, Lage 10). Sie kann mindestens bis in die Untere *detortus*-Zone nachgewiesen werden, aus der nach dem Conodonten-Befund (GZG 301, coll. Walliser, Probe 3398) auch die „Göttinger Platte" stammt. Die mehr als 75 (sichtbaren) meist adulten Kronen unterschiedlicher Größe und einzelnen sehr kleinen (juvenilen) Individuen dieser „Kolonie" (Abb. 2) sind mit Resten von Cirren-Lobolithen assoziiert und gehören

wahrscheinlich als neue Art von (?)*Camarocrinus* in die Stammlinie der Camarocrininae (mit *Camarocrinus* und *Marhoumacrinus*, Haude 1989). Fragmente adulter Kronen, die sowohl *Carolicrinus* als auch *Marhoumacrinus* zugeordnet werden könnten, gehören aufgrund ihrer Assoziation ausschließlich mit Cirren-Lobolithen (z. B. in Profil Atrous 3, Lage 21) sicher zu *Carolicrinus*. Demnach kommt diese Gattung von der Unteren bis in die Obere *detortus*-Zone vor und alterniert dort ein- bis zweimal mit Lagen von *Marhoumacrinus* sp. bzw. z. T. wohl auch mit *Camarocrinus* sp. In der *hesperius*-Zone des unteren Lochkoviums sind offenbar nur noch Formen mit Platten-Lobolith vorhanden, die vielleicht nur noch eine dieser beiden Gattungen als damit letzte Vertreter der Scyphocrinoiden repräsentieren − jedenfalls in Marokko. Bei Kronen aus dem Lochkovium, die *Scyphocrinites elegans* zugeordnet wurden (Prokop & Petr 1986), dürfte es sich aufgrund der dort allein assoziierten Reste von Platten-Lobolithen eher um eine Art von *Camarocrinus* handeln. Denn eine morphologisch so spektakuläre evolutive Entwicklung wie der Wandel von einer Form mit Cirren-Lobolith in eine solche mit Platten-Lobolith ist kaum im Rahmen einer einfachen Art-Aufspaltung (in diesem Fall von *Scyphocrinites*) zu begründen. Ein solcher Wandel betrifft auch die Formen der Gattungen *Carolicrinus* (mit Cirren-Lobolith) und *Marhoumacrinus* (mit Platten-Lobolith). Für Prokop & Petr (1986: 202) stellt sich das anders dar, weil anhand des böhmischen Materials eine durch lokale Assoziation abgesicherte taxonomische Zuordnung der Lobolithen-Typen offenbar nicht möglich ist. Aufgrund des ähnlichen Armbaus halten sie (und im Anschluss daran auch Hess 2010) *Marhoumacrinus legrandi* für den „direkten phylogenetischen Vorläufer von *Carolicrinus barrandei*" (innerhalb einer Familie Marhoumacrinidae); dementsprechend nehmen sie, ohne empirischen Beleg, auch für *Carolicrinus* einen Platten-Lobolithen an.

Paläobiologie der Scyphocrinoiden

Die Scyphocrinoiden entwickelten sich im höheren Silur aus benthonisch lebenden Vorläufern mit einer Wurzel aus gegliederten, reich verzweigten Cirren (nach Donovan 1993: „Radicen", da „Cirren" als aktiv bewegliche, unverzweigte Anhänge des Stiels definiert werden, die erst seit dem Mesozoikum nachgewiesen sind). Im Silur bildeten sich in epikontinentalen Gebieten der niederen bis mittleren Paläobreiten weit verbreitet schwarze bituminöse Sedimente, die euxinische Bedingungen bei geringem Wasseraustausch in Bodennähe und eine hohe Planktonproduktion im Oberflächenwasser anzeigen. Durch die in eine Schwimmboje umgewandelte Wurzel konnten die driftenden Scyphocrinoiden dort das reiche Angebot an planktonischer Nahrung nutzen, schneller wachsen und beträchtliche Größen erreichen (Abb. 10). Eine Berechnung des Gewichts der Skelettmasse unter Wasser (spezifisches Gewicht von Echinodermen-Stereom ca. 0,3 g)
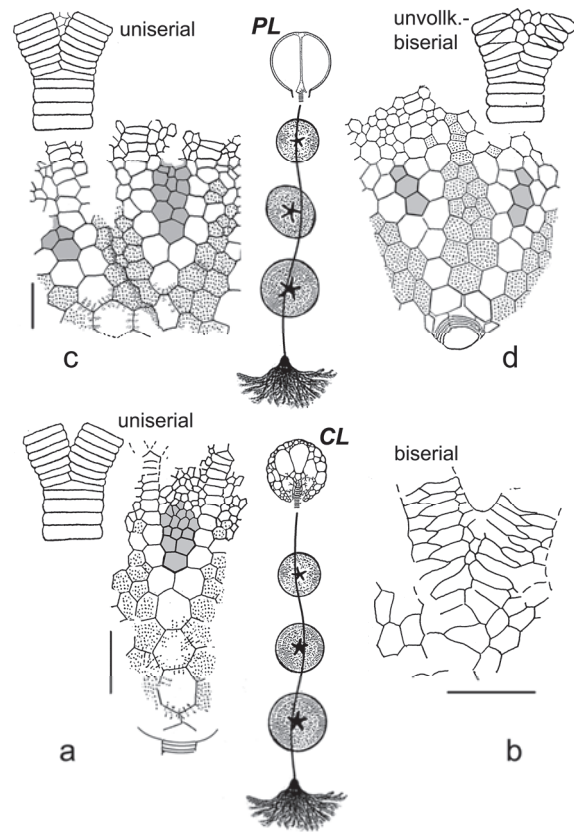

Abb. 8: Diagramm der identifizierten Scyphocrinoiden-Gattungen mit einigen diagnostisch relevanten Merkmalen. (**a**) *Scyphocrinites* cf. *elegans* (GZG 1612-474-12-101, vgl. Abb. 9c) mit längeren scharfen Rippen auf den Rändern der proximalen Kelchplatten und uniserialer Anordnung der Armglieder; (**b**) *Carolicrinus* cf. *barrandei* (vgl. Abb. 9e), Kelchwand mit biserialer Anordnung der Glieder des inkorporierten distalen Secundibrachiums und der folgenden Armbereiche; (**c**) *Camarocrinus* cf. *subornatus* (vgl. Abb. 9g) mit der Abfolge 1-2-2/3 der Intersecundibrachial-Platten (dunkel gerastert) in der Kelchwand und meist uniserial bis unvollkommen biserial angeordneten Armgliedern; (**d**) *Marhoumacrinus legrandi* [aus Prokop & Petr 1987: Abb. 4, verändert] mit der bei dieser Gattung typischen Abfolge 1-1-1/2 der Intersecundibrachial-Platten (dunkel gerastert) in der Kelchwand und unvollkommen biserialer Armstruktur. − Bei (a) und (b) Cirren-Lobolith (CL) und durchgehend runder Stielquerschnitt; bei (c) und (d) Platten-Lobolith (PL) und − typisch − im Mittelstielbereich ovaler Stielquerschnitt. − Punktraster = Interradial-Bereiche; grau = Intersecundibrachial-Bereiche; Maßstäbe = 1 cm.

Fig. 8: Diagram of identified genera of scyphocrinoids with some of the diagnostically relevant characters. (**a**) *Scyphocrinites* cf. *elegans* (GZG 1612-474-12-101, see Fig. 9c) with relative long, sharp ridges across the margins of proximal plates, and uniserial brachials; (**b**) *Carolicrinus* cf. *barrandei* (see Fig. 9e), calyx wall with biserially arranged brachial elements of incorporated distal secundibrachium and following parts of arms; (**c**) *Camarocrinus* cf. *subornatus* (see Fig. 9g) with sequence of intersecundibrachs 1-2-2/3 (grey) in the calyx wall, and mostly uniserial or incompletely biserial brachials; (**d**) *Marhoumacrinus legrandi* [from Prokop & Petr 1987: fig. 4, modified] with the typical sequence of intersecundibrachials 1-1-1/2 (grey) in the calyx wall, and incompletely biserial structure of arms. − In (a) and (b) cirrus lobolith (CL) and round columnals in the whole stem; in (c) and (d) plate lobolith (PL) and − exclusively the middle part of the stem − consisting of elliptical columnals. − Dotted = interradial area, grey = intersecundibrachial area; scale bars = 1 cm.
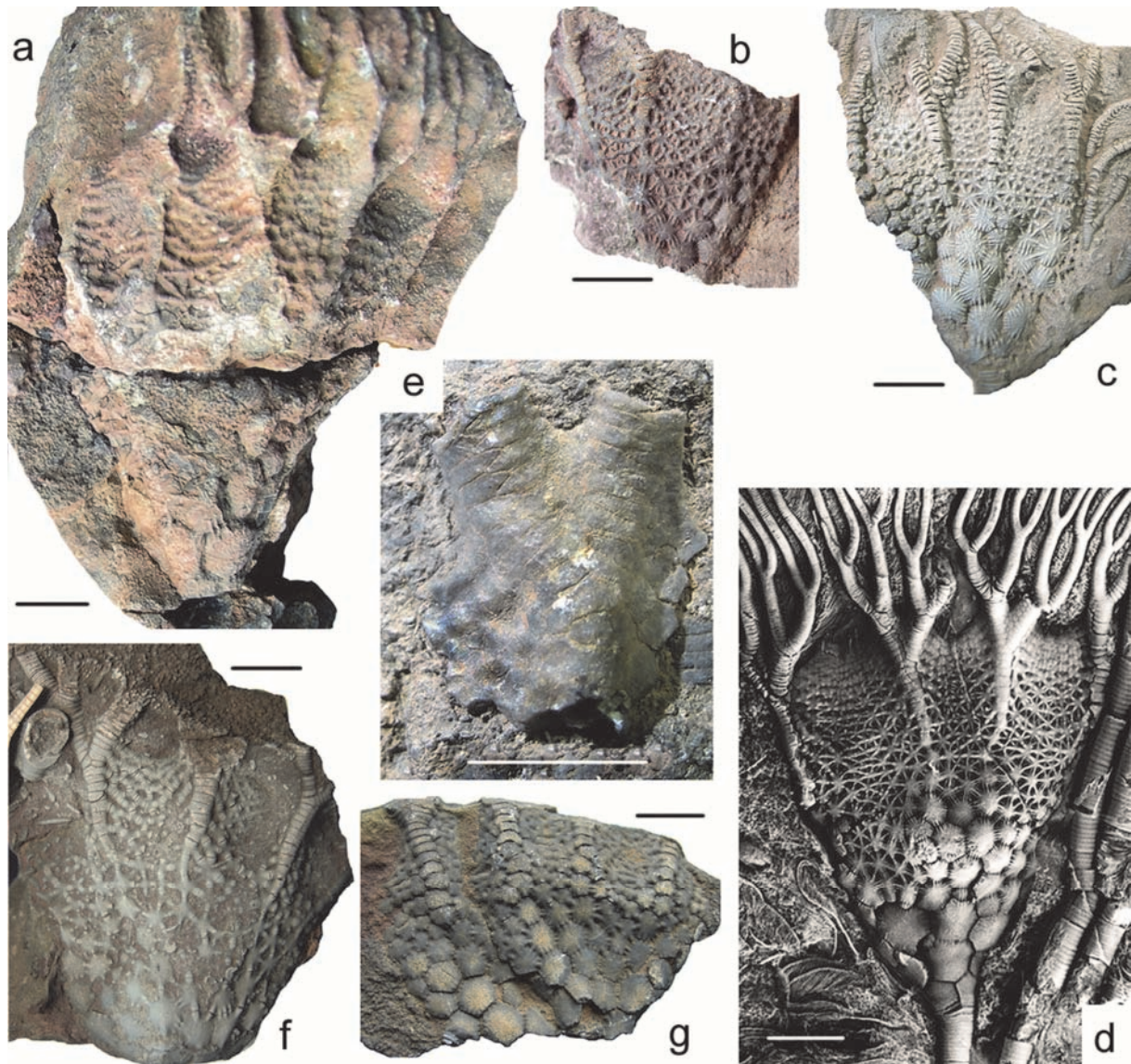
Abb. 9: (**a-c**) *Scyphocrinites* cf. *elegans*. (**a**) (GZG 1612-477-11-108); (**b**) (GZG 1612-474-10-114); (**c**) (vgl. Abb. 8a; GZG 1612- 474-12-101). (**d**) *Camarocrinus*? n. sp.? ("Gö-3") aus der Göttinger Scyphocrinoiden-„Kolonie" in Abb. 2a **(Ausschnitt b; GZG 103-1-3)**; (**e**) *Carolicrinus* cf. *barrandei,* Bruchstück einer Kelchwand (vgl. Abb. 8b; GZG 1612-477-20-109); (**f–g**) *Camarocrinus* cf. *subornatus*. (**f**) (GZG 1612-474-14-107); (**g**) (vgl. Abb. 8c; GZG 1612-474-14-013). – Maßstäbe = 1 cm.

Fig. 9: (**a-c**) *Scyphocrinites* cf. *elegans*. (**a**) (GZG 1612-477-11-108); (**b**) (GZG 1612-474-10-114); (**c**) (see Fig. 8a; GZG 1612- 474-12-101). (**d**) *Camarocrinus*? n. sp.? ("Gö-3") in the Göttingen scyphocrinoid "colony" see Fig. 2a **(detail b; GZG 103-1-3)**; (**e**) *Carolicrinus* cf. *barrandei,* fragment of calyx wall (see Fig. 8b; GZG 1612-477-20-109); (**f–g**) *Camarocrinus* cf. *subornatus*. (**f**) (GZG 1612-474-14-107); (**g**) (see Fig. 8c; GZG 1612-474-14-013). – Scale bars = 1 cm.

von einem Modell-Scyphocrinoiden mit definierten Skelett-Einheiten ergibt, dass selbst ein nicht vollständig mit Gas gefüllter Lobolith von 10 cm Durchmesser einen mehrere Meter langen Stiel mit großer Krone an der Wasseroberfläche halten konnte (Haude 1998). Die horizontweise weite Verbreitung der wahrscheinlich bei Sturmereignissen abgesunkenen Linsen-förmigen Massen-Vorkommen mit Kronen von z. T. beträchtlichen Größenunterschieden in den bekannten „Kolonien" (s. o.), sowie häufige Funde von Jungtieren (Abb. 2d, 11) zeigen außerdem eine hohe Reproduktionsrate an.

Juvenile Scyphocrinoiden und Lobolithen-Bildung

Vor allem aber können bei Cirren- und Platten-Lobolithen auf der (beim lebenden Tier) nach unten gerichteten Kugel-Kalotte, hauptsächlich im Bereich ihres Stielansatzes, mehrere kleine, angeheftete Crinoidenwurzeln mit anzementiertem Stielende erhalten sein, die mit dem Stielansatz des Lobolithen gleichgerichtet sind (Springer 1917: Abb. 7-10; Haude 1972: Abb: 18; 1992: Abb. 3, Taf. 1, Fig. G, H; Prokop & Petr 2001: Abb. 2, 3ff.). Sie wurden bereits von Strimple (1963) als Haftwurzeln juveniler Scyphocrinoiden − vor Ausbildung ihres Lobolithen − gedeutet. Der Stielteil von der Anheftungsstelle bis zur Ablösungsstelle des Lobolithen wäre damit vergleichbar dem

„*Pentacrinus*-Stiel" rezenter, sekundär ungestielter Comatuliden. Für dessen Natur als post-larvaler Stiel von Scyphocrinoiden spricht der pentagonale Zentralkanal, das völlige Fehlen anderer Crinoiden in den betreffenden Schichten sowie die Tatsache, dass im Stielstumpf der Lobolithen (der v. a. bei Platten-Lobolithen regelhaft U-förmig gekrümmt und mit den Primär-Cirren stets bilateral-symmetrisch gebaut ist) das Stielende ausnahmslos als Resorptionsnarbe erscheint, die die Abbruchstelle zu einem postlarvalen Stiel sein könnte. Danach hätte sich die Scyphocrinoiden-Larve an einem driftenden Substrat festgesetzt (hier: an einem Lobolithen); der sich entwickelnde Crinoide bildete dann zunächst eine Haftwurzel aus flächigem bis ungegliedert-ästigem Stereom-Zement und einen isomorphen (aus gleichförmigen Gliedern bestehenden) Primär- oder Post-Larvalstiel. Nach beträchtlicher Größenzunahme dieses Stiels (Durchmesser bis zu 3 mm) würde dann in größerem Abstand von der Haftwurzel [gemäß bekannten Längen des Post-Larvalstiels von mehr als 8 cm (s. Haude 1972: Abb. 18)] Längenwachstum auch durch Interkalation neuer Glieder (Internodalia) zwischen die älteren einsetzen, so dass dieser Stielbereich eine heteromorphe Struktur erhielte (Wechsel von Gliedern unterschiedlicher Größe, Abb. 2d, 11). Hier erst würden sich an den Nodalia (nur an der Kelchbasis angelegten Gliedern) segmentierte Primär-Cirren und von deren vielfachen Gabelungen ausgehend der Lobolith gebildet haben [Abb. 12; s. auch Prokop & Petr (2001: fig. 1b, c)]. Nach einiger Zeit besäße der juvenile Lobolith genügend Stabilität und Gas-Inhalt, dass bei Lösung seiner Verbindung zum Post-Larvalstiel die pelagische Lebensweise des jungen Scyphocrinoiden beginnen würde.

Allerdings stehen zwei wichtige Befunde nicht im Einklang mit diesem Modell: Die Stiele fast vollständig erhaltener Jungtiere mit bereits ausgebildeten Primär-Cirren samt Lobolithenrest [auf einer marokkanischen Scyphocrinoiden-Platte im Naturhistorischen Museum Basel (Hess 1999: Abb. 110)] und die Stielereste juveniler Kronen (s. Abb. 11) sind (a) wesentlich dünner (Durchmesser ca. 1 mm) als die der meisten juvenilen Haftwurzeln (Durchmesser bis zu 3 mm) und (b) heteromorph gebaut. Danach erscheint die ontogenetische Entwicklung von Scyphocrinoiden mit direkter Lobolithen-Bildung ohne eine vorangehende angeheftete Phase mit Post-Larvalstiel plausibler (Abb. 13). Hatten angeheftete Scyphocrinoiden mit ihrem vergleichsweise dicken und wohl auch relativ langen Post-Larvalstiel vielleicht eine andere Funktion, so dass sie gar keine Lobolithen entwickelten? Für eine Klärung solcher Fragen wäre eine gezielte Suche auf vorhandenen, gut präparierten Platten erfolgversprechend.

Paläobiologische Bedeutung struktureller Veränderungen bei Lobolithen und zugehörigen Stielen

Von den beiden Lobolithen-Typen ist der Cirren-Lobolith mit Wänden aus dichtem Geflecht von Wurzel-Cirren, den vielen blasenartigen, geschlossenen Kammern und

den ganz unregelmäßig angeordneten Primär-Cirren zweifellos die ursprünglichere Bauform (Abb. 6). Das zeigt sich in den marokkanischen Tonschiefern auch in seinem erheblich früheren (ca. 70 m tieferen) Auftreten vor Scyphocrinoiden mit dem bautechnisch höher entwickelten Platten-Lobolith (Abb. 7). Bei diesem sind die ursprünglichen Cirren-Ossikel an den Oberflächen der Wände (Außenfläche des Lobolithen und Innenfläche seiner Kammern) in plattige Elemente verbreitert und nur noch in den Zwickeln der so gebildeten Doppelwand sehr dünne Cirren vorhanden. Vor allem aber werden statt der zahlreichen geschlossenen, blasenartigen Kammern bei dem Cirren-Lobolith nur noch wenige, nach unten offene Kammern gebildet, deren Öffnung sich innerhalb einer Kragen-artigen Wand jeweils in der ersten oder zweiten Gabelung der vier bis sechs(?) primären, regelhaft bilateral-symmetrisch angeordneten Wurzel-Cirren des U-förmig gekrümmten Stielendes befindet (Haude 1972: Abb. 10). Von dort aus blähen sie sich durch den Auftriebsdruck des zunehmenden Gas-Volumens in den Kammern nach oben auf.
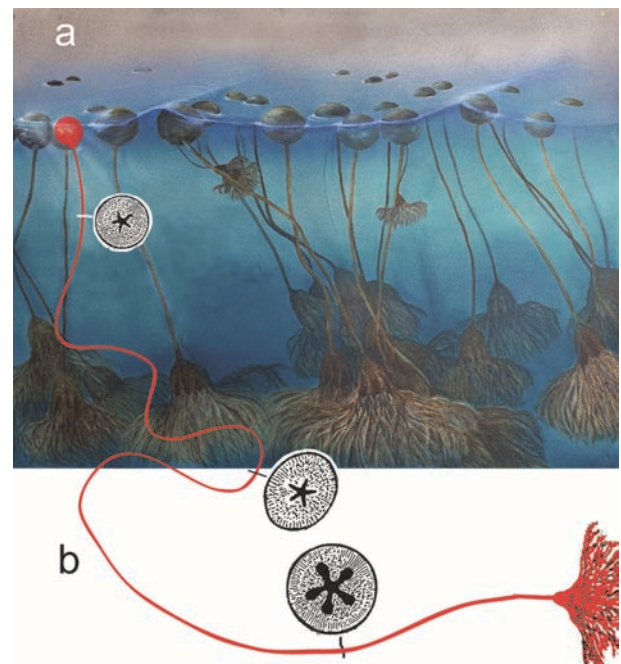

Abb. 10: (**a**) Lebensbild einer Scyphocrinoiden-"Kolonie" (Stiele aus Platzgründen stark verkürzt dargestellt; Geowissenschaftliches Museum, Universität Göttingen); (**b**) Modell eines Scyphocrinoiden mit realistischer Mindest-Länge des Stiels bezogen auf die berechnete Mindest-Tragkraft des eingezeichneten Lobolithen (Haude 1998); die im mittleren Stielbereich (zur Platz-Ersparnis übertrieben dargestellte) erhöhte Biegsamkeit – in einer Ebene(!) – bezieht sich auf den dort ovalen Stielquerschnitt bei Taxa mit Platten-Lobolith (vgl. Abb. 8c, d).

Fig. 10: (**a**) Presentation of a living scyphocrinoid "colony" (stems figured very short for practical reasons; Geoscience Museum, University of Göttingen); (**b**) scyphocrinoid with realistic minimal length of stem derived from the physical bearing capacity of a lobolith oft he figured size (Haude 1998); the – planar(!) – flexibility of the middle part oft he stem with elliptical columnals in taxa with plate lobolith (cf. Fig. 8c, d) exaggerated for size reduction of the graphic.
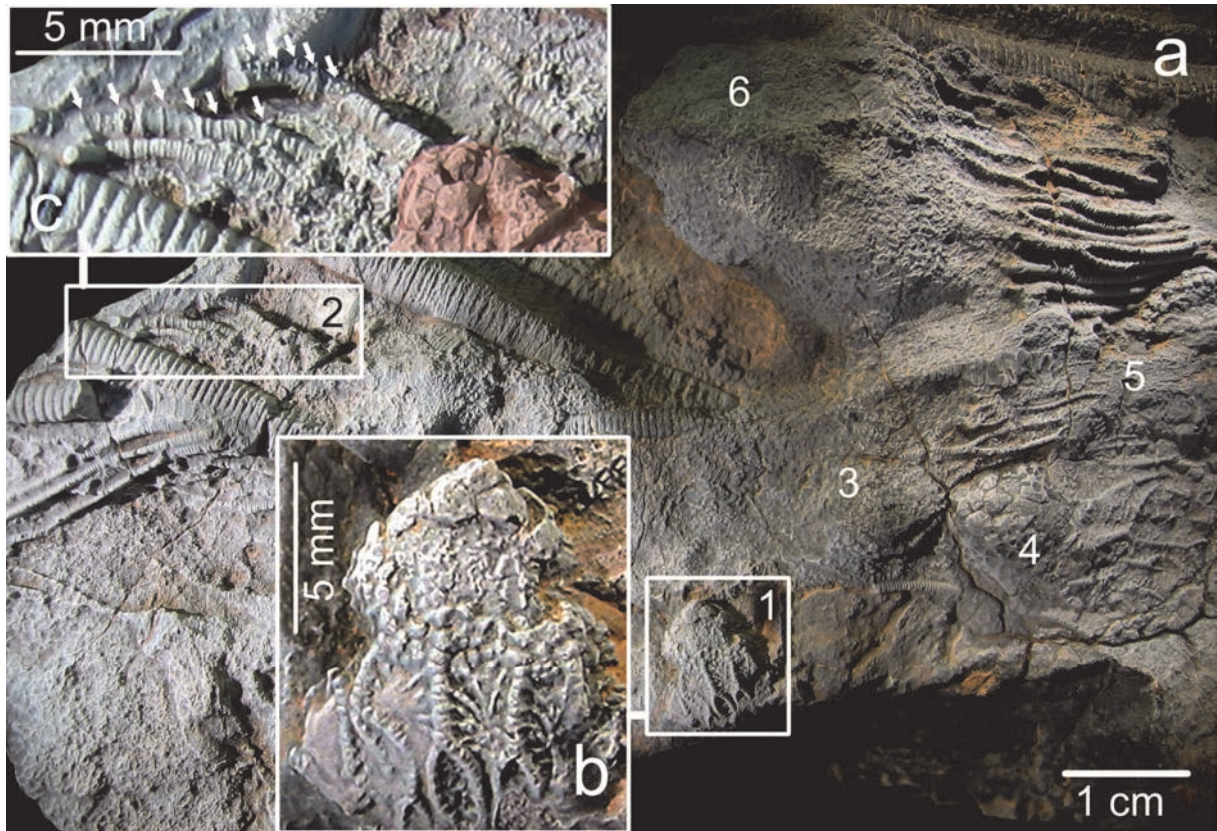
Abb. 11: (**a**) Mehrere juvenile Scyphocrinoiden [(?)*Scyphocrinites* cf. *elegans*] unterschiedlicher Größe (stärker verwittert; GZG 1612-477-11-101); (**b**) Krone „1" (Rechteck) mit anscheinend noch nicht fest in die Kelchwand inkorporierten Pinnulae der Sekundibrachia; (**c**) juvenile, heteromorphe Stiele mit breiteren Gliedern (einige „Nodalia": Pfeile) als mögliche Sprossungsorte von Primär-Cirren zur Anlage eines Lobolithen; „2" zugehörige, stark verwitterte Krone (Kelchrest: farbig).

Fig. 11: (**a**) several juvenile scyphocrinoids [(?)*Scyphocrinites* cf. *elegans*] (considerably eroded; GZG 1612-477-11-101); (**b**) crown "1" with pinnules of secundibrachs obviously still not incorporated into the calyx wall; (**c**) juvenile heteromorphic stems with the broader columnals as possible "nodals" from where may develop the primary cirri and the lobolith; strongly eroded crown "2" (relict of calyx stained).

Der Platten-Lobolithen ist zweifellos auch bautechnisch „besser"; denn statt des individuellen Spitzenwachstums in jeder Cirren-Verästelung bei dem Cirren-Lobolith kann nun die bei Echinodermen typische Plattenbauweise in einer durchgehenden Epithelschicht erfolgen. Das zeigt sich auch in der wahrscheinlichen Blütephase der Scyphocrinoiden. Denn das durch das reiche Nahrungsangebot bedingte schnellere Wachstum und die daraufhin beträchtliche Größenzunahme dieser Crinoiden, erforderte auch eine entsprechende Zunahme des Auftrieb-Volumens. Die im Gelände gemessenen Cirren-Lobolithen waren zwar deutlich größer [Durchmesser von über 16 cm; möglicherweise handelt es sich bei dem von Hess (2010) erwähnten nordafrikanischen Exemplar ebenfalls um diesen Bautyp] als die zahlreicher erhaltenen Platten-Lobolithen, diese haben aber eine wesentlich dünnere, dabei festere Wand und könnten mit den nach unten offenen Kammern auch eine Ökonomisierung der (symbiontischen?) Gasproduktion andeuten. Vielleicht sind solche Verbesserungen der Bojen-Funktion auch der Grund dafür, dass vor dem Aussterben im untersten Devon nur noch Arten mit Platten-Lobolith nachgewiesen sind: Ein in der unteren Lochkov-Stufe einsetzender Wechsel der Lithofazies könnte verschlechterte Lebensbedingungen im

Oberflächenbereich andeuten, denen nur diese Scyphocrinoiden etwas länger standgehalten haben.

Zu den biotechnischen Verbesserungen der Scyphocrinoiden mit Platten-Lobolith gehört auch der ovale Querschnitt des Mittelstiels bei *Camarocrinus* und *Marhoumacrinus*. Dadurch ist zwar die Biegsamkeit dort höher, jedoch nur in zweidimensionaler Ausrichtung, in der Ebene der kurzen Achse der ovalen Stielglieder. Torsions-Beanspruchungen bei Änderung der Ausrichtung eines gekrümmten Stiels, etwa infolge turbulenter Wellenbewegung, sind aber bei der frei-hängenden Lebensweise minimal bzw. werden durch widerstandsloses Mit-Rotieren des Lobolithen kompensiert.

Die Bojen-Funktion des Lobolithen an der Wasseroberfläche erscheint dann problematisch, wenn die wahrscheinlich starke physiologische Belastung durch Sonnenstrahlung und Austrocknung des exponierten, über die Wasseroberfläche reichenden Teils des Lobolithen zu berücksichtigen ist. Denn wie bei allen Echinodermen bestehen die Skelettelemente der Lobolithenwand aus Stereom-Kalzit, einem schwammartig-mikroporösen Innenskelett, das von Zellgewebe durchsetzt und gewöhnlich außen von einer dünnen Epidermis bedeckt ist. Die große Zahl kleiner Skelettelemente vor allem im oberen Teil der Lo-
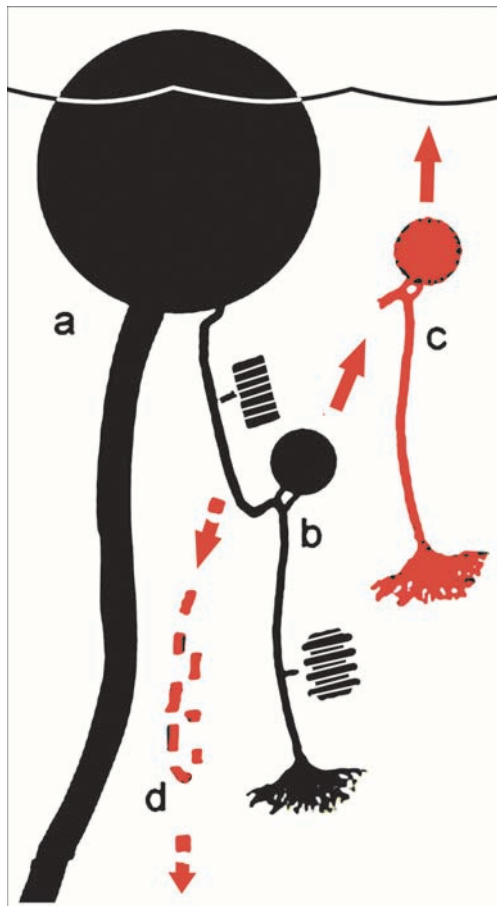
Abb. 12: Modell der Lobolithen-Bildung (hier nicht vertreten). (**a**) Lobolith eines adulten Scyphocrinoiden; (**b**) angehefteter juveniler Scyphocrinoide, am Übergang vom isomorphen Post-Larvalstiel zum heteromorphen Juvenil-Stiel Sprossung von Primär-Cirren mit Bildung eines Lobolithen an breiteren Gliedern („Nodalia"); (**c**) Ablösung des nun pelagisch lebenden Crinoiden; (**d**) Zerfall des Post-Larvalstiels.

Fig. 12: Model of lobolith development (not supported). (**a**) lobolith of adult scyphocrinoid; (**b**) attached juvenile scyphocrinoid, at the transition from isomorphic to heteromorphic growth of a juvenile stem, primary cirri at the broader columnals ("nodals"?); (**c**) detachment of the now pelagic crinoid; (**d**) disintegration of the postlarval stem.

bolithenwand zeigt, dass hier verstärktes Wand-Wachstum durch Interkalation stattfand. Seilacher & Hauff (2004: Abb. 1) versuchten, dieses Problem dadurch zu lösen, dass sie eine Anpassung der Scyphocrinoiden an eine Sprungschicht in gewisser Tiefe annehmen, den Grenzbereich zwischen einem dichteren und weniger dichten Wasserkörper darüber. Der Lobolithen-Auftrieb sollte deshalb regulierbar gewesen sein. Außerdem hätte dadurch das dichte Armgitter der stark verzweigten Krone bei Relativbewegungen dieser Wasserkörper eine Schleppnetz-Funktion ("townet filtration") gehabt.

So plausibel eine solche Erklärung zunächst erscheint, sprechen doch mindestens zwei Gründe dagegen: (**1**) Die nicht selten an Lobolithen erhaltenen Wurzelstümpfe kleiner Scyphocrinoiden (s. o.) befinden sich fast ausschließlich an der nach unten gerichteten Kalotte und dort

überwiegend im Bereich des Stielansatzes (Haude 1992: Abb. 3A, B; Taf. 1, Fig. H; Prokop & Petr 2001: fig. 1 ff.). Deren anzementierte Stielenden sind weitgehend mit dem Stielteil des Lobolithen gleichgerichtet; beim Driften an einer Sprungschicht in einiger Tiefe wäre zu erwarten, dass zumindest einige Larven auch die obere Seite besiedelt hätten. (**2**) Es ist höchst unwahrscheinlich, dass der Wurzelbereich eines Crinoiden je das erforderliche, höchst differenzierte physiologische Potential zum Ausgleich von Änderungen des Gasvolumens − etwa bei Schwankungen des hydrostatischen Drucks − erwerben konnte; denn schon eine geringe Volumen-Reduktion des Auftriebsmittels hätte Absinken zur Folge gehabt.

Es kann deshalb vorläufig nur angenommen werden, dass die Lobolithen einen irgendwie gearteten Schutz vor dem Expositionsstress ihres oberen Wandbereichs besaßen. Immerhin zeigen viele Lobolithen gerade auf den Wandplättchen des exponierten Kalottenbereichs oft eine starke Pustulierung, bei der es sich wahrscheinlich um resorbierte, aus der Oberfläche der Wandplättchen herausgetretene Spitzen ursprünglicher Cirren-Verästelungen handelt (Haude 1998: Abb. 4C); vielleicht deutet sich darin eine Struktur an, die einem wuchernden organischen Belag (Algen, Bakterien?) Halt bot, der die Belastung durch Strahlung verminderte bzw. diese absorbierte.

Einige Wandteile der marokkanischen Platten-Lobolithen zeigen deutliche Lücken in der äußeren Plattenlage der Doppelwand im Bereich der oberen Kalotte (Abb. 7d), während die Plattenlage der inneren Wand völlig dicht zu sein scheint. War die äußere Lage evtl. bereits frei von Stroma, der organischen Skelett-Substanz (also „tot"), so dass sie partiell als Schutzschild wirkte?

Das im oberen Bereich der marokkanischen Profile nachgewiesene, alternierende Auftreten von monospezifischen Scyphocrinoiden-„Kolonien" (assoziiert entweder mit Cirren- oder mit Platten-Lobolithen) zeigt, dass diese Scyphocrinoiden-Arten lange Zeit gleichzeitig, aber in der Regel in voneinander getrennten Assoziationen gelebt haben (Haude & Walliser 1998). Demnach haben dort offenbar normalerweise ruhige Strömungsregime in Form großräumiger Wirbel (Gyren; Prokop & Petr 2001) bei extrem günstigen Lebensbedingungen im Oberflächenbereich des Wassers geherrscht.

Ergebnisse

Die Scyphocrinoiden-Schichten (Grenzbereich Silur–Devon) in der Tafilalet-Region von SE-Marokko können in vier Conodonten-Zonen untergliedert werden. Danach treten die ersten Scyphocrinoiden in der tieferen *eosteinhornensis* s. l.-Zone auf, einige Meter darüber folgen weitere Formen, die in der Unteren und Oberen *detortus*-Zone der obersten Přídolí-Stufe zwei- bis dreimal alternieren; die letzten reichen bis in die *hesperius*-Zone der untersten Lochkov-Stufe.
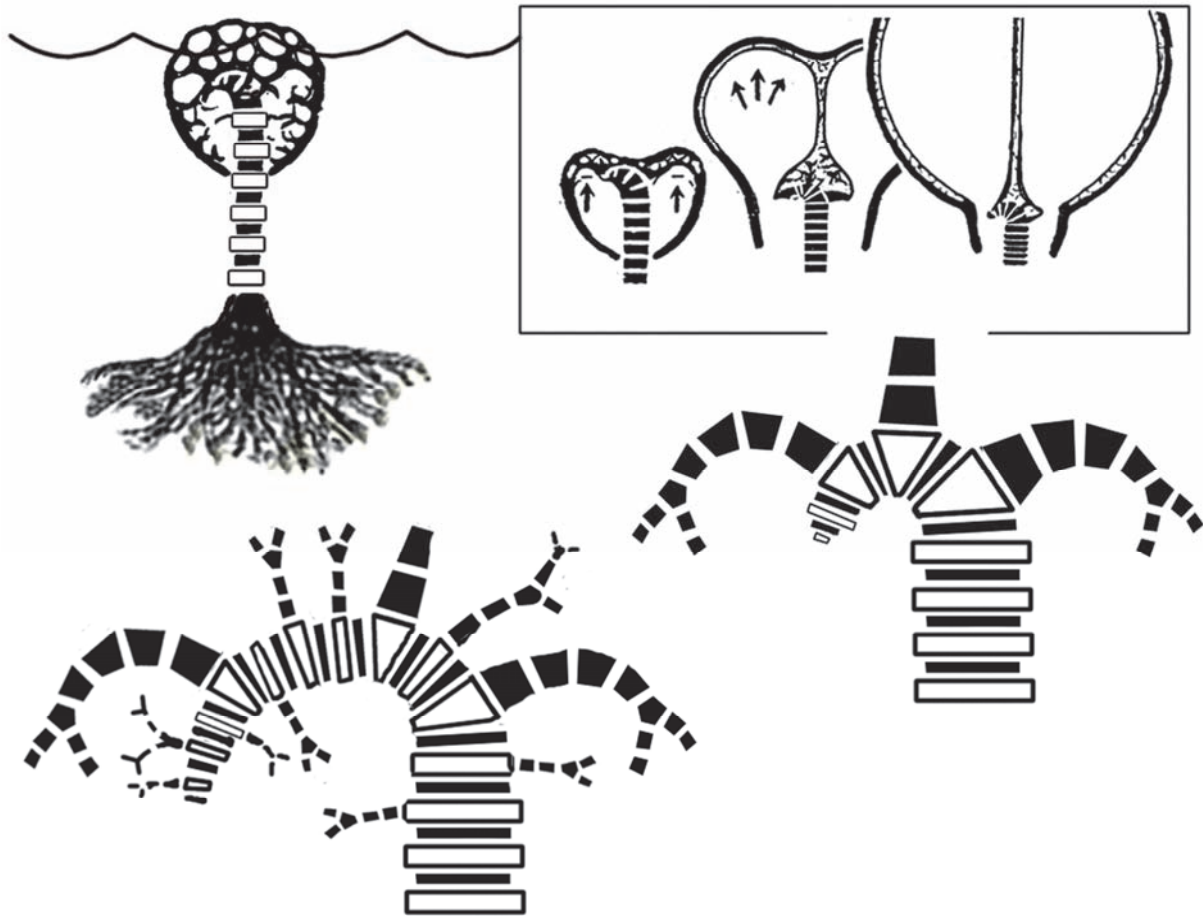
Abb. 13: Modell der direkten Lobolithen-Bildung ohne längeres Wachstum nach der Larvalphase. (**a**) Juveniler Scyphocrinoide mit Cirren-Lobolith an einem kurzen heteromorphen Stiel; (**b**) Stielansatz eines Cirren-Lobolithen mit unregelmäßig an „Nodalia" gesprossten Primär-Cirren; (**c**) Stielansatz eines Platten-Lobolithen mit regelmäßig (hier nicht dargestellt) bilateral-symmetrisch an dem jeweils übernächsten „Nodale" paarig gesprossten Primär-Cirren; (**d**) Aufblähung (hier: bei einem Platten-Lobolithen) durch Auftriebsdruck bei Kammer-interner Gas-Produktion.

Fig. 13: Model of direct lobolith development without growth of a longer post-larval stem. (**a**) juvenile scyphocrinoid with cirrus lobolith developing at a short heteromorphic stem; (**b**) distal stem with irregular growth of primary cirri of a cirrus lobolith; (**c**) distal stem with regular growth (of pairs, not shown) of primary cirri at every second "nodal"; (**d**) inflation (here: in a plate lobolith) by hydrostatic stress induced by increasing gas contents within basally open chambers.

Die lagenweise weite Verbreitung, chaotische Lagerung und dichte Packung der Scyphocrinoiden-Skelettteile über vollständig erhaltenen Kronen auf der Unterseite, die an Tonschiefer grenzt, sind wahrscheinlich die Folge von Sturmwetter-Ereignissen: Durch das Abbrechen der Lobolithen als Schwimmbojen zahlreicher, eng benachbart driftender und wahrscheinlich durch lange Algenteile zusammen gehaltener Scyphocrinoiden müssen solche „Kolonien" ihren Gesamt-Auftrieb verloren haben und abgesunken sein.

Da die einzelnen Scyphocrinoiden-Lagen meist durch einige Dezimeter bis mehrere Meter dicke Ton-/Alaunschiefer getrennt sind, kam es bei ihrem seit Jahren umgehenden Abbau in der Regel nicht zu sekundärer Vermischung der im Aushub zurück gelassenen Reste. Dadurch können taxonomisch wichtige Skelettteile ausgewertet und hinreichend sicher systematisch zugeordnet werden. So

gehören die Scyphocrinoiden-Teile einer Lage jeweils nur einer Gattung bzw. Art an. Das zeigte sich schon im Gelände an den gut unterscheidbaren Cirren- und Platten-Lobolithen und deren zerfallenen Resten, die dort nie zusammen in der gleichen Lage vorkommen. Die in den untersuchten Profilen festgestellten Assoziationen von Lobolithen-Typen mit bestimmten Kronen-Taxa bestätigen frühere Ergebnisse in überregionalen Vorkommen. Danach hatten die Gattungen *Scyphocrinites* und *Carolicrinus* einen Cirren-Lobolithen, *Marhoumacrinus* und *Camarocrinus* einen Platten-Lobolithen. Eine Familie Marhoumacrinidae Prokop & Petr, 1987, die auch mit *Carolicrinus* begründet wurde (weil diese Autoren dort einen zugehörigen Platten-Lobolithen vermuteten), ist deshalb irreführend (s. Diskussion in Haude 1999).

Wegen der oft nur fragmentarischen Erhaltung der aufgesammelten Kronen und auch der z. T. beträchtlichen

morphologischen Variabilität im Kelchbau, die sowohl in einzelnen Kelchen, als auch in großen Kolonien, etwa der Göttinger Scyphocrinoiden-Platte zu beobachten ist, erweist sich die genauere Bestimmung der Scyphocrinoiden z. T. als problematisch. So sind die Strukturen im höheren Kelchbereich bei Resten von *Carolicrinus* und *Marhoumacrinus*, sowie bei *Scyphocrinites* und *Camarocrinus* z. T. recht ähnlich. Sie lassen sich aber – bei Ausschluss biostratinomischer Vermischung verschiedener Formen – anhand der Assoziation mit jeweils typischen Lobolithen- und Stielteilen mit hinreichender Sicherheit taxonomisch differenzieren.

Die günstigen Lebensverhältnisse im Plankton-reichen Oberflächenwasser ermöglichten auch eine hohe Reproduktionsrate. Die oft zahlreich an gut erhaltenen Lobolithen anzementierten Haftwurzeln von Jungtieren scheinen anzuzeigen, dass die Scyphocrinoiden erst nach einer längeren gestielten Juvenil-Phase einen eigenen Lobolithen entwickelten. Gegen dieses Modell spricht aber, dass die Stiele von Jungtieren mit bereits ausgebildetem Lobolith bzw. Primär-Cirren deutlich dünner sind als der Stielrest vieler Haftwurzeln. Außerdem sind die Stiele aller an einem Lobolithen haftenden Wurzeln juveniler Individuen isomorph, während die Stielreste freier juveniler Individuen heteromorph sind. Deshalb ist eine direkte Entwicklung wahrscheinlicher, bei der der Lobolith bereits sehr früh mit der Anlage von Primär-Cirren an Nodal-Gliedern beginnt.

Danksagung

Literaturverzeichnis

Alleman, V. (1958): Contribution à la connaissance morphologique et paléobiologique du genre *Scyphocrinites* Zenker, 1833 (Crinoidea Camerata). *Mémoire de Licence, Institut de Paléontologie Animale, Année académique 1957-1958, Université de Liège*: vi + 44 pp.

Baumiller, T. K. (2002): Multi-snail infestation of Devonian crinoids and the nature of platyceratid-crinoid interactions. *Acta Palaeontologica Polonica* **47** (1): 133-139.

Beyer, A. K. (1952): Zur Stratigraphie des oberen Gotlandiums in Mitteleuropa. *Wissenschaftliche Zeitschrift der Universität Greifswald (Mathematisch-naturwissenschaftliche Reihe)* **[1951/1952]** (1): 1-33.

Chen Zhong-tai & Yao Ji-hui (1990): First discovery of *Scyphocrinites* in China. *Acta Palaeontographica Sinica* **29**: 228-236.

Chlupáč, I. & Vacek, F. (2003): Thirty years of the first international stratotype: The Silurian-Devonian boundary at Klonk and its present status. *Episodes* **26** (1): 10-15.

Corradini, C. & Corriga, M. G. (2012): A Přídolí–Lochkovian conodont zonation in Sardinia and the Carnic Alps: implications for a global zonation scheme. *Bulletin of Geosciences* **87** (4): 635-650.

Corradini, C.; Corriga, M. G. & Männik, P. (2013): Revised conodont stratigraphy of the Silurian of Cellon, Carnic Alps. In: Lindskog, A. & Mehlqvist, K. (eds.): *Proceedings of the 3rd IGCP 591 Annual Meeting, Lund, Sweden, 9-19 June 2013*: 69-70.

Corriga, M. G.; Corradini, C.; Haude, R. & Walliser, O. H. (2013): Conodont and crinoid stratigraphy of the upper Silurian and Lower Devonian scyphocrinoid beds of Tafilalt, southeastern Morocco. *GFF* **136** (1): 65-69. http://dx.doi.org/10.1080/11035897.2013.862849

Hall, J. (1879): Notice of some remarkable crinoidal forms from the Lower Helderberg group. *New York State Museum, Annual Report* **28**: 205-210.

Haude, R. (1972): Bau und Funktion der *Scyphocrinites*-Lobolithen. *Lethaia* **5** (1): 95-125. http://dx.doi.org/10.1111/j.1502-3931.1972.tb00844.x

Haude, R. (1981): Mechanik, Morphogenese und paläokologische Bedeutung der "Pelmatozoen"-Stiele. In: Reif, W. (Hrsg.): Funktionsmorphologie. *Paläontologische Kursbücher* **1**: 187-203.

Haude, R. (1989): The scyphocrinoids *Carolicrinus* and *Camarocrinus*. In: Jahnke, H. & Shi, Y.: The Silurian–Devonian boundary strata and the Early Devonian of the Shidian-Baoshan area (W. Yunnan, China). *Courier Forschungsinstitut Senckenberg* **110**: 170-178.

Haude, R. (1992): Scyphocrinoiden, die Bojen-Seelilien im hohen Silur–tiefen Devon. *Palaeontographica (A: Paläozoologie, Stratigraphie)* **222**: 141-187.

Haude, R. (1998): Seelilien mit Schwimmboje: Die Scyphocrinoiden. *Fossilien* **15** (4): 217-225.

Haude, R. (1999): Phylogeny of scyphocrinoids (U. Silurian - L. Devonian) with respect to their extraordinary root construction. In: Candia Carnevali, M. D. & Bonasoro, F. (eds.): *Echinoderm Research 1998. Proceedings of the 5th European Conference on Echinoderms, Milan 7-12 September 1998*. Rotterdam (A. A. Balkema): 279-284.

Haude, R.; Jahnke, H. & Walliser, O. H. (1994): Scyphocrinoiden an der Wende Silur/Devon. *Aufschluß* **45** (2): 49-55.

Haude, R. & Walliser, O. H. (1998): Conodont-based Upper Silurian - Lower Devonian range of scyphocrinoids in SE-Morocco. In: Gutiérrez-Marco, J. C. & Rábano, I. (eds.): *Proceedings of the 6th International Graptolite Conference & 1998 Field Meeting IUGS Subcommission on Silurian Stratigraphy*. ITGE Temas Geológico-Mineros **23**: 94-96.

Hess, H. (1999): Scyphocrinitids from the Silurian-Devonian boundary of Morocco. In: Hess, H.; Ausich, W. I.; Brett, C. E. & Simms, M. J. (eds.): *Fossil crinoids*. Cambridge (University Press): 93-102.

Hess, H. (2010): Paleoecology of pelagic crinoids. In: Selden, P. (ed.) & Ausich, W. (coord. author): *Treatise-online, **T** (revised), **1** (16)*: 1-33.

Hollard, H. (1962): État des recherches sur la limite Siluro-Dévoniennne dans le sud du Maroc. In: Erben, H. K. (ed.): *2. Internationale Arbeitstagung über die Silur/Devon-Grenze und die Stratigraphie von Silur und Devon, Bonn – Bruxelles 1960. Symposiums-Band*. Stuttgart (E. Schweizerbart): 95-97.

Hollard, H. (1977): Le domaine de l'Anti-Atlas au Maroc. In: Martinsson, A. (ed.): The Silurian-Devonian boundary. *Final report of the Committee on the Silurian-Devonian Boundary within IUGS Commission on Stratigraphy and a state of the art report for Project Ecostratigraphy. IUGS Series* **A 5**. Stuttgart (E. Schweizerbart): 168-194.

Horný, R.J. (2000): Mode of life of some Silurian and Devonian platyceratids. *Bulletin of Geosciences* **75** (2): 135-143.

Jaeger, H. (1962): Das Silur (Gotlandium) in Thüringen un dam Ostrand des Rheinischen Schiefergebirges (Kellerwald, Marburg, Giessen). In : Erben, H. K. (ed.): *2. Internationale Arbeitstagung über die Silur/Devon-Grenze und die Stratigraphie von Silur und Devon, Bonn – Bruxelles 1960. Symposiums-Band.* Stuttgart (E. Schweizerbart): 108-135.

Jahnke, H. & Shi, Y. (1989): The Silurian-Devonian boundary strata and the Early Devonian of the Shidian-Baoshan area (W. Yunnan, China). *Courier Forschungsinstitut Senckenberg* **110**: 137-193.

Legrand, P. (1962): Connaissances aquises sur la limite des systèmes Siluriens et Dévoniens au Sahara septentrional. In: Erben, H. K. (ed.): *2. Internationale Arbeitstagung über die Silur/Devon-Grenze und die Stratigraphie von Silur und Devon, Bonn – Bruxelles 1960. Symposiums-Band.* Stuttgart (E. Schweizerbart): 151-159.

Massa, D.; Combaz, A. & Manderscheid, G. (1965): Observations sur les séries siluro-dévoniennes des confins algéro-marocains du Sud. *Notes et Mémoires de la Compagnie Française des Pétroles* **8**: 188 pp.

Plodowski, G. (1996): Das Exponat des Monats: Eine Platte mit 44 Kronen freischwimmender Seelilien aus Marokko. *Natur und Museum* **126** (5): 165-167.

Poueyto, A. (1952): Terrains Gothlandiens. In: Alimen, A.; Le Maitre, D.; Menchikoff, N.; Petter, G. & Poueyto, A.: Les chaines d´Ougarta et la Saoura. *19. Congres Géologique International, Monographies Regionales 1, Algérie* **15**: 37-47.

Prokop, R. J. & Petr, V. (1986): Revision of Superfamily Melocrinitacea d'Orbigny, 1852 (Crinoidea, Camerata) in Silurian and Devonian of Bohemia. *Sborník Národního Muzea v Praze (B)* **42** (3/4): 197-219.

Prokop, R. J. & Petr, V. (1987): *Marhoumacrinus legrandi*, gen. et sp. n., (Crinoidea, Camerata) from Upper Silurian - Lowermost Devonian of Algeria. *Sborník Národního Muzea v Praze (B)* **43**: 1-14.

Prokop, R. J. & Petr, V. (1994): A note on the phylogeny of scyphocrinitid crinoids. *Acta Universitatis Carolinae, Geologica* **[1992]** (1/2): 31-36.

Prokop, R. J. & Petr, V. (2001): Remarks on palaeobiology of juvenile scyphocrinitids and marhoumacrinids (Crinoidea, Camerata) in the Bohemian uppermost Silurian and lowermost Devonian. *Journal of the Czech Geological Society* **46** (3-4): 259–268.

Ray, B.S. (1980): A study of the crinoid genus *Camarocrinus* in the Hunton group of Pontotoc County, Oklahoma. *Baylor Geological Studies, Bulletin* **39**: 6-16.

Reed, F. R. C. (1906): The Lower Palaeozoic fossils of the northern Shan states, Burma. *Palaeontologia Indica (N. S.)* **2** (3): 1-154.

Reed, F. R. C. (1917): Ordovician and Silurian fossils from Yunnan. *Palaeontologia Indica (N. S.)* **6** (3): 1-84.

Schuchert, C. (1904): On Siluric and Devonic Cystidea and *Camarocrinus. Smithsonian Miscellaneous Collections* **47**: 201-272.

Seilacher, A. & Hauff, R. (2004): Constructional morphology of pelagic crinoids. *Palaios* **19** (1): 3-16.
http://dx.doi.org/10.1669/0883-1351(2004)019<0003:CMOPC>2.0.CO;2

Springer, F. (1917): On the crinoid genus *Scyphocrinus* and its bulbous root, *Camarocrinus. Smithsonian Institution, Publication* **2440**: 74 pp.

Strimple, H. L. (1963): Crinoids of the Hunton Group (Devonian-Silurian) of Oklahoma. *Oklahoma Geological Survey, Bulletin* **100**: 169 pp.

Waagen, W. & Jahn, J. (1899): Classe des echinodermes, famille des crinoides. In: Barrande, J. (ed.): *Système Silurien du Centre de la Bohème. I: Recherches Paléontologiques, 7, Classe des Echinodermes* **2**: 215 pp.

Yakovlev, N. N. (1953): O nakhodke lobolitov v SSSR i o biologicheskom znachnii ikh. [Über die Entdeckung von Lobolithen in der UdSSR und deren biologische Bedeutung]. *Vsesoyuznyi Paleontologicheskii Obshch Ezhegodnik* **14**: 18-37.

Zenker, J. C. (1833): Organische Reste (Petrefacten) aus der Altenburger Braunkohlen-Formation, dem Blankenburger Quadersandtein, jenaischen bunten Sandstein und böhmischen Übergangsgebirge. *Beiträge zur Naturgeschichte der Urwelt.* Jena (F. Mauke): 1-67.

Santonian sea cucumbers (Echinodermata: Holothuroidea) from Sierra del Montsec, Spain

Mike Reich[1,2] * & Jörg Ansorge[3]

[1]Geoscience Museum, Georg-August University Göttingen, Goldschmidtstr. 1-5, 37077 Göttingen, Germany; Email: mreich@gwdg.de

[2]Department of Geobiology, Geoscience Centre, Georg-August University Göttingen, Goldschmidtstr. 3, 37077 Göttingen, Germany

[3]Institute for Geography and Geology, Ernst-Moritz-Arndt University Greifswald, F.-L.-Jahn-Str. 17a, 17489 Greifswald, Germany; Email: ansorge@uni-greifswald.de

* corresponding author

Recent discovery of disarticulated sea cucumber material from Font de la Plata (Sierra del Montsec, Lleida, Catalonia, Spain) resulted in the identification of at least six holothurian taxa, belonging to the Apodida (Synaptidae, Chiridotidae), Molpadiida (?stem group Molpadiidae), and Aspidochirotida (Holothuriidae). Three new genera (*Cruxopadia*, *Eoleptosynapta*, *Eorynkatorpa*) and four new species (*Cruxopadia mesozoica*, *C. reitneri*, *Eoleptosynapta jaumei*, *Eorynkatorpa catalonica*) are described from Late Cretaceous sediments of Spain, and in part from the Late Jurassic of France. The new fauna increases our knowledge of holothuroid echinoderms from Santonian strata worldwide.

Introduction

The Sierra del Montsec, situated in the southern marginal zone of Pyrenees, presents classical outcrops and excellent preserved fossils of early and late Cretaceous age. Among them are also members of eleutherozoan echinoderms, such as echinoids, asteroids, and ophiuroids; only holothurians were missing up to now.

Holothuroid echinoderms are not common as fossils in general (e.g., Frizzell & Exline 1956, 1966; Gilliland 1993), the skeleton is rarely robust and consists of microscopic ossicles embedded in the body wall as well as of larger calcareous ring elements, encircling the pharynx at the inner side of the mouth. Consequently they disarticulate rapidly after death and have left a rather poor fossil record (e.g., Reich 2013a).

Santonian holothurians have so far been recorded only from Germany and the U.K. Lommerzheim (1976, 1991) reported their occurrence from Westphalia (Germany), but, unfortunately, without any descriptions. Upton (1917) mentioned a chiridotid wheel (Apodida) from the "Upper Chalk" of Purley (Surrey, England). Recently, a nearly articulated find from the "Upper Chalk" of England, belonging to the Holothuriidae (Aspidochirotida), was presented by Reich (2008, 2013b) and is currently under description by Reich & Gale.
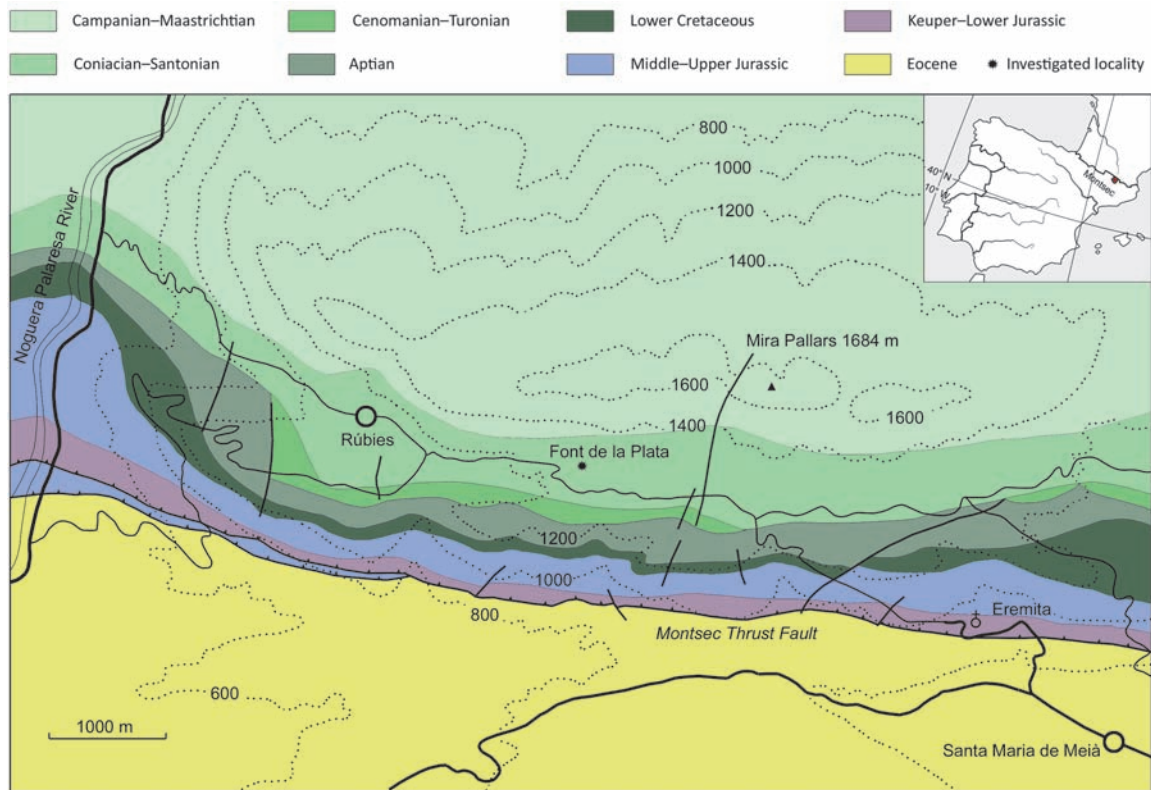
Fig. 1: Location of the sampled outcrop at Font de la Plata, east of Rúbies, Sierra del Montsec, Catalonia, Spain. Geological map from Ansorge (1991, modified).

Geological setting and material

The studied microfossil material from the late Santonian ("Santon E" of Krusat 1966) of the Font de la Plata (Montsec de Rúbies; Figs. 1–2) was sampled by JA in September 1996 and includes around 50 isolated holothurian ossicles. This formation (> 100 m) contains grey and/or yellowish calcareous marls and marly limestones interbedded by limestones and sandstones (Krusat 1966: 60f.). It can be correlated with the "Unit 5" of Caus & Cornella (1983) or with the "Montsec marls" of Caus & Gómez-Garrido (1989).

The rich associated fauna (e.g., Krusat 1966) comprises abundant scleractinian corals and rudist bivalves, calcareous algae, chaetetid sponges, decapod crustaceans, bivalves, gastropods, cephalopods, articulate brachiopods, larger foraminifera and teleost fishes (e.g., Bataller 1937a, 1953; Hottinger 1966; Cornella 1977; Caus et al. 1978; Hottinger et al. 1989; Nolf 2003; Garassino et al. 2009; Hottinger & Caus 2009). Echinoderms are also reported with representatives of the Echinoidea and Asteroidea (e.g., Bataller 1937b: 590, 1953: 57ff.; Krusat 1966: 58; Neumann & Hess 2001: 7ff.).

The pachydont bivalves *Hippuritella maestrei* (Vidal), *Hippuritella sulcatissima* (Douvillé), and *Vaccinites galloprovincialis* (Matheron) (systematics updated after Vicens 1992, Vicens et al. 1998 and Steuber 2002) reported by Krusat

(1966: 84) are biostratigraphically useful and are considered to be late Santonian in age, which is in agreement with other fossils (see Llompart 1979; Caus et al. 1999). This Santonian environment corresponds to an open shallow-water platform (e.g., Llompart 1979).

The studied samples include besides the isolated holothurian ossicles also typical other calcareous microfossils, such as foraminifera and ostracods, as well as microscopic remains of macrofossils, like octocoral scleres (Alcyonacea), echinoid spines, and ophiuroid ossicles (lateral side shields, vertebrae etc.).

In the systematic description we also introduce a new molpadiid genus (*Cruxopadia* Reich gen. nov.) with its genotype *C. mesozoica* Reich sp. nov. from the early Oxfordian of Villers-sur-Mer (Calvados, France). Early Oxfordian mudstones of the *Quenstedtoceras mariae* Zone are exposed at longer cliff sections of the English Channel coast between Houlgate and Villers-sur-Mer, Normandy (e.g., Dugué et al. 1998; Merle 2011). Holothurians from the Oxfordian marls of Villers-sur-Mer are known for a long time (e.g., Deflandre-Rigaud 1946, 1962). Samples were taken by MR in 1999 and 2012.

Methods

The microscopic fossils from clayey and calcareous marls were isolated using hot water and/or hydrogen peroxide (10 %). After washing (sieve sizes: >0.063 mm, 0.1 mm and 1 mm), the residues were dehydrated at a temperature of ~70°C (cf. Wissing & Herrig 1999). All specimens were studied under a binocular microscope first and later mounted on stubs and coated with Au/Pd or Au for investigation and documentation using scanning electron microscopy (SEM).

All figured specimens are deposited at the Geoscience Centre of the Georg-August University Göttingen, Germany (GZG).

Systematic palaeontology

Phylum **Echinodermata** Bruguière, 1791 [ex Klein, 1734]
Subphylum **Eleutherozoa** Bell, 1891
Class **Holothuroidea** de Blainville, 1834
Subclass **Holothuriacea** Smirnov, 2012
Order **Molpadiida** Haeckel, 1896

Family (?stem group) **Molpadiidae** J. Müller, 1850

Genus *Cruxopadia* Reich gen. nov.

Type species. – *Cruxopadia mesozoica* Reich sp. nov. from the early Oxfordian of Normandy, France.

Etymology. – Named after Latin *crux, crŭcis* = cross, and in remembrance of the modern holothurian genus *Molpadia*. The generic name is of feminine gender.

Diagnosis. – Solid cross-shaped plates with four central perforations.

Comparison. – The new genus differs from the related *Priscolongatus* Górka & Luszczewska, 1969 (syn. *Fletcherina* Soodan, 1975; *Brianella* Huddleston, 1982; *Hannaina* Soodan, 1975; *Koteshwaria* Tandon & Saxena, 1983) in being not table-like and therefore in having no spire or stirrup. The synonymy of genera/paragenera within this 'Priscolongatus group' was briefly discussed by Gilliland (1993: 81–82).

Occurrence. – Hitherto known only from the late Jurassic (Oxfordian) to the late Cretaceous (Santonian) of Europe (France, Spain).

Cruxopadia mesozoica Reich sp. nov.
Figs. 3A–B

Material. – One cross-shaped ossicle (GZG.INV.91405; holotype; Fig. 3A); two further (broken) ossicles (GZG.INV.91406–91407; paratypes).

Fig. 2: Outcrop at Font de la Plata, east of Rúbies, showing the interbedded strata of calcareous marls and limestones (September 1996).

Type locality. – Villers-sur-Mer, Normandy, France.

Type horizon. – "Marnes de Villers", *Quenstedtoceras mariae* Zone (late Jurassic: early Oxfordian).

Etymology. – Species name refers to the "Mesozoic" era.

Diagnosis. – A species of *Cruxopadia* with the following characteristics: ossicle in one plane, four solid radiating arms at (nearly) right angles, medium-sized in length and tapering distally. All arms are more or less of equal length. Four central perforations are cross-shaped arranged, and medium-sized in diameter.

Description. – The ossicles of *C. mesozoica* are cross-shaped (Fig. 3A; diameter ~250–260 μm) and in one plane with four solid radiating arms at nearly right angles (±90°) or so with respect to each other. These arms are medium-sized (~100–110 μm) and more or less of equal length and tapering distally. Four central perforations with a medium-sized diameter (~16–17 μm) are cross-shaped arranged and circular to suboval in outline. The square of these perforations is covering approx. 20 % of the whole central portion of the ossicle. The central portion takes approx. 60 % of the total ossicle area (diameter). No spire or stirrup is present. The surface is fine-grained (Fig. 3A).

Comparison. – *C. mesozoica* differs from *C. reitneri* Reich sp. nov. in having shorter and more robust arms as well as in having much larger central perforations. Also the central portion is much larger, by covering more than 60 % of the total ossicle area (diameter).

Remarks. – The new material extends the fossil record of the 'fusiform rod' molpadiid morphotype back to the Mesozoic, and furthermore shows that Cenozoic and modern 'fusiform rods' probably evolved from primarily cross-shaped ossicles with an evolutionary trend to decrease the number of central perforations (4 to 3) and the formation

Fig. 3:   Representative ossicles of molpadiid sea cucumbers. **(A–B)** *Cruxopadia mesozoica* gen. et sp. nov.; **(A)** GZG.INV.91405, holotype, upper side; **(B)** Schematic drawing, upper side. **(C–D)** *Cruxopadia reitneri* gen. et sp. nov.; **(C)** GZG.INV.91408, holotype, upper side; **(D)** Schematic drawing, upper side. Early Oxfordian; Villers-sur-Mer, Normandy, France (A–B). Late Santonian; Font de la Plata, east of Rúbies, Catalonia, Spain (C–D). Scale bar = 0.1 mm.

of arms (4 to 2). Modern molpadiid members with 'fusiform rods' have 2–3(4) arms and (2)3–4 prominent central perforations (e.g., Pawson 1977; Pawson et al. 2001).

The new species bearing this type of ossicles lived probably, as all other members of the Molpadiida, infaunal as an active burrower and deposit feeder.

Occurrence. – The new species occurs in the "Marnes de Villers" of Calvados (Normandy), early Oxfordian of France.

Cruxopadia reitneri Reich sp. nov.

Figs. 3C–D

Material. – One cross-shaped ossicle (GZG.INV.91408; holotype; Fig. 3C); one further (broken) ossicle (GZG.INV.91409; paratype).

Type locality. – Font de la Plata, Sierra del Montsec, Catalonia, Spain.

Type horizon. – Marly limestones of the "Santon E", (Cretaceous: late Santonian).

Etymology. – Named after Joachim Reitner (*1952), Göttingen, in recognition of his contributions to the study of Spanish Mesozoic strata and in celebration of his 60th birthday.

Diagnosis. – A species of *Cruxopadia* with the following characteristics: ossicle in one plane, four delicate and solid radiating arms at (nearly) right angles; arms long and tapering distally. Four central perforations are cross-shaped arranged, and small in diameter.

Description. – The ossicles of *C. reitneri* are cross-shaped (Fig. 3C) and in one plane with four solid radiating arms at nearly right angles ($\pm 90°$) or so with respect to each other. These arms are long and delicate, 110–120 μm in length and tapering distally. Four central perforations with a small diameter (~9–11 μm) are cross-shaped arranged and circular to suboval in outline. The square of these perforations are covering approx. 20 % of the whole central portion of the ossicle. The central portion takes approx. 30 % of the total ossicle area (diameter). No spire or stirrup is present. The surface is coarse-grained (Fig. 3C).

Comparison. – *C. reitneri* differs from *C. mesozoica* in having longer and more delicate arms as well as in having much smaller central perforations. Also the central portion is much smaller, in covering only 30 % of the total ossicle area (diameter). No spire or stirrup is present.

Remarks. – See under *C. mesozoica.*

Occurrence. – The new species occurs in the late Santonian of Spain.

Order **Aspidochirotida** Grube, 1840
Family **Holothuriidae** Burmeister, 1837

[p. p.] Paragenus *Priscopedatus* Schlumberger, 1890

Type species. – *Priscopedatus pyramidalis* Schlumberger, 1890 from the Middle Eocene (Lutetian) of Chaussy, Paris Basin, France.

Remarks. – The paragenus *Priscopedatus* (cf. Soodan 1975) needs a comprehensive revision, since table-like ossicles are present in species of all orders of the Holothuriacea (Aspidochirotida, Molpadiida, Dendrochirotida). A modern comprehensive overview of these table-like ossicles (including SEM pictures) is, however, missing so far. We therefore use the paragenus name in quotation marks.

'Priscopedatus' sp.

Fig. 4A

Material. – One incomplete table ossicle (GZG.INV.91449).

Description. – Incomplete table-like ossicle (diameter ~165 µm), nearly suboval in outline with a short stirrup over a suboval central hole with around 8–10 peripheral perforations.

Remarks. – The described ossicle taxon belongs to the *Priscopedatus/Feddenella* group of Gilliland (1993: 66ff.), and can clearly be assigned to the Holothuriidae (Aspidochirotida) due to the typical "holothuriid cross".

Occurrence. – This taxon occurs in the late Santonian of Spain.

[p. p.] Paragenus *Parvispina* Kornicker & Imbrie, 1958

Type species. – *Stichopites spinosus* Frizzell & Exline, 1956 from the Mississippian of Illinois, U.S.A.

Remarks. – The paragenus *Parvispina* also needs to be revised in comparison to other members (e.g., *Rhabdotites*, *Stichopites*) of the paraphyletic parafamily Stichopitidae (e.g., Gilliland 1993: 65-66). We therefore use the paragenus name in quotation marks.

'Parvispina' sp.

Fig. 4B

Material. – One holothuriid rod (GZG.INV.91447).
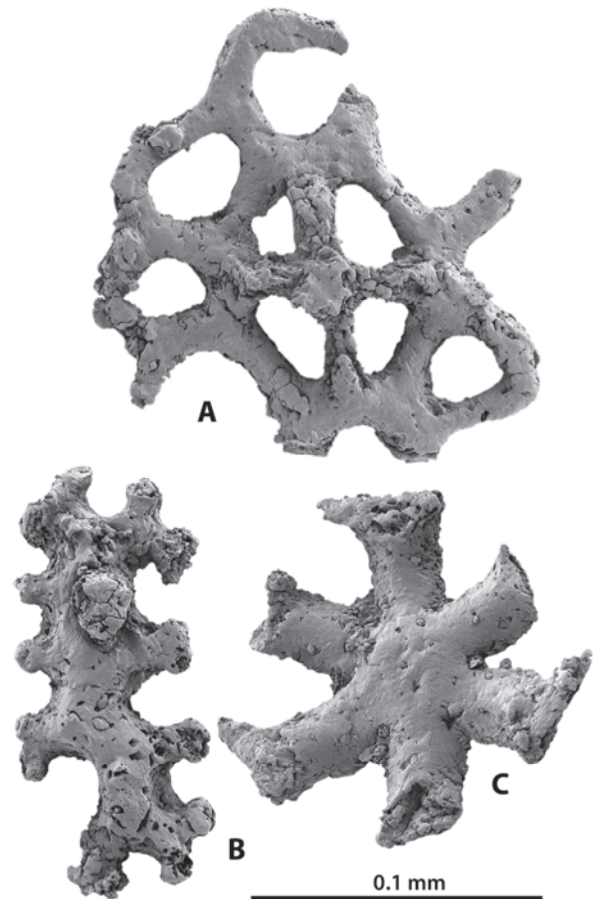
Fig. 4:   Representative ossicles of holothuriid **(A–B)** and chiridotid **(C)** sea cucumbers. **(A)** incomplete table ossicle *'Priscopedatus'* sp. (Holothuriidae), GZG.INV.91449, upper side; **(B)** rod-like ossicle *'Parvispina'* sp. (Holothuriidae), GZG.INV.91447. **(C)** not fully developed wheel, gen. et sp. indet. (Chiridotinae), GZG.INV.91448, upper side.
All from the late Santonian; Font de la Plata, east of Rúbies, Catalonia, Spain. Scale bar = 0.1 mm.

Description. – Straight and slightly arched rod, around 150 µm in length, and short dichotomously branched, not spinose.

Remarks. – This ossicle taxon can be clearly assigned to the Holothuriidae, where most ancient members, like *Actinopyga*, *Bohadschia* and *Holothuria (Halodeima)* (Samyn et al. 2005) bear this type of rod in the body-wall and (partly) tube-feet (e.g., Rowe 1969; Massin 1996, 1999; Samyn 2003).

Occurrence. – This taxon occurs in the late Santonian of Spain.

Both holothuriid taxa lived probably, as (nearly) all other members of the Holothuriidae, as epibenthic deposit feeders.

Subclass **Synaptacea** Cuénot, 1891
Order **Apodida** Brandt, 1835 [= Synaptida Cuénot, 1891 *sensu* Smirnov, 2012]
Suborder **Synaptina** Smirnov, 1989

Family **Chiridotidae** Östergren, 1898
Subfamily **Chiridotinae** Östergren *sensu* Smirnov, 1998

gen. et sp. indet.

Fig. 4C

Material. – One (not fully developed) wheel (GZG.INV.91448).

Description. – The single specimen is a typical, not fully developed, (6-spoked) chiridotid wheel. The diameter is ~123 μm.

Remarks. – Further statements are not possible due to the missing rim (dentation etc.). This small wheel-ossicle represents the first record of a member of the Chiridotidae (Chiridotinae) from Santonian strata worldwide (cf. Fig. 8).

Occurrence. – This taxon occurs in the late Santonian of Spain.

Family Synaptidae Burmeister, 1837 *sensu* Östergren, 1898

Paragenus *Calcancora* Frizzell & Exline, 1956

Type species. – *Calcancora mississippiensis* Frizzell & Exline, 1956 from the Paleogene (Oligocene) of Mississippi, U.S.A.

Calcancora sp. 1

Fig. 6A

Material. – One incomplete anchor (GZG.INV.91410).

Description. – Incomplete anchor ossicle, with preserved flukes only, which are long (~115 μm) and serrated with 8–10 teeth on each fluke.

Remarks. – The described anchor ossicle probably belongs to *Eorynkatorpa catalonica* gen. et sp. nov. (Rynkatorpinae), where such serrated anchors (with >5 teeth on each fluke) are common.

Occurrence. – This taxon occurs in the late Santonian of Spain.

Calcancora sp. 2

Fig. 6B

Material. – One incomplete anchor (GZG.INV.91411).

Description. – Incomplete anchor ossicle of medium length (~250 μm) with two moderately long (~95 μm) flukes, and 4–5 small teeth on lower side of each fluke. Knob not branched and with no visible denticulation.

Remarks. – The described anchor ossicle probably belongs to *Eoleptosynapta jaumei* gen. et sp. nov. (?stem Leptosynaptinae), where such sparsely serrated anchors combined with this type of (unbranched) knob are known.

Occurrence. – This taxon occurs in the late Santonian of Spain.

Family **Synaptidae** Burmeister, 1837 *sensu* Östergren, 1898
Subfamily **Rynkatorpinae** Smirnov, 1989

Genus *Eorynkatorpa* Reich gen. nov.

Type species. – *Eorynkatorpa catalonica* Reich sp. nov. from the late Santonian of Catalonia, Spain.

Etymology. – Named after Greek ἕως = dawn, and in remembrance of the modern holothurian genus *Rynkatorpa*. The generic name is of feminine gender.

Diagnosis. – Synaptid sea cucumbers with distinct anchor plates, which are more or less elongate and slightly irregular in outline; with less than 15 perforations, of which the two in the center of the plate are prominent, much larger and elongated. All perforations have smooth margins.

Comparison. – The new genus differs from the related modern *Rynkatorpa* Rowe & Pawson, 1967 in having less than 25 perforations and even a different articulation area (cf. also Clark 1908; Rowe & Pawson 1967; Smirnov 1997; Pawson & Vance 2005). No fossil representatives or relatives of *Rynkatorpa* are known up to now.

Occurrence. – Hitherto known only from the late Cretaceous (Santonian) of Spain.

Eorynkatorpa catalonica Reich sp. nov.

Figs. 5A–D

Material. – One cluster of two anchor plate ossicles (GZG.INV.91450; holotype); one further anchor plate (GZG.INV.91451; paratype).
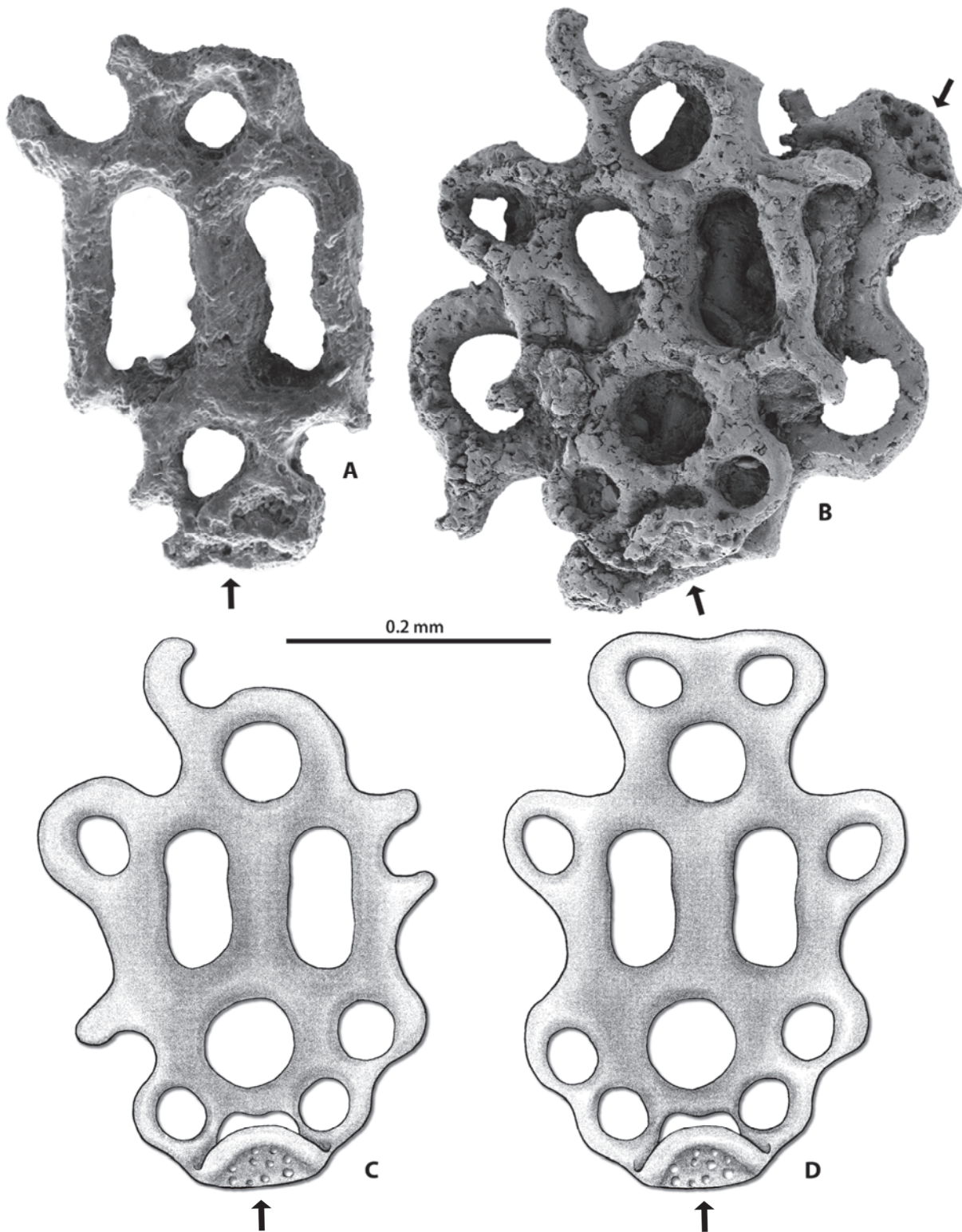
Fig. 5: Representative ossicles of a new synaptid sea cucumber **(A–D)**, *Eorynkatorpa catalonica* gen. et sp. nov. **(A)** incomplete anchor plate GZG.INV.91451, paratype, upper side; **(B)** cluster of two anchor plates GZG.INV.91450, holotype, upper side; **(C–D)** schematic (interpretative) drawing of the upper side, showing a more irregular **(C)** or a regular **(D)** outline of the anchor ossicle.
The arrows mark the articulation areas for the anchor ossicles. All from the late Santonian; Font de la Plata, east of Rúbies, Catalonia, Spain. Scale bar 0.2 mm.

Type locality. – Font de la Plata, Sierra del Montsec, Catalonia, Spain.

Type horizon. – Marly limestones of the "Santon E", (Cretaceous: late Santonian).

Etymology. – Named after the region ("Catalonia") where the new species, described in this paper, was found.

Diagnosis. – As for the genus.

Description. – The new anchor plates are more or less elongate and slightly irregular in outline, 420–450 μm long and 280–300 μm wide. All ossicles with 8–13 perforations, of which the two central perforations are very prominent, angular in outline and three times larger than any other present perforation. The articular end is simple, forming a turned over edge, slightly curved and finely perforated. All perforations have smooth margins.

Comparison. – See under *Eorynkatorpa*.

Remarks. – The two large prominent perforations in the centre are typical for representatives of the extant genus *Rynkatorpa* Rowe & Pawson, 1967. Members of this genus are currently known with around a dozen species from bathyal [*R. albatrossi* (Fisher); *R. bicornis* (Sluiter); *R. challengeri* (Théel); *R. coriolisi* Smirnov; *R. duodactyla* (Clark); *R. felderi* Pawson & Vance; *R. pawsoni* Martin; *R. sluiteri* (Fisher); *R. timida* (Koehler & Vaney)] and shallow-water [*R. bisperforata* (Clark); *R. gibbsi* Rowe; *R. hickmani* Rowe & Pawson; *R. uncinata* (Hutton)] depths, mostly from the Pacific Ocean (e.g., Clark 1908; Rowe & Pawson 1967; Smirnov 1983a, 1983b; Pawson & Vance 2005). Only one representative was reported from the Atlantic Ocean (*R. felderi* Pawson & Vance, 2005).

All species of *Rynkatorpa* are detritus/deposit feeders with specimen lengths between 0.5 and 13 cm, living as burrowers in soft substrates.

The present new species represents the oldest unequivocal record related to this group (cf. also Fig. 8). Smirnov (2012: 811) also assigned the sclerite association of *Rigaudites punctatus* Mutterlose, 1982 and *Calcancora michaeli* Mutterlose, 1982 (both from the Albian of northern Germany) to the extant genus *Rynkatorpa*, which is, in opinion of the first author, not clearly supportable. The anchor plate *R. punctatus* with its four medium-sized central perforations surrounded by numerous smaller perforations does not match the definition of the subfamily Rynkatorpinae (Smirnov 1998: 520, 2012: 811) or the genus *Rynkatorpa* (Rowe & Pawson 1967: 31; Pawson & Vance 2005: 16). Our new species *Eorynkatorpa catalonica* is rather a *Rynkatorpa*-stem group representative, in which the two typical central large (angular) perforations were formed by fusion of four central medium-sized perforations (e.g., *Rigaudites punctatus*, cf. Mutterlose 1982: pl. 8.6-2, fig. 23).

Occurrence. – The new species occurs in the late Santonian of Spain.

Subfamily (?stem group) **Leptosynaptinae** Burmeister, 1837 *sensu* Östergren, 1898

Genus *Eoleptosynapta* Reich gen. nov.

Type species. – *Eoleptosynapta jaumei* Reich sp. nov. from the late Santonian of Catalonia, Spain.

Etymology. – Named after Greek ἕως = dawn, and in remembrance of the modern holothurian genus *Leptosynapta*. The generic name is of feminine gender.

Diagnosis. – Synaptid sea cucumbers with distinct anchor plates, which are more or less reverse pear-shaped in outline; with 3(–4) horizontal rows of prominent medium-sized perforations (8–15), and an inconspicuous ledge for the articulation of the anchor. All perforations have smooth margins.

Comparison. – The new genus differs from related modern genera like *Leptosynapta* Verrill, 1867, *Epitomapta* Heding, 1928, and *Eupatinapta* Heding, 1928 (e.g., Clark 1924; Heding 1928; Cherbonnier 1953b, 1988; Thandar & Rowe 1989) in having smooth perforation margins. Only *Patinapta* Heding, 1928 has (in part) no serrations at the margins of perforations (e.g., Heding 1928, 1929; Cherbonnier 1953a, 1954, 1955, 1988), but can be distinguished from *Eoleptosynapta* gen. nov. by a different arrangement of anchor plate perforations. Within the Leptosynaptinae only members of *Eupatinapta* have more than the 7 (6 + 1) perforations in the main part of anchor plates, but these are serrated. In contrast to Reich (2003b: 81, 86), Smirnov (2012: 811) also assigned the sclerite association of *Rigaudites nudus* Reich, 2003b and *Calcancora pomerania* Reich, 2003b (both from the early Maastrichtian of northern Germany) to the Leptosynaptinae, which is, in opinion of the first author, not convincing. No related Mesozoic representatives are known up to now, however, members of the Leptosynaptinae from Cenozoic strata are well-known (e.g., Frizzell & Exline 1956, 1957; cf. Smirnov 2012).

Occurrence. – Hitherto known only from the late Cretaceous (Santonian) of Spain.

Eoleptosynapta jaumei Reich sp. nov.
Figs. 6C–F, 7A–C

Material. – 35 nearly complete or partly broken anchor plates (GZG.INV.91412–91446).

Type locality. – Font de la Plata, Sierra del Montsec, Catalonia, Spain.

Type horizon. – Marly limestones of the "Santon E", (Cretaceous: late Santonian).
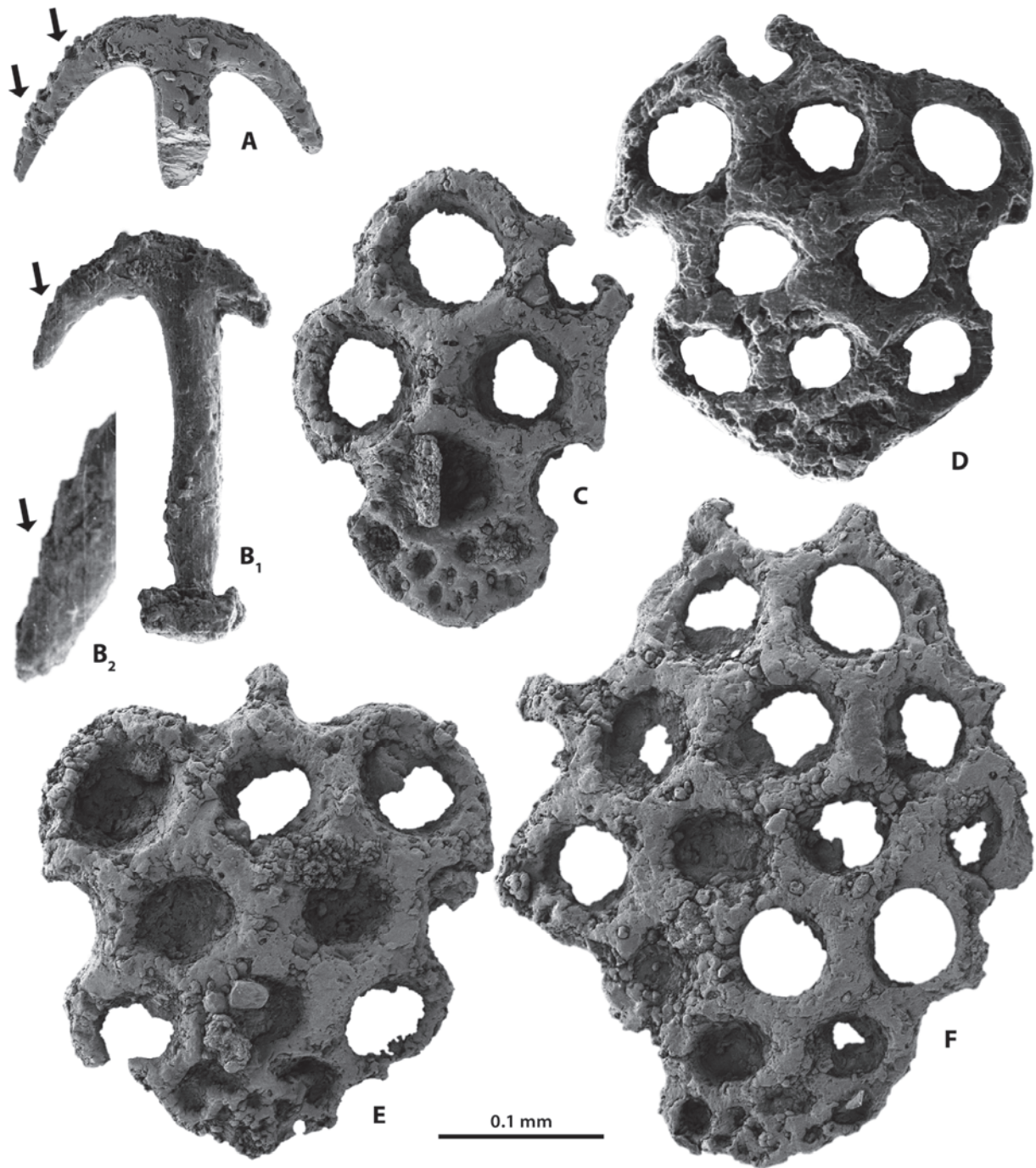
Fig. 6: Representative ossicles of synaptid sea cucumbers. **(A)** *'Calcancora'* sp. 1 (Rynkatorpinae), incomplete anchor GZG.INV.91410, upper side, **(A₁)** total view, **(A₂)** detail of one fluke showing few fine denticles; **(B)** *'Calcancora'* sp. 2 (Rynkatorpinae), incomplete anchor GZG.INV.91411, upper side; **(C–F)** *Eoleptosynapta jaumei* gen. et sp. nov.; **(C)** juvenile anchor plate GZG.INV.91412, paratype, lower side; **(D)** ?subadult/adult anchor plate GZG.INV.91413, paratype, lower side; **(E)** ?subadult/adult anchor plate GZG.INV.91414, holotype, lower side; **(F)** incomplete adult anchor plate GZG.INV.91415, paratype, lower side.

Perforations in anchor plates are partly filled with sediment. The arrows in (A) and (B) mark the preserved teeth at anchor flukes. All specimens from the late Santonian; Font de la Plata, east of Rúbies, Catalonia, Spain. Scale bar 0.1 mm.
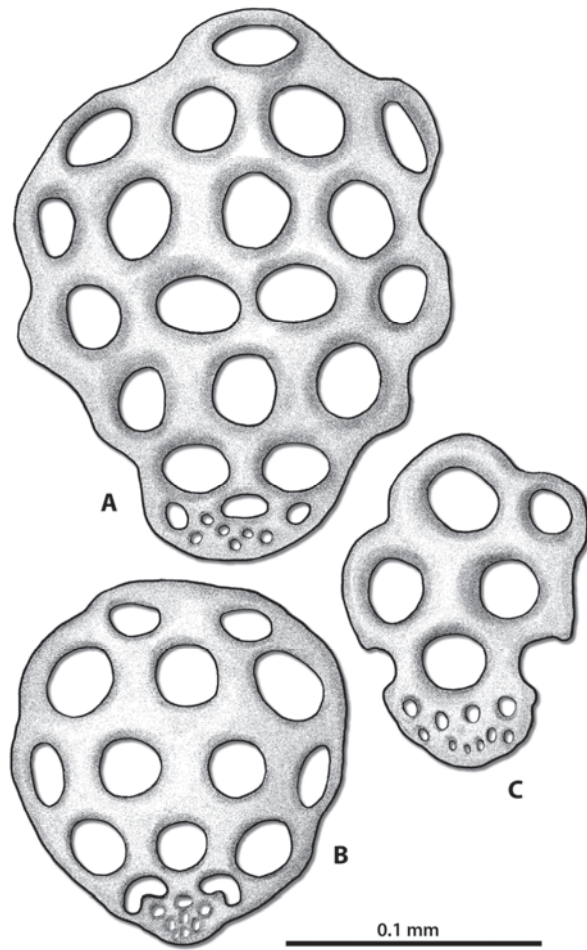
Fig. 7: Schematic drawings of representative ossicles of a new synaptid sea cucumber **(A–C)**, *Eoleptosynapta jaumei* gen. et sp. nov. **(A)** adult anchor plate, lower side; **(B)** ?subadult anchor plate, lower side; **(C)** juvenile anchor plate, lower side.
All from the late Santonian; Font de la Plata, east of Rúbies, Catalonia, Spain. Scale bar 0.1 mm.

Etymology. – Named after Jaume Gallemí (*1954), Barcelona, in recognition of his contributions to Cretaceous echinoderms from Spain.

Diagnosis. – As for the genus.

Description. – The new anchor plate ossicles are more or less pear-shaped in outline, and ~250–430 μm long and ~200–330 μm wide, with 3(–4) rows of medium-sized perforations. These rows contain altogether 8–15 perforations (each 45–55 μm in diameter) with smooth margins. The articulation area for the anchor ossicle is build up by an inconspicuous ledge with numerous very small perforations of subcircular and suboval outline.

Comparison. – See under *Eoleptosynapta*.

Remarks. – The present ossicle association probably presents a stem group member of the Leptosynaptinae, due to the clearly arranged medium-sized perforations of the anchor plates. Representatives of the more Cenozoic and modern Leptosynaptinae + Synaptinae (cf. Frizzell & Exline 1957; Smirnov 1999) normally contain 6 + 1 prominent perforations in the main part of anchor ossicles (see Smirnov 2012: 811f.). It would be conceivable that two rows were reduced during early diversification and later evolution (cf. also Fig. 8).

Species of related leptosynaptid sea cucumbers are quite larger than rynkatorpid species, with specimen lengths normally between 10 and 20(30) cm. They developed different lifestyles; most modern species are infaunal deposit feeders ("funnel-feeders") living in U- or L-shaped tubes (e.g., Roberts et al. 2000), but also facultative swimmers are known (e.g., Costello 1946; Glynn 1965).

Occurrence. – This taxon occurs in the late Santonian of Spain.

Discussion

The species described and discussed herein belong to three holothurian groups: Apodida, Aspidochirotida, and Molpadiida. There are six recognised taxa: (1) *Cruxopadia mesozoica* gen. et sp. nov., (2) *C. reitneri* gen. et sp. nov. (both Molpadiida: ?stem group Molpadiidae), (3) *Eorynkatorpa catalonica* gen. et sp. nov. (Apodida: Synaptidae: Rynkatorpinae), (4) *Eoleptosynapta jaumei* gen. et sp. nov. (Apodida: Synaptidae: Leptosynaptinae), (5) gen. et sp. indet. (Apodida: Chiridotidae: Chiridotinae), and (6) gen. et sp. indet. (Aspidochirotida: Holothuriidae). The two different described anchor ossicles (paragenus *Calcancora*) probably belong either to *Eorynkatorpa catalonica* (*Calcancora* sp. 1) or to *Eoleptosynapta jaumei* (*Calcancora* sp. 2). The both holothuriid ossicles (table = '*Priscopedatus*' sp. and rod = '*Parvispina*' sp.) probably also form a biological species. Most of the fossil species encountered herein were infaunal detritus/deposit feeders (1–5); only holothuriid sea cucumbers normally live as epibenthic detritus/deposit feeders (6).

The sea cucumber material reported in our paper represents the first Santonian holothurian fauna ever described worldwide, helping to fill in some gaps in the fossil record (cf. Fig. 8). Especially the synaptid (Figs. 5–7) and probably also the molpadiid (Fig. 3) holothurians underwent a period of rapid diversification in the Cretaceous. Our results provide new insight in the early diversification of the Synaptidae (Apodida) as well as will help to improve calibration points of divergence times for sea cucumber groups in future studies.
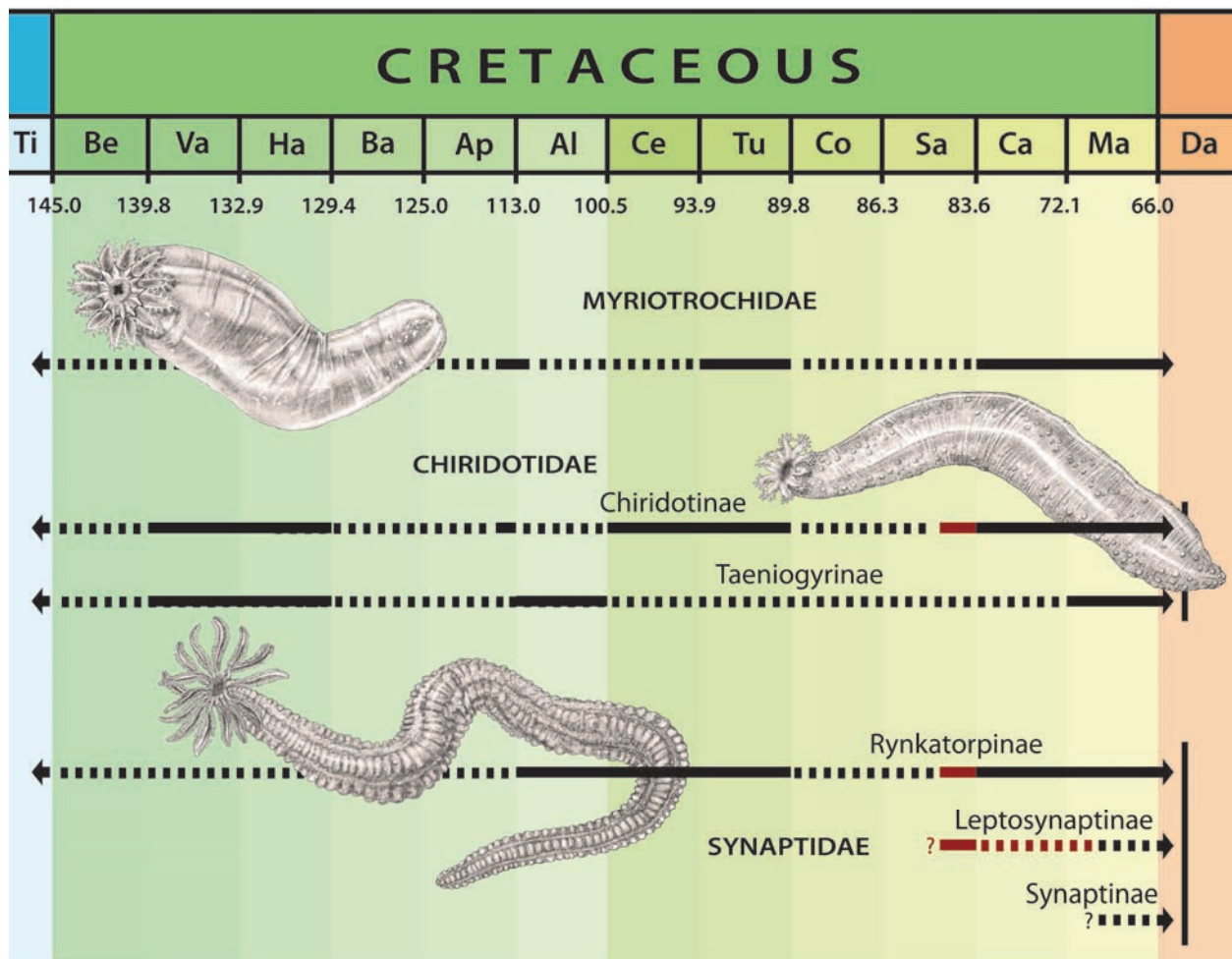
Fig. 8: Evolutionary history of Cretaceous apodid sea cucumbers. Red bars showing the filled gaps in the Fossil Record due to the here described Santonian fauna (Fossil Record of Apodida after Reich in Herrig et al. 1997; Reich 2002, 2003a, 2003b; Reich & Wiese 2010 and Reich unpubl., modified).

References

Ansorge, J. (1991): Zur Sedimentologie und Paläontologie des unterkretazischen Plattenkalkaufschlusses „La Cabrua" (Sierra del Montsec; Provinz Lerida/NE-Spanien) unter besonderer Berücksichtigung der fossilen Insekten. *Unpublished Diploma thesis, Ernst-Moritz-Arndt University Greifswald, Department of Geosciences*: 83 pp., 59 figs., 9 pls.

Bataller, J. R. (1937a): La fauna coral·lina del Cretàcic de Catalunya i regions limítrofes. *Arxius de l'Escola Superior d'Agricultura* **3** (1): 5-299.

Bataller, J. R. (1937b): Catàleg de les espècies fòssils noves del cretàcic de Catalunya i d'altres regions. *Arxius de l'Escola Superior d'Agricultura* **3** (3): 581-619.

Bataller, J. R. (1953): *Mapa Geológico de España, Escala 1 : 50.000. Explicación de la Hoja n.° 290 Isona (Lérida).* Madrid (Instituto Geológico y Minero de España con la colaboración de la Excma. Diputación Provincial de Lérida): 113 pp.

Bell, F. J. (1891): On the Arrangement and Inter-relations of the Classes of Echinodermata. *Annals and Magazine of Natural History (6th series)* **8**: 206-215.

Blainville, H. M. D. de (1834): *Manuel d'Actinologie et de Zoophytologie. 2 vols.* Paris & Strasbourg (Levrault): viii + 694 pp., 99 pls. [pp. 188–197]

Brandt, J. F. (1835): Prodromus descriptionis animalium ab H. Mertensio in orbis terrarum circumnavigatione observatorum. In: *Animalia Mertensii 1.* Petropoli (Graeff) & Lipsiae (Leop. Voss): 1-75.

Bruguière, J. G. (1791): *Encyclopédie méthodique, ou par ordre de matières: par une Société de Gens de Lettres, de Savans et d'Artistes. Précédée d'un Vocabulaire universel, servant de Table pour tout l'Ouvrage, ornée des Portraits de MM. Diderot & d'Alembert, premiers éditeurs de l'Encyclopédie. Tableau encyclopédique et méthodique des trois règnes de la nature. [5] L'helminthologie, ou les vers infusoires, les vers intestins, les vers mollusques, etc. - Vers Echinodermes.* Paris (Panckoucke): viii + 132 pp.

Burmeister, H. (1837): *Handbuch der Naturgeschichte. Zweiter Band. [Dritte Abtheilung Zoologie].* Berlin (T. C. Friedrich): 858 pp.

Caus, E. & Cornella, A. (1983): Macroforaminifères du Crétacé supérieur du bassin sud-pyrénéen. *Géologie Méditerranéenne* **10** (3/4): 137-142.

Caus, E. & Gómez-Garrido, A. (1989): Upper Cretaceous biostratigraphy of the south-central Pyrenees (Lleida, Spain). *Geodinamica Acta: Revue de géologie dynamique et de géographie physique* **3** (3): 221-228.

Caus, E.; Cornella, A. & Pons, M. J. (1978): Foraminíferos bentónicos del Santoniense sudpirenaico (Montsec de Rubies, prov. de Lérida, España). Nueva adscripción genérica de *Dictyopsella chalmasi* Schlumberger. *Revista Española de Micropaleontología* **10** (3): 453-460.

Caus, B.; Llompart, C.; Rosell, J. & Bernaus, J. M. (1999): El Coniaciense superior–Santoniense inferior de la Sierra del Montsec (Pirineos, NE de España). *Revista de la Sociedad Geológica de España* **12** (2): 269-280.

Cherbonnier, G. (1953a): Note sur une nouvelle espèce de Synapte de l'Ile Maurice: *Patinapta vaughani* n. sp. *Bulletin du Muséum National d'Histoire Naturelle (2e série)* **25** (5): 501-504.

Cherbonnier, G. (1953b): Recherches sur les Synaptes (Holothuries Apodes) de Roscoff. *Archives de Zoologie Expérimentale et Générale* **90** (3): 163-186.

Cherbonnier, G. (1954): Note préliminaire sur les Holothuries de la Mer Rouge. *Bulletin du Muséum National d'Histoire Naturelle (2e série)* **26** (2): 252-260.

Cherbonnier, G. (1955): Les Holothuries de la Mer Rouge. In: Résultats scientifiques des campagnes de la "Calypso": I Campagne en Mer Rouge (1951-1952). *Annales de l'Institut Océanographique (N. S.)* **30**: 129-183.

Cherbonnier, G. (1988): Echinodermes: Holothurides. In: *Faune de Madagascar 70.* Paris (Editions de l'ORSTOM): 1-292.

Clark, H. L. (1908): The Apodous holothurians. A monograph of the Synaptidæ and Molpadiidæ. *Smithsonian Contributions to Knowledge* **35** (2): 1-231.

Clark, H. L. (1924): The Holothurians of the Museum of Comparative Zoölogy. The Synaptinae. *Bulletin of the Museum of Comparative Zoölogy at Harvard College* **65** (13): 459-501.

Cornella, A. (1977): Foraminíferos bentónicos del Santoniense del Bco. de la Font de la Plata. Montsec de Rubies (Prov. de Lérida). *Publicaciones de Geología, Universidad Autónoma Bellaterra* **8**: 1-45.

Costello, D. P. (1946): The swimming of *Leptosynapta. The Biological Bulletin* **90** (2): 93-96.

Cuénot, L. (1891): Études Morphologiques sur les Échinodermes. *Archives de Biologie* **11**: 313-680.

Deflandre-Rigaud, M. (1946): Sur les divers types de sclérites d'Holothurides oxfordiens des marnes de Villers-sur-Mer. *Memoires, Comptes Rendus de l'Académie des Sciences* **223** (14): 513-515.

Deflandre-Rigaud, M. (1962): Contribution à la connaissance des sclérites d'Holothurides fossiles. *Mémoires du Muséum National d'Histoire Naturelle (N. S., Série C: Sciences de la Terre)* **11** (1): 1-123.

Dugué, O.; Fily, G. & Rioult, M. (1998): Jurassique des côtes du Calvados. *Bulletin de la Société géologique de Normandie* **85** (2): 3-132.

Frizzell, D. L. & Exline, H. (1956): Monograph of Fossil Holothurian Sclerites. *Bulletin of School of Mines and Metallurgy (Technical Series)* **89** [1955] (1): 1-204.

Frizzell, D. L. & Exline, H. (1957): Revision of the family Synaptitidae, fossil holothurian sclerites (Echinodermata, Holothuroidea). In: Primer Congreso Nacional de Geologia, Anales – Parte II. *Boletino de la Sociedad Geologica del Peru* **32**: 97-119.

Frizzell, D. L. & Exline, H. (1966): Holothuroidea – Fossil Record. In: Moore, R. C. (ed.): *Treatise on Invertebrate Paleontology, U, Echinodermata 3 [Asterozoa–Echinozoa] (2).* Lawrence, Kans. (University of Kansas Press) & Boulder, Colo. (Geological Society of America): U646-U672.

Garassino, A.; Artal, P. & Pasini, G. (2009): New records of decapod macrurans from the Cretaceous of Catalonia and the Province of Castellón (Spain). *Bulletin of the Mizunami Fossil Museum* **35**: 87-95.

Gilliland, P. M. (1993): The skeletal morphology, systematics and evolutionary history of holothurians. *Special Papers in Palaeontology* **47**: 1-147.

Glynn, P. W. (1965): Active movements and other aspects of the biology of *Astichopus* and *Leptosynapta* (Holothuroidea). *The Biological Bulletin* **129** (1): 106-127.

Górka, H. & Łuszczewska, L. (1969): Holothurian sclerites from the Polish Jurassic and Tertiary. *Rocznik Polskiego Towarzystwa Geologicznego [= Annales de la Société Géologique de Pologne]* **39** (1-3): 361-402.

Grube, A. E. (1840): *Aktinien, Echinodermen und Würmer des Adriatischen- und Mittelmeers nach eigenen Sammlungen beschrieben.* Königsberg (J. H. Bon): 92 pp.

Haeckel, E. (1896): Systematische Phylogenie der Echinodermen. In: Haeckel, E.: *Entwurf eines Natürlichen Systems der Organismen auf Grund ihrer Stammesgeschichte. Zweiter Theil: Systematische Phylogenie der Wirbellosen Thiere (Invertebrata).* Berlin (G. Reimer): 348-504.

Heding, S. G. (1928): Synaptidæ. In: Papers from Dr. Th. Mortensen's Pacific Expedition 1914–16. XLVI. *Videnskabelige Meddelelser fra Dansk naturhistorisk Forening i København* **85**: 105-323.

Heding, S. G. (1929): Contributions to the Knowledge of the Synaptidæ I. *Videnskabelige Meddelelser fra Dansk naturhistorisk Forening i København* **88**: 139-154.

Herrig, E.; Frenzel, P. & Reich, M. (1997): Zur Mikrofauna einer Ober-Campan-Scholle von der Halbinsel Wittow (NW Rügen/Ostsee). *Freiberger Forschungshefte (C: Paläontologie, Stratigraphie, Fazies)* **468** (5): 129-169.

Hottinger, L. (1966): Foraminifères rotaliformes et Orbitoïdes du Sénonien inférieur pyrénéén. *Eclogae Geologicae Helvetiae* **59** (1): 277-302.

Hottinger, L.; Drobne, K. & Caus, E. (1989): Late Cretaceous, Larger, Complex Miliolids (Foraminifera) Endemic in the Pyrenean Faunal Province. *Facies* **21**: 99-134.

Hottinger, L. & Caus, E. (2009): Meandropsinidae, an ophtalmidid family of Late Cretaceous K-strategist foraminifera endemic in the Pyrenean Gulf. *Neues Jahrbuch für Geologie und Paläontologie* **253** (2-3): 249-279. http://dx.doi.org/10.1127/0077-7749/2009/0253-0249

Huddleston, R. W. (1982): New generic names for two groups of fossil holothurian sclerites. *Geoscience Journal* **3** (1): 81-82.

Klein, J. T. (1734): *Naturalis Dispositio Echinodermatum: Accessit Lucubratiuncula De Aculeis Echinorum Marinorum, Cum Spicilegio De Belemnitis.* Gedani (Schreiber): 78 + 36 pp.

Kornicker, L. & Imbrie, J. (1958): Holothurian sclerites from the Florena shale (Permian) of Kansas. *Micropaleontology* **4** (1): 93-96.

Krusat, G. (1966): Beitrag zur Geologie und Paläontologie der Sierra del Monsech (Provincia de Lérida, Spanien). *Unpublished Diploma thesis, Free University Berlin, Faculty of Mathematics and Natural Sciences*: 118 pp., 45 figs.

Llompart, C. (1979): Aportacione al conocimiento de la paleogeografía y paleoecología de los nivels fosilíferos del Santoniense del Montsec (prov. de Lleida). *Estudios Geológicos* **35** (1-2): 311-318.

Lommerzheim, A. (1976): Zur Palaeontologie, Fazies, Palaeogeographie und Stratigraphie der turonen Grünsande (Oberkreide) im Raum Mülheim/Broich/Speldorf (Westfalen) mit einer Beschreibung der Cephalopodenfauna. *Decheniana* **129**: 197-244.

Lommerzheim, A. (1991): Biofazielle Analyse des Makrobenthos der Bohrung Metelen 1001 (Santon/Campan; Münsterland, NW-Deutschland). *Facies* **24**: 135-146.

Massin, C. (1996): Results of the Rumphius Biohistorical Expedition to Ambon (1990). Part 4. The Holothurioidea (Echinodermata) collected at Ambon during the Rumphius Biohistorical Expedition. *Zoologische Verhandelingen* **307**: 1-53.

Massin, C. (1999): Reef-dwelling Holothuroidea (Echinodermata) of the Spermonde Archipelago (South-West Sulawesi, Indonesia). *Zoologische Verhandelingen* **329**: 1-114.

Merle, B. (2011): *Les falaises des Vaches Noires de Cuvier au Paléospace.* Rouen (PTC – Éditions des Falaises): 128 pp.

Müller, J. (1850): Anatomische Studien über die Echinodermen. + Berichtigung und Nachtrag zu den anatomische Studien über die Echinodermen. *Archiv für Anatomie, Physiologie und wissenschaftliche Medicin* **[1850]**: 117-155, 225-233.

Mutterlose, J. (1982): Holothuriensklerite aus der höheren Unterkreide Nordwestdeutschlands. In: Kemper, E. (ed.): Das späte Apt und frühe Alb Nordwestdeutschlands. *Geologisches Jahrbuch, (A: Allgemeine und regionale Geologie BR Deutschland und Nachbargebiete, Tektonik, Stratigraphie, Paläontologie)* **65**: 597-615.

Neumann, C. & Hess, H. (2001): *Coulonia parva* n. sp., a new species of Astropectinidae (Asteroidea; Echinodermata) from the Santonian (Upper Cretaceous) of Sierra de Montsech (southern Pyrenees, Spain). *Paläontologische Zeitschrift* **75** (1): 7-11.

Nolf, D. (2003): Fish otoliths from the Santonian of the Pyrenean faunal province, and an overview of all otolith-documented North Atlantic Late Cretaceous teleosts. *Bulletin de l'institut royal des sciences naturelles de Belgique (Sciences de la terre) [= Bulletin van het Koninklijk Belgisch Instituut voor Natuurwetenschappen (Aardwetenschappen)]* **73**: 155-173.

Östergren, H. J. (1898): Das System der Synaptiden (Vorläufige Mitteilung). *Öfversigt Kongliga Vetenskaps-Akademiens Förhandlingar* **55** (2): 111-120.

Pawson, D. L. (1977): Molpadiid Sea Cucumbers (Echinodermata: Holothuroidea) of the Southern Atlantic, Pacific and Indian Oceans. In: Pawson, D. L. (ed.): Biology of the Antarctic Seas VI. *Antarctic Research Series* **26**: 97-123.

Pawson, D. L. & Vance, D. J. (2005): *Rynkatorpa felderi*, new species, from a bathyal hydrocarbon seep in the northern Gulf of Mexico (Echinodermata: Holothuroidea: Apodida). *Zootaxa* **1050**: 15-20.

Pawson, D. L.; Vance, D. J. & Ahearn, C. (2001): Western Atlantic sea cucumbers of the Order Molpadiida (Echinodermata: Holothuroidea). *Bulletin of the Biological Society of Washington* **10**: 311-327.

Reich, M. (2002): Holothurien (Echinodermata) aus der Oberkreide des Ostseeraumes: Teil 1. Myriotrochidae Théel, 1877. *Neues Jahrbuch für Geologie und Paläontologie, Abhandlungen* **224** (3): 373-430.

Reich, M. (2003a): Holothurien (Echinodermata) aus der Oberkreide des Ostseeraumes: Teil 3. Chiridotidae Östergren, 1898. *Neues Jahrbuch für Geologie und Paläontologie, Abhandlungen* **228** (3): 363-397.

Reich, M. (2003b): Holothurien (Echinodermata) aus der Oberkreide des Ostseeraumes: Teil 4. Synaptidae Burmeister, 1837. *Neues Jahrbuch für Geologie und Paläontologie, Abhandlungen* **229** (1): 75-94.

Reich, M. (2008): A nearly articulated holothurian specimen from the Santonian of England. In: Löffler, S.-B. & Freiwald, A. (eds.): Jahrestagung der Paläontologischen Gesellschaft. 8.-10. September 2008, Erlangen. *Erlanger Geologische Abhandlungen, Sonderband* **6**: p. 109.

Reich, M. (2013a): How many species of fossil holothurians are there ? In: Johnson, C. (ed.): *Echinoderms in a Changing World. Proceedings of the 13th International Echinoderm Conference, University of Tasmania, Hobart Tasmania, Australia, 5-9 January 2009.* Boca Raton / London / New York / Leiden (CRC Press, Taylor & Francis Group): 23-51. http://dx.doi.org/10.1201/b13769-5

Reich, M. (2013b): A nearly articulated aspidochirote holothurian from the Late Cretaceous (Santonian) of England. In: Johnson, C. (ed.): *Echinoderms in a Changing World. Proceedings of the 13th International Echinoderm Conference, University of Tasmania, Hobart Tasmania, Australia, 5-9 January 2009.* Boca Raton / London / New York / Leiden (CRC Press, Taylor & Francis Group): 299-300. http://dx.doi.org/10.1201/b13769-38

Reich, M. & Wiese, F. (2010): Apodid sea cucumbers (Echinodermata: Holothuroidea) from the Upper Turonian of the Isle of Wolin, NW Poland. *Cretaceous Research* **31** (4): 350-363. http://dx.doi.org/10.1016/j.cretres.2010.03.001

Roberts, D.; Gebruk, A.; Levin, V. & Manship, B. A. D. (2000): Feeding and digestive strategies in deposit-feeding holothurians. *Oceanography and Marine Biology: An Annual Review* **38**: 257-310.

Rowe, F. W. E. (1969): A Review of the Family Holothuriidae (Holothurioidea: Aspidochirotida). *Bulletin of the British Museum of Natural History (Zoology)* **18** (4): 119-170.

Rowe, F. W. E. & Pawson, D. L. (1967): A new genus in the holothurian family Synaptidae, with a new species from Tasmania. *Papers and Proceedings of the Royal Society of Tasmania* **101**: 31-35.

Samyn, Y. (2003): Shallow-water Holothuroidea (Echinodermata) from Kenya and Pemba Island, Tanzania. *Studies in Afrotropical Zoology* **292**: 1-158.

Samyn, Y.; Appeltans, W. & Kerr, A. M. (2005): Phylogeny of *Labidodemas* and the Holothuriidae (Holothuroidea: Aspidochirotida) as inferred from morphology. *Zoological Journal of the Linnean Society* **144** (1): 103-120. http://dx.doi.org/10.1111/j.1096-3642.2005.00158.x

Schlumberger, C. (1890): Second note sur les Holothuridées fossiles du Calcaire Grossier. *Bulletin de la Société géologique de France (sér. 3)* **18**: 191-206.

[Smirnov, A. V.] Смирнов, А. В. (1983a): *Rynkatorpa duodactyla* (Apoda, Synaptidae) – новый для фауны СССР вид голотурий из части тихого океана. [*Rynkatorpa duodactyla* (Apoda, Synaptidae) – novyj dlâ fauny SSSR vid goloturij iz časti tihogo okeana; *Rynkatorpa duodactyla* (Apoda, Synaptidae), a sea cucumber from the North Pacific new for the fauna of the USSR]. *Зоологический журнал [Zoologičeskij žurnal]* **62** (1): 75-82.

[Smirnov, A. V.] Смирнов, А. В. (1983b): Изменчивость якорных пластинок голотурии *Rynkatorpa duodactyla* (Apoda, Synaptidae). [Izmenčivost' ākornyh plastinok goloturii *Rynkatorpa duodactyla* (Apoda, Synaptidae); The variability of anchor plates in *Rynkatorpa duodactyla* (Apoda, Synaptidae)]. *Зоологический журнал [Zoologičeskij žurnal]* **62** (4): 546-552.

[Smirnov, A. V.] Смирнов, А. В. (1989): Соотношение систем ископаемых и современных голотурий семейства Synaptidae. [Sootnošenie sistem iskopaemyh i sovremennyh goloturij semejstva Synaptidae; Coordination of modern and fossil synaptid holothurians.]. In: Кальо, Д. Л. [Kaľo, D. L.] (ed.): *Проблемы изучения ископаемых и современных иглокожих. [Problemy izučeniā iskopaemyh i sovremennyh iglokožih; Fossil and Recent Echinoderm Researches.].* Таллинн [Tallinn] (Академия наук Эстонской ССР [Akademiā nauk Èstonskoj SSR]): 203-217.

Smirnov, A. V. (1997): New apodid holothurians (Holothurioidea, Apodida) from the New Caledonian continental slope collected during "BIOGEOCAL" expedition 1987. *Zoosystema* **19** (1): 15-26.

Smirnov, A. V. (1998): On the classification of the apodid holothurians. In: Mooi, R. & Telford, M. (eds.): *Echinoderms: San Francisco. Proceedings of the Ninth International Echinoderm Conference on Echinoderms, San Francisco / California / USA / 5–9 August 1996.* Rotterdam (A. A. Balkema): 517-522.

Smirnov, A. V. (1999): The origin of the order Apodida (Holothuroidea) and its families. In: Candia Carnevali, M. D. & Bonasoro, F. (eds.): *Echinoderm Research 1998. Proceedings of the Fifth European Conference on Echinoderms, Milan, Italy, 7–12 September 1998.* Rotterdam (A. A. Balkema): 393-395.

Smirnov, A. V. (2012): System of the Class Holothuroidea. *Paleontological Journal* **46** (8): 793-832. http://dx.doi.org/10.1134/S0031030112080126

Soodan, K. S. (1975): Revision of fossil Holothuroidea family Priscopedatidae FRIZZELL and EXLINE, 1955 and some new genera from Kutch, India. *Geophytology* **5** (2): 213-224.

Steuber, T. (2002): A palaeontological database of RUDIST BIVALVES (Mollusca: Hippuritoidea, Gray 1848). www.paleotax.de/rudist/intro.htm [last access 03/2013]

Tandon, K. K. & Saxena, R. K. (1983): Fossil holothuroids from Middle Eocene rocks of Kutch, India. *Geophytology* **7** (2): 229-259.

Thandar, A. S. & Rowe, F. W. E. (1989): New species and new records of apodous holothurians (Echinodermata, Holothuroidea) from southern Africa. *Zoologica Scripta* **18** (1): 145-155.

Upton, C. (1917): Notes on *Chirodota*-spicules from the Lias and Inferior Oolite. *Proceedings of the Cotteswold Naturalists' Field Club* **19** (2): 115-117.

Verrill, A. E. (1867): On the Geographical Distribution of the Echinoderms of the West Coast of America. *Transactions of the Connecticut Academy of Arts and Sciences* **1** (2): 323-351.

Vicens, E. (1992): Intraspecific variability in Hippuritidae in the southern Pyrenees, Spain: taxonomic implications. *Geologica Romana (N. S.)* **28**: 119-161.

Vicens, E.; López, G. & Obrador, A. (1998): Facies successions, biostratigraphy and rudist faunas of Coniacian to Santonian platform deposits in the Sant Corneli anticline (Southern Central Pyrénées). In: Masse, J.-P. & Skelton, P. W. (eds.): Quatrième Congrès international sur les Rudistes. *Geobios (Mémoire spécial)* **22**: 403-427.

Wissing, F.-N. & Herrig, E. with cooperation of M. Reich (1999): *Arbeitstechniken der Mikropaläontologie. Eine Einführung.* Stuttgart (Enke-Verlag): 191 pp.

Supplement to: 'How many species of fossil holothurians are there?'

Mike Reich[1,2]

[1]Geoscience Museum, Georg-August University Göttingen, Goldschmidtstr. 1-5, 37077 Göttingen, Germany;
Email: mreich@gwdg.de
[2]Department of Geobiology, Geoscience Centre, Georg-August University Göttingen, Goldschmidtstr. 3,
37077 Göttingen, Germany

My 'How many species of fossil holothurians are there?' checklist covered all published fossil holothurian names through 01 June 2012. This supplement includes new fossil species (7) described through 01 August 2013, a few addenda missing (4), and correction of errors discovered in the original. With these additions, I number the named fossil sea cucumber species of the world at 959 species/paraspecies. The need for more study of fossil holothurians is again demonstrated by the fact that large areas worldwide, e.g. Africa, Asia, Australia, South America, still remain unstudied.

Introduction

'How many species of fossil holothurians are there?' (Reich 2013) covered all published fossil holothurian names described through 01 June 2012. In this supplement I correct errors discovered in the my check list (Reich 2013), list 7 new fossil species described since, and include also 3 nomina nova and 1 ?manuscript name missing in Reich (2013).

Taxa described since the last checklist

The detailed list includes the species, original genus, author(s), type stratum and locality. A few fossil species are designated in part as follows: * sclerite assemblage, ** body fossil, *** non-Holothuroidea or very probably non-Holothuroidea (Reich 2013: 32-51). The numbering of species/paraspecies from Reich (2013) is continued here.

Correction

45.   *annulata* Giebel, 1857**/***; <u>*Protholoturia¹*</u> [Jurassic: Lower Tithonian; Germany]

61.   *armata* Giebel, 1857**/***; <u>*Protholoturia¹*</u> [Jurassic: Lower Tithonian; Germany]

380.   *ingridae* Mostler in Krainer et al., 1994; *Neomicro-antyx* [Jurassic: <u>Toarcian</u>; Austria]

¹ = *Protholothuria* Giebel nom. correct. Giebel 1866: 36 (pro *Protholoturia* Giebel, 1857)

Addendum

949.   *catalonica* Reich in Reich & Ansorge, 2014; *Eorynkatorpa* [Cretaceous: Santonian; Spain]

950.   *frankwiesei* Reich, 2012; *Palaeolaetmogone* [Cretaceous: Turonian; Poland]

951.   *jaumei* Reich in Reich & Ansorge, 2014; *Eoleptosynapta* [Cretaceous: Santonian; Spain]

952.   *latifolia* Mostler, 1972; *Protocaudina* [Jurassic; other details unknown]

953.   *mesozoica* Reich in Reich & Ansorge, 2014; *Cruxopadia* [Jurassic: Oxfordian; France]

954.   *oloughlini* Reich, 2012; *Priscolaetmogone* [Cretaceous: Maastrichtian; Germany/Baltic Sea]

955.   *reitneri* Reich in Reich & Ansorge, 2014; *Cruxopadia* [Cretaceous: Santonian; Spain]

956.   *rioulti* Smirnov, 1989; *Croneisites*? [Paleogene: Eocene: Lutetian; France]

957.   *rugia* Reich, 2012; *Palaeocaudina* [Cretaceous: Maastrichtian; Germany]

958.   *sadeddini* Reich, 2003; *Calcligula* [Cretaceous: Albian; U.S.A.: Texas]

959.   *saidi* Reich, 2003; *Calcligula* [Jurassic: Bajocian; Egypt]

Acknowledgements

References

Giebel, C. [G. A.] (1857): Zur Fauna des lithographischen Schiefers von Solenhofen. *Zeitschrift für die Gesammten Naturwissenschaften* **9**: 373-388.

Giebel, C. [G. A.] (1866): *Repertorium zu Goldfuss' Petrefakten Deutschlands. Ein Verzeichniss aller Synonymen und literarischen Nachweise zu den von Goldfuss abgebildeten Arten.* Leipzig (List & Francke): iv + 122 pp.

Krainer, K.; Mostler, H. & Haditsch, J. G. (1994): Jurassische Beckenbildung in den Nördlichen Kalkalpen bei Lofer (Salzburg) unter besonderer Berücksichtigung der Manganerz-Genese. In: Festschrift zum 60. Geburtstag von Erik Flügel. *Abhandlungen der Geologischen Bundesanstalt in Wien* **50**: 257-293.

Mostler, H. (1972): Holothuriensklerite aus dem Jura der Nördlichen Kalkalpen und Südtiroler Dolomiten. *Geologisch-Paläontologische Mitteilungen Innsbruck* **2** (6): 1-29.

Reich, M. (2003): Holothurien (Echinodermata) aus der Oberkreide des Ostseeraumes: Teil 5. Molpadiidae J. Müller, 1850. *Neues Jahrbuch für Geologie und Paläontologie, Abhandlungen* **229** (2): 231-253.

Reich, M. (2012): On Mesozoic laetmogonid sea cucumbers (Echinodermata: Holothuroidea: Elasipodida). In: Kroh, A. & Reich, M. (eds.): Echinoderm Research 2010: Proceedings of the Seventh European Conference on Echinoderms, Göttingen, Germany, 2-9 October 2010. *Zoosymposia* **7**: 185-212.

Reich, M. (2013): How many species of fossil holothurians are there? In: Johnson, C. (ed.): *Echinoderms in a Changing World. Proceedings of the 13th International Echinoderm Conference, University of Tasmania, Hobart Tasmania, Australia, 5-9 January 2009.* Boca Raton / London / New York / Leiden (CRC Press, Taylor & Francis Group): 23-51. http://dx.doi.org/10.1201/b13769-5

Reich, M. & Ansorge, J. (2014): Santonian sea cucumbers (Echinodermata: Holothuroidea) from Sierra del Montsec, Spain. In: Wiese, F.; Reich, M. & Arp, G. (eds.): "Spongy, slimy, cosy & more…". Commemorative volume in celebration of the 60th birthday of Professor Joachim Reitner. *Göttingen Contributions to Geosciences* **77**: 147-160. http://dx.doi.org/10.3249/webdoc-3926

[Smirnov, A. V.] Смирнов, А. В. (1989): Соотношение систем ископаемых и современных голотурий семейства Synaptidae. [Sootnošenie sistem iskopaemyh i sovremennyh goloturij semejstva Synaptidae; Coordination of modern and fossil synaptid holothurians.]. In: Кальо, Д. Л. [Kal'o, D. L.] (ed.): *Проблемы изучения ископаемых и современных иглокожих. [Problemy izučeniā iskopaemyh i sovremennyh iglokožih; Fossil and Recent Echinoderm Researches.].* Таллинн [Tallinn] (Академия наук Эстонской ССР [Akademiā nauk Èstonskoj SSR]): 203-217.

Shallow-water brittle-star (Echinodermata: Ophiuroidea) assemblages from the Aptian (Early Cretaceous) of the North Atlantic: first insights into bathymetric distribution patterns

Ben Thuy[1] *; Andrew S. Gale[2]; Sabine Stöhr[3] & Frank Wiese[4]

[1]*Natural History Museum Luxembourg, 24, rue Münster, 2160 Luxembourg-city, Luxembourg; Email: nebyuht@yahoo.com*
[2]*School of Earth and Environmental Sciences, University of Portsmouth, Burnaby Building, Burnaby Road, Portsmouth PO1 3QL, UK*
[3]*Department of Invertebrate Zoology, Swedish Museum of Natural History, Box 50007, SE-10405 Stockholm, Sweden*
[4]*Department of Geobiology, Geoscience Centre, Georg-August University Göttingen, Goldschmidtstr. 3, 37077 Göttingen, Germany*

* corresponding author

In spite of their excellent preservation potential and abundance, brittle-star microfossils are still an underexploited source of alpha-taxonomical data. Knowledge on the Lower Cretaceous fossil record of the ophiuroids is particularly patchy, hampering the use of the ophiuroids as a model organism to explore macroevolutionary, taphonomic and other further-reaching aspects. Here, we describe three ophiuroid assemblages mostly based on dissociated lateral arm plates from the early Aptian of Cuchía (Cantabria, northern Spain), and the latest Aptian of Wizard Way (Texas, USA). A total of eleven species were identified. Ten species are new to science, three of which (*Ophioleuce sanmigueli* sp. nov., *Ophiozonella eloy* sp. nov. and *Ophiodoris holterhoffi* sp. nov.) are formally described as new. The two Spanish assemblages are dominated by an ophionereidid and an ophiolepidid, and the Texan one by an ophionereidid and, to a much lesser extent, an ophiacanthid assemblage. Our analysis reveals that the eastern (Cuchía) and western (Texas) North Atlantic faunal spectra were not fundamentally different from each other during the Aptian. We furthermore present the first clear bathymetric gradient in the ophiuroid fossil record, comparing the Texan assemblage with a recently discovered coeval fauna from middle bathyal palaeodepths of Blake Nose, western North Atlantic, and show that Aptian shallow-water (<200 m) and deep-sea ophiuroid communities were clearly distinct. Finally, we argue that the Aptian shallow-water assemblages, although dominated by families which typically occur in present-day mid- to low-latitude shallow seas, have no modern equivalents in terms of family-level composition.

Introduction

Echinoderms are among the most important invertebrate fossil groups. In fact, their skeletal plates quite conveniently combine a high fossilisation potential and sufficient morphological disparity for taxonomic identification (e.g., Donovan 1996, 2001; Gale 2011). As a result, echinoderms have been successfully used in the past as model organisms to explore large-scale palaeoecologic, palaeoclimatologic and macroevolutionary patterns (e.g., Aronson 1987; Baumiller & Gahn 2004; Kroh 2007; Hunter & Underwood 2009; Thuy & Meyer 2012). Recently, dissociated lateral arm plates of ophiuroids have been suggested as a particularly promising yet largely unexplored source of evidence in this respect, mostly because they abundantly occur as microfossils in most marine sediments and are determinable to genus and even species level (Thuy & Stöhr 2011). Indeed, ophiuroid lateral arm plates have provided key evidence to explore the geological history of the modern deep-sea fauna (Thuy et al. 2012) and the macroevolutionary patterns in the bathymetric distribution of a modern deep-sea ophiuroid family (Thuy 2013).

Yet, the fossil record of the ophiuroids, unlike that of other echinoderm groups (e.g., Hess 2011), is still only patchily known, in spite of fairly numerous taxonomic studies (e.g., Hess 1962, 1964, 1965a, 1965b, 1966, 1975a, 1975b; Kutscher & Hary 1991; Kutscher 1996; Kutscher & Jagt 2000; Kutscher & Villier 2003; Thuy 2005; Thuy 2011; Thuy & Kroh 2011; Thuy 2013). For some stratigraphic stages, fewer than 20 fossil ophiuroid species are known, which corresponds to less than 1 percent of the present-day diversity of the class, amounting to 2064 currently recognised species (Stöhr et al. 2012).

The Aptian is one of these blank areas with respect to ophiuroid palaeodiversity, with, until recently, only a single nominal ophiuroid species described (Taylor 1966). Smith & Rader (2009), Thuy et al. (2012) and Thuy (2013) added another five nominal ophiuroid species and eight unnamed species reports for the Aptian, resulting in as few as 14 species in total for the entire stage. Clearly, much more data are needed until even an approximate picture of Aptian ophiuroid diversity becomes discernible. This is all the more desirable considering that the Early Cretaceous was a crucial time in the evolution of the Ophiuroidea, witnessing the divergence of a number of important modern groups (Stöhr et al. 2012).

Here, we report on three ophiuroid assemblages mostly based on lateral arm plates from Aptian shallow-water deposits of the North Atlantic, two from Spain and one from Texas. The main purpose of this study is to contribute to a better understanding of ophiuroid diversity in the Aptian in particular and in the Early Cretaceous in general, and thus to expand the alpha-taxonomic basis for further-reaching studies. In addition, we compare the here described shallow-water assemblages with the near-coeval, middle bathyal North Atlantic ophiuroid assemblage described by Thuy et al. (2012) and Thuy (2013) presenting

first insights into the bathymetric distribution of Lower Cretaceous ophiuroids.

Fig. 1: Palaeogeographic reconstruction for the late Aptian (from Erbacher et al. 2001, modified) with the position of the studied assemblages (Cuchía, Spain, and Wizard Way, Texas) in the western North Atlantic. Thick lines denote palaeocoastlines and grey areas represent emerged land. The star indicates the position of the middle bathyal Blake Nose assemblage of Thuy et al. (2012).

Geological context

The ophiuroid assemblages described herein were extracted from bulk sediment samples from two localities. One sample was retrieved from the Echinoid Marker Bed of Smith & Rader (2009), at the base of Unit 2 of the Lower Member of the Glen Rose Formation, Texas, United States of America, near Wizard Way, southwest of Austin, on the western side of the palaeo-North Atlantic. This site has been dated to a latest Aptian age (Stricklin et al. 1971; Smith & Rader 2009), thus postdating OAE (Oceanic Anoxic Event) 1a but predating OAE 1b. The Echinoid Marker Bed is an orbitoline-rich, marly wackestone that underlies rudist bioherm limestones. It was presumably deposited in a peri-reefal setting below normal wave base (Smith & Rader 2009).

Further samples were retrieved from the Cuchía section in Cantabria, Spain, ca. 5 km E of Suances at the Playa de los Caballos, on the eastern side of the palaeo-North Atlantic (Fig. 1). It exposes superbly a transgressive-regressive sequence of a Lower (–Middle?) Albian age. Dark transgressive/maximum flooding marls of ca. 55 m thickness are referred to as Marl Member of the Caranceja Formation *sensu* Garcia-Mondejar 1982 (see Wilmsen 2005), which is equivalent to the Patrocinio Formation of Najarro et al. (2011). The marls rest with a sharp contact on coarse-grained calcarenites (Calcarenite Member of the Caranceja Formation; Wilmsen 2005). They show frequent intercalations of blood-red to brown weathering clay-ironstone layers, in which ammonites occur frequently in two levels (Collignon 1979). The succession grades progressively *via* highly fossiliferous, massively bedded silty

marls into prodelta turbidites and fluvial sandstones with wood remains and abundant ichnofossils *Ophiomorpha nodosa* (Lundgren). A detailed description of the section is given by Wilmsen (2005).

Five samples from the Marl Member were processed. It turned out that the bathymetrically deepest part of the section yielded only scarce material. However, some 20 m above the base of the section (ca. 2 m above the second ammonite level), microfauna becomes abruptly abundant. Thus, we considered two samples from an interval above the second ammonite layer (Cuchía 1: 1.5 m above the second ammonite layer, and Cuchía 2: 10 m above the second ammonite layer). Biostratigraphically, the fauna derives from a critical interval close or within the OAE 1a. Collignon (1979) and Wilmsen (2005) regarded the second ammonite level to represent already the *Deshayesites deshayesi* Zone (late Early Aptian). This would then mean that the here described fauna from Cuchía postdates OAE 1a. Najarro et al. (2010), however, re-interpreted the fauna as *D. weissi* Zone (middle Lower Aptian), and δ¹³C correlations seem to confirm this assessment. Thus, our fauna appears to coincide stratigraphically with the OAE 1a (Selli Event).

Material and methods

The ophiuroid remains described herein were retrieved from the sieving residues of bulk sediment samples. Micropalaeontological sample processing involved immersion in 10 percent hydrogen peroxide and soaking in an oversaturated, hot soda solution respectively for the two Spanish samples, and washing in a clay processing device (Ward 1981) for the Texan sample. The ophiuroid remains were picked from the >250 μm residue fraction using a dissecting microscope. Selected specimens were cleaned using an ultrasonic tank. They were then mounted on aluminium stubs and coated with platinum or palladium for scanning electron microscopy. Lateral arm plates of modern ophiuroids, used for morphological comparison, were extracted from complete specimens using household bleach (NaOCl), as described by Thuy & Stöhr (2011).

The material from the Texan sample includes both disarticulated skeletal plates and articulated arm fragments, mostly displaying pristine preservation of even the finest stereom structures. The specimens from the Spanish samples are all fully disarticulated and show signs of pre-burial abrasion and/or diagenetic alteration, blurring some of the finer structures of the stereom.

Identifications, ideally to species level, were almost exclusively based on the lateral arm plates (abbreviated in the descriptions as LAPs), following the terminology and guidelines of Thuy & Stöhr (2011). In the exceptional case of the Texan assemblage, it was possible to extract additional taxonomic evidence from vertebrae, oral plates and ventral and dorsal arm plates by combining these with a

particular type of lateral arm plates. This was possible on the one hand thanks to the co-occurrence of articulated arm fragments, and on the other hand because the lateral arm plates in question were by far the most abundant in the sample. Higher-level classification follows Smith et al. (1995) and the amendments by Martynov (2010) and Thuy et al. (2012).

A detrended correspondence analysis was computed using the PAST software (Hammer et al. 2001) in order to compare the studied ophiuroids assemblages quantitatively with a coeval middle bathyal assemblage from the western North Atlantic (Thuy et al. 2012) and with modern ophiuroid communities from various depths. This analysis was based on the dataset of Thuy et al. (2012) (minus the Cretaceous shallow-water assemblages) and the relative abundances on family level of the here described assemblages, deduced from lateral arm plate counts. As in the analysis of Thuy et al. (2012), the ubiquitous Ophiuridae were removed from the dataset in order to enhance bathymetric trends in family-level compositions.

All types, figured and additional specimens were deposited in the collection of the Geoscientific Museum at the University of Göttingen (GZG.INV.).

Systematic palaeontology

Class **Ophiuroidea** Gray, 1840
Order **Ophiurida** Müller & Troschel, 1840

Family **Ophiacanthidae** Ljungman, 1867

Genus *Ophiacantha* Müller & Troschel, 1842

Type species. – *Ophiacantha spinulosa* Müller & Troschel, 1842 [junior synonym of *Ophiacantha bidentata* (Bruzelius, 1805)]

Diagnosis for LAPs. – Ophiacanthid with dorsal and ventral lobes of spine articulations fused into continuous volute; ventral part of LAPs not protruding ventro-proximalwards; generally no more than one spur on the outer proximal and inner distal edges; ridge on inner side composed of long, oblique, straight to slightly bent main part with a pointed dorsal tip and with ventralward pointing, vertical to slightly oblique or bent extension generally at least as long as half of the main part; in many cases, main part and ventralwards pointing extension fused into large, irregularly triangular knob; tentacle notch small.

Ophiacantha sp. nov.

Figs. 2.1–2

Material examined. – GZG.INV.78820 (figured dissociated LAP), GZG.INV.78821 (figured dissociated LAP) and GZG.INV.78822 (6 dissociated LAPs) from Cuchía 2,

and GZG.INV.78823 (2 dissociated LAPs from Cuchía 1).

Description. – Relatively small, dissociated LAPs of stout aspect, proximal ones slightly higher than wide, distal ones slightly wider than high; dorsal edge concave as a result of a moderately well developed constriction; distal edge evenly convex; proximal edge evenly concave, devoid of spurs, kinks or protrusions; ventral portion of LAP weakly protruding ventro-proximalwards; outer surface stereom coarsely meshed, with trabeculae thickened into small tubercles; narrow band of much more finely meshed stereom along proximal edge of LAP. Seven (proximal LAPs) to five (distal LAPs) large, ear-shaped spine articulations freestanding on elevated distal portion of LAP, bordered proximally by poorly defined, knobby and irregularly wavy, vertical ridge; dorsal and ventral lobes of spine articulations merged into continuous, coarsely meshed volute with well developed sigmoidal fold; dorsalward increase in size of spine articulations and of gaps separating them; gap between spine articulations and distal edge of LAP narrower than half a spine articulation. Ventral edge of LAP weakly concave; tentacle notch invisible in external view.

Inner side of LAP with large, wide, prominent but poorly defined ridge composed of a nearly straight, oblique central part with pointed dorsal tip and vertical, ventralwards pointing dorsal extension nearly parallel to the proximal edge of the LAP; central part of the ridge and ventralwards pointing dorsal extension merged into vertically elongate, nearly triangular knob with concave ventral edge; ventral portion of main ridge part with rounded kink and ventro-proximalwards pointing extension not merged with ventral portion of LAP; inner side of distal edge of LAP devoid of spurs; very poorly defined, almost indiscernible, shallow tentacle notch between ventro-distal tip of LAP and slightly thickened ventro-proximal portion of LAP; single, small, poorly defined perforation discernible near distal edge of kink of ridge, in wide, shallow, almost indiscernible vertical furrow.

Remarks. – The large, ear-shaped spine articulations with a well developed sigmoidal fold in combination with the absence of a single, conspicuous, large perforation on the inner side unequivocally place the above described LAPs in the family Ophiacanthidae. On genus level, closest affinities are shared with the LAPs of *Ophiacantha* in its proper sense as defined by Thuy (2013), mainly on account of the general shape of the LAPs devoid of a strongly ventro-proximalwards protruding ventral portion, the absence of spurs on the outer proximal and inner distal edges, the continuous lobe of the spine articulations and the shape of the ridge on the inner side. There are superficial similarities with the LAPs of the extinct genus *Ophiogaleus* Thuy, 2013, assumed to share very close phylogenetic ties with *Ophiacantha* (Thuy 2013), in particular concerning the knobby rather than vertically striated outer surface. The absence of spurs on the outer proximal and

inner distal edges of the above described LAPs as well as the absence of a kink between the straight, oblique part of the ridge on the inner side and its widened, nearly triangular dorsal portion, however, preclude assignment to *Ophiogaleus*.

Among the fossil LAP types currently assigned to *Ophiacantha* according to the revised ophiacanthid fossil record (Thuy 2013), closest similarities are shared with *Ophiacantha jaegeri* Thuy, 2013, from the Hauterivian of Germany, especially on account of the outer surface ornamentation and the shape and arrangement of the spine articulations. LAPs of the species in question, however, differ from the above described specimens in their more fragile general appearance, the slightly lower number of spine articulations and the spur on the outer proximal and inner distal edges. The above described LAPs almost certainly belong to a new species, which, however, we refrain from formally describing here on account of the limited and poorly preserved material available.

The genus *Ophiacantha*, even if restricted as by Thuy (2013), includes several types of LAP morphologies, many of which most likely represent yet undescribed genera in the *Ophiacantha* lineage. On the basis of the observation that LAP morphology reflects phylogenetic relationships in ophiuroids (Thuy & Stöhr 2011), it can be assumed that *Ophiacantha jaegeri* and the new Aptian species represent another one of these groups.

Occurrence. – Early Aptian of Cuchía, Spain.

Genus *Dermocoma* Hess, 1964

Type species. – *Dermocoma wrighti* Hess, 1964.

Diagnosis for LAPs. – Ophiacanthid with LAPs commonly displaying a fine vertical striation on their outer surface; well developed spurs on the inner distal and, in some cases to a lesser extent, outer proximal edge; ventral portion of LAP strongly protruding ventro-proximalwards; up to six moderately large, ear-shaped spine articulations with continuous volute in notches of elevated distal portion of LAP; ridge on inner side of LAPs simple, continuous, generally slender, devoid of sharp kinks or conspicuously thickened parts; tentacle notch small to moderately large.

Dermocoma sp. nov.

Fig. 2.3

Material examined. – GZG.INV.78824 (figured dissociated LAP) and GZG.INV.78825 (6 dissociated LAPs) from Cuchía 2, and GZG.INV.78826 (one dissociated LAP) from Cuchía 1.

Description. – Relatively small dissociated LAPs, proximal one slightly more than 1.5 times higher than wide, median one slightly lower; ventral third to quarter of LAP strongly protruding ventro-proximalwards, with convex ventral edge; dorsal edge nearly straight; distal edge slightly wavy;

proximal edge concave, slightly wavy, with poorly defined, weakly prominent and protruding swollen central area, no clearly defined spurs discernible. Outer surface of LAPs with very finely meshed, seemingly smooth stereom, no vertical striation discernible. Five (proximal LAPs) to four (median ones) moderately large, ear-shaped spine articulations in notches of weakly elevated distal portion of LAP; spine articulations nearly equidistant and approximately of similar size except for slightly larger median ones; ventral lobes with weak connection with distalwards projecting tip of outer surface stereom separating notches, and merged with dorsal lobe into continuous volute; spine articulations proximally sharply bordered by edge of notches; gap between spine articulations and distal edge of LAP very narrow. Ventro-distal edge of LAP with large, rather shallow tentacle notch.

Inner side of LAPs with relatively thin, poorly defined and weakly prominent ridge devoid of conspicuously thickened parts or extensions, composed of oblique and slightly dorsalwards bent dorsal portion, and shorter ventral portion, connected with dorsal one by gentle kink and seemingly merged with ventral portion of LAP; inner side of distal edge devoid of spurs; no perforation or vertical furrow discernible. Inner side of tentacle notch concave, well defined.

Remarks. – The above described LAPs are clearly assignable to the Ophiacanthidae on account of the spine articulation structure and the absence of a single, large perforation on the inner side. Within this family, greatest affinities are shared with the LAPs of the extinct genus *Dermocoma* as suggested by the relatively small size, the continuous volute, the regular arrangement and the position within notches of the slightly elevated distal LAP edge of the spine articulations, the conspicuous ventro-proximalward pointing ventral portion of the LAPs as well as the shape of the ridge on the inner side (Thuy 2013). Among all the species and unnamed LAP types assigned to *Dermocoma*, none is compatible with the above described specimens. In fact, the lack of both a well developed vertical striation and spurs on the outer proximal and inner distal edges is a unique combination of characters in the genus *Dermocoma* (Thuy 2013). Thus, the above described material most probably belongs to a new species of *Dermocoma*. In the light of the limited amount and the poor preservation of the material available to date, however, we refrain from formally naming the new species.

The here described occurrence narrows down a lengthy stratigraphic gap in the fossil record of the genus between an unnamed new species of *Dermocoma* from the late Valanginian of Austria and another unnamed congener from the early Albian of the United Kingdom (Thuy 2013).

Occurrence. – Early Aptian of Cuchía, Spain.

Genus *Ophiojagtus* Thuy, 2013

Type species. – *Ophiojagtus acklesi* Thuy, 2013

Diagnosis for LAPs. – Ophiacanthid with stout, thick, strongly curved LAPs generally with a high height/width ratio; outer surface devoid of ornamentation elements; no spurs on outer proximal and inner distal edges; ventral portion of LAPs long to extremely long, strongly protruding ventralwards and often with widened ventral tip; proximal edge commonly with proximalwards pointing protrusion; large, ear-shaped spine articulations composed of thick, continuous volute, freestanding on bulging distal portion of LAP and not bordered proximally by a ridge-like structure; broad, well defined ridge on the inner side of the LAPs, generally with dorso-proximalwards pointing dorsal part; tentacle notch large but poorly defined and generally shallow.

Ophiojagtus acklesi Thuy, 2013

*2013 *Ophiojagtus acklesi* Thuy, p. 219; figs. 38: 5-7.

Diagnosis. – Species of *Ophiojagtus* with relatively small LAPs displaying four to five spine articulations, a very long ventral portion and a very short ridge on the inner side not extending onto the ventral portion of the LAP but with a strongly widened dorsal tip projecting onto the inner side of the well developed protrusion of the proximal LAP edge.

Remarks. – This species was described and figured in detail by Thuy (2013) on the basis of specimens which are part of the assemblage described herein.

Occurrence. – Latest Aptian of Wizard Way, Texas, U.S.A.

Ophiojagtus sp. nov.
Fig. 2.4

Material examined. – GZG.INV.78827 (figured dissociated LAP) and GZG.INV.78828 (one dissociated LAP) from Cuchía 1, and GZG.INV.78829 (three dissociated LAPs) from Cuchía 2.

Description. – Moderately large, dissociated LAPs, at most 1.5 times higher than wide; of stout and massive aspect; dorsal edge slightly concave, with conspicuously pointed dorso-proximal tip of LAP; distal edge evenly convex; proximal edge with large, rounded, non-prominent central protrusion; ventral portion of LAP very narrow, tongue shaped, devoid of thickened ventral tip, accounting for one quarter of the total LAP height. Outer surface with very finely meshed stereom, devoid of conspicuous ornamentation elements; slightly more coarsely meshed stereom on ventral portion of LAP; outer surface stereom arranged in fine, weakly developed horizontal stripes close to protrusion of proximal edge in some LAPs. Four large,

ear-shaped spine articulations freestanding on strongly bulging distal portion of LAP, and composed of a thick, continuous and slightly rugose volute; very weak dorsalward increase in size of gaps separating spine articulations; two median spine articulations larger than dorsal and ventral ones; gap between spine articulations and distal edge of LAP narrower than one spine articulation. Ventrodistal edge of LAP with very large but rather shallow tentacle notch.

Inner side of LAP with moderately wide, prominent, well defined ridge, composed of oblique, slightly proximalwards bent dorsal part with a rounded, tongue-shaped dorsal tip slightly extending onto the inner side of the protrusion of the proximal LAP edge, and a much narrower ventral part extending onto the inner side of the ventral portion of the LAP and almost reaching the ventral tip of the latter; no spurs on the inner side of the distal edge of the LAP; inner side of the tentacle notch very large but shallow and very poorly defined. No perforations discernible; very shallow, poorly defined vertical furrow distally lining ridge.

Remarks. – The above described LAPs display the highly distinctive combination of characters which is uniquely found in the extinct ophiacanthid genus *Ophiojagtus*, as described by Thuy (2013). Within this genus, no currently known species or unnamed LAP type displays a similarly narrow and short ventral portion devoid of widened ventral tip combined with a narrow ventral part of the ridge on the inner side extending well onto the inner side of the ventral LAP portion. The above described LAP type most probably belongs to a new species of *Ophiojagtus* but the limited amount and the poor preservation of the material at hand preclude a meaningful formal description.

Occurrence. – Early Aptian of Cuchía, Spain.

Family **Amphiuridae** Ljungman, 1867

Genus ***Amphilimna*** Verrill, 1899

Type species. – *Ophiocnida olivacea* Lyman, 1869

Diagnosis for LAPs. – Small to medium-sized, fragile, conspicuously triangular and strongly arched LAPs; outer surface with coarsely meshed stereom, devoid of tubercles or striation; diffuse, non-prominent and non-protruding area of more finely meshed stereom on outer proximal edge of LAP; highly distinctive, medium-sized spine articulations composed of two horizontally elongate, straight, parallel lobes separated proximally by a single lens-shaped knob extending beyond the two lobes proximally; inner side of LAP with a small, relatively short, strongly bent ridge with a ventro-distalwards pointing tip and a ventro-proximalwards pointing tip.

Amphilimna sp. nov.

Fig. 2.5

Material examined. – GZG.INV.78830 (figured dissociated LAP) and GZG.INV.78831 (8 dissociated LAPs) from Cuchía 2, and GZG.INV.78832 (3 dissociated LAPs) from Cuchía 1.

Description. – Very small, dissociated LAPs, proximal ones slightly higher than wide, distal ones nearly as high as wide; LAP outline triangular and strongly arched; dorsal edge straight to weakly convex; distal edge strongly convex; proximal edge strongly concave; ventral quarter of LAP conspicuously ventro-proximalwards protruding; outer surface with coarsely meshed stereom, becoming finer towards spine articulations; diffuse are of more finely meshed stereom in the centre of the proximal edge, non-prominent and non-protruding. Five equal-sized, nearly equidistant spine articulations integrated into outer surface stereom of distal LAP edge; spine articulations composed of two straight, parallel horizontally elongate equal-sized lobes separated proximally by a single, lens-shaped knob extending beyond lobes proximally; ventralmost spine articulation on ventro-distal tip of LAP; gap between spine articulations and distal edge of LAP very narrow.
Inner side of LAP with moderately well defined, short, strongly bent ridge with ventro-distalwards pointing tip and higher, slightly less well defined ventro-proximalwards pointing tip; no spurs on inner side of distal edge; no clearly defined perforation but very weakly defined, shallow, vertical furrow between distal tip of ridge and distal edge of LAP; inner side of tentacle notch moderately well defined, deep.

Remarks. – The above described LAPs display the highly distinctive, triangular, strongly bent outline combined with coarsely meshed outer surface stereom, spine articulations composed of two parallel lobes separated proximally by a single lens-shaped knob extending beyond the lobes proximally, and a strongly bent ridge, which unequivocally places them in the extant amphiurid genus *Amphilimna* (Fig. 2.6). Although the material available is sparse and rather poorly preserved, precluding a formal description, the find is remarkable. In fact, it represents the first fossil record of the genus, and one of the very few Lower Cretaceous occurrences of the Amphiuridae. It even marks the second oldest amphiurid record, after *Xanthamphiura hauteriviensis* Hess, 1970 from the Hauterivian of Switzerland, thus endorsing the assumption that much of the early divergence of the family took place in the Early Cretaceous (Stöhr et al. 2012).

*Occurrence.* – Early Aptian of Cuchía, Spain.
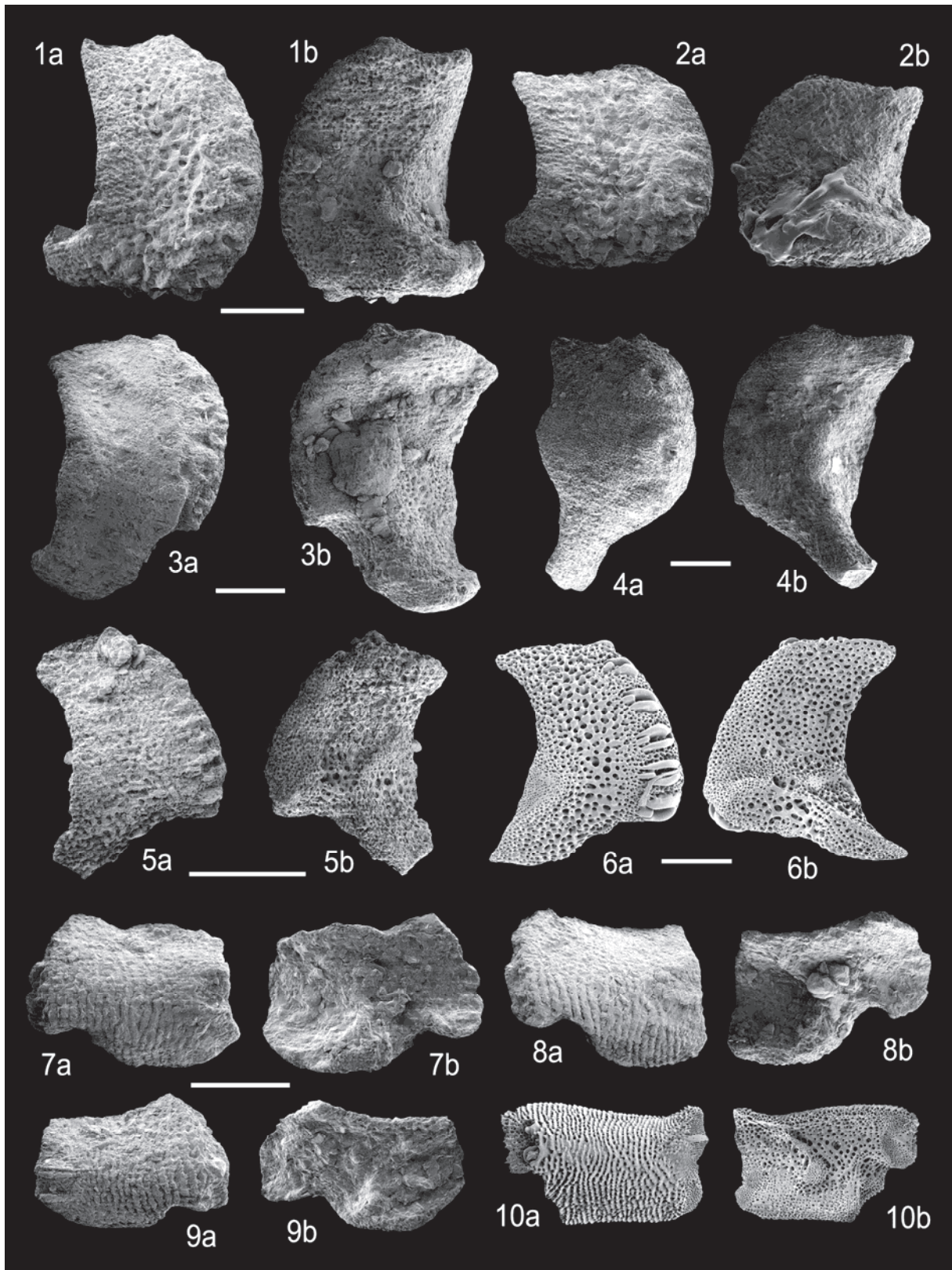
Fig. 2: **(1–2)** *Ophiacantha* sp. nov., dissociated LAPs in external (a) and internal (b) views from the early Aptian of Cuchía, Spain; **(1)** proximal LAP (GZG.INV.78820), **(2)** distal LAP (GZG.INV.78821) (both Cuchía 2 sample). **(3)** *Dermocoma* sp. nov., dissociated proximal LAP (GZG.INV.78824) in external (a) and internal (b) views from the early Aptian of Cuchía, Spain (Cuchía 2 sample). **(4)** *Ophiojagtus* sp. nov., dissociated proximal LAP (GZG.INV.78827) in external (a) and internal (b) views from the early Aptian of Cuchía, Spain (Cuchía 2 sample). **(5)** *Amphilimna* sp. nov., dissociated proximal LAP (GZG.INV.78830) in external (a) and internal (b) views from the early Aptian of Cuchía, Spain (Cuchía 2 sample). **(6)** *Amphilimna olivacea*, recent, proximal LAP in external (a) and internal (b) views. **(7–9)** *Ophioleuce sanmigueli* sp. nov., dissociated LAPs in external (a) and internal (b) views; **(7)** proximal LAP (holotype, GZG.INV.78833) (Cuchía 1 sample), **(8)** median LAP (paratype, GZG.INV.78835) (Cuchía 2 sample), **(9)** distal LAP (paratype, GZG.INV.78834) (Cuchía 1 sample). **(10)** *Ophioleuce brevispinum*, Recent, median LAP in external (a) and internal (b) views. All scale bars equal 250 μm.

Family **Ophiuridae** Müller & Troschel, 1840
Subfamily **Ophioleucinae** Matsumoto, 1915

Genus *Ophioleuce* Koehler, 1904

Type species. – *Ophioleuce seminudum* Koehler, 1904
Diagnosis for LAPs. – Small, fragile LAPs generally with a low height/width ratio; outer surface ornamentation commonly consisting in a vertical striation composed of overlapping lamellae; commonly well developed, horizontally elongate spurs on the outer proximal and inner distal edges; tentacle notch moderately deep, with ventro-distal tip of LAP weakly projecting ventralwards; inner side of LAP generally with a simple, narrow ridge, in some cases continuous, in some cases divided in two parts.

Ophioleuce sanmigueli sp. nov.

Figs. 2.7–9

Etymology. – The species is dedicated to the family of Basilio Coz San Miguel in Boo de Piélagos (Cantabria, northern Spain) for the friendship and support throughout the years to one of us (FW).

Diagnosis. – Species of *Ophioleuce* with very small, fragile LAPs; proximal LAPs 1.5 times wider than high; weakly developed constriction; two well defined, horizontally elongate spurs on the outer proximal and inner distal edges; outer surface almost completely covered by fine, regular vertical striation composed of overlapping lamellae with smooth distal edge proximally, and coarsely denticulate distal edge distally; three small spine articulations with dorsalward decrease in size; tentacle notch moderately deep, with ventro-distal tip of LAP weakly projecting ventralwards; inner side of LAP with simple, continuous, narrow ridge devoid of widened parts.

Type locality and horizon. – Cuchía 1 sample, Marl Member of the Caranceja Formation, *Deshayesites weissi* Zone, middle early Aptian of Cuchía, Cantabria, Spain.

Type material. – GZG.INV.78833 (holotype); GZG.INV. 78834 (paratype) from Cuchía 1 and GZG.INV.78835 (paratype) from Cuchía 2.

Additional material. – GZG.INV.78836 (8 dissociated LAPs) from Cuchía 2, and GZG.INV.78837 (5 dissociated LAPs) from Cuchía 1.

Description of holotype. – GZG.INV.78833 is a very small, dissociated proximal LAP of very fragile aspect; approximately 1.5 times wider than high; dorsal edge slightly fragmented, originally concave as a result of a weak constriction; ventral quarter of LAP protruding ventralwards, with slightly angular, convex ventral edge; distal edge irregularly convex; proximal edge nearly straight, with two sharply defined, lens-shaped, horizontally elongate, prominent but only very weakly protruding spurs; dorsal spur

slightly larger than ventral one; slightly depressed area between spurs; outer surface predominantly covered by fine, regular vertical striation composed of distalwards overlapping, thin lamellae; distal edge of lamellae smooth in proximal lamellae, and coarsely denticulate in distal ones; lamellae replaced by finely meshed stereom in dorso-proximal area of outer surface; ventral portion of LAP entirely covered by striation. Three small, inconspicuous spine articulations inserted in deep notches of the distal LAP edge; weak dorsalward decrease in size of spine articulations and of gaps separating them; spine articulations composed of a small, thin, vertically elongate and nearly straight proximal lobe overlapped by distalmost lamella of outer surface striation, and slightly larger, higher, vertically elongate but bent distal lobe; gap between spine articulations and distal edge of LAP composed of very thin stereom, narrower than one spine articulation, widest ventrally and rapidly decreasing in width dorsalwards. Tentacle notch large, comparatively deep and well defined, with ventro-distal tip of LAP slightly projecting ventralwards.
Inner side of LAP with sharply defined, narrow simple ridge devoid of thickened parts and composed of a nearly straight, oblique dorsal portion; ventral portion of the ridge half as long as the dorsal one, connected with the latter by a gentle kink and with ventral tip sharply separated from inner side of ventral LAP portion; inner side of distal edge with two well defined, horizontally elongate, prominent but not protruding spurs; ventral spur larger than dorsal one; inner side of tentacle notch sharply defined, distally and proximally bordered by slightly thickened edge. No perforations or vertical furrow discernible.

Paratype supplements and variation. – GZG.INV.78835 is a very small, dissociated proximal to median LAP, approximately 1.5 times wider than high; dorsal edge evenly concave; ventral portion amounting for almost one third of the total LAP height; spurs on proximal edge of LAP similar to those of holotype but dorsal spur slightly smaller than ventral one; outer surface ornamentation as in holotype. Three spine articulations similar in shape, size, position and arrangement to those of holotype. Tentacle notch slightly deeper than in holotype, with ventro-distal tip of LAP slightly more strongly projecting ventralwards.
Inner side well in agreement with that of holotype. Ridges on inner distal edge slightly smaller and less well defined than in holotype.

GZG.INV.78834 is a very small, dissociated distal LAP, almost two times wider than high; dorsal edge evenly concave; ventral portion accounting for one fifth of the total LAP height; spurs on outer proximal edge as in holotype but dorsal one much larger than ventral one; outer surface ornamentation as in holotype, with slightly better developed coarsely denticulate distal edge of the distal lamellae. Three spine articulations similar in size, shape, position and arrangement to those of holotype. Inner side partly obscured by sediment but well in agreement with holotype as far as discernible.
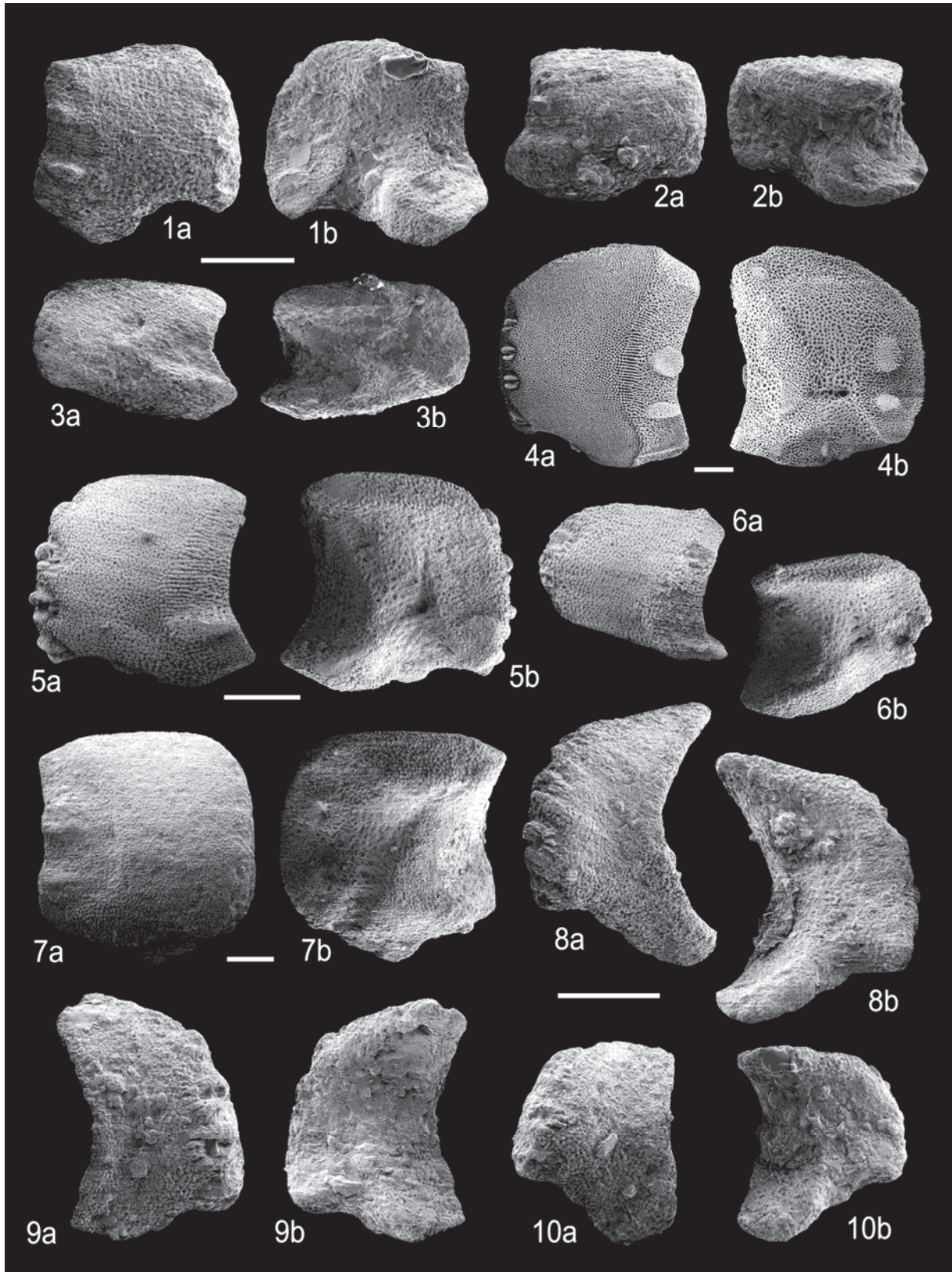
Fig. 3: **(1–3)** *Ophiozonella eloy* sp. nov., dissociated LAPs in external (a) and internal (b) views, from the early Aptian of Cuchía, Spain; **(1)** proximal LAP (holotype, GZG.INV.78838), (2) median LAP (paratype, GZG.INV.78839) (both Cuchía 1 sample), **(3)** distal LAP (paratype, GZG.INV.78840) (Cuchía 2 sample). **(4)** *Ophiozonella nivea*, recent, proximal LAP in external (a) and internal (b) views. **(5–6)** *Ophiozonella thomasi* sp. nov., dissociated LAPs from the latest Aptian of Wizard Way, Texas; **(5)** proximal LAP (holotype, GZG.INV.78843), **(6)** distal LAP (paratype, GZG.INV.78844). **(7)** *Ophiotitanos*? sp., dissociated median(?) LAP (GZG.INV.78845) in external (a) and internal (b) views, from the early Aptian of Cuchía, Spain (Cuchía 2 sample). **(8–10)** *Ophiodoris*? sp. nov., dissociated LAPs in external (a) and internal (b) views, from the early Aptian of Cuchía, Spain; **(8)** proximal LAP (GZG.INV.78848), **(9)** proximal LAP (GZG.INV.78849) (both Cuchía 2 sample), **(10)** median to distal LAP (GZG.INV.78851) (Cuchía 1 sample). All scale bars equal 250 μm.

Remarks. – The very fragile nature of the above described LAPs, the fine vertical striation, the comparatively deep tentacle notches as well as the spine articulations composed of a straight vertical proximal lobe and a slightly larger, bent vertical distal lobe, defined by Martynov (2010) as irregular rhombic spine articulation, strongly favours an assignment to the ophiurid subfamily Ophioleucinae (Fig. 2.10). Knowledge on the fossil record of this group has been rather sparse so far. Hess (1964) introduced the new genus *Sinosura* for fossil ophiuroid remains from the Pliensbachian of the United Kingdom and discussed possible ophioleucinin affinities of the new genus.

Smith et al. (1995) tentatively placed *Sinosura* in the Ophioleucinae, a view later challenged by Hess & Meyer (2008) but then again explicitly endorsed by Thuy et al. (2011) on the basis of new observations on pristinely preserved material. *Ophiopinna* Hess, 1960 from the Callovian of France is another fossil ophiuroid for which ophioleucinin affinities have been suggested (Hendler & Miller 1991). A third fossil ophiuroid with supposed ophioleucinin affinities was described by Thuy (2011) as *Eirenura papillata* Thuy, 2011, from the Pliensbachian of France. Recently, ophiuroid material from Aptian deep-sea sediment cores were assigned to the extant genus *Ophioleuce* on the basis of striking similarities in LAP morphology with recent *Ophioleuce brevispinum* (H. L. Clark, 1911) (Thuy et al. 2012).

The above described ophioleucinin occurrence thus significantly adds to the rather fragmentary knowledge of the fossil record of a seemingly ancient but poorly documented ophiuroid group. On genus level, the LAPs in question are incompatible with any of the currently known fossil genera with supposed ophioleucinin affinities. LAPs of *Sinosura* generally have significantly more spine articulations, deeper tentacle notches and differently shaped ridges on the inner side. In *Ophiopinna*, some of the LAPs display highly distinctive articulations for the feather-shaped arm spines, and *Eirenura* has relatively high, rectangular LAPs with numerous spine articulations and a very weak vertical outer surface striation composed of small scales arranged in vertical rows. Among the extant representatives of the Ophioleucinae, however, striking similarities in LAP morphology are shared with *Ophioleuce*. The above described LAPs are thus assigned to this genus. Confusion with the probable congener from the Aptian deep-sea sediments of the North Atlantic (Thuy et al. 2012) is precluded on account of the discontinuous ridge on the inner side of the latter.

Recent representatives of the Ophioleucinae are restricted to deep-sea settings (Thuy et al. 2012). The here described material from shallow marine deposits represents the youngest record of the family at shelf depths.

Occurrence. – Early Aptian of Cuchía, Spain.

Family **Ophiolepididae** Ljungman, 1867

Genus *Ophiozonella* Matsumoto, 1915

Type species. – *Ophiozonella longispina* H. L. Clark, 1908

Diagnosis for LAPs: Ophiolepidid with rather stout, compact LAPs with straight to evenly convex rather than pointed dorsal edge; relatively small ventral portion protruding ventro-proximalwards; outer proximal and inner distal edges generally with one or two well developed, horizontally elongate spurs composed of densely meshed but not massive stereom; relatively small spine articulations composed of nearly parallel dorsal and ventral lobes connected proximally by one to three minute knobs; large and deep tentacle notch; inner side of LAPs with poorly defined and weakly prominent, vertical, slightly proximalwards bent ridge.

Ophiozonella eloy sp. nov.

Figs. 3.1–3

Etymology. – Species named after the Family Eloy in Liénceres (Cantabria). The Bar Eloy and the Autoservicio Eloy have been important alimentation, information and social centres for one of the authors (F.W.) during his large number of field campaigns to the area since 1990.

Diagnosis. – Species of *Ophiozonella* with relatively small LAPs, two spurs on the outer proximal and inner distal edges; ventral spurs larger than the dorsal one; fine horizontal striation between the spurs, at least in proximal LAPs; up to four small, nearly equal-sized spine articulations integrated into the outer surface stereom of the distal LAP edge; relatively deep tentacle notch; ridge on inner side poorly defined, weakly prominent, proximalwards bent; inner side of tentacle notch encompassed distally and proximally by thickened edges.

Type locality and horizon. – Cuchía 1 sample, Marl Member of the Caranceja Formation, *Deshayesites weissi* Zone, middle early Aptian of Cuchía, Cantabria, Spain.

Type material. – GZG.INV.78838 (holotype); GZG.INV. 78839 (paratype) from Cuchá 1 and GZG.INV.78840 (paratype) from Cuchía 2.

Additional material. – GZG.INV.78841 (43 dissociated LAPs) from Cuchía 1, and GZG.INV.78842 (141 dissociated LAPs) from Cuchía 2.

Description of holotype. – GZG.INV.78838 is a small, dissociated proximal LAP, nearly as high as wide; dorsal edge straight; distal edge evenly convex; ventral fifth of LAP protruding ventro-proximalwards; proximal edge concave with two well defined, oval, horizontally elongate, prominent but only weakly protruding spurs, ventral one larger than dorsal one; proximal edge of LAP lined by an area of finely meshed stereom, encompassing spurs, and with fine

horizontal striation between the spurs; remaining outer surface of LAP with moderately coarsely meshed stereom. Four small spine articulations integrated into outer surface stereom near distal edge of LAP; spine articulations nearly equidistant and of similar size except for slightly smaller dorsalmost one; small, short, horizontally elongate dorsal and ventral lobes of spine articulation proximally connected by two to three small, round knobs; gap between spine articulations and distal edge of LAP slightly narrower than one spine articulation. Tentacle notch large, well defined and relatively deep, with ventro-distal tip of LAP projecting ventralwards.

Inner side of LAP with poorly defined, weakly prominent, slightly proximalwards bent vertical ridge; ventral part of ridge not merged with thickened ventral edge of LAP, better defined and more strongly prominent than dorsal part of ridge; inner side of distal edge with two well defined, oval, horizontally elongate spurs, ventral one of which clearly larger than dorsal one; inner side of tentacle notch conspicuously well defined, large, deep, distally and proximally encompassed by thickened edges. No perforations or vertical furrow discernible.

Paratype supplements and variation. – GZG.INV.78839 is a small, dissociated median LAP, slightly wider than high; generally well in agreement with holotype; dorsal edge weakly convex; two spurs on proximal edge, slightly larger but less well defined than in holotype; fine horizontal striation between spurs not discernible. Three small, poorly preserved spine articulations seemingly similar to those of holotype; dorsal gap between spine articulations slightly larger than ventral one. Tentacle notch shallower than in holotype. Ridge on inner side of LAP very poorly defined, slightly shorter and more strongly bent than in holotype; spurs on inner side of distal edge hardly discernible; inner side of dorsal thickened.

GZG.INV.78840 is a small, dissociated distal LAP, approximately 1.5 times wider than high; dorsal edge weakly convex; two spurs on outer proximal edge, much larger than in holotype but less sharply defined; ventral spurs conspicuously larger than dorsal one; no fine horizontal striation discernible between spurs; Three small, nearly equidistant spine articulations similar to those of holotype. Tentacle notch much shallower than in holotype. Ridge on inner side as in holotype but more strongly oblique; two spurs on inner distal edge large but very weakly defined; inner side of dorsal edge thickened.

Remarks. – The above described LAPs show striking similarities with those of extant ophiolepidid *Ophiozonella*, in particular *O. nivea* (Lyman, 1875) (Fig. 3.4) on account of the shape, number and size of the spine articulations, the two spurs on the outer proximal and inner distal edges, the presence of a fine horizontal striation associated the spurs, and the shape of the ridge on the inner side. The material in question is thus assigned to the extant genus *Ophiozonella*. Very similar LAPs were described as *Ophiozonella stoehrae* Thuy & Kroh, 2011 from the Barremian of

France. These differ, however, in displaying much larger spine articulations, a single spur on the outer proximal and inner distal edges and a much more sharply defined ridge on the inner side. The same holds true for the LAPs of the slightly younger *Ophiozonella thomasi* sp. nov. (see below).

The here described Aptian specimens share similarities with some of the dissociated LAPs assigned to the extinct genus *Ophiopetra* Enay & Hess, 1962, in particular *Ophiopetra bathonica* Hess, 1964 and some of the LAP types described as *Ophiopetra? oertlii* Hess, 1965 (Hess 1965a; Kutscher 1996). The type species *Ophiopetra lithographica* Enay & Hess, 1962, in contrast, most probably belongs to the Ophiacanthidae, as a recent re-examination of the type material surprisingly revealed (previously unpublished). Disentangling the *Ophiopetra*-complex and correctly re-assigning the different species and LAP types exceeds the scope of the present study. The relevant point here is that assignment of the above described LAPs to *Ophiopetra* can be excluded on account of the probably ophiacanthid affinities of the type species.

Occurrence. – Early Aptian of Cuchía, Spain.

Ophiozonella thomasi sp. nov.

Figs. 3.5–6

Etymology. – Species named in honour of Thomas Daniel, for his friendship and his inestimable support to one of the authors (BT) of this study during the years in Göttingen.

Diagnosis. – Species of *Ophiozonella* with medium-sized LAPs of rounded squarish outline; ventral sixth of LAP protruding ventro-proximalwards; single well defined spur on the outer proximal and inner distal edges; outer surface with finely meshed stereom, with trabecular intersections transformed into tiny, polygonal tubercles; up to four relatively large spine articulations; inner side with moderately well defined, weakly prominent ridge with slightly widened dorsal tip.

Type locality and horizon. – Wizard Way, Texas, USA; Echinoid Marker Bed of Smith & Rader (2009), base of Unit 2 of the Lower Member of the Glen Rose Formation, latest Aptian.

Type material. – GZG.INV.78843 (holotype); GZG.INV. 78844 (paratype).

Description of holotype. – GZG.INV.78843 is a medium-sized, dissociated proximal LAP, nearly as high as wide and of rounded squarish aspect; dorsal edge weakly convex; distal edge evenly convex; proximal edge evenly concave, with a single, large, well defined, prominent but not protruding, horizontally elongate spur composed of slightly more densely meshed stereom than remaining proximal edge and positioned in the middle of the ventral half of the edge; band of conspicuous, fine horizontal striation lining

proximal edge, widest in the middle of the proximal edge, more quickly narrowing dorsalwards than ventralwards; ventral sixth protruding ventro-proximalwards; outer surface with finely meshed stereom, with trabecular intersections developed into small polygonal tubercles. Four relatively large, nearly equal-sized spine articulations in shallow notches of distal edge of LAP, composed of parallel, horizontal dorsal and ventral lobes connected proximally by one to three small knobs; weak dorsalward increase in size of gaps separating spine articulations; gap between spine articulations and distal edge extremely narrow. Large, well defined but relatively shallow tentacle notch, with conspicuous, convex, ventralwards pointing protrusion in the proximal half of the notch.

Inner side of LAP with narrow, moderately well defined, weakly prominent, slightly oblique ridge with weakly widened dorsal tip; ventral tip of ridge not merged with thickened ventral edge of LAP; dorsal and ventral parts of the ridge connected by a very gently kink; inner side of distal edge with relatively small, poorly defined, slightly horizontally elongate, oval, weakly prominent knob; large, slightly irregular perforation between the kink of the ridge and the distal edge of the LAP, with well defined, short, dorsalwards projecting vertical furrow; inner side of tentacle notch large, well defined, distally and proximally bordered by thickened edges.

Paratype supplements. – GZG.INV.78844 is a medium-sized, dissociated distal LAP, approximately 1.5 times wider than high; generally well in agreement with holotype; spur on proximal edge less well defined and very close to the ventro-proximal tip of the LAP; band of fine horizontal striation lining proximal edge less well developed than in holotype; three spine articulations similar in shape, size, position and arrangement to those of holotype; ventralmost spine articulation largely lost due to fragmentation of the plate; tentacle notch very shallow.

Ridge on inner side of LAP similar to that of holotype but shorter and slightly more strongly bent; ventro-distal edge of LAP broken, no spur discernible; perforation between kink of ridge and distal edge of LAP slightly smaller than in holotype and dorsally bordered by two smaller perforations rather than furrow; tentacle notch as in holotype.

Remarks. – Assignment of the above described LAPs to *Ophiozonella* is based on the striking similarities with the LAPs of modern representatives of the genus, in particular with respect to the shape of the LAPs, the size, position and shape of the spine articulations, the ornamentation of the outer proximal edge, the shape of the ridge on the inner side and the development of the tentacle notch. LAPs of the slightly older congener *Ophiozonella eloy* sp. nov. from Spain (see above) can be easily distinguished since they display two spurs on the outer proximal and inner distal edges, much smaller spine articulations, deeper tentacle notches and a less well defined ridge on the inner side. Greatest similarities are shared with the LAPs of

Ophiozonella stoehrae from the Barremian of France (Thuy & Kroh 2011). These differ in the larger ventro-proximalwards projecting ventral portion, the irregular vertical striation on the outer surface, the absence of the band of fine horizontal striation lining the outer proximal edge, and the more strongly prominent ridge on the inner side.

Although the amount of material is very limited, the LAPs at hand are so clearly distinctive, also thanks to the excellent preservation, that they are taken here as a basis for the description of a new species.

Occurrence. – Latest Aptian of Wizard Way, Texa, U.S.A.

Family **Ophiodermatidae** Ljungman, 1867

Genus *Ophiotitanos* Spencer, 1907

Type species. – *Ophiotitanos tenuis* Spencer, 1907

Diagnosis for LAPs. – Ophiodermatid with large LAPs of stout, massive aspect; two well defined, prominent and protruding spurs on outer proximal edge, paralleled by two well defined, weakly prominent spurs on inner distal edge; no fine horizontal striation on outer proximal edge; numerous (generally more than six) small spine articulations sunken in shallow notches of distal edge; inner side ventral tip of LAP devoid of strongly prominent knobs; tentacle notch commonly developed as within-plate perforation in distal and, in some cases, even median LAPs.

Ophiotitanos? sp.
Fig. 3.7

Material examined. – GZG.INV.78845 (figured LAP) and GZG.INV.78846 (8 dissociated LAPs) from Cuchía 2, and GZG.INV.78847 (one dissociated LAP) from Cuchía 1.

Description. – Large, dissociated median to distal LAPs of very stout and massive aspect, rounded squarish in outline; nearly as high as wide to slightly wider than high; dorsal, ventral and distal edges evenly convex; proximal edge concave with two large, nearly equal-sized, moderately well defined, prominent but weakly protruding, horizontally elongate spurs in slightly sunken, semicircular depression of proximal edge; outer surface with very finely meshed stereom with trabecular intersections transformed into tiny tubercles in some plates merged into short vertical rows near ventral edge of LAP; up to five very small, nearly equal-sized and equidistant spine articulations sunken into shallow notches of distal edge of LAP; spine articulations composed of two oblique lobes, a slightly curved dorsal one and a smaller, straight ventral one; gap between spine articulations and distal edge of LAP narrower than one spine articulation. Tentacle notch invisible in external view.

Inner side of LAPs with relatively large, moderately well defined, prominent, tongue-shaped, vertical ridge, with rounded proximalwards bent dorsal tip and slightly widened, ventralwards pointing ventral tip not merged with ventral edge of LAP; inner side of distal edge of LAP with two large, nearly equal-sized, poorly defined and weakly prominent spurs composed of slightly more finely meshed stereom; dorsal and ventral edges of LAP thickened; tentacle notch developed as narrow, sharply defined, oblique furrow. No perforations discernible.

Remarks. – The above described LAPs share greatest similarities with the LAPs figured by Thuy & Kroh (2011: pl. 4, figs. 2-3) as *Ophiotitanos* sp., with respect to the stout and massive general aspect, the rounded squarish outline, the shape, size and position of the spine articulations, the two spurs on the outer proximal and inner distal edges, the shape of the ridge on the inner side and the development of the tentacle notch. Assuming that the here described LAPs are, indeed, median to distal ones, they are best assigned to the extinct genus *Ophiotitanos*. Given the sparse nature of the material available, however, it cannot be ruled out that the LAPs in question are, in fact, proximal ones of a yet unknown genus. In the light of these uncertainties, the LAPs at hand are best treated as an unnamed record tentatively assigned to *Ophiotitanos*.

In any case, spine articulation morphology in combination with the two spurs on the outer proximal and inner distal edges and the tongue-shaped ridge on the inner side strongly suggest ophiodermatid affinities. Thuy & Kroh (2011) transferred *Ophiotitanos* to the Ophiuridae, arguing that the distal tentacle openings developed as within LAP perforations challenge assignment to the Ophiodermatidae. New investigations on distalmost LAPs of recent ophiodermatids, however, revealed that within-plate perforations are not uncommon in a number of genera, among others *Ophiarachnella* Ljungman, 1872. We thus re-transfer *Ophiotitanos* to the Ophiodermatidae, in agreement with Kutscher & Jagt (2000), stressing, however, that the general skeletal morphology of *Ophiotitanos* is in need of reappraisal in order to definitely clarify its higher taxonomic position.

Occurrence. – Early Aptian of Cuchía, Spain.

Family **Ophionereididae** Ljungman, 1867

Genus *Ophiodoris* Koehler, 1904

Type species. – *Ophiodoris malignus* Koehler, 1904

Diagnosis for LAPs. – Ophionereidid with relatively small, fragile LAPs displaying a large, ventro-proximalwards protruding ventral portion; outer surface covered by small to medium-sized tubercles; large spine articulations in shallow notches of weakly bulging distal portion of LAP; spine articulations composed of a large, horizontally elongate, slightly bent dorsal lobe and a smaller, horizontally elongate, straight ventral lobe; both lobes proximally separated by one to three slightly horizontally elongate knobs; inner side of LAPs with well defined ridge composed of a nearly vertical dorsal part with a ventralwards pointing extension on its ventral tip, a strongly oblique median part and a less well defined ventro-proximalwards pointing ventral part; single, large perforation near kink between median and ventral ridge parts.

Ophiodoris? sp. nov.

Figs. 3.8–10

Material examined. – GZG.INV.78848 (figured LAP), GZG.INV.78849 (figured LAP) and GZG.INV.78850 (148 dissociated LAPs) from Cuchía 2, and GZG.INV.78851 (figured LAP) and GZG.INV.78852 (91 dissociated LAPs) from Cuchía 1.

Description. – Very small, dissociated LAPs, proximal ones slightly higher than wide, sickle-shaped; median and distal ones as wide as long to slightly wider than long, not sickle-shaped; dorsal edge oblique, straight in proximal LAPs, weakly convex in median to distal ones; dorso-proximal tip conspicuously pointed in proximal LAPs; distal edge evenly convex; proximal edge evely concave, with poorly defined, almost indiscernible and very weakly protruding thickened central part; ventral third protruding ventro-proximalwards, conspicuously narrow in proximal LAPs; outer surface covered by very small tubercles, merged into very weak, irregular vertical rows near spine articulations. Four (proximal LAPs) to three (distal LAPs) large spine articulations in very shallow notches of slightly bulging distal portion of LAPs; spine articulations composed of a large, horizontally elongate, slightly bent dorsal lobe and a smaller, horizontally elongate, straight ventral lobe; both lobes proximally separated by two to three small, elongate knobs; spine articulations nearly equidistant, separated by tubercules of outer surface stereom; median spine articulations slightly larger than dorsalmost and ventralmost ones. Tentacle notch very large, relatively shallow.

Inner side of LAPs with moderately well defined, narrow ridge composed in proximal LAPs of a nearly vertical, straight dorsal part, a more strongly oblique, poorly defined median part and a similarly poorly defined ventro-proximalwards pointing ventral part not merged with ventral edge of LAP; ventral tip of dorsal part with poorly defined ventralwards pointing extension; all parts connected with rounded kinks; inner side of distal LAPs too poorly preserved to allow for distinction of ridge morphology; single, relatively large perforation near kink between median and ventral parts of ridge, with weakly defined, shallow vertical furrow projecting dorsalwards from perforation; inner side of tentacle notch large, well defined, distally and proximally encompassed by thickened edges.

Remarks. – The above described LAPs display a highly distinctive spine articulation morphology exclusively found in the LAPs of extant Ophionereididae and in some representatives of the Ophiochitonidae (Martynov 2010). The shape of the ridge on the inner side in combination with a single large perforation further endorses these affinities. The sickle-shaped outline of the LAPs, the outer surface ornamentation and the rather shallow tentacle notch not encompassed distally by a ventralwards protruding ventro-distal tip of the LAP favour assignment to the Ophionereididae. Within this family, similarities are greatest with *Ophiodoris* on account of the more fragile aspect of the LAPs but assignment to any of the other four ophionereidid genera cannot be satisfyingly ruled out as long as the respective LAPs have not been examined in detail. On account of this preliminary observation as well as the striking similarities with the LAPs of slightly younger *Ophiodoris holterhoffi* sp. nov. (see below), known from more conclusive material, we tentatively refer the above described LAPs to *Ophiodoris*. They can be easily told apart from the LAPs of *Ophiodoris holterhoffi* sp. nov. due to the pointed dorso-proximal tip, the two to three knobs separating the dorsal and ventral lobes of the spine articulations, and the outer surface ornamentation.

Occurrence. – Early Aptian of Cuchía, Spain.

Ophiodoris holterhoffi sp. nov.

Figs. 4.1–8

Etymology. – Species named in honour of Frank Holterhoff, who kindly assisted one of the authors (A.S.G.) during fieldwork in Texas.

Diagnosis. – Species of *Ophiodoris* with very small, fragile LAPs; dorso-proximal tip of LAP truncated; outer surface with coarse tuberculation; up to four large spine articulations on slightly bulging distal edge of LAP, with dorsal and ventral lobes proximally separated by up to two medium-sized to large knobs.

Type locality and horizon. – Wizard Way, Texas, USA; Echinoid Marker Bed of Smith & Rader (2009), base of Unit 2 of the Lower Member of the Glen Rose Formation, latest Aptian.

Type material. – GZG.INV.78853 (holotype); GZG.INV. 78854, GZG.INV.78855, GZG.INV.78856, GZG.INV. 78857, GZG.INV.78858, GZG.INV.78859 and GZG. INV.78860 (paratypes).

Additional material. – GZG.INV.78861 (374 dissociated LAPs), GZG.INV.78862 (23 dissociated vertebrae) and GZG.INV.78863 (5 dissociated oral plates).

Description of holotype. – GZG.INV.78853 is a small, dissociated proximal LAP, slightly higher than wide; dorsal edge nearly straight; dorso-proximal tip truncated in external view; distal edge gently convex; proximal edge weakly concave, with very weak, slightly prominent, poorly defined central protrusion; narrow band of fine, irregular horizontal striation lining proximal edge except for ventral quarter, widest around central protrusion; small, poorly defined, weakly prominent and non-protruding, horizontally elongate, thin spur near ventro-proximal tip of LAP; ventral quarter of LAP conspicuously protruding ventro-proximalwards; outer surface with coarse, tightly packed, slightly vertically elongate tubercles, coarsest around and between spine articulations, less densely packed on ventral portion of LAP. Four large, conspicuous, nearly equidistant spine articulations composed of a smooth, vertically elongate, slightly bent dorsal lobe and a smaller, smooth, vertically elongate and nearly straight ventral lobe; both lobes separated proximally by single, large knob; spine articulations in very shallow notches of weakly bulging distal portion of LAP; second ventralmost spine articulation largest, dorsalmost one smallest; gap between spine articulations and distal edge of LAP very narrow. Tentacle notch very large and deep.

Inner side of LAP with conspicuous, sharply defined, relatively narrow ridge composed of three parts; dorsal part slightly oblique, almost vertical, with widened ventralwards pointing extension on ventral tip; median part oblique, connected with dorsal and ventral parts by gentle kinks; ventral part well defined dorsally, becoming decreasingly prominent and well defined ventralwards but not merged with ventral edge of LAP; dorso-proximal tip pointed in internal view; inner side of distal edge devoid of spurs; single, medium-sized perforation distally bordering kink between median and ventral parts of ridge, with poorly defined, shallow, vertical furrow projecting dorsalwards from perforation; inner side of tentacle notch well defined, with coarsely meshed, slightly horizontally elongate stereom, encompassed distally and proximally by thickened edges.

Paratype supplements and variation. – GZG.INV.78854 is a small, dissociated proximal LAP; very well in agreement with holotype; dorsal and ventral lobes of spine articulations proximally separated by two medium-sized knobs rather than a single large one. Inner side as in holotype.

GZG.INV.78855 is a small, dissociated median LAP, nearly as high as wide; dorsal edge gently convex; proximal edge and outer surface ornamentation as in holotype, except for better defined, more strongly prominent small spur near ventro-proximal tip of LAP; ventral third of LAP protruding ventro-proximalwards. Three spine articulations similar in shape and position to those of holotype, except for two medium-sized knobs proximally separating dorsal and ventral lobes of spine articulations; median spine articulation slightly larger than ventral and dorsal ones. Inner side as in holotype, except for larger perforation but almost indiscernible vertical furrow dorsalwards projecting from the perforation.
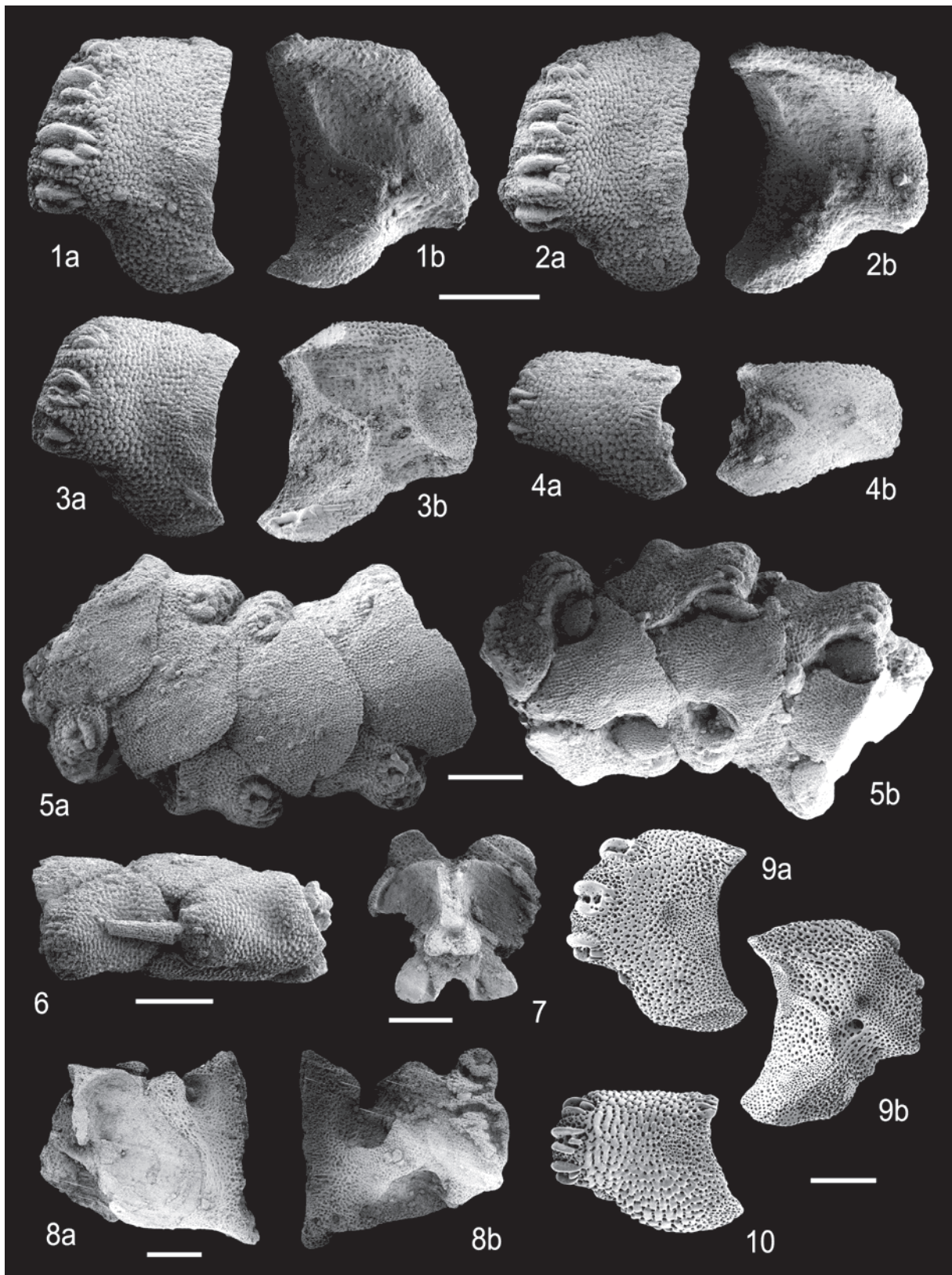
Fig. 4: **(1–8)** *Ophiodoris holterhoffi* sp. nov. from the latest Aptian of Wizard Way, Texas. **(1)** proximal LAP (holotype, GZG.INV.78853), **(2)** proximal LAP (paratype, GZG.INV.78854), **(3)** median LAP (paratype, GZG.INV.78855), **(4)** distal LAP (paratype, GZG.INV.78856) [all in external (a) and internal (b) views], **(5)** proximal arm fragment (paratype, GZG.INV.78857) in dorsal (a) and ventral (b) views, **(6)** distal arm fragment (paratype, GZG.INV.78858) in lateral view, **(7)** vertebra (paratype, GZG.INV.78859) in dorso-distal view, **(8)** oral plate (paratype, GZG.INV.78860) in adradial (a) and abradial (b) views. **(9–10)** *Ophionereis porrecta*, recent; **(9)** proximal LAP in external (a) and internal (b) views, **(10)** distal LAP in external view. All scale bars equal 250 µm.

Table 1: Faunal spectra of the three assemblages described herein and of the Blake Nose assemblage described by Thuy et al. (2012) with additional data from Thuy (2013).

Family	Cuchía 1 & 2 (early Aptian)	Texas (latest Aptian)	Blake Nose (latest Aptian)
Ophiacanthidae	*Ophiacantha* sp. nov.	*Ophiojagtus acklesi*	*Ophiologimus martynovi*
	Ophiojagtus sp. nov.		*Ophiologimus aiodipius*
	Dermocoma sp. nov.		*Ophiotoma incredibilis*
			Ophiolimna kucerai
			Ophiacantha sp. nov. 1
			Ophiacantha sp. nov. 2
			Ophiotreta sp. nov.
			Ophiacanthid indet.
Ophiomycetidae			*Ophiotholia* sp. nov.
Ophiolepididae	*Ophiozonella eloy*	*Ophiozonella thomasi*	*Ophiomusium* sp. nov.
Ophiuridae	*Ophioleuce sanmigueli*		*Ophioleuce* sp. nov.
Ophiodermatidae	*Ophiotitanos*? sp.		
Amphiuridae	*Amphilimna* sp. nov.		
Ophionereididae	*Ophiodoris*? sp. nov.	*Ophiodoris holterhoffi*	

GZG.INV.78856 is a small, dissociated distal LAP; almost 1.5 times wider than high; dorsal edge very weakly convex; no spur discernible near ventro-proximal edge of LAP; ventral quarter of LAP protruding ventro-proximalwards. Three nearly equal-sized spine articulations similar in shape and position to those of holotype. Tentacle notch large but very shallow. Ridge on inner side relatively narrow, sharply defined, prominent, composed of an oblique, proximalwards bent dorsal part with a widened dorsal tip displaying a ventralwards projecting extension, and a less well defined ventral part; both parts of the ridge connected by a rounded kink; large, poorly defined perforation between kink and distal edge of LAP; no vertical furrow discernible; inner side of tentacle notch very large, well defined, encompassed distally and proximally by thickened edges.

GZG.INV.78857 is an articulated arm fragment composed of three proximal to median arm segments; LAP morphology well in agreement with holotype and other paratypes; dorsal arm plates very large, slightly wider than long, wider than half the total width of the arm; with rounded obtuse distal angle, pointed right lateral angles, and straight to slightly convex, latero-proximal edges; proximal angle not discernible, covered by neighbouring dorsal arm plates; outer surface of dorsal arm plates uniformly covered by tubercles, slightly smaller than tubercles covering outer surface of LAPs; neighbouring dorsal arm plates overlapping. No accessory dorsal arm plates. Ventral arm plates large, slightly longer than wide, widest distally, with weakly convex distal edge, pointed latero-distal tips, deeply concave tentacle notches on lateral edges, slightly concave latero-proximal edges and pointed proximal angles; outer surface of ventral arm plates uniformly covered by tubercles slightly smaller than those covering the outer surface of the LAPs; tentacle openings covered by a large, leaf-like, very weakly longitudinally striated scale; at least one much smaller additional scale on lateral edge of ventral arm plate. No arm spines preserved.

GZG.INV.78858 is an articulated arm fragment composed of two distal segments; LAP morphology well in agreement with distal paratype LAPs; dorsal arm plates slightly longer than wide, fan-shaped, with an evenly convex distal edge and an acute proximal angle; neighbouring dorsal arm plates separated by LAPs; ventral arm plates as in above described paratype except for higher length/width ratio; no tentacle scales discernible; one arm spine preserved, conical, with fine, irregular longitudinal striation; tip broken; preserved part of spine as long as half an arm segment; original spine length not exceeding the length of an arm segment.

GZG.INV.78859 is a small, dissociated vertebra with large, dorso-distal and dorso-proximal muscular fossae, and small ventro-proximal and small, distalwards protruding ventro-distal fossae; well developed keel projecting distalwards, associated with a deep groove on the proximal face.

GZG.INV.78860 is a dissociated oral plate, nearly as high as wide; very large, entire, kidney-shaped abradial muscular area forming a weak wing distally; adradial muscular area nearly half as high as oral plate, entire, narrow, ventro-proximalwards bent; ring nerve notch deep.

Remarks. – The highly distinctive spine articulation morphology combined with the coarse tuberculation of the outer surface, the single large perforation and the ridge on the inner side composed of three parts, and the large but rather shallow tentacle notch unequivocally place the above described LAPs in the family Ophionereididae (Figs. 5.9–10). The presence of distinctively keeled vertebrae (Stöhr et al. 2012) and oral plates strongly reminiscent of those of recent *Ophionereis variegata* Duncan, 1879 (Murakami 1963) co-occurring with the LAPs in question further endorse the ophionereidid affinities. The fortunate presence of articulated arm fragments leaves no doubt as to the genus-level placement of the material in question. In fact, *Ophiodoris* is the only extant ophionereidid genus lacking accessory dorsal arm plates. The here described fossil material thus either belongs to *Ophiodoris* or to a very

closely related yet unknown fossil genus. In the light of the striking similarities in dorsal and ventral arm plate morphology and tentacle scale pattern shared with the type species *Ophiodoris malignus*, assignment to *Ophiodoris* seems to be the best option at the present state of knowledge.

Occurrence. – Latest Aptian of Wizard Way, Texas, U.S.A.

Faunal analysis

The assemblages described herein include a total of eleven species, eight in the two Spanish assemblages and three in the Texan one (Table 1). Ten of the species reported herein are new. The two Spanish assemblages seemed to yield the same faunal spectrum, albeit in slightly different relative abundances. They are thus treated as one assemblage (Cuchía 1 & 2) when presence/absence data are concerned, but are considered separately (Cuchía 1 and Cuchía 2) in the relative abundances analysis. Cuchía 1 & 2 is one of the most diverse Lower Cretaceous ophiuroid assemblages known to date, only outmatched by the Barremian shallow-water assemblage from France described by Thuy & Kroh (2011) (nine species) and the Aptian bathyal assemblage described by Thuy et al. (2012) and Thuy (2013) (eleven species).

Surprisingly, Cuchía 1 & 2 and the Texan assemblage do not have a single species in common. On genus level, however, all genera found in the Texan assemblage also occur in Cuchía 1 & 2. In the present-day North Atlantic, it is not uncommon that ophiuroid genera which occur on both sides of the ocean fall into eastern and western species (Paterson 1985). Thus, it could be that the here described Aptian records document a similar longitudinal separation on species level of genera occurring on both sides of the ancient North Atlantic. Other factors than longitude, in particular time (early Aptian versus latest Aptian ~4 Ma) or differences in depositional setting (silty basinal marls *versus* peri-reefal debris), however, might have contributed at least as much to the differences in species-level composition. In any case, the similarities on genus level clearly show that the eastern and western North Atlantic shallow-water ophiuroid communities were not fundamentally different in the Aptian.

In contrast, the latest Aptian middle bathyal ophiuroid assemblage from Blake Nose (western North Atlantic) described by Thuy et al. (2012) and Thuy (2013) displays a strikingly different faunal spectrum. Not a single species is shared with the Aptian shallow-water assemblages, and only two of the eight genera (*Ophiacantha* and *Ophioleuce*) in total also occur in Cuchía 1 & 2. The case of the Texan assemblage is particularly intriguing. In fact, it is stratigraphically and geographically closest to the Blake Nose assemblage but fails to share a single genus with latter.

While, for Cuchía 1 & 2, concurrence of time and longitude cannot be ruled out, the faunal differences between the Texan and the Blake Nose assemblages most probably reflect a true bathymetric signal between mid-shelf (sublittoral) and mid-slope (middle bathyal). Depth-related patterns in faunal composition are only rarely detectable as such in the fossil record because taxonomically assessable deep-sea assemblages are extremely scarce (Thuy et al. 2012), and even if they occur they have to be paralleled with stratigraphically and geographically close shallow-water equivalents. To our knowledge, the here described bathymetric gradient, although limited to two data points, is the first for the ophiuroid fossil record.

On family-level composition, all three shallow-water assemblages studied herein are dominated by the Ophionereididae (Cuchía 1: 60.1 %; Cuchía 2: 44.5 %; Texas: 84.0 %) followed by the Ophiolepididae in the Spanish assemblages (Cuchía 1: 29.4 %; Cuchía 2: 42.1 %) and the Ophiacanthidae in the Texan one (15.6 %). All other families identified account for less than 6 % each in all three assemblages. This differs markedly from the family-level composition of the middle bathyal Blake Nose assemblage (Thuy et al. 2012) dominated by the Ophiacanthidae (54.9 %), followed by the Ophiuridae (35.6 %) and the Ophiolepididae (9.5 %). It thus seems as if shelf and slope ophiuroid communities, in general clearly distinct in present-day oceans (Stöhr et al. 2012), were differentiated already in the Aptian.

While the middle bathyal Blake Nose ophiuroid assemblage was astonishingly similar to its present-day equivalents (Thuy et al. 2012), the here described shallow-water assemblages seem to lack modern counterparts in terms of family-level composition. In fact, a detrended correspondence analysis reveals that the three Aptian shallow-water assemblages studied herein plot outside the present-day ophiuroid communities, on the margin of the mid- to low-latitude shallow (0–200 m) ones (Fig. 5). The non-analogue composition of the shallow-water Aptian assemblages is due to the co-dominance of the Ophionereididae and the Ophiolepididae. In spite of the low palaeo-latitudes of the assemblages in question (Fig. 1), the Ophiocomidae, Ophiotrichidae and Ophiactidae, which commonly dominate present-day equivalent communities (Stöhr et al. 2012), completely lack, and the Amphiuridae, another typical and abundant component of modern shallow assemblages (Stöhr et al. 2012), are very rare.

A more detailed analysis of the composition of the shallow-water Aptian assemblages further endorses their non-analogue composition: the Ophiolepididae are represented by the extant genus *Ophiozonella* which, in present-day oceans, typically occurs at bathyal depths (e.g., H. L. Clark 1911; Matsumoto 1915). Even the representative of the otherwise typically shallow Ophionereididae (e.g., Hendler et al. 1995) in the Aptian assemblages, the extant genus *Ophiodoris*, almost exclusively occurs at bathyal depths in modern seas (Koehler 1904; H. L. Clark 1911). Thus, the Aptian shallow-water ophiuroid communities are in no way comparable to their modern counterparts, in spite of the dominance of typically shallow families.
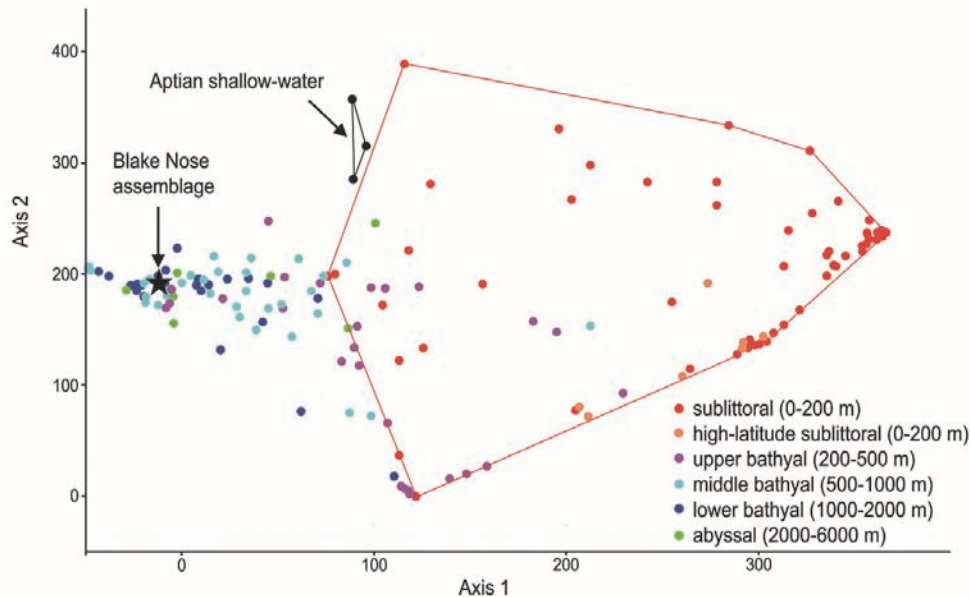
Fig. 5: Detrended correspondence analysis of the three shallow-water (<200 m) Aptian assemblages from Spain and Texas in comparison with modern ophiuroid assemblages and the middle bathyal Aptian assemblage from Blake Nose, western North Atlantic, described by Thuy et al. (2012). The shallow-water Aptian assemblages differ markedly from the Blake Nose one, and plot outside the modern communities, next to the mid- to low-latitude shallow ones. The analysis is based on the relative abundances of the 17 extant ophiuroid families minus the Ophiuridae. Modern community and Blake Nose data from Thuy et al. (2012).

References

Aronson, R. B. (1987): Predation on fossil and Recent ophiuroids. *Paleobiology* **13** (2): 187-192.

Baumiller, T. K. & Gahn, F. J. (2004): Testing predator-driven evolution with Paleozoic crinoid arm regeneration. *Science* **305** (5689): 1453-1455. http://dx.doi.org/10.1126/science.1101009

Bruzelius, N. (1805): *Dissertatio sistens species cognitas asteriarum, quam, … sub præsidio D. M. And. J. Retzii.* Lundæ (Literis Berlingianis): 1-37. [formerly known as R. J. Retzius]

Clark, H. L. (1908): Some Japanese and East Indian Echinoderms. *Bulletin of the Museum of Comparative Zoology* **51**: 279-311.

Clark, H. L. (1911): North Pacific Ophiurans in the collection of the Unites States National Museum. *Bulletin of the United States National Museum* **75**: 1-302.

Collignon, M.; Pascal, A.; Peybernès, B. & Rey, J. (1979): Faunes d'ammonites de l'Aptien de la région de Santander (Espagne). *Annales de Paléontologie (Invertébrés)* **65**: 139-156.

Donovan, S. K. (1996): Use of the SEM in interpreting ancient faunas of sea urchins. *European Microscopy and Analysis* **54**: 35-36.

Donovan, S. K. (2001): Evolution of the Caribbean echinoderms during the Cenozoic: moving towards a complete picture using all of the fossils. *Palaeogeography, Palaeoclimatology, Palaeoecology* **166** (1-2): 177-191. http://dx.doi.org/10.1016/S0031-0182(00)00208-X

Duncan, P. M. (1879): On some Ophiuroidea from the Korean Seas. *Journal of the Linnean Society, Zoology* **14**: 445-482. http://dx.doi.org/10.1111/j.1096-3642.1879.tb02443.x

Enay, R. & Hess, H. (1962): Sur la découverte d'Ophiures (*Ophiopetra lithographica* n. g. n. sp.) dans le Jurassique supérieur de Haut-Valromey (Jura méridional). *Eclogae Geologicae Helvetiae* **55** (2): 657-673.

Erbacher, J.; Huber, B. T.; Norris, R. D. & Markey, M. (2001): Increased thermohaline stratification as a possible cause for an ocean anoxic event in the Cretaceous period. *Nature* **409** (6818): 325-327. http://dx.doi.org/10.1038/35053041

Gale, A. S. (2011): The phylogeny of post-Paleozoic asteroidea (Neoasteroidea, Echinodermata). *Special Papers in Palaeontology* **85**: 1-112.

Garcia-Mondejar, J. (1982): Tectónica sinsedimentaria en el Aptiense y Albiense de la región Vasco-Cantábria occidental. *Cuadernos de Geología Ibérica* **8**: 23-36.

Gray, J. E. (1840): A synopsis of the genera and species of the class Hypostoma (*Asterias* Linnaeus). *Annals of the Magazine of Natural History* **6**: 175-184, 275-290.

Hammer, Ø.; Harper, D. A. T. & Ryan, P. D. (2001): PAST: Paleontological Statistics Software Package for Education and Data Analysis. *Palaeontologia Electronica* **4**: 1-9.

Hendler, G. & Miller, J. E. (1991): Swimming ophiuroids – real and imagined. In: Yanagisawa, T.; Yasumasu, I.; Oguro, C.; Suzuki, N. & Motokawa, T. (eds.): *Biology of Echinodermata.* Rotterdam (A.A. Balkema): 179-190.

Hendler, G.; Miller, J. E.; Pawson, D. L. & Kier, P. M. (1995): *Sea Stars, Sea Urchins, and Allies*. Washington, DC (Smithsonian Institution Press): 390 pp.

Hess, H. (1962): Mikropaläontologische Untersuchungen an Ophiuren II: Die Ophiuren aus dem Lias (Pliensbachien-Toarcien) von Seewen (Kt. Solothurn). *Eclogae geologicae Helvetiae* **55** (2): 609-656.

Hess, H. (1964): Die Ophiuren des englischen Jura. *Eclogae Geologicae Helvetiae* **57** (2): 756-801.

Hess, H. (1960): Neubeschreibung von *Geocoma elegans* (Ophiuroidea) aus dem unteren Callovien von La Voulte-sur-Rhône (Ardèche). *Eclogae geologicae Helvetiae* **53** (1): 335-385.

Hess, H. (1965a): Mikropaläontologische Untersuchungen an Ophiuren IV: Die Ophiuren aus dem Renggeri-Ton (Unter-Oxford) von Chapois (Jura) und Longecombe (Ain). *Eclogae geologicae Helvetiae* **58** (2): 1059-1082.

Hess, H. (1965b): Trias-Ophiurien aus Deutschland, England, Italien und Spanien. *Mitteilungen der Bayerischen Staatssammlung für Paläontologie und Historische Geologie* **5**: 151-177.

Hess, H. (1966): Mikropaläontologische Untersuchungen an Ophiuren V: Die Ophiuren aus dem Argovien (unteres Ober-Oxford) vom Guldental (Kt. Solothurn) und von Savigna (Dépt. Jura). *Eclogae geologicae Helvetiae* **59** (2): 1025-1063.

Hess H (1970): Schlangensterne und Seesterne aus dem oberen Hauterivien „Pierre jaune" von St-Blaise bei Neuchâtel. *Eclogae Geologicae Helvetiae* **63** (3): 1069-1091.

Hess, H. (1975a): Mikropaläontologische Untersuchungen an Ophiuren VI: Die Ophiuren aus den Günsberg-Schichten (oberes Oxford) vom Guldental (Kt. Solothurn). *Eclogae geologicae Helvetiae* **68** (3): 591-601.

Hess, H. (1975b): Mikropaläontologische Untersuchungen an Ophiuren VII: Die Ophiuren aus den Humeralis-Schichten (Ober-Oxford) von Raedersdorf (Ht-Rhin). *Eclogae geologicae Helvetiae* **68** (3): 603-612.

Hess, H. (2011): *Treatise on Invertebrate Paleontology, Part T, Revised, Echinodermata 2, volume 3, Crinoidea Articulata*. Lawrence (KU Paleontological Institute, University of Kansas): xxix + 261 pp.

Hess, H. & Meyer, C. A. (2008): A new ophiuroid (*Geocoma schoentalensis* sp. nov.) from the Middle Jurassic of northwestern Switzerland and remarks on the family Aplocomidae Hess, 1965. *Swiss Journal of Geosciences* **101** (1): 29-40. http://dx.doi.org/10.1007/s00015-008-1253-5

Hunter, A. W. & Underwood, C. J. (2009): Palaeoenvironmental control on distribution of crinoids in the Bathonian (Middle Jurassic) of England and France. *Acta Palaeontologica Polonica* **54** (1): 77-98.

Koehler, R. (1904): Ophiures de l'expédition du Siboga. Part 1. Ophiures de mer profonde. *Siboga Expeditie* **45a**: 1-176.

Kroh, A. (2007): Climate changes in the Early to Middle Miocene of the Central Paratethys and the origin of its echinoderm fauna. *Palaeogeography, Palaeoclimatology, Palaeoecology* **253** (1-2): 169-207. http://dx.doi.org/10.1016/j.palaeo.2007.03.039

Kutscher, M. (1996): Echinodermata aus dem Ober-Toarcium und Aalenium Deutschlands II. Ophiuroidea. *Stuttgarter Beiträge zur Naturkunde, Serie B* **242**: 1-33.

Kutscher, M. & Hary, A. (1991): Echinodermen im Unteren Lias (Bucklandi- und Semicostatum-Zone) zwischen Ellange und Elvange (SE-Luxemburg). *Neues Jahrbuch für Geologie und Paläontologie, Abhandlungen* **182** (1): 37-72.

Kutscher, M. & Jagt, J. W. M. (2000): Early Maastrichtian ophiuroids from Rügen (northeast Germany) and Møn (Denmark); In: Jagt, J. M. W., Late Cretaceous-Early Paleocene echinoderms and the K/T boundary in the southeast Netherlands and the northeast Belgium. part 3: Ophiuroids. *Scripta Geologica* **21**: 45-107.

Kutscher, M. & Villier, L. (2003): Ophiuroid remains from the Toarcian of Sainte-Verge (Deux-Sèvres, France): paleobiological perspectives. *Geobios* **36** (2): 179-194. http://dx.doi.org/10.1016/S0016-6995(03)00005-6

Ljungman, A. V. (1867): Ophiuroidea viventia huc usque cognita enumerat. *Öfversigt af Kongliga Vetenskaps-Akademiens Förhandlingar* **23**: 303-336.

Ljungman, A. V. (1872): Förteckning öfver uti Vestindien af Dr. A Goës samt under korvetten Josefinas expedition i Atlantiska Oceanen samlade Ophiurider. *Öfversigt af Kungliga Vetenskaps-Akademiens Förhandlingar* **28**: 615-658.

Lyman, T. (1869): Preliminary report on the Ophiuridea and Astrophytidae dredged in deep water between Cuba and the Florida Reef, by L.F. de Pourtales, Assist. U.S. Coast Survey. *Bulletin of the Museum of Comparative Zoology, Harvard University* **1**: 309-354.

Lyman, T. (1875): Zoological results of the Hassler Expedition. II. Ophiuridae and Astrophytidae. *Illustrated Catalogue of the Museum of Comparative Zoology* **8**: 1-34.

Martynov, A. (2010): Reassessment of the classification of the Ophiuroidea (Echinodermata), based on morphological characters. I. General character evaluation and delineation of the families Ophiomyxidae and Ophiacanthidae. *Zootaxa* **2697**: 1-154.

Matsumoto, H. (1915): A new classification of the Ophiuroidea, with description of new genera and species. *Proceedings of the Academy of Natural Sciences of Philadelphia* **68**: 43-92.

Müller, J. & Troschel, F. H. (1840): Über die Gattungen der Ophiuren. *Archiv für Naturgeschichte* **6**: 327-330.

Müller, J. & Troschel, F. H. (1842): *System der Asteriden. 1. Asteriae. 2. Ophiuridae*. Braunschweig (Vieweg): 134 pp.

Murakami, S. (1963): The dental and oral plates of Ophiuroidea. *Transactions of the Royal Society of New Zealand, Zoology* **4**: 1-48.

Najarro, M.; Rosales, I. & Martín-Chivelet, J. (2010): Major palaeoenvironmental perturbation in an Early Aptian carbonate platform: prelude of the Oceanic Anoxic Event 1a? *Sedimentary Geology* **235** (1-2): 50-71. http://dx.doi.org/10.1016/j.sedgeo.2010.03.011

Najarro, M.; Rosales, I.; Moreno-Bedmar, J. A.; Gea, G. A. de; Barrón, E.; Company, M. & Delanoy, G. (2011): High-resolution chemo- and biostratigraphic records of the Early Aptian oceanic anoxic event in Cantabria (N Spain): Palaeoceanographic and palaeoclimatic implications. *Palaeogeography, Palaeoclimatology, Palaeoecology* **299**: 137-158. http://dx.doi.org/10.1016/j.palaeo.2010.10.042

Paterson, G. L. J. (1985): The deep-sea Ophiuroidea of the North Atlantic Ocean. *Bulletin of the British Museum (Natural History), Zoology Series* **49**: 1-162.

Smith, A. B.; Paterson, G. L. J. & Lafay, B. (1995): Ophiuroid phylogeny and higher taxonomy: morphological, molecular and palaeontological perspectives. *Zoological Journal of the Linnean Society* **114**: 213-243. http://dx.doi.org/10.1006/zjls.1995.0024

Smith, A. B. & Rader, W. I. (2009): Echinoid diversity, preservation potential and sequence stratigraphical cycles in the Glen Rose Formation (early Albian, Early Cretaceous), Texas, USA. *Palaeobiodiversity and Palaeoenvironments* **89** (1-2): 7-52. http://dx.doi.org/10.1007/s12549-009-0002-8

Spencer, W. K. (1907): A monograph on the British fossil Echinodermata from the Cretaceous formations 2: The Asteroidea and Ophiuroidea, Part 4. *Monograph of the Palaeontographical Society, London* **[1907]**: 91-132.

Stöhr, S.; O'Hara, T. D. & Thuy, B. (2012): Global diversity of brittle stars (Echinodermata: Ophiuroidea). *PLoS ONE* **7** (3): 1-14 [e31940]. http://dx.doi.org/10.1371/journal.pone.0031940

Stricklin, F. L.; Smith, C. I. & Lozo, F. E. (1971): Stratigraphy of Lower Cretaceous Trinity deposits of central Texas. *University of Texas at Austin Bureau of Economic Geology Report of Investigations* **71**: 1-63.

Taylor, B. J. (1966): Taxonomy and morphology of Echinodermata from the Aptian of Alexander Island. *British Antarctic Survey Bulletin* **8**: 1-18.

Thuy, B. (2005): Les Ophiures de l'Hettangien inférieur de Vance (B), Bereldange/Bridel et Bourglinster (L). *Memoirs of the Geological Survey of Belgium* **51**: 33-57.

Thuy, B. (2011): Exceptionally well-preserved brittle stars from the Pliensbachian (Early Jurassic) of the French Ardennes. *Palaeontology* **54** (1): 215-233.

Thuy, B. (2013): Temporary expansion to shelf depths rather than an onshore-offshore trend: the shallow-water rise and demise of the modern deep-sea brittle star family Ophiacanthidae (Echinodermata: Ophiuroidea). *European Journal of Taxonomy* **48**: 1-242. http://dx.doi.org/10.5852/ejt.2013.48

Thuy, B. & Kroh, A. (2011): Barremian ophiuroids from the Serre de Bleyton (Drôme, SE France). *Annalen des Naturhistorischen Museums in Wien, Serie A* **113**: 777-807.

Thuy, B. & Meyer, C. A. (2012): The pitfalls of extrapolating present-day depth ranges to fossil communities: new insights from brittle stars (Echinodermata: Ophiuroidea) from the Middle Jurassic of Switzerland. *Swiss Journal of Palaeontology* **132** (1): 5-21. http://dx.doi.org/10.1007/s13358-012-0048-5

Thuy, B. & Stöhr, S. (2011): Lateral arm plate morphology in brittle stars (Echinodermata: Ophiuroidea): new perspectives for ophiuroid micropalaeontology and classification. *Zootaxa* **3013**: 1-47.

Thuy, B.; Gale, A. S.; Kroh, A.; Kucera, M.; Numberger-Thuy, L. D.; Reich, M. & Stöhr, S. (2012): Ancient origin of the modern deep-sea fauna. *PLoS ONE* **7** (10): 1-11 [e46913]. http://dx.doi.org/10.1371/journal.pone.0046913

Thuy, B.; Gale A. S. & Reich, M. (2011): A new echinoderm Lagerstätte from the Pliensbachian (Early Jurassic) of the French Ardennes. *Swiss Journal of Palaeontology* **130** (1): 173-185. http://dx.doi.org/10.1007/s13358-010-0015-y

Verrill, A. E. (1899): Report on the Ophiuroidea collected by the Bahama expedition in 1893. *Bulletin of the Laboratories of Natural History of the State of Iowa* **5**: 1-88.

Ward, D. J. (1981): A simple machine for bulk processing of clays and silts. *Tertiary Research* **3**: 121–124.

Wilmsen, M. (2005): Stratigraphy and biofacies of the Lower Aptian of Cuchía (Cantabria, northern Spain). *Journal of Iberian Geology* **31**: 253-275.

A new species of the barnacle genus *Tesseropora* (Crustacea: Cirripedia: Tetraclitidae) from the Early Pliocene of Fuerteventura (Canary Islands, Spain)

Jahn J. Hornung[1,2]

[1]*Department of Geobiology, Geoscience Centre, Georg-August University Göttingen, Goldschmidtstr. 3, 37077 Göttingen, Germany; Email: jhornun@gwdg.de*
[2]*Geoscience Museum, Georg-August University Göttingen, Goldschmidtstr. 1-5, 37077 Göttingen, Germany*

A new barnacle species, *Tesseropora canariana* sp. nov., from Lower Pliocene shoreline deposits of western Fuerteventura is described. It represents the first record of the genus *Tesseropora* from the Canary Islands. The compartment of the new species is morphologically very similar to *T. dumortieri* (Fischer, 1866) from the Miocene of the western Tethys and eastern Atlantic coast and to *T. sulcata* Carriol, 1993 from the Upper Pliocene French Atlantic coast. It is an early example of an Atlantic island population of this genus and documents its Neogene transatlantic dispersal. Lithofacies, taphonomy and faunal association at the type locality indicate epiphytical fixation of the barnacles under warm-subtropical conditions at a high-energy, rocky shoreline.

Introduction

Fossil barnacles from uplifted Neogene shore sediments at the Canary Islands have so far been reported only by Simonelli (in Rothpletz & Simonelli 1890) in their classical monograph on the Lower Pliocene Las Palmas Formation of Gran Canaria. He noticed several compartments of a balanid which he tentatively referred to the extant species *Perforatus* cf. *perforatus* (Bruguière, 1789), and a single radial plate of a second taxon. The latter was described under a new binomen, *Chenolobia hemisphaerica* Simonelli (in Rothpletz & Simonelli 1890: 724, pl. XXXVI, figs. 2, 2a-b).

Since Simonelli introduced the new taxon explicitly as "n. sp." and stressed the similarity of his new species to extant members of the coronulid genus *Chelonibia* Leach, 1817, '*Chenolobia*' is apparently an "error typographicus" and represents technically a "nomen nudum". '*Chenolobia*' *hemisphaerica* was intentionally a member of the genus *Chelonibia* in the original description, where it currently resides in the most recent overviews (Ross & Frick 2007; Epibiont Research Cooperative 2007: 31, as *C. hemispherica* [sic!]).
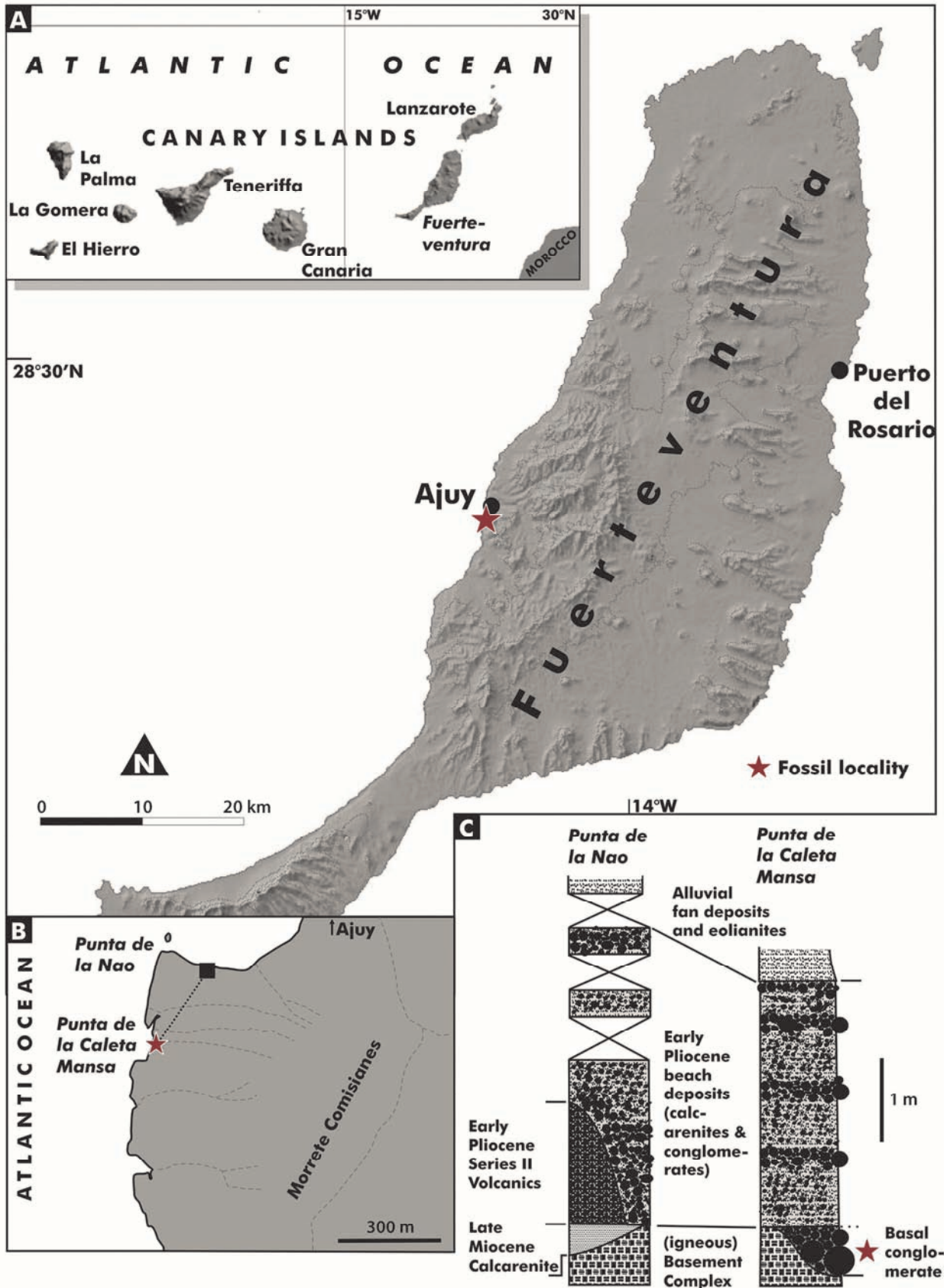
Fig. 1: **(A–B)** Location of the sampled outcrop at Punta de la Caleta Mansa, south of Ajuy, Fuerteventura, Canary Islands, Spain. **(C)** Lithostratigraphy of the type strata of *T. canariana* sp. nov. The Basal Complex is Jurassic to Miocene, the alluvial fan deposits and eolianites are Pliocene to Recent in age (see text).

In this study, the first record of the tetraclitid genus *Tesseropora* Pilsbry, 1916 from the Canary Islands is described, which originates from Lower Pliocene beds of western Fuerteventura. Fossil species of the genus *Tesseropora* have been so far described from the Mediterranean-Tethyan (Oligocene–Miocene), eastern Atlantic (Late Pliocene) and eastern Pacific (Pliocene) realms (Zullo 1968; Carriol 1993, 2005, 2008). Extant members of this genus inhabit the Indopacific and island shores in the Atlantic Ocean (e.g., Nilsson-Cantell 1921; Newman & Ross 1977; Young 1998; Southward 1998; Wirtz et al. 2006).

Material and methods

Material collection and geological setting

The material was collected from uplifted shore sediments (Meco & Stearns 1981; Meco & Pomel 1985; Meco et al. 2007) at the western coast of the Island of Fuerteventura ~1.5 km south of the village of Ajuy (Puerto de la Peña, Figs. 1A–B).

In this area, the Jurassic to Neogene sedimentary-magmatic Basement Complex (LeBas et al. 1986; Balogh et al. 1999) was truncated by a Miocene shore-plate, today elevated to 6–12 m a.s.l. (Fig. 1C). This erosive surface was subsequently overlain by ~1 m of Upper Miocene (Upper Tortonian, Rona & Nawalk 1970) shallow-water calcarenites.

The calcarenitic unit is south of Ajuy covered by basaltic lava flows of the volcanic Series II (*sensu* Fúster et al. 1968, 1984), which erupted during the Plio-Pleistocene subaerial volcanic phase of the island (Stillman 1999). The lava flows intercalate distally with coeval hyaloclastites and coarse-grained beach deposits. Subsequent erosion locally reactivated the pre-Upper Miocene shore-plate on top of the Basement Complex. This reactivated shore-plate and the lava flows of Series II are overlain by onlapping coarse-grained, clastic beach deposits. These are ranging in grainsize from micritic mudstone and coarse-grained sand to boulders up to 70 cm in diameter. The units, which contain the material described herein, can be subdivided into several subunits. The basal unit (Fig. 1C) consists of a highly fossiliferous, clast supported, cobble to large boulder conglomerate. The clasts derive mainly from the underlying basal complex rocks and in minor parts from epiclastic volcanics of the island edifice. The matrix consists of a buff-colored, sandy biomicrite. Double-valved specimens of the deep-burrowing bivalve *Eastonia* sp. are preserved in vertical life-position within matrix-filled cavities between large blocks. Other molluscs include *Nerita emiliana* (Mayer, 1872) and *Persististrombus coronatus* (Defrance, 1827). Younger subunits of the beach-deposits (Fig. 2) consist of smaller sized clasts (small granules to pebbles), and macrofossils are reworked to pebble- to sand-sized bioclasts.

This succession is interpreted to represent initial deposition on a rocky shore-plate, strewn with blocks of eroded basement, that was subsequently inundated by a rapid sea-level rise, allowing finer-grained sediment to settle between the boulders and colonisation by burrowing infauna (basal conglomerate). Finally, adecrease in the rate of sea-level rise resulted in the formation of a pebbly bioclast sand beach (younger subunits).

Based on the occurrence of similar mollusc faunas, Meco and Stearns (1981) and Meco et al. (2007) correlated the Neogene emergent shore-line deposits of western Fuerteventura with similar units at Gran Canaria and Lanzarote islands. Generally, palaeontological evidence and absolute radiometric dating indicate a Late Miocene to Early Pliocene age for these sediments. The radiometric ages obtained by Coello et al. (1992) for the locally underlying lava flows (5.0–5.8 Ma) and the presence of *Nerita emiliana* suggest an Early Pliocene (Zanclean) age for the fossiliferous conglomerate and sandstone at the sampling locality. They are overlain by Pliocene to Holocene alluvial fan deposits and aeolian calcarenites, palaeosoils and soils.

The barnacle material has been collected from the basal conglomerate a few cm above the shore-plate discontinuity surface. The cirripedians are not rare at the locality, but extraction from the matrix is difficult due to the brittle preservation and dense surrounding rock matrix. The barnacle compartments were not attached to a substrate but freely embedded in random orientation in the matrix.

Methods and repository

The specimens have been cleaned from matrix as far as possible given their delicate preservation and photographed. Descriptive terminology follows Newman et al. (1969). The specimens are stored in the invertebrate fossil collection of the Geoscience Centre, University of Göttingen, Germany (GZG.INV.).

Systematic palaeontology

Subclass **Cirripedia** Burmeister, 1834
Superorder **Thoracica** Darwin, 1854
Order **Sessilia** Lamarck, 1818
Suborder **Balanomorpha** Pilsbry, 1916
Superfamily **Coronuloidea** Leach, 1817
Family **Tetraclitidae** Gruvel, 1903
Subfamily **Tetraclitinae** Gruvel, 1903

Genus ***Tesseropora*** Pilsbry, 1916

Tesseropora canariana sp. nov.

Figs. 2–3

Holotype. – GZG.INV.003333 (Figs. 2A–C, 3), complete compartment of adult individual, length: 24 mm, width: 22 mm, height: >21 mm.
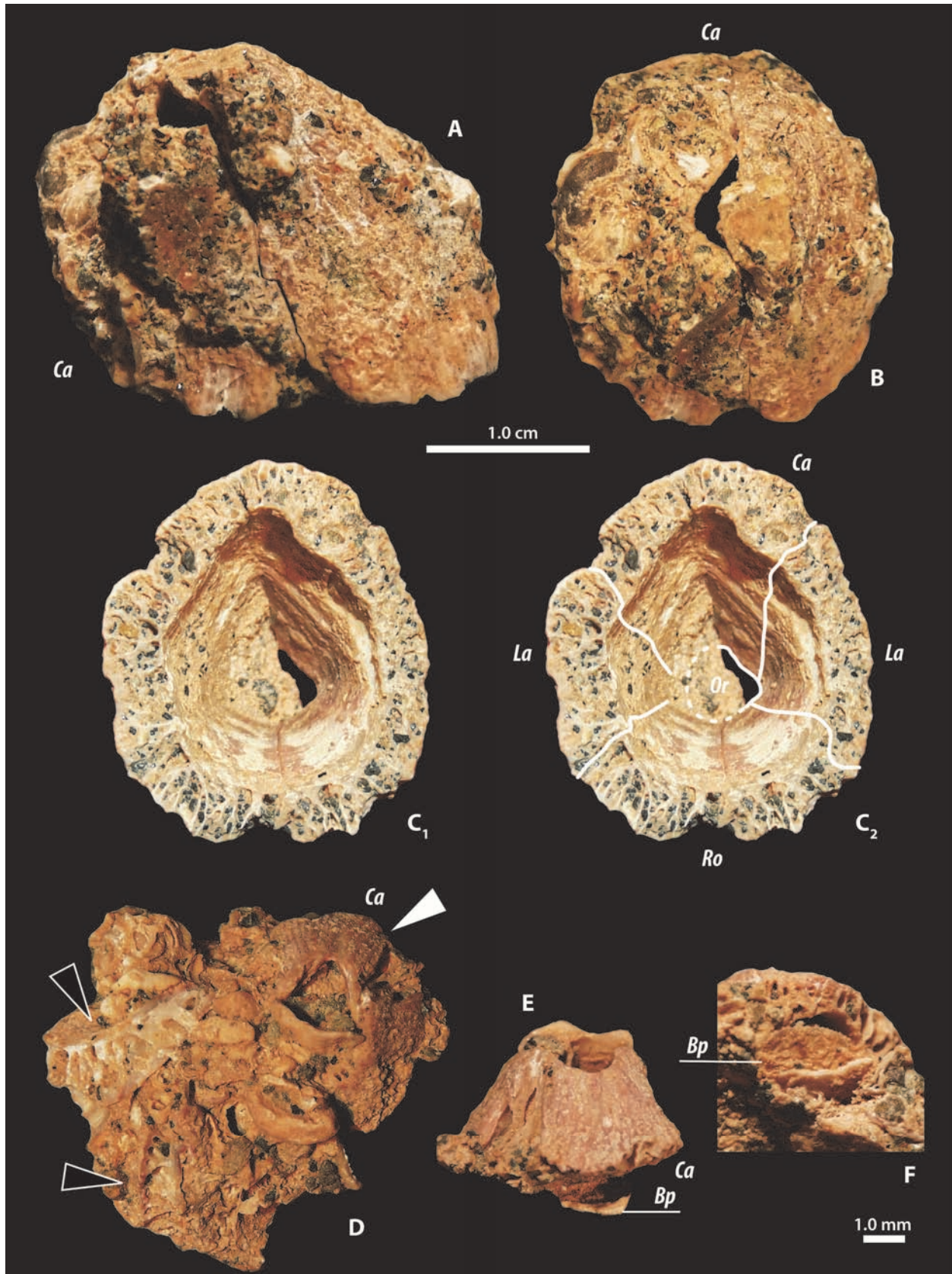
Fig. 2: *Tesseropora canariana* sp. nov., Early Pliocene, western Fuerteventura, Canary Islands, Spain. **(A–C)** GZG.INV.003333, holotype, adult compartment, in **(A)** lateral, **(B)** apical, and **(C)** basal view (C₁ = unlabelled and C₂ = labelled). **(D–F)** GZG.INV.003334, paratype, subadult compartment, **(D)** paratype specimen in apical view (white arrow) with associated compartment fragments of larger specimens (black arrows), **(E)** paratype specimen in lateral view, **(F)** paratype specimen in basal view with fragment of calcareous basal plate. Abbreviations: *Bp*: basal plate, *Ca*: carina, *La*: lateral, *Ro*: rostral, *Or*: orifice. Scale bars: (A–E) = 1.0 cm, (F) = 1.0 mm.

Paratype. – GZG.INV.003334 (Figs. 2D–F), slightly damaged compartment of subadult individual, length: >12 mm, width: ~16 mm, height: >9 mm.

Further material examined. – Compartment fragments in matrix associated to GZG.INV.003334.

Locus typicus. – Punta de la Caleta Mansa, ~1.5 km S of Puerto de la Peña, western Fuerteventura, Canary Islands, Spain.

Stratum typicum. – Unnamed Lower Pliocene (Zanclean) shoreline-deposits, overlying subaerial basalts of the Volcanic Series II (of Fúster et al. 1968).

Etymology. – After the occurrence on the Canary Islands.

Diagnosis. – Only the compartment is known. A large species of *Tesseropora*, showing the following combination of characters: compartment plates robust and rigidly articulating, radii and alae narrow, secondary and tertiary parietal tube rows are present, horizontally striated sheath very well developed, covering the upper ~60–80 % of the parietes and the radii.

Fig. 3: *Tesseropora canariana* sp. nov., GZG.INV.003333, holotype. **(A)** Longitudinal section through the compartment showing the sheath and radii; **(B)** Detail of compartment wall (rostral) with parietal tubes and intraparietal septals. Abbreviations as in Fig. 2. Scale bars = 5.0 mm.

Description. – A large species with a shell in form of a steep-sided, truncated cone in adult specimen. In subadults, the cone is proportionally lower and wider. The base cross-section of the shell is oval; the side formed by the carina is protruding (Fig. 2C). The compartment plates are very rigidly connected, forming a robust shell. At the outer surface of the compartment, plate sutures are not visible and all known specimens are fully articulated. The outer surface is ornamented with basiapically oriented, coarse, rugged ribs (2–4 per mm). The orifice margin is oval to subpentagonal and enlarged by erosion (Figs. 2A–E).

The inner and outer lamina of the compartment plates are connected by intraparietal septals, which join the smooth inner lamina in normal angle. In large (adult) specimens, the interparietal septals are anastomosing one or two times before contacting the outer lamina, thus forming secondary and eventually tertiary rows of parietal tubes (Fig. 3B). The sheath is closely attached to the inner lamina, extending downwards for ~80 % of the compartment height on the rostral and lateral and to ~60 % on the carina, and shows an ornamentation consisting of faint horizontal striae. Alae and radii are narrow (less than 15 % of the width of the compartment plates to which they attach, Fig. 3A). A calcareous basal plate is present (Figs. 2E–F).

Discussion

The assignment of the barnacles from Fuerteventura to the genus *Tesseropora* Pilsbry, 1916 is based upon the development of the intraparietal septals, joining the inner lamina in normal angles, the development of only 2–3 rows of parietal tubes in large (adult) specimens and the presence of a calcareous basal plate. These features distinguish it from the otherwise similar genus *Tetraclita* Schumacher, 1817 (compare Newman & Ross 1977).

The new species is very similar to *T. dumortieri* (Fischer, 1866) from Miocene deposits of the Rhone Valley and the eastern Atlantic and to *T. sulcata* Carriol, 1993 from the Late Pliocene of the French Atlantic coast. These two species can only be distinguished by details of their opercular valves (Carriol 1993). However, since only the compartment plates of *T. canariana* sp. nov. are known, it can not be compared in this feature. The close relationship to these forms is mainly based on the development of secondary and tertiary parietal tubes, the narrow radii and alae, the solid and compact habitus (sutures of compartment plates can hardly be traced in external view) and the size. It differs from both significantly in the extension and ornamentation of the sheath.

Among the living *Tesseropora* species it shares the development of multiple parietal tube rows with *T. wireni* (Nilsson-Cantell, 1921) (tropical Indopacific), but the latter differs in having wider alae and radii, and is smaller and less rigidly build. From the extant species *T. atlantica* Newman & Ross, 1977 (Bermuda), *T. arnoldi* Young, 1998 (Azores, considered conspecific with *T. atlantica* by Southward 1998, Costa & Jones 2000), *T. rosea* (Krauss, 1848)

(southern, temperate Indopacific), and the fossil *T. isseli* (de Alessandri, 1895) (Oligocene, Italy), and *T. unisemita* Zullo, 1968 (Pliocene, Mexico) it differs in the presence of multiple parietal tube rows. However, in *T. arnoldi* the sheath is very similar to *T. canariana* sp. nov.

Recent identifications of *T. dumortieri* from the "Faluns de Touraine" (Carriol 2005, 2008) showed that populations of this genus entered the Atlantic Ocean from the Mediterranean as early as during the Middle Miocene. In the present-day Atlantic barnacle fauna, *Tesseropora* is represented only by isolated, island-bound occurrences (Bahamas, Madeira, Azores, Saint Paul's Rock; Newman & Ross 1977; Edwards & Lubbock 1983; Young 1998; Wirtz et al. 2006). Probably *T. canariana* sp. nov. represents an early case of insular endemism similar to those of other Atlantic archipelagos. Cardigos et al. (2006) have proposed an anthropogenic introduction of the extant *T. atlantica* (?=*T. arnoldi*) to the Azores, based upon a very short larval dispersal phase of this species. However, Winkelmann et al. (2010) argued for a natural dispersion and this is supported by *T. canariana* sp. nov. from Fuerteventura, showing transatlantic insular occurrence as early as Pliocene. The Neogene populations from the European shore regions (*T. sulcata*) and Fuerteventura apparently became extinct since the Pliocene, most probably due to the decrease of water temperature towards the end of the Pliocene.

The new species from western Fuerteventura lived in the high energy, well oxygenated, shore-line or shore-face zone of a rocky shore. Dispersed embedding in the matrix and the preservation of a calcareous basal plate in the paratype suggests epiphytical colonisation, e.g., on thallophytes. The good quality of preservation precludes a long transport distance, and the robustness of the shell suggests a substrate in a high-energy environment. This is consistent with the habitat of extant species of this genus (Denley & Underwood 1979; Anderson & Anderson 1985). The abundant presence of the gastropod *Persististrombus coronatus* and other molluscs indicates warm water temperatures, with minimum sea surface temperatures not falling below 15–16°C (Meco 1977, Harzhauser & Kronenberg 2013).

Acknowledgements

References

Anderson, D. T. & Anderson, J. T. (1985): Functional morphology of the balanomorph barnacles *Tesseropora rosea* (Krauss) and *Tetraclitella purpurascens* (Wood) (Tetraclitidae). *Australian Journal of Marine and Freshwater Research* **36** (1): 87-113. http://dx.doi.org/10.1071/MF9850087

Balogh, K.; Ahijado, A.; Casillas, R. & Fernandez, C. (1999): Contributions to the chronology of the Basal Complex of Fuerteventura, Canary Islands. *Journal of Volcanology and Geothermal Research* **90** (1-2): 81-101. http://dx.doi.org/10.1016/S0377-0273(99)00008-6

Bruguière, M. (1789): *Encyclopédie méthodique, ... Histoire naturelle des vers. Tome 1 (1)*. Paris (Panckoucke): 344 pp.

Burmeister, C. H. (1834): *Beiträge zur Naturgeschichte der Rankenfüsser (Cirripedia)*. Berlin (C. Reimer): viii + 60 pp.

Cardigos, F.; Tempera, F.; Ávila, S. P.; Gonçalves, J.; Colaço, A. & Santos, R. S. (2006): Non-indigenous marine species of the Azores. *Helgoland Marine Research* **60** (2): 160-169. http://dx.doi.org/10.1007/s10152-006-0034-7

Carriol, R.-P. (1993): *Tesseropora* (Cirripedia, Thoracica) du Néogène de France. *Geobios* **26** (6): 709-713. http://dx.doi.org/10.1016/S0016-6995(93)80052-S

Carriol, R.-P. (2005): Re-examination and new species of Cirripeds (Thoracica, Tetraclitidae, and Balanidae) from the Middle Miocene of the faluns de Touraine (France). *Annales de Paléontologie* **91** (1): 117-126. http://dx.doi.org/10.1016/j.annpal.2004.11.002

Carriol, R.-P. (2008): New genus and new species of Cirripedia (Chthamalidae, Tetraclitidae, Archaeobalanidae and Balanidae) from the Middle Miocene of the faluns of Touraine (France). *Zootaxa* **1675**: 31-48.

Coello, J.; Cantagrel, J. M.; Hernán, F.; Fúster, J. M.; Ibarrola, E.; Ancochea, E.; Casquet, C.; Jamond, C.; Díaz de Téran, J.-R. & Cendrero, A. (1992): Evolution of the eastern volcanic ridge of the Canary Islands based on new K-Ar data. *Journal of Volcanology and Geothermal Research* **53**: 251-274. http://dx.doi.org/10.1016/0377-0273(92)90085-R

Costa, A. C. & Jones, M. B. (2000): The genus *Tesseropora* (Cirripedia: Tetraclitidae) from São Miguel, Azores. *Arquipélago. Life and Marine Sciences, Suppl.* **2** (A): 71-78.

Darwin, C. (1854): *A Monograph on the Fossil Balanidæ and Verrucidæ of Great Britain*. London (The Palaeontographical Society): 44 pp.

De Alessandri, G. (1895): Contribuzione allo studio dei Cirripedia fossili d'Italia. *Società Geologica Italiana, Bolletino* **13**: 234-314.

Defrance, J. L. M. (1827): *Dictionnaire des sciences naturelles, 51*. Paris (Levrault & Normat): 534 pp.

Denley, E. J. & Underwood, A. J. (1979): Experiments on factors influencing settlement, survival and growth of two species of barnacles in New South Wales. *Journal of Experimental Marine Biology and Ecology* **36**: 269-294. http://dx.doi.org/10.1016/0022-0981(79)90122-9

Edwards, A. & Lubbock, R. (1983): The ecology of Saint Paul's Rock (equatorial Atlantic). *Journal of Zoology* **200**: 51-69. http://dx.doi.org/10.1111/j.1469-7998.1983.tb06108.x

Epibiont Research Cooperative (2007): A Synopsis of the Literature on the Turtle Barnacles (Cirripedia: Balanomorpha: Coronuloidea) 1758-2007. *Epibiont Research Cooperative, Special Publication* **1**: 1-62.

Fischer, P. (1866): Note E. Description des nouvelles espèces d'invertébrés fossiles dans les bassin du Rhône, (formation tertiaire moyenne). In: Falsan, A. & Locard, A. (eds.): *Monographie Géologique du Mont-d'Or Lyonnais et ses dépendances*. Lyon (Pitrar Ainé): 434-440.

Fúster, J. M.; Cendrero, A.; Gastesi, P. & Lopez Ruiz, J. (1968): *Geología y vulcanología de las Islas Canarias. Fuerteventura*. Madrid (Inst. "Lucas Mallada"): 239 pp.

Fúster, J. M.; Barrera, J. L.; Muñoz, M.; Sagredo, J. & Yebenes, A. (1984): *Mapa geologica de Espagna (1 : 25 000). 1106/III Pajara.* Madrid (Instituto Geologico y Minero de Espagna): 61 pp.

Gruvel, A. (1903): Révision des Cirrhipèdes appartenant à la collection du Muséum d'Histoire Naturelle. Operculés. I. Partie systématique. *Nouvelles Archives du Muséum d'Histoire Naturelle (sér. 4)* **5**: 95-170.

Harzhauser, M. & Kronenberg, G. C. (2013): The Neogene strombid gastropod *Persististrombus* in the Paratethys Sea. *Acta Palaeontologica Polonica* **58** (4): 785-802.

Krauss, F. (1848): *Die südafrikanischen Mollusken; ein Beitrag zur Kenntniss der Mollusken des Kap- und Natallandes und zur geographischen Verbreitung derselben, mit Beschreibung und Abbildung der neuen Arten.* Stuttgart (Ebner & Seubert): 134 pp.

Lamarck, J. B. de (1818): *Histoire naturelle des animaux sans vertèbres. Tome V.* Paris (Deterville & Verdière): 612 pp.

Leach, W. E. (1817): *The Zoological Miscellany, being descriptions of new or interesting animals. Vol. 3.* London (B. McMillan): 157 pp.

LeBas, M. J.; Rex, D. C. & Stillman, C. J. (1986): The early magmatic history of Fuerteventura, Canary Islands. *Geological Magazine* **123**: 287-298. http://dx.doi.org/10.1017/S0016756800034762

Mayer, M. C. (1872): Description des Coquilles fossiles des terraines tertiaires supérieurs (suite). *Journal de Conchyliologie (sér. 3)* **20** (12): 227-238.

Meco, J. (1977): *Paleontologia de Canarias I: Los "Strombus" neógenos y cuaternarios del Atlántico euroafricano.* Gran Canaria (Ediciones des Excmo, Cabildo Insular de Gran Canaria): 92 pp.

Meco, J & Pomel, R. (1985). Les formations marines et continentales intervolcaniques des Iles Canariens Orientales, Grand Canarie, Fuerteventura et Lanzarote; stratigraphie et signification paleoclimatique. *Estudios Geológicos* **41**: 223-227.

Meco, J. & Stearns, C. E. (1981): Emergent Littoral Deposits in the Eastern Canary Islands. *Quarternary Research* **15** (2): 199-208. http://dx.doi.org/10.1016/0033-5894(81)90104-6

Meco, J.; Scaillet, S.; Gouillou, H.; Lomoschitz, A.; Carracedo, J. C.; Ballester, J.; Betancort, J.-F. & Cilleros, A. (2007): Evidence for long-term uplift on the Canary Island from emergent Mio-Pliocene littoral deposits. *Global and Planetary Change* **57** (3-4): 222-234. http://dx.doi.org/10.1016/j.gloplacha.2006.11.040

Newman, W. A. & Ross, A. (1977): A living *Tesseropora* (Cirripedia; Balanomorpha) from Bermuda and the Azores, first records from the Atlantic since the Oligocene. *Transactions of the San Diego Natural History Museum* **18** (12): 207-216.

Newman, W. A.; Zullo, W. A. & Withers, T. H. (1969): Cirripedia. In: Moore, R. C. (ed.): *Treatise on Invertebrate Paleontology, Part R, Arthropoda 4, Volume 1.* Boulder, Colo. (The Geological Society of America) & Lawrence, Kans. (University of Kansas): R206-R294.

Nilsson-Cantell, C. A. (1921): Cirripedien-Studien. Zur Kenntnis der Biologie, Anatomie und Systematik dieser Gruppe. *Zoologiska Bidrag från Uppsala* **7**: 75-395.

Pilsbry, H. A. (1916): The sessile barnacles (Cirripedia) contained in the collections of the U.S. National Museum; including a monograph of the American species. *Bulletin of the United States National Museum* **93**: 1-366.

Rona, A. & Nawalk, A. J. (1970): Post-early Pliocene unconformity on Fuerteventura, Canary Islands. *Bulletin of the Geological Society of America* **81**: 2117-2122. http://dx.doi.org/10.1130/0016-7606(1970)81[2117:PPUOFC]2.0.CO:2

Ross, A. & Frick, M. G. (2007): Systematics of the coronuloid barnacles. *Epibiont Research Cooperative, Special Publication* **1**: 23-29.

Rothpletz, A. & Simonelli, V. (1890): Die marinen Ablagerungen auf Gran Canaria. *Zeitschrift der Deutschen Geologischen Gesellschaft* **42**: 677-737.

Schumacher, C. F. (1817): *Essai d'un nouveau système des habitations des vers testacés.* Copenhague (Schultz): 287 pp.

Southward, A. (1998): Notes on Cirripedia of the Azores Region. *Arquipélago, Life and Marine Sciences* **16** (A): 11-27.

Stillman, C. J. (1999): Giant Miocene landslides and the evolution of Fuerteventura, Canary Islands. *Journal of Volcanology and Geothermal Research* **94** (1-4): 89-104. http://dx.doi.org/10.1016/S0377-0273(99)00099-2

Winkelmann, K.; Buckeridge, J. S.; Costa, A. C.; Manso Dionísio, M. A.; Medeiros, A.; Cachão, M. & Ávila, S. P. (2010): *Zullobalanus santamariaensis* sp. nov., a new late Miocene barnacle species of the family Archaeobalanidae (Cirripedia: Thoracica), from the Azores. *Zootaxa* **2680**: 33-44.

Wirtz, P.; Araújo, R. & Southward, A. (2006): Cirripedia of Madeira. *Helgoland Marine Research* **60** (3): 207-212. http://dx.doi.org/10.1007/s10152-006-0036-5

Young, P. S. (1998) Cirripedia (Crustacea) from the "Campagne Biaçores" in the Azores region, including a generic revision of the Verrucidae. *Zoosystema* **20** (1): 31-92.

Zullo, V. A. (1968): *Tesseropora* Pilsbry (Cirripedia, Thoracica) from the Pliocene of the Gulf of California. *Crustaceana* **15** (3): 272-274.

A large ichthyosaur vertebra from the lower Kössen Formation (Upper Norian) of the Lahnewiesgraben near Garmisch-Partenkirchen, Germany

Hans-Volker Karl[1] *; Gernot Arp[2]; Eva Siedersbeck[3] & Joachim Reitner[2]

[1]*Thuringian State Office for Monument Conservation and Archaeology, Humboldtstr. 11, 99423 Weimar, Germany; Email: KarlHV@tlda.thueringen.de*

[2]*Department of Geobiology, Geoscience Centre, Georg-August University Göttingen, Goldschmidtstr. 3, 37077 Göttingen, Germany*

[3]*Martinswinkelstr. 10, 82467 Garmisch-Partenkirchen, Germany*

* corresponding author

A posterior dorsal centrum of a large ichthyosaur is described and discussed. The vertebra was found in the lower Kössen Formation (Hochalm Member, Upper Norian) of the Lahnewiesgraben near Garmisch-Partenkirchen, Bavaria. The large dimension of the vertebra is remarkable and suggests at total length of the ichthyosaur similar to the giant *Shonisaurus* of the same age. The colonization by a low-diverse, small-sized bivalve community suggests that this vertebra served as an island-like hard substrate on the seafloor for about some years prior to final embedding.

Introduction

Ichthyosaurs are prominent components of Mesozoic marine vertebrate communities (e.g., Maisch 2010). While isolated vertebrae of small to medium-sized ichthyosaurs are common in many shallow-marine deposits, large specimens are rare and have always attracted much attention (e.g., Theodori 1854; Zapfe 1976). Isolated vertebral centra of ichthyosaurs can readily be identified in terms of their approximate position in the vertebral series (McGowan & Motani 2003). Vertebrae in which the dia-pophysis (dp) and parapophysis (pp) lie in the lower half of the centrum probably have to be attributed to the posterior half of the dorsal series. In this article we describe an ichthyosaur vertebra from the Upper Triassic Kössen Formation from the Northern Calcareous Alps with affinities to *Shonisaurus*. The enormous size of the vertebra, its stratigraphic position and rareness is of scientific importance.
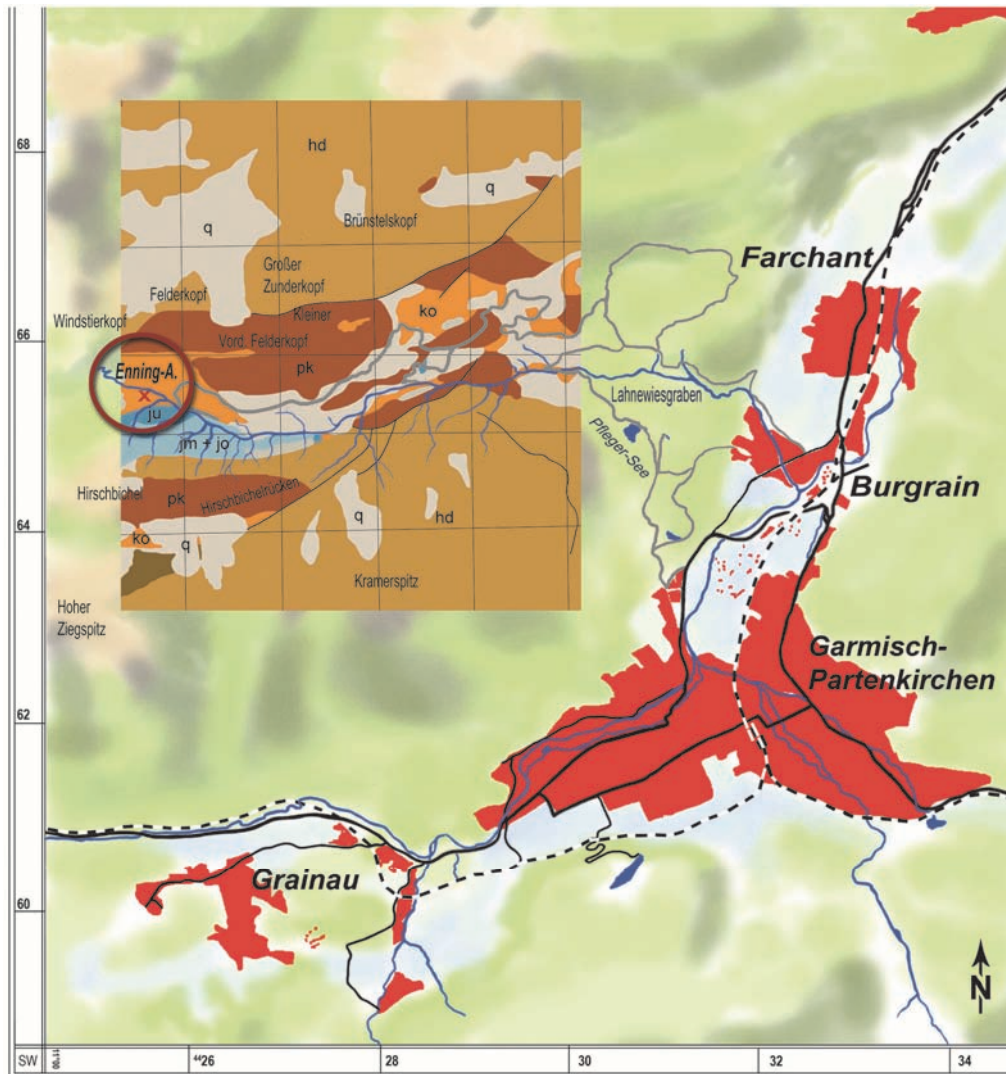
Fig. 1: Locality of the described giant Upper Norian ichthyosaur vertebra (GZG.V.26007), Fleckgraben, creek into the Lahnewiesgraben (Enning-Alm) near Garmisch-Partenkirchen, Bavaria, Germany [GPS 47311916 N; 11004870 E]. Geological map of the Lahnewiesgraben area. **hd:** Hauptdolomit Formation, **pk:** Plattenkalk Formation, **ko:** Kössen Formation, **ju:** Lower Jurassic formations, **jm + jo:** Middle and Upper Jurassic formations, **q:** Quaternary deposits.

Geological setting and stratigraphy

The Lahnewiesgraben is an alpine creek 2 km NW of Garmisch-Partenkirchen, Northern Calcareous Alps, Bavaria (Fig. 1). The upper Triassic to lower Cretaceous series of the Lahnewiesgraben area were deposited at the northern margin of the Tethys and incorporated into the upper Austroalpine nappe system (for review see e.g., Mandl 2000), specifically the Lechtal Nappe (Kuhnert 1967), during the Alpine Orogeny. One important structural geological element of the Lechtal Nappe system is the Lahnewies-Neidernach syncline. Due to the tectonically incompetent Kössen facies this syncline exhibits a strong special faulting and folding which makes it difficult to find complete stratigraphic sections. The uppermost Triassic of the Lahnewies–Neidernach syncline is represented by dark shale, marly limestones and limestones of the Kössen Formation being considered deposits of intraplatform basins

due to extensional tectonics and successive desintegration of the vast Norian Austroalpine carbonate platform. Lower facies of the Kössen Formation (Hochalm Member; Golebiowski 1990) is characterized by highly fossiliferous shallowing upward-cycles of marls and calcareous tempestites with a rich and diverse community of bivalves like *Rhaetavicula contorta* (Portlock), *Bakevellia praecursor* (Quenstedt), *Gervillaria inflata* (Schafhäutl), *Modiolus minutus* (Goldfuss), *Atreta intusstriata* (Emmrich), abundant brachiopods *Rhaetina gregaria* (Suess) (Kuss 1983, Tomašových 2006), and further invertebrates. Plant remains like horsetails (e.g., *Equisetites muensteri*, *Equisetites intermedius* and *Equisetites grosphodon*) have been swept into these intraplatform basins by storm events (Kühn 1940; Friebe 2000). Near the basis of the Hochalm Member, at the transition to the Plattenkalk Member of the Hauptdolomit Formation, vertebrate remains and accumulations of conchostraca have been described from shallow marine often bituminous carbonates (e.g., Faupl 2000).

Lahnewiesgraben-Enning
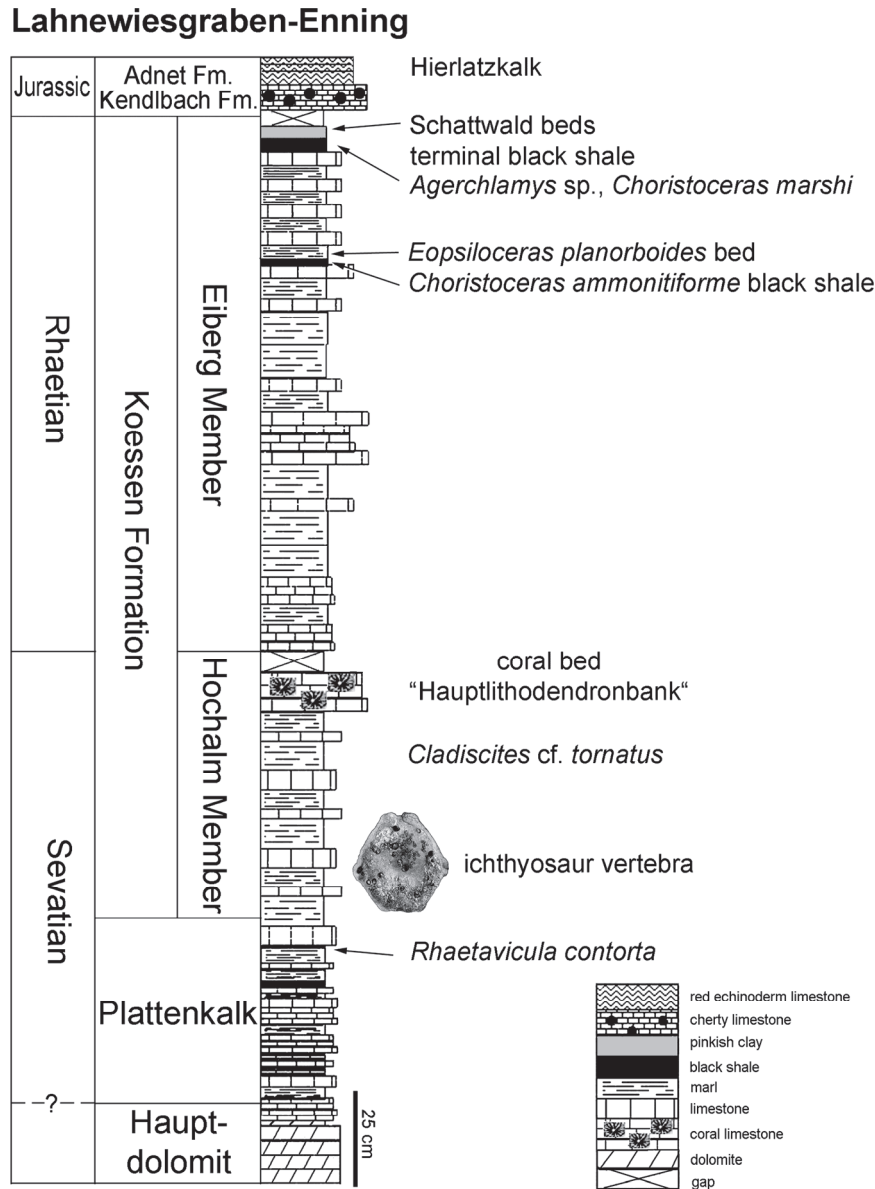
Fig. 2:   Complied stratigraphic section of the Upper Triassic of the Lahnewies–Neidernach syncline.

The top of the Hochalm Member is marked by a widespread, thick coral bed (Hauptlithodendronbank). The following Eiberg Member (Golebiowski 1990) finally reflects a further deepening with less fossiliferous marl-limestone alternations characterized by deeper-water trace fossil associations (e.g., *Zoophycos*) and a few cephalopod beds, within the Lahnewies–Neidernach syncline specifically with *Eopsiloceras planorboides* (Gümbel), *Choristoceras* cf. *ammonitiforme* (Gümbel) and *Choristoceras marshi* (Hauer). Remarkable are a couple of cephalopod-bearing beds near the top of Eiberg facies which is characteristic for the Lahnewies–Neidernach syncline (Reitner 1978) (Fig. 2). This couple is composed of a black shale with abundant small *Choristoceras* cf. *ammonitiforme* and small *Agerchlamys*-type bivales followed up a grey bioturbated marly limestone with abundant *Eopsiloceras planorboides* specimens, the only known finding site in the Kössen beds of the North-

ern Calcareous Alps. The top of the section is characterized by a 20 cm thick oil shale with *Choristoceras marshi* and abundant *Agerchlamys* bivales and the red to pink coloured Schattwald beds, similar to other sections of the western Eiberg Basin (Hillebrandt et al. 2007, Hillebrandt & Kment 2009). The Kössen Formation has approximately 200 m thickness (Linke 1963). However, a number of faults and folds inhibit the presentation of a continuous section. The presented section is a simplified sedimentological and stratigraphic compilation of tectonically isolated small sections of the Lahnewies–Neidernach syncline.

The vertebra described in this paper was found in September 2003 in a tributary in the eastern part of the Lahnewiesgraben (Fleckgraben) *ex situ* at basal parts of the Hochalm Member. The Upper Norian age of these basal parts is indicated by the finding of a *Cladiscites* cf. *tornatus* (Bronn) (Wiedmann et al. 1979) (Fig. 2).
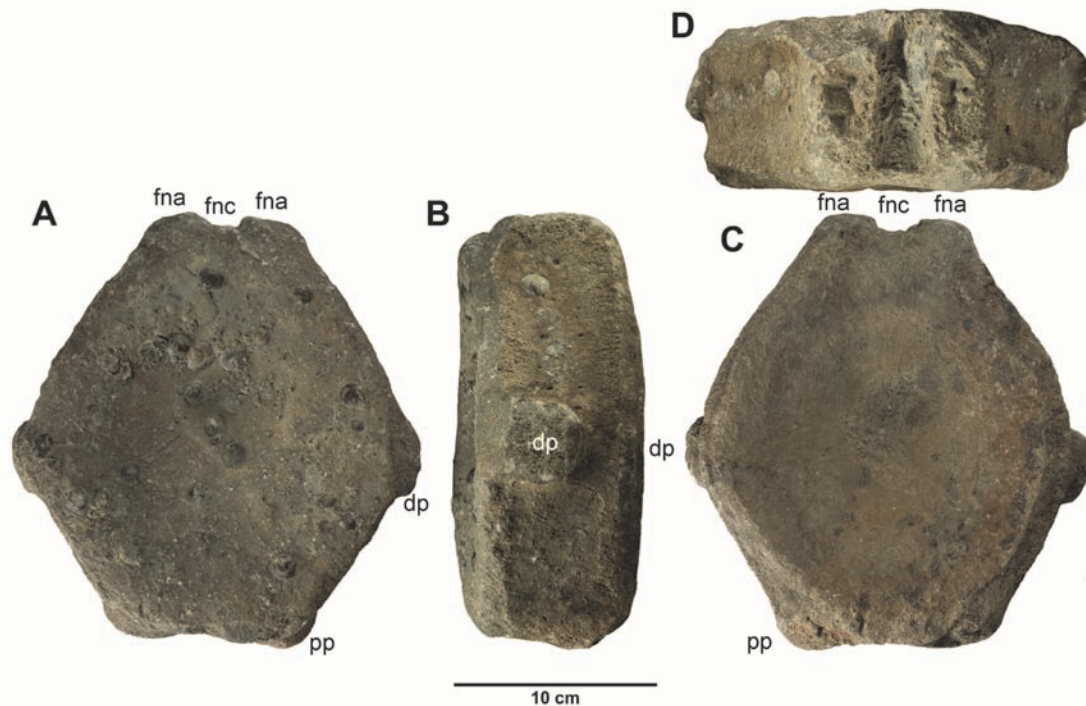
Fig. 3: Ichthyosauria gen. et sp. indet., presacral trunk vertebra from the lower Kössen Formation (Hochalm Mb; Upper Norian) of the Lahnewiesgraben near Garmisch-Partenkirchen (Geoscience Museum Göttingen collection number: GZG.V.26007). **(A)** anterior views, **(B)** lateral view, **(C)** posterior view, **(D)** dorsal view [Abbreviations: fnc = floor of neural canal, fna = facet of neural arch, dp = diapophysis, pp = parapophysis].

Short review on Triassic ichthyosaurs

Ichthyosaurs were important large marine Triassic vertebrates and their record is starting in the lower Triassic, e.g., first taxa are known from the Sticky Keep Formation in Svalbard (Olenekian). However, they were abundantly found in organic-rich sediments of the middle Triassic (Anisian–Ladinan). Important sites are known form the southern Alps of Switzerland and northern Italy (Monte San Giorgio Grenzbitumen zone and lower Meride Limestone) (e.g., Maisch & Matzke 2005; Furrer 1995; Wirz 1945), Guanling Formation of Guizhou, southern China (e.g., Li 1999), and the Ladinian/early Carnian Tschermakfjellet Formation of Svalbard (e.g., Riis et al. 2008). Haubold (2002) summarizes the known ichthyosaur taxa of the Alpine and German Triassic. Most important are the findings from the Anisian/Ladinian Grenzbitumenzone and lower Meride Limestone of the Monte San Giorgio realm with taxa of Mixosauridae (*Mixosaurus cornalianus, M. kuhnschnyderi, Wimanius odontopalatus*) and Shastasauridae (*Besanosaurus leptorhynchus, Cymbospondylus buchseri*). From the German Basin (Anisian Röt Formation/Lower Muschelkalk), diverse remains of Mixosauridae (*Contectopalatus/Mixosaurus atavus*), questionable Omphalosauridae (*Tholodus schmidi)* are known, and from Ladinian upper Muschelkalk taxa of Mixosauridae (*Contectopalatus/Mixosaurus atavus, Phalarodon major*), Cymbospondylidae (*Phantomosaurus/Shastasaurus neubigi*), and Omphalosauridea (*Omphalosaurus* sp.) are known (von Meyer 1848; Peyer

1939). Nicholls & Makoto (2004) described remains of a large *Shonisaurus* from the Norian of British Columbia.

However, upper Triassic sites with ichtyosaur remains are sparse and all new findings are of great phylogenetic importance. A general survey on the palaeobiogeography of ichthyosaurs is given by Sander & Faber (1998) and Sander & Mazin (1993), as well as on the phylogeny by Lawrence (2008) and Maisch (2010).

A large ichthyosaur vertebra (*Leptopterygius* sp.) is already known from the Kössen Formation with a diameter of 16 cm from the Neumühle quarry near Vienna (Zapfe 1976). Before, two small ichthyosaur vertebrae from the Kössener Schichten of Schleimser Joch in the Achental (Austria) were described by von Meyer (1856) like that of *Ichtyosaurus tenuirostris*. Up to now the following species were found in the same horizon of the present specimen in the upper Norian to Rhaetian (arrangement according to McGowan & Motani, in 2003):

(1) *Macgowania janiceps* from upper Norian of British Columbia, only anterior skeleton parts known;

(2) *Leptonectes tenuirostris* from upper Rhaetian of England, with round vertebrae (ca. 2.5 m);

(3) *Leptonectes solei* from upper Rhaetian of England, with round vertebrae (large form, skull 1 m);

(4) *Leptonectes moorei* from upper Rhaetian of England, only anterior skeleton parts known (small form);

(5) *Ichthyosaurus communis* from Triassic–Jurassic boundary from England, moderate large form up to 2.5 m.
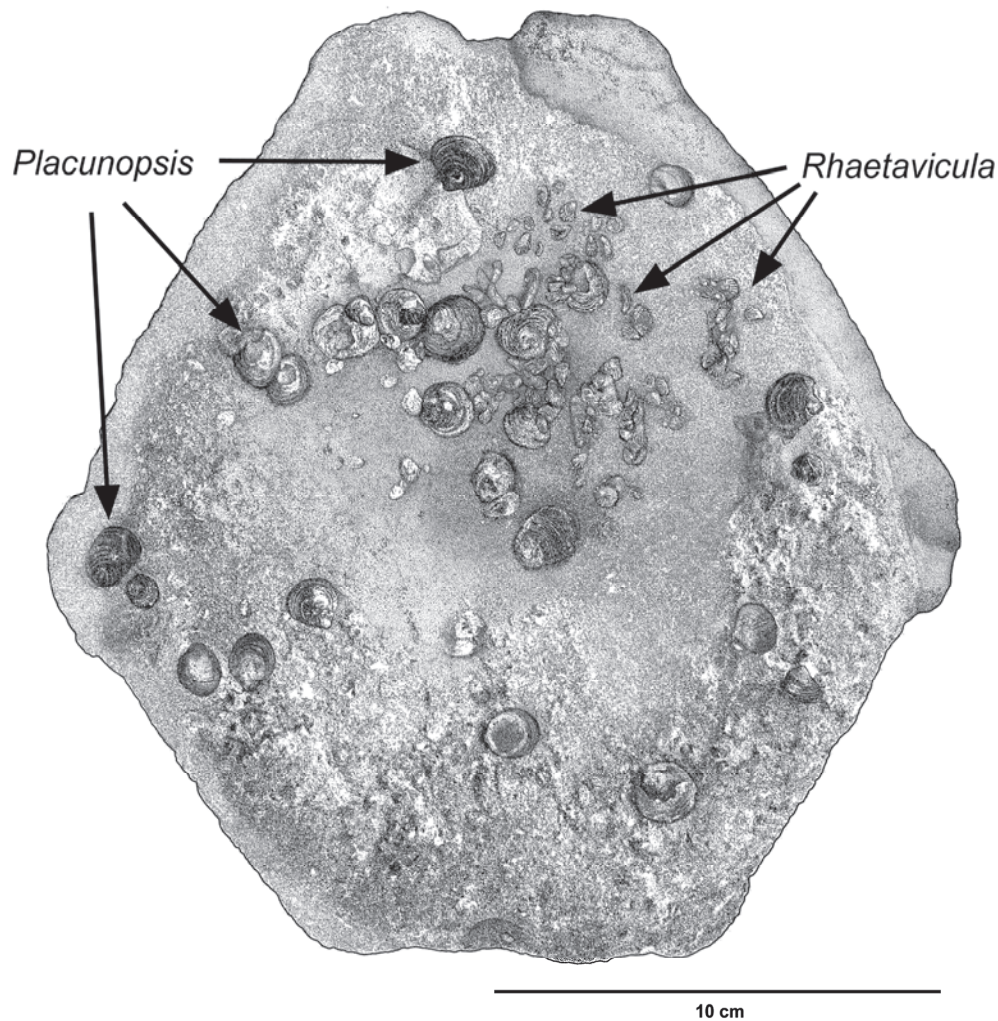
Fig. 4:   Drawing of the vertebra showing the attached bivalve species *Placunopsis alpine* and *Rhaetavicula contorta*.

Description of the new ichthyosaur vertebra

It is not possible to erect a valid new taxon based on one vertebra. However, the vertebra is well preserved and exhibits some significant anatomical characters which have affinities to the *Shonisaurus* group.

The here described presacral trunk vertebra, (Fig. 3; GZG.V.26007, leg. Eva Siedersbeck, Garmisch-Partenkirchen) was found in the Fleckgraben, a side creek of the Lahnewiesgraben close the Enning-Alm near Garmisch-Partenkirchen (Bavaria, Germany; Fig. 1). Exposed in the Fleckgraben is the Lower Kössen Formation (Upper Norian, Hochalm Member).

The general outline resembles that of the specimen depicted by McGowan & Motani (2003) and named *Omphalosaurus* sp. (BMNH 24684 d). Such vertebrae can be identified as originating from the posterior dorsal region of *Omphalosaurus* or *Ophthalmosaurus* and should clearly be used with great caution concerning taxonomy (McGowan & Motani, 2003). In comparison with the measurements of TMP 94.378.2, *Shonisaurus sikanniensis,* a large ichthyosaur of 21 meters in length, possibly like our new specimen, *Shonisaurus popularis*, *Leptopterygius rheticus*, and *Leptopterygius* sp. from the Kössen Formation show the much higher compactness of our vertebra from the Lahnewiesgraben. Based on the presence of a single apophysis located on the lateral surface of the bone, the vertebra is caudal in origin and many large ichthyosaurs from the time frame in question have hexagonal caudals. Among Triassic vertebrae, only Middle Triassic and later ichthyosaurs have short vertebrae with H/L ratio greater than 1.5. The more primitive forms have H/L ratios of 0.9 to 1.2 (Motani 2000). Vertebral body size and proportions similar to *Shonisaurus sikanniensis* presacral or posterior trunk vertebra, but in contrast to clear hexagonal outline. Also for the ichthyosaur from Lahnewiesgraben can be assumed that this was a large animal with a body length of more than 20 meters.

Table 1: Measurements and ratios of the trunk vertebra.

L	H	W	H/L	W/L
7.8	21.0	18.5	2.7	2.4

Epibiontic colonization of the vertebra

The surface of the vertebra shows a number of attached bivalve shells (Fig. 4). One intervertebral surface as well as side faces of the centrum show about 25 specimen of the fixosessile, cemented *Placunopsis alpina* (Winkler, 1859) with shell heights not exceeding 1 cm. In addition, about 150 small specimen of the epibyssate *Rhaetavicula contorta* (Portlock, 1843) with maximum shell heights of 5 mm are attached. Specimens of both bivalve species are commonly articulated and are here considered as an autochthonous association. In contrast, two valves of the shallow infaunal *Myophoriopis isoceles* (Stoppani, 1857) which are also attached to the vertebra are clearly par-autochthonous. Attached benthos of the other intervertebral surface was removed during preparation. The observed bivalve community is typical for the Hochalm Member (Mb) of the Lower Kössen Formation.

Discussion

The vertebral body size and proportions of the here presented specimen are comparable to *Shonisaurus sikanniensis* presacral or posterior trunk vertebra. It is a very large ichthyosaur with a length of more than 20 meters The cluster belongs to the Lahnewiesgraben specimen, and shows the same type of vertebra in the proportions as the two corresponding of *Shonisaurus sikanniensis*. On the other hand, it clearly differs in its shape.

The low diverse, small-sized bivalve epibiontic association suggests that the vertebra surface was exposed to the water column for about some years prior to final embedding. During that time, the vertebra constituted a hard substrate for benthic colonizers on the seafloor, similar to present-day whale vertebra in shelf and deep-see environments (Smith & Baco 2003).

Acknowledgements

References

Faupl, P. (2000): *Historische Geologie – Eine Einführung*. Wien (Facultas Universitätsverlag): 271 pp.

Friebe, G. (2000): Schachtelhalme (Equisetaceae) aus der Kössen-Formation (Rhaetium) der Nördlichen Kalkalpen Vorarlbergs. *Vorarlberger Naturschau* **8**: 191-200.

Furrer, H. (1995): The Kalkschieferzone (Upper Meride Limestone; Ladinian) near Meride (Canton Ticino, Southern Switzerland) and the evolution of a Middle Triassic intraplatform basin. *Eclogae geologicae Helvetiae* **88** (3): 827-852.

Golebiowski, R. (1990): The Alpine Kössen Formation, a key for European topmost Triassic correlations. *Albertiana* **8**: 25-35.

Haubold, H. (2002): Literaturbericht-Ichthyosaurier und Sauropterygier. *Zentralblatt für Geologie und Paläontologie (II: Paläontologie)* **[2002]** (5/6): 367-410.

Hillebrandt, A. von & Kment, K. (2009): Die Trias/Jura-Grenze und der Jura in der Karwendelmulde und dem Bayerischen Synklinorium. *Deutsche Stratigraphische Kommission (DSK) Subkommission für Jurastratigraphie. Exkursionsführer zur Jahrestagung in Fall vom 10.-13.06.2009.* Erlangen (Druckladen): 45 pp.

Hillebrandt, A. von; Krystyn, L. & Kuerschner, W. M. (2007): A candidate GSSP for the base of the Jurassic in the Northern Calcareous Alps (Kuhjoch section, Karwendel Mountains, Tyrol, Austria). *ISJS Newsletter* **34** (1): 2-20.

Kühn, O. (1940): Zur Kenntnis des Rhät von Vorarlberg. *Mitteilungen des Alpenländischen geologischen Vereins* **33**: 111-157.

Kuhnert, C. [with contrib. of K. Bader; K. Cramer; T. Diez; E. Hohenstatter; M. Schuch & A. Lohr] (1967): *Erläuterungen zur geologischen Karte von Bayern. Blatt Nr. 8432 Oberammergau*. München (Bayerisches Geologisches Landesamt): 128 pp.

Kuss, J. (1983): Faziesentwicklung in proximalen Intraplattform-Becken: Sedimentation, Palökologie und Geochemie der Kössener Schichten (Ober-Trias, Nördliche Kalkalpen). *Facies* **9** (1): 61-171. http://dx.doi.org/10.1007/BF02536659

Lawrence, J. D. (2008): A total evidence analysis of the evolutionary history of the thunnosaur ichthyosaurs. *Unpublished Master Thesis, Graduate College of Bowling Green State University*. Bowling Green, Ohio: 82 pp.

Li Chun (1999): Ichthyosaur from Guizhou, China. *Chinese Science Bulletin* **44** (14): 1329-1333.

Linke, G. (1963): Neue Ergebnisse zur Stratigraphie und Tektonik der Lahnenwies-Mulde und ihrer näheren Umgebung. *Unpublished PhD thesis, FU Berlin*. Berlin: 114 pp.

Maisch, M. W. & Matzke, A. T. (2005): Observations on Triassic ichthyosaurs. Part XIV: The Middle Triassic mixosaurid Phalarodon major (v. Huene, 1916) from Switzerland and a reconstruction of mixosaurid phylogeny. *Neues Jahrbuch für Geologie und Paläontologie, Monatshefte* **[2005]** (10): 597-613.

Maisch, M. W. (2010): Phylogeny, systematics, and origin of the Ichthyosauria – the state of the art. *Palaeodiversity* **3**: 151-214.

Mandl, G. W. 2000. The Alpine sector of the Tethyan shelf – Examples of Triassic to Jurassic sedimentation and deformation from the Northern Calcareous Alps. *Mitteilungen der Österreichischen Geologischen Gesellschaft* **92** [1999]: 61-77.

McGowan, C. & Motani, R. (2003): Ichthyopterygia. In: Suess, H.-D. (ed.): *Handbook of Paleoherpetology* **8**: 175 pp.

Meyer, H. von (1848): *Tholodus Schmidi. Neues Jahrbuch für Mineralogie etc.* **[1848]**: 467.

Meyer, H. von (1856): Mittheilungen an Professor Bronn gerichtet. *Neues Jahrbuch für Mineralogie etc.* **[1856]**: 824-825.

Motani, R. (2000): Is *Omphalosaurus* ichthyopterygian? – A phylogenetic perspective. *Journal of Vertebrate Paleontology* **20** (2): 295-301. http://dx.doi.org/1671/0272-4634(2000)020[0295:IOIAPP]2.0.CO;2

Nicholls, E. L. & Makoto, M. (2004): Giant ichthyosaurs of the Triassic - a new species of *Shonisaurus* from the Pardonet Formation (Norian: Late Triassic) of British Columbia. *Journal of Vertebrate Paleontology* **24** (4): 838-849. http://dx.doi.org/1671/0272-4634(2004)024[0838: GIOTTN]2.0.CO;2

Peyer, B. (1939): Über *Tholodus schmidi* H. v. Meyer. *Palaeontographica (A: Paläozoologie, Stratigraphie)* **90** (1-2): 1-47.

Portlock, J. E. (1843): *Report on the geology of the county of Londonderry and parts of Tyrone and Fermanagh.* Dublin (Milliken): 784 pp.

Reitner, J. (1978): Ein Teuthiden-Rest aus dem Obernor (Kössener Schichten) der Lahnewies-Neidernachmulde bei Garmisch-Partenkirchen (Bayern). *Paläontologische Zeitschrift* **52** (3/4): 205-212. http://dx.doi.org/10.1007/BF02987702

Riis, F.; Lundschien, B. A.; Høy, T.; Mørk, A. & Mørk, M. B. E. (2008): Evolution of the Triassic shelf in the northern Barents Sea region. *Polar Research* **27**: 318-338. http://dx.doi.org/10.1111/j.1751-8369.2008.00086.x

Sander, P. M. & Faber, C. (1998): New finds of *Omphalosaurus* and a review of Triassic ichthyosaur paleobiogeography. *Paläontologische Zeitschrift* **72** (1/2):149-162. http://dx.doi.org/10.1007/BF02987823

Sander, P. M. & Mazin, J. M. (1993): The palaeobiogeography of Middle Triassic ichthyosaurs: five major faunas. *Paleontologia Lombarda (N.S.)* **2**: 145-152.

Smith, C. R. & Baco, A. R. (2003): Ecology of whale falls at the deep-sea floor. *Oceanography and Marine Biology: an Annual Review* **41**: 311-354.

Stoppani, A. (1857): *Studii geologici e paleontologici sulla Lombardia.* Milano (Turati): 461 pp.

Theodori, C. (1854): *Beschreibung des kolossalen* Ichthyosaurus trigonodon *in der Lokal-Petrefakten-Sammlung zu Banz, nebst synoptischer Darstellung der übrigen* Ichthyosaurus-*Arten in derselben.* München (G. Franz): xiv + 81 pp.

Tomašových, A. (2006): Brachiopod and Bivalve Ecology in the Late Triassic (Alps, Austria): Onshore-Offshore Replacements Caused by Variations in Sediment and Nutrient Supply. *Palaios* **21** (4): 344-368. http://dx.doi.org/10.2110/palo.2005.P05-53e

Wiedmann, J.; Fabricius, F.; Krystyn, L.; Reitner, J. & Urlichs, M. (1979): Über Umfang und Stellung des Rhaet. *Newsletters on Stratigraphy* **8** (2): 133-152.

Winkler, G. G. (1859): *Die Schichten der* Avicula contorta *inner- und ausserhalb der Alpen. Palaeontologisch-geognostische Studie.* München (Joh. Palm's Hofbuchhandlung): 51 pp.

Wirz, A. (1945): Die Triasfauna der Tessiner Kalkalpen. XV. Beiträge zur Kenntnis des Ladinikums im Gebiete des Monte San Giorgio. *Schweizerische Paläontologische Abhandlungen* **65**: 1-84.

Zapfe, H. (1976): Ein großer Ichthyosaurier aus den Kössener Schichten der Nordalpen. *Annalen des Naturhistorischen Museums Wien* **80**: 239-250.

Göttingen Contributions to Geosciences 77

This volume contains papers presented in part at a symposium held in May 2012 at Göttingen University, to honour Professor Joachim Reitner for his numerous contributions to the fields of geobiology, geology, and palaeontology. Our present volume reflects the breadth of Reitner's interests and accomplishement with tributes and research or review papers by his students, former students, collaborators, and friends.
The symposium was held in conjunction with Joachim Reitner's 60th birthday.

GEORG-AUGUST-UNIVERSITÄT GÖTTINGEN

Universitätsverlag Göttingen